CHEMICAL & PHARMACEUTICAL BULLETIN

Vol. 35, No. 11 November 1987

Regular Articles

[Chem. Pharm. Bull. 35(11)4377—4394(1987)]

# Correlation between Molecular Orbital Distributions in Drug-Receptor Interaction: Diels–Alder Reaction Systems and Dihydrofolate Reductase System

HIDEO KUBODERA and HIDEAKI UMEYAMA*

*School of Pharmaceutical Sciences, Kitasato University, Shirokane, Minato-ku, Tokyo 108, Japan*

(Received March 2, 1987)

An index which corresponds to charge transfer interaction is presented as a tool to study the correlation of molecular orbital (MO) distributions. The MO distribution correlation (MODIC) index was applied to Diels–Alder reaction systems (1-methoxy-1,3-butadiene–acrolein system and cyclopentadiene–maleic acid anhydride system), and the dihydrofolate reductase (DHFR) system. In the Diels–Alder reaction systems, the positions of reaction centers and orientations of substitutional groups predicted by the index were consistent with experimental findings. In the DHFR system, the reactivities of different ligands were explained by the index.

Frontier electron theory provides some indexes to predict reactivities, based on the molecular orbital coefficients of the isolated molecule in its ground state. The MODIC index has the advantage that it contains information on the three-dimensional distribution of MO's. It can predict the MO's in the transition state of a reaction.

**Keywords**——drug-receptor interaction; charge transfer interaction; molecular orbital distribution; *ab initio*; molecular surface; Diels–Alder reaction; dihydrofolate reductase; methotrexate; NADPH

## Introduction

To evaluate the drug-receptor interaction correctly is of great importance when the structure–activity relationship is discussed. The overall interaction can be categorized into electrostatic interaction, exchange repulsion, polarization interaction, dispersion force, charge transfer interaction, hydrophobic interaction and so on. As regards the electrostatic interaction, it has been reported that the distributions of electrostatic potentials of enzyme and ligand show a good complementarity.[1~3] Such distributions can not be expressed precisely by using so-called Mulliken charges[4] of molecules. For this reason, we developed a new set of charges to reproduce the results of *ab initio* molecular orbital (MO) calculation.[5,6] The exchange repulsion and dispersion force can be estimated by assuming, for example, Lennard–Jones potential function, if the interactomic distances are known. It is very difficult to evaluate the "real" hydrophobic interaction energy, because it includes the problem of entropy. Some practical ways of estimation, however, have been reported.[7,8]

The afore-mentioned interactions do not include the effect of intermolecular charge

transfer. This effect, however, should be taken into consideration when chemical reactions such as enzymatic reactions are discussed. If *ab initio* MO theory is employed, the charge transfer interaction can be evaluated properly based on appropriate methodology and basis set functions. However, the molecules of interest in biological and pharmaceutical studies are too large in general for the theory to be applicable in practice. In such a situation, an index which corresponds to intermolecular charge transfer interaction is necessary.

The molecular orbital distribution correlation (MODIC) index is introduced here and applied to Diels–Alder reaction systems (1-methoxy-1,3-butadiene–acrolein system and cyclopentadiene–maleic acid anhydride system), and the dihydrofolate reductase (DHFR) system. In the Diels–Alder reaction systems, the positions of reaction centers and orientations of substitutional groups predicted by the index were consistent with experimental findings. In the DHFR system, dihydrofolate molecules, which are protonated and not protonated at the 5-position, and methotrexate (MTX) were used as ligand molecules. Experimental results on the reactivities of these different ligands were explained reasonably by the index.

## Method

The MODIC index was estimated on the van der Waals surface of one molecule in the interacting system in the fashion described below. *Ab initio* molecular orbital calculations were applied to these models. In the present paper RHF-LCAO-*ab initio* calculations were performed based on the STO-3G[9] or 4-31G[10] basis set using the GAUSSIAN GENERAL program.[11] The van der Waals molecular surface of one molecule, which is numbered 2,

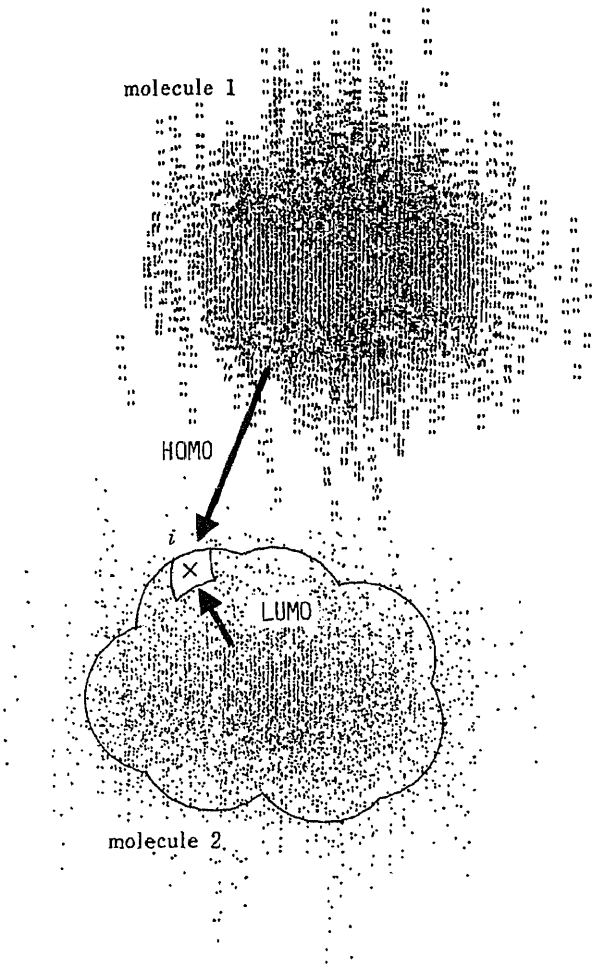


Fig. 1. Interacting Molecules

The values of MO's of the two molecules are evaluated at the same point on the molecular surface of the one molecule.

for example, was expressed with many patches. The value of the $m$-th MO of molecule 2 (guest molecule), $P^i_{2,m}$, was evaluated at each point $i$ on this "guest" molecular surface (see Fig. 1). The value of the $n$-th MO of molecule 1 (host molecule), $P^i_{1,n}$, was also evaluated at the same point, $i$, on the guest molecular surface.

The energetically scaled product of $P^i_{1,n}$ and $P^i_{2,m}$ is calculated as the MODIC parameter. The absolute value of the average of the MODIC parameter over the whole or specific region of the surface was calculated as the MODIC index according to the next equations.

$$\text{MODIC parameter} = P^i_{1,n}P^i_{2,m}/|e_{1,n}-e_{2,m}|^{1/2}$$

$$\text{averaged MODIC parameter} = \sum_i (P^i_{1,n}P^i_{2,m}/|e_{1,n}-e_{2,m}|^{1/2})s_i/\sum_i s_i$$

$$= \sum_i (\text{MODIC parameter})s_i/\sum_i s_i$$

$$\text{MODIC index} = |\sum_i (P^i_{1,n}P^i_{2,m}/|e_{1,n}-e_{2,m}|^{1/2})s_i/\sum_i s_i|$$

$$= |\text{averaged MODIC parameter}|$$

where $e_{1,n}$ and $e_{2,m}$ are the energy levels of the $n$-th and $m$-th molecular orbitals of molecules 1 and 2, respectively; $s_i$ is the patch area which is assigned to each point $i$. The MODIC index shows the correlation of molecular orbital distributions. The molecular surface was expressed[1-3,5-8] as an assembly of spheres having van der Waals radii.[12] We took up here energetically closest combinations of the highest occupied molecular orbital (HOMO) and the lowest unoccupied molecular orbital (LUMO). A modified version of GAUSSIAN GENERAL was used for evaluation of the MODIC indexes.

Firstly, the Diels–Alder reaction systems (1-methoxy-1,3-butadiene–acrolein, and cyclopentadiene–maleic acid anhydride systems) were treated. Each molecular geometry was taken from experimental data.[13] For the 1-methoxy-1,3-butadiene–acrolein system, the dependency of the index on geometrical change was tested with reference to the transition state structure of the ethylene–butadiene system.[14]

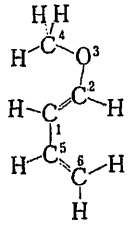

1-methoxy-1,3-butadiene

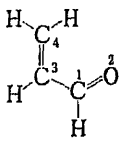

acrolein

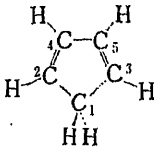

cyclopentadiene

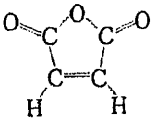

When the orientations of substitutional groups were considered, exponents of Gaussian-type functions were enlarged so as to make each atomic orbital contribution clear in the calculation of the above equation (see Results and Discussion).

As examples of applications to biological systems, the DHFR system was taken up: system A, dihydrofolate (protonated at the 5-position)–reduced nicotinamide adenine dinucleotide phosphate (NADPH); system B, dihydrofolate (non-protonated)–NADPH; system C, MTX–NADPH. Dihydrofolate and methotrexate, which are a substrate and an inhibitor, respectively, were modeled as shown below. The molecule of NADPH was also modeled only by a nicotinamide ring.

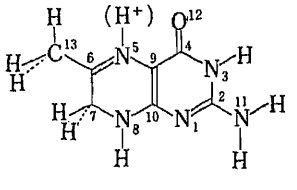

dihydrofolate

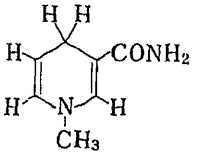

NADPH

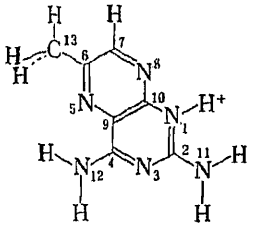

methotrexate (MTX)

The coordinates of MTX and NADPH were taken from an entry in the Protein Data Bank (PDB)[15] registered as 3DFR.[16] As for dihydrofolates (protonated and not protonated), MNDO calculations[17] were applied to optimize their geometries. After that, based on the report by Bolin *et al.*,[16] their atoms were superimposed to get the best least-squares fit to corresponding atoms of MTX (Fig. 2).

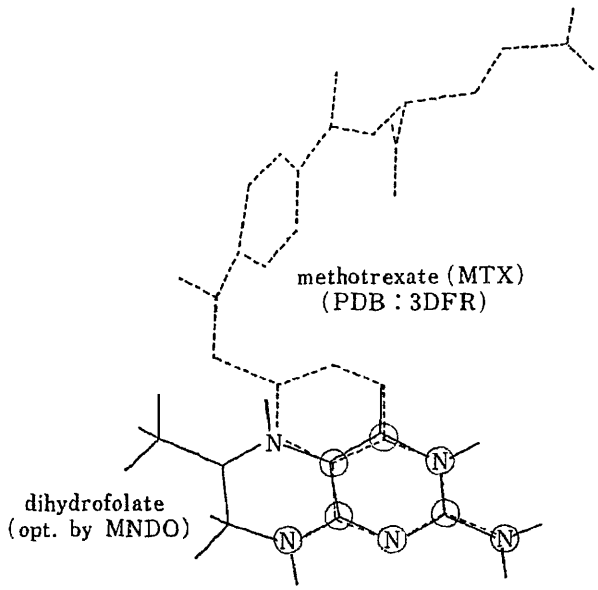


Fig. 2. Least-Squares Fit of Dihydrofolate Molecule to Methotrexate

The solid line stands for the geometries of dihydrofolates (protonated at the 6-position and not protonated), while the dashed line represents methotrexate. The geometries of dihydrofolates were optimized by MNDO calculations. The geometry of methotrexate was taken from the protein data bank (registered number 3DFR). The encircled atoms were used for the fitting.

The energy decomposition method[18-25] was employed to analyze intermolecular interactions. Molecular orbital calculations were done at the computer center of the University of Tokyo and at the computer center of the Institute for Molecular Science. The calculations of MODIC indexes were performed at the computer center of the University of Tokyo. In the calculation procedure, only the graphical part was performed with a program, which is a modified version of TERAS.[26]

## Results and Discussion

### 1-Methoxy-1,3-butadiene–Acrolein System

The geometries of the 1-methoxy-1,3-butadiene–acrolein system are shown in Fig. 3. The distance $R$ connecting the centers of reaction sites in both molecules is changed to 2.1, 3.4 and 4.9 Å. Distances of 2.1 and 3.4 Å correspond to the intermolecular distances of the transition state structure[14] and van der Waals contact of the ethylene–1,3-butadiene reaction system, respectively. The angle theta is changed to 0, 76 and 90 degrees. An angle of 76 degrees is obtained from the transition state structure of ethylene–1,3-butadiene.[14] Both molecules

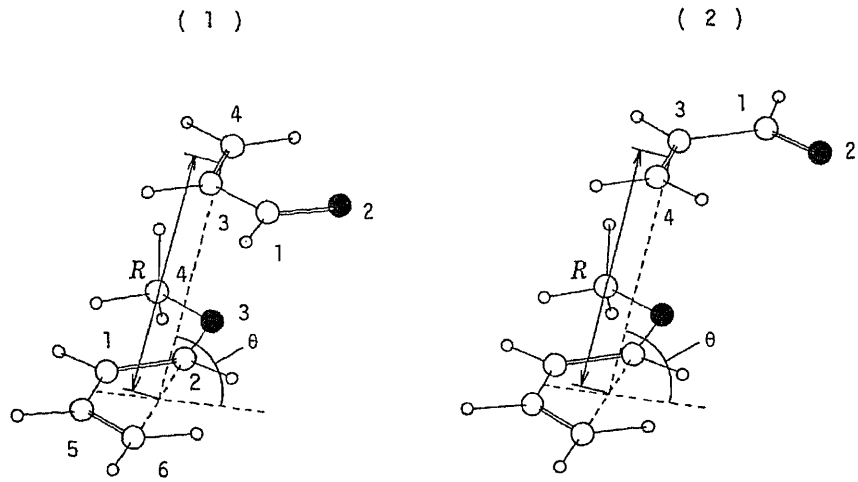


Fig. 3. The Geometry of the 1-Methoxy-1,3-butadiene–Acrolein System

$R$: 2.1, 3.4, 4.9 Å. $\theta$: 0.0, 76.0, 90.0°.
○, carbon; ●, oxygen; o, hydrogen.

TABLE I. Averaged MODIC Parameters (Bohr$^{-3}$ Hartree$^{-1/2}$) for 1-Methoxy-1,3-butadiene and Acrolein

| Atom | 0 degrees | | 76 degrees | | 90 degrees | |
|---|---|---|---|---|---|---|
| | MTBE–ACL1 | MTBE–ACL2 | MTBE–ACL1 | MTBE–ACL2 | MTBE–ACL1 | MTBE–ACL2 |
| 3.4 Å | | | | | | |
| | $\times 10^{-5}$ | $\times 10^{-5}$ | $\times 10^{-5}$ | $\times 10^{-5}$ | $\times 10^{-5}$ | $\times 10^{-5}$ |
| 1 | 0.000222 | 0.000194 | 0.537 | 0.460 | 2.00 | 1.74 |
| 2 | 0.0 | 0.0 | −0.0000675 | −0.0000433 | −0.00227 | −0.00176 |
| 3 | 0.0586 | 0.0514 | 2.96 | 2.83 | 3.82 | 4.16 |
| 4 | 0.0662 | 0.0772 | 2.94 | 2.99 | 4.31 | 3.78 |
| Total | 0.108 | 0.112 | 1.02 | 1.00 | 1.53 | 1.45 |
| 4.9 Å | | | | | | |
| | $\times 10^{-7}$ | $\times 10^{-7}$ | $\times 10^{-7}$ | $\times 10^{-7}$ | $\times 10^{-7}$ | $\times 10^{-7}$ |
| 1 | 0.00000108 | 0.000000949 | 0.118 | 0.105 | 0.830 | 0.769 |
| 2 | 0.0 | 0.0 | −0.00000639 | −0.00000502 | −0.000778 | −0.000654 |
| 3 | 0.00577 | 0.00502 | 1.13 | 1.06 | 1.57 | 1.74 |
| 4 | 0.00706 | 0.00841 | 1.10 | 1.16 | 1.75 | 1.51 |
| Total | 0.0317 | 0.0329 | 0.357 | 0.357 | 0.612 | 0.584 |
| 2.1 Å | | | | | | |
| | | | $\times 10^{-4}$ | $\times 10^{-4}$ | | |
| 1 | | | 0.541 | 0.313 | | |
| 2 | | | 0.0000279 | 0.000114 | | |
| 3 | | | 3.65 | 3.33 | | |
| 4 | | | 3.41 | 3.58 | | |
| Total | | | 1.26 | 1.20 | | |

Planar. MTBE, 1-methoxy-1,3-butadiene (HOMO); ACL1 and ACL2, acrolein from (1) and (2) in Fig. 3, respectively (LUMO); Total, including hydrogens. Evaluation was done on the van der Waals surface of acrolein with the STO-3G basis set.

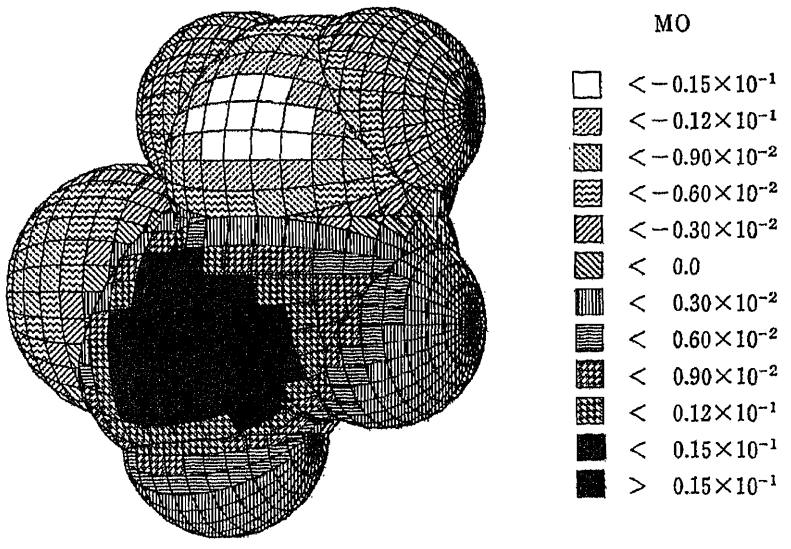


Fig. 4. The LUMO of Acrolein on Its Surface

maintain planar forms and the two planes are parallel. Two types of orientations (1) and (2) in Fig. 3 are considered here to check the predictability of orientation by the MODIC index.

The MODIC indexes for the LUMO of acrolein and the HOMO of 1-methoxy-1,3-butadiene are tabulated in Table I. The uppermost part of the table contains the angular dependency for a distance of 3.4 Å. The positions numbered as 3 and 4 in Fig. 3 have greater

TABLE II. Energy Level and LCAO-MO Coefficients[a]

| | HOMO of 1-methoxy-1,3-butadiene | LUMO of acrolein |
|---|---|---|
| Energy level[b] | −0.2267 | 0.2211 |
| Atom[c] | | |
| 1 | −0.4973 | −0.4976 |
| 2 | −0.4235 | 0.5769 |
| 3 | 0.4558 | −0.4354 |
| 4 | −0.0263 | 0.6484 |
| 5 | 0.3062 | |
| 6 | 0.4831 | |

*a*) The STO-3G basis set was used. *b*) In Hartree unit. *c*) See Fig. 3.

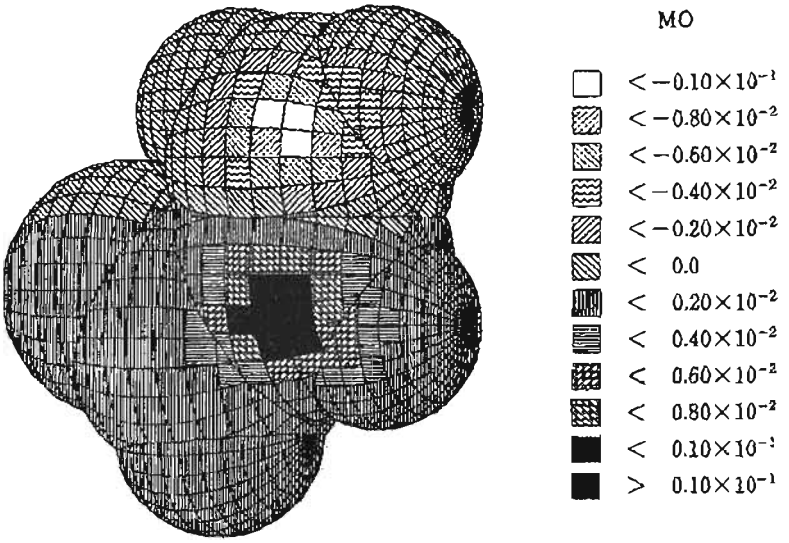


Fig. 5. The HOMO of 1-Methoxy-1,3-butadiene on the Surface of Acrolein
The conformation corresponds to 3.4 Å and 76 degrees (MTBE-ACL1 in Table I).

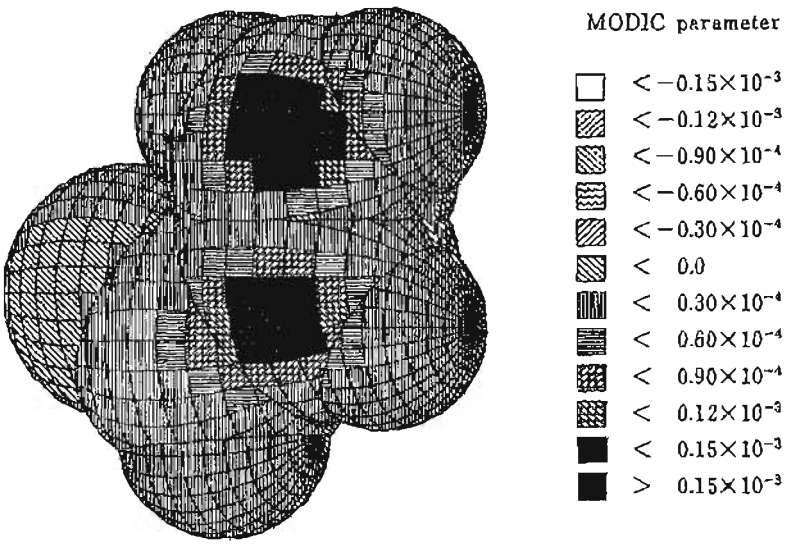


Fig. 6. The MODIC Parameter Distribution on the Surface of Acrolein
The conformation corresponds to 3.4 Å and 76 degrees (MTBE-ACL1 in Table I).

values, which is indicative of the predictability of the reaction center by the index. The value of the index increases a little as the angle becomes larger, because the overlap of the orbitals may increase.

A graphical representation of the LUMO of acrolein on the molecular surface of the guest molecule is depicted in Fig. 4. The molecular surface corresponds to the geometry of the acrolein moiety of Fig. 3, and it faces 1-methoxy-1,3-butadiene. The coefficient of LCAO approximation is largest at the atom numbered 4, as shown in Table II. Graphically considered, however, the MO distribution is rather larger around atoms 1 and 3. This may be due to the contributions from orbitals of atoms 1 and 3, whose LCAO coefficients are not the largest.

The distribution of the HOMO of 1-methoxy-1,3-butadiene is shown on the same molecular surface of acrolein in Fig. 5. The largest values are localized at some narrow regions.

The calculated MODIC parameters between the HOMO of 1-methoxy-1,3-butadiene and the LUMO of acrolein are shown in Fig. 6. It is clear that only the reaction centers have large contributions. This allows us to comprehend the values listed in Table I easily.

Table I also contains the angular dependence at a distance of 4.9 Å. The overall tendency

TABLE III. Effect of Basis Set on Averaged MODIC Parameters ($Bohr^{-3}\,Hartree^{-1/2}$) for 1-Methoxy-1,3-butadiene and Acrolein

| Atom | STO-3G | | 4-31G | |
|---|---|---|---|---|
| | MTBE–ACL1 | MTBE–ACL2 | MTBE–ACL1 | MTBE–ACL2 |
| | $\times 10^{-5}$ | $\times 10^{-5}$ | $\times 10^{-5}$ | $\times 10^{-5}$ |
| 1 | 0.537 | 0.460 | 3.63 | 2.67 |
| 2 | −0.0000675 | −0.0000433 | −0.00176 | −0.000767 |
| 3 | 2.96 | 2.83 | 14.8 | 12.8 |
| 4 | 2.94 | 2.99 | 15.1 | 16.8 |
| Total | 1.02 | 1.00 | 5.49 | 5.39 |

3.4 Å distant, 76 degrees, planar. MTBE, 1-methoxy-1,3-butadiene (HOMO); ACL1, acrolein from (1) in Fig. 3 (LUMO); ACL2, acrolein from (2) in Fig. 3 (LUMO); Total, including hydrogens. Evaluation was done on the van der Waals surface of acrolein.

TABLE IV. Averaged MODIC Parameters ($Bohr^{-3}\,Hartree^{-1/2}$) for 1-Methoxy-1,3-butadiene and Acrolein

| Atom | On acrolein | | On methoxybutadiene | |
|---|---|---|---|---|
| | MTBE–ACL1 | MTBE–ACL2 | MTBE–ACL1 | MTBE–ACL2 |
| | $\times 10^{-4}$ | $\times 10^{-4}$ | $\times 10^{-4}$ | $\times 10^{-4}$ |
| 1 | 0.0589 | 0.0513 | 0.0411 | 0.0214 |
| 2 | 0.0000247 | 0.0000210 | 1.69 | 1.26 |
| 3 | 1.43 | 1.31 | −0.000740 | −0.00303 |
| 4 | 1.30 | 1.41 | −0.000558 | −0.000400 |
| 5 | — | — | 0.0161 | 0.0267 |
| 6 | — | — | 1.06 | 1.39 |
| Total | 0.404 | 0.407 | 0.276 | 0.277 |

3.4 Å distant, 76 degrees, deformed by 0.29 Å. MTBE, 1-methoxy-1,3-butadiene (HOMO); ACL1, acrolein from (1) in Fig. 3 (LUMO); ACL2, acrolein from (2) in Fig. 3 (LUMO); Total, including hydrogens. Evaluation was done on the van der Waals surface of acrolein with the STO-3G basis set.

is the same as in the case of 3.4 Å. The intermolecular distance dependency is also seen from the same table. The value itself changes drastically as the distance changes. The predictability of the reaction center, however, is not affected at all.

The purpose of Table I is to check the dependence of the MODIC upon the intermolecular location. When one actually applies the present method, the locations of molecules must be determined along a well-determined standard, *e.g.* molecular-mechanically. The geometry with 3.4 Å and 76 degrees in Table I may be most stable. The appropriate evaluation of the MODIC is possible if a reasonable geometry is used.

When one performs *ab initio* calculations, the dependency of the result on the choice of basis set functions should be checked. Here we employed the 4-31G basis set as well as the STO-3G basis set and compared the results (Table III). In the case of the 4-31G basis set, the values are approximately five times as large as those with STO-3G, but the predictability of the reaction centers by the index is not changed.

Next we concentrated on the predictability of orientation of substituent groups. It is known experimentally that form (2) is more advantageous than form (1) in Fig. 3,[27] but this

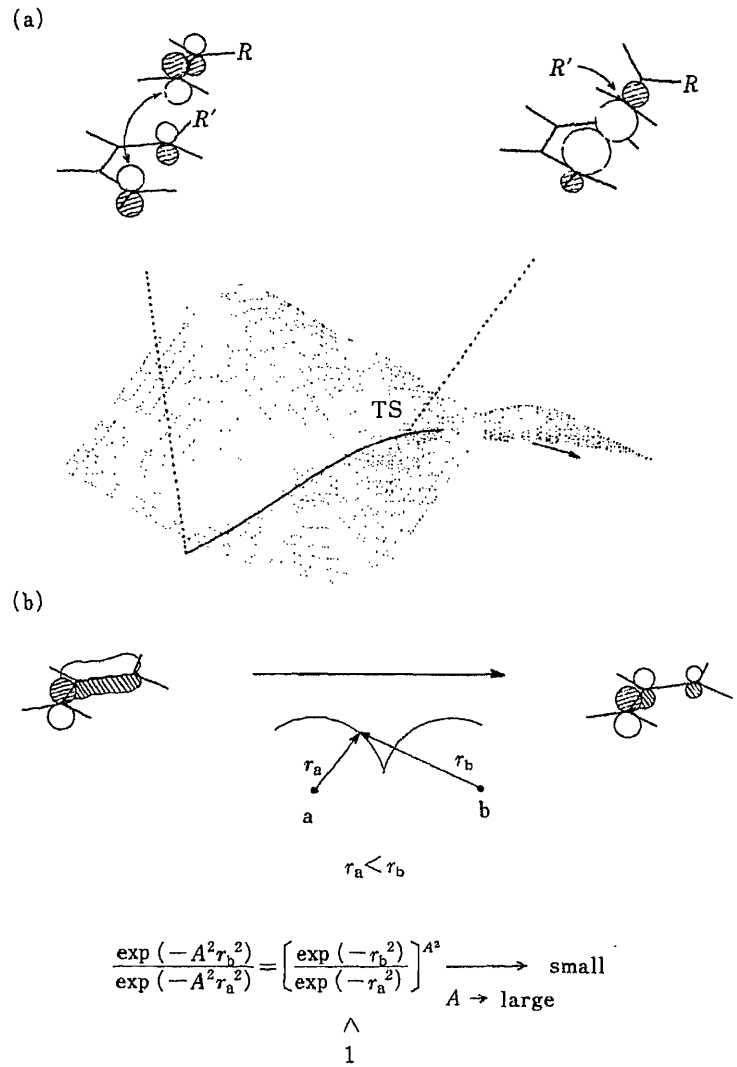


Fig. 7. A Schematic Picture of the Orbital Change along the Reaction Coordinate and the Corresponding Effect of the Scaling Factor

See the text for details.

TABLE V. Interaction Energies between 1-Methoxy-1,3-butadiene and Acrolein

| | STO-3G (kcal/mol) | | 4-31G (kcal/mol) | |
|---|---|---|---|---|
| | MTBE–ACL1 | MTBE–ACL2 | MTBE–ACL1 | MTBE–ACL2 |
| CT | −0.3 | −0.3 | −1.4 | −1.5 |
| Total | 0.3 | 0.3 | −0.4 | −0.6 |

3.4 Å distant, 76 degrees, planar. MTBE, 1-methoxy-1,3-butadiene; ACL1, acrolein from (1) in Fig. 3; ACL2, acrolein from (2) in Fig. 3; CT, charge transfer energy; Total, total interaction energy.

fact is not reflected in the MODIC index (see Tables I and III).

In the transition state of the ethylene–1,3-butadiene system, the geometry of each molecule is deformed from the planar form, and the reaction sites are positioned out of the plane. Considering this, in the 1-methoxy-1,3-butadiene–acrolein system, the reaction centers (four carbon atoms) were deformed inward vertically to the molecular planes by 0.29 Å. The result of evaluation of the MODIC index is summarized in Table IV. The index corresponding to form (2) in Fig. 3 is a little larger than that for form (1) in Fig. 3, in accordance with experiment.[27] This tendency is the same if the surface of 1-methyl-1,3-butadiene is taken for evaluation (Table IV).

Frontier electron theory[28] makes predictions only from the coefficients of molecular orbitals in the LCAO approximation such as in Table II. For example, the atoms numbered 3 and 4 of acrolein are predicted to become attached to the atoms numbered 2 and 6 of 1-methoxy-1,3-butadiene, respectively. This may indicate that the theory anticipates the transition structure from the initial structure (*cf.* Fig. 7(a)). However, in the case of the MODIC index, which takes into account the three-dimensional distribution, *i.e.* all the coefficients of the LCAO approximation, the transition state structure is not considered appropriately.

Actually the situation is very delicate energetically. Table V shows the charge transfer and the total interaction energies for both orientations in Fig. 3 (3.4 Å, 76 degrees, and planar forms are assumed), calculated with the STO-3G and 4-31G basis sets. In the case of the STO-3G basis set, the energies of the total and charge transfer interactions for both orientations are exactly the same. The 4-31G calculation gave only slight differences of 0.2 and 0.1 kcal/mol for total and charge transfer energies, respectively.

In such a situation, we had to devise a way to cope with geometrical and orbital changes in the transition state on the basis of the initial state information. As is seen from a comparison between the results in Fig. 4 and Table II, it is difficult to elucidate each contribution to a molecular orbital from an atomic orbital, only by considering three-dimensional molecular orbital distribution. Therefore, some modification of orbital functions was introduced as follows.

In our MO calculations, each atomic orbital is expressed with some Gaussian-type functions such as $\exp(-A^2r^2)$. The ratio of contribution from an atomic orbital, belonging to the same kind of atom b as a, to that from another atomic orbital belonging to atom a, at a certain point on the surface of atom a is (see Fig. 7(b))

$$R=\exp(-A^2r_b^2)/\exp(-A^2r_a^2)$$

$$=(\exp(-r_b^2)/\exp(-r_a^2))^{A^2}$$

At this point,

$$r_a<r_b$$

and hence,

$$\exp(-r_b^2)/\exp(-r_a^2) < 1$$

Therefore when $A$ becomes large enough, $R$ approaches zero, which means the contribution from atom b is neglibible compared with that from atom a, at the point in question. This device gives rise to the same effect as that seen in Table IV with geometrical deformation (see Fig. 7(a)). Accordingly, the large scaling factor corresponds to the geometrical change of

TABLE VI. Effect of Scaling Factor on Averaged MODIC Parameters (Bohr$^{-3}$ Hartree$^{-1/2}$) for 1-Methoxy-1,3-butadiene and Acrolein

| Atom | Scaling factor 1.0× | | 1.5× | | 2.0× | |
|---|---|---|---|---|---|---|
| | MTBE–ACL1 | MTBE–ACL2 | MTBE–ACL1 | MTBE–ACL2 | MTBE–ACL1 | MTBE–ACL2 |
| | $\times 10^{-5}$ | $\times 10^{-5}$ | $\times 10^{-7}$ | $\times 10^{-7}$ | $\times 10^{-10}$ | $\times 10^{-10}$ |
| 1 | 0.537 | 0.460 | 0.0766 | 0.0671 | 0.00367 | 0.00321 |
| 2 | 0.0 | 0.0 | 0.0 | 0.0 | 0.0 | 0.0 |
| 3 | 2.96 | 2.83 | 2.54 | 2.31 | 1.24 | 1.09 |
| 4 | 2.94 | 2.99 | 2.43 | 2.66 | 1.16 | 1.32 |
| Total | 1.02 | 1.00 | 0.747 | 0.757 | 0.350 | 0.359 |

| Atom | 2.5× | | 4.0× | |
|---|---|---|---|---|
| | MTBE–ACL1 | MTBE–ACL2 | MTBE–ACL1 | MTBE–ACL2 |
| | $\times 10^{-15}$ | $\times 10^{-15}$ | $\times 10^{-35}$ | $\times 10^{-35}$ |
| 1 | 0.00070 | 0.00061 | 0.0 | 0.0 |
| 2 | 0.0 | 0.0 | 0.0 | 0.0 |
| 3 | 4.45 | 3.91 | 5.62 | 4.93 |
| 4 | 4.15 | 4.74 | 5.25 | 5.98 |
| Total | 1.25 | 1.28 | 1.58 | 1.62 |

3.4 Å distant, 76 degrees, planar. MTBE, 1-methoxy-1,3-butadiene (HOMO); ACL1 and ACL2, acrolein from (1) and (2) in Fig. 3, respectively (LUMO); Total, including hydrogens. Evaluation was done on the van der Waals surface of acrolein with the STO-3G basis set.

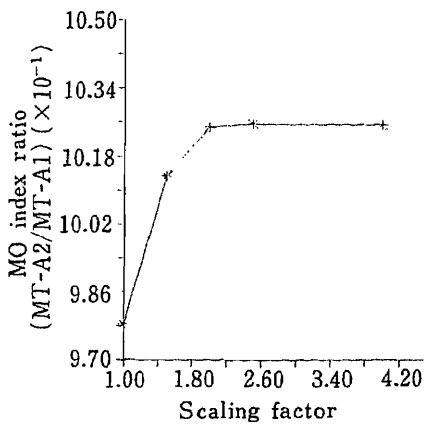


Fig. 8. The Ratio of the Total MODIC Indexes for the 1-Methoxy-1,3-butadiene System Plotted against the Scaling Factor

The plotted data correspond to the values in Table VI.

TABLE VII. Charge Transfer Interaction Energies between Orbitals of 1-Methoxy-1,3-butadiene and Acrolein

| MO of MTBE | MO of ACL1 | Charge transfer energy (kcal/mol) |
|---|---|---|
| All orbitals | All orbitals | −0.308[a)] |
| All occupied | All unoccupied | −0.201 |
| All unoccupied | All occupied | −0.102 |
| HOMO | LUMO | −0.089 |
| HOMO | Next LUMO | −0.032 |
| Next HOMO | LUMO | −0.004 |
| LUMO | HOMO | 0.0 |
| LUMO | Next HOMO | 0.0 |
| Next LUMO | HOMO | 0.0 |

3.4 Å distant, 76 degrees, planar. MTBE, 1-methoxy-1,3-butadiene; ACL1, acrolein. The STO-3G basis set was used. *a*) Corresponds to Table V.

molecules.

The MODIC indexes with larger scaling factor, which corresponds to $A$ in the above equation, are listed in Table VI for the geometries with 3.4 Å and 76 degrees (Fig. 3). The scaling factors were taken to be 1.0, 1.5, 2.0, 2.5, and 3.0. As the scaling factor increases, the value of the MODIC index decreases drastically, but its ratio for the geometry in Fig. 3 (2) against that in Fig. 3 (1) gradually increases in accordance with experiment.[27]

The ratio is plotted against the scaling factor in Fig. 8. The ratio increases steeply as the scaling factor increases from 1.0 to 2.0, and then it reaches a plateau. Therefore, the value of 2.0 may be a good candidate as a scaling factor, when the transition state is considered.

As discussed above, the MODIC index, with some scaling if needed, can predict the orientations of substitutional groups, as well as the location of reaction centers in the Diels–Alder reaction of the 1-methoxy-2,3-butadiene–acrolein system.

In this section we have discussed the system composed of the HOMO of 1-methoxy-1,3-butadiene and the LUMO of acrolein. In order to check the validity of this selection of orbitals, we performed a detailed analysis of charge transfer energy. The charge transfer interaction energies were evaluated for the system in Fig. 3 (1) with the STO-3G basis set (*cf.* Table VII).

The total charge transfer energy is −0.3 kcal/mol. To this energy, the charge transfer energy from all occupied orbitals of 1-methoxy-1,3-butadiene to all unoccupied orbitals of acrolein contributes −0.2 kcal/mol, while the reverse charge transfer contributes −0.1 kcal/mol. More detailed numerical analysis on the interaction between individual orbitals[29,30] revealed that the charge transfer from the HOMO of 1-methoxy-1,3-butadiene to the LUMO of acrolein was −0.089 kcal/mol, while that from the HOMO of the latter to the LUMO of the former was practically zero. Beside the frontier orbitals, only the next combinations of orbitals make a contribution: the HOMO of 1-methoxy-1,3-butadiene to the next LUMO of acrolein (−0.032 kcal/mol), and the next HOMO of the former to the LUMO of the latter (−0.004 kcal/mol). Considering these energetical analyses, the criterion for selecting the HOMO–LUMO combination stated in the Method section is considered to be valid.

**Cyclopentadiene–Maleic Acid Anhydride System**

Next, the results for the cyclopentadiene–maleic acid anhydride system will be discussed. Two orientations are considered for each value of theta, 90 or 76 degrees (Fig. 9). The two planes are parallel and distant by 3.4 Å, which corresponds to van der Waals contact. Experimentally, the orientation in Fig. 9 (1) is favorable for the reaction,[31] which is predicted

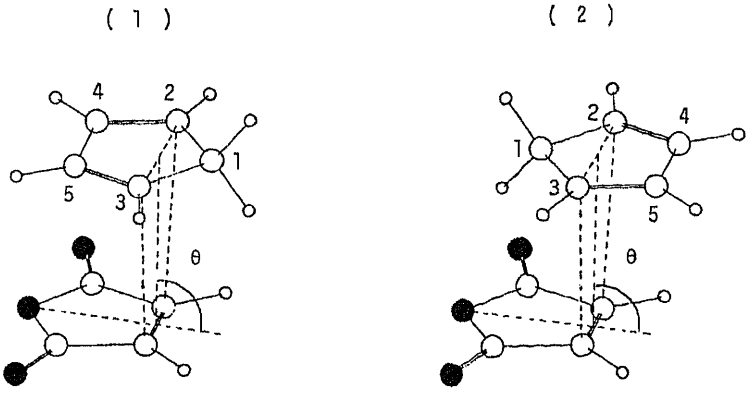


Fig. 9. The Geometry of the Cyclopentadiene–Maleic Acid Anhydride System

Distance between two molecular planes: 3.4 Å.
○, carbon; ●, oxygen; ○, hydrogen. $\theta$: 76.0, 90.0°.

TABLE VIII. Effect of Scaling Factor on Averaged MODIC Parameters (Bohr$^{-3}$ Hartree$^{-1/2}$) for Cyclopentadiene and Maleic Acid Anhydride

| Atom | Scaling factor 1.0× | | 2.0× | |
|---|---|---|---|---|
| | CPD1–MLAH | CPD2–MLAH | CPD1–MLAH | CPD2–MLAH |
| 90 degrees[a] | | | | |
| | $\times 10^{-5}$ | $\times 10^{-5}$ | $\times 10^{-10}$ | $\times 10^{-10}$ |
| 1 | 0.758 | 1.28 | 0.233 | 0.267 |
| 2 | 5.08 | 5.19 | 3.25 | 3.26 |
| 3 | 5.08 | 5.18 | 3.24 | 3.26 |
| 4 | 3.60 | 1.20 | 2.11 | 0.227 |
| 5 | 3.60 | 1.20 | 2.11 | 0.227 |
| Total | 2.03 | 1.64 | 1.20 | 0.799 |
| Ratio | 1.24 | 1.00 | 1.50 | 1.00 |
| 76 degrees[a] | | | | |
| | $\times 10^{-5}$ | $\times 10^{-5}$ | $\times 10^{-10}$ | $\times 10^{-10}$ |
| 1 | 0.262 | 1.60 | 0.0189 | 1.19 |
| 2 | 3.61 | 3.76 | 2.78 | 2.64 |
| 3 | 3.60 | 3.76 | 2.78 | 2.63 |
| 4 | 5.53 | 0.266 | 8.75 | 0.00302 |
| 5 | 5.53 | 0.266 | 8.75 | 0.00302 |
| Total | 2.07 | 1.21 | 2.53 | 0.712 |
| Ratio | 1.71 | 1.00 | 3.56 | 1.00 |

3.4 Å distant. CPD1, cyclopentadiene from (1) in Fig. 9 (HOMO); CPD2, cyclopentadiene from (2) in Fig. 9 (HOMO); MLAH, maleic acid anhydride (LUMO); Total, including hydrogens. Evaluation was done on the van der Waals surface of cyclopentadiene with the STO-3G basis set. *a*) See Fig. 9.

TABLE IX. Charge Transfer Energy between Dihydrofolate (Protonated) and NADPH

| Basis set | Charge transfer energy (kcal/mol) |
|---|---|
| STO-3G | −6.8 |
| 4-31G | −8.7 |

correctly by the frontier electron theory.

The results are summarized in Table VIII. The left half of the table corresponds to a scaling factor of 1.0. The MODIC index is larger for Fig. 9 (1) than for Fig. 9 (2), in accordance with experiment.[31] The reaction centers are also clear, because the two positions numbered 2 and 3 have the largest values of the index. Furthermore, in this system, the MODIC indexes around the atoms numbered 4 and 5 are not negligible, which is indicative that the secondary effect is large in this system.

Similar considerations apply to the case of a scale factor of 2.0 in the right half of Table VIII. Moreover, the ratio of the total MODIC index (Fig. 9 (1) against Fig. 9 (2)) increases from 1.24 to 1.50, when the scaling factor is changed from 1.0 to 2.0. The predictability of orientation is improved by changing the scaling factor, as is the case with the 1-methoxy-1,3-butadiene–acrolein system. The above discussion is equally valid for theta of 90 and 76 degrees.

**Dihydrofolate Reductase System**

As an application to biological systems, we treated the DHFR system. For dihydrofolate, two types are considered: protonated at the 5-position and not protonated.

TABLE X. Averaged MODIC Parameters (Bohr$^{-3}$ Hartree$^{1/2}$) for Dihydrofolate Reductase Systems

| Atom | NADPH-substrate | | NADPH-inhibitor |
|---|---|---|---|
| | NADPH–PTC | NADPH–PTN | NADPH–MTC |
| | $\times 10^{-5}$ | $\times 10^{-5}$ | $\times 10^{-5}$ |
| 1 | −0.0235 | −0.0362 | −0.00613 |
| 2 | 0.0323 | 0.0436 | −0.0634 |
| 3 | −0.00723 | 0.00294 | 0.0186 |
| 4 | −0.216 | 0.333 | 17.9 |
| 5 | 6.10 | 3.70 | −30.9 |
| 6 | −385. | −176. | −0.432 |
| 7 | 49.7 | −20.9 | 0.0377 |
| 8 | −2.02 | −1.08 | −0.00464 |
| 9 | −5.76 | 7.10 | 8.57 |
| 10 | −11.8 | −7.32 | −0.394 |
| 11 | 0.000000433 | 0.00000148 | −0.000000298 |
| 12 | 0.00230 | 0.00121 | −2.46 |
| 13 | −3.11 | −2.14 | −0.232 |
| Total | −26.3 | −12.0 | −1.39 |

PTC, dihydrofolate (protonated, LUMO); PTN, dihydrofolate (not protonated, LUMO); MTC, methotrexate (protonated); Total, including hydrogens. Evaluation was done on the van der Waals surface of PTC, PTN or MTC with the STO-3G basis set.

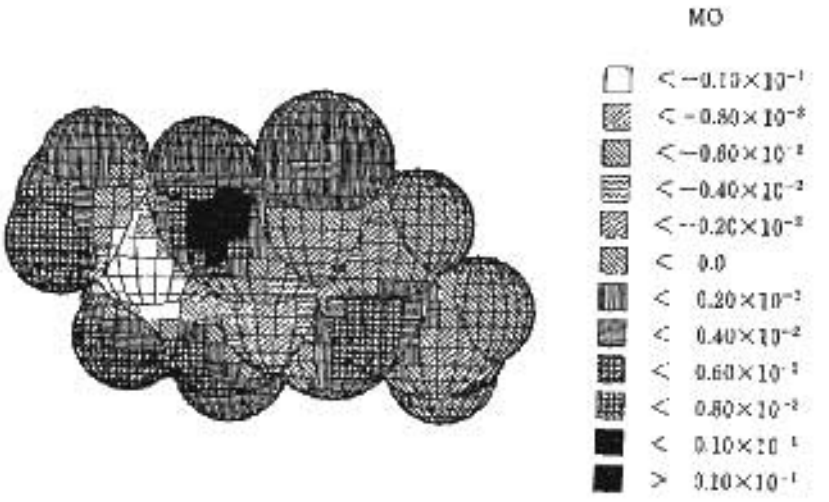


Fig. 10. The LUMO of Protonated Dihydrofolate on Its Surface

**System A**——If dihydrofolate is protonated at the 5-position, the charge transfer interaction energy is calculated to be −6.8 kcal/mol with the STO-3G basis set and −8.7 kcal/mol with the 4-31G basis set (Table IX). Since the values are rather large compared with those for the 1-methoxy-1,3-butadiene–acrolein system (see Table V), the MODIC index deserves to be discussed.

The averaged MODIC parameters for the system are summarized in Table X. According to this table, the protonated dihydrofolate has the largest value at the carbon atom of the 6-position (numbered 6; see Method section). This situation reflects the real enzymatic reaction in which hydride ion attacks at the 6-position, and can be observed graphically in accordance with the experiment.

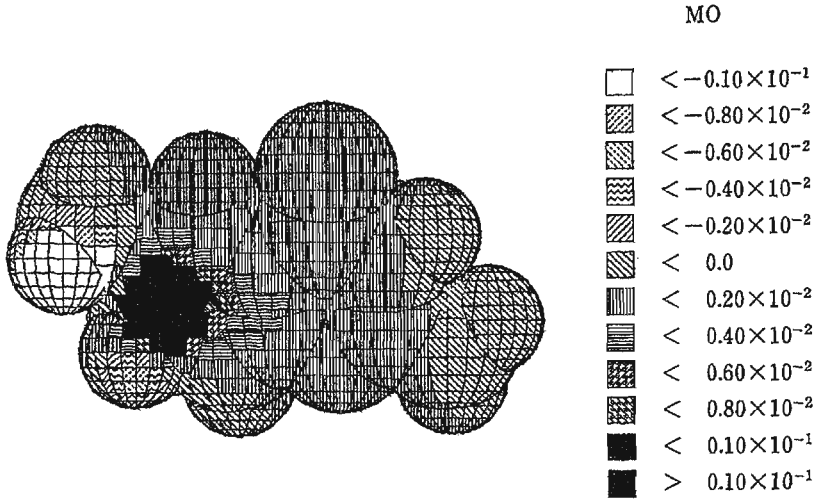


Fig. 11. The HOMO of NADPH on the Surface of Protonated Dihydrofolate

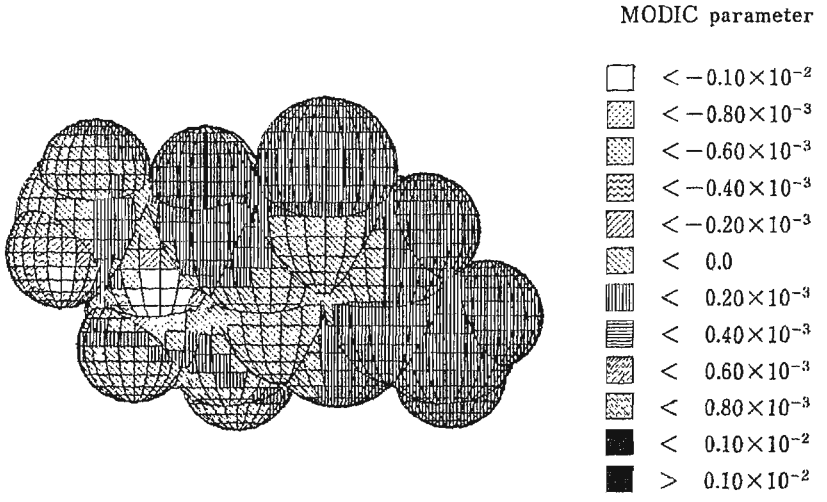


Fig. 12. The MODIC Parameter Distribution on the Surface of Protonated Dihydrofolate

Figure 10 shows the LUMO of the dihydrofolate on its van der Waals surface. It is very clear that the distribution is thickest at the 6-position, where the hydride ion from NADPH attacks from the front of the paper. Therefore, the 6-position is most favorable for the charge transfer interaction.

However, the reactivity also depends on the distribution of the counterpart, *i.e.* the HOMO of NADPH. As is seen in Fig. 11, the MO distribution is also thickest around the 6-position of dihydrofolate. Needless to say, this distribution of the MO on the surface depends upon the locations of the two molecules. Suitable location is essential for biological reactions. Therefore, the geometries determined in the Method section were taken as the starting point of discussion. The correlation is indeed best at the position in question, as shown in Table X and Fig. 12.

**System B**——In the case of non-protonated dihydrofolate, the same position as on the protonated dihydrofolate has the largest value (Table X). The magnitude, however, is much smaller than that for the protonated dihydrofolate. The situation is readily understood from the distribution of the LUMO of the non-protonated dihydrofolate. As is depicted in Fig. 13,

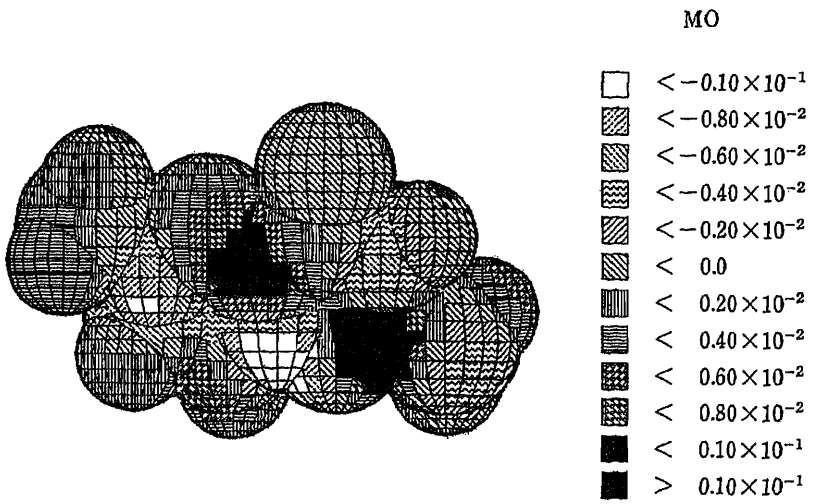


Fig. 13. The LUMO of Non-protonated Dihydrofolate on Its Surface

TABLE XI. Energy Levels for Dihydrofolate Systems[a]

| Molecule | MO | Energy level (Hartree) |
|---|---|---|
| NADPH | HOMO | −0.2041 |
| Dihydrofolate (protonated) | LUMO | −0.0039 |
| Dihydrofolate (not protonated) | LUMO | 0.2051 |
| Methotrexate | LUMO | −0.0105 |

*a*) The STO-3G basis set was used.

TABLE XII. Energies of MTX

| Protonation | Energy[a] (Hartree) |
|---|---|
| At 1-position | −589.3363 |
| At 5-position | −589.2693 |
| Difference | 0.0670 |
| | (42.1 kcal/mol) |

*a*) The STO-3G basis set was used.

the distribution of the orbital is not so dense at the 6-position. Furthermore, the energy level of the LUMO is higher than that for the protonated dihydrofolate (Table XI). The MODIC index reflects the combination of these effects. The result obtained here, that the protonated dihydrofolate reacts more favorably than the non-protonated one, is in good agreement with the report by Gund *et al.*[32] stating that the reduction proceeds with the first protonation at the 5-position and then with hydride ion transfer to the 6-position.

**System C**——On the other hand, the correlation between MTX and NADPH is much worse. This corresponds to the fact that MTX prevents the reduction catalysis by acting as an inhibitor. The LUMO of MTX, the HOMO of NADPH, and their correlation are depicted graphically in Figs. 14, 15, and 16, respectively.

As stated above, the reduction is considered to be a two-step reaction (protonation in the first place and hydride ion transfer in the next step). In MTX, the proton affinity is greater at the 1-position than at the 5-position by 42.1 kcal/mol (Table XII). Therefore the protonation

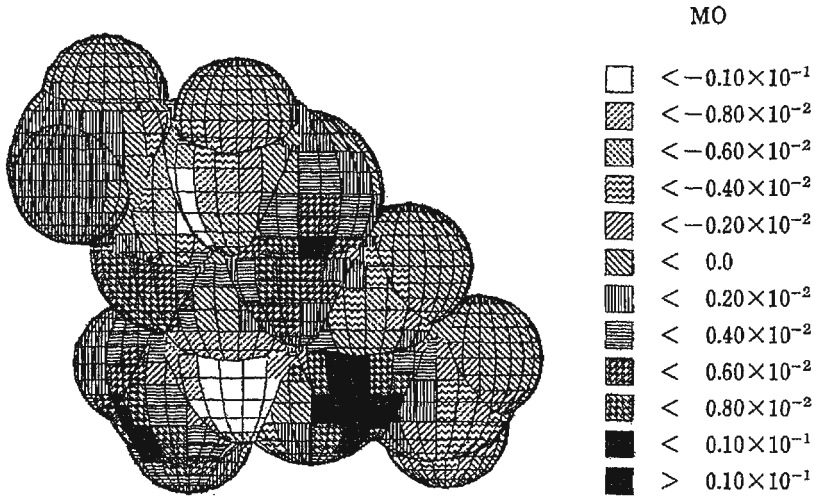


Fig. 14. The LUMO of Methotrexate on Its Surface

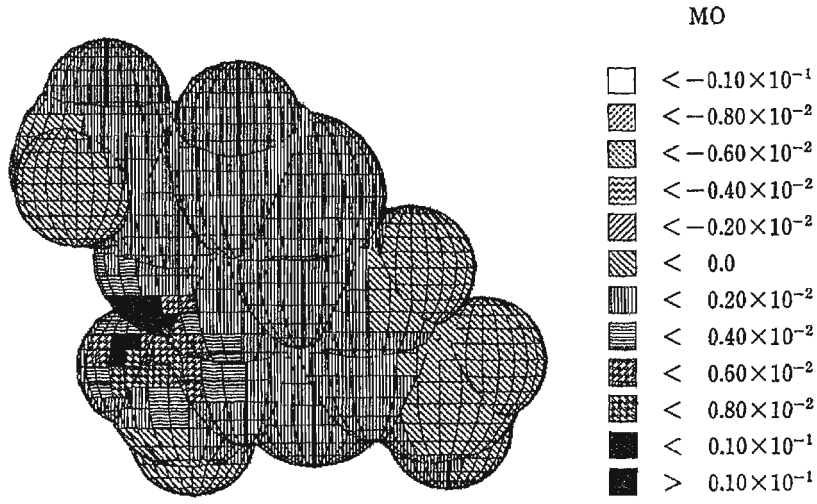


Fig. 15. The HOMO of NADPH on the Surface of Methotrexate

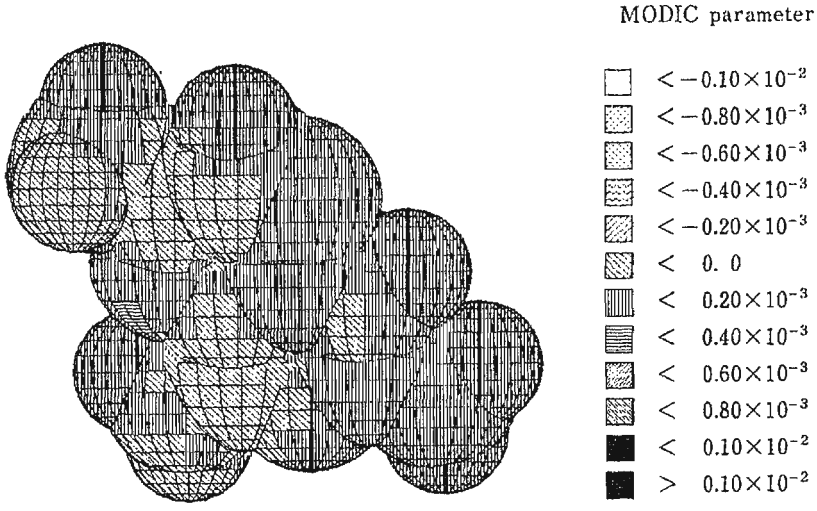


Fig. 16. The MODIC Parameter Distribution on the Surface of Methotrexate

takes place at the 1-position, whereas the protonation takes place at the 5-position in the case of dihydrofolate. Because of that, the three-dimensional structure may become different due to the interaction with the enzyme, and the next step of the catalysis is prohibited (*cf.* Table X).

In the enzymatic reaction, the effect of surrounding residues is known to be important for the ligand-receptor interaction.[33,34] This effect may affect the MODIC index. We are now preparing to examine this problem. Furthermore, the distribution may need to be considered in three-dimensional space. However, the treatment on the molecular surface as stated above provides a very useful picture which is quite consistent with chemical considerations.

## Conclusion

In the present paper, an index referred to as the MO distribution correlation index, the MODIC index for short, is presented as a tool to obtain a deeper insight into drug-receptor interactions for possible application to drug designing. The index was applied to Diels–Alder reaction systems and the DHFR system.

In Diels–Alder reaction systems, the following results were obtained.

1. Reaction centers are predicted by the MODIC index.
2. The transition state can be assumed simply from the initial molecular structures and molecular orbitals, by enlarging the scaling factor which determines the extents of the distributions of individual atomic orbitals.
3. Orientations of substitutional groups are predictable owing to the effect stated just above.

In the DHFR system, the reactivities of ligands are interpreted rationally. The results may be summarized as follows.

4. The MODIC index is larger for protonated dihydrofolate than for non-protonated dihydrofolate, which is in agreement with another report.[32]
5. Methotrexate has a much smaller MODIC index compared with dihydrofolates, which is consistent with the fact that MTX is a strong inhibitor of DHFR.

Our method reported here represents a well-defined procedure based on the three-dimensional distribution of molecular orbitals, and may overcome the arbitrariness of the frontier electron theory, which discusses the reactivity based on the numerical LCAO coefficients.

### References


1) K. Komatsu, S. Nakagawa, H. Umeyama, and H. Nakamura, *Chem. Pharm. Bull.*, **35**, 1880 (1987).
2) K. Komatsu, H. Nakamura, S. Nakagawa, and H. Umeyama, *Chem. Pharm. Bull.*, **32**, 3313 (1984).
3) H. Nakamura, K. Komatsu, S. Nakagawa, and H. Umeyama, *J. Mol. Graph.*, **3**, 2 (1985).
4) R. S. Mulliken, *J. Chem. Phys.*, **23**, 1841 (1955).
5) H. Kubodera, S. Nakagawa, and H. Umeyama, *Chem. Pharm. Bull.*, **35**, 1673 (1987).
6) H. Kubodera and H. Umeyama, *Chem. Pharm. Bull.*, **35**, 3087 (1987).
7) D. Eisenberg and A. D. McLachlan, *Nature* (London), **319**, 199 (1986).
8) K. Akahane and H. Umeyama, *Chem. Pharm. Bull.*, **34**, 3492 (1986).
9) W. J. Hehre, R. F. Stewart, and J. A. Pople, *J. Chem. Phys.*, **51**, 2657 (1969).
10) R. Ditchfield, W. J. Hehre, and J. A. Pople, *J. Chem. Phys.*, **54**, 724 (1971).
11) S. Nakagawa, K. Morokuma, S. Kato, K. Kitaura, I. Ohmine, S. Sakai, and S. Obara, unpublished; program package containing GAUSSIAN 70, HONDO, *etc.*
12) A. Bondi, *J. Phys. Chem.*, **68**, 441 (1964).
13) Geometries were taken mainly from "Landolt-Boernstein Numerical Data and Functional Relationships in Science and Technology," New series, Group II, Vol. 7, Structure Data of Free Polyatomic Molecules, ed. by K.-H. Hellwege and A. M. Hellwege, Springer-Verlag Berlin-Heidelberg-New York, 1976.
14) F. Bernardi, A. Bottoni, M. A. Robb, M. J. Field, I. H. Hillier, and M. F. Guest, *J. Chem. Soc., Chem.*

*Commun.*, **1985**, 1051.
15) F. C. Bernstein, T. F. Koetzle, G. J. B. Williams, E. F. Meyer, Jr., M. D. Brice, J. R. Rodgers, O. Kennard, T. Shimanouchi, and M. Tasumi, *J. Mol. Biol.*, **112**, 535 (1977).
16) J. T. Bolin, D. J. Filman, D. A. Matthews, R. C. Hamlin, and J. Kraut, *J. Biol. Chem.*, **257**, 13650 (1982).
17) M. J. S. Dewar and W. Thiel, *J. Am. Chem. Soc.*, **99**, 4899 (1977); *idem*, *ibid.*, **99**, 4907 (1977).
18) K. Morokuma, *J. Chem. Phys.*, **55**, 1236 (1971).
19) S. Iwata and K. Morokuma, *J. Am. Chem. Soc.*, **95**, 7563 (1973).
20) W. A. Lathan and K. Morokuma, *J. Am. Chem. Soc.*, **97**, 3615 (1974).
21) H. Umeyama, K. Kitaura, and K. Morokuma, *Chem. Phys. Lett.*, **36**, 11 (1975).
22) H. Umeyama and K. Morokuma, *J. Am. Chem. Soc.*, **98**, 4400 (1976).
23) K. Kitaura and K. Morokuma, *Int. J. Quantum Chem.*, **10**, 325 (1976).
24) H. Umeyama, K. Morokuma, and S. Yamabe, *J. Am. Chem. Soc.*, **99**, 330 (1977).
25) H. Umeyama and K. Morokuma, *J. Am. Chem. Soc.*, **99**, 1316 (1977).
26) H. Nakamura, M. Kusunoki, and N. Yasuoka, *J. Mol. Graph.*, **2**, 14 (1984).
27) O. Wichterle, *Coll. Czech. Chem. Comm.*, **10**, 497 (1938).
28) K. Fukui, T. Yonezawa, and H. Shingu, *J. Chem. Phys.*, **20**, 722 (1952).
29) H. Umeyama and T. Matsuzaki, *Chem. Pharm. Bull.*, **27**, 1626 (1979).
30) H. Umeyama and T. Kudo, *Chem. Pharm. Bull.*, **29**, 554 (1981).
31) I. Fleming, "Frontier Orbitals and Organic Chemical Reactions," Kodansha, Tokyo, 1978, p. 122.
32) P. Gund, J. D. Andose, J. B. Rhodes, and G. M. Smith, *Science*, **208**, 1425 (1980).
33) S. Nakagawa, H. Kubodera, and H. Umeyama, *J. Infer. Deduct. Biol.*, **1**, 67 (1987).
34) S. Nakagawa and H. Umeyama, *J. Mol. Biol.*, **179**, 103 (1984).

[Chem. Pharm. Bull. 35(11)4395—4404(1987)]

# *Ab Initio* Molecular Orbital Study of Reactivity of Active Alkyl Groups. I. Deprotonation of Acetaldehyde with Amide, Hydroxide or Fluoride Ions

TOKIHIRO NIIYA, MIHO YUKAWA, HIROKI MORISHITA and YOSHINOBU GOTO*

*Faculty of Pharmaceutical Sciences, Fukuoka University, Nanakuma, Jonan-ku, Fukuoka 814-01, Japan*

(Received March 18, 1987)

The reactions of acetaldehyde with amide ($NH_2^-$), hydroxide ($OH^-$) or fluoride ($F^-$) ions were investigated by *ab initio* calculations. Acetaldehyde, which has an active methyl group, was taken as the model compound. The hydrogen-abstraction steps were studied in detail in terms of the energies and the structures of all the complexes in the reaction process. It became clear that the order of the deprotonation ability, *i.e.*, $NH_2^- > OH^- > F^-$ can be reasonably explained when deformation energy is taken into account in the calculation of the energies of the complexes in each reaction pathway. The reactions of methane with these three anions are also discussed as reference reactions.

**Keywords**——deprotonation; active methyl group; *ab initio* calculation; acetaldehyde; methane; amide ion; hydroxide ion; fluoride ion

Many reactions in organic and biological chemistry are initiated with the deprotonation of active alkyl groups,[1] but their mechanisms are still not known in detail. In these reactions, the deprotonation step is often crucial, *i.e.*, the proton transfer itself presents the major energy barrier.[2]

For several years, we have been investigating the chemical reactivities of active alkyl groups in nitrogen-containing aromatic heterocycles.[3] The reactivities of the active alkyl groups of the heterocycles toward electrophilic reagents vary in a very complicated way depending on the type of heterocycle and the positions of substituents on the heterocycle. It would be particularly interesting to elucidate the nature of the reactivities of these active alkyl groups, because such information would be useful in designing synthetic methods in organic chemistry.

It is considered that the reactions of the active alkyl groups of pyridine or pyrimidine derivatives with electrophilic reagents proceed *via* the following general reaction mechanisms. As shown in Chart 1, the following sequence of steps is assumed for this electrophilic reaction: in the first step the abstraction of a hydrogen atom occurs from the active methyl group by the negatively charged atom of a base ($B^-$), followed by the attack of an electrophilic reagent (E) on the carbanion thus generated as the second step.

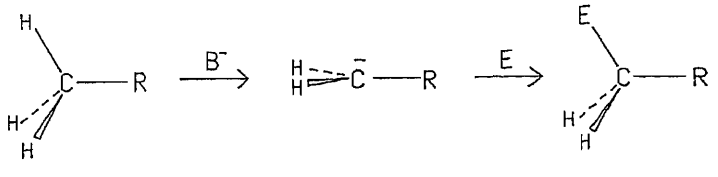


Chart 1

It is generally believed that the first step shown in Chart 1 consists of the following three steps, *i.e.*, (1) formation of an H-bonded encounter complex, A-H···B$^-$, (2) proton transfer to form a new complex, A$^-$···H-B, and (3) separation into products, A$^-$ + HB, as shown in Chart 2.[4)]

$$\underset{\text{reactants}}{A-H+B^-} \rightleftharpoons \underset{\text{C-I}}{A-H\cdots B^-} \rightleftharpoons \underset{\text{TS}}{[A\cdots H\cdots B]^-} \rightleftharpoons \underset{\text{C-II}}{A^-\cdots H-B} \rightleftharpoons \underset{\text{products}}{A^- + H-B}$$

Chart 2

Many theoretical and experimental studies have been done on proton abstraction reactions[5)] and on solvation effects[6)] on anions. We have carried out an *ab initio* molecular orbital (MO) study on the gas phase deprotonation reactions shown in Chart 2 in order to clarify the fundamental deprotonation reaction profiles. Acetaldehyde ($CH_3CHO$) as a model of an active methyl compound, and amide ($NH_2^-$), hydroxide ($OH^-$) or fluoride ($F^-$) ions as an ionic base were employed. The deprotonation reactions of methane ($CH_4$) with these three anions are regarded as reference reactions.

## Computational Procedure

*Ab initio* LCAO SCF MO calculations were carried out using the Gaussian 80[7a)] and 82[7b)] series of programs. All structures of the monomers were fully optimized using the 6-31G[7a,b)] and 6-31+G[7c)] basis sets by employing a gradient optimization technique as shown in Table I. The effect of electron correlation was incorporated at the level of second-order Møller–Plesset (MP2) perturbation theory in these calculations. The geometry optimizations and the energy calculations of all complexes were performed using the 6-31+G basis set, which incorporates diffuse functions not only on first row atoms of anionic bases, but also on those of $CH_4$, $CH_3CHO$ and conjugate acids (HB) of bases, because in the HOMO of the methide anion $^-C^1H_2C^2HO$ the carbon atom ($C^1$) of the methylene group has a larger coefficient than the other atoms of this anion. Diffuse functions were incorporated only on the carbon atom ($C^1$) of the methyl group of $C^1H_3C^2HO$ in these calculations.

## Results and Discussion

The optimized geometries and the total energies of the monomers are shown in Table I. The incorporation of diffuse functions into the basis set contributes to the energy stabilization of the anions more than to that of the neutral molecules. All optimized geometries of each molecule at any level of the basis sets show good agreement with the experimental values. The differences ($\Delta E°$) between the energies of the reactants [($CH_4$ or $CH_3CHO$)+$B^-$] and those of the products [($CH_3^-$ or $^-CH_2CHO$)+HB] in the ground state are shown in Table II. All the energies of the products calculated using any basis set are higher than those of the reactants in the reaction of $CH_4$ with $NH_2^-$, $OH^-$ or $F^-$.

On the other hand, in the reaction of $CH_3CHO$ with $NH_2^-$ or $OH^-$ ion the energies of the products calculated using any basis set are lower than those of the reactants, and the $\Delta E°$ values decrease in the order of the values shown in the columns from left to right in Table II. On the contrary, in the case of the reaction with $F^-$ the energies of the products calculated using the HF/6-31+G or MP2/6-31+G basis set are higher than those of the reactants and the $\Delta E°$ values increase in the order of the values shown in the columns from left to right in Table II. An electron correlation should be incorporated into energy calculations of chemical reactions; in this report however we will discuss the results calculated using the HF/6-31+G basis set, because the results calculated using the HF/6-31+G basis set are similar in

TABLE I. Optimized Geometries and Total Energies of Monomers at Various Level of Calculation

| Monomer | Point group | $E_{total}$ (a.u.) | | | $r$ (Å) / ∠ (°) | Optimized geometries | | | Exptl |
|---|---|---|---|---|---|---|---|---|---|
| | | HF/6-31G | HF/6-31+G | MP2/6-31+G | | HF/6-31G | HF/6-31+G | MP2/6-31+G | |
| $NH_2^-$ | $C_{2v}$ | −55.45586 | −55.49842 | −55.63644 | $r$ (N–H) | 1.040 | 1.023 | 1.044 | |
| | | | | | ∠HNH | 101.7 | 107.5 | 108.4 | |
| $OH^-$ | $C_{\infty v}$ | −75.31175 | −75.36094 | −75.51482 | $r$ (O–H) | 0.981 | 0.969 | 0.999 | 0.984[a] |
| $F^-$ | | −99.35018 | −99.41607 | −99.56779 | | | | | |
| $CH_3^-$ | $C_{3v}$ | −39.43991 | −39.48892 | −39.60259 | $r$ (C–H) | 1.085 | 1.097 | 1.100 | |
| | | | | | ∠HCH | 118.3 | 110.4 | 114.7 | |
| $^-CH_2CHO$ | $C_s$ | −152.22365 | −152.23396 | −152.54550 | $r$ ($C^1$–$C^2$) | 1.364 | 1.377 | 1.411 | |
| | | | | | $r$ ($C^2$–O) | 1.285 | 1.278 | 1.306 | |
| | | | | | $r$ ($C^1$–$H^2$) | 1.077 | 1.078 | 1.095 | |
| | | | | | $r$ ($C^1$–$H^3$) | 1.078 | 1.077 | 1.094 | |
| | | | | | $r$ ($C^2$–$H^4$) | 1.106 | 1.102 | 1.125 | |
| | | | | | ∠$C^1C^2O$ | 130.4 | 130.1 | 129.9 | |
| | | | | | ∠$C^1C^2H^4$ | 113.5 | 113.6 | 113.1 | |
| | | | | | ∠$C^2C^1H^3$ | 120.9 | 121.4 | 121.7 | |
| | | | | | ∠$C^2C^1H^2$ | 121.4 | 120.6 | 120.4 | |
| $NH_3$ | $C_{3v}$ | −56.16552 | −56.17138 | −56.28951 | $r$ (N–H) | 0.991 | 0.991 | 1.010 | 1.012[b] |
| | | | | | ∠HNH | 116.1 | 117.5 | 116.3 | 106.7[b] |
| $H_2O$ | $C_{2v}$ | −75.98536 | −75.99260 | −76.12575 | $r$ (O–H) | 0.950 | 0.950 | 0.977 | 0.957[b] |
| | | | | | ∠HOH | 111.5 | 112.8 | 111.3 | 104.52[b] |
| HF | $C_{\infty v}$ | −99.98343 | −99.99473 | −100.13024 | $r$ (H–F) | 0.921 | 0.923 | 0.953 | 0.917[c] |
| $CH_4$ | $T_d$ | −40.18055 | −40.18133 | −40.28023 | $r$.(C–H) | 1.096 | 1.082 | 1.082 | 1.094[b] |
| $CH_3CHO$ | $C_s$ | −152.84307 | −152.84399 | −153.15415 | $r$ ($C^1$–$C^2$) | 1.496 | 1.496 | 1.514 | 1.501[d] |
| | | | | | $r$ ($C^2$–O) | 1.214 | 1.214 | 1.261 | 1.216[d] |
| | | | | | $r$ ($C^1$–$H^1$) | 1.090 | 1.090 | 1.101 | |
| | | | | | $r$ ($C^1$–$H^3$) | 1.081 | 1.081 | 1.096 | |
| | | | | | $r$ ($C^2$–$H^4$) | 1.086 | 1.085 | 1.105 | 1.114[d] |
| | | | | | ∠$C^1C^2O$ | 124.1 | 124.1 | 124.0 | 123.9[d] |
| | | | | | ∠$C^1C^2H^4$ | 116.3 | 116.3 | 116.1 | 117.5[d] |
| | | | | | ∠$C^2C^1H^3$ | 110.1 | 110.2 | 109.7 | |
| | | | | | ∠$C^2C^1H^1$ | 109.9 | 109.8 | 110.2 | |

*a*) "Tables of Interatomic Distances," ed. by L. E. Sutton, The Chemical Society London, London, supplement 1965. *b*) G. Herzberg, "Molecular Spectra and Molecular Structure III. Electronic Spectra and Electronic Structure of Polyatomic Molecules," Van Nostrand, New York, N. Y., 1966. *c*) G. A. Knipers, D. F. Smith, and A. N. Nielsen, *J. Chem. Phys.*, **25**, 275 (1956). *d*) R. W. Kilb, C. C. Lin, and E. B. Wilson, Jr., *J. Chem. Phys.*, **26**, 1695 (1957).

TABLE II. The Differences ($\Delta E°$) between the Energies of the Reactants and Those of the Products (kcal·mol$^{-1}$)

| | $CH_4$ | | | $CH_3CHO$ | | |
|---|---|---|---|---|---|---|
| | HF/6-31G | HF/6-31+G | MP2/6-31+G | HF/6-31G | HF/6-31+G | MP2/6-31+G |
| $NH_2^-$ | 19.4 | 12.1 | 15.4 | −57.3 | −39.5 | −27.9 |
| $OH^-$ | 42.1 | 38.0 | 41.9 | −34.0 | −13.6 | −1.4 |
| $F^-$ | 67.4 | 71.3 | 72.3 | −8.7 | 19.7 | 29.0 |

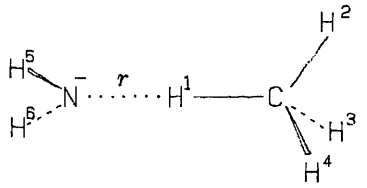


Fig. 1. The Coordinate System Assumed for Hydrogen Abstraction by a Base from $CH_4$

TABLE III. Comparison of Calculated Energies in the Reaction of $CH_4$ with Bases (a.u.)

| | Base | | |
|---|---|---|---|
| | $NH_2^-$ | $OH^-$ | $F^-$ |
| $E_{total}$ | | | |
| $CH_4+B^-$ | −95.67955 | −115.54207 | −139.59740 |
| C-U | −95.68568 | −115.55023 | −139.60417 |
| C-I | −95.68580 | −115.55037 | −139.60429 |
| TS | −95.65797 | — | — |
| C-II | −95.67181 | — | — |
| $CH_3^-+HB$ | −95.66030 | −115.48151 | −139.48365 |
| $\Delta E_{int}$ | −0.00613 | −0.00816 | −0.00697 |
| | (−3.8) | (−5.1) | (−4.4) |

Values in parentheses are in kcal·mol$^{-1}$.

magnitude to those calculated using the MP2/6-31+G basis set, and performing the geometry optimization of the complex I(C-I) and II(C-II) shown in Chart 2 at the MP2 level is too time-consuming. The calculations at the SCF level presented here will test the level at which reasonably quantitative results can be obtained.

**Reaction of $CH_4$ with Bases**

As shown in Fig. 1, the base ($B^-$) approached the hydrogen atom of $CH_4$ along the axis of the C–$H^1$ bond. Only the distance $r$ between the heteroatom of $B^-$ and the hydrogen atom of $CH_4$ was optimized, while the optimized geometries of $CH_4$ and $B^-$ in the ground states remained unchanged. Such complexes are indicated by C-U (undeformed complex). The energies of the system ($CH_4+B^-$) represent the sum of the total energies of $CH_4$ and each base, and the difference in the energy values of the system ($CH_4+B^-$) and C-U, *i.e.*, the interaction energies between $CH_4$ and $B^-$ ($\Delta E_{int}$), are shown in Table III. The total energies of the fully geometry-optimized complexes, C-I, C-II and transition state (TS), are also shown in Table III.

The energy diagrams of the deprotonation reaction of $CH_4$ with bases are shown in Fig.

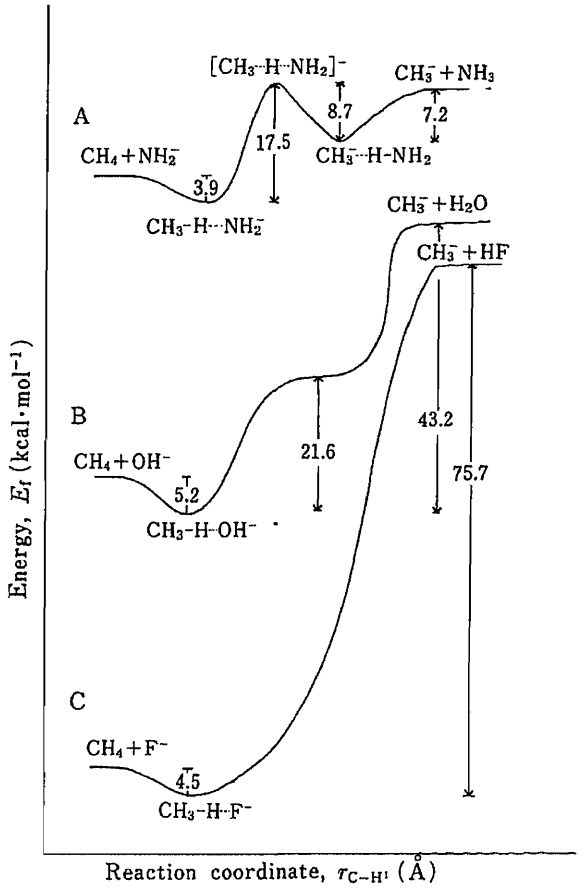


Fig. 2. Comparison of Reaction Profiles for the Deprotonation of $CH_4$ by Bases

The values in the figure are $\Delta E_f$ (kcal·mol$^{-1}$) and the differences in energy between the three systems are arbitrary.

TABLE IV. Optimized Geometries of Complexes between $CH_4$ and Bases

| Geometrical parameter | Optimized geometries $r$ (Å) ∠ (°) | | | | | | | |
|---|---|---|---|---|---|---|---|---|
| | $NH_2^-$ | | | | $OH^-$ | | $F^-$ | |
| | C-U | C-I | TS | C-II | C-U | C-I | C-U | C-I |
| Bond length | | | | | | | | |
| $r$ (C–$H^1$) | 1.082 | 1.092 | 1.490 | 2.379 | 1.082 | 1.091 | 1.082 | 1.091 |
| $r$ (C–$H^2$) | 1.082 | 1.087 | 1.099 | 1.093 | 1.082 | 1.087 | 1.082 | 1.087 |
| $r$ (C–$H^3$) | 1.082 | 1.087 | 1.098 | 1.094 | 1.082 | 1.087 | 1.082 | 1.087 |
| $r$ (C–$H^4$) | 1.082 | 1.087 | 1.100 | 1.094 | 1.082 | 1.087 | 1.082 | 1.087 |
| $r1$ | 2.320 | 2.295 | 1.249 | 1.017 | 2.064 | 2.048 | 2.078 | 2.058 |
| $r2$ | 1.023 | 1.022 | 1.004 | 0.998 | 0.969 | 0.964 | — | — |
| $r3$ | 1.023 | 1.022 | 1.004 | 0.998 | — | — | — | — |
| Bond angle | | | | | | | | |
| ∠$H^2CH^1$ | 109.5 | 109.9 | 110.5 | 130.1 | 109.5 | 110.0 | 109.5 | 110.0 |
| ∠$H^3CH^1$ | 109.5 | 109.9 | 110.3 | 94.5 | 109.5 | 110.0 | 109.5 | 110.0 |
| ∠$H^4CH^1$ | 109.5 | 109.9 | 110.1 | 94.8 | 109.5 | 110.0 | 109.5 | 110.0 |
| A1 | 126.3 | 126.5 | 123.2 | 112.0 | 180.0 | 179.9 | — | — |
| A2 | 107.5 | 107.1 | 113.4 | 112.6 | — | — | — | — |
| Dihedral angle | | | | | | | | |
| ∠$H^3CH^1H^2$ | 120.0 | 120.1 | 120.4 | 123.7 | 120.0 | 120.0 | 120.0 | 120.0 |
| ∠$H^4CH^1H^2$ | −120.1 | −120.0 | −119.9 | −124.0 | −120.0 | −120.0 | −120.0 | −120.0 |
| D1 | −60.0 | −59.9 | −59.9 | −60.1 | — | — | — | — |
| D2 | −180.0 | −180.1 | −180.1 | −127.5 | — | — | — | — |

$r1$, $r$ (N(O, F)–$H^1$); $r2$, $r$ (N(O)–$H^5$); $r3$, $r$ (N–$H^6$); A1, ∠$H^5N(O)H^1$; A2, ∠$H^6NH^5$; D1, ∠$H^5NH^1H^2$; D2, ∠$H^6NH^5H^1$.

2. In the reaction of $CH_4$ with $NH_2^-$, its reaction coordinate has the form shown in Fig. 2A; the minima in this reaction coordinate are two hydrogen-bonded complexes, C-I and C-II, and the central barrier is the highest energy point on the minimum energy reaction path from C-I to C-II and can be identified with the TS. As shown in Fig. 2B, the reaction of $CH_4$ with $OH^-$ shows a single-well potential-energy surface, which has a flat region corresponding to a merging of TS and C-II. The reaction of $CH_4$ with $F^-$ also has a single-well potential-energy surface, and only one minimum point of the energy corresponding to C-I is shown in Fig. 2C. The values of the energy differences between each system are given in kcal·mol$^{-1}$.

From the $\Delta E_{int}$ values the deprotonation ability at the initial step of the reaction decreases in the following order: $OH^- > F^- > NH_2^-$. The energies of formation of C-I ($\Delta E_f$) in the reactions of $CH_4$ with $NH_2^-$, $OH^-$, and $F^-$ are 3.9, 5.2 and 4.5 kcal·mol$^{-1}$, respectively (Fig. 2). These energies are nearly equal to the values of $\Delta E_{int}$, and this result means that the intramolecular deformation energy in the step of formation of C-I is very small.

In the case of the reaction of $CH_4$ with $NH_2^-$, if C-I could gain energy of more than 17.5 kcal·mol$^{-1}$, it would change into the products *via* TS and C-II (Fig. 2A).[8] In the reaction of $CH_4$ with $OH^-$, a flat region corresponding to merging of TS and C-II is observed, and rather higher energy than that in the case of the reaction with $NH_2^-$ would be necessary to obtain the products (Fig. 2B).[8] In the reaction of $CH_4$ with $F^-$, neither the step of TS nor C-II is observed, and a very high energy (75.7 kcal·mol$^{-1}$) is required to form the products (Fig. 2C).[9]

Table IV shows the optimized geometries of the complexes, *i.e.*, C-U, C-I, TS and C-II. The structure of C-I is very similar to that of C-U in all cases. In TS, the C–H$^1$ bond is elongated, and the N–H$^1$ bond becomes appreciably shortened. The structures of the monomers comprising C-II are almost the same as those of the products, *i.e.*, the N–H$^1$ bond length is very similar to the N–H bond length in the ammonia molecule.

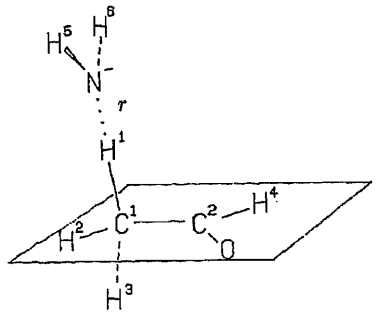


Fig. 3. The Coordinate System Assumed for Hydrogen Abstraction by a Base from $CH_3CHO$

TABLE V. Comparison of Calculated Energies in the Reaction of $CH_3CHO$ with Bases (a.u.)

| | Base | | |
|---|---|---|---|
| | $NH_2^-$ | $OH^-$ | $F^-$ |
| $E_{total}$ | | | |
| $CH_3CHO + B^-$ | −208.34241 | −228.20493 | −252.26006 |
| C-U | −208.36837 | −228.23324 | −252.28533 |
| C-I | — | — | −252.28626 |
| C-II | −208.41474 | −228.24890 | — |
| $^-CH_2CHO + HB$ | −208.40534 | −228.22655 | −252.22869 |
| $\Delta E_{int}$ | −0.02596 | −0.02831 | −0.02527 |
| | (−16.3) | (−17.8) | (−15.9) |

Values in parentheses are in kcal·mol$^{-1}$.

From the results described above, it seems very difficult for the deprotonation reaction of $CH_4$ with $NH_2^-$, $OH^-$, or $F^-$ to occur, and the deprotonation ability of these bases is in the following order: $NH_2^- > OH^- > F^-$.

**Reaction of $CH_3CHO$ with Bases**

In analogy with the reaction of $CH_4$ with bases, a base was considered to approach the hydrogen atom of the methyl group along the axis of the C–H[1] bond as shown in Fig. 3, and the interaction energies between undeformed reactants ($\Delta E_{int}$) and the total energies of each complex are listed in Table V.

The energy diagrams of the deprotonation reaction of $CH_3CHO$ with bases are shown in Fig. 4. The single-well potential-energy surface is observed in all three reactions. In the case of the reaction of $CH_3CHO$ with $NH_2^-$ or $OH^-$ (Fig. 4A, B), the minimum point of the energy corresponds to C-II. On the other hand, in the case of the reaction with $F^-$, the minimum point of the energy corresponds to C-I, and the flat region in the proton-transfer surface corresponds to a merging of TS and C-II (Fig. 4C).

In the initial step of the reaction, the $\Delta E_{int}$ values alone indicate that the deprotonation ability decreases in the following order: $OH^- > NH_2^- > F^-$. On the other hand, the results taking into account the intramolecular deformation energies are as follows. As shown in Fig. 4, in the reaction of $CH_3CHO$ with $NH_2^-$ or $OH^-$, the proton-transfer *via* C-I and TS occurs very easily, and the corresponding C-II is obtained. The C-II may be transformed more readily into the products, because the difference between the total energy of C-II and that of the products is rather small. The energies of formation of C-II ($\Delta E_f$) are 45.4 and 27.6 kcal·mol$^{-1}$, while the energies needed to change from C-II to the products are 5.9 and 14.0 kcal·mol$^{-1}$, respectively. Consequently, the difference (39.5 kcal·mol$^{-1}$) between the energy

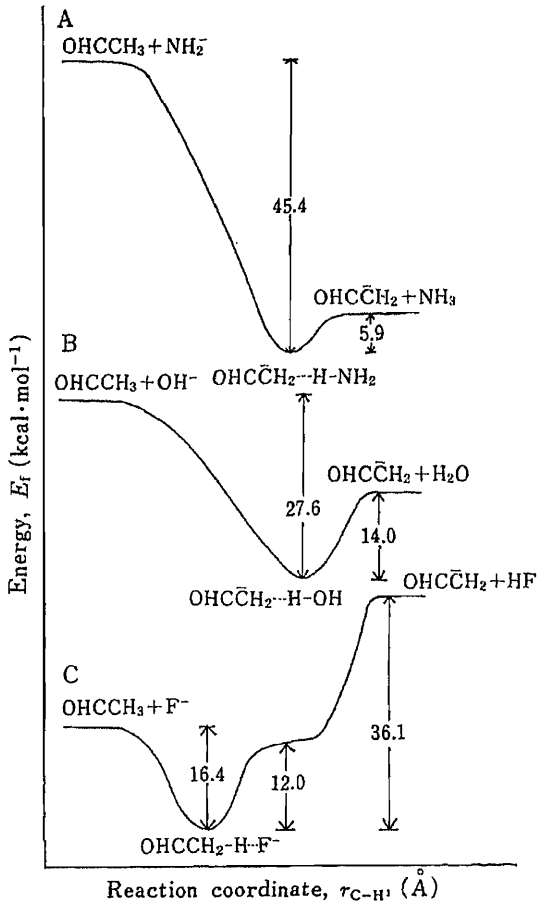


Fig. 4. Comparison of Reaction Profiles for the Deprotonation of $CH_3CHO$ by Bases

The values in the figure are $\Delta E_f$ (kcal·mol$^{-1}$) and the differences in energy between the three systems are arbitrary.

of formation of C-II and that needed to change from C-II to the products in the reaction with $NH_2^-$ is larger than that (13.6 kcal·mol$^{-1}$) in the reaction with $OH^-$. This result means that the deprotonation ability of $NH_2^-$ is larger than that of $OH^-$.

As shown in Fig. 4C, in the reaction with $F^-$, the most stable C-I is first formed, and in the next step a flat region corresponding to a merging of TS and C-II is observed, and finally the complex changes into the products that have a total energy higher than that of the

TABLE VI. Optimized Geometries of Complexes between $CH_3CHO$ and Bases

| Geometrical parameters | Optimized geometries $r$ (Å) ∠ (°) | | | | | |
|---|---|---|---|---|---|---|
| | $NH_2^-$ | | $OH^-$ | | $F^-$ | |
| | C-U | C-II | C-U | C-II | C-U | C-I |
| Bond length | | | | | | |
| $r$ ($C^1$–$H^1$) | 1.090 | 2.606 | 1.090 | 2.215 | 1.090 | 1.160 |
| $r$ ($C^1$–$H^2$) | 1.090 | 1.077 | 1.090 | 1.077 | 1.090 | 1.090 |
| $r$ ($C^1$–$H^3$) | 1.081 | 1.078 | 1.081 | 1.078 | 1.081 | 1.082 |
| $r$ ($C^2$–$H^4$) | 1.085 | 1.100 | 1.085 | 1.099 | 1.085 | 1.088 |
| $r$ ($C^1$–$C^2$) | 1.496 | 2.606 | 1.496 | 1.377 | 1.496 | 1.482 |
| $r$ ($C^2$–O) | 1.214 | 1.279 | 1.214 | 1.278 | 1.214 | 1.224 |
| $r1$ | 1.991 | 1.002 | 1.824 | 1.033 | 1.822 | 1.796 |
| $r2$ | 1.023 | 0.996 | 0.970 | 0.951 | — | — |
| $r3$ | 1.023 | 0.996 | — | — | — | — |
| Bond angle | | | | | | |
| ∠$H^1C^1C^2$ | 109.8 | 90.0 | 109.8 | 90.0 | 109.8 | 109.9 |
| ∠$H^2C^1C^2$ | 109.8 | 120.6 | 109.8 | 120.5 | 109.8 | 109.1 |
| ∠$H^3C^1C^2$ | 109.8 | 121.6 | 109.8 | 121.1 | 109.8 | 110.9 |
| ∠$H^4C^2C^1$ | 116.3 | 114.1 | 116.3 | 114.3 | 116.3 | 115.2 |
| ∠$OC^2C^1$ | 124.1 | 129.4 | 124.1 | 129.1 | 124.1 | 126.2 |
| A1 | 123.4 | 112.5 | 181.3 | 109.1 | — | — |
| A2 | 107.5 | 113.7 | — | — | — | — |
| Dihedral angle | | | | | | |
| ∠$H^2C^1C^2O$ | 0.0 | 179.9 | 0.0 | 180.1 | 0.0 | 244.1 |
| ∠$H^3C^1C^2O$ | 120.1 | −5.0 | 120.1 | −9.7 | 120.1 | 4.5 |
| ∠$H^4C^2C^1H^1$ | 59.9 | −128.3 | 59.9 | −113.1 | 59.9 | −52.0 |
| ∠$OC^2C^1H^1$ | −120.1 | 50.1 | −120.1 | 63.9 | −120.1 | 127.8 |
| D1 | 70.5 | 100.1 | 170.2 | −24.7 | — | — |
| D2 | 183.2 | −29.8 | — | — | — | — |

$r1$, $r$ (N(O, F)–$H^1$); $r2$, $r$ (N(O)–$H^5$); $r3$, $r$ (N–$H^6$); A1, ∠$H^5N(O)H^1$; A2, ∠$H^6NH^5$; D1, ∠$H^5N(O)C^1C^2$; D2, ∠$H^6NC^1C^2$.

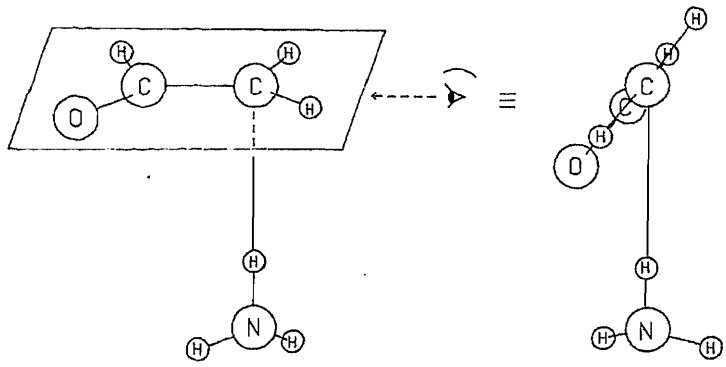


Fig. 5. The Conformation of C-II in the Reaction of $CH_3CHO$ with $NH_2^-$

reactants. This energy diagram shows that the equilibrium of this reaction lies far towards C-I, and this reaction does not proceed easily.

The full optimized geometries of each complex in the reaction of $CH_3CHO$ with $NH_2^-$, $OH^-$ or $F^-$ are shown in Table VI. Figure 5 shows the conformation of C-II in the case of the reaction of $CH_3CHO$ with $NH_2^-$. In the complex of $CH_3CHO$ with $NH_2^-$ corresponding to C-II, the original structures of each monomer are considerably changed, *i.e.*, the $H^1$ atom is combined with the N atom of $NH_2^-$ practically to form the ammonia molecule and the rest, the methide anion, has a nearly planar structure. The structure of the complex of $CH_3CHO$ with $OH^-$ is also quite similar to that of the complex with $NH_2^-$. However, in the complex of $CH_3CHO$ with $F^-$ corresponding to C-I, the original structure of $CH_3CHO$ remains almost unaltered. From the results described above, the order of the deprotonation ability of these bases is as follows: $NH_2^- > OH^- > F^-$.

**Concluding Remarks**

It has been reported[10] that the experimental values of the proton affinities of $NH_2^-$, $OH^-$ and $F^-$ are 403.6, 390.8 and 371.5 kcal·mol$^{-1}$, respectively. It is assumed that the proton affinity mentioned above parallels the deprotonation ability of the base, and thus it is clear that the order of the deprotonation ability, *i.e.*, $NH_2^- > OH^- > F^-$ can be reasonably explained, when deformation energy is taken into account in the calculations of the energies of the complexes in each reaction pathway. The reaction pathways can be classified into three categories as follows.

(1) The formation of C-I is observed, and the difference between the energy of C-I and that of C-II or the products is so large that the reaction does not proceed easily (Fig. 2B, C and 4C). The calculated system has a single-well surface behavior, and the structure of C-I is very similar to that of the reactants.

(2) Both C-I and C-II are formed, and TS is observed. The reaction diagram shows a double-well potential-energy surface behavior (Fig. 2A). If the reaction could proceed to the point of C-II *via* TS, it would be possible to obtain products. The structure of C-I is very similar to those of the reactants, while that of C-II is similar to that of the products.

(3) The energy of the products is rather lower than that of reactants, and the formation of C-II is observed, while the points of C-I and TS are not apparent (Fig. 4A, B). The calculated system has a single-well surface behavior, and the structure of C-II is very similar to those of the products.

The classification of reactions into the above three categories arises from the combination of the reactivity of an active methyl group and the deprotonation ability of a base.

An investigation on the reactions of $CH_4$ and $CH_3CHO$ with various bases with the use of the same technique as in this report is in progress.

**Acknowledgement** The authors are grateful to Professor K. Morokuma and Dr. M. Hanamura of the Institute for Molecular Science for valuable advice and stimulating discussions. Thanks are also due to the Computer Center, Institute for Molecular Science, Okazaki National Research Institutes for the use of HITAC M-680H and S810/10 computers, and to the Computation Center of Fukuoka University for the use of FACOM M-200 and M-380R computers.

**References**

1) W. P. Jencks, "Catalysis in Chemistry and Enzymology," McGraw-Hill, Inc., New York, 1969.
2) *a*) A. A. Frost and R. G. Pearson, "Kinetics and Mechanism," John Wiley & Sons, Inc., New York, 1961, pp. 335—350; *b*) M. L. Bender, "Mechanisms of Homogeneous Catalysis from Protons to Proteins," John Wiley & Sons, Inc., New York, 1971.
3) *a*) Y. Goto, T. Niiya, H. Yamanaka, T. Sakamoto, T. Kubota, K. Ezumi and R. Shimada, *Chem. Pharm. Bull.*, **28**, 1117 (1980); *b*) Y. Goto, T. Niiya, N. Honjo, T. Sakamoto, H. Yoshizawa, H. Yamanaka and T. Kubota, *ibid.*, **30**, 1126 (1982); *c*) T. Sakamoto, H. Yoshizawa, H. Yamanaka, Y. Goto, T. Niiya and N. Honjo,

*Heterocycles*, **17**, 73 (1982).
4) *a*) M. Eigen, *Angew. Chem.*, **75**, 489 (1963); *b*) F. G. Bordwell and D. L. Hughes, *J. Am. Chem. Soc.*, **107**, 4737 (1985).
5) *a*) K. Morokuma, *Acc. Chem. Res.*, **10**, 294 (1977); *b*) S. Nagase and K. Morokuma, *J. Am. Chem. Soc.*, **100**, 1666 (1978); *c*) G. Klass and J. H. Bowie, *Aust. J. Chem.*, **33**, 2271 (1980); *d*) J. C. Sheldon, *ibid.*, **34**, 1189 (1981); *e*) J. C. Sheldon and J. H. Bowie, *ibid.*, **36**, 289 (1983); *f*) H. F. Koch, *Acc. Chem. Res.*, **17**, 137 (1984); *g*) T. Minato and S. Yamabe, *J. Am. Chem. Soc.*, **107**, 4621 (1985).
6) *a*) D. K. Bohme and G. I. Mackay, *J. Am. Chem. Soc.*, **103**, 978 (1981); *b*) D. K. Bohme and A. B. Raksit, *ibid.*, **106**, 3447 (1984); *c*) K. Ohta and K. Morokuma, *J. Phys. Chem.*, **89**, 5845 (1985).
7) *a*) J. S. Binkley, R. A. Whiteside, R. Krishnan, R. Seeger, D. J. DeFrees, H. B. Schlegel, S. Topiol, L. R. Kahn and J. A. Pople, *QCPE*, **13**, 406 (1981); *b*) J. S. Binkley, M. J. Frisch, D. J. DeFrees, R. Krishnan, R. A. Whiteside, R. Seeger, H. B. Schlegel and J. A. Pople, GAUSSIAN 82 from Carnegie-Mellon University, Pittsburgh, PA; *c*) H. F. Schaefer III, "Methods of Electronic Structure Theory," Plenum Press, New York, 1977, p. 10.
8) H. Z. Cao, M. Allavena, O. Tapia and E. M. Evleth, *J. Phys. Chem.*, **89**, 1581 (1985).
9) L. P. Davis, L. W. Burggraf, M. S. Gordon and K. K. Baldridge, *J. Am. Chem. Soc.*, **107**, 4415 (1985).
10) *a*) J. E. Bartmess and R. T. McIver, Jr., *Gas Phase Ion Chem.*, **2**, 88 (1979); *b*) J. Chandrasekhar, J. G. Andrade and P. v. R. Schleyer, *J. Am. Chem. Soc.*, **103**, 5609 (1981).

[Chem. Pharm. Bull. 35(11)4405—4409(1987)]

# A Velocity-Gradient Flow Cell for Raman and Emission Spectroscopy of a Deoxyribonucleic Acid-Drug Solution

MASAMICHI TSUBOI,*[,a,1)] TERUKI IKEDA,[b] and HEIZABURO SHINDO[c]

*Department of Chemistry, Meisei University,[a] Hodokubo 2-1-1, Hino-shi, Tokyo 191, Japan, Application Laboratory, Japan Spectroscopic Co., Ltd.,[b] 2967-5, Ishikawa-cho, Hachioji-shi, Tokyo 192, Japan, and Division of Analytical Chemistry, Tokyo College of Pharmacy,[c] Horinouchi, Hachioji-shi, Tokyo 192-03, Japan*

(Received April 28, 1987)

A deoxyribonucleic acid (DNA) solution was placed in the gap (1 mm) between two coaxial cylinders; the inside diameter of the outer cylinder was 12 mm, and the outside diameter of the inner cylinder was 10 mm. When the inside cylinder was rotated at 2500 revolutions per minute, a sufficiently large velocity gradient of the liquid flow was produced across the gap so that the DNA molecules were oriented along the flow direction. Anisotropy of the Raman scatterings of the DNA molecule was examined by passing an exciting laser beam into the gap from the bottom of the cylinder in the direction parallel to the cylinder axis. An antitumor drug, aclacinomycin A (HCl salt), was added to the DNA solution, and the anisotropy of its emission and Raman spectra was also examined. It has been established that aclacinomycin binds to DNA with its chromophore oriented parallel to the base plane of the DNA duplex.

**Keywords**——aclacinomycin; DNA; Raman spectrum; emission spectrum; flow cell

In ordinary solutions, the molecules are randomly oriented. In a spectroscopic measurement on such a solution, therefore, information on the anisotropic properties of the molecules in question is obscured. It is true that a spectroscopic measurement on a single crystal has a number of advantages in this respect. However, it is often difficult to obtain crystalline samples in biological and pharmaceutical studies. In addition, what is usually relevant in such studies is information on the molecules in solution rather than in crystals, where the molecular environment may be greatly different from that in a living system. Thus it is desirable to have molecules oriented in solution. This is known to be possible for the deoxyribonucleic acid (DNA) duplex by placing its solution in a flow with a velocity gradient of $10^3$ cm $s^{-1}$/cm order of magnitude.[2,3)] Wada and Kozawa,[3)] for example, produced such a velocity gradient in the flow of a solution placed in the gap between two coaxial cylinders, one of which was rapidly rotated. Wada *et al.* examined the anisotropy of the 260 nm absorption of DNA, and of the 445 nm absorption of actinomycin D bound to DNA.[3,4)] In our present study, a similar technique has been applied to Raman and fluorescence spectroscopy. This has proved to be a powerful technique for characterizing the Raman lines of DNA, and for elucidating the geometry of a DNA-drug interaction.

## Description of the New Cell: a Velocity-Gradient Flow Cell for Laser Raman and Emission Spectroscopy[5)]

A solution container has been constructed, in which a flow of the sample solution, having a uniform velocity gradient, can be produced. It consists of two coaxial cylinders (inner and outer cylinders) whose dimensions are given in Fig. 1. As may be seen in the figure, a gap of 1 mm is produced when the inner cylinder is inserted into the outer cylinder along the common vertical axis. The sample solution is placed in this gap. When the inner cylinder is

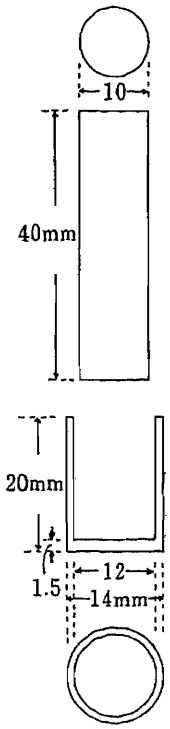


Fig. 1. Two Coaxial Glass Cylinders, Which Form the Essential Portion of the New Flow Cell

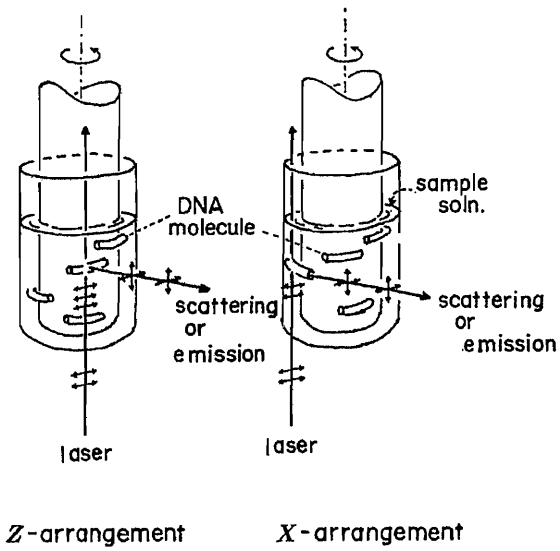


Fig. 2. Two Different Scattering or Emission Geometries for the New Flow Cell

rotated at the rate of 2500 revolutions per minute (rpm) with the outer cylinder fixed, a flow of the solution is produced along the horizontal circles. The flow velocity is zero at the outer wall, whereas it is about 1300 mm/s at the other end of the gap (at the surface of the inner cylinder). Therefore, the velocity gradient here, which would be nearly uniform, should be $1300\,s^{-1}$.

For examining the Raman and/or emission spectrum of the sample solution, the exciting laser beam is passed from the bottom vertically along the gap through the solution. The light scattered or emitted from the sample solution along the horizontal direction through the outer cylinder is collected and led to the entrance slit of a spectrometer. Two different modes of passing the laser beam were adopted: in one of them, the electric vector of the laser beam was directed along the flow of the solution (*Z*-arrangement, see Fig. 2); in the other, the laser beam was polarized along the perpendicular direction to the flow (*X*-arrangement, see Fig. 2). For locating the outer and inner cylinders relative to each other and relative to the laser and spectrometer positions, it is essential to have micropositioners for both cylinders which should be operated independently of each other.

**Example I: Effect of Aligning DNA Molecules on the Raman Spectrum**

A sample of salmon sperm DNA was obtained from PL Biochemicals Inc., and used after being purified as follows: DNA was dissolved in 10 mM Tris + 0.1 mM EDTA (ethylenediaminetetraacetic acid) solution (pH 7.5) and stirred overnight; 2 volumes of ethanol were added to precipitate DNA, which was dried in the atmosphere and then dissolved in 0.1 M NaCl + 0.1 mM EDTA overnight. Finally the solution was subjected to centrifugation at 20000 rpm for 2 h to remove precipitates.

This DNA solution (concentration = 0.5%) was placed in the cell and the Raman spectrum was observed, by the use of a Jasco NR-1000 Raman spectrometer, with the *X*- and

*Z*-arrangements of the 488.0 nm beam of an NEC GLG 3200 Ar ion laser. As may be seen in Fig. 3, the intensities of some observed Raman lines are markedly different for *X*- and *Z*-arrangements. This fact indicates that the sample solution is anisotropic, and this is considered to be caused by alignment of the DNA molecules along the flow. For a DNA duplex with its axis along the *Z*-direction (flow direction), we can expect four different components of each Raman scattering tensor, namely *xx*, *xy*, *xz*, and *zz* components. The optical system collecting the scattering light has no polarizer, and the spectrometer has a scrambler. Therefore, the scattering light should involve mainly the *xx* and *xy* components in the *X*-arrangement, and the *xz* and *zz* components in the *Z*-arrangement (see Fig. 2). It is understandable that the 1375 $cm^{-1}$ line, assignable to the $CH_3$ symmetric deformation vibration of the thymine residue, and the 1090 $cm^{-1}$ line, assignable to the $PO_2^-$ symmetric stretching vibration, have relatively large *zz* components. Thus, both of these vibrations have appreciable atomic displacements along the *z*-direction (axis of the DNA double helix), and therefore may cause large polarizability oscillation along the *z*-direction. On the other hand, the 1490, 1338, 1310, and 1270 $cm^{-1}$ lines, all assignable to in-plane skeletal stretching vibrations of the base residues, would have large *xx* and *xy* components, but only a smaller *zz* component. This explains why these lines are weak in the spectrum with the *Z*-arrangement of the exciting laser.

**Example II: Effects on the Raman and Emission Spectra of Aclacinomycin Bound to DNA**

Aclacinomycin A has antitumor activity,[6] and is known to be bound strongly to DNA in

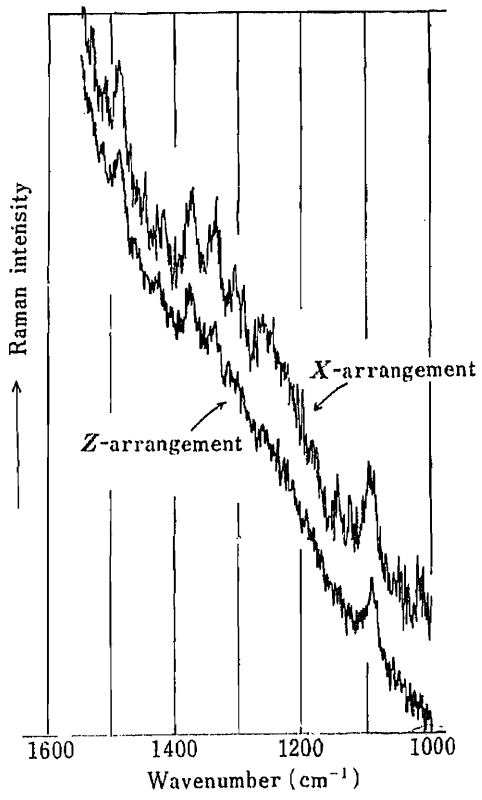


Fig. 3. Raman Spectra of Salmon Sperm DNA in 0.5% Aqueous Solution at pH 7.5 (No Buffer), and at 20 °C

Exciting light, 488.0 nm beam of an Ar ion laser (100 mW at the sample point). Two different modes of incidence are adopted (see Fig. 2).

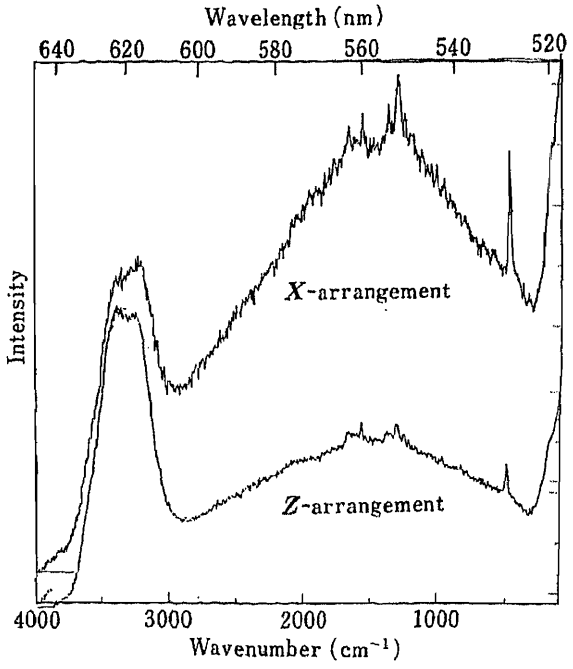


Fig. 4. Raman and Fluorescence Spectra of an Aqueous Mixture of Salmon Sperm DNA (0.15 M in Nucleotide) and Aclacinomycin A HCl (0.0005 M), at pH 6 and at 20 °C

Exciting light, 514.5 nm beam of Ar ion laser (30 mW at the sample point). Two different modes of incidence are adopted (see Fig. 2).

aqueous solution.[7,8] This drug is strongly fluorescent but the fluorescence is markedly quenched on binding to DNA. Is the residual fluorescence caused by the drug bound to DNA? Does this quenching enable us to observe the Raman spectrum of aclacinomycin? What is the geometry of the chromophore of this drug with respect to DNA in the complex? These questions were all answered by a spectroscopic examination by the use of the present new "velocity gradient flow cell."

Aclacinomycin A HCl was added to the above-mentioned DNA solution, so that the final concentrations of DNA and drug were 0.15 M and 0.0005 M, respectively. This mixture solution was placed in the cell, and the scattering and emission were examined with a Jasco NR-1100 Raman spectrometer, for the *X*- and *Z*-arrangements of the 514.5 nm beam of an NEC GLG 3200 Ar ion laser. The results are shown in Fig. 4. As may be seen here, the fluorescence background is much stronger for the *X*-arrangement than for the *Z*-arrangement. This is clearly seen by using the $H_2O$ Raman band at around 3300 $cm^{-1}$ (at 620 nm) as an internal standard; the water molecules in the solution would be directed randomly even under the flow, and the Raman band should have equal intensities for the *X*- and *Z*-arrangements of the laser. Thus, the transition moment of the 558 nm emission band of the aclacinomycin chromophore has now been shown to be directed dominantly along the *X*-direction (perpendicular to the flow, or to the axis of the aligned DNA duplex) rather than the *Z*-direction. It has been indicated, in other words, that the fluorescence in question arises from the aclacinomycin molecule bound to DNA, and that its chromophore is located parallel to the DNA base plane. This gives support to the idea that the chromophore is intercalated in the stacked base-pairs of the DNA molecule.

Superimposed on the fluorescence background just mentioned, several prominent Raman lines are evident (see Fig. 4). They are at 500, 1300, 1380, 1590, and 1700 $cm^{-1}$, and are assignable to ring vibrations of the aclacinomycin chromophore. These are considered to be resonance-enhanced by the 437 nm absorption, whereas the Raman lines of DNA are much weaker so that they are buried in the fluorescence background. All of the observed Raman lines of aclacinomycin are stronger for the *X*-arrangement of the laser than for the *Z*-arrangement. This is understandable, because these Raman lines should be caused by in-plane vibrations of the chromophoric portion of the aclacinomycin molecule, and here every Raman scattering should have a greater $xx$ component than $zz$ component.

## Discussion

The experiments described in the preceding two sections (Examples I and II) have proved that the present velocity-gradient flow cell is useful (1) in aligning the DNA molecules unidirectionally in solution, to obtain knowledge of the anisotropy of the DNA Raman lines, (2) for judging whether a given drug molecule is bound to DNA, and (3) if so, for obtaining information on the geometry of the complex. The cell would also be useful (4) for aligning any rod-shaped macromolecules or their complexes, including some viruses such as tobacco mosaic virus. This may allow us to obtain information on the relative orientations of the constituent molecules. Lastly, the cell should be useful (5) for examining in detail the dynamic behavior of macromolecules and for deriving their elastic constants in a quantitative manner. When the velocity gradient of the flow of a sample solution is continuously changed, and when the anisotropy of its emission, for example, is quantitatively determined as a function of the velocity gradient and as a function of ionic strength and other properties of the solvent, the results would represent valuable data on the dynamic properties of macromolecule or a macromolecular complex.

**Acknowledgements** Our thanks are due to Professor Akiyoshi Wada, University of Tokyo, for his valuable

advice, to Dr. Tomio Takeuchi (Institute of Microbial Chemistry) and Dr. Hiroshi Tone (Sanraku-Ocean Co., Ltd.) for the aclacinomycin A HCl sample, and to Mr. Tadashi Miyazaki (President, Japan Spectroscopic Co., Ltd.) for his interest, encouragement, and support. This work was partly supported by a grant (No. 62840014) from the Ministry of Education, Science, and Culture.

## References and Notes

1) Present address: *Faculty of Science and Engineering, Iwaki-Meisei University, Chuodai-Iino 5-5-1, Iwaki, Fukushima 970, Japan.*
2) A. Wada, *Applied Spectroscopy Reviews*, **6**, 1 (1972).
3) A. Wada and S. Kozawa, *J. Polym. Sci.*, **A2**, 853 (1964).
4) M. Tsuboi, S. Higuchi, Y. Kyogoku, K. Matsuo, and A. Wada, *Chem. Pharm. Bull.*, **12**, 501 (1964).
5) Patent pending.
6) T. Oki, Y. Matsuzawa, A. Yoshimoto, K. Numata, I. Kitamura, S. Hori, A. Takamatsu, H. Umezawa, M. Ishizuka, H. Naganawa, H. Suda, M. Hamada, and T. Takeuchi, *J. Antibiot.*, **28**, 830 (1975).
7) H. Yamaki, H. Suzuki, T. Nishimura, and N. Tanaka, *J. Antibiot.*, **31**, 1149 (1978).
8) S. Takahashi, N. Nagashima, Y. Nishimura, and M. Tsuboi, *Chem. Pharm. Bull.*, **34**, 4494 (1986).

[Chem. Pharm. Bull. 35(11)4410—4417(1987)]

# Control of Antipyrine Release Rate by Plasma Coating Using Tetrafluoroethylene and Propargyl Alcohol Blend Monomer

TATSUYA KITADE, KEISUKE KITAMURA, and KEI HOZUMI*

*Kyoto Pharmaceutical University, Misasagi, Yamashina-ku, Kyoto 607, Japan*

(Received April 30, 1987)

Antipyrine powder was coated by deposition of a polymer thin film within a glow discharge of tetrafluoroethylene and propargyl alcohol blend monomer under reduced pressure (plasma polymerization) and drug release from the product was investigated. A dissolution test revealed that the use of the blend monomer was superior to that of the individual plain monomer. The plasma coating of the powder was done with intermittent agitation or with continuous mixing under electromechanical vibration; in the former case the product gave slow drug release, but the reproducibility was poor, while in the latter case, reproducibility was good, but the release rate was faster. It was found that the release rate could be fairly well controlled by changing the film thickness of the plasma polymer, and was not influenced by the pH of the dissolution medium.

**Keywords**——plasma polymerization; tetrafluoroethylene; propargyl alcohol; blend monomer; polymer thin film; slow release; antipyrine

Plasma polymerization of organic monomers proceeds in a glow discharge under reduced pressure and the resultant polymers slowly deposit onto solid materials directly from the vapor phase forming polymer thin films. Because the gas can diffuse readily, powdered materials can be plasma-coated if the materials are mixed intermittently or continuously during the polymerization process.[1-8] Solid and dense plasma polymer was uniformly formed around individual particles,[9-11] so that this method may be available to control the release rate of powdered pharmaceuticals in dissolution media. The technique has the advantages that a thinner coating film than usual can be prepared, and the release rate can be freely controlled by changing the film thickness. Antipyrine was chosen as a model pharmaceutical having suitable solubility and high stability in aqueous media, while tetrafluoroethylene (TFE) and propargyl alcohol (PA) were employed as hydrophobic and hydrophilic monomers, respectively.[9,12-14] The release rate of antipyrine was investigated after plasma coating of the powder with polymers derived from either plain or blend monomer.

## Experimental

**Plasma-Coating Apparatus**——A schematic diagram of the plasma-coating apparatus is shown in Fig. 1. A glass bell jar having a diameter of 25 cm and a height of 30 cm was set up on a stainless steel base and the interior was evacuated with a rotary pump (300 l/min). Two stainless steel parallel electrodes having a diameter of 10 cm were installed horizontally in the bell jar and a 13.56 MHz electric current was supplied. The upper electrode was drum-shaped, having 12 nozzles through which monomer gas diffused downwards, while the material being coated was placed on the lower electrode. The TFE monomer gas, stored in a pressurized tank, was passed to the upper electrode *via* a needle valve and a mass flow meter. Liquid propargyl alcohol was stored in a small glass reservoir and its vapor was slowly drawn towards the upper electrode *via* a stop valve under reduced pressure. The pressure in the plasma apparatus was monitored by a thermocouple vacuum gauge and was regulated by a pressure control valve installed on the vacuum line.

Coating of the antipyrine powder was carried out by two methods (stationary condition with intermittent agitations and electromechanical vibrational mixing during plasma polymerization). In the former case, the powder was spread on a watch glass and the plasma polymerization was interrupted every 20 or 30 min for manual agitation,

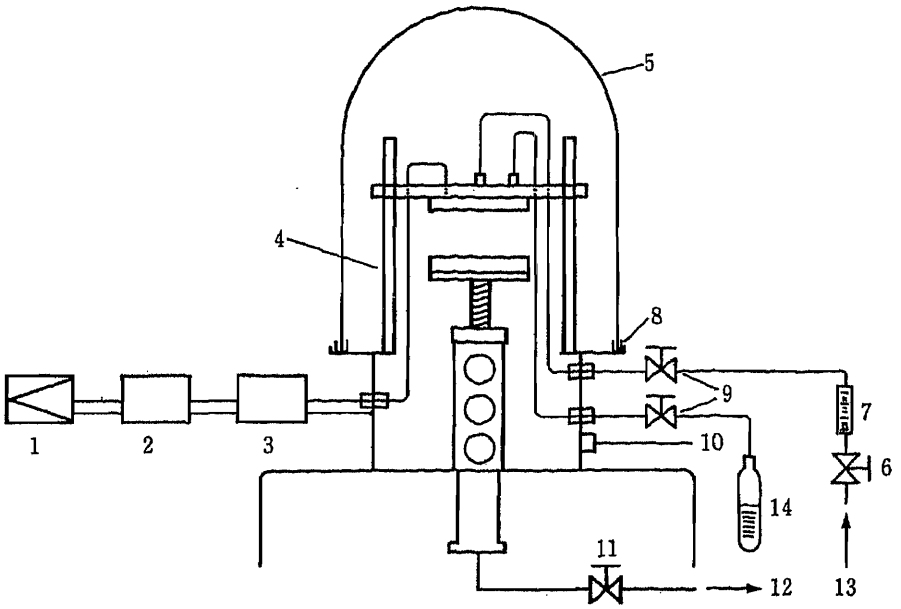


Fig. 1. Schematic Diagram of Plasma-Coating Apparatus

1, 13.56 MHz power generator; 2, power meter; 3, matching network; 4, insulator rod; 5, glass bell jar; 6, needle valve; 7, flow meter; 8, rubber ring; 9, stop valve; 10, thermocouple vacuum gauge; 11, pressure control valve; 12, rotary pump; 13, TFE; 14, propargyl alcohol.

while in the latter case the powder was put in a light plastic vessel which was connected to a resonance bar synchronized at 60 Hz by an electric vibrator.[6,8,11]

Dissolution studies were carried out using the puddle method in 1000 ml of distilled water at 37 °C with stirring at 150 rpm. The concentration of antipyrine in the aqueous medium was determined spectrophotometrically at a wavelength of 242 nm.

**Materials**——TFE: Presented by courtesy of Daikin Kogyo Inc. Propargyl alcohol: Nakarai Chemicals Ltd., EP Reagent. Antipyrine: Kanto Chemical Co., Inc., EP Reagent.

**Measuring Apparatus**——Dissolution test apparatus: Toyama Sangyo NTR-55. Spectrophotometer: Shimadzu UV-210A double-beam scanning spectrophotometer.

## Results and Discussion

### Monomers and Method of Coating

Since plasma-polymerized tetrafluoroethylene (PPTFE) has a highly cross-linked and three-dimensionally compact molecular structure,[6] the polymer membrane is rather rigid and fragile. On the other hand, plasma-polymerized propargyl alcohol (PPPA) is comparatively flexible[13] because of its low degree of cross-linking with a concomitant abundance of free-rotation sites in the molecule. Therefore a preliminary study was conducted on the choice of monomers and of the methods for coating. Figure 2 shows the dissolution curves of antipyrine powder plasma-coated with various plain and blend monomers under the stationary condition. Coating film thickness of all the samples was approximately 0.5 $\mu$m. The film thickness mentioned hereafter is the monitoring film thickness on a slide glass placed near the sample and coated under the same conditions. The film thickness was measured by using a reflection interferometer in the conventional manner. Since the deposition of the polymer film was confined to the surface layer of the powder material being mixed, the actual film thickness grown during the plasma process was considered to be much thinner than the monitoring values on the slide glass. However, the latter values were useful as a guide to obtain reproducible film thickness on the powder material.[6,8,11]

The figure shows that the antipyrine coated with the TFE plain monomer gave faster

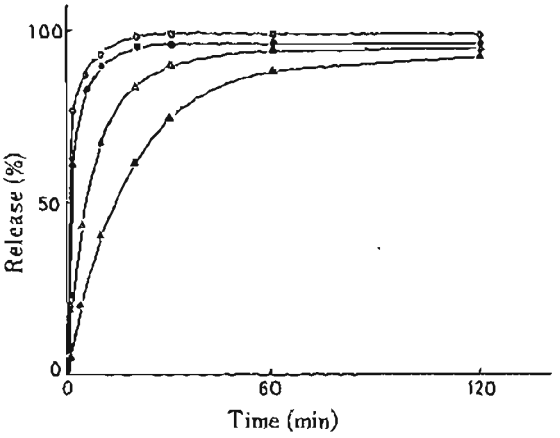


Fig. 2. Mean Release Profiles of Antipyrine Powder Plasma-Coated with Various Monomers

○, TFE; ●, PA; △, TFE–PA bilayer; ▲, TFE–PA (1 : 10) copolymer. Film thickness: 0.5 μm.

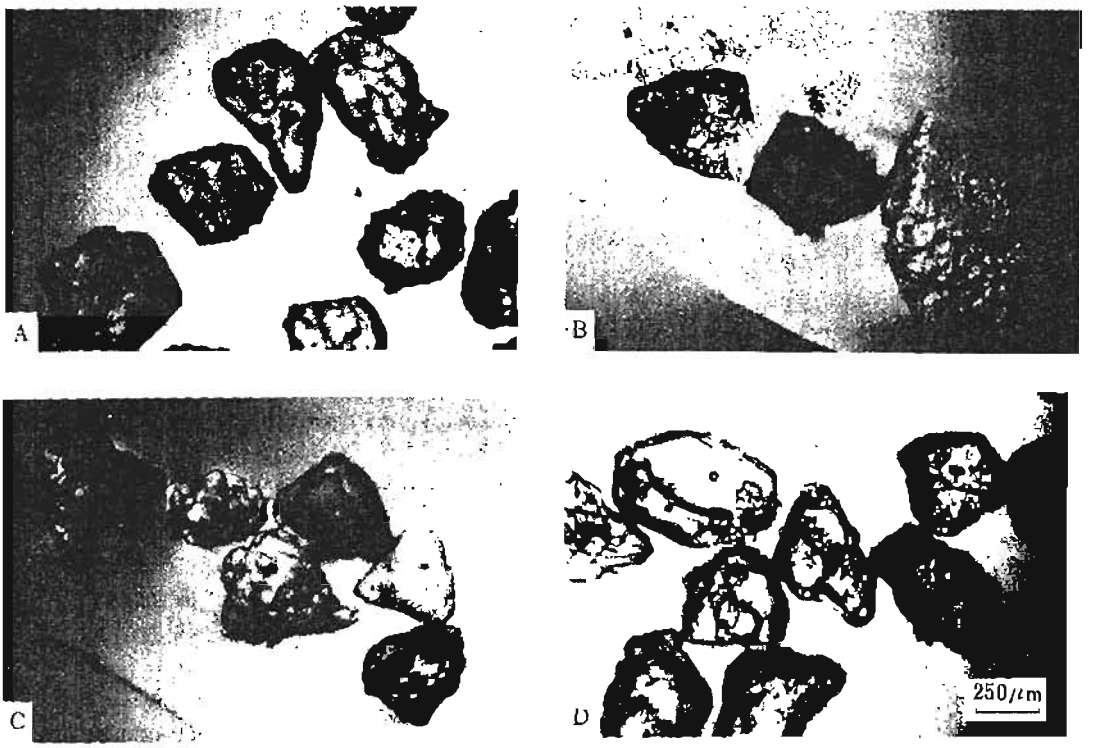


Fig. 3. Optical Micrographs of Microencapsulated Antipyrine Powder

A) PA plasma-coated, original; B) TFE plasma-coated, half-dissolved; C) PA plasma-coated, half-dissolved; D) TFE–PA (1 : 10) plasma-coated (copolymer), half-dissolved.

dissolution than that coated with the PA plain monomer. However, either dissolution rate was significantly slower than that of uncoated antipyrine, which dissolved within a few seconds. It was also observed that the TFE plasma-coated particles tended to float on water during the dissolution test due to their highly hydrophobic surface, and a number of fragments considered to be derived from the coating film were seen. The latter finding suggested that the antipyrine was released not by permeation through the coating film but directly through cracks or by destruction of the film.[8] The relatively high release rate of the TFE plasma-coated particles was therefore understandable. In the case of PA plain monomer, the encapsulated particles dispersed well in water because of the hydrophilic surface and no fragment of the coating film was observed. It was presumed that the PPPA film was relatively flexible and the antipyrine

was released essentially by permeation through the polymer film. A high rate of permeation through the PPPA film was apparent.

To overcome the disadvantages of the use of plain monomers, antipyrine powder was first plasma-coated with TFE and then with PA to form a bilayer film. It was found that the antipyrine powder was uniformly dispersed in water and no fragment of the coating film was seen during the dissolution test. The dissolution rate was remarkably retarded in comparison with the use of plain monomers.

A further trial using TFE and PA blend monomer at a molar ratio of 1 : 10 resulted in the most effective retardation among all the cases tested. Thus, TFE–PA copolymer seemed to be the most promising material for coating antipyrine powder in order to control the release rate.

Figure 3 shows optical micrographs of encapsulated antipyrine powder with different coating films. Picture A illustrates the antipyrine particles plasma-coated with PA plain monomer. Because of the extremely thin film, the appearance of the coated particles was practically the same as that of the uncoated ones. This was also true in the cases of other monomers. Picture B shows the sample plasma-coated with TFE plain monomer and half-dissolved in the dissolution test. Some of the coating film was broken up by swelling of the hydrated core drug, leaving empty polymer capsules. It was therefore considered that the plasma coating with TFE plain monomer yielded fragile and easily breakable polymer capsules from which relatively fast dissolution occurred.

The PA plain monomer formed a flexible coating film which could tolerate swelling of core drug, as shown in picture C. A number of prominences as a result of such expansion were seen on the coated surface, while no empty capsule was observed. The results support permeation of the drug through PPPA film as the route of the dissolution.

The TFE–PA blend monomer exhibited an excellent particle profile during the dissolution test, as illustrated in picture D. Neither destruction nor deformation of the encapsulated particles was observed throughout the course of dissolution, and the core drug was released smoothly through the polymer film by permeation.

**Composition of the Blend Monomer**

It was naturally thought that the properties of the polymer derived from the blend monomer would be altered by changing the composition of the gas mixture. Prior to the study

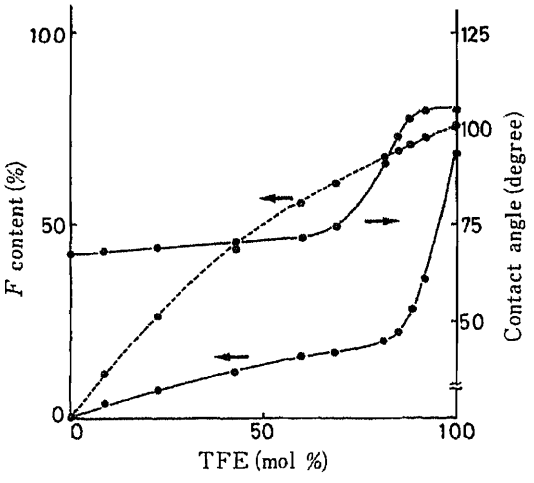


Fig. 4. Relationship of F Content and Contact Angle of Plasma Polymers Produced at Various TFE–PA Compositions

------, theory; ——, experiment. Pressure, 0.2 mbar; power, 5 W; mean diameter of particles, 214 μm; coating time, 20 min × 4.

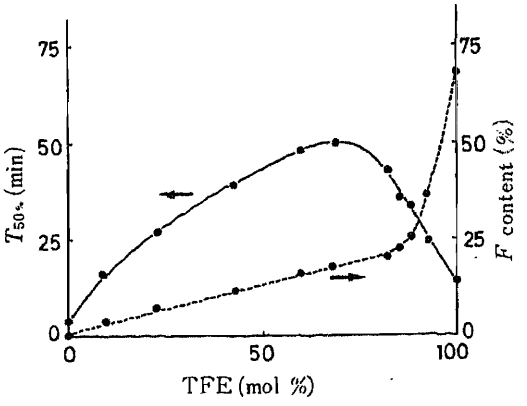


Fig. 5. The 50% Release Times of Antipyrine Powder Plasma-Coated at Various TFE–PA Compositions

Pressure, 0.2 mbar; power, 5 W; mean diameter of particles, 214 μm; coating time, 20 min × 4.

of release control, the relationship between fluorine content and contact angle of water on a glass surface in regard to the plasma polymers formed from different compositions of the blend monomer was investigated. The results are shown in Fig. 4. The fluorine content in the plasma polymers was consistently lower than the theoretical value and in the range of TFE mole percent below 80% it was less than one-third of the theoretical content. The result suggested that the PA fraction in the blend monomer was preferably polymerized until its mole percent became particularly low. The fluorine content in the polymer exhibited a strong correlation with the contact angle of water.

The relationship between the time required for 50% drug release from antipyrine powder plasma-coated with various TFE–PA compositions and the fluorine content in the resultant plasma polymer was also investigated. Increasing fluorine content increased the time required for 50% release ($T_{50\%}$), but when the TFE composition in the blend monomer exceeded 80%, the fluorine content in the polymer suddenly increased while the $T_{50\%}$ was abruptly shortened (Fig. 5). It seemed therefore that the TFE–PA blend monomer at a molar ratio of approximately 4:1 was the most effective in regard to slow release. It has been experienced, however, that plasma polymers formed from blend monomer with a high content of TFE sometimes exhibited faster release than usual, probably because of behavior similar to that described for the coating with TFE plain monomer (Fig. 2B). The optimum composition of the blend monomer requires further research.

**Coating under Stationary and Vibrational Mixing Conditions**

Coating of the antipyrine powder under the stationary condition resulted in the formation of a nonuniform or imperfect coating film, namely, the particles in the upper layer are coated with a thicker film than those in the lower layer and also the upper side of each particle forms a thicker film than the lower side. Therefore repeated intermittent manual agitations were necessary in the course of the coating process. Another technique, involving electromechanical vibrational mixing of the powder during the coating process, was employed to ensure the deposition of a uniform coating layer all around the particles.[6,8,11] Since the polymer film grew on all the vibrating particles, the growth rate was expected to be slower than under the stationary condition.

Figure 6 shows the dissolution curves of antipyrine powder plasma-coated with both processes. In the case of coating under the stationary condition, the sample (100 mg) was uniformly spread on a watch glass having a diameter of 9 cm and the watch glass was placed on the lower electrode for plasma coating. The coating process was interrupted every 20 or 30 min to remove the watch glass from the plasma chamber and agitate the sample powder manually. This unit process was repeated four times to complete the plasma coating. The release profiles of the products showed reasonable changes of release rate depending upon the

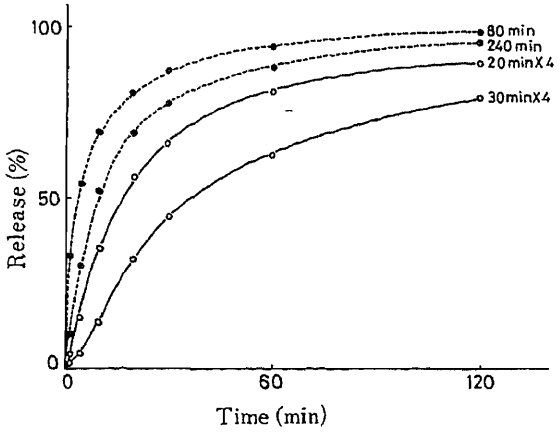


Fig. 6. Mean Release Profiles of TFE–PA Plasma-Coated Antipyrine Powder Processed under Stationary and Vibrational Mixing Conditions

——, fourfold coated under the stationary condition with intermittent agitations. ------, coated under the vibrational mixing condition. Pressure, 0.4 mbar; power, 5 W; mean diameter of particles, 359 μm; blend monomer, TFE–PA (1 : 10).

total coating time.

Release profiles of the product derived from the vibrational mixing condition are shown in the same figure for comparison. In this technique 100 mg of sample powder was put in a shallow plastic vessel having a diameter of approximately 6 cm and was shaken with a resonance bar energized by a 60 Hz electric vibrator. The sample coated in this manner for either 80 or 240 min exhibited faster drug release than those processed under the stationary condition, as expected.

These two procedures were compared for reproducibility of $T_{50\%}$ of TFE–PA plasma-coated antipyrine powder. The results are shown in Table I. In the case of vibrational mixing, the relative standard deviation of the release time was 12.1%, and in the case of the stationary condition it was 40.7%. Therefore it was concluded that coating under the stationary condition induced a slower release rate than under the vibrational mixing condition, while the latter technique resulted in higher reproducibility of the release rate than the former.

## Particle Size

The influence of particle size of antipyrine powder on $T_{50\%}$ was investigated. Results for

TABLE I. Reproducibility of 50% Release Time of TFE–PA Plasma-Coated Antipyrine Powder Processed under Stationary and Vibrational Mixing Conditions

| Fourfold coated under stationary condition with intermittent agitations[a] | | Coated under vibrational mixing condition[b] | |
|---|---|---|---|
| $T_{50\%}$ (min) | RSD (%) | $T_{50\%}$ (min) | RSD (%) |
| 10.0 | | 8.0 | |
| 4.5 | | 9.8 | |
| 3.5 | 40.7 | 11.0 | 12.1 |
| 6.4 | | 10.5 | |
| 8.2 | | 9.2 | |

Pressure, 0.4 mbar; power, 5 W; mean particle diameter, 359 $\mu$m; blend monomer, TFE–PA (1 : 10); coating time, *a*) 10 min × 4 or *b*) 240 min.

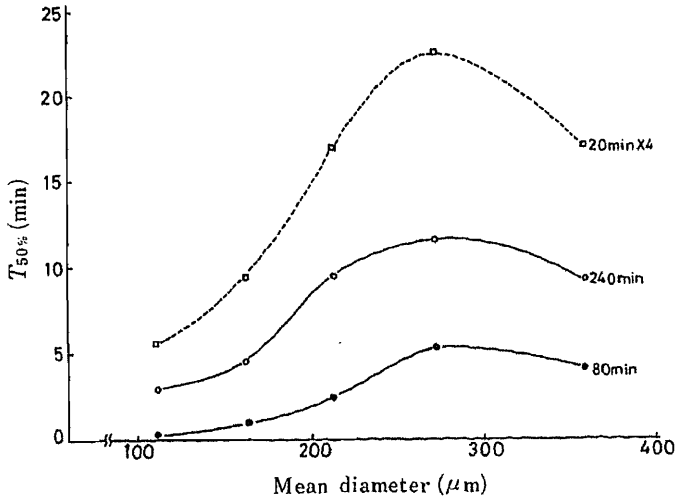


Fig. 7. Effect of Particle Size on 50% Release Time of Antipyrine Powder Plasma-Coated with TFE–PA Blend Monomer

——, Coated under the vibrational mixing condition. ------, Fourfold coated under the stationary condition with intermittent agitations. Pressure, 0.4 mbar, power, 5 W; blend monomer, TFE–PA (1 : 10).

particle sizes in the range of 110 to 360 $\mu$m before coating are shown in Fig. 7. In all cases coated under various conditions, $T_{50\%}$ was maximum at approximately 274 $\mu$m particle diameter, and either smaller or larger particle size gave a shorter release time. This characteristic phenomenon was thought to be the result of large surface area of the sample at smaller particle size and a relatively thin polymer film at larger particle size, in which case the film would be readily cracked by swelling of the particles. It was also found that the release rate was controllable by changing the particle size.

**Film Thickness**

The relation between the film thickness and the release rate is shown in Fig. 8. It was clear that the release rate was almost directly proportional to the film thickness. Since the film thickness could be simply controlled by adjusting the time of the coating process,[9] it seemed possible to prepare microcapsules with a desirable release rate.

**Temperature and pH of the Dissolution Medium**

Figures 9 and 10 show the dissolution curves at various temperatures and pH values of the dissolution medium. An increase of temperature accelerated the release rate, but the

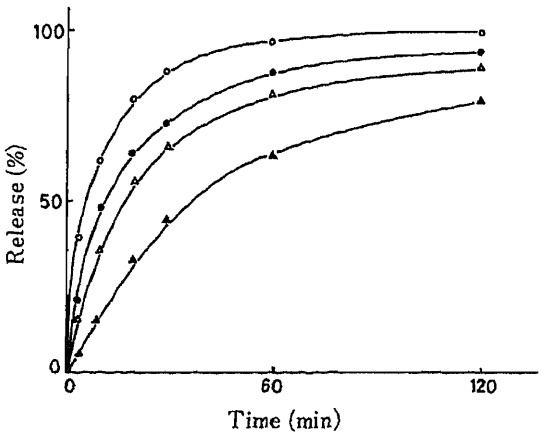


Fig. 8. Mean Release Profiles of Antipyrine Powder Plasma-Coated with TFE–PA (1 : 10) Blend Monomer to Various Film Thicknesses

Film thickness ($\mu$m): ○, 0.25; ●, 0.50; △, 1.00; ▲, 1.50.

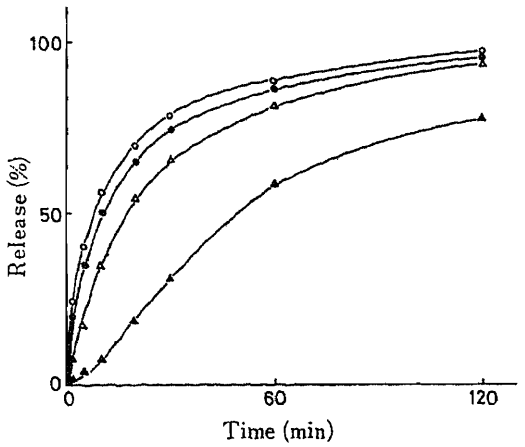


Fig. 9. Mean Drug Release Profiles from Antipyrine Powder Plasma-Coated with TFE–PA (3 : 10) Blend Monomer in Dissolution Medium at Various Temperatures

Temperature (°C): ○, 60; ●, 50; △, 40; ▲, 30. Film thickness, 1 $\mu$m.

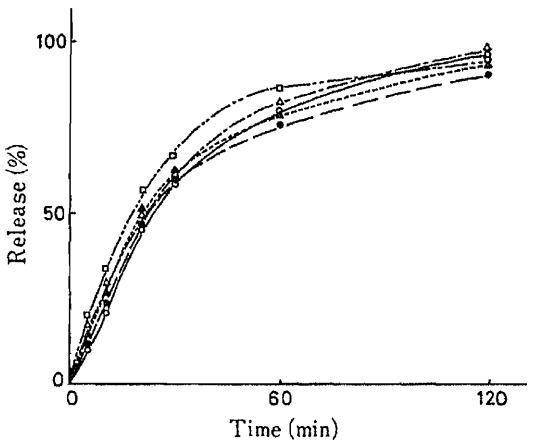


Fig. 10. Mean Drug Release Profiles from Antipyrine Powder Plasma-Coated with TFE–PA (3 : 10) Blend Monomer in Dissolution Medium at Various pH Values

pH: ○, 2; ●, 4; △, 6; ▲, 8; □, 10. Film thickness, 1 $\mu$m.

polymer film may act more effectively as a diffusion barrier at higher flux of antipyrine, so that the release rate varied nonlinearly with the temperature change. Since the polymer film was neutral, the pH change only influenced the amine character of antipyrine. It is clear from Fig. 10 that a wide range of pH variation produced no significant difference of the release rate, because the antipyrine flux was essentially controlled by movement of the molecules through the polymer network, and not by the solvation energy in the dissolution medium.

## Conclusion

The results reported here may be summarized as follows. a) Plasma coating of the model pharmaceutical using TFE–PA blend monomer was most effective for producing slow drug release among the methods using TFE and/or PA monomers. The optimum TFE content of the blend monomer for the slowest release rate was found at the highest content at which the resultant plasma polymer still maintained a hydrophilic nature. b) Due to the fast growth rate of the polymer film, coating under the stationary condition resulted in slower release than under the vibrational mixing conditions, while the former technique yielded inferior reproducibility of the release rate to the latter. c) There was an optimum particle size of approximately 274 $\mu$m in diameter for the slowest release rate of the model pharmaceutical. Larger or smaller particle size resulted in a faster release rate. d) The release rate could be controlled readily by changing the film thickness, which is strongly dependent upon the time of plasma coating at a given particle size. e) Increasing the temperature of the dissolution medium accelerated the release rate, but changes of pH did not significantly alter the release rate.

### References

1) K. Hozumi (ed.), "Low-Temperature Plasma Chemistry," Nankodo, Tokyo, 1976.
2) K. Hozumi, *Membrane*, **5**, 24 (1980).
3) K. Hozumi, *Polymer*, **30**, 114 (1981).
4) O. Tsuji, T. Wydeven, and K. Hozumi, *Microchem. J.*, **22**, 229 (1977).
5) K. Hozumi, K. Kitamura, T. Kitade, and S. Iwagami, *Microchem. J.*, **28**, 215 (1983).
6) T. Kitade, K. Hozumi, and K. Kitamura, *Bunseki Kagaku*, **32**, 368 (1983).
7) T. Kitade, K. Hozumi, and K. Kitamura, *Yakugaku Zasshi*, **103**, 719 (1983).
8) K. Hozumi, K. Kitamura, and T. Kitade, *Nippon Kagaku Kaishi*, **10**, 1558 (1984).
9) K. Hozumi, K. Kitamura, and T. Kitade, *Yakugaku Zasshi*, **99**, 521 (1979).
10) K. Hozumi, K. Kitamura, and T. Kitade, *Bull. Chem. Soc. Jpn.*, **54**, 1392 (1981).
11) T. Kitade, K. Hozumi, and K. Kitamura, *Yakugaku Zasshi*, **103**, 726 (1983).
12) K. Hozumi, K. Kitamura, T. Kitade, M. Kuriyama, A. Takekawa, and K. Fujii, *Kobunshi Ronbunshu*, **42**, 55 (1985).
13) K. Hozumi, K. Kitamura, T. Kitade, and K. Yoshimura, *Kobunshi Ronbunshu*, **42**, 881 (1985).
14) K. Yoshimura, K. Hozumi, K. Kitamura, T. Kitade, and Y. Okamoto, *Bunseki Kagaku*, **35**, 496 (1986).

[Chem. Pharm. Bull. 35(11)4418—4428(1987)]

# Degradation of 1,3-Diaryl-1-nitrosoureas in Aqueous Solutions and in Organic Solvents

MAKOTO MIYAHARA,*[a] NAOKI MIYATA,[a] MASAAKI HIROBE,[b] and SHOZO KAMIYA[a]

*National Institute of Hygienic Sciences,[a] 1-18-1 Kamiyoga, Setagaya-ku, Tokyo 158, Japan and Faculty of Pharmaceutical Sciences,[b] University of Tokyo, 7-3-1 Hongo, Bunkyo-ku, Tokyo 113, Japan*

(Received March 3, 1987)

The degradation of 1,3-di(*p,p'*-disubstituted)aryl-1-nitrosoureas (I) in aqueous buffer solutions (at 0 °C over pH −0.5 to 5.4) and in several organic solvents (benzene, chloroform, *etc.*) has been kinetically studied. In aqueous solution, the overall rates of degradation followed pseudo-first-order kinetics at constant pH. The decomposition reaction of 1,3-diphenyl-1-nitrosourea (Ia) was first-order in hydrogen ion over the pH range of −0.5 to 1.5 and denitrosated 1,3-diphenylurea (IIa) was formed predominantly. In the range of pH 1.5 to 5.4, the degradation of Ia was catalyzed by hydroxide ion and the main product was IIa, which was formed by the recombination of reactive products. In organic solvents, thermal degradation of Ia obeyed first-order kinetics and gave similar products to those yielded in the base-catalyzed degradation. The acid- and base-catalyzed and thermal degradations of Ia were about $10^2$ to $10^3$ times more rapid than those of related 1,3-dialkyl-1-nitrosoureas. The reaction mechanisms are discussed.

**Keywords**——1,3-diaryl-1-nitrosourea; kinetics; acid catalysis; base catalysis; pyrolysis; denitrosation; degradation

It is well known that *N*-nitrosoureas [RN(NO)CONHR'] generally act on deoxyribonucleic acid (DNA) of cells as alkylating reagents and that the alkyl derivatives [R = $CH_3$, $C_2H_5$, $C_3H_7$, $C_4H_9$] are carcinogenic, while on the other hand, some of the 2-chloroethyl derivatives [R = $ClCH_2CH_2$] are highly carcinostatic. The relationship between their chemical properties and biological activities (including carcinogenicity and antitumor activity), has been studied for more than ten years.[1] A few years ago, we reported that some 1,3-diaryl-1-nitrosoureas (I)

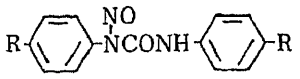

Ia—c

a : R=H, b : R=$CH_3$, c : R=Cl

IIa—c

a : R=H, b : R=$CH_3$, c : R=Cl

are highly effective against rat asites hepatoma AH-13 cells.[2] It was shown that they were fairly reactive as compared with the 1,3-dialkyl-1-nitrosoureas, and their chemical properties were also very different from those of the corresponding 1,3-dialkyl-1-nitrosoureas. Consequently, based on their chemical actions on DNA and protein model compounds, it was proposed that the manifestation of their antitumor activities is mainly due to the formation of active chemical species, a phenyldiazonium salt and a phenyl isocyanate, in tumor cells.[3] However, the mode of degradation of 1,3-diaryl-1-nitrosoureas in aqueous solution, that may be closer to cellular conditions, is still not clear.

This paper describes kinetic studies on the degradation of 1,3-diaryl-1-nitrosoureas in

aqueous solutions and in organic solvents, in comparison with that of related 1,3-dialkyl-1-nitrosoureas.

## Experimental

**Materials**——All 1,3-diaryl-1-nitrosoureas [1,3-diphenyl-1-nitrosourea (Ia), 1,3-bis(4-tolyl)-1-nitrosourea (Ib), 1,3-bis(4-chlorophenyl)-1-nitrosourea (Ic)] used in this study were prepared by the method reported in our previous paper.[4] Other organic chemicals used were purchased from Wako Pure Chemical Industries Co., Ltd. and Tokyo Kasei Industry Co., Ltd., "extra pure" grade. Organic solvents used were purchased from Wako Pure Chemical Industries Co., Ltd. and Ishizu Seiyaku Co., Ltd., "guaranteed" grade.

**Kinetics**——Rate constants for degradation were determined in the following manner. In aqueous solution: 1,3-diaryl-1-nitrosoureas and internal standard were dissolved in acetone at 0 °C. The buffer solutions were cooled at 0 °C and mixed with the acetone solution. A volume of 2 $\mu$l of the reaction mixture was taken at timed intervals and immediately subjected to analysis by means of high-performance liquid chromatography (HPLC). In organic solvent: 1,3-diaryl-1-nitrosoureas and an internal standard were dissolved in organic solvent at the indicated temperature. The degradation of 1,3-diaryl-1-nitrosoureas was monitored by using HPLC as described below.

**HPLC Analysis**——Chromatography was performed with a system consisting of a Shimadzu model LC-6A pump equipped with a reverse phase column (Whatman Partisil 5-ODS-3, 4.6 × 150 mm) and a Shimadzu model SPD-6AV UV-Vis spectrophotometric detector monitor. Peak areas of 1,3-diphenyl-1-nitrosourea were analyzed with a Shimadzu model C-R3A data processor. The mobile phase consisted of acetonitrile-water and the flow rate was 2 ml/min. The injection volume was 2 $\mu$l, and an appropriate compound was used as an internal standard.

## Results

### Acid-Catalyzed Degradation

1,3-Diphenyl-1-nitrosourea (Ia) was decomposed at 0 °C in mixtures of acid solution (pH < 1.5) and acetone (50%, v/v). The rates of disappearance of Ia were measured by means of HPLC. As shown in Fig. 1 and Table I, the rate data adhere to a first-order rate law over the entire reaction process. The rate of disappearance of Ia depended upon the acid strength over

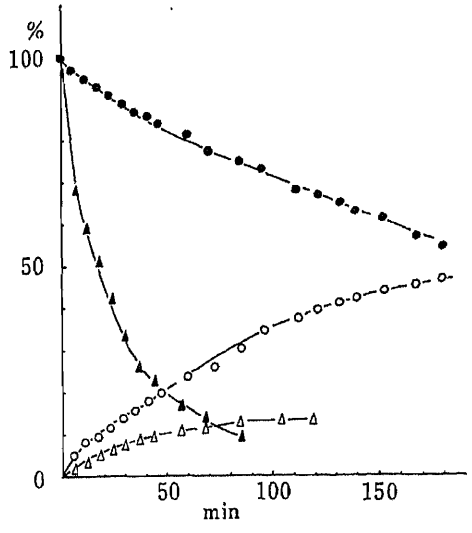


Fig. 1. Time Course of Disappearance of 1,3-Diphenyl-1-nitrosourea (Ia) and Formation of 1,3-Diphenylurea (IIa)

●, disappearance of 1,3-diphenyl-1-nitrosourea (Ia) at pH 0.3; ○, formation of 1,3-diphenylurea (IIa) at pH 0.3; ▲, disappearance of 1,3-diphenyl-1-nitrosourea (Ia) at pH 4.2; △, formation of 1,3-diphenylurea (IIa) at pH 4.2.

Table I. Degradation Rates[a] of 1,3-Diphenyl-1-nitrosourea in Various pH Buffer[b]

| pH | $k_{obs}$[c] ($s^{-1}$) | $\log k_{obs}$ | $r$[d] |
|---|---|---|---|
| 5.4 | $3.53 \times 10^{-3}$ | −2.45 | −0.972 |
| 4.2 | $6.13 \times 10^{-4}$ | −3.21 | −0.990 |
| 3.5 | $1.73 \times 10^{-4}$ | −3.76 | −0.997 |
| 2.5 | $3.73 \times 10^{-5}$ | −4.42 | −0.987 |
| 1.5 | $5.75 \times 10^{-6}$ | −5.24 | −0.984 |
| 1.1 | $1.04 \times 10^{-5}$ | −4.98 | −0.995 |
| 0.3 | $5.25 \times 10^{-5}$ | −4.27 | −0.999 |
| 0.0 | $8.97 \times 10^{-5}$ | −4.05 | −0.999 |
| −0.2 (1.5 N HCl) | $3.13 \times 10^{-4}$ | −3.50 | −0.992 |
| −0.5 (3 N HCl) | $8.70 \times 10^{-4}$ | −3.06 | −0.995 |

*a*) Determined by using HPLC. The mobile phase consisted of acetonitrile–water (5:5) and the flow rate was 2 ml/min. Naphthalene was used as an internal standard. 1,3-Diphenyl-1-nitrosourea (I) had an elution time of 3.0 min. *b*) Each run was carried out at 0 °C ± 0.2 °C. The reactions were initiated by mixing 1,3-diphenyl-1-nitrosourea (Ia) (1—2 mg) in acetone (2.5 ml) with Walpole's buffer (HCl–acetate buffer) (2.5 ml) or diluted HCl (2.5 ml). *c*) Rate constants were calculated by means of the least-squares method. *d*) Correlation coefficient between time and concentration of 1,3-diphenyl-1-nitrosourea (Ia).

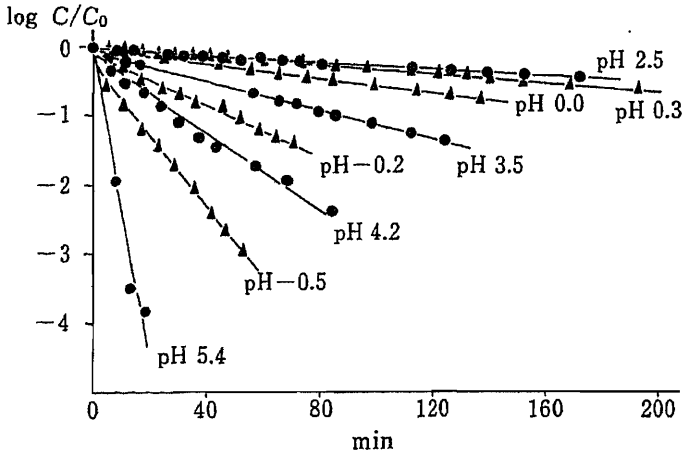


Fig. 2. First-Order Plots of Disappearance of 1,3-Diphenyl-1-nitrosourea (Ia) at Several pH Values

▲, acid-catalyzed reaction; △, base-catalyzed reaction.

TABLE II. Substitution Effects of Degradation[a] of 1,3-Diaryl-1-nitrosoureas (Ia—c)

| Compd. No. | R | $\sigma$ | pH 2.5 $k$ ($s^{-1}$)[b] ($r$)[c] | pH 2.5 $\log k$ | pH 2.5 $\log k/k_0$ | pH 0.3 $k$ ($s^{-1}$)[b] ($r$)[c] | pH 0.3 $\log k$ | pH 0.3 $\log k/k_0$ |
|---|---|---|---|---|---|---|---|---|
| Ia | H | 0.00 | $3.73\times10^{-5}$ | −4.43 | — | $5.25\times10^{-5}$ | −4.28 | — |
| | | 0.00 | (−0.987) | | | (−0.999) | | |
| Ib | $CH_3$ | −0.17 | $2.33\times10^{-5}$ | −4.63 | −0.200 | $8.12\times10^{-5}$ | −4.05 | 0.225 |
| | | −0.12 | (−0.987) | | | (−0.998) | | |
| Ic | Cl | 0.23 | $5.17\times10^{-4}$ | −3.29 | 1.14 | $1.28\times10^{-4}$ | −3.89 | 0.388 |
| | | 0.28 | (−0.997) | | | (−0.998) | | |

*a*) Each run was carried out at 0 °C ± 0.2 °C. The reactions were initiated by mixing 1,3-diaryl-1-nitrosourea (1—2 mg) in acetone (5 ml) with Walpole's buffer (HCl–acetate buffer, pH 0.3 or 2.5) (5 ml). *b*) Determined by using HPLC. The mobile phase consisted of acetonitrile–water (H, 5:5; $CH_3$, 55:45; Cl, 6:4). 1,3-Diphenyl-1-nitrosourea (Ia), 1,3-di(4-tolyl)-1-nitrosourea (Ib) and 1,3-bis(4-chlorophenyl)-1-nitrosourea (Ic) had elution times of 4.7, 3.0, and 4.8 min, respectively. Naphthalene or biphenyl was used as an internal standard. Rate constants were calculated by means of the least-squares method. *c*) Correlation coefficient between time and concentration of 1,3-diaryl-1-nitrosoureas.

pH 1.5. The base-catalyzed reaction of Ia is discussed later.

The only detectable product was 1,3-diphenylurea (IIa), a denitrosated urea. The time courses of degradation of Ia and formation of IIa at 0 °C in pH 0.3 buffer solution were measured by means of HPLC. As shown in Fig. 2, the amount of IIa increased proportionally as the reaction proceeded. When 14% of Ia had disappeared, 12% of IIa had been formed. At the half-life time of Ia (220 min), the yield of IIa was about 50%.

The isolated yield of IIa at pH 0.3 and 0 °C was 91% at 1 d after the reaction had started. The structure was confirmed by means of melting point determination and infrared (IR), proton nuclear magnetic resonance ($^1$H-NMR) and HPLC analyses.

The *p*-substitution effects on the rates were examined at pH 0.3 and the results are shown in Table II. The disappearance rates of Ia and Ib were $5.25\times10^{-5}$ and $12.8\times10^{-5}\,s^{-1}$, which are similar to each other. It can be concluded that substitution effects are small in the acid-

TABLE III. Comparison of the Stability of 1,3-Diaryl-1-nitrosourea (Ia) with Those of Related 1,3-Dialkyl-1-nitrosoureas in Acidic Solution[a] (1.5 N HCl)

| No. | Compounds | Temp.[b] (°C) | $k_{obs}$[c] ($s^{-1}$) | $r$[d] |
|---|---|---|---|---|
| Ia | 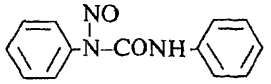 | 25 | $5.35 \times 10^{-3}$ [e] | −0.972 |
| | | 0 | $3.13 \times 10^{-4}$ [e] | −0.990 |
| III | 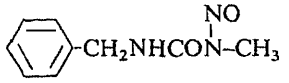 | 25 | $8.70 \times 10^{-5}$ [g] | −0.999 |
| IV | 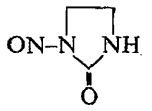 | 25 | $1.50 \times 10^{-4}$ [h] | −0.998 |
| V | 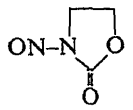 | 25 | $9.70 \times 10^{-4}$ [f] | −0.999 |

*a*) The reaction was initiated by mixing an *N*-nitroso compound (1—2 mg) in acetone (5 ml) with Walpole's buffer (HCl–acetate buffer) (5 ml). *b*) ±0.4 °C. *c*) Rate constants were calculated by means of the least-squares method. *d*) Correlation coefficient between time and concentration of *N*-nitroso compounds. *e*) Determined by using HPLC. *f*) Determined spectrophotometrically. Degradation was monitored with a Shimadzu UV-240 spectrophotometer at 419 nm. *g*) Determined by using HPLC. The monitoring wavelength was 392 nm, and *p*-nitrotoluene was used as an internal standard. The mobile phase consisted of acetonitrile–water (5:5). Compound III had an elution time of 3.6 min. *h*) Determined spectrophotometrically at (392 nm).

catalyzed degradation of 1,3-diaryl-1-nitrosoureas.

Degradation rates of 1,3-diaryl-1-nitrosoureas under the same conditions were compared with those of the related 1,3-dialkyl-1-nitrosoureido derivatives. As shown in Table III, at 25 °C in 1.5 N HCl, the observed rate constant of Ia was $5.35 \times 10^{-3}\,s^{-1}$. On the other hand, those of 1-nitroso-1-methyl-3-benzylurea (III) and a cyclic *N*-nitrosourea, 1-nitroso-2-imidazolidinone (IV), were $8.70 \times 10^{-5}$ and $15.0 \times 10^{-5}\,s^{-1}$. Thus, under acid-catalyzed conditions, Ia degrades $10^2$ fold more rapid than the related 1,3-dialkyl-1-nitrosoureido derivatives. 3-Nitroso-2-oxazolidinone (V), related to a cyclic *N*-nitrosourea IV, degraded with a rate constant of $9.70 \times 10^{-4}\,s^{-1}$.

**Base-Catalyzed Degradation**

The base-catalyzed reaction of 1,3-diphenyl-1-nitrosourea (Ia) could be studied by means of HPLC over a wide pH range. However, the reaction of Ia is quite rapid at pH 5.4 and, therefore, the pseudo-first degradation rates of 1,3-diaryl-1-nitrosoureas were measured in the range from pH 2 to 5. As shown in Fig. 1, the rate data for each of these reactions obeyed pseudo first-order kinetics over the entire reaction process. The product distribution for the reaction of Ia was studied in the buffer solution (pH 4.2) by using HPLC. The time courses of degradation of Ia and formation of IIa are shown in Fig. 2. When 32% of Ia had disappeared, less than 2% of IIa had been formed. Compound Ia had a half-life time of 19 min, and at this time the yield of IIa was only about 5%. Thus, the contribution of denitrosation is not important in the base-catalyzed pH region.

The degradation products of Ia were determined by using HPLC. Though the final set of products was complicated, the main product was IIa (42%) at one day after the reaction had started. The intermediates in the base catalysis seem to be mainly a diazonium ion and an isocyanate, and the urea should be produced by coupling of the isocyanate. To test this hypothesis, we tried to find recombined products of two 1,3-diaryl-1-nitrosoureas bearing

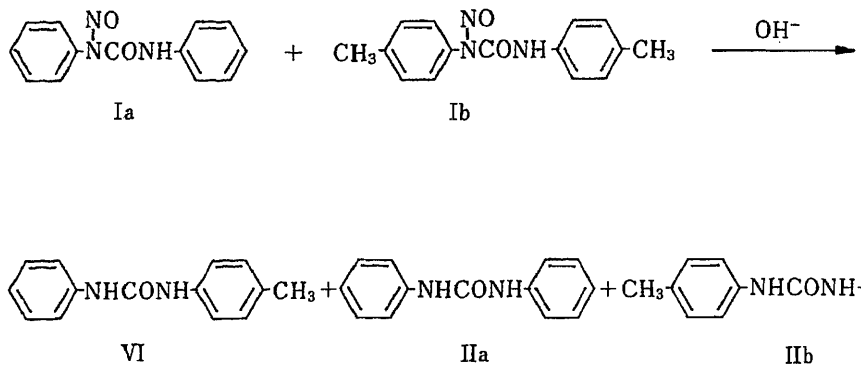


Chart 1. Formation of Different Ureas from Two Kinds of 1,3-Diaryl-1-nitrosoureas (Ia, b)

different substituents in a reaction mixture: when mixture of Ia and Ib (1 : 1) was decomposed in pH 4.2 buffer-acetone solution at 0 °C (Chart 1), the formation of a recombined urea (1-(4-tolyl)-3-phenylurea, VI) was indeed observed, accompanied with IIa and IIb. The ratio of 1,3-di(4-tolyl)urea (IIb), 1-(4-tolyl)-3-phenylurea (VI) and 1,3-diphenylurea (IIa) was about 1 : 1.8 : 1.

The substitution effects on the rates of base-catalyzed degradation were examined at pH 2.5 and the results are shown in Table II. The degradation rates were in order of the substituent effect. Plots of $\log k_{obs}$ against $\sigma$ and $\sigma^0$ gave positive slopes ($\rho = 3.45$, $r = 0.915$ and $\rho = 3.41$, $r = 0.97$, respectively) indicating that decreasing electron density at the nitrogen atom results in increasing degradation rate of 1,3-diaryl-1-nitrosoureas. This result is different from that at pH 0.3, and means that the reaction mechanism at pH 2.5 was different from that at pH 0.3.

The stability of 1,3-diphenyl-1-nitrosourea (Ia) was compared with those of the related 1,3-dialkyl-1-nitrosoureido derivatives at pH 5.4. At 0 °C, the rate of disappearance of Ia was $3.53 \times 10^{-3}\,s^{-1}$ and that of 3-benzyl-1-methyl-1-nitrosourea (III) at 50 °C was $8.70 \times 10^{-5}\,s^{-1}$. The degradation reaction of Ia is more than $10^3$ fold more rapid than those of 1,3-dialkyl-1-nitrosoureido derivatives.

**Thermal Degradation in Organic Solvents**

Thermal degradation of Ia in organic solvents was studied by means of HPLC. The products of thermal decomposition have already been reported and they were derivatives of the reactive intermediates, such as aryldiazonium salts and arylisocyanates.[3] The degradation of 1,3-diphenyl-1-nitrosourea (Ia) obeyed first-order kinetics in several organic solvents (Table IV). In benzene and chloroform at 20—40 °C, the rate constants of Ia were $3.08 \times 10^{-4}$—$3.10 \times 10^{-5}\,s^{-1}$. Compared with the degradation in aqueous solutions, the thermal degradation rates of Ia in nonpolar solvents were very slow.

In acetone and dimethylsulfoxide (DMSO), the degradation rates of Ia were $4.58 \times 10^{-6}\,s^{-1}$ (at 5 °C) and $1.26 \times 10^{-4}\,s^{-1}$ (at 10 °C), respectively. In aprotic polar solvents, the degradation rates of Ia were almost the same as those in nonpolar solvents.

In methanol, Ia was very unstable and its degradation rate was $2.00 \times 10^{-3}\,s^{-1}$ at 0 °C. It gave IIa and methyl *N*-phenylcarbamate [$C_6H_5NHCOOCH_3$]. Those results suggest that methanol may play a role as a scavenger of nitrosonium ion and phenyl isocyanate.[3]

In chloroform, the rates of disappearance of Ib and Ic bearing methyl and chloro groups on the phenyl ring at the *para* position, were $1.95 \times 10^{-4}\,s^{-1}$ (at 40 °C) and $9.85 \times 10^{-5}\,s^{-1}$ (at 30 °C), respectively (Table IV). Considering the difference of the temperature examined, these data suggest that there is little substituent effect on the degradation rates of 1,3-diaryl-1-

TABLE IV. Degradation[a] Rates of 1,3-Diaryl-1-nitrosoureas in Organic Solvents

| Compd. No. | Substituent | Temp.[b] (°C) | Solvent[c] | $k_{obs}$ ($s^{-1}$) | $r$[d] |
|---|---|---|---|---|---|
| Ia | H | 40 | Benzene | $3.08\times10^{-4}$ | −0.997 |
| | | 20 | Benzene | $3.10\times10^{-5}$ | −0.984 |
| | | 30 | Chloroform[e] | $1.32\times10^{-4}$ | −0.989 |
| | | 5 | Acetone | $4.58\times10^{-6}$ | −0.949 |
| | | 10 | DMSO | $1.26\times10^{-4}$ | −0.968 |
| | | 0 | Methanol | $2.00\times10^{-3}$ | −0.997 |
| Ib | $CH_3$ | 40 | Chloroform[e] | $1.95\times10^{-4}$ | −0.983 |
| Ic | Cl | 30 | Chloroform[e] | $9.85\times10^{-4}$ | −0.988 |

*a*) The reactions were initiated by dissolving a 1,3-diaryl-1-ureido derivative (1—2 mg) in an organic solvent (5 ml) at the indicated temperature. In the case of degradation in DMSO, Ia was dissolved in acetone (5 ml, at 10 °C). The reaction was initiated by mixing the solution and DMSO (10 ml). Determined by using HPLC. In the case of degradation in benzene, the monitoring wavelength was 392 nm and *p*-nitrotoluene was used as an internal standard. The mobile phase consisted of acetonitrile–water (Ia, 5 : 5; Ib, 55 : 45; Ic, 6 : 4). Ia, Ib and Ic had elution times of 3.0, 4.7, and 4.8 min, respectively. Naphthalene or biphenyl was used as an internal standard. Rate constants were calculated by means of the least-squares method. *b*) ±0.2 °C. *c*) All solvents used were of reagent grade. *d*) Correlation coefficient between time and concentration of 1,3-diaryl-1-nitrosoureas. *e*) The chloroform used contained about 0.5% methanol as a stabilizer.

TABLE V. Comparison of the Stability of 1,3-Diaryl-1-nitrosourea with Related *N*-Nitroso Compounds in Chloroform[a]

| No. | Compounds | Temp.[b] (°C) | $k_{obs}$[c] ($s^{-1}$) | $r$[d] |
|---|---|---|---|---|
| Ia | 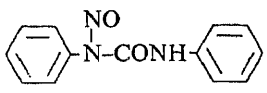 | 30 | $1.32\times10^{-4}$ [e] | −0.989 |
| III | 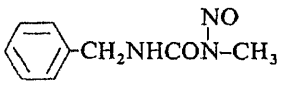 | 25 | —[g] | |
| IV | 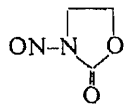 | 25 | $8.77\times10^{-5}$ [f] | −0.999 |

*a*) The reactions were initiated by dissolving an *N*-nitroso compound (1—2 mg) in an organic solvent (5 ml) at the indicated temperature. *b*) ±0.4 °C. *c*) Rate constants were calculated by means of the least-squares method. *d*) Correlation coefficient between time and concentration of *N*-nitroso compounds. *e*) Determined by using HPLC. *f*) Determined spectrophotometrically. Degradation was monitored with a Shimadzu model UV-240 spectrophotometer (cell length = 10 mm) at 419 nm. *g*) Determined by using HPLC. The monitoring wavelength was 392 nm and *p*-nitrotoluene was used as an internal standard. The mobile phase consisted of acetonitrile–water (5 : 5). 1-Nitroso-1-methyl-3-benzylurea had an elution time of 3.6 min. The degradation rate was too slow to measure.

nitrosoureas.

Degradation rates of III and IV were measured in chloroform for comparison with those of 1,3-diaryl-1-nitrosoureas (Table V). The observed degradation rate of Ia was $1.32\times10^{-4}\,s^{-1}$ at 30 °C. The degradation rate of III under the same conditions was too slow to be determined ($<10^{-8}\,s^{-1}$). The observed degradation rate of IV was $3.68\times10^{-5}\,s^{-1}$.

Thus, 1,3-diaryl-1-nitrosoureas are very unstable compounds in organic solvents as compared with these related 1,3-dialkyl-1-nitrosoureido compounds.

## Discussion

1,3-Diphenyl-1-nitrosourea (Ia) was decomposed at 0 °C in the mixtures of acid solution

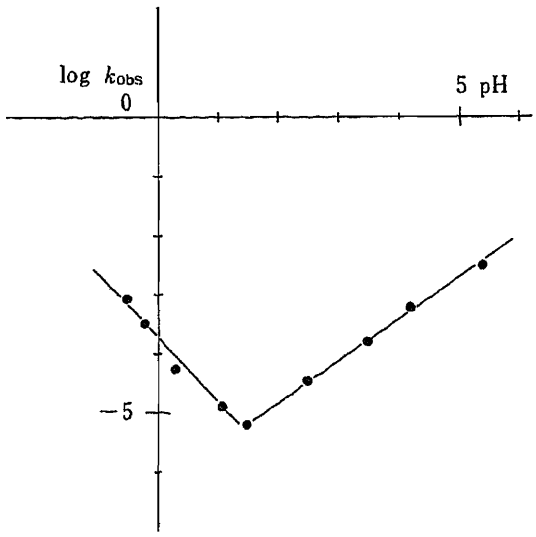


Fig. 3. The Relationship between the Logarithms of the Observed First-Order Rate Constants for 1,3-Diphenyl-1-nitrosourea (Ia) and the pH Values

and acetone (50%, v/v). In any pH, the degradation followed first-order kinetics. The relationship between the logarithms of the observed first-order rate constants ($k_{obs}$) and the pH values is shown in Fig. 3. The data indicate that the rate of disappearance of Ia is greatly dependent on the pH value of the reaction medium. From the plots, the minimum rate constant among the observed first-order rate constants is $5.25 \times 10^{-6}\,s^{-1}$ at pH 1.5. In the region of pH 1.5—5.4, the pH profile for the degradation of Ia was linear with a slope of about 0.703, which means that the contribution of specific base catalysis is predominant in this region. On the other hand, in the region of pH $< -1.5$, the profile was linear with a slope about $-1.05$, which means that the contribution of specific acid catalysis is predominant. The following rate expression is derived, where $[H^+]$ and $[OH^-]$ are hydrogen ion and hydroxide ion concentrations, respectively, $k_0$ is the zero-order rate constant of pyrolysis of Ia, and, $k_1$ and $k_2$ are the first-order rate constants for specific acid and base catalysis, respectively. From Fig. 3, the following parameters are calculated: $n' = -1.05$, $n'' = 0.703$, $k_1 = 1.6 \times 10^{-4}\,s^{-1}$, and $k_2 = 3.91 \times 10^{-7}\,s^{-1}$. In the region of pH 1.5—5.4, the reaction medium was a mixture of acetone and water, causing the reaction order to be fractional.

$$k_{obs} = k_0 + k_1[H^+]^{n'} + k_2[OH^-]^{n''}$$

Compared with related 1,3-dialkyl-1-nitrosoureido derivatives (Table III), the pH profiles of 1,3-diaryl-1-nitrosoureas are very different. Degradation of 1,3-diaryl-1-nitrosoureas was about $10^2$ fold more rapid under acid catalysis and about $10^3$ fold more rapid under base catalysis,[6] as compared with 1,3-dialkyl-1-nitrosoureido derivatives. The most stable pH regions of 1,3-dialkyl-1-nitrosoureas are quite different from those of 1,3-diaryl-1-nitrosoureas. The disappearance of 1-methyl-1-nitrosourea (MNU) is independent of the acid strength from pH 2 to 4 and inversely proportional to the acid strength at higher pH values. In contrast, the rate of disappearance of 1,1,3-trimethyl-3-nitrosourea (TMNU) is proportional to the acid strength at lower than pH 7, and inversely proportional to the acid strength at higher than pH 7. The minimum observed rate constants of MNU and TMNU were $7.08 \times 10^{-7}\,s^{-1}$ at pH 2—4 and $4.03 \times 10^{-8}\,s^{-1}$ at pH 7, respectively.[6]

On the other hand, the rate of disappearance of Ia is entirely dependent on pH, and the minimum observed rate constant of Ia was $5.25 \times 10^{-6}\,s^{-1}$ at pH 1.5. This means that, even at such a low pH, base-catalyzed degradation can occur. These properties of Ia should be due to the specific conformation of 1,3-diaryl-1-nitrosoureas and the remarkable electron deficiency at the nitrogen atoms of the ureido group. The rate constants of 1-alkyl-3-aryl-1-nitrosoureas

and 1-alkyl-3-aryl-3-nitrosoureas were in the range of $1.01—2.63\times10^{-4}\,s^{-1}$ at 25 °C at pH 6.95[7] and $0.33—2.6\times10^{-5}\,s^{-1}$ at 33 °C in chloroform.[8] These reports show that the stability of *N*-nitrosoalkylarylureas is almost the same as that of 1,3-dialkyl-1-nitrosoureas, and suggest that the benzene ring attached to the ureido nitrogen atom does not affect the stability. On the other hand, in 1,3-diaryl-1-nitrosoureas in which both nitrogen atoms of the ureido group are substituted by benzene rings, they may restrict free rotation around the amide bond of the ureido group and force the *N*-nitrosoureas to adopt a rotamer form which is very easily attacked by hydroxide ion. This rotamer also readily undergoes thermal degradation. The electron-withdrawing effect of the benzene ring may also make 1,3-diaryl-1-nitrosoureas unstable. In the entire pH region in which acid-catalyzed degradation of TMNU occurs, 1,3-diaryl-1-nitrosoureas were decomposed by base catalysis. This means that the reaction site in 1,3-diaryl-1-nitrosoureas should have much greater positive charge than that of TMNU. These two effects make 1,3-diaryl-1-nitrosoureas more unstable than related 1,3-dialkyl-1-nitrosoureas in the base-catalyzed pH region and in organic solvents.

The pH profile and final products of acid-catalyzed degradation of 1,3-diaryl-1-nitrosoureas are not similar to those of 1,3-alkyl-1-nitrosoureas. In the acid-catalyzed pH region, Ia gave the denitrosated urea quantitatively. This is presumably because the diarylureas formed are insensitive to acids and nitrous acid, and, therefore, the hydrolysis of IIa was negligible. This fact helps us to analyze the reaction clearly. On the other hand, the final degradation product of MNU was methanol, and those of TMNU were methanol and *N*,*N*′-dimethylamine.[5,6] This means that the denitrosated ureas formed from the degradation of these 1,3-dialkyl-1-nitrosoureas are unstable. It appears that the degradation products of 1,3-diaryl-1-nitrosoureas are essentially the same as the initial degradation products of 1,3-dialkyl-1-nitrosoureas, and the reaction mechanism for degradation of 1,3-diaryl-1-nitrosoureas may be the same as that of 1,3-dialkyl-1-nitrosoureas in this pH region.

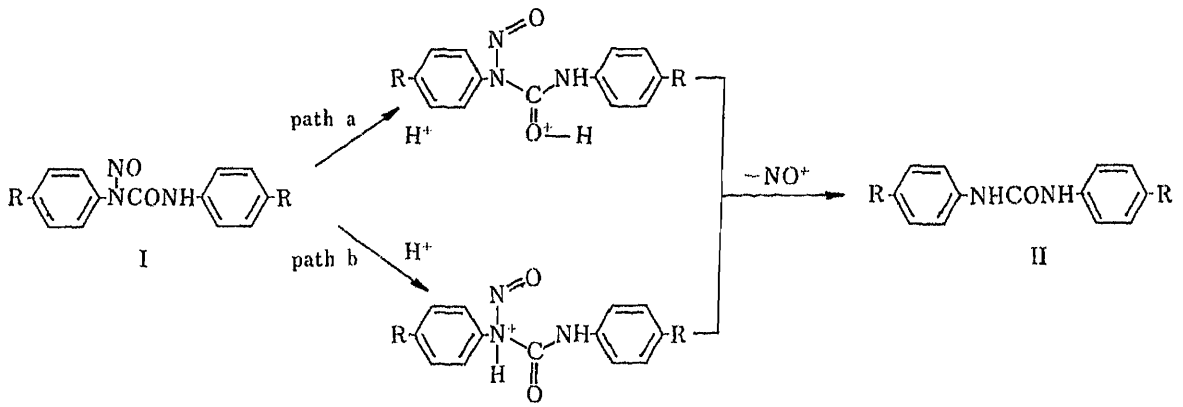


Chart 2. A Possible Mechanism of Acid-Catalyzed Degradation

Two possible reaction mechanisms could be proposed for the acid-catalyzed denitrosation of I, as shown in Chart 2. One involves proton attack on the nitrogen atom on which the nitroso group is attached, followed by degradation of this intermediate to give the denitrosated urea II (path b). Path b seems to apply to denitrosation of *N*-nitrosoamines.[5] The other involves initial protonation on the carbonyl oxygen atom, to produce an enolic type urea and nitrosonium ion (path a). These two types of mechanism can account for the denitrosation of 1,3-diaryl-1-nitrosoureas. The mechanism of acid-catalyzed denitrosation of 1,3-diaryl-1-nitrosoureas can not be settled at the present time, but may involve an ionic key step. If the reaction site is near a benzene ring (path b), substituents should affect the rate of degradation. Since substituent effects on the degradation rate are relatively small, path a is

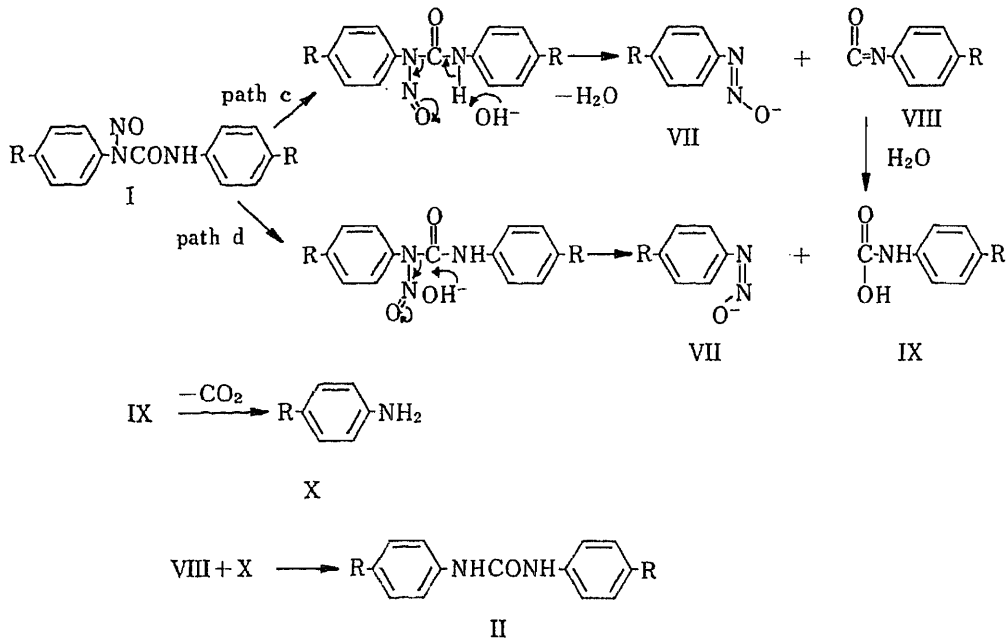


Chart 3. A Possible Mechanism of Base-Catalyzed Degradation

more likely. These results do not correspond with the results obtained in the study of three types of 1,3-dialkyl-1-nitrosoureas reported by Snyder *et al.*[6]

Two mechanisms for base-catalyzed degradation could also be proposed, as shown in Chart 3. One involves initial abstraction of the ureido hydrogen atom by hydroxide ion to produce a phenyldiazohydroxide (VII) and an isocyanate (VIII) (path c). The other involves attack of a hydroxide ion on the carbonyl carbon of I to give a tetrahedral intermediate which produces phenyldiazohydroxide (VII) and *N*-phenylcarbamic acid (IX) (path d). The following evidence suggests that path c is more likely. 1. As mentioned above, considerable amounts of 1,3-diarylureas (II) were formed from 1,3-diaryl-1-nitrosoureas. These products can be easily derived from aryl isocyanates (VIII) in aqueous solution. Path c accounts for this product (II), but path d can not. 2. These reaction rates are affected by substitution on the benzene ring, which means that the reaction site is relatively near the phenyl ring and/or a considerable negative charge is placed on the benzene ring in the transition state. 3. As shown

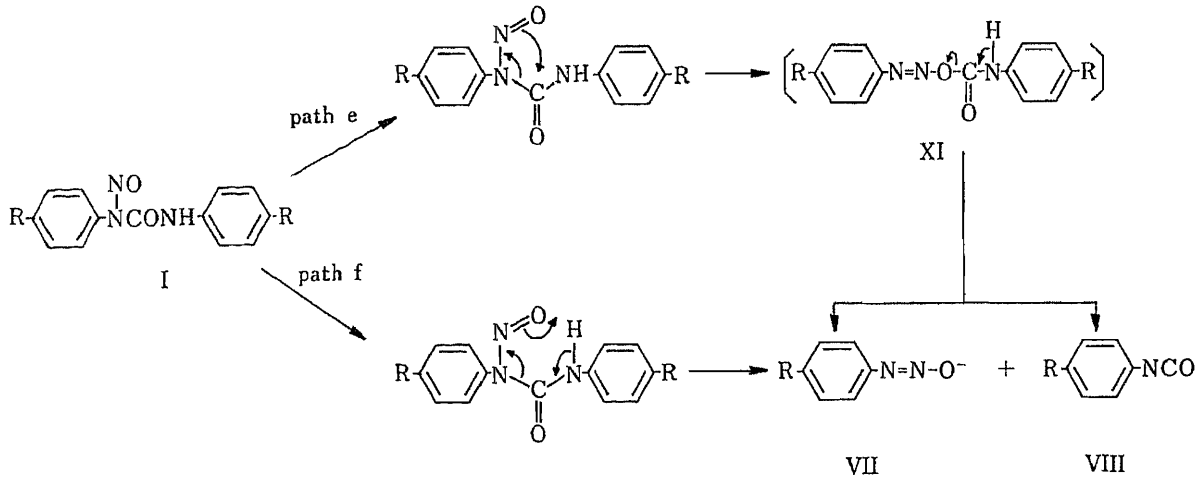


Chart 4. A Possible Mechanism of Thermal Decomposition in Organic Solvents

in Fig. 1, there is a time lag between the decrease of Ia and increase of the combination urea (IIa). This mechanism accounts for the slow formation of the urea. This conclusion is contrary to results obtained in a study on 1,3-dialkyl-1-nitrosoureas[6] but consistent with results obtained in the studies of 1-methyl-1-nitroso-3-arylureas.[7,9]

On the basis of thermal degradation product analysis,[3] two possible mechanisms were presented (Chart 4). One involves intramolecular rearrangement through a 4-membered ring to afford a phenyldiazo carbamate (XI), which decomposes to give a phenyldiazonium ion (VII) and a phenyl isocyanate (VIII) (path e). The other involves internal prototropy through a 6-membered ring followed by intramolecular rearrangement to give a phenyl isocyanate (VIII) and a diazonium ion (VII) (path f). Since the kinetic results show no substitution effects, the reaction site may be located far from the phenyl ring and/or a phenyldiazohydroxide ion is not involved in the rate-determining step.[10] The base-catalyzed degradation of I involves intermediates similar to those in the pyrolysis in organic solvents, but the rate of this reaction depends strongly on the substituents on the benzene rings. If the reaction proceeded *via* path f, substituents should influence the rate constants, because the acidity of the NH proton is controlled by substituents on the phenyl rings.[11]

## Conclusion

In aqueous solutions, in the pH range of $-0.5$ to 1.5, the degradation of Ia was first-order in hydrogen ion and yielded denitrosated IIa as the main product. Our kinetic data show that a slow protonation at the carbonyl oxygen atom is the key step in the reaction. In the range of pH 1.5—5.4, the degradation of Ia was catalyzed by hydroxide ion, but the products were II, formed by recombination of the reactive intermediate. The analysis of reaction products and our kinetic data support the conclusion that the reaction occurs *via* initial proton abstraction.

In organic solvents, I was more stable than in aqueous solutions, and the first-order rate constant for Ia was greater than those of 1,3-dialkyl-1-nitrosoureas. Thermal degradation of I could proceed *via* a 4-membered ring intermediate to give phenyldiazo *N*-phenylcarbamate (XI) as a reactive intermediate.

Compared with related 1,3-dialkyl-1-nitrosoureas, degradation of I is several hundred fold more rapid under all the conditions we examined. This can be interpreted in terms of a special conformation of I and the electron-withdrawing effect of the benzene rings.

This work has shown that 1,3-diaryl-1-nitrosoureas (I) undergo base-catalyzed degradation, even at low pH, much more readily than 1,3-dialkylureido derivatives and generate active chemical species. Accordingly, similar degradation reactions may proceed in AH-13 tumor cells and antitumor-active chemical species may be formed effectively. This might result in high activity for killing the tumor cells.

### References and Notes


1) S. Kamiya, *Eisei Shikenjo Hokoku*, **104**, 1 (1986).
2) Mi. Miyahara, M. Miyahara and S. Kamiya, *Chem. Pharm. Bull.*, **32**, 564 (1984).
3) *a*) M. Miyahara and S. Kamiya, *Chem. Pharm. Bull.*, **30**, 3466 (1982); *b*) S. Kamiya, Mi. Miyahara and M. Miyahara, Abstracts of Papers, 13th Symposium on Progress in Organic Reactions and Synthesis, Tokushima, Nov. 1986, p. 87.
4) M. Miyahara, S. Kamiya and M. Nakadate, *Chem. Pharm. Bull.*, **31**, 41 (1983).
5) *a*) E. Aldred and D. L. H. Williams, *J. Chem. Soc., Perkin Trans. 2*, **1982**, 777; *b*) S. S. Singer and B. B. Cole, *J. Org. Chem.*, **46**, 3461 (1981); *c*) I. D. Biggs and D. L. H. Williams, *J. Chem. Soc., Perkin Trans. 2*, **1975**, 107.
6) J. K. Snyder and L. M. Stock, *J. Org. Chem.*, **45**, 1990 (1980).
7) K. Yoshida and K. Yano, *Bull. Chem. Soc. Jpn.*, **55**, 2200 (1982).
8) M. Tanno, private communication.

9) S. M. Hecht and J. W. Kozarich, *J. Org. Chem.*, **38**, 1821 (1973).
10) R. Fuchs and E. S. Lewis, "Investigation of Rates and Mechanisms of Reaction," 3rd ed., Part 1, ed. by E. S. Lewis, "Techniques of Chemistry," series, Vol. 6, ed. by A. Weissberger, John Wiley, New York,1974, Chapter 14.
11) M. Miyahara, *Chem. Pharm. Bull.*, **34**, 1950 (1986).

[Chem. Pharm. Bull. 35(11)4429—4435(1987)]

# Flavonoids from *Andrographis paniculata*

MASANORI KUROYANAGI,*[,a] MAKOTO SATO,[a] AKIRA UENO[a] and KOUZABURO NISHI[b]

*Shizuoka College of Pharmacy,[a] 2-2-1, Oshika, Shizuoka 422, Japan and Izu Medicinal Plant Research Station, National Institute of Hygienic Sciences,[b] 155, Shimokamo Minamiizu-machi, Kamo-gun, Shizuoka 415-03, Japan*

(Received March 20, 1987)

A new flavanone glucoside, named andrographidine A (**1**), and five new flavone glucosides, named andrographidines B (**2**), C (**3**), D (**4**), E (**5**) and F (**6**), were isolated from the root of *Andrographis paniculata*. Their structures were determined on the basis of spectral data, especially carbon-13 and proton nuclear magnetic resonance spectra, and chemical derivatization. They have uncommon O-substitution patterns involving 5-, 7-, 8-, 2'-, 3'- and 4'-O-substituents.

**Keywords**——*Andrographis paniculata*; Acanthaceae; flavone glucoside; flavanone glucoside; andrographidine A; andrographidine B; $^{13}$C-NMR; methylglucopyranoside per-*p*-bromobenzoate; *A*-value

*Andrographis paniculata* (Japanese name "senshinren," Acanthaceae) is widely used as a folk medicine in China and South-East Asia. The aerial part of the title plant has a very bitter taste. From the plant several kinds of labdan-type diterpenoids, andrographolide,[1] 14-deoxyandrographolide[2] and neoandrographolide,[3] and their glucosides[4] have been isolated as bitter principles, as well as several kinds of flavone derivatives.[5,6] We also isolated these diterpenoids from the aerial part of the plant as cell differentiation inducers.[7]

From the root of the plant, six new flavone glucosides, named andrographidines A (**1**), B (**2**), C (**3**), D (**4**), E (**5**) and F (**6**), were isolated along with 5-hydroxy-7,8,2',3'-tetramethoxyflavone (**7**)[5] and 7,8-dimethoxy-5-hydroxyflavone (**8**).[6] This paper deals with the isolation and the structural elucidation of the flavone glucosides.

The ethyl acetate (AcOEt)-soluble fraction of the root of the title plant was separated by repeated column chromatography and high-performance liquid chromatography (HPLC) as described in the experimental section to give a new flavanone glucoside (**1**) and five new flavone glucosides, **2**—**6**, along with **7** and **8**.

The structures of compound **7**, mp 150—152 °C, $C_{19}H_{18}O_7$, and **8**, mp 183—184 °C, $C_{17}H_{14}O_5$, were determined as 5-hydroxy-7,8,2',3'-tetramethoxyflavone and 7,8-dimethoxy-5-hydroxyflavone, respectively, from their proton and carbon-13 nuclear magnetic resonance ($^1$H- and $^{13}$C-NMR) spectra, which were identical with the reported data.

Andrographidine A (**1**), mp 168—169 °C, gave the molecular formula $C_{23}H_{26}O_{10}$ from mass spectrum (MS) and elemental analysis, and this was supported by the $^{13}$C-NMR spectrum. The $^1$H- and $^{13}$C-NMR spectra of **1** showed the presence of a phenyl group ($\delta$ 6.9—7.5 (5H, m) and 126.6 (d), 129.1 (d) 128.8 (d) and 139.5 (s)), two methoxyl groups ($\delta$ 3.60 (3H, s), 3.68 (3H, s), and 56.2, 60.8), a flavanone skeleton ($\delta$ 5.29 (1H, dd, $J$=5.4, 10.3 Hz), 2.69 (1H, dd, $J$=5.4, 17.8 Hz), 2.87 (1H, dd, $J$=10.3, 17.8 Hz), and 77.8 (d), 45.8 (t)) and a glucopyranosyl moiety (as shown in Table I). The presence of the flavanone skeletone was supported by the ultraviolet (UV) spectrum (237 nm log $\varepsilon$ (4.16), 285 (4.23), 320 (3.79)).[8] The characteristic chemical shift (60.8) of a methoxyl group showed that one of the two methoxyl

groups had substituents at both neighboring carbons. The $^1$H-NMR spectrum of **1** indicated that andrographidine A had no chelated hydroxyl group. Methanolysis of **1** gave an aglycone (**1a**), mp 98—100 °C, $C_{17}H_{16}O_5$, along with α-methylglucopyranoside, which was shown to be identical with an authentic sample (as the per-*p*-bromobenzoate) by HPLC. This was further confirmed by determination of the *A*-value, which was obtained from the circular dichroism (CD) spectrum.[9] The $^1$H-NMR spectrum of **1a** showed the typical double-doublet signal at C-2 ($\delta$ 5.47 (1H, dd, $J$=4.6, 10.9 Hz)) and two double-doublet signals at C-3 ($\delta$ 3.13 (1H, dd, $J$= 10.9, 17.5 Hz), 2.85 (1H, dd, $J$= 17.5, 4.6 Hz) of the flavanone ring and a chelated hydroxyl group ($\delta$ 11.96 (s)). In the $^{13}$C-NMR spectra of **1a** and its acetate (**1b**), the C-6 carbon signal was shifted to lower field by acetylation ($\delta$ 93.2→101.2). These results indicated that **1** is 7,8-dimethoxy-5-D-glucopyranosyloxyflavanone, and $^1$H- and $^{13}$C-NMR spectra of an acetate (**1c**) of **1** also supported the structure. The CD spectrum of **1a** showed a positive maximum at 310 nm ([$\theta$]+7500) and a negative maximum at 254 nm ([$\theta$]−32400), characteristic of flavanones.[10] From the CD spectral data, C-2 configuration of **1a** was concluded to be *S*. Thus, the structure of andrographidine A was concluded to be (2*S*)-7,8-dimethoxy-5β-D-glucopyranosyloxyflavanone.

Andrographidine B (**2**), mp 230 °C, gave the molecular formula $C_{23}H_{24}O_{12}$ from elemental analysis and MS, and this was supported by the $^{13}$C-NMR spectrum. The $^1$H- and $^{13}$C-NMR spectra of **2** showed the presence of two methoxyl groups ($\delta$ 3.58 (3H, s), 3.73 (3H, s), and $\delta$ 56.4, 61.7), a chelated hydroxyl group ($\delta$ 13.5) and a glucopyranosyl moiety (Table I). The characteristic signals of C-3 of the flavone appeared at $\delta$ 6.69 (1H, s) and $\delta$ 106.7. The signals at $\delta$ 6.39 ($^1$H-NMR) and $\delta$ 96.3 ($^{13}$C-NMR) suggested that the substitution pattern of the A ring was 5,7,8-tri-O- or 5,6,7-tri-O-. Andrographidine B was methanolyzed to give an aglycone (**2a**) and α-methyl-D-glucopyranoside. α-Methyl-D-glucopyranoside was identified by HPLC and CD comparisons with an authentic sample (as the per-*p*-bromobenzoate). Andrographidine B was acetylated to give a pentaacetate (**2b**). The $^1$H-NMR spectra of **2a** and **2b** showed the presence of a 2′,3′-di-O-substituted B ring (as described in the experimental section). The $^1$H- and $^{13}$C-NMR signal patterns of the A and C rings of **2a** showed almost the same chemical shifts as those of **7** (Table I and the experimental section). On acetylation of **2**, the carbon signals at $\delta$ 96.3 (C-6) and 112.1 (C-1′) shifted to lower fields ($\delta$ 104.9 and 125.8, respectively), and in the $^1$H-NMR spectrum of **2b**, the H-5′ signal appeared as a triplet at lower field ($\delta$ 7.47, t, $J$=8.3 Hz) in comparison with H-4′ ($\delta$ 6.96, dd,

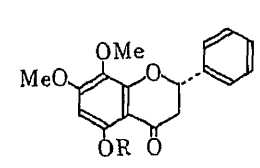

1 : R=glc
1a : R=H
1b : R=Ac
1c : R=glc-Ac

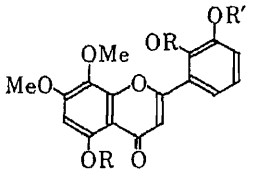

2 : R=H, R′=glc
2a : R=R′=H
2b : R=Ac, R′=glc-Ac

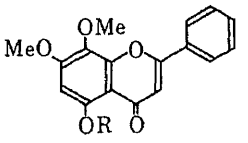

3 : R=glc
8 : R=H

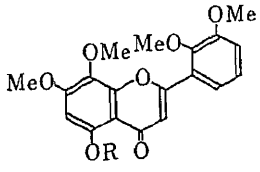

4 : R=glc
4a : R=glc-Ac
7 : R=H

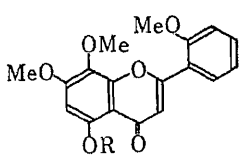

5 : R=glc
5a : R=H
5b : R=glc-Ac

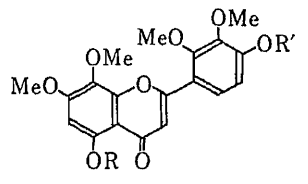

6 : R=glc, R′=H
6a : R=R′=H
6b : R=glc-Ac, R′=Ac

Chart 1

$J$=1.1, 8.3 Hz) and H-6′ ($\delta$ 7.28 dd, $J$=1.1, 8.3 Hz). These results indicate that hydroxy groups are located at C-5 and C-2′, so **2** is 5,2′-dihydroxy-7,8-dimethoxy-3′$\beta$-D-glucopyranosyloxyflavone.

Andrographidine C (**3**), mp 196—201 °C, gave the molecular formula $C_{23}H_{24}O_{10}$ from elemental analysis, and this was supported by the $^{13}$C-NMR spectrum. The $^{1}$H- and $^{13}$C-NMR spectra of **3** showed the presence of a phenyl group ($\delta$ 7.84 (2H, dd, $J$=6.8, 3.0 Hz), 7.1—7.3 (3H, m, H-3′, 4′, 5′), and 126.5×2, 129.3×2, 131.7), two methoxyl groups and a glucopyranosyl moiety. Of the two methoxyl groups, one methoxyl group showed the characteristic chemical shift ($\delta$ 61.3) for a methoxyl group substituted at both neighboring carbons. The $^{1}$H-NMR spectrum of **3** showed the presence of two singlet aromatic proton signals ($\delta$ 6.77, 7.37) assignable to H-3 and H-6. Acid hydrolysis of **3** gave the aglycone, which was identical with an authentic sample of **8**. These data suggested that **3** is 7,8-dimethoxy-5$\beta$-D-glucopyranosyloxyflavone.

Andrographidine D (**4**), mp 181—184 °C, gave the molecular formula $C_{25}H_{28}O_{12}$ from elemental analysis, and this was supported by the $^{13}$C-NMR spectrum. The $^{1}$H- and $^{13}$C-NMR spectra of **4** showed the presence of four methoxyl groups and a glucopyranosyl moiety. Of the four methoxyl groups, two were substituted at both neighboring carbons ($\delta$ 60.8, 61.3). Two singlet aromatic protons appeared at 6.86 and 7.38 ppm as in the case of **3**. The remaining three protons were considered to be on the B ring and were assignable as being at C-4′, C-5′ and C-6′, ($\delta$ 7.05 (1H, dd, $J$=2.2, 7.5 Hz), 7.19 (1H, t, $J$=7.4 Hz) and 7.49 (1H, dd, $J$=2.2, 7.4 Hz), respectively). This substitution pattern was supported by the $^{13}$C-NMR spectrum (Table I). These results suggested that the structure of andrographidine D is represented by **4**. Acetylation gave a pentaacetate (**4a**). The $^{1}$H-NMR spectrum of **4a** showed

Table I. $^{13}$C-NMR Data for the Flavonoids **1**—**8**

| | 1[a] | 2[a] | 3[a] | 4[a] | 5[a] | 6[a] | 7[b] | 8[b] |
|---|---|---|---|---|---|---|---|---|
| C-2 | 77.8 | 163.0 | 161.6 | 160.6 | 159.7 | 160.6 | 162.3 | 163.9 |
| 3 | 45.8 | 106.7 | 108.6 | 113.1 | 113.5 | 111.4 | 110.1 | 105.4 |
| 4 | 190.6 | 183.3 | 178.3 | 178.5 | 178.7 | 178.8 | 183.0 | 182.7 |
| 5 | 159.6 | 158.9 | 154.7 | 154.6 | 154.7 | 154.6 | 158.6 | 158.7 |
| 6 | 97.3 | 96.3 | 102.0 | 102.2 | 102.2 | 102.3 | 95.7 | 95.9 |
| 7 | 156.4 | 158.3 | 157.2 | 157.2 | 157.2 | 157.1 | 157.6 | 157.6 |
| 8 | 133.0 | 129.6 | 133.5 | 133.6 | 133.6 | 133.8 | 129.1 | 129.1 |
| 9 | 156.7 | 158.3 | 157.2 | 157.2 | 157.2 | 157.1 | 157.6 | 157.6 |
| 10 | 108.0 | 105.7 | 110.6 | 110.7 | 110.6 | 110.9 | 105.0 | 105.0 |
| 1′ | 139.5 | 112.1 | 133.5 | 108.5 | 120.7 | 116.9 | 110.4 | 131.4 |
| 2′ | 126.6 | 158.0 | 126.5 | 154.6 | 158.5 | 154.0 | 153.4 | 126.4 |
| 3′ | 129.1 | 157.7 | 129.3 | 153.8 | 112.6 | 142.5 | 149.8 | 129.1 |
| 4′ | 128.8 | 110.7 | 131.7 | 116.1 | 133.0 | 154.6 | 115.6 | 131.9 |
| 5′ | 129.1 | 132.7 | 129.3 | 121.0 | 129.4 | 113.5 | 124.2 | 129.1 |
| 6′ | 126.6 | 113.5 | 126.5 | 121.0 | 121.3 | 124.7 | 120.8 | 126.4 |
| G-1 | 105.7 | 102.3 | 106.6 | 106.6 | 106.6 | 106.7 | | |
| 2 | 75.0 | 74.7 | 75.2 | 75.2 | 75.3 | 75.3 | | |
| 3 | 79.5 | 78.9 | 79.5 | 79.5 | 79.5 | 79.4 | | |
| 4 | 71.7 | 71.4 | 71.6 | 71.7 | 71.8 | 71.8 | | |
| 5 | 79.5 | 78.7 | 77.9 | 77.9 | 78.0 | 78.0 | | |
| 6 | 62.8 | 62.5 | 62.7 | 62.8 | 62.8 | 62.9 | | |
| OMe | 56.2 | 56.4 | 56.3 | 56.1 | 55.8 | 56.5 | 56.3 | 56.3 |
| | 60.8 | 61.7 | 61.3 | 56.5 | 56.5 | 60.6 | 56.1 | 61.7 |
| | | | | 60.8 | 61.4 | 61.0 | 61.0 | |
| | | | | 61.3 | | 61.4 | 61.5 | |

*a*) Measured in pyridine-$d_5$. *b*) Measured in $CDCl_3$.

an ABC type signal pattern due to the B ring ($\delta$ 7.05 (1H, dd, $J$=2.2, 7.4 Hz, H-4'), 7.19 (1H, t, $J$=7.4 Hz, H-5') and 7.40 (1H, dd, $J$=2.2, 7.4 Hz, H-6')). The structure of **4** was further confirmed by methanolysis to give **7**, which was identified by comparison with authentic **7**.

Andrographidine E (**5**), mp 126—130 °C, gave the molecular formula $C_{24}H_{26}O_{11}$ from elemental analysis, and this was supported by the $^{13}$C-NMR spectrum. The $^{13}$C-NMR spectrum of **5** showed the presence of three methoxyl groups and the same A- and C-ring system (including the glucopyranosyl moiety) as **3** and **4** (Table I). The remaining carbon signals were assignable to the B ring. The $^1$H-NMR spectrum of **5** showed the characteristic signal of H-6' ($\delta$ 7.87 (1H, dd, $J$=1.5, 7.6 Hz). Compound **5** gave an aglycone (**5a**) on methanolysis along with α-methyl-D-glucopyranoside, which was identified by HPLC (as the per-*p*-bromobenzoate). The $^1$H-NMR spectrum of **5a** showed the characteristic signal pattern of the 2'-mono-O-substituted B ring ($\delta$ 7.96 (1H, dd, $J$=1.8, 8.1 Hz at H-6'), 7.49 (1H, dt, $J$=1.8, 8.1 Hz at H-4'), 7.0—7.2 (2H, m, at H-3' and H-5')). These data indicated the structure **5** for andrographidine E. The $^1$H-NMR spectrum of an acetate (**5b**) of **5** also showed characteristic signals of the B ring having an O-functional group at C-2'.

Andrographidine F (**6**), mp 135—140 °C, gave the molecular formula $C_{25}H_{28}O_{13}$ from the fast atom bombardment (FAB) MS and elemental analysis, and this was supported by the $^{13}$C-NMR spectrum. The $^{13}$C-NMR spectrum of **6** showed the presence of four methoxyl groups and the same A-ring and C-ring system (including the glucopyranosyl moiety) as **3**, **4** and **5**. Three of the four methoxyl groups resonated at characteristic fields ($\delta$ 60.6, 61.0 and 61.4). Andrographidine F gave a pentaacetate (**6b**). The $^1$H-NMR spectrum of **6b** showed the presence of a phenolic acetyl group ($\delta$ 2.37) and AB-type aromatic protons on the B-ring ($\delta$ 7.57 (1H, d, $J$=8.7 Hz at H-6') and 7.15 (1H, d, $J$=8.7 Hz at H-5')). On methanolysis, andrographidine F gave an aglycone (**6a**), whose $^1$H-NMR spectrum also showed similar AB-type signals ($\delta$ 7.57 (1H, d, $J$=8.9 Hz at H-6') and 6.90 (1H, d, $J$=8.9 Hz at H-5')). These results indicate that the structure of andrographidine F is **6**.

The flavone glucosides isolated from the root of *A. paniculata* have uncommon O-substitution patterns, involving C-5, C-7, C-8, C-2', C-3' and C-4', and glucosylation at C-5. The diterpenes isolated from the aerial parts of the plant have not been isolated from the root. On the other hand, these flavone glucosides have not been isolated from the aerial part.

## Experimental

All melting points were determined on a Yanagimoto micro melting point apparatus and are uncorrected. Infrared (IR) spectra were recorded on a JASCO A-202 grating infrared spectrometer and UV spectra on a Shimadzu UV-210 spectrometer. CD spectra were measured on a JASCO J-20A spectropolarimeter. $^1$H- and $^{13}$C-NMR spectra were recorded on a JEOL JNM-FX 90Q FT (90 MHz and 22.5 MHz, respectively) NMR spectrometer with tetramethylsilane (TMS) as an internal standard ($\delta$ value). MS were recorded on JEOL JMS D-100 and JEOL JMS DX-303 instruments. Thin layer chromatography (TLC) was carried out on precoated Silica gel $60F_{254}$ plates (Merck). Column chromatography was carried out on Silica gel type 60 (Merck). HPLC were carried out using TSK gel type ODS-80 Tm (Toyo Soda).

**Extraction and Isolation of Constituents**——The dried roots of *A. paniculata* (1 kg) were extracted with MeOH under reflux to give the MeOH extract (100 g), which was partitioned between AcOEt and water to give an AcOEt-soluble fraction (50 g) and an aqueous fraction. The AcOEt-soluble fraction was chromatographed on a silica gel column; elution was carried out with a hexane–AcOEt gradient solvent system, AcOEt and an AcOEt–MeOH gradient system successively to give five fractions, Fr. 1 (5.5 g), 2 (4.2 g), 3 (2.2 g), 4 (23 g) and 5 (8 g). Fraction 2 was repeatedly chromatographed on a silica gel column with a chloroform ($CHCl_3$)–MeOH gradient solvent system to give 5-hydroxy-7,8,2',3'-tetramethoxyflavone (**7**) (500 mg) and 7,8-dimethoxy-5-hydroxyflavone (**8**) (100 mg). Fraction 4 was chromatographed on a silica gel column with a $CHCl_3$–MeOH gradient solvent system to give andrographidines A (**1**) (1.5 g), B (**2**) (300 mg) and F (**6**) (150 mg), and a mixture of andrographidines C, D and E (1.6 g). The mixture was purified by HPLC (column, YMC-Pack D-ODS-7; 30% $CH_3CN$) to give andrographidines C (**3**) (130 mg), D (**4**) (150 mg) and E (**5**) (120 mg).

**Andrographidine A (1)**——Colorless needles, mp 168—169 °C (AcOEt). MS *m/z*: 462 ($M^+$) ($C_{23}H_{26}O_{10}$), 300

($M-C_6H_{10}O_5$). *Anal.* Calcd for $C_{23}H_{26}O_{10}\cdot 1/2H_2O$: C, 58.59; H, 5.77. Found: C, 58.69; H, 5.66. IR $\nu_{max}^{KBr}$ $cm^{-1}$: 3400, 1672, 1603, 1594, 1205, 1145, 1075. UV $\lambda_{max}^{MeOH}$ nm ($\log\varepsilon$): 237 (4.16), 285 (4.23), 320 (3.79). $^1$H-NMR (pyridine-$d_5$): 2.69 (1H, dd, $J$=17.8, 5.4 Hz, H-3), 2.87 (1H, dd, $J$=17.8, 10.3 Hz, H-3), 3.60 (3H, s, MeO), 3.68 (3H, s, OMe), 5.29 (1H, dd, $J$=10.3, 5.4 Hz, H-2), 6.9—7.5 (6H, m, arom-H). $^{13}$C-NMR as shown in Table I.

**Andrographidine B (2)**——Pale yellow needles, mp 230 °C (acetone). *Anal.* Calcd for $C_{23}H_{24}O_{12}\cdot 1/2H_2O$: C, 55.00; H, 4.99. Found: C, 54.95; H, 4.84. IR $\nu_{max}^{KBr}$ $cm^{-1}$: 3470, 1662, 1610, 1580, 1476, 1080, 1035. UV $\lambda_{max}^{MeOH}$ nm ($\log\varepsilon$): 264 (4.48), 334 (3.78). $^1$H-NMR (pyridine-$d_5$): 3.58 (3H, s, OMe), 3.73 (3H, s, OMe), 5.50 (1H, d, $J$=6.5 Hz, anomeric H), 6.39 (1H, s, H-6), 6.69 (1H, s, H-3), 13.50 (1H, s, chelated OH at C-5). $^{13}$C-NMR as shown in Table I.

**Andrographidine C (3)**——Colorless needles, mp 196—201 °C (MeOH). *Anal.* Calcd for $C_{23}H_{24}O_{10}\cdot H_2O$: C, 57.74; H, 5.48. Found: C, 57.90; H, 5.15. IR $\nu_{max}^{KBr}$ $cm^{-1}$: 3390, 1640, 1600, 1345, 1122, 1070, 1030. UV $\lambda_{max}^{MeOH}$ nm ($\log\varepsilon$): 265 (4.49), 306 (4.12), 327 (4.06). $^1$H-NMR (pyridine-$d_5$): 3.68, 3.76 (3H each, s, OMe), 6.77 (1H, s, H-3), 7.1—7.3 (3H, m, H-3′, 4′, 5′), 7.37 (1H, s, H-6), 7.84 (2H, dd, $J$=3.0, 6.8 Hz, H-2′, 6′). $^{13}$C-NMR as shown in Table I.

**Andrographidine D (4)**——Colorless needles, mp 181—184 °C (MeOH). MS $m/z$: 358 ($M-C_6H_{10}O_5$)$^+$, 343 (358−Me)$^+$. *Anal.* Calcd for $C_{25}H_{28}O_{12}\cdot 1/2H_2O$: C, 56.92; H, 5.16. Found: C, 56.70; H, 5.29. IR $\nu_{max}^{KBr}$ $cm^{-1}$: 3420, 3220, 1636, 1470, 1340, 1070, 1038. UV $\lambda_{max}^{MeOH}$ nm ($\log\varepsilon$): 263 (4.48), 335 (3.78). $^1$H-NMR (pyridine-$d_5$): 3.70, 3.57 (3H each, s, OMe × 2), 6.86 (1H, s, H-3), 7.05 (1H, dd, $J$=2.2, 7.5 Hz, H-4′), 7.19 (1H, t, $J$=7.4 Hz, H-5′), 7.40 (1H, dd, $J$=2.2, 7.4 Hz, H-6′), 7.38 (1H, s, H-6). $^{13}$C-NMR as shown in Table I.

**Andrographidine E (5)**——Colorless needles, mp 126—130 °C (MeOH). MS $m/z$: 328 ($M-C_6H_{10}O_5$)$^+$, 313 (328—Me). *Anal.* Calcd for $C_{24}H_{26}O_{11}\cdot H_2O$: C, 56.69; H, 5.55. Found: C, 56.79; H, 5.25. IR $\nu_{max}^{KBr}$ $cm^{-1}$: 3400, 1635, 1610, 1575, 1256, 1130, 1072, 1030. UV $\lambda_{max}^{MeOH}$ nm ($\log\varepsilon$): 264 (4.39), 333 (4.16). $^1$H-NMR (pyridine-$d_5$): 3.52, 3.74 (3H each, s, OMe), 6.83 (1H, s, H-6), 6.97 (1H, s, H-3), 7.87 (1H, dd, $J$=1.5, 7.6 Hz, H-6′). $^{13}$C-NMR as shown in Table I.

**Andrographidine F (6)**——Colorless needles, mp 135—140 °C (MeOH). FABMS $m/z$: 537 (M+H)$^+$. 375. *Anal.* Calcd for $C_{25}H_{28}O_{13}\cdot H_2O$: C, 54.15; H, 5.45. Found: C, 53.98; H, 5.06. IR $\nu_{max}^{KBr}$ $cm^{-1}$: 3380, 1630, 1470, 1334, 1310, 1123, 1070, 1035. UV $\lambda_{max}^{MeOH}$ nm ($\log\varepsilon$): 249 (4.31), 263 (4.30), 336 (4.36). $^1$H-NMR (pyridine-$d_5$): 3.73 (3H, s, OMe), 3.76 (9H, s, OMe), 6.90 (1H, d, $J$=8.9 Hz, H-5′), 6.98 (1H, s, H-3), 7.37 (1H, s, H-6), 7.57 (1H, d, $J$=8.9 Hz, H-6′). $^{13}$C-NMR as shown in Table I.

**5-Hydroxy-7,8,2′,3′-tetramethoxyflavone (7)**——Yellow needles, mp 150—152 °C (hexane–AcOEt). MS $m/z$: 358 (M)$^+$ ($C_{19}H_{18}O_7$). IR $\nu_{max}^{KBr}$ $cm^{-1}$: 3450, 1610, 1585, 1095. UV $\lambda_{max}^{MeOH}$ nm ($\log\varepsilon$): 271 (4.47), 311 (3.98), 344 (3.87). $^1$H-NMR ($CDCl_3$): 3.90, 3.92, 3.94 (3H each, s, OMe × 3), 6.42 (1H, s, H-6), 6.89 (1H, s, H-3), 7.06 (1H, dd, $J$=2.4, 8.1 Hz, H-4′), 7.19 (1H, t, $J$=8.1 Hz, H-5′), 7.42 (1H, dd, $J$=2.4, 8.1 Hz, H-6′). $^{13}$C-NMR as shown in Table I.

**7,8-Dimethoxy-5-hydroxyflavone (8)**——Pale yellow needles, mp 183—184 °C (hexane). MS $m/z$: 298 (M)$^+$ ($C_{17}H_{14}O_5$). IR $\nu_{max}^{KBr}$ $cm^{-1}$: 3450, 1668, 1592, 1450, 1375, 1122. UV $\lambda_{max}^{MeOH}$ nm ($\log\varepsilon$): 274 (4.52), 315 (3.85), 346 (3.78). $^1$H-NMR ($CDCl_3$): 3.95 (6H, s, OMe), 6.43 (1H, s, H-6), 6.66 (1H, s, H-3), 7.4—7.7 (3H, m, H-3′, 4′, 5′), 7.93 (2H, dd, $J$=2.2, 7.4 Hz, H-2′, 6′), 12.55 (1H, s, OH). $^{13}$C-NMR as shown in Table I.

**Methanolysis of Andrographidine A (1)**——Compound 1 (90 mg) was refluxed in 10% HCl–MeOH (4 ml) for 1 h. The reaction solution was neutralized with $AgCO_3$. The neutralized solution was evaporated to dryness *in vacuo* and purified by preparative layer chromatography (PLC) to give an aglycone part (45 mg) and a methyl sugar (30 mg). The crude aglycone was recrystallized from hexane to give **1a** as colorless needles, (25 mg), mp 98—100 °C. MS $m/z$: 300 (M)$^+$. IR $\nu_{max}^{KBr}$ $cm^{-1}$: 3450, 1640, 1380, 1315, 1110. UV $\lambda_{max}^{MeOH}$ nm ($\log\varepsilon$): 238 sh (4.06), 289 (4.27), 343 (3.80). CD ($c$=0.02): $[\theta]_{310}$ +7500, $[\theta]_{254}$ −32400. $^1$H-NMR ($CDCl_3$): 2.85 (1H, dd, $J$=4.6, 17.5 Hz, H-3), 3.13 (1H, dd, $J$=10.9, 17.5 Hz, H-3), 3.78 3.89 (3H each, s, OMe), 5.47 (1H, dd, $J$=10.9, 4.6 Hz, H-2), 6.11 (1H, s, H-6), 7.44 (5H, br s, phenyl). $^{13}$C-NMR ($CDCl_3$): 43.5 (C-3), 56.2 (OMe), 61.3 (OMe), 79.2 (C-2), 93.2 (C-6), 107.5 (C-10), 126.1 (C-2′, 6′), 128.7 (C-4′), 128.8 (C-3′, 5′), 133.3 (C-8), 138.6 (C-1′), 159.9 (C-7, 9), 159.9 (C-4), 161.7 (C-5).

The methyl sugar fraction (2 mg) was *p*-bromobenzoylated and analyzed by HPLC (TSK gel ODS 80 Tm, 90% $CH_3CN$, detection at 247 nm), and identified as α-methyl-D-glucopyranoside-per-*p*-bromobenzoate. The CD spectrum of the purified α-methylglucopyranoside-per-*p*-bromobenzoate was measured to obtain the *A*-value (+20).

**Acetate (1b) of 1a**——The aglycone (**1a**) (12 mg) was acetylated in the usual way to give an acetate (**1b**). $^1$H-NMR ($CDCl_3$): 2.38 (3H, s, Ac), 2.77 (1H, dd, $J$=4.4, 17.6 Hz, H-3), 3.13 (1H, dd, $J$=11.2, 17.6 Hz, H-3), 3.84, 3.90 (3H each, s, OMe), 5.50 (1H, dd, $J$=4.4, 11.2 Hz, H-2), 6.33 (1H, s, H-6), 7.42 (5H, br s, phenyl). $^{13}$C-NMR ($CDCl_3$): 21.1 (Ac), 45.2 (C-3), 56.3 (OMe), 61.1 (OMe), 79.5 (C-2), 101.2 (C-6), 126.0 (C-2′, 6′), 128.7 (C-4′), 128.8 (C-3′, 5′), 138.6 (C-8), 158.2 (C-7), 159.8 (C-9), 189.0 (C-4); other carbons were not identified because of the small amount of the sample.

**Acetate (1c) of Andrographidine A (1)**——Compound **1** (45 mg) was acetylated in the usual way to give an acetate (**1c**), amorphous powder (60 mg). IR $\nu_{max}^{KBr}$ $cm^{-1}$: 1760, 1693, 1605, 1370, 1225, 1130, 1065, 1040. $^1$H-NMR ($CDCl_3$): 2.05 (9H, s, Ac), 2.11 (3H, s, Ac), 2.80 (1H, dd, $J$=16.2, 5.4 Hz, H-3), 3.00 (1H, dd, $J$=16.2, 10.1 Hz, H-3), 3.81, 3.92 (3H each, s, OMe), 4.25 (2H, d, $J$=3.6 Hz, H-6″), 5.0—5.6 (5H, m, H-2, 2″, 3″, 4″, 5″), 6.53 (1H, s, H-6), 7.41 (5H, s, phenyl). $^{13}$C-NMR ($CDCl_3$): 20.5 (Ac), 45.7 (C-3), 56.3 (OMe), 61.1 (OMe), 62.3 (G-6), 68.8 (G-4), 70.9 (G-2), 72.4 (G-5), 72.7 (G-3), 79.2 (C-2), 97.7 (C-6), 100.2 (G-1), 107.3 (C-10), 126.0 (C-2′, 6′), 128.5 (C-4′), 128.7 (C-3′, 5′), 134.1 (C-8), 138.9 (C-1′), 153.5 (C-9), 155.9 (C-7), 158.1 (C-5), 169.3, 169.6, 170.0, 170.3 (Ac), 188.1 (C-4).

**Methanolysis of Andrographidine B (2)**——Compound **2** (34 mg) was methanolyzed to give an aglycone (**2a**) and

α-methyl-D-glucopyranoside. The aglycone (**2a**) was recrystallized from MeOH to give yellow needles (15 mg), mp 297—299 °C. MS *m/z*: 330 $(M)^+$ ($C_{17}H_{14}O_7$). IR $\nu_{max}^{KBr}$ $cm^{-1}$: 3490, 3000, 1666, 1610, 1570, 1460, 1280, 1130, 1018, 790. UV $\lambda_{max}^{MeOH}$ nm (log ε): 264 (4.42), 308 (3.92), 332 (3.88). $^1$H-NMR (pyridine-$d_5$): 3.54, 3.72 (3H each, s, OMe), 6.41 (1H, s, H-6), 6.60 (2H, d, $J$=8.0 Hz, H-4′, 6′), 6.73 (1H, s, H-3), 7.08 (1H, t, $J$=8.0 Hz, H-5′), 13.19 (1H, s, chelated OH at C-5). $^{13}$C-NMR (pyridine-$d_5$): 56.3 (OMe), 61.4 (OMe), 96.2 (C-6), 105.7 (C-10), 107.7 (C-3, 4′), 110.5 (C-1′), 113.1 (C-6′), 129.6 (C-8), 132.6 (C-5′), 158.0 (C-3′), 158.6 (C-7, 2′), 158.9 (C-5), 164.0 (C-2), 183.3 (C-4).

**Acetate (2b) of Andrographidine B (2)**——Compound **2** was acetylated in the usual way to give a pentaacetate (**2b**), viscous oil. $^1$H-NMR ($CDCl_3$): 1.78, 1.93, 2.03, 2.09, 2.18, 2.42 (3H each, s, Ac), 3.92, 3.98 (3H each, s, OMe), 6.14 (1H, s, H-3), 6.69 (1H, s, H-6), 6.96 (1H, dd, $J$=1.1, 8.3 Hz, H-4′), 7.08 (1H, dd, $J$=1.1, 8.3 Hz, H-6′), 7.47 (1H, t, $J$=8.3 Hz, H-5′). $^{13}$C-NMR ($CDCl_3$): 20.0, 20.4, 20.5, 20.8, 21.0 (Ac), 56.6, 61.7 (OMe), 62.0 (G-6), 68.5 (G-4), 70.8 (G-2), 72.4 (G-5), 72.5 (G-3), 99.7 (G-1), 104.9 (C-6), 111.3 (C-10), 113.9 (C-3), 114.6 (C-4′), 118.3 (C-6′), 125.8 (C-1′), 131.8 (C-5′), 135.3 (C-8), 145.3 (C-2′), 149.6 (C-5), 155.7 (C-7, 9), 156.1 (C-3′), 156.9 (C-2), 168.7, 168.9, 169.2, 169.5, 169.9, 170.3 (Ac), 176.1 (C-4).

**Methanolysis of Andrographidine C (3)**——Compound **3** was methanolyzed to give an aglycone (**3a**) and α-methyl-D-glucopyranoside. **3a**, MS *m/z*: 298 $(M)^+$ ($C_{17}H_{14}O_5$), identical with **8** (IR spectrum, TLC and $^1$H-NMR spectrum).

**Methanolysis of Andrographidine D (4)**——Compound **4** was methanolyzed to give an aglycone (**7**) and α-methyl-D-glucopyranoside. **7**, MS *m/z*: 358 $(M)^+$ ($C_{19}H_{18}O_7$), identical with 5-hydroxy-7,8,2′,3′-tetramethoxyflavone (IR spectrum, TLC and $^1$H-NMR spectrum).

**Acetate (4a) of Andrographidine D (4)**——Compound **4** was acetylated to give an acetate (**4a**). $^1$H-NMR ($CDCl_3$): 2.05 (9H, s, Ac), 2.19 (3H, s, Ac). 3.90, 3.97 (3H each, s, OMe), 3.93 (6H, s, OMe), 4.22 (2H, d, $J$=4.0 Hz, H-6′′), 5.2—5.5 (4H, m, H-1′′, 2′′, 3′′, 4′′), 6.81 (1H, s, H-3), 6.84 (1H, s, H-6), 7.05 (1H, dd, $J$=2.2, 7.4 Hz, H-4′), 7.19 (1H, t, $J$=7.4 Hz, H-5′), 7.40 (1H, dd, $J$=2.2, 7.4 Hz, H-6′). $^{13}$C-NMR ($CDCl_3$): 20.6, 21.0 (Ac), 56.1, 56.5, 60.9, 61.5 (OMe), 62.0 (G-6), 68.9 (G-4), 70.1 (G-2), 72.2 (G-5), 72.7 (G-3), 100.8 (G-1), 103.6 (C-6), 113.0 (C-3), 115.2 (C-4′), 120.8 (C-6′), 124.2 (C-5′), 126.4 (C-8), 151.2 (C-3′), 153.4 (C-2′), 155.7 (C-7, 9), 159.3 (C-2), 169.4, 170.0, 170.1, 170.3 (Ac), 177.0 (C-4).

**Methanolysis of Andrographidine E (5)**——Compound **5** was methanolyzed to give an aglycone (**5a**) and α-methyl-D-glucopyranoside. **5a**, MS *m/z*: 328 $(M)^+$ ($C_{18}H_{16}O_6$). $^1$H-NMR ($CDCl_3$): 3.91 (3H, s, OMe), 3.94 (6H, s, OMe), 6.42 (1H, s, H-6), 7.04 (1H, s, H-3), 7.0—7.2 (2H, m, H-3′, 5′), 7.49 (1H, dt, $J$=1.8, 8.1 Hz, H-4′), 7.96 (1H, dd, $J$=1.8, 8.1 Hz, H-6′). $^{13}$C-NMR ($CDCl_3$): 55.7, 56.3, 61.7 (OMe), 95.6 (C-6), 104.9 (C-10), 110.5 (C-3), 111.8 (C-3′), 120.5 (C-1′), 121.0 (C-6′), 129.4 (C-5′), 132.7 (C-4′), 134.4 (C-8), 157.6 (C-7, 9), 158.2 (C-2′), 158.5 (C-5), 161.5 (C-2), 183.1 (C-4).

**Acetate (5b) of Andrographidine E (5)**——Compound **5** was acetylated to give an acetate (**5b**). $^1$H-NMR ($CDCl_3$): 2.03, 2.19 (3H each, s, Ac), 2.05 (6H, s, Ac), 3.93, 3.94, 3.97 (3H each, s, OMe), 4.22 (2H, d, $J$=4.3 Hz, H-6′′), 5.0—5.5 (5H, m, H-1′′, 2′′, 3′′, 4′′, 5′′), 6.83 (1H, s, H-6), 6.97 (1H, s, H-3), 7.00—7.22 (2H, m, H-3′, 5′), 7.48 (1H, dt, $J$=1.8, 7.9 Hz, H-4′), 7.94 (1H, dd, $J$=1.8, 7.9 Hz, H-6′). $^{13}$C-NMR ($CDCl_3$): 20.6, 21.0 (Ac), 55.6, 56.4, 61.5 (OMe), 62.0 (G-6), 68.9 (G-4), 71.0 (G-2), 72.2 (G-5), 72.7 (G-3), 100.8 (G-1), 103.3 (C-6), 111.2 (C-10), 111.8 (C-3′), 113.2 (C-3), 120.7 (C-1′), 120.9 (C-6′), 129.2 (C-5′), 132.2 (C-4′), 134.0 (C-8), 151.2 (C-2′), 155.6 (C-7, 9), 158.1 (C-5), 158.5 (C-2), 169.4, 170.0, 170.1, 170.3 (Ac), 177.2 (C-4).

**Methanolysis of Andrographidine F (6)**——Compound F was methanolyzed to give an aglycone (**6a**) and α-methyl-D-glucopyranoside. **6a** was recrystallized to give pale yellow needles, mp 236—237 °C. MS *m/z*: 374 $(M)^+$ ($C_{19}H_{18}O_8$). IR $\nu_{max}^{KBr}$ $cm^{-1}$: 3450, 3150, 1660, 1610, 1550, 1503, 1323, 1220, 1028. UV $\lambda_{max}^{MeOH}$ nm (log ε): 251 (4.19), 271 (4.30), 300 (4.16), 326 (4.24). $^1$H-NMR ($CDCl_3$+$CD_3OD$): 3.90, 3.92 (3H each s, OMe), 3.98 (6H, s, OMe), 6.46 (1H, s, H-6), 6.93 (1H, s, H-3), 6.90 (1H, d, $J$=8.9 Hz, H-5′), 7.57 (1H, d, $J$=8.9 Hz, H-6′). $^{13}$C-NMR ($CDCl_3$+$CD_3OD$): 55.9, 60.2, 60.4, 61.2 (OMe), 95.3 (C-6), 107.6 (C-3), 111.9 (C-5′), 113.3 (C-10), 124.1 (C-6′), 141.2 (C-3′), 158.4 (C-5), 162.4 (C-2), 183.0 (C-4).

**Acetate (6b) of Andrographidine F (6)**——Compound **6** was acetylated to give an acetate (**6b**). $^1$H-NMR ($CDCl_3$): 2.05 (9H, s, Ac), 2.19, 2.37 (3H each, s, Ac), 3.90, 3.92, 3.94, 3.98 (3H each, s, OMe), 4.23 (2H, d, $J$=4.3 Hz, H-6′′), 5.0—5.5 (5H, m, H-1′′, 2′′, 3′′, 4′′, 5′′), 6.80 (1H, s, H-3), 6.85 (1H, s, H-6), 7.15 (1H, d, $J$=8.7 Hz, H-5′), 7.57 (1H, d, $J$=8.7 Hz, H-6′). $^{13}$C-NMR ($CDCl_3$): 20.6, 21.0 (Ac), 56.5, 60.8, 61.2, 61.5 (OMe), 62.1 (G-6), 68.9 (G-4), 71.0 (G-2), 72.2 (G-5), 72.7 (G-3), 100.8 (G-1), 103.5 (C-6), 112.8 (C-3), 118.5 (C-5′), 123.6 (C-6′), 124.6 (C-1′), 146.0, 146.8, 151.3 (not assignable), 155.8 (C-7, 9), 158.4 (C-5), 168.6, 169.5, 170.0, 170.1, 170.3 (Ac), 176.8 (C-4).

**Acknowledgements** We wish to thank Dr. K. Yokoi, SS Pharmaceutical Co., Ltd., for measurement of FABMS. We also thank Dr. M. Uchida and Mrs. H. Kitamura of the Analysis Center of this college for mass spectral measurement and elemental analysis.

## References

1) M. P. Cava, W. R. Chan, R. P. Stein and C. R. Willis, *Tetrahedron*, **21**, 2617 (1965).

2) A. Balmain and J. D. Connolly, *J. Chem. Soc., Perkin Trans. 1*, **1973**, 1247.
3) W. R. Chan, D. R. Taylor, C. R. Willis, R. L. Bodden and H. W. Fehlhaben, *Tetrahedron*, **27**, 5081 (1971).
4) T. Fujita, R. Fujitani, Y. Takeda, Y. Takaishi, T. Yamada, M. Kido and I. Miura, *Chem. Pharm. Bull.*, **32**, 2117 (1984).
5) I. R. Govindachari, P. C. Parthasarathy, B. R. Pai and P. S. Subramaniam, *Tetrahedron*, **21**, 3237 (1965).
6) M. F. Jalal, K. H. Overton and D. S. Rycroft, *Phytochemistry*, **18**, 149 (1979).
7) T. Taki, M. Kuroyanagi, H. Maeda, M. Miyachi, M. Sato, M. Matsumoto and S. Fukushima, The 6th Symposium on the Development and Application of Naturally Occurring Drug Materials, Nagoya, July 1986, p. 62.
8) A. I. Scott, "Interpretation of the Ultraviolet Spectra of Natural Products," Pergamon Press, Oxford, 1964, p. 135.
9) H. W. Liu and K. Nakanishi, *J. Am. Chem. Soc.*, **104**, 1178 (1982); K. Nakanishi, M. Kuroyanagi, H. Nanbu, E. M. Oltz, R. Takeda, G. L. Verdine and A. Zask, *Pure Appl. Chem.*, **56**, 1031 (1984).
10) W. Gaffield, *Tetrahedron*, **26**, 4093 (1970).

[Chem. Pharm. Bull. 35(11)4436—4441(1987)]

# Lipid A and Related Compounds. XIV.[1] A New Synthesis of Lipid Y, the Reducing Sugar Moiety of *Salmonella*- and *Proteus*-Type Lipid A

KIYOSHI IKEDA, SHIN-ICHI NAKAMOTO, TOSHIO TAKAHASHI, and KAZUO ACHIWA*

*School of Pharmaceutical Science, University of Shizuoka, Oshika 2-2-1, Shizuoka 422, Japan*

(Received March 26, 1987)

An efficient synthesis of lipid Y by the use of chemoselective debenzylation as a key step is described.

**Keywords**——lipid A; lipid Y; glucosamine derivative; chemoselective debenzylation; lipid Y synthesis

Lipid A, a constituent of lipopolysaccharide (LPS) of gram-negative bacteria, has been shown to play an important role in the various biological activities[2] of LPS, such as pyrogenicity, lethal toxicity, adjuvant activity and so on. The chemical structure of lipid A consists of a $\beta(1\rightarrow6)$ linked D-glucosamine disaccharide which carries phosphate residues at positions 1 and 4′ as well as amide-bound and ester-bound D-3-hydroxy and/or acyloxy fatty acids,[3] as indicated in Chart 1.

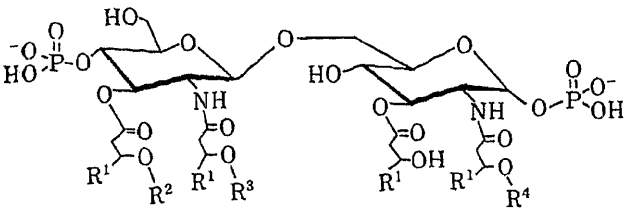

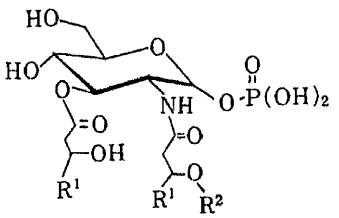

**1a**: $R^1=CH_3(CH_2)_{10}-$, $R^2=R^3=R^4=H$ (*Salmonella* mutant)

**1b**: $R^1=CH_3(CH_2)_{10}-$, $R^2=CH_3(CH_2)_{12}CO-$, $R^3=CH_3(CH_2)_{10}CO-$, $R^4=H$ (*Escherichia coli*)

**1c**: $R^1=CH_3(CH_2)_{10}-$, $R^2=CH_3(CH_2)_{12}CO-$, $R^3=CH_3(CH_2)_{10}CO-$, $R^4=CH_3(CH_2)_{14}CO-$ (*Salmonella minnesota*)

**1d**: $R^1=CH_3(CH_2)_{10}-$, $R^2=CH_3(CH_2)_{12}CO-$, $R^3=CH_3(CH_2)_{12}CO-$, $R^4=CH_3(CH_2)_{14}CO-$ (*Proteus mirabilis*)

lipid Y (**2**): $R^1=CH_3(CH_2)_{10}-$, $R^2=CH_3(CH_2)_{14}CO-$

Chart 1

Although synthetic procedures have been developed, improved methods for chemoselective protection and deprotection of 2-amino-2-deoxy-D-glucose derivatives remain important, especially in the field of lipid A synthesis.[1,4]

In a recent communication,[1d] we reported an efficient synthesis of lipid Y,[5] which

corresponds to the reducing glucosamine unit of *Salmonella minnesota* (**1c**)[3c] and *Proteus mirabilis* lipid A (**1d**),[3c] using a chemoselective debenzylation of the glycosidic benzyl group of a 2-amino-2-deoxy-D-glucose derivative that carries another benzyl group protecting a 3-hydroxytetradecanoyl substituent at O-3. In our strategy, the key intermediate (**3**) that we designed is useful for the synthesis of two precursors of lipid A, *i.e.*, the non-reducing unit and the reducing unit. This paper describes in detail the successful application of the key intermediate (**3**) to lipid Y synthesis.

In the initial stage of the synthesis of lipid Y, the key intermediate (**3**) was prepared starting from benzyl 2-chloroacetamido-2-deoxy-β-D-glucopyranoside (**4**)[6] in two steps (Chart 2). The latter compound (**4**) was treated with 2,2-dimethoxypropane in dimethylformamide (DMF) in the presence of a catalytic amount of *p*-toluenesulfonic acid (*p*-TSA) to afford compound (**5**) in 87% yield. Removal of the chloroacetyl group of **5** was effected by forming a pyridinium salt with pyridine as a base, followed by hydrolysis to give the key intermediate (**3**) in 80% yield. The proton nuclear magnetic resonance ($^1$H-NMR) spectrum of **3** showed the presence of a doublet ($J$=8.1 Hz) at 4.35 ppm assigned to the anomeric proton and an AB quartet ($J$=7.9 Hz) at 4.57 and 4.90 ppm due to the methylene protons of the glycosidic benzyl group.

The key intermediate (**3**) thus obtained was applied for the synthesis of lipid Y as follows. The free amino group of **3** was acylated with optically pure (*R*)-3-hexadecanoyloxytetradecanoic acid and dicyclohexylcarbodiimide (DCC) in $CH_2Cl_2$ to afford the *N*-acylated compound (**6**) in 90% yield. The remaining hydroxyl group of **6** was acylated with optically pure (*R*)-3-benzyloxytetradecanoic acid, DCC, and a catalytic amount

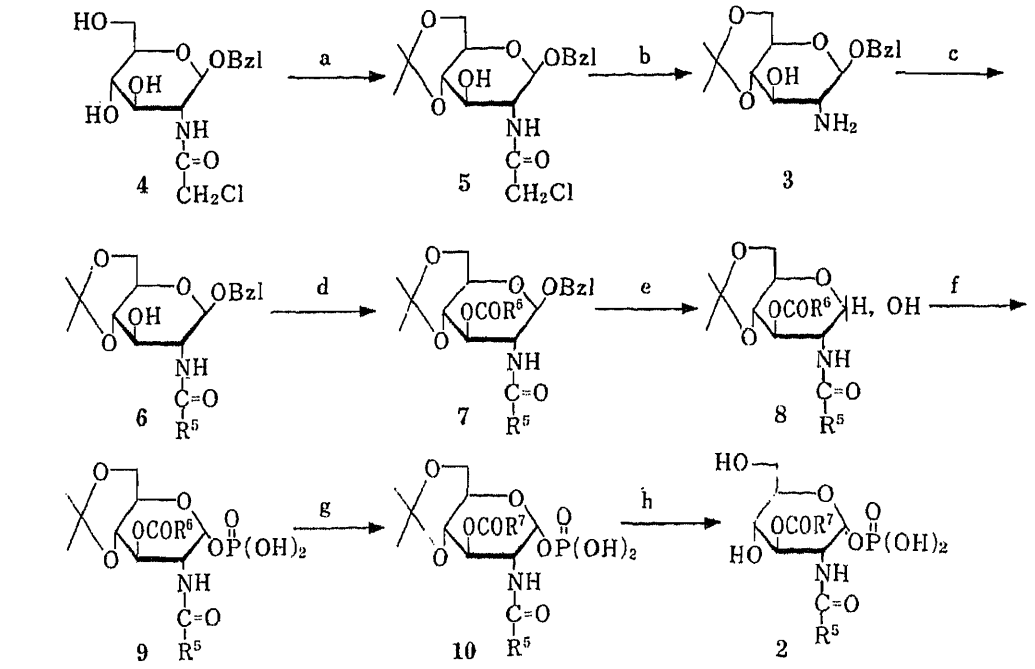


$R^5$=$CH_3(CH_2)_{10}$CH(OC(=O)$(CH_2)_{14}CH_3$)$CH_2$– (*R*), $R^6$=$CH_3(CH_2)_{10}$CH(OBzl)$CH_2$– (*R*), $R^7$=$CH_3(CH_2)_{10}$CH(OH)$CH_2$– (*R*)

a) $(CH_3)_2C(OCH_3)_2$, *p*-TSA; b) i) pyridine, ii) 5% aq. NaOH–MeOH (1 : 1); c) $R^5CO_2H$, DCC; d) $R^6CO_2H$, DCC, 4-dimethylaminopyridine; e) 10% Pd/C, $H_2$ in THF–EtOH (1 : 1); f) i) *n*-BuLi, $(BzlO)_2POCl$, ii) 10% Pd/C, $H_2$; g) Pd-black, $H_2$; h) 90% AcOH

Chart 2

of 4-dimethylaminopyridine (DMAP) in $CH_2Cl_2$ to afford the triacylated compound (**7**) in 72% yield.

Selective hydrogenolysis of the glycosidic benzyl group of **7** was examined under various conditions, as follows. At first, when a solution of **7** in benzene–MeOH (5:1) was hydrogenated for 30 h at room temperature under slight pressure in the presence of 10% Pd-on-carbon, the starting compound (**7**) was recovered unchanged. When a solution of **7** in tetrahydrofuran (THF)–MeOH (5:1) was hydrogenated for 15 h at room temperature under atmospheric pressure in the presence of 10% Pd-on-carbon, the desired product (**8**) was obtained in poor yield, together with a considerable amount of the compound didebenzylated at glycosidic and O-3 protecting groups. A small amount of unchanged starting material (**7**) was recovered. When a solution of **7** in THF was hydrogenated for 72 h at 30 °C under 50 atm in the presence of 10% Pd-on-carbon, the expected 1-debenzylated compound (**8**) was isolated in 59% yield as a single anomer. NMR and thin-layer chromatographic (TLC) analyses of this 1-debenzylated product (**8**) indicated high chemoselectivity. The $^1$H-NMR spectrum of **8** showed the presence of the methylene proton signal of the benzyl group protecting the 3-(3-benzyloxy)tetradecanoyl substituent at 4.50 ppm (singlet) and the disappearance of the signal attributed to the glycosidic benzyl group. In addition, the carbon-13 nuclear magnetic resonance ($^{13}$C-NMR) spectrum of **8** showed a signal at 92.3 ppm (doublet) suggestive of the $\alpha$-anomeric configuration. As a result of the improvement of chemoselectivity of the debenzylation of **7**, the most promising result was obtained as follows. When a solution of **7** in THF–EtOH (1:1) was hydrogenated for 38 h at 30 °C under slight pressure in the presence of 10% Pd-on-carbon, the desired product (**8**) was obtained in an acceptable yield of 64% as a mixture of anomers ($\alpha:\beta=3:1$). This method is satisfactory for practical use. In the $^1$H-NMR spectrum of **8**, two sets of doublet at 6.14 and 6.54 ppm were assigned to the amide protons of the $\alpha$-anomer and the $\beta$-anomer, respectively.

This assignment was verified by observing the disappearance of the $^1$H-NMR signal of the $\beta$-anomer after treatment with an anomerization reagent. The $\alpha/\beta$ ratio of **8** was determined by integration of the amide proton signals in the $^1$H-NMR spectrum. Complete conversion of $\beta$- into $\alpha$-anomer was observed when the mixture was dissolved in THF–AcOH (3:1) and stirred for 48 h at 45 °C.

The glycosidic hydroxyl group of **8** was then phosphorylated with dibenzylphosphorochloridate and *n*-butyllithium in THF at −70 °C.[7] The reaction mixture was directly hydrogenolyzed with 10% Pd-on-carbon to afford the 1-phosphate (**9**) in 48% yield after purification by preparative TLC ($CHCl_3$–MeOH = 5:1). Deprotection of the remaining benzyl group of **9** was carried out by hydrogenolysis over Pd-black in THF–MeOH (1:3) to afford **10** in 63% yield after purification by preparative TLC ($CHCl_3$–MeOH = 5:1). Finally, deprotection of **10** by treatment with 90% AcOH gave **2** in 91% yield after purification by preparative TLC ($CHCl_3$–MeOH = 5:1). The triacylglucosamine-1-phosphate (**2**) was clearly positive with the specific spray reagent for the phosphoric group.[8] The structure of **2** was assigned on the basis of the positive fast atom bombardment mass spectrometry (FAB MS), which showed an $(M+Na)^+$ ion at *m/z* 973, $(M-H_2PO_4)^+$ at 853, $(M-C_{16}+Na+H)^+$ at 734, and $(M-C_{16}-OH-C_{14}-H_2PO_4+2H)^+$ at 388. The specific rotation of **2** was in good agreement with that of lipid Y reported by Shiba's group.[9] The structures of all compounds were characterized by $^1$H- and $^{13}$C-NMR spectroscopies, as well as infrared (IR) spectroscopy and elemental analyses.

In order to check the limitations of this chemoselective debenzylation, we examined the hydrogenation of **12** in THF at 30 °C for 24 h in the presence of 10% Pd-on-carbon. In the case of **12**, the benzyl group protecting the 2-(3-benzyloxy)tetradecanamido substituent was removed as readily as the glycosidic benzyl group, to give **13** in 68% yield. These results suggested that the order of reactivity of debenzylation is the benzyl group on an amide

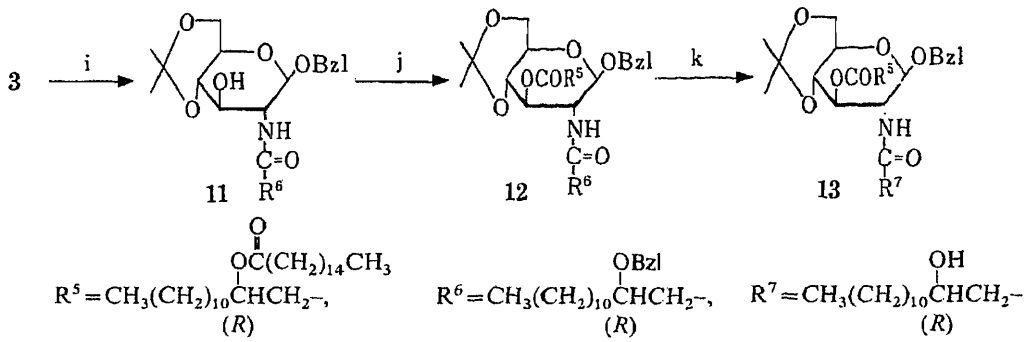


i) $R^6CO_2H$, DCC; j) $R^5=CO_2H$, DCC, 4-dimethylaminopyridine; k) 10% Pd/C, $H_2$ in THF

Chart 3

substituent ≈ the glycosidic benzyl group > the benzyl group on an ester substituent.

This method of chemoselective removal of the benzyl group should be of great help for the synthesis of natural products such as complex carbohydrates.

## Experimental

All melting points are uncorrected. $^1$H-NMR spectra were recorded on a JEOL JNM-FX (90 MHz) FT-NMR spectrometer with tetramethylsilane (in $CDCl_3$) as an internal standard. $^{13}$C-NMR spectra were recorded on a JEOL JNM-FX90Q (22.5 MHz) FT-NMR spectrometer with tetramethylsilane (in $CDCl_3$) as an internal standard reference. Abbreviations are as follows: s, singlet; br s, broad singlet; d, doublet; t, triplet; q, quartet; m, multiplet. IR spectra were recorded on a JASCO A-202 infrared spectrophotometer. Optical rotations were determined with a JASCO DIP-140 digital polarimeter.

Column chromatography was carried out on silica gel (Kiesel gel-60, 70—230 mesh, Merck). TLC on Kiesel gel 60-F (Merck) was used to monitor the reaction and to ascertain the purity of reaction products. The spots were visualized by spraying with aqueous sulfuric acid and then heating.

**Benzyl 2-Chloroacetamido-2-deoxy-4,6-*O*-isopropylidene-β-D-glucopyranoside (5)**——2,2-Dimethoxypropane (24.9 g, 240 mmol) was added to a stirred solution of benzyl 2-chloroacetamido-2-deoxy-β-D-glucopyranoside (4) (24.4 g, 71 mmol), prepared as described in the literature,[6] and *p*-TSA (1.38 g, 8 mmol) in DMF (150 ml) at room temperature under nitrogen. After 12 h, the reaction mixture was poured into a solution of water (1200 ml) and 5% aqueous sodium hydroxide (13 ml). The whole was extracted with three 150 ml portions of ethyl acetate. The organic extracts were combined, washed with water (100 ml), and dried ($MgSO_4$). After removal of the solvent, the residue was purified by crystallization from *n*-hexane to furnish **5** (23.9 g, 87%) as a white powder, mp 173—176 °C. $[\alpha]_D^{22}$ −91.4° (*c* = 1.15, $CHCl_3$). IR (KBr): 3456 (OH), 3330 (NH), 1694 (amide), 853 ($Me_2C$), 700 (Ph) $cm^{-1}$. $^1$H-NMR ($CDCl_3$) δ: 1.42 and 1.52 (each 3H, s, $Me_2C$), 3.99 (2H, s, $COCH_2$), 4.44—4.98 (3H, m, $CH_2Ph$ and H-1), 7.31 (5H, s, Ph). *Anal.* Calcd for $C_{18}H_{24}ClNO_6$: C, 56.03; H, 6.27; N, 3.63. Found: C, 55.95; H, 6.28; N, 3.68.

**Benzyl 2-Amino-2-deoxy-4,6-*O*-isopropylidene-β-D-glucopyranoside (3)**——A solution of **5** (23.9 g, 62 mmol) in pyridine (120 ml) was heated at 85—90 °C for 1.5 h, then allowed to cool. The solvent was evaporated off and the residue was dissolved in a solution (152 ml) of 5% aqueous sodium hydroxide and methanol (1 : 1), then stirred at 30 °C for 16 h. After removal of the solvent, the residue was dissolved in chloroform (180 ml), washed with water, and dried ($MgSO_4$). After removal of the solvent, the residue was purified by crystallization from MeOH to furnish **3** (15.3 g, 80%) as a white powder, mp 132—133 °C. $[\alpha]_D^{22}$ −98.0° (*c* = 1.25, $CHCl_3$). IR (KBr): 3572 (OH), 3376 (NH), 854 ($Me_2C$), 692 (Ph) $cm^{-1}$. $^1$H-NMR ($CDCl_3$) δ: 1.42 and 1.50 (each 3H, s, $Me_2C$), 4.35 (1H, d, *J* = 8.1 Hz, H-1), 4.57 and 4.90 (each 1H, d, *J* = 7.9 Hz, $CH_2Ph$), 7.33 (5H, s, Ph). *Anal.* Calcd for $C_{16}H_{23}NO_5$: C, 62.12; H, 7.49; N, 4.52. Found: C, 61.94; H, 7.44; N, 4.55.

**Benzyl 2-Deoxy-2-[(*R*)-3-hexadecanoyloxytetradecanamido]-4,6-*O*-isopropylidene-β-D-glucopyranoside (6)**——DCC (0.297 g, 1.44 mmol) was added to a stirred solution of **5** (0.371 g, 1.20 mmol) and (*R*)-3-hexadecanoyloxytetradecanoic acid (0.695 g, 1.44 mmol) in dry dichloromethane (8 ml) at 0 °C under nitrogen. The mixture was stirred for 5 h at 0 °C, then at room temperature for 12 h. The resulting suspension was filtered through Celite and evaporated. The residue was chromatographed on silica gel with chloroform–ether (20 : 1) to give **6** (0.840 g, 90%), mp 72—74 °C. $[\alpha]_D^{20}$ −41.1° (*c* = 1.13, $CHCl_3$). IR (KBr): 3440 (OH), 3376 (NH), 1731 (ester), 1673 (amide), 853 ($Me_2C$), 697 (Ph) $cm^{-1}$. $^1$H-NMR ($CDCl_3$) δ: 0.89 (6H, t, *J* = 5.4 Hz, $(CH_2)_{10}CH_3$ and $(CH_2)_{14}CH_3$), 1.25 (48H, br s, $(CH_2)_{10}CH_3$ and $(CH_2)_{14}CH_3$), 1.44 and 1.53 (each 3H, s, $Me_2C$), 2.13—2.52 (4H, m, $COCH_2 \times 2$), 4.61 and 4.89

(each 1H, d, $J$=8.1 Hz, $CH_2Ph$), 6.19 (1H, br d, $J$=7.8 Hz, NH), 7.32 (5H, s, Ph). $^{13}$C-NMR ($CDCl_3$) $\delta$: 99.9 (d, C-1 and s, $Me_2\underline{C}$), 171.3, 174.0 (s, $>C=O \times 2$). *Anal.* Calcd for $C_{46}H_{79}NO_8 \cdot 1/2H_2O$: C, 70.55; H, 10.30; N, 1.79. Found: C, 70.83; H, 10.22; N, 2.17.

**Benzyl 3-*O*-[(*R*)-3-Benzyloxytetradecanoyl]-2-deoxy-2-[(*R*)-3-hexadecanoyloxytetradecanamido]-4,6-*O*-isopropylidene-β-D-glucopyranoside (7)**——DCC (0.161 g, 0.78 mmol) was added to a stirred solution of **6** (0.503 g, 0.65 mmol), (*R*)-3-benzyloxytetradecanoic acid (0.261 g, 0.78 mmol) and 4-dimethylaminopyridine (0.032 g, 0.26 mmol) in dry dichloromethane (5 ml) at 0 °C under nitrogen. The mixture was stirred for 5 h at 0 °C, then at room temperature for 12 h. The resulting suspension was filtered through Celite and evaporated. The residue was chromatographed on silica gel with chloroform–isopropyl ether (20 : 1) to give **7** (0.508 g, 72%) as a syrup. $[\alpha]_D^{20}$ −21.1° ($c$=1.80, $CHCl_3$). IR (neat): 3332 (NH), 1732 (ester), 1659 (amide), 860 ($Me_2C$), 696 (Ph) cm$^{-1}$. $^1$H-NMR ($CDCl_3$) $\delta$: 0.88 (9H, t, $J$=4.9 Hz, $(CH_2)_{10}\underline{CH_3} \times 2$ and $(CH_2)_{14}\underline{CH_3}$), 1.26 (68H, br s, $(\underline{CH_2})_{10}CH_3 \times 2$ and $(\underline{CH_2})_{14}CH_3$), 1.46 and 1.58 (each 3H, s, $\underline{Me_2}C$), 2.05—2.70 (6H, m, $COCH_2 \times 3$), 4.49 (2H, s, $-\underline{CH_2}-CH-OCH_2Ph$), 4.57 and 4.87 (each 1H, d, $J$=7.6 Hz, $-O-CH-OC\underline{H_2}Ph$), 5.89 (1H, br d, $J$=9.0 Hz, NH), 7.29 (10H, s, Ph × 2). $^{13}$C-NMR ($CDCl_3$) $\delta$: 99.7 (d, C-1), 100.7 (s, $Me_2C$), 169.6, 171.5, 173.5 (s, $>C=O \times 3$). *Anal.* Calcd for $C_{67}H_{111}NO_{10}$: C, 73.79; H, 10.26; N, 1.28. Found: C, 74.05; H, 10.12; N, 1.30.

**3-*O*-[(*R*)-3-Benzyloxytetradecanoyl]-2-deoxy-2-[(*R*)-3-hexadecanoyloxytetradecanamido]-4,6-*O*-isopropylidene-α-D-glucopyranose (8)**——Compound **7** (0.105 g, 0.105 mmol) was dissolved in THF–EtOH (1 : 1) (10 ml) and the solution was stirred under atmospheric pressure of $H_2$ in the presence of 10% Pd-on-carbon (87 mg) for 38 h at 30 °C. The catalyst was filtered off and the filtrate was evaporated *in vacuo*. The residue was again dissolved in THF–AcOH (3 : 1) (2.5 ml) and the mixture was kept at 45 °C for 48 h. After removal of the solvent, the residue was chromatographed on neutral aluminium oxide W200 with ether–hexane (10 : 1) to give **8** (0.082 g, 64%) as a syrup. $[\alpha]_D^{23}$ +12.7° ($c$=1.07, $CHCl_3$). IR (neat): 3320 (OH, NH), 1739 (ester), 1659 (amide), 858 ($Me_2C$), 694 (Ph) cm$^{-1}$. $^1$H-NMR ($CDCl_3$) $\delta$: 0.88 (9H, t, $J$=6.0 Hz, $(CH_2)_{10}\underline{CH_3} \times 2$ and $(CH_2)_{14}\underline{CH_3}$), 1.25 (68H, br s, $(\underline{CH_2})_{10}CH_3 \times 2$ and $(\underline{CH_2})_{14}CH_3$), 1.43 (6H, s, $Me_2C$), 2.17—2.73 (6H, m, $COCH_2 \times 3$), 4.50 (2H, s, $-CH_2-CH-OC\underline{H_2}Ph$), 6.14 (1H, br d, $J$=9.0 Hz, NH), 7.31 (5H, s, Ph). $^{13}$C-NMR ($CDCl_3$) $\delta$: 92.3 (d, C-1), 99.8 (s, $Me_2\underline{C}$), 170.1, 172.2, 173.4 (s, $>C=O \times 3$). *Anal.* Calcd for $C_{60}H_{105}NO_{10}$: C, 72.03; H, 10.58; N, 1.40. Found: C, 71.83; H, 10.51; N, 1.48.

**3-*O*-[(*R*)-Benzyloxytetradecanoyl]-2-deoxy-2-[(*R*)-3-hexadecanoyloxytetradecanamido]-4,6-*O*-isopropylidene-α-D-glucopyranosyl-1-phosphate (9)**——*n*-Butyllithium (1.6 M in *n*-hexane) (0.13 ml, 0.21 mmol) was added to a stirred solution of **8** (0.172 g, 0.17 mmol) in dry THF (4.0 ml) at −65 °C under nitrogen. After 2 min, dibenzylphosphorochloridate (0.072 g, 0.26 mmol) in dry THF (0.5 ml) was added at the same temperature and then the mixture was stirred for a further 10 min at −50 °C. The whole mixture was immediately subjected to hydrogenolysis over 10% Pd-on-carbon (80 mg) for 20 h at 30—40 °C under 50 atm to give **9** (0.089 g, 48%) as a syrup after purification by preparative TLC ($CHCl_3$–$CH_3OH$=5 : 1). $[\alpha]_D^{22}$ +17.4° ($c$=0.76, $CHCl_3$). IR (neat): 3450 (OH, NH), 1733 (ester), 1660 (amide), 1260 (>P=O), 865 ($Me_2C$) cm$^{-1}$. $^1$H-NMR ($CDCl_3$) $\delta$: 0.89 (9H, t, $J$=6.1 Hz, $(CH_2)_{10}\underline{CH_3} \times 2$ and $(CH_2)_{14}\underline{CH_3}$), 1.25 (68H, br s, $(\underline{CH_2})_{10}CH_3 \times 2$ and $(\underline{CH_2})_{14}CH_3$), 1.43 (6H, s, $\underline{Me_2}C$), 2.11—2.61 (6H, m, $COCH_2 \times 3$), 7.30 (5H, br s, Ph). *Anal.* Calcd for $C_{60}H_{106}NO_{13}P$: C, 66.70; H, 9.89; N, 1.30. Found: C, 66.39; H, 9.43; N, 1.09.

**2-Deoxy-2-[(*R*)-3-hexadecanoyloxytetradecanamido]-3-*O*-[(*R*)-3-hydroxytetradecanoyl]-4,6-*O*-isopropylidene-α-D-glucopyranosyl-1-phosphate (10)**——Compound **9** (0.038 g, 0.035 mmol) was dissolved in THF–MeOH (1 : 3) (5 ml) and hydrogenolyzed at 30—35 °C under slight pressure in the presence of Pd-black (22 mg) for 48 h. The catalyst was filtered off and the filtrate was evaporated *in vacuo*. The residue was purified by preparative TLC ($CHCl_3$–MeOH=5 : 1) to afford **10** (0.022 g, 63%) as a colorless powder, mp 89—92 °C. $[\alpha]_D^{24}$ +15.0° ($c$=0.44, $CHCl_3$). IR (KBr): 3450 (OH, NH), 1733 (ester) (amide), 1260 (>P=O), 865 ($Me_2C$) cm$^{-1}$. *Anal.* Calcd for $C_{53}H_{100}NO_{13}P \cdot 2H_2O$: C, 62.02; H, 10.21; N, 1.36. Found: C, 61.77; H, 10.23; N, 1.67.

**2-Deoxy-2-[(*R*)-3-hexadecanoyloxytetradecanamido]-3-*O*-[(*R*)-3-hydroxytetradecanoyl]-2-deoxy-α-D-glucopyranosyl-1-phosphate (2)**——A solution of **10** (0.022 g, 0.022 mmol) in acetic acid and water (9 : 1) (0.5 ml) was heated at 85 °C for 15 min. After removal of the solvent the residue was subjected to preparative TLC with $CHCl_3$–$CH_3OH$ (5 : 1) to give **2** (0.019 g, 91%) after lyophilization from dioxane, mp 88—90 °C. $[\alpha]_D^{26}$ +11.7° ($c$=0.24, $CHCl_3$). [lit.[9] $[\alpha]_D^{13}$ +10.0° ($c$=0.53, $CHCl_3$)]. IR (KBr): 3400 (OH, NH), 1735 (ester), 1658 (amide) cm$^{-1}$. Positive FAB MS $(M+Na)^+$ at $m/z$ 973, $(M-H_2PO_4)^+$ at $m/z$ 853, $(M-C_{16}+Na+H)^+$ at $m/z$ 734, $(M-C_{16}-H_2PO_4+H)^+$ at $m/z$ 614, $(M-C_{16}-OH-C_{14}-H_2PO_4+2H)^+$ at $m/z$ 388. *Anal.* Calcd for $C_{50}H_{96}NO_{13}P \cdot 3H_2O$: C, 59.80; H, 10.24; N, 1.39. Found: C, 59.70; H, 9.86; N, 1.35.

**Benzyl 2-[(*R*)-3-Benzyloxytetradecanoyloxytetradecanamido]-2-deoxy-4,6-*O*-isopropylidene-β-D-glucopyranoside (11)**——DCC (0.149 g, 0.72 mmol) was added to a stirred solution of **3** (0.185 g, 0.60 mmol) and (*R*)-3-benzyloxytetradecanoic acid (0.241 g 0.72 mmol) in dry dichloromethane (2 ml) at 0 °C under nitrogen. The mixture was stirred for 5 h at 0 °C, then at room temperature for 18 h. The resulting suspension was filtered through Celite and the filtrate was evaporated. The residue was chromatographed on silica gel with chloroform–acetone (40 : 1) to give **10** (0.273 g, 73%), mp 60—63 °C. IR (neat): 3440 (OH), 3284 (NH), 1652 (amide), 861 ($Me_2C$), 692 (Ph) cm$^{-1}$. *Anal.* Calcd for $C_{37}H_{55}NO_7$: C, 71.01; H, 8.86; N, 2.24. Found: C, 70.88; H, 8.75; N, 2.34.

**Benzyl 2-[(*R*)-3-Benzyloxytetradecanamido]-2-deoxy-3-*O*-[(*R*)-3-hexadecanoyloxytetradecanoyl]-4,6-*O*-iso-**

**propylidene-β-D-glucopyranoside (12)**——DCC (0.064 g, 0.31 mmol) was added to a stirred solution of **11** (0.162 g, 0.26 mmol), (*R*)-3-hexadecanoyloxytetradecanoic acid (0.150 g, 0.31 mmol) and DMAP (0.013 g, 0.11 mmol) in dry dichloromethane (2 ml) at 0 °C under nitrogen. The mixture was stirred for 5 h at 0 °C, then at room temperature for 12 h. The resulting suspension was filtered through Celite and the filtrate was evaporated. The residue was chromatographed on silica gel with chloroform–isopropyl ether (10 : 1) to give **11** (0.253 g, 90%) as a syrup. $[\alpha]_D^{22}$ −25.6° ($c$=2.05, $CHCl_3$). *Anal.* Calcd for $C_{67}H_{111}NO_{10}$: C, 73.79; H, 10.26; N, 1.28. Found: C, 73.63; H, 10.30; N, 1.18.

**Benzyl 2-Deoxy-3-*O*-[(*R*)-3-hexadecanoyloxytetradecanoyl]-2-[(*R*)-3-hydroxytetradecanamido]-4,6-*O*-isopropylidene-β-D-glucopyranoside (13)**——Compound **12** (0.090 g, 0.083 mmol) was dissolved in THF (6 ml) and stirred under 50 atm of $H_2$ in the presence of 10% Pd-on-carbon (65 mg) for 24 h at 30 °C. The catalyst was filtered off and the filtrate was evaporated *in vacuo*. The residue was chromatographed on neutral aluminium oxide W200 with ether–hexane (2 : 1) to give **13** (0.060 g, 68%), mp 79—83 °C. $[\alpha]_D^{20}$ −27.5° ($c$=0.36, $CHCl_3$). IR (neat): 3296 (OH, NH), 1739 (ester), 1655 (amide), 860 ($Me_2C$) $cm^{-1}$. $^1$H-NMR ($CDCl_3$) $\delta$: 0.87 (9H, t, $J$=4.4 Hz, $(CH_2)_{10}CH_3$ × 2 and $(CH_2)_{14}CH_3$), 1.25 (68H, brs, $(CH_2)_{10}CH_3$ × 2 and $(CH_2)_{14}CH_3$), 1.43 (6H, s, $Me_2C$), 2.50—2.66 (6H, m, $COCH_2$ × 3), 4.58 and 4.87 (each 1H, d, $J$=11.7 Hz, -O-CH-$OCH_2$Ph), 6.13 (1H, brd, $J$=8.6 Hz, NH), 7.30 (5H, brs, Ph). $^{13}$C-NMR ($CDCl_3$) $\delta$: 99.7 (d, C-1), 100.5 (s, $Me_2C$). *Anal.* Calcd for $C_{60}H_{105}NO_{10}\cdot 5H_2O$: C, 66.08; H, 10.63; N, 1.28. Found: C, 66.09; H, 10.72; N, 1.63.

**Acknowledgment** The authors are indebted to Dr. K. Narita and the staff of the Analysis Center of this college for microanalysis. This work was supported in part by a Grant-in-Aid from Tokyo Biochemical Research Foundation.

## References

1) *a*) T. Takahashi, C. Shimizu, S. Nakamoto, K. Ikeda, and K. Achiwa, *Chem. Pharm. Bull.*, **33**, 1760 (1985); *b*) S. Nakamoto, T. Takahashi, K. Ikeda, and K. Achiwa, *ibid.*, **33**, 4098 (1985); *c*) T. Shimizu, S. Akiyama, T. Masuzawa, Y. Yanagihara, S. Nakamoto, T. Takahashi, K. Ikeda, and K. Achiwa, *ibid.*, **33**, 4621 (1985); *d*) K. Ikeda, S. Nakamoto, T. Takahashi, and K. Achiwa, *Carbohydr. Res.*, **145**, C5 (1986); *e*) T. Takahashi, S. Nakamoto, K. Ikeda, and K. Achiwa, *Tetrahedron Lett.*, **27**, 1819 (1986); *f*) S. Nakamoto and K. Achiwa, *Chem. Pharm. Bull.*, **34**, 2302 (1986); *g*) T. Shimizu, S. Akiyama, T. Masuzawa, Y. Yanagihara, S. Nakamoto, and K. Achiwa, *ibid.*, **34**, 2310 (1986); *h*) T. Shimizu, S. Akiyama, T. Masuzawa, Y. Yanagihara, S. Nakamoto, T. Takahashi, K. Ikeda, and K. Achiwa, *ibid.*, **34**, 5169 (1986); *i*) T. Shimizu, S. Akiyama, T. Masuzawa, Y. Yanagihara, S. Nakamoto, and K. Achiwa, *ibid.*, **35**, 873 (1987); *j*) K. Ikeda, T. Takahashi, H. Kondo, and K. Achiwa, *ibid.*, **35**, 1311 (1987); *k*) K. Ikeda, T. Takahashi, C. Shimizu, S. Nakamoto, and K. Achiwa, *ibid.*, **35**, 1383 (1987); *l*) T. Shimizu, S. Akiyama, T. Masuzawa, Y. Yanagihara, K. Ikeda, T. Takahashi, H. Kondo, and K. Achiwa, *Microbiol. Immunol.*, **31**, 381 (1987); *m*) T. Shimizu, S. Akiyama, T. Masuzawa, Y. Yanagihara, S. Nakamoto, and K. Achiwa, *Infection and Immunology*, **55**, 2287 (1987).
2) O. Westphal and O. Lüderitz, *Angew. Chem.*, **66**, 407 (1954); O. Lüderitz, C. Galanos, V. Lehmann, H. Mayer, E. T. Rietschel, and J. Weckesser, *Naturwissenschaften*, **65**, 578 (1978).
3) *a*) K. Takayama, N. Qureshi, and P. Mascagni, *J. Biol. Chem.*, 12801 (1983); *b*) M. Imoto, S. Kusumoto, T. Shiba, H. Naoki, T. Iwashita, E. Th. Rietschel, H. W-. Wollenweber, C. Galanos, and O. Lüderitz, *Tetrahedron Lett.*, **24**, 4017 (1983); *c*) U. Seydel, B. Lindner, H. W-. Wollenweber, and E. T. Rietschel, *Eur. J. Biochem.*, **145**, 505 (1984).
4) M. Imoto, H. Yoshimura, M. Yamamoto, S. Kusumoto, and T. Shiba, *Tetrahedron Lett.*, **25**, 2667 (1984); M. Imoto, H. Yoshimura, N. Sakaguchi, S. Kusumoto, and T. Shiba, *ibid.*, **26**, 1545 (1985).
5) K. Takayama, N. Qureshi, P. Mascagni, L. Anderson, and C. R. H. Raetz, *J. Biol. Chem.*, **258**, 14245 (1983).
6) P. H. Gross and R. W. Jeanloz, *J. Org. Chem.*, **32**, 2759 (1967).
7) M. Inage, H. Chaki, S. Kusumoto, and T. Shiba, *Chem. Lett.*, **1982**, 1281.
8) J. C. Dittmer and R. L. Lester, *J. Lipid Res.*, **5**, 126 (1964).
9) S. Kusumoto, M. Yamamoto, and T. Shiba, *Tetrahedron Lett.*, **25**, 3727 (1984).

[Chem. Pharm. Bull. 35(11)4442—4453(1987)]

# Studies on Griseolic Acid Derivatives. V.[1] Synthesis and Phosphodiesterase Inhibitory Activity of Substituted Derivatives of the Hydroxy Group at the 2′- or 7′-Position in Griseolic Acid

YOSHINOBU MUROFUSHI,[a] MISAKO KIMURA,[a] YASUTERU IIJIMA,[b] MITSUO YAMAZAKI,[b] and MASAKATSU KANEKO*,[a]

*Chemical Research Laboratories,[a] Biological Research Laboratories,[b] Sankyo Co., Ltd., 2–58, Hiromachi 1-chome, Shinagawa-ku, Tokyo 140, Japan*

(Received April 10, 1987)

Substituted derivatives of the hydroxy group at the 2′- or 7′-position in griseolic acid (**1**) were synthesized by selective substitution in order to study the relationship between structure and inhibitory activity against adenosine 3′,5′-cyclic monophosphate (cAMP) or guanosine 3′,5′-cyclic monophosphate (cGMP) phosphodiesterase (PDE). All of the derivatives which had a configurationally inverted substituent at the 2′-position instead of the hydroxy group were almost equal to natural griseolic acid in cAMP PDE inhibitory activity, except when the substituent was an amino group. On the other hand, substitution of 7′-OH with inversion tended to reduce the inhibitory activity a little.

**Keywords**——griseolic acid; 2′-substituted griseolic acid derivatives; 7′-substituted griseolic acid derivatives; adenosine 3′,5′-cyclic monophosphate; guanosine 3′,5′-cyclic monophosphate; phosphodiesterase; cAMP phosphodiesterase inhibitory activity; cGMP phosphodiesterase inhibitory activity

## Introduction

Severin *et al.*[2] have reported the structure–activity relationship between adenosine 3′,5′-cyclic monophosphate (cAMP) derivatives and their inhibitory activity against phosphodiesterase (PDE). However, this inhibitory activity depends on two parameters; namely, the affinity of the cAMP derivative for the receptor site of PDE and the hydrolyzability by PDE. Therefore, the relationship based only on the affinity for the receptor site cannot be investigated. On the other hand, griseolic acid (**1**) cannot be a substrate of PDE, but inhibits the hydrolyses of cAMP and guanosine 3′,5′-cyclic monophosphate (cGMP) competitively.

Consequently, we planned to study the inhibitory activity against PDE using griseolic acid derivatives and thus to establish the structure–activity relationship based only on the affinity. We have already reported synthetic procedures for griseolic acid derivatives which are partially or fully acylated at the $N^6$-, $O^{2'}$- or $O^{7'}$-position and the PDE inhibitory activity of the products.[1] It was revealed that acylation of the amino group of the adenine moiety greatly reduced the inhibitory activity. On the other hand, acylation of the hydroxy groups at the 7′- and 2′-positions had relatively little effect on the inhibitory activity.

In the present work, we have synthesized derivatives of griseolic acid (**1**) with various substituents at the 2′- or 7′-position instead of OH, and have investigated the structure–activity relationship for PDE inhibitory activity.

## Results and Discussion

### Synthesis

The following methods are available introducing a variety of substituents into the sugar

moiety of a purine-type nucleoside[4]: (a) by using 2-acetoxyisobutylyl bromide,[5] (b) by using a *ortho* ester as an intermediate,[6] (c) by using a cyclonucleoside, in which the 8-position and sugar moiety are cyclized, as an intermediate,[7] (d) by using a 2′,3′-epoxide as an intermediate, (e) *via* a methanesulfonylated or toluenesulfonylated compound,[8,9] (f) *via* a trifluoromethanesulfonylated compound,[9-11] (g) by direct halogenation, (h) *via* a ketone which is synthesized by oxidation of the hydroxy group, (i) by addition across a double bond which is introduced by dehydration.[9] Methods (a) and (b) can introduce only a restricted range of substituents. In method (c), the purine compound must be substituted at the 8-position first, so this method needs many steps and is not convenient. Moreover, this method cannot give substitution at the 7′-position. Method (d) cannot be used because griseolic acid does not have a hydroxy group at the 3′-position and at the position next to 7′. Method (e) is inferior to method (f) in reactivity. As for method (g), the reactivity is low and only a halogen atom can be introduced. Method (h) can only introduce a hydroxy group. Method (i) cannot be employed as it is difficult to introduce a double bond into griseolic acid because of structural strain. For the above reasons, we synthesized the derivatives substituted at the 2′- or 7′-position according to method (f).

The structures of all derivatives were confirmed by nuclear magnetic resonance (NMR) spectroscopy and elemental analyses unless otherwise stated and yields were calculated based on the immediately preceding starting material.

**Synthesis of Derivatives Substituted at the 2′-Position**

We synthesized these derivatives according to the method shown in Fig. 1. Griseolic acid (**1**) was converted to the $O^{2'}$-benzoylated derivative (**2**) by the method already reported.[1] Then, we attempted to synthesize the dimethyl ester derivative (**3**). Takahashi *et al.* have reported the esterification of the carboxy group in griseolic acid with diazomethane,[12] but, this method is not suited to mass production because the $O^{2'}$-methylated derivative is formed as a by-product. As a result of detailed investigation using griseolic acid as a starting material, we found that the dimethyl ester could be synthesized in good yield by allowing griseolic acid to stand with benzoyl chloride in methanol. This reaction was thought to occur by way of the mixed anhydride followed by methanolysis. Thus, we synthesized **3** in good yield from **2** using this method. The $O^{7'}$-pyranyl derivative (**4**) was obtained in 88% yield by reacting **3** with 2,3-dihydropyran in the presence of *p*-toluenesulfonic acid in dioxane.[13] The methyl ester function was not considered to be a good protecting group in these syntheses, because the desired compounds, with various substituents at the 2′-position in griseolic acid, might not be obtained because of decomposition at the stage of removing the methyl groups. We therefore selected the benzhydryl group, which was easily removed under acidic conditions, as the protecting group. Compound **4** was allowed to stand in 1 N aqueous sodium hydroxide to remove the benzoyl group at the 2′-position and the methyl groups. Except in salt form, this compound is not stable and the pyranyl group was easily lost. Consequently, this compound was subjected, without purification, to benzhydrylation with diphenyldiazomethane to give **5** in 46% yield. Compound **5** was allowed to react with trifluoromethanesulfonyl chloride in the presence of dimethylaminopyridine to give **6** in 71% yield. Compound **6** was allowed to react with sodium azide in the presence of hexamethylphosphoramide and the pyranyl group of this compound **7** was converted to give **8** in 96% yield.[14] This compound was visualized on a thin the benzhydryl groups were removed to give **7** in 18% yield. According to Fukukawa *et al.*,[11] compound **7** was converted to give **8** in 96% yield.[14] This compound was visualized on a thin layer chromatography (TLC) plate by spraying with a solution of cysteine–sulfuric acid followed by heating. Compound **6** was allowed to react with anhydrous lithium halogenide (*e.g.*, lithium iodide, lithium bromide, and lithium chloride) in hexamethylphosphoramide and the pyranyl group and the benzhydryl groups were removed in the same manner as

described above to give **10a**, **10b**, and **10c** in 23.4%, 36.5% and 14.2% yields through **9a**, **9b**, and **9c**, respectively.

Compound **9a** was allowed to react with *n*-butyltin hydride in the presence of azoisobutyronitrile (AIBN) in benzene under reflux, and the benzhydryl groups were removed in the same manner as described above to give **11** in 69.2% yield (Fig. 1).

If an acetoxy group could be introduced at the 2′-position, the corresponding arabino-type derivative could be synthesized by removing the acetyl group. Thus, we investigated the substitution reaction of the acetoxy group with sodium acetate under various reaction conditions, but all the reaction mixtures turned brown and complicated decompositions occurred without giving the desired compound. Furthermore, all efforts to synthesize an arabino-type compound with sodium benzoate instead of sodium acetate were in vain, because the same type of decomposition again occurred. This complicated decomposition was thought to result from the acetoxy group, substituted at the 2′-position, migrating toward the

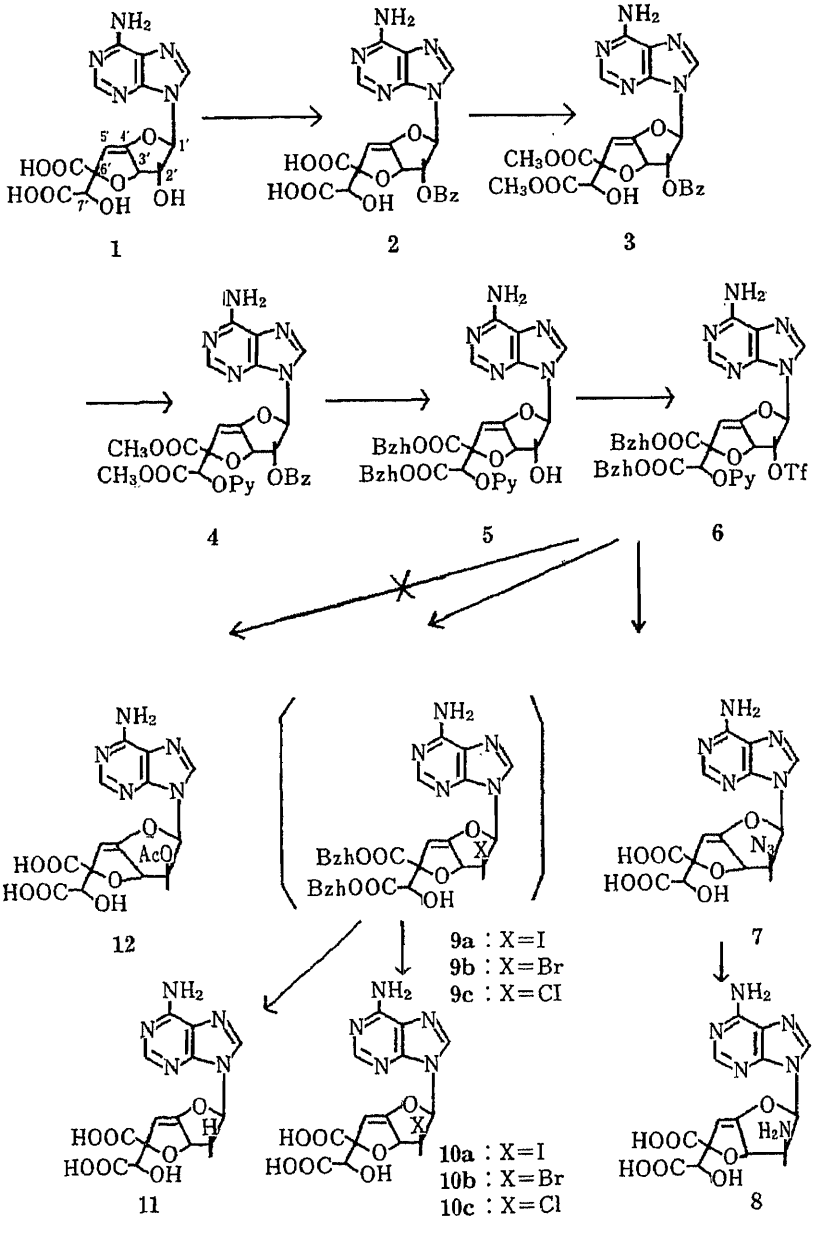


Fig. 1

3′- or 4′-position through a mechanism similar to that of the acyl migration reaction.

**Synthesis of Derivatives Substituted at the 7′-Position**

We synthesized these derivatives according to the methods shown in Figs. 2 and 3. Compound **13**, which has already been reported,[1] was allowed to react with trifluoromethanesulfonyl chloride in the presence of dimethylaminopyridine in methylene chloride to give **15** in 80% yield (Figs. 2 and 3).

Compound **15** was allowed to react with well-dried sodium azide in the presence of hexamethylphosphoramide to give **16** in 55% yield. The benzhydryl groups of compound **16** were removed with trifluoroacetic acid and the benzoyl group was removed by using a 20% methanolic solution of ammonia to give **17** in 49% yield.

According to the manner of Fukukawa *et al.*,[11] compound **16** was converted to **18** in 43% yield. This compound was visualized on a TLC plate by spraying with a solution of cysteine–sulfuric acid followed by heating. The benzhydryl group and the benzoyl group of compound **18** were removed in the same manner as described above to give **19** in 66% yield. Compound **15** was allowed to react with well-dried anhydrous lithium chloride or lithium bromide in anhydrous dimethylformamide under protection from moisture to give **20a** in 70% yield or **20b** in 53% yield, and each compound was deprotected in the conventional manner to give **21a** in 82% yield or **21b** in 57% yield. Compound **20b** was allowed to react with *n*-butyltin hydride (2.5 eq) in the presence of AIBN in anhydrous benzene, after which the benzoyl group and the benzhydryl groups were deprotected in the conventional manner to give **22** in 82% yield. This compound was identical with the natural product, the structure of which was

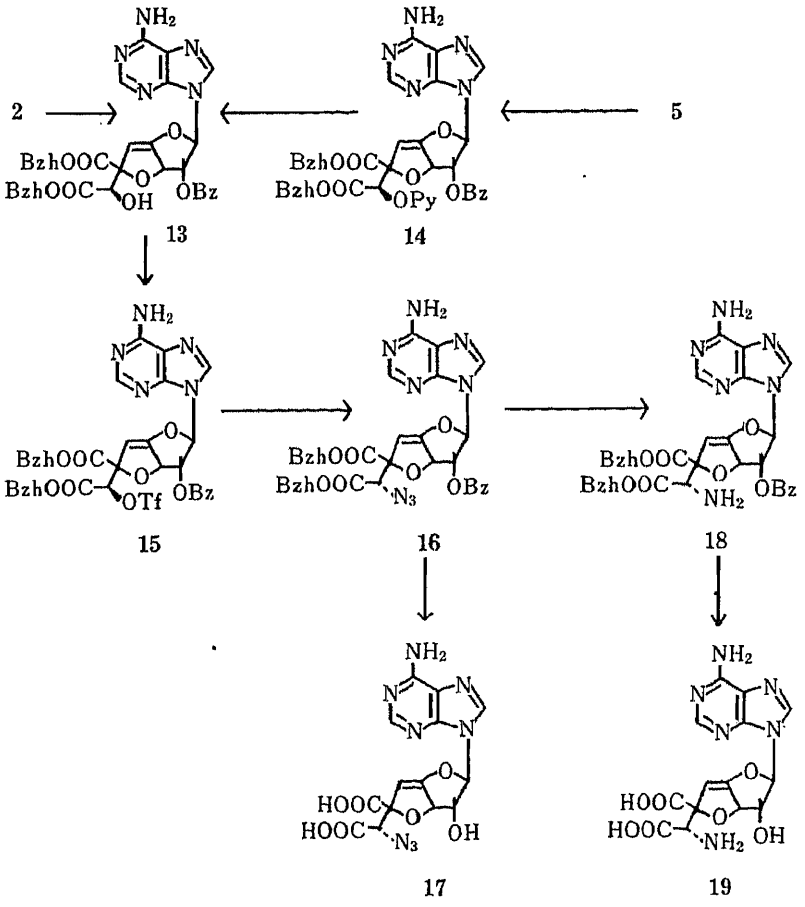


Fig. 2

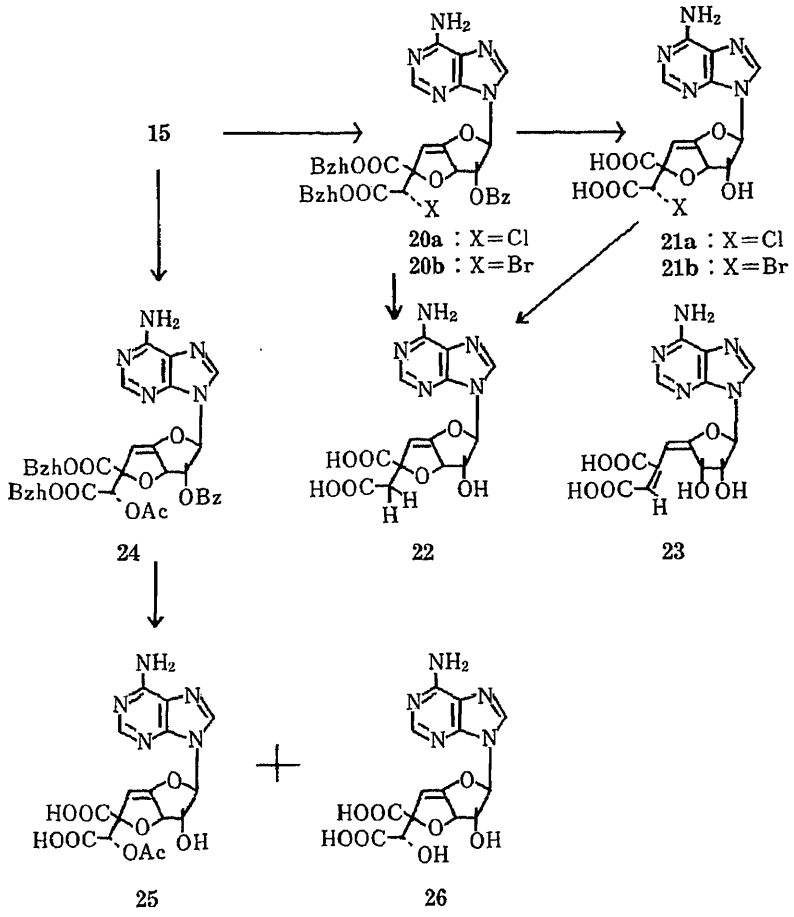


Fig. 3

determined by X-ray analysis, in all physical properties examined. Furthermore, compound **22** was also obtained by reducing **21b** with 80% aqueous acetic acid and zinc powder (16% yield).[15] This poor yield was a result of the generation of compound **23** as a by-product. The mechanism for the formation of **23** was thought to be that the furan ring was cleaved by the bromo atom in a $\beta$-elimination mechanism to generate the double bond between the 6′- and 7′-positions. Compound **24** was obtained by reacting **15** with well-dried sodium acetate which was dried by melting, in acetic acid, followed by protection with diphenyldiazomethane (68% yield). The stereoisomer of compound **1** (30%) was obtained by removing the benzhydryl groups of **24** with trifluoroacetic acid followed by treatment with a 20% methanolic solution of ammonia overnight. In this reaction, compound **25**, in which the acetyl group at the 7′-position was configurationally inverted, was also obtained in 18% yield.

**PDE-Inhibitory Activity**

On the whole, the PDE-inhibitory activities of the $\beta$-oriented derivatives at the 2′-position were almost equal to that of griseolic acid, and those of the substituted derivatives with inverted configuration at the 7′-position were a little lower than that of griseolic acid (Tables I and II).

The stereoisomer of griseolic acid (**26**) showed almost the same inhibitory activity against PDE as griseolic acid (**1**). These facts suggest that the configuration and the substituent at the 7′-position do not influence the affinity for the receptor site of PDE, and the PDE probably only recognizes the carboxy group of the sugar moiety of griseolic acid. Characteristic features were that the 2′-*epi*-bromo derivative (**9b**) showed a 1.7 times stronger activity than griseolic

TABLE I. PDE-Inhibitory Activity of 2′-Substituted Derivatives of Griseolic Acid

| Compound No. | | 1 | 7 | 8 | 10a | 10b | 10c | 11 |
|---|---|---|---|---|---|---|---|---|
| 2′-Substituent | | OH | $N_3$ | $NH_2$ | I | Br | Cl | H |
| $IC_{50}$ ($\mu$M) | cAMP | 0.16 | 0.45 | 3.20 | 0.40 | 0.09 | 0.15 | 0.19 |
| | cGMP | 0.63 | 6.40 | 12.7 | 2.80 | 4.10 | 2.50 | 1.10 |
| | cAMP/cGMP | 0.25 | 0.07 | 0.25 | 0.14 | 0.02 | 0.06 | 0.17 |

TABLE II. PDE-Inhibitory Activity of 7′-Substituted Derivatives of Griseolic Acid

| Compound No. | | 17 | 19 | 21a | 21b | 22 | 25 | 26 |
|---|---|---|---|---|---|---|---|---|
| 7′-Substituent | | $N_3$ | $NH_2$ | Cl | Br | H | OAc | OH |
| $IC_{50}$ ($\mu$M) | cAMP | 4.40 | 2.00 | 1.50 | 3.40 | 0.16 | 0.76 | 0.22 |
| | cGMP | 13.0 | 4.20 | 14.8 | 19.0 | 0.63 | 2.80 | 1.05 |
| | cAMP/cGMP | 0.34 | 0.48 | 0.10 | 0.18 | 0.25 | 0.27 | 0.21 |

acid and the 2′-*epi*-amino-derivative (**8**) showed a 1/50 weaker activity. Accordingly, electron-withdrawing groups seemed to be better than electron-donating groups as the $\beta$-oriented substituent at the 2′-position (Tables I and II).

## Conclusion

Considered as a whole, the inhibitory activities of the 2′$\beta$-substituted derivatives were almost equal to that of griseolic acid itself. However, the compound in which the substituent at the 2′-position was an amino group showed a weaker activity. Consequently, it was suggested that electron-withdrawing groups are more suitable for the 2′$\beta$-substituent than electron-donating groups for inhibitory activity. An electron-withdrawing 2′$\beta$-substituent may interact with the base, changing the conformation to one better suited for approaching the receptor site of PDE. On the other hand, substitution of 7′-OH with inverted configuration tended to reduce the inhibitory activity a little. Accordingly, it could be considered that the substituents with inverted configuration at the 7′-position show decreased affinity to the PDE because of the change in stereostructure around the 7′-position. From this result, it was suggested that the hydroxy groups in the sugar moiety do not play a significant role in interaction with the receptor site of PDE. This conclusion is consistent with that of Severin *et al.*[2]

### Experimental

**General**——Melting points were determined on a Yanagimoto melting point apparatus and are uncorrected. NMR spectra were obtained with a Varian EM-390 spectrometer (90 MHz) and the chemical shifts are expressed in ppm from tetramethylsilane as internal standard: s, singlet; d, doublet; t, triplet; dd, doublet of doublets; m, multiplet; br d, broad doublet; br m, broad multiplet; br s, broad singlet. Ultraviolet (UV) spectra were obtained with a Hitachi 200-20 spectrophotometer. TLC was carried out on Merck Silica gel $F_{254}$ precoated TLC plates with 0.25-mm layer thickness, and spots were visualized by UV irradiation or by spraying with 30% sulfuric acid followed by heating. Ordinary chromatography was performed by the rapid chromatography method[16] on Merck silica gel (Kieselgel 60, Art 9385).

**Dimethyl $O^{2'}$-Benzoylgriseolate (3)**——$O^{2'}$-Benzoylgriseolic acid (28.6 g, 59.2 mmol)[11] was suspended in 500 ml of methanol, and 41.2 ml (355 mmol) of benzoyl chloride was added dropwise over a period of about 15 min under ice-cooling and stirring. The mixture was stirred for an additional 1 h under the same conditions and then stirred for another 26 h at room temperature. The solvent was distilled off and the residue was dissolved in a mixture of ethyl acetate and 10% (w/v) aqueous sodium bicarbonate. The organic layer was separated from the aqueous layer, washed

with water, and dried over anhydrous magnesium sulfate, and the solvent was distilled off. The residue was dissolved in a mixture of ethyl acetate and ethanol and the solvents were distilled off, whereupon crystals were precipitated. These crystals were collected by filtration in a yield of 13.8 g (45.6%). Further, the mother liquor was concentrated to approximately 100 ml and poured into 1 l of hexane with stirring. The precipitated powder was collected by filtration and purified by silica gel column chromatography (5% methanol–methylene chloride) to yield 12.5 g of **3**. UV $\lambda_{max}^{methanol}$ nm ($\varepsilon$): 229.5 (19300), 256.5 (17400). NMR (DMSO-$d_6$) $\delta$: 8.41 (1H, s), 8.30 (1H, s), 7.02 (1H, s, 1′-H), 5.86 (1H, d, $J$=5.4 Hz, 2′-H), 6.40 (1H, dd, $J$=5.4, 2.4 Hz, 3′-H), 5.25 (1H, d, $J$=2.4 Hz, 5′-H), 4.65 (1H, s, 7′-H), 7.3—8.3 (7H, m, benzoyl+$NH_2$), 3.58 (3H, s, $CH_3$), 3.76 (3H, s, $CH_3$).

**Dimethyl $O^{2'}$-Benzoyl-$O^{7'}$-(tetrahydropyran-2-yl)griseolate (4)**——Compound **3** (25.6 g, 50 mmol) was suspended in 250 ml of dioxane and 10.5 g (55.2 mmol) of *p*-toluenesulfonic acid was added to the suspension to yield a clear yellow solution. 2,3-Dihydropyran (137 ml, 1.5 mol) was added to this clear solution and the mixture was stirred for 2.5 h at room temperature. Anhydrous potassium carbonate was added to the reaction mixture and the solvent was distilled off. The residue was dissolved in a mixture of ethyl acetate and saturated aqueous sodium bicarbonate. The organic layer was separated from the aqueous layer, washed with water, and dried over anhydrous magnesium sulfate. The drying agent was removed by filtration, after which the solvent was distilled off. Hexane was added to the residue and the supernatant was removed. The remaining solution was purified by silica gel column chromatography (5% methanol–methylene chloride) to yield 26.1 g (87.6%) of **4** as a colorless foam. UV $\lambda_{max}^{methanol}$ nm ($\varepsilon$): 230 (18100), 257 (17000). NMR (DMSO-$d_6$) $\delta$: 8.40 (1H, s), 8.28 (1H, s), 7.07 (1H, s, 1′-H), 5.84 (1H, d, $J$=5.4 Hz, 2′-H), 6.41 (1H, dd, $J$=5.4, 2.4 Hz, 3′-H), 5.19, 5.36 (1H, d, $J$=2.4 Hz, 5′-H), 4.54, 4.81 (1H, s, 7′-H), 7.3—8.3 (7H, m, benzoyl+$NH_2$), 3.06 (3H, s, $CH_3$), 3.76 (3H, s, $CH_3$), 1.0—2.0 (9H, br m, tetrahydropyranyl).

**Dibenzhydryl $O^{7'}$-(Tetrahydropyran-2-yl)griseolate (5)**——Methanol (175 ml) and 175 ml of 1 N aqueous sodium hydroxide were added to 26.1 g (43.8 mmol) of compound **4**, the mixture was reacted for about 20 h with stirring at room temperature, and the pH of the solution was adjusted to about 7.0. The solvent was distilled off at a temperature below 30 °C and the residue was dissolved in 500 ml of acetone and 100 ml of water. Three equivalents of diphenyldiazomethane was added to this solution. The pH of the mixture was adjusted to 1.5 with 3 N hydrochloric acid and stirring was continued (the pH gradually rose to 3) while protecting the mixture from light. After 2.5—4 h, the solvent was distilled from the mixture. The residue was dissolved in a mixture of ethyl acetate and water. The organic layer was separated from the aqueous layer, washed with water, and dried over anhydrous magnesium sulfate. The drying agent was removed by filtration and the residue was purified by silica gel chromatography (5% methanol–methylene chloride) to yield 16.0 g (46.0%) of **5** as a colorless foam. UV $\lambda_{max}^{methanol}$ nm ($\varepsilon$): 257 (17000). NMR (DMSO-$d_6$) $\delta$: 8.36 (1H, s), 8.17 (1H, s), 4.67 (1H, d, $J$=5.4 Hz, 2′-H), 6.55 (1H, s, 1′-H), 6.3—6.5 (1H, br m, 3′-H), 5.20, 5.30 (1H, d, $J$=2.4 Hz, 5′-H), 5.00, 4.83 (1H, s, 7′-H), 1.3—2.0 (9H, br m, tetrahydropyranyl), 7.2—7.6 (22H, m, benzhydryl+$NH_2$), 6.80 (2H, s, CH).

**Dibenzhydryl $O^{7'}$-(Tetrahydropyran-2-yl)-$O^{2'}$-trifluoromethanesulfonylgriseolate (6)**——Compound **5** (12.8 g, 16.1 mmol) and 5.9 g (48.3 mmol) of 4-(dimethylamino)pyridine were dissolved in 300 ml of dry methylene chloride. Trifluoromethanesulfonyl chloride (5.17 ml, 48.6 mmol) was added to the solution under a stream of nitrogen gas and under cooling with dry ice/acetone. The mixture was then stirred at room temperature for 2—2.5 h, after which ice-water was added to the reaction mixture. The organic layer was separated from the aqueous layer, washed successively with saturated aqueous sodium bicarbonate and saturated aqueous sodium chloride, and dried over anhydrous magnesium sulfate. The drying agent was removed by filtration and the solvent was distilled off. The residue was purified by silica gel column chromatography (5% methanol–methylene chloride) to yield 10.54 g (70.6%) of **6**. UV $\lambda_{max}^{methanol}$ nm ($\varepsilon$): 257.5 (17600). NMR (DMSO-$d_6$) $\delta$: 8.40 (1H, s), 8.13 (1H, s), 7.1—7.8 (23H, m, 1′-H, overlapping with benzhydryl+$NH_2$), 6.10 (1H, d, $J$=5.4 Hz, 2′-H), 6.7—6.9 (3H, m, 3′-H, overlapping with CH), 5.29, 5.53 (1H, d, $J$=2.4 Hz, 5′-H), 4.90, 5.08 (1H, s, 7′-H), 1.0—2.0 (9H, br m, tetrahydropyranyl).

***S*-2′-Azido-2′-deoxygriseolic Acid (7)**——Compound **6** (2.0 g, 2.2 mmol) was dissolved in 8 ml of hexamethylphosphoric triamide. Sodium azide (0.28 g, 4.3 mmol) was added to the solution and the mixture was stirred for 3 h at room temperature. The reaction mixture was poured into ice-water containing sodium chloride. The precipitate was collected by filtration, washed with water, dissolved in ethyl acetate, and dried over anhydrous magnesium sulfate. The solvent was distilled off and the residue was purified by silica gel chromatography (3% methanol–methylene chloride) to yield 0.86 g (1.07 mmol) of dibenzhydryl *S*-2′-azido-2′-deoxy-$O^{7'}$-(tetrahydropyran-2-yl)griseolate. This compound (0.86 g, 1.07 mmol) and 0.13 g (0.52 mmol) of pyridine *p*-toluenesulfonate were dissolved in 1 ml of methylene chloride and 5 ml of ethanol and the mixture was heated at 50 °C for 12 h. A further 0.13 g (0.52 mmol) of pyridine *p*-toluenesulfonate was added and the mixture was allowed to react for a further 17 h at 60 °C. The solvent was distilled off and the residue was dissolved in methylene chloride. The resulting solution was washed with water and dried over anhydrous magnesium sulfate. The solvent was then distilled off and the residue was purified by silica gel chromatography (5% methanol–methylene chloride) to yield 0.36 g of dibenzhydryl *S*-2′-azido-2′-deoxygriseolate. This compound (0.36 g, 0.49 mmol) was dissolved in 3 ml of anisole and 3 ml of trifluoroacetic acid was added under ice-cooling. The mixture was left standing for 15 min. Dry toluene was then added and the solvent was distilled from the reaction mixture. Acetone and toluene were added to the residue and then distilled off. This process was repeated twice. The residue was dissolved in a small quantity of acetone and hexane was added to precipitate a powder. The

powder was collected by filtration and dissolved in saturated aqueous sodium bicarbonate. The pH of this solution was adjusted to 2.4 and the solution was purified by Rp-8 prepacked column (Merck) chromatography (5% (v/v) aqueous acetonitrile containing 0.02% (v/v) acetic acid) to yield 0.16 g (18.3%) of **7**. UV $\lambda_{max}$ nm ($\varepsilon$): ($H_2O$) 257 (15800); (0.1 N NaOH) 258 (16300); (0.1 N HCl) 255.5 (16000). IR: 2125 $cm^{-1}$ ($N_3$). NMR (DMSO-$d_6$) $\delta$: 8.29 (1H, s), 8.20 (1H, s), 7.06 (1H, d, $J$=8.3 Hz, 1'-H), 4.8—5.2 (2H, m, 2'- and 5'-H), 6.08 (1H, dd, $J$=9.0, 2.4 Hz, 3'-H), 4.51 (1H, s, 7'-H), 7.69 (2H, br s, $NH_2$). $[\alpha]_D^{20}$ −53.8° ($c$=0.5, DMSO).

***S*-2'-Amino-2'-deoxygriseolic Acid (8)**——Water (1.5 ml) and 6 ml of pyridine were added to compound **7** (0.14 g, 0.25 mmol). The air in the flask was replaced by nitrogen gas and then the solution was saturated with hydrogen sulfide at room temperature. The container was tightly stoppered and left standing at room temperature for 7—8 h and then at 5 °C overnight. The solvent was distilled off, and water was added to the residue, and then distilled off. This process was repeated and the residue was dissolved in 0.1 N hydrochloric acid. The insoluble matter was removed by filtration and the pH of the filtrate was adjusted to 2.3 with saturated aqueous sodium bicarbonate. The solution was purified by chromatography through an Rp-8 prepacked column (Merck) (3% (v/v) acetonitrile–0.02% (v/v) acetic acid–96.98% (v/v) water) to yield 93 mg (96%) of **8**. UV $\lambda_{max}$ nm ($\varepsilon$): ($H_2O$) 256.5 (15600); (0.1 N NaOH) 258 (16300); (0.1 N HCl) 254 (16400). NMR (DMSO-$d_6$) $\delta$: 8.24 (1H, s), 8.20 (1H, s), 6.76 (1H, br d, 1'-H), 3.7—4.44 (1H, br s, overlapping with $H_2O$, 2'-H), 5.86 (1H, br m, 3'-H), 4.95 (1H, d, $J$=2.4 Hz, 5'-H), 4.44 (1H, s, 7'-H), 7.34 (2H, br s, $NH_2$). $[\alpha]_D^{20}$ −73.6° ($c$=0.5, DMSO).

**2'-Deoxy-*S*-2'-iodogriseolic Acid (10a)**——Compound **6** (1.37 g, 1.48 mmol) was dissolved in 4 ml of hexamethylphosphoric triamide, and 0.8 g (6 mmol) of anhydrous lithium iodide was added. The mixture was left standing for 5—6 h at room temperature. A further 1 ml of hexamethylphosphoric triamide was added to the reaction mixture and the mixture was allowed to react for 6—7 h on an ultrasonic bath (up to 40 °C). The reaction mixture was then poured into ice-water. The precipitate was collected by filtration, washed with water, and dissolved in ethyl acetate; this solution was dried over anhydrous magnesium sulfate. The solvent was distilled off and the residue was purified by silica gel column chromatography (3% methanol–methylene chloride) to yield 0.5 g of dibenzhydryl 2'-deoxy-*S*-2'-iodo-*O*$^{7'}$-(tetrahydropyran-2-yl)griseolate. A 0.5 g (0.56 mmol) portion of this compound was dissolved in 1 ml of methylene chloride, and 0.14 g (0.56 mmol) of pyridine *p*-toluenesulfonate and 10 ml of ethanol were added to the solution. The mixture was heated at 60 °C for 8 h. The solvent was distilled from the reaction mixture and the residue was dissolved in a mixture of ethyl acetate and water. The organic layer was separated from the aqueous layer and dried over anhydrous magnesium sulfate. The solvent was then distilled off and the residue was purified by silica gel column chromatography (5% methanol–methylene chloride) to yield 0.35 g of dibenzhydryl 2'-deoxy-*S*-2'-iodogriseolate. A 0.32 g (0.39 mmol) portion of this compound was dissolved in 3 ml of anisole, to which 3 ml of trifluoroacetic acid was then added under ice-cooling. The mixture was left standing for 30 min. Dry toluene was then added and the solvent was distilled from the reaction mixture. Acetone and toluene were added to the residue and distilled off. This process was repeated twice. The residue was suspended in a small quantity of acetone, to which hexane was added. The resulting precipitate was collected by filtration. This precipitate was dissolved in saturated aqueous sodium bicarbonate and the insoluble matter was removed. The pH of the residue was adjusted to 2.4 with 3 N hydrochloric acid and the precipitate was collected by filtration, washed with water and dried to yield 160 mg (22.1%) of **10a**. The mother liquor was purified by chromatography through an Rp-8 prepacked column (Merck) (5% (v/v) aqueous acetonitrile containing 0.02% (v/v) acetic acid) to yield a further 0.01 g (1.3%) of **10a**. UV $\lambda_{max}$ nm ($\varepsilon$): ($H_2O$) 258 (15900); (0.1 N NaOH) 258 (17200); (0.1 N HCl) 257.5 (16200). NMR (DMSO-$d_6$) $\delta$: 8.34 (1H, s), 8.22 (1H, s), 6.96 (1H, d, $J$=7.5 Hz, 1'-H), 5.00 (1H, dd, $J$=9.0, 7.5 Hz, 2'-H), 6.29 (1H, dd, $J$=9.0, 2.4 Hz, 3'-H), 5.18 (1H, d, $J$=2.4 Hz, 5'-H), 4.52 (1H, s, 7'-H), 7.40 (2H, br s, $NH_2$). $[\alpha]_D^{20}$ −56.8° ($c$=0.5, DMSO).

**2'-Deoxy-*S*-2'-bromogriseolic Acid (10b)**——Compound **6** (2.5 g, 2.69 mmol) was dissolved in 12 ml of hexamethylphosphoric triamide and 1.18 g (13.5 mmol) of anhydrous lithium bromide was added. The mixture was allowed to react for 4—5 h on an ultrasonic bath (up to 35 °C). The reaction product was stirred overnight at room temperature. It was then slowly poured into ice-water containing sodium chloride. The precipitate was collected by filtration, washed successively with ice-water and hexane, and dissolved in ethyl acetate; this solution was dried over anhydrous magnesium sulfate. The drying agent was filtered off and the filtrate was evaporated to yield 2.26 g (2.69 mmol) of dibenzhydryl 2'-deoxy-*S*-2'-bromo-*O*$^{7'}$-(tetrahydropyran-2-yl)griseolate, which was dissolved in 5 ml of methylene chloride. Ethanol (20 ml) and 0.73 g (2.9 mmol) of pyridine *p*-toluenesulfonate were added to this solution and the mixture was allowed to react at 60 °C for 12 h. The solvent was distilled off and the residue was dissolved in methylene chloride. The solution was washed with water and dried over anhydrous magnesium sulfate. The drying agent was removed by filtration and the solvent was distilled off. The residue was purified by silica gel chromatography (5% methanol–methylene chloride) to yield 0.9 g (43%) of dibenzhydryl 2'-deoxy-*S*-2'-bromogriseolate. The procedures described for the synthesis of **10a** were repeated to yield 436 mg (36.5%) of **10b**. UV $\lambda_{max}$ nm ($\varepsilon$): ($H_2O$) 257.5 (15400); (0.1 N NaOH) 257.5 (16200); (0.1 N HCl) 255 (15300). NMR (DMSO-$d_6$) $\delta$: 8.36 (1H, s), 8.23 (1H, s), 7.10 (1H, d, $J$=7.5 Hz, 1'-H), 5.17 (1H, dd, $J$=9.0, 7.5 Hz, 2'-H), 6.30 (1H, dd, $J$=9.0, 2.4 Hz, 3'-H), 5.21 (1H, d, $J$=3.0 Hz, 5'-H), 4.52 (1H, s, 7'-H), 7.39 (2H, br s, $NH_2$). $[\alpha]_D^{20}$ −58° ($c$=0.5, DMSO).

***S*-2'-Chloro-2'-deoxygriseolic Acid (10c)**——The procedures described for the synthesis of **10a** were repeated except that compound **6** (2 g, 2.16 mmol) was reacted with anhydrous lithium chloride (1.4 g, 33 mmol) in place of the

bromide and the reaction mixture was heated at 60 °C for 4 h to yield 0.18 g (21.0%) of **10c**. UV $\lambda_{max}$ nm (ε): ($H_2O$) 257 (15000); (0.1 N NaOH) 257 (15200); (0.1 N HCl) 254.5 (14800). NMR (DMSO-$d_6$) δ: 8.36 (1H, s), 8.22 (1H, s), 7.14 (1H, d, $J$=7.5 Hz, 1'-H), 5.21 (1H, dd, $J$=9.0, 7.5 Hz, 2'-H), 6.25 (1H, dd, $J$=9.0, 2.4 Hz, 3'-H), 5.22 (1H, d, $J$=2.4 Hz, 5'-H), 4.54 (1H, s, 7'-H), 7.42 (2H, br s, $NH_2$).

**2'-Deoxygriseolic Acid (11)**——Compound **9a** (0.83 g, 1.07 mmol) and about 10 mg of α,α'-azobisisobutyronitrile were dissolved in 20 ml of benzene, and 0.7 ml (2.6 mmol) of tributyltin hydride was added under a stream of nitrogen gas. The mixture was refluxed for 45 min. The solvent was distilled off and the residue was purified by silica gel column chromatography (5% methanol–methylene chloride) to yield 0.72 g (96.3%) of dibenzhydryl 2'-deoxygriseolate. This compound (0.72 g, 1.03 mmol) was dissolved in 5 ml of anisole, and 5 ml of trifluoroacetic acid was added under ice-cooling. The mixture was left standing for 15 min, after which dry toluene was added and the solvent was distilled off. Acetone and toluene were added to the residue and then distilled off. This process was repeated again, after which the residue was suspended in a small quantity of acetone. Hexane was added to the suspension to turn the solid matter into powder. This powder was collected by filtration and dissolved in saturated aqueous sodium bicarbonate. The pH of the solution was adjusted to 2.3 with 3 N hydrochloric acid and the solution was purified by chromatography through an Rp-8 prepacked column (Merck) (3% (v/v) aqueous acetonitrile containing 0.02% (v/v) acetic acid) to yield 0.269 g (69.2%) of **11**. UV $\lambda_{max}$ nm (ε): ($H_2O$) 257.5 (15800); (0.1 N NaOH) 257.5 (15800); (0.1 N HCl) 255 (16700). NMR (DMSO-$d_6$) δ: 8.40 (1H, s), 8.24 (1H, s), 6.90 (1H, br m, 1'-H), 2.76 (2H, br m, 2'-H), 6.05 (1H, br m, 3'-H), 4.94 (1H, d, $J$=3.0 Hz, 5'-H), 4.50 (1H, s, 7'-H), 7.43 (2H, br s, $NH_2$). $[\alpha]_D^{20}$ −17.6° ($c$=0.5, DMSO).

**Dibenzhydryl *O*$^{2'}$-Benzoyl-*O*$^{7'}$-trifluoromethanesulfonylgriseolate (15)**——Compound **13** (7.99 g, 9.79 mmol) and 1.46 g (12.0 mmol) of 4-(dimethylamino)pyridine were introduced into a 100 ml three-necked round-bottomed flask and dried under reduced pressure in the presence of phosphorus pentoxide. Also in the presence of phosphorus pentoxide, 50 ml of methylene chloride was separately distilled and added to the flask. Trifluoromethanesulfonyl chloride (2.02 ml, 19.0 mmol) was then added under ice-cooling and protection from moisture, and the mixture was stirred for 2 h under the same conditions. After addition of 10 ml of water, the mixture was stirred for a further 15 min under ice-cooling. The reaction mixture was transferred to a separating funnel, to which 20 ml of 0.1 N hydrochloric acid was added to wash the organic layer. This layer was washed successively with saturated aqueous sodium chloride and saturated aqueous sodium bicarbonate, and dried over anhydrous sodium sulfate. The solvent was distilled off under reduced pressure. The resulting residue was purified by silica gel column chromatography (1% (v/v) methanol–methylene chloride). The fraction containing the main product was collected and concentrated to yield 7.38 g (79.5%) of **15** as a pale yellow foam. UV $\lambda_{max}^{methanol}$ nm (ε): 257 (17100). NMR (DMSO-$d_6$) δ: 8.33 (1H, s), 8.08 (1H, s), 7.1—8.2 (28H, m, 1'-H overlapping with benzhydryl, benzoyl and $NH_2$), 6.00 (1H, d, $J$=5.4 Hz, 2'-H), 6.93 (1H, dd, $J$=2.4, 5.4 Hz, 3'-H), 5.21 (1H, d, $J$=2.4 Hz, 5'-H), 6.05 (1H, s, 7'-H), 6.88 (2H, CH).

**Dibenzhydryl *S*-7'-Azido-*O*$^{2'}$-benzoyl-7'-deoxygriseolate (16)**——Compound **15** (935 mg, 0.99 mmol) was dissolved in 5 ml of well-dried hexamethylphosphoric triamide, to which 68.3 mg (1.05 mmol) of well-dried sodium azide (obtained by lyophilization from water) was added. The mixture was allowed to react at room temperature for 2 h under protection from moisture. The reaction mixture was poured into ice-water and the resulting insoluble matter was collected by filtration, washed with water and dried. The resulting solid material was purified by silica gel preparative TLC (1% methanol–methylene chloride). The main band was extracted with methylene chloride to yield 455 mg (54.9%) of **16** in the form of a pale yellow powder. The compound showed an extremely strong infrared (IR) spectral peak due to azide at 2100 $cm^{-1}$. UV $\lambda_{max}^{methanol}$ nm (ε): 257 (18900). NMR (DMSO-$d_6$) δ: 8.36 (1H, s), 8.11 (1H, s), 6.93 (1H, s, 1'-H), 5.85 (1H, d, $J$=5.4 Hz, 2'-H), 6.5—6.8 (1H, m, 3'-H), 5.34 (1H, d, $J$=2.4 Hz, 5'-H), 4.87 (1H, s, 7'-H), 7.1—8.2 (29H, m, $NH_2$, benzhydryl, benzoyl and 1/6 benzene), 6.58 (1H, s, CH), 6.71 (1H, s, CH).

***S*-7'-Azido-7'-deoxygriseolic Acid (17)**——Compound **16** (300 mg, 0.36 mmol) was dissolved in 5 ml of anisole. Trifluoroacetic acid (5 ml) was added to the resulting solution under ice-cooling and the mixture was left standing for 30 min in a tightly stoppered vessel. The solvent was distilled off under reduced pressure. The residue was dissolved in acetone, to which toluene was added and the solvent was distilled off. This process was repeated 3 times. The residue was dissolved in 10 ml of acetone and the solution was poured into 100 ml of hexane. The resulting precipitate was collected by filtration, thoroughly washed with hexane, and dried. The resulting pale yellow solid was dissolved in 20 ml of a 20% (v/v) solution of ammonia in methanol and the mixture was left standing overnight. The solvent was distilled off under reduced pressure and the resulting residue was dissolved in a small quantity of water. The pH of the resulting solution was adjusted to 2.0 and the solution was washed with a small quantity of ether and purified by Rp-8 (Merck) column chromatography (water containing 10% (v/v) acetonitrile). The main peaks were collected and the solvent was distilled off to yield 70 mg (48.5%) of **17** in the form of a pale yellow granular substance. The IR spectrum of this compound showed a strong peak at 2110 $cm^{-1}$ which was ascribable to azide. UV $\lambda_{max}^{H_2O}$ nm (ε): 258 (15000). NMR (DMSO-$d_6$) δ: 8.36 (1H, s), 8.21 (1H, s), 6.50 (1H, s, 1'-H), 4.61 (1H, d, $J$=5.4 Hz, 2'-H), 6.08 (1H, dd, $J$=2.4, 5.4 Hz, 3'-H), 5.01 (1H, d, $J$=2.4 Hz, 5'-H), 4.27 (1H, s, 7'-H), 7.36 (2H, br s, $NH_2$). $[\alpha]_D^{20}$ −31.6° ($c$=0.25, DMSO).

**Dibenzhydryl *O*$^{2'}$-Benzoyl-*S*-7'-amino-7'-deoxygriseolate (18)**——Compound **16** (1.20 g, 1.43 mmol) was dissolved in 15 ml of pyridine, to which 5 ml of water was added. Nitrogen gas was passed through the mixture for approximately 5 min, and hydrogen sulfide gas was passed through it for a further 30 min under ice-cooling. The flask

was flushed with nitrogen gas and the reaction mixture was left standing at room temperature for 17 h in a tightly stoppered vessel. Nitrogen gas was passed through the reaction mixture for 1 h at room temperature to remove excess hydrogen sulfide gas. Acetic acid (10 ml) was added to the reaction product and the solvent was distilled off under reduced pressure. Ethanol (10 ml) was added to the residue and distilled off. This process was repeated twice. The residue was dissolved in 30 ml of ethyl acetate and 20 ml of water and subjected to fractionation of the organic and aqueous layers. The organic layer was washed successively with 20 ml each of 0.1 N hydrochloric acid, 5% (w/v) aqueous sodium bicarbonate, and saturated aqueous sodium chloride in that order, and dried over anhydrous magnesium sulfate. The solvent was distilled off under reduced pressure to yield a pale yellow residue. This residue was purified by prepacked silica gel column (Merck) chromatography (2% (v/v) methanol–methylene chloride) to yield 494 mg (42.7%) of **18** in the form of a pale yellow powder. UV $\lambda_{max}^{methanol}$ nm ($\varepsilon$): 260 (18300). NMR (DMSO-$d_6$) $\delta$: 8.43 (1H, s), 8.15 (1H, s), 6.63 (1H, s, 1′-H), 5.90 (1H, d, $J$=6.8 Hz, 2′-H), 6.66, 6.63 (1H, dd, $J$=6.8, 2.4 Hz, 3′-H), 5.47 (1H, d, $J$=2.4 Hz, 5′-H), 4.01 (1H, s, 7′-H), 7.0—8.2 (28H, m, $NH_2$, benzhydryl, benzoyl and 1/6 benzene), 6.76 (1H, s, CH), 6.90 (1H, s, CH).

***S*-7′-Amino-7′-deoxygriseolic Acid (19)**——Compound **18** (434 mg, 0.53 mmol) was dissolved in 5 ml of anisole. Trifluoroacetic acid (5 ml) was added to the resulting solution under ice-cooling and the mixture was left standing for 30 min at room temperature in a tightly stoppered vessel. The solvent was distilled off under reduced pressure. Acetone (5 ml) and 5 ml of toluene were added to the residue and then distilled off. This process was repeated 3 times. The resulting residue was dissolved in 5 ml of ethanol and 5 ml of acetone, and the solution was slowly poured into 50 ml of a 1 : 1 (v/v) mixture of hexane and acetone with stirring. The resulting precipitate was collected by filtration, washed with hexane, and dried. The resulting ochre-colored powder was dissolved in 20 ml of 20% (v/v) methanolic ammonia and left standing for 17 h at room temperature in a tightly stoppered vessel. The solvent was distilled off under reduced pressure and 20 ml of water was added to the residue to dissolve it. The resulting solution was gradually acidified with 1 N hydrochloric acid, whereupon insoluble matter appeared but then dissolved when the pH reached 1. The solution was washed with 20 ml of ethyl acetate. The pH of the aqueous layer was adjusted to about 7.0 by adding sodium bicarbonate. The aqueous layer was then purified by chromatography through an Rp-8 prepacked column (Merck) (10% aqueous acetonitrile) to yield 133 mg (66.0%) of **19** in the form of a pale yellow powder. UV $\lambda_{max}$ nm ($\varepsilon$): ($H_2O$) 257.5 (15300); (0.1 N NaOH) 259 (15600); (0.1 N HCl) 255.7 (15300).

**Dibenzhydryl *O*$^{2'}$-Benzoyl-*S*-7′-chloro-7′-deoxygriseolate (20a)**——Compound **15** (2.84 g, 3.0 mmol) was dissolved in 50 ml of dimethylformamide, and 1.27 g (30 mmol) of anhydrous lithium chloride was added. The mixture was stirred under heating at 100 °C for 1 h. The solvent was distilled off under reduced pressure. The resulting residue was dissolved in 30 ml of water and 50 ml of ethyl acetate and the organic layer was separated. This was washed with water and dried over anhydrous magnesium sulfate, and the solvent was evaporated off to yield a pale brown residue. The residue was separated and purified by silica gel column chromatography (5% (v/v) methanol–methylene chloride) to yield 1.74 g (69.5%) of **20a** as a pale yellow caramel-like substance. UV $\lambda_{max}^{methanol}$ nm ($\varepsilon$): 257 (16500). NMR (DMSO-$d_6$) $\delta$: 8.39 (1H, s), 8.09 (1H, s), 6.64 (1H, s, 1′-H), 5.92 (1H, d, $J$=5.4 Hz, 2′-H), 6.72 (1H, dd, $J$=2.4, 5.4 Hz, 3′-H), 5.39 (1H, d, $J$=2.4 Hz, 5′-H), 5.21 (1H, s, 7′-H), 7.1—8.1 (27H, m, $NH_2$, benzhydryl and benzoyl), 6.88 (1H, s, CH), 6.97 (1H, s, CH).

***S*-7′-Chloro-7′-deoxygriseolic Acid (21a)**——Compound **20a** (1.34 g, 1.61 mmol) was dissolved in 10 ml of anisole. Trifluoroacetic acid (10 ml) was added to the resulting solution under ice-cooling, and the mixture was left standing for 30 min in a tightly stoppered vessel at room temperature. The solvent was distilled off under reduced pressure. The residue was dissolved in acetone, to which toluene was added, and the solvent was distilled off. This process was repeated 3 times. The residue was dissolved in a small quantity of acetone and the solution was slowly poured into 100 ml of hexane with stirring. The resulting white precipitate was collected by filtration, thoroughly washed with hexane, and then dried. The resulting pale yellow solid was dissolved in 20 ml of a 20% (v/v) methanolic ammonia, and the solution was left standing for 2 h at room temperature in a tightly stoppered vessel. The solvent was distilled off under reduced pressure and the resulting residue was dissolved in 30 ml of water. The water solution was washed twice with 20-ml portions of ether, and then its pH was adjusted to 2.0 using concentrated hydrochloric acid. The solution was purified by chromatography through an Rp-8 prepacked column (Merck) (10% aqueous acetonitrile) to yield 525 mg (82.0%) of **21a** in the form of a pale yellowish powder. UV $\lambda_{max}$ nm ($\varepsilon$): ($H_2O$) 257 (15300); (0.1 N NaOH) 259.5 (15200); (0.1 N HCl) 257.5 (15100). NMR (DMSO-$d_6$) $\delta$: 8.42 (1H, s), 8.31 (1H, s), 6.58 (1H, s, 1′-H), 4.70 (1H, d, $J$=5.4 Hz, 2′-H), 6.10 (1H, dd, $J$=2.4, 5.4 Hz, 3′-H), 5.25 (1H, d, $J$=2.4 Hz, 5′-H), 4.97 (1H, s, 7′-H). $[\alpha]_D^{20}$ −31.6° ($c$=0.25, DMSO).

**Dibenzhydryl *O*$^{2'}$-Benzoyl-*S*-7′-bromo-7′-deoxygriseolate (20b)**——Compound **15** (14.1 g, 14.87 mmol) was dissolved in 50 ml of dimethylformamide, and 13 g (149 mmol) of anhydrous lithium bromide was added. The mixture was stirred under heating at 95 °C for 22 min. The same procedure as described for the synthesis of compound **20a** was repeated to yield 6.9 g (52.8%) of **20b**. UV $\lambda_{max}^{methanol}$ nm ($\varepsilon$): 258 (17500). NMR (DMSO-$d_6$) $\delta$: 8.40 (1H, s), 8.09 (1H, s), 6.67 (1H, s, 1′-H), 5.97 (1H, d, $J$=5.4 Hz, 2′-H), 6.75 (1H, dd, $J$=2.1, 5.4 Hz, 3′-H), 5.40 (1H, d, $J$=2.1 Hz, 5′-H), 5.13 (1H, s, 7′-H), 7.0—8.2 (28H, m, $NH_2$, benzhydryl, benzoyl and 1/6 benzene), 6.67 (1H, s, CH), 6.75 (1H, s, CH).

***S*-7′-Bromo-7′-deoxygriseolic Acid (21b)**——Compound **20b** (878 mg, 1 mmol) was dissolved in 10 ml of anisole.

The same procedure as described for the synthesis of compound **21a** was repeated to yield 250 mg (56.5%) of **21b**. UV $\lambda_{max}^{H_2O}$ nm (ε): 257 (16000). NMR (DMSO-$d_6$) $\delta$: 8.47 (1H, s), 8.26 (1H, s), 6.80 (1H, s, 1'-H), 4.83 (1H, d, $J$=5.7 Hz, 2'-H), 6.52 (1H, dd, $J$=2.1, 5.7 Hz, 3'-H), 6.31 (1H, d, $J$=2.1 Hz, 5'-H), 5.13 (1H, s, 7'-H).

**7'-Deoxygriseolic Acid (22)**——**21a**→**22**: Compound **21a** (500 mg, 1.26 mmol) was dissolved in 30 ml of 80% aqueous acetic acid. Zinc powder (600 mg, 9.2 mol) was added in three approximately equal portions at intervals of 1 h with vigorous stirring. The stirring was continued under the same conditions. The insoluble matter was removed by filtration and the filtrate was evaporated to dryness. The pH of the resulting residue was adjusted to 2.0 with 1 N hydrochloric acid. The solution was purified on an Rp-8 prepacked column (Merck) (5% aqueous acetonitrile) to yield 250 mg (54.6%) of **22** in the form of a white powder. UV $\lambda_{max}$ nm (ε): ($H_2O$) 257.5 (15600); (0.1 N NaOH) 258.4 (15700); (0.1 N HCl) 255.5 (15600). NMR (DMSO-$d_6$) $\delta$: 8.40 (1H, s), 8.27 (1H, s), 6.51 (1H, s, 1'-H), 4.62 (1H, d, $J$=4.9 Hz, 2'-H), 6.03 (1H, dd, $J$=2.4, 4.9 Hz, 3'-H), 5.10 (1H, d, $J$=2.4 Hz, 5'-H), 2.92 (2H, dd, $J$=16.5, 27 Hz, 7'-H). $[\alpha]_D^{20}$ −3.8° ($c$=0.5, DMSO).

**20b**→**22**: Compound **20b** (3.51 g, 3.99 mmol) was dissolved in 40 ml of 80% aqueous acetic acid, and zinc powder (2.6 g, 39 mol) was added to the reaction solution with vigorous stirring at room temperature. The stirring was continued for 20 min. The insoluble matter was removed by filtration and the filtrate was evaporated to dryness. Addition and evaporation of toluene (30 ml) and acetone (30 ml) were repeated 3 times. The residue was dissolved in 140 ml of a 1 : 1 solution of ethyl acetate and 0.1 N hydrochloric acid. The organic layer was washed successively with 5% aqueous sodium bicarbonate (70 ml) and saturated aqueous sodium chloride (70 ml), and dried over anhydrous magnesium sulfate. The solvent was distilled off under reduced pressure to yield 3.18 g of a pale yellow caramel. This contained two main products and was purified by preparative silica gel TLC developed with methylene chloride containing 5% methanol. The more mobile material was deprotected by using the same procedure as described for the synthesis of **21a** to give 250 mg (16.4%) of **22**. The less mobile material was deprotected by using the same procedure as described for the synthesis of **21a** to give 150 mg (10.3%) of **23**.

**23**: NMR (DMSO-$d_6$) $\delta$: 8.43 (1H, s), 8.23 (1H, s), 7.37 (2H, brs, $NH_2$), 6.18 (1H, d, $J$=6.6 Hz, 1'-H), 4.6—5.3 (2H, m), 2.3—2.8 (2H, m).

**20b**→**22**: Compound **20b** (5.5 g, 6.26 mmol) and 30 mg of α,α'-azobis-isobutyronitrile were dissolved in 100 ml of benzene, and 4.2 ml (15.6 mmol) of tributyltin hydride was added under a stream of nitrogen gas. The mixture was refluxed for 55 min. The solvent was distilled from the reaction mixture, and the residue was purified by silica gel column chromatography (5% methanol–methylene chloride) to yield 4.8 g (98%) of dibenzhydryl $O^{2'}$-benzoyl-7'-deoxygriseolate. This compound (4.8 g, 6.00 mmol) was dissolved in 40 ml of anisole, and 5 ml of trifluoroacetic acid was added under ice-cooling. The mixture was left standing for 15 min, after which dry toluene was added and the solvent was distilled off. Acetone and toluene were added to the residue and distilled off. This process was repeated, after which the residue was dissolved in 50 ml of 0.5 N aqueous sodium hydroxide, and the mixture was left standing at room temperature for 3.5 h. The pH of the solution was adjusted to 2.3 with 3 N hydrochloric acid, and the solution was purified by chromatography through an Rp-8 prepacked column (Merck) (10% (v/v) aqueous acetonitrile containing 0.02% (v/v) acetic acid) to yield 1.84 g (82.4%) of **22**.

**Dibenzhydryl $O^{2'}$-Benzoyl-*S*-7'-acetoxy-7'-deoxygriseolate (24)**——Sodium acetate (which had previously been melted and dried) [3.2 g, 40 mmol] was dissolved in 50 ml of acetic acid with heating at 95 °C. Compound **15** (3.79 g, 4.0 mmol) was added and the mixture was stirred for 1 h at 95 °C under protection from moisture. The solvent was distilled off under reduced pressure and 10 ml each of acetone and toluene were added to the residue and distilled off. This process was repeated 3 times. The residue was dissolved in 90% (v/v) aqueous acetone. The pH of the solution was adjusted to a value no greater than 1 with 1 N hydrochloric acid, and diphenyldiazomethane was added to the mixture until the reddish color disappeared. The mixture was allowed to react at room temperature for approximately 1 h, and excess diphenyldiazomethane was decomposed with acetic acid. The solvent was distilled off under reduced pressure. The residue was dissolved in 50 ml of ethyl acetate and 50 ml of water and subjected to fractionation. The organic layer was washed successively with 5% (w/v) aqueous sodium bicarbonate and saturated aqueous sodium chloride, and dried over anhydrous magnesium sulfate. The drying agent was removed by filtration and the solvent was distilled off. The residue was purified by silica gel column chromatography (5% methanol–methylene chloride) to yield 2.33 g (67.9%) of **24** in the form of a pale yellow caramel-like substance. UV $\lambda_{max}^{methanol}$ nm (ε): 257 (18100). NMR (DMSO-$d_6$) $\delta$: 8.38 (1H, s), 8.14 (1H, s), 7.18 (1H, s, 1'-H), 5.91 (1H, d, $J$=5.4 Hz, 2'-H), 6.79 (1H, dd, $J$=2.4, 5.4 Hz, 3'-H), 5.32 (1H, d, $J$=2.4 Hz, 5'-H), 6.00 (1H, s, 7'-H), 7.0—8.3 (27H, m, $NH_2$, benzhydryl and benzoyl), 6.79 (1H, s, CH), 6.91 (1H, s, CH), 1.88 (3H, s, $CH_3$).

***S*-7'-Hydroxy-7'-deoxygriseolic Acid (26)**——Compound **24** (2.23 g, 2.60 mmol) was dissolved in 20 ml of anisole and 20 ml of trifluoroacetic acid. The same procedure as described for the synthesis of compound **21b** was repeated to yield 300 mg (30.4%) of **26** in the form of a pale yellow powder. The NMR spectrum of the compound was identical with that of griseolic acid.[1] $[\alpha]_D^{20}$ −6.8° ($c$=0.5, DMSO) [*cf.* griseolic acid +6.9° ($c$=0.1, DMSO)].

***S*-7'-Acetoxy-7'-deoxygriseolic Acid (25)**——In the process of purification with an Rp-8 column described in connection with the synthesis of compound **26**, the second peak material eluted with water containing 10% (v/v) acetonitrile was collected to yield 200 mg (18.3%) of **25** in the form of a pale yellow powder. UV $\lambda_{max}$ nm (ε): ($H_2O$) 257 (16100); (0.1 N NaOH) 258.2 (16500); (0.1 N HCl) 255 (16100). NMR (DMSO-$d_6$) $\delta$: 8.38 (1H, s), 8.23 (1H, s),

6.56 (1H, s, 1′-H), 4.63 (1H, d, $J$=4.6 Hz, 2′-H), 6.07 (1H, q, $J$=1.9, 4.6 Hz, 3′-H), 5.13 (1H, d, $J$=1.9 Hz, 5′-H), 5.40 (1H, s, 7′-H), 7.42 (2H, br s, $NH_2$), $[\alpha]_D^{20}$ −22° ($c$=0.5, DMSO).

**PDE Inhibitory Activity**

The test was carried out essentially following the method of Pichard and Cheung.[17] Rat brains were homogenized in glass-glass or glass-Teflon homogenizers with four volumes of cold 0.17 M Tris–HCl buffer (pH 7.4), containing 5 mM aqueous $MgSO_4$. The homogenate was then centrifuged at 100000×$g$ at 0 °C for 1 h. The clear supernatant solution was stored at −20 °C and used as a cAMP PDE preparation. Prior to use, this solution was diluted 100—150 times with 40 mM Tris–HCl buffer (pH 7.5). The reaction mixture (total volume, 0.1 ml), consisting of 40 mM Tris–HCl buffer (pH 7.5), 5 mM $MgSO_4$, 50 μM $CaCl_2$, 20 μM snake venom (*Crotalus atrox*, Sigma), 0.14 μM [$^{14}$C] cAMP, test material and enzyme solution, was incubated at 30 °C for 20 min. At the end of this time, the reaction mixture was treated with Amberlite IRP-58 resin, and the level of residual radioactivity of adenosine was determined. The experiment was carried out at a number of concentration levels of each active compound, and from the results, the 50% inhibition value ($IC_{50}$) was calculated.

A similar experiment was carried out with cGMP as the substrate instead of cAMP. The $IC_{50}$ value toward cGMP PDE was also calculated. The results are summarized in Tables I and II.

**Acknowledgment** The authors wish to express their thanks to Dr. H. Nakao, the Director of the Chemical Research Laboratories, for his encouragement and to Drs. T. Hiraoka and T. Miyadera for their valuable suggestions.

## References and Notes

1) Paper IV in this series, Y. Murofushi, M. Kimura, Y. Iijima, M. Yamazaki, and M. Kaneko, *Chem. Pharm. Bull.*, **35**, 1036 (1987).
2) E. S. Severin, N. N. Gulyaev, T. V. Bulargina, and M. N. Kochetkava, *Ad. Enzyme Regul.*, **17**, 251 (1979).
3) F. Nakagawa, T. Okazaki, A. Naito, Y. Iijima, and M. Yamazaki, *J. Antibiot.*, **38**, 823 (1985).
4) J. A. Wright, N. T. Taylor, and J. J. Fox, *J. Org. Chem.*, **34**, 2632 (1969); K. Kondo, T. Adachi, and I. Inoue, *ibid.*, **42**, 3967 (1977); R. Mengel and H. Wiedner, *Chem. Ber.*, **109**, 1395 (1976); R. Ranganathan and D. Larwood, *Tetrahedron Lett.*, **45**, 4341 (1978).
5) A. F. Russell, S. Greenberg, and J. G. Moffatt, *J. Am. Chem. Soc.*, **95**, 4025 (1973); S. Greenberg and J. G. Moffatt, *ibid.*, **95**, 4016 (1973).
6) M. J. Robins, R. Mengel, R. A. Jones, and Y. Fouron, *J. Am. Chem. Soc.*, **98**, 8204 (1976); T. C. Jain, I. D. Jenkins, A. F. Russell, J. P. H. Verheyden, and J. G. Moffatt, *J. Org. Chem.*, **39**, 30 (1974).
7) M. Ikehara, H. Tada, and M. Kaneko, *Tetrahedron*, **24**, 3489 (1968); M. Ikehara and M. Kaneko, *Chem. Pharm. Bull.*, **18**, 2401 (1968); M. Ikehara and Y. Ogiso, *Tetrahedron*, **28**, 3695 (1972); M. Ikehara and T. Maruyama, *ibid.*, **31**, 1369 (1975); J. B. Chattopadhyaya and C. B. Reese, *J. Chem. Soc., Chem. Commun.*, **1977**, 414; M. Ikehara, Y. Ogiso, T. Maruyama, and M. Kaneko, "Nucleic Acid Chemistry," Part 2, ed. by L. B. Townsend and R. S. Tipson, John Wiley and Sons, Inc., New York, 1978, p. 485.
8) W. W. Lee, A. Benitez, L. Goodman, and B. R. Baker, *J. Am. Chem. Soc.*, **82**, 2648 (1960); W. W. Lee, A. Benitez, C. D. Anderson, L. Goodman, and B. R. Baker, *ibid.*, **83**, 1906 (1961); E. J. Reist, A. Benitez, L. Goodman, B. R. Baker, and W. W. Lee, *J. Org. Chem.*, **27**, 3274 (1962); R. Mengel and H. Wiedner, *Chem. Ber.*, **109**, 433 (1976); M. Ikehara, T. Maruyama, and H. Miki, *Tetrahedron Lett.*, **1976**, 4485; R. Mengel and H. Griesser, *ibid.*, **1977**, 1177; M. Ikehara, T. Maruyama, H. Miki, and Y. Takatsuka, *Chem. Pharm. Bull.*, **25**, 754 (1977); M. Ikehara, T. Maruyama, and H. Miki, "Chemistry and Biology of Nucleosides and Nucleotides," ed. by R. E. Harmon, R. K. Robins and L. B. Townsend, Academic Press, New York, 1978, p. 387; *idem*, *Tetrahedron*, **34**, 1133 (1978); M. Ikehara and T. Maruyama, *Chem. Pharm. Bull.*, **26**, 240 (1978); A. V. Azhayev and J. Smrt, *Collect. Czech. Chem. Commun.*, **43**, 1520 (1970); D. Wagner, J. P. H. Verheyden, and J. G. Moffatt, *J. Org. Chem.*, **39**, 24 (1974).
9) R. Ranganathan, *Tetrahedron Lett.*, **15**, 1291 (1977).
10) R. Ranganathan, *Tetrahedron Lett.*, **13**, 1185 (1975).
11) K. Fukukawa, T. Ueda, and T. Hirano, *Chem. Pharm. Bull.*, **31**, 1582 (1983).
12) S. Takahashi, F. Nakagawa, K. Kawazoe, Y. Furukawa, S. Sato, C. Tamura, and T. Naito, *J. Antibiot.*, **38**, 830 (1985).
13) I. Hirano, S. Nishino, K. Kamaike, S. Nishiyama, S. Ueda, H. Yamamoto, and Y. Ishido, *Nucleic Acids Research Symposium Series*, **12**, 71 (1983).
14) M. L. Wolfrom and M. W. Winkley, *J. Org. Chem.*, **32**, 1823 (1967).
15) T. McCreadie, K. Overton, and A. J. Allison, *J. Chem. Soc. (C)*, **1971**, 317.
16) E. J. Prishe, J. Smejkal, J. P. H. Verheyden, and J. G. Moffatt, *J. Org. Chem.*, **41**, 1836 (1976).
17) A. L. Pichard and W. Y. Cheung, *J. Biol. Chem.*, **251**, 5726 (1976).

[Chem. Pharm. Bull. 35(11)4454—4459(1987)]

# Application of Microorganisms and Enzymes to the Synthesis of Chiral Cyclopentane and Bicyclo[3.3.0]octane Derivatives

ZHUO-FENG XIE, HIROSHI SUEMUNE, IZUMI NAKAMURA, and KIYOSHI SAKAI*

*Faculty of Pharmaceutical Sciences, Kyushu University, Fukuoka 812, Japan*

(Received April 23, 1987)

Optically active cyclopentane and bicyclo[3.3.0]octane derivatives were synthesized by utilizing biochemical methods. *Pseudomonas fluorescens* lipase was found to be an effective enzyme for the enantioselective hydrolysis of monoacetoxy- and diacetoxycyclopentanes such as (±)-**4a**, (±)-**5a**, (±)-**6a**, and **7a**. However, hydrolysis of bicyclo[3.3.0]octane *trans*-acetate ((±)-**8a**) using this enzyme resulted in low enantioselectivity. Optically pure (+)-**8b** for the synthesis of carbacyclin was obtained from (±)-**8a** by using porcine pancreatic lipase. Reduction of 3-acetyl-7-oxobicyclo[3.3.0]-oct-2-ene with baker's yeast afforded a useful intermediate ((+)-**11b**) for the synthesis of hirsutic acid.

**Keywords**——enzymatic hydrolysis; enantioselective hydrolysis; bicyclo[3.3.0]octane; baker's yeast; carbacyclin; hirsutic acid

Bicyclo[3.3.0]octane derivatives are useful synthons, because, for example, they are key intermediates in the synthesis of biologically active carbacyclin (**1**)[1] and triquinanes.[2] Carbacyclin is a potent inhibitor of platelet aggregation as well as a vasodilator, and triquinanes such as hirsutic acid have antitumor activity.

As a part of our studies on the conversion of chiral natural products to biologically active compounds, we previously reported on the conversion[3] of (+)-limonen-10-ol into the key intermediate (**3**) in the synthesis of **1** *via* the enone (**2**).

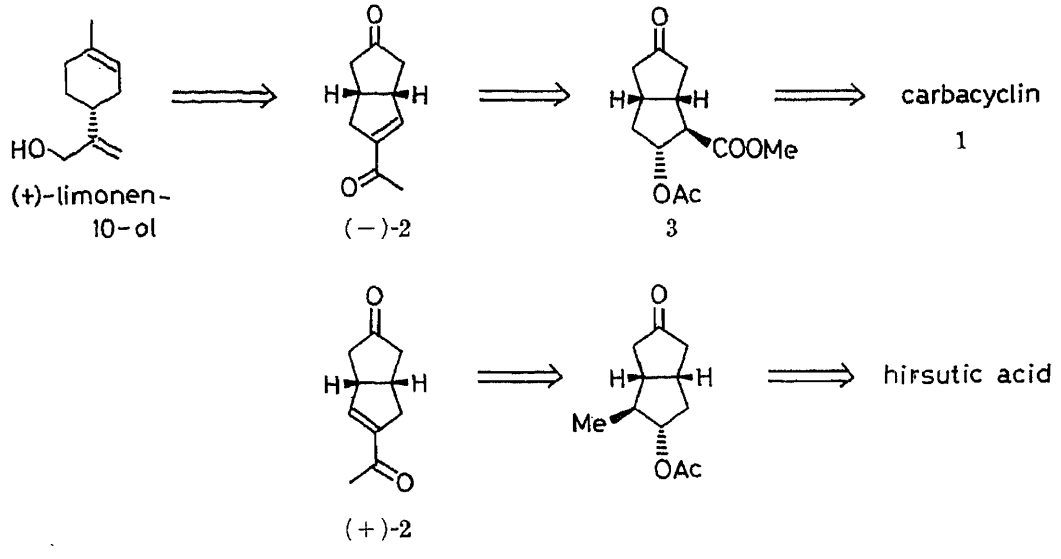


Chart 1

TABLE I. *P. fluorescens* Lipase-Catalyzed Hydrolysis of Acetates (±)-(**4a**—**8a**)

| Entry | Substrate | Reaction time (h) | Hydrolyzed product | | | Recovered acetate | |
|---|---|---|---|---|---|---|---|
| | | | Compd. | Yield (%) | ee (%) | Yield (%) | ee (%) |
| 1 | (±)-**4a** | 6 | (1*R*,2*R*)-(−)-**4b** | 30 | >99 | 65 | 30 |
| 2 | (±)-**5a** | 1.5 | (1*S*,2*R*)-(−)-**5b** | 42 | >99 | 50 | 90 |
| 3 | (±)-**6a** | 8 | (1*R*,2*R*)-(+)-**6b** | 43 | >99 | 42 | 95 |
| 4 | **7a** | 3 | (1*R*,2*S*)-(−)-**7b** | 39 | >99 | 42 | — |
| 5 | (±)-**8a** | 56 | (1*S*,2*R*,3*R*,5*R*)-(+)-**8b** | 13 | 45 | 76 | 2 |

In connection with this research, we have undertaken the preparation of optically active bicyclo[3.3.0]octane and cyclopentane derivatives utilizing biochemical methods. Recently, Schneider *et al.* reported that the enzymatic hydrolysis of *trans*-1,2-diacetoxycyclopentane ((±)-**6a**) with pig liver esterase (PLE),[4] showed low enantioselectivity (63% ee), as did that of dimethyl cyclopentane-1,2-dicarboxylate (*meso*) (17% ee),[5] in contrast to the highly enantioselective hydrolysis of *trans*-1,2-diacetoxycyclobutane (95% ee) and *trans*-1,2-diacetoxycyclohexane (95% ee). During our studies on enzymatic hydrolysis,[6] we have found that the *trans*-diacetate ((±)-**6a**), as well as the *trans*-monoacetate ((±)-**4a**) and the *cis*-monoacetate ((±)-**5a**), was hydrolyzed with *Pseudomonas fluorescens* lipase (PFL) to afford the corresponding alcohols with high optical purities (Table I). It is noteworthy that the *meso*-diacetate (**7a**) was also hydrolyzed with PFL to the optically pure monoacetate (1*R*,2*S*)-(−)-**7b** (>99% ee). This finding is in contrast to the fact that the *cis*-1,2-diacetoxycycloalkanes (4-, 5-, and 6-membered ring) were hydrolyzed to the optically inactive monoacetates with PLE.[4] The hydrolysis of bicyclo[3.3.0]octane acetate ((±)-**8a**) using PFL resulted in low enantioselectivity (45% ee). Thus, PFL seems to be effective for the enantioselective hydrolysis of monocyclic five-membered cycloalkane acetates.

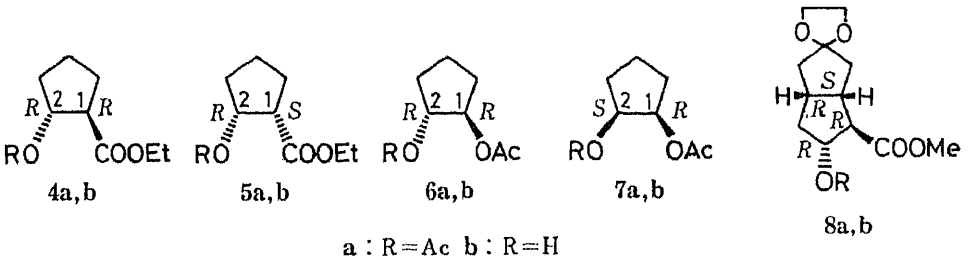


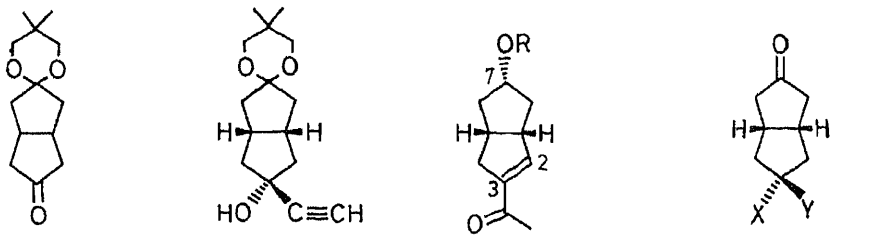


Chart 2

Enantioselective hydrolysis of (±)-**8a** was examined with several enzymes, and it was found that porcine pancreatic lipase (PPL) affords the optically pure alcohol ((+)-**8b**) with the desired absolute stereochemistry for the synthesis of **1**, although in unsatisfactory conversion yield. The prolonged hydrolysis time induced a decrease of enantioselectivity, while the conversion yield increased. As shown in Table II, the high enantioselectivity (entry 4) of PPL-catalyzed hydrolysis of (±)-**8a** was remarkably reduced in the cases of the monocyclic five-membered cycloalkane *trans*-acetates ((±)-**4a** and (±)-**6a**), which afforded (−)-**4b** (67%ee) and (+)-**6b** (28% ee), respectively. However, the hydrolysis of the *cis*-monoacetate ((±)-**5a**) proceeded faster and with high enantioselectivity to afford (−)-**5b** (>99% ee). From the absolute stereochemistry of the hydrolyzed products, it may be concluded that the acetoxy group hydrolyzed with PPL is of the *R*-configuration. This finding is in agreement with the result of hydrolysis with PFL except for the *meso*-diacetate (**7a**) having $\sigma$-symmetry (see Table I).

Compound (−)-(**2**) is important for the synthesis of **1**, and its enantiomer (+)-**2** is also a promising key intermediate for the synthesis of hirsutic acid. Thus, our attention was directed to enzymatic hydrolysis of the monoacetate ((±)-**11a**), in which there is no ester group at the $\beta$-position to the acetoxy group. The substrate ((±)-**2**) was synthesized as follows. Treatment of bicyclo[3.3.0]octanone (**9**) with lithium acetylide–ethylenediamine in tetrahydrofuran (THF) at room temperature afforded the *endo*-alcohol (**10**) as a sole product. Exposure of **10** to 85% formic acid at 90 °C yielded (±)-**2** in 65% overall yield from **9**. The structure of (±)-**2** was supported by the signals of the $\beta$-hydrogen ($C_2$-H) of $\alpha,\beta$-unsaturated ketone at $\delta$ 6.55 (1H, d, $J$=2.4 Hz) and $C_3$–$COCH_3$ at $\delta$ 2.36 (3H, s) in the proton nuclear magnetic resonance ($^1$H-NMR) spectrum, in addition to the absorption bands at 1740, 1660 (carbonyl), and 1610 (olefin) $cm^{-1}$ in the infrared (IR) spectrum. Reduction of (±)-**2** with $NaBH_4$ in the presence of $CeCl_3$ in MeOH, followed by the oxidation of the allylic alcohol with $MnO_2$, and

Table II. Enzymatic Hydrolysis of Acetates

| Entry | Substrate | Origin of lipase | Reaction time (h) | Hydrolyzed product | | |
|---|---|---|---|---|---|---|
| | | | | Compd. | Yield (%) | ee (%) |
| 1 | (±)-**4a** | Porcine pancreas | 27 | (1*R*,2*R*)-**4b** | 28 | 67 |
| 2 | (±)-**5a** | Porcine pancreas | 6 | (1*S*,2*R*)-**5b** | 30 | >99 |
| 3 | (±)-**6a** | Porcine pancreas | 72 | (1*R*,2*R*)-**6b** | 25 | 28 |
| 4 | (±)-**8a** | Porcine pancreas | 24 | (1*S*,2*R*,3*R*,5*R*)-**8b** | 14 | >99 |
| 5 | (±)-**8a** | Porcine pancreas | 40 | (1*S*,2*R*,3*R*,5*R*)-**8b** | 34 | 40 |
| 6 | (±)-**8a** | *Mucol javanicus* | 44 | (1*S*,2*R*,3*R*,5*R*)-**8b** | 32 | 34 |
| 7 | (±)-**8a** | *Aspergillus niger* | 3 | (1*S*,2*R*,3*R*,5*R*)-**8b** | 44 | 41 |

Table III. Enzymatic Hydrolysis of (±)-**11a**

| Entry | Origin of lipase | Reaction time (h) | Hydrolyzed product (**11b**) | | |
|---|---|---|---|---|---|
| | | | Absolute config. | Yield (%) | ee (%) |
| 1 | *P. fluorescens* | 120 | 1*S*,5*R*,7*S* | 24 | 45 |
| 2 | Porcine pancreas | 120 | 1*R*,5*S*,7*R* | 12 | 16 |
| 3 | *Rhizopus delemar* | 120 | 1*R*,5*S*,7*R* | 18 | 8 |
| 4 | *Candida cylindracea* | 2 | 1*S*,5*R*,7*S* | 16 | 70 |

subsequent acetylation in a standard manner afforded (±)-**11a**.

Among the tested lipases (Table III), *Candida cylindracea* lipase afforded (−)-**11b**[3] in the highest optical yield (70% ee, isolated yield 16%). PPL, which gave high optical purity in the hydrolysis of (±)-**8a**, showed only 16% ee (isolated yield 12%). The low enantioselectivity and poor conversion yield in the hydrolysis with PPL suggest that the ester group at the β-position with respect to the acetoxy group plays an important role in the hydrolysis.

Next, enantioselective reduction of (±)-**2** with baker's yeast was examined. Treatment of (±)-**2** with baker's yeast at 30 °C for 20 h afforded two fractions, in addition to the recovered (+)-**2**. They could be separated by column chromatography on silica gel. The less polar, optically inactive fraction (10% yield) was identified as a mixture (1 : 2) of **12** and **13** by comparison with authentic samples, which were prepared by catalytic hydrogenation of (±)-**2** followed by epimerization with $K_2CO_3$ in MeOH. The polar fraction (25% yield) with high optical purity (>99% ee, $[\alpha]_D^{29}$ +95.8° ($CHCl_3$)) was found to be the *endo*-alcohol ((1*R*,5*S*,7*R*)-(+)-**11b**) by comparison with the enantiomer ((−)-**11b**).[3] The absolute stereochemistry of the recovered (+)-**2** (49% ee) was determined by comparison with the pyridinium chlorochromate (PCC) oxidation product of (+)-**11b**. Optically pure (+)-**11b** is available as an intermediate with the desired absolute stereochemistry for the synthesis of hirsutic acid. The formation of **12**, **13** and the recovery of (+)-**2** suggest that the double bond of (−)-**2** was enzymatically hydrogenated in marked preference to that of the enantiomer (+)-**2**.

Thus, we found that biochemical methods are effective for the synthesis of chiral cyclopentane and bicyclo[3.3.0]octane derivatives.

## Experimental

IR spectra were measured with a JASCO A-202 spectrometer. $^1$H-NMR spectra were measured on JEOL JNM-FX 100 and JEOL JNM-GX 270 spectrometers. Mass spectra (MS) were taken on a JEOL JMS-D 300 spectrometer. Specific rotations were measured on a JASCO DIP-400 polarimeter. For column chromatography, silica gel (Merck, Kieselgel 60, 70—230 mesh) was used. For enzymatic hydrolysis, *P. fluorescens* lipase (Amano Pharmaceutical Co., "Amano P"), PPL (Sigma, type II (pfs)), *Mucol javanicus* lipase (Amano Pharmaceutical Co., "Amano M-10"), *Aspergillus niger* lipase (Amano Pharmaceutical Co., "Amano A"), *Rhizopus delemar* lipase (Seikagaku Kogyo, fine grade) and *Candida cylindracea* lipase (Sigma, type VII (pfs)) were used. All organic solvent extracts were washed with saturated brine and dried on anhydrous sodium sulfate.

**Preparation of the Acetates ((±)-4a through (±)-8a)**——These compounds were synthesized by usual acetylation with $Ac_2O$–pyridine of the racemic alcohols ((±)-**4a**, (±)-**5a** and (±)-**8a**)[7,8] and *cis*- or *trans*-cyclopentane-1,2-diol[9] in quantitative yields as colorless oils.

**General Procedure of Lipase-Catalyzed Hydrolysis of the Acetates ((±)-4a through (±)-8a)**——Lipase (50 mg) was added to a stirred suspension of a substrate (100 mg) in phosphate buffer (pH 7.0, 0.1 M) (20 ml). The reaction mixture was stirred at 33 °C for a fixed time as shown in Tables I and II. The whole was extracted with AcOEt (100 ml × 2), and the combined extracts were dried. After removal of the solvent *in vacuo*, the crude product was purified by column chromatography on silica gel (5 g). Hydrolyzed products were obtained as colorless oils. The results of the reactions are summarized in Tables I and II.

Optical purities of hydrolyzed products were determined from the 270 MHz $^1$H-NMR spectra of their (+)-α-methoxy-α-trifluoromethylphenylacetic acid (MTPA)[10] esters. The absolute stereochemistries of the products were also determined by comparison of the specific rotations with those of authentic samples (Tables IV and V).

The absolute stereochemistry of (+)-**6b** (entry 3 in Table I) was determined by hydrolysis with $K_2CO_3$–MeOH to afford the known (*R*,*R*)-(−)-cyclopentane-1,2-diol ($[\alpha]_D^{20}$ −15.0°(*c*=0.7, $CHCl_3$), reported value[12] $[\alpha]_D$ −33.8° ($H_2O$)). In addition circular dichroism (CD) spectra of the corresponding bis(*p*-methoxy)benzoate showed a negative first Cotton effect. (*R*,*R*)-(−)-1,2-Bis(*p*-methoxybenzoyloxy)cyclopentane: $[\alpha]_D^{26}$ −190° (*c*=1.23, $CHCl_3$). CD (*c*=2.05 × $10^{-5}$, MeOH) $\Delta\varepsilon^{25}$: −18.9 (262) (negative maximum), +5.8 (242) (positive maximum).

The absolute stereochemistry of compound (−)-**7b** was established by conversion of (*R*,*R*)-(−)-cyclopentane-1,2-diol into (1*S*,2*R*)-(+)-1-acetoxy-2-hydroxycyclopentane, (1*S*,2*R*)-(+)-**7b** (51% yield, $[\alpha]_D^{25}$ +9.3° (*c*=0.3, $CHCl_3$)) by treatment with a mixture of AcOH (1 eq), triphenylphosphine (1 eq), and diethyl azodicarboxylate (1 eq).

**7,7-(2,2-Dimethylpropylenedioxy)-3β-ethynyl-3α-hydroxy-1βH,5βH-bicyclo[3.3.0]octane (10)**——A solution of the ketone **9** (10.3 g) was added dropwise with stirring to a suspension of lithium acetylide–ethylenediamine complex

TABLE IV. Specific Rotation of Hydrolyzed Product

| Compd. | $[\alpha]_D^{20}$ ($c$, solvent) | Reported value | | |
|---|---|---|---|---|
| | | Compd. | $[\alpha]_D$ | (Temp., $c$, solvent) |
| (1*R*,2*R*)-**4b** | −64.0° (1.20, MeOH) | (1*S*,2*S*)-**4b** | +66.0° | (20 °C, 1.13, MeOH)[11] |
| (1*S*,2*R*)-**5b** | −14.3° (0.63, $CHCl_3$) | (1*R*,2*S*)-**5b** | +14.1° | (22 °C, 1.70, $CHCl_3$)[11] |
| (1*R*,2*R*)-**6b** | +22.3° (1.12, $CHCl_3$) | | — | |
| (1*R*,2*S*)-**7b** | −8.9° (0.60, $CHCl_3$) | | — | |
| (1*S*,2*R*,3*R*,5*R*)-**8b** | +27.3° (1.15, $CHCl_3$) | (1*S*,2*R*,3*R*,5*R*)-**8b** | +29.0° | (23 °C, 1.50, $CHCl_3$)[8] |

TABLE V. Chemical Shifts of Methoxy Signals of (+)-MTPA Esters (270 MHz $^1$H-NMR)

| Alcohol | $\delta$ ($CDCl_3$) (ppm) | Alcohol | $\delta$ ($CDCl_3$) (ppm) |
|---|---|---|---|
| (1*R*,2*R*)-**4b** | 3.553 | (1*S*,2*S*)-**4b** | 3.537 |
| (1*S*,2*R*)-**5b** | 3.495 | (1*R*,2*S*)-**5b** | 3.506 |
| (1*R*,2*R*)-**6b** | 3.562 | (1*S*,2*S*)-**6b** | 3.531 |
| (1*R*,2*S*)-**7b** | 3.608 | (1*S*,2*R*)-**7b** | 3.549 |
| | 2.014 (OAc) | | 2.068 (OAc) |
| (1*S*,2*R*,3*R*,5*R*)-**8b** | 3.548 | (1*R*,2*S*,3*S*,5*S*)-**8b** | 3.534 |
| | 3.679 (COOMe) | | 3.605 (COOMe) |

(21.1 g) in THF (500 ml) at 0 °C under an $N_2$ atmosphere. After being stirred for 24 h at room temperature, the reaction mixture was poured into ice-water (300 ml) and extracted with ether (200 ml × 3). The combined extracts were successively washed with 5% $H_2SO_4$, 5% aqueous $NaHCO_3$ and brine, then dried. Removal of the solvent *in vacuo* gave a colorless solid, which was chromatographed on silica gel (150 g). The fraction eluted with 5% AcOEt in hexane (v/v) afforded **10** (8.05 g, 81%) as colorless needles, mp 111—112 °C, recrystallized from hexane. IR (Nujol): 3400, 3300, 1460, 1110 $cm^{-1}$. $^1$H-NMR ($CDCl_3$) $\delta$: 0.96 (6H, s, $CH_3 \times 2$), 2.46 (1H, s, C≡CH), 3.48 (4H, s, $OCH_2 \times 2$). MS *m/z*: 250 ($M^+$), 232, 208, 128.

**3-Acetylbicyclo[3.3.0]oct-2-en-7-one ((±)-2)**——A mixture of **10** (4.0 g) and 85% HCOOH (50 ml) was heated at 90 °C for 9 h with stirring. Removal of formic acid *in vacuo* afforded an oily residue, which was purified by flash column chromatography on silica gel (Merck, Kieselgel 230—400 mesh, 60 g). The fraction eluted with 50% AcOEt in hexane (v/v) afforded (±)-**2** (2.08 g, 80%) as a colorless oil. IR (neat): 1740, 1670, 1610, 1400, 1370 $cm^{-1}$. $^1$H-NMR ($CDCl_3$) $\delta$: 2.36 (3H, s, $COCH_3$), 3.64 (1H, m, $C_1$-H), 6.55 (1H, d, $J$=2.4 Hz, $C_2$-H). MS *m/z*: 164 ($M^+$), 149, 121.

**3-Acetyl-7α-hydroxy-1βH,5βH-bicyclo[3.3.0]oct-2-ene ((±)-11b)**——$NaBH_4$ (50 mg) was added portionwise to a stirred suspension of (±)-**2** (200 mg) and $CeCl_3 \cdot 7H_2O$ (440 mg) in MeOH (5 ml) at 0 °C. The mixture was stirred for 5 min at room temperature, then acetone (0.5 ml) was added. The whole was diluted with brine (10 ml) and extracted with ether (25 ml × 3). The combined extracts were dried. Removal of the solvent *in vacuo* afforded an oily residue (196 mg), which was dissolved in $CHCl_3$ (1 ml) and added to a stirred suspension of $MnO_2$ (1 g) in $CHCl_3$ (5 ml). The reaction mixture was stirred for 24 h at room temperature. After filtration, the filtrate was concentrated *in vacuo* to leave an oily residue, which was chromatographed on silica gel (3 g). The fraction eluted with 5% AcOEt in hexane (v/v) afforded (±)-**11b** (180 mg, 90%) as a colorless oil. IR (neat): 3400, 1655, 1610 $cm^{-1}$. $^1$H-NMR ($CDCl_3$) $\delta$: 2.32 (3H, s, $COCH_3$), 3.35 (1H, m, $C_1$-H), 4.24 (1H, tt, $J$=5, 5 Hz, $C_7$-H), 6.63 (1H, d, $J$=2.5 Hz, $C_2$-H). MS *m/z*: 166 ($M^+$), 148, 105.

**7α-Acetoxy-3-acetyl-1βH,5βH-bicyclo[3.3.0]oct-2-ene ((±)-11a)**——$Ac_2O$ (306 mg) was added dropwise to a stirred solution of (±)-**11b** (255 mg) in pyridine (3 ml). After being stirred for 2 h at room temperature, the reaction mixture was diluted with brine (5 ml) and extracted with AcOEt (20 ml × 3). The combined extracts was successively washed with 1% aqueous HCl, 5% aqueous $NaHCO_3$ and brine, then dried. Removal of the solvent afforded an oily residue, which was chromatographed on silica gel (10 g). The fraction eluted with 30% AcOEt in hexane (v/v) gave (±)-**11a** (305 mg, 96%) as a colorless oil. IR (neat): 1735, 1665, 1617, 1375, 1250 $cm^{-1}$. $^1$H-NMR ($CDCl_3$) $\delta$: 1.94 (3H, s, $OCOCH_3$), 2.32 (3H, s, $COCH_3$), 3.38 (1H, m, $C_1$-H), 5.07 (1H, tt, $J$=5.5, 5.5 Hz, $C_7$-H), 6.58 (1H, d, $J$=2.2 Hz, $C_2$-H). MS *m/z*: 208 ($M^+$), 166, 148.

**Lipase-Catalyzed Hydrolysis of (±)-11a**——Enzymatic hydrolysis was examined in the same manner as before.

The optical purity and absolute stereochemistry of the reaction product were determined from the specific rotation of authentic samples.[3]

**Reduction of (±)-2 with Baker's Yeast**——Compound (±)-**2** (1.0 g) was added to a stirred suspension of glucose (100 g), baker's yeast (100 g, Oriental Yeast Co., Ltd.), and water (500 ml). The mixture was stirred for 20 h at 30 °C, then AcOEt (500 ml) was added, and the whole was filtered through Celite. An aqueous layer of filtrate was extracted with AcOEt (300 ml × 2). The combined extracts were washed with brine and dried. Removal of the solvent *in vacuo* afforded an oily residue, which was chromatographed on silica gel (25 g). The fraction eluted with 10% AcOEt in hexane (v/v) afforded a mixture of **12** and **13** (1 : 2) (100 mg, 10%), (±)-**2** (220 mg, 22% yield, 49% ee): $[\alpha]_D^{26}$ +71.3° ($c$ = 0.80, $CHCl_3$), and (+)-**11b** (250 mg, 25% yield, >99% ee), $[\alpha]_D^{29}$ +95.8° ($c$ = 1.27, $CHCl_3$). The optical purities of (+)-**2** and (+)-**11b** were estimated from the specific rotation.[3]

**3α-Acetyl-1βH,5βH-bicyclo[3.3.0]octan-7-one (12)**——Compound (±)-**2** (100 mg) was subjected to catalytic hydrogenation using 5% Pd–C (80 mg) in MeOH (10 ml). The catalyst was filtered off, and the filtrate was evaporated *in vacuo* to afford an oily residue, which was chromatographed on silica gel (2 g). The fraction eluted with 10% AcOEt in hexane (v/v) afforded **12** (92 mg, 92%) as a colorless oil. IR (neat): 1738, 1700, 1400, 1360 $cm^{-1}$. 270 MHz $^1$H-NMR ($CDCl_3$) $\delta$: 1.65 (2H, m), 2.05—2.35 (4H, m), 2.18 (3H, s, $COCH_3$), 2.50 (2H, m), 2.78 (2H, m), 3.07 (1H, tt, $J$ = 9.9, 8.2 Hz, $C_3$-H). MS $m/z$: 166 ($M^+$), 123, 95.

**Epimerization of 12 to 13**——$K_2CO_3$ (200 mg) was added to a stirred solution of **12** (80 mg) in MeOH (5 ml). After being stirred for 4 h at room temperature, the reaction mixture was diluted with brine (10 ml), and extracted with ether (20 ml × 3). The combined extracts were dried. Removal of the solvent *in vacuo* afforded an oily residue, which was chromatographed on silica gel (2 g). The fraction eluted with 10% AcOEt in hexane (v/v) afforded a mixture (1 : 1) of **12** and **13** (75 mg). 270 MHz $^1$H-NMR ($CDCl_3$) $\delta$: 3.07 (tt, $J$ = 9.9, 8.2 Hz, $C_3$-H of **12**), 3.12 (tt, $J$ = 7.7, 7.7 Hz, $C_3$-H of **13**).

**PCC Oxidation of (+)-11b to (1*R*,5*S*)-(+)-2**——PCC (210 mg) was added to a stirred solution of (+)-**11b** (110 mg, >99% ee) in $CH_2Cl_2$ (5 ml) at 0 °C. After 2 h at room temperature, ether (20 ml) was added and the precipitate was filtered off through Celite. The filtrate was concentrated *in vacuo* to afford an oily residue, which was purified by chromatography on silica gel (2 g). The fraction eluted from 10% AcOEt in hexane (v/v) afforded (+)-**2**: $[\alpha]_D^{23}$ +142° ($c$ = 1.5, $CHCl_3$).

**Acknowledgement** The authors are grateful to Amano Pharmaceutical Co., Ltd., Japan for generously providing lipase.

## References and Notes

1) *a*) W. Bartmann and G. Bech, *Angew. Chem., Int. Ed. Engl.*, **21**, 751 (1982); *b*) Z.-F. Xie, K. Funakoshi, H. Suemune, T. Oishi, H. Akita, and K. Sakai, *Chem. Pharm. Bull.*, **34**, 3058 (1986), and references cited therein.
2) B. M. Trost and F. Dininno, *J. Am. Chem. Soc.*, **96**, 1083 (1974).
3) Z.-F. Xie, Y. Ichikawa, H. Suemune, and K. Sakai, *Chem. Pharm. Bull.*, **35**, 1812 (1987).
4) D. H. G. Grout, V. S. D. Gaudet, K. Laumen, and M. Schneider, *J. Chem. Soc., Chem. Commun.*, **1986**, 808.
5) P. Mohr, N. W. Sarcevic, and C. Tamm, *Helv. Chim. Acta*, **66**, 251 (1983).
6) H. Suemune, K. Okano, H. Akita, and K. Sakai, *Chem. Pharm. Bull.*, **35**, 1741 (1987).
7) J. Pascual and J. Castells, *J. Am. Chem. Soc.*, **74**, 2899 (1952).
8) K. Kojima, S. Amemiya, K. Koyama, and K. Sakai, *Chem. Pharm. Bull.*, **33**, 2688 (1985).
9) *a*) G. A. Olah, A. P. Fung, and D. Meidar, *Synthesis*, **1981**, 280; *b*) W. D. Lloyd, B. J. Navarette, and M. F. Shaw, *ibid.*, **1972**, 610.
10) J. A. Dale and H. S. Mosher, *J. Am. Chem. Soc.*, **95**, 512 (1973).
11) D. Buisson and R. Azerad, *Tetrahedron Lett.*, **27**, 2634 (1986).
12) B. Helferich and R. Hiltmann, *Chem. Ber.*, **1937**, 308.

[Chem. Pharm. Bull. 35(11)4460—4464(1987)]

# Studies on the Constituents of Umbelliferae Plants. XVI.[1] Isolation and Structures of Three New Ligustilide Derivatives from *Angelica acutiloba*

TAKASHI TSUCHIDA, MASARU KOBAYASHI,* KO KANEKO, and HIROSHI MITSUHASHI

*Faculty of Pharmaceutical Sciences, Hokkaido University, Sapporo 060, Japan*

(Received April 30, 1987)

Three new ligustilide derivatives (**3**—**5**) were isolated from the crude drug toki, the dried roots of the Umbelliferae plant *Angelica acutiloba*, together with a known ligustilide dimer, levistolide A (**2**), and four known oxygenated ligustilide derivatives, senkyunolide E (**6**), senkyunolide F (**7**), senkyunolide H (**8**) and senkyunolide I (**9**). Compound **3** was shown to be the angeloyl ester of **7**. Compounds **4** and **5**, designated tokinolide A and tokinolide B, are dimeric ligustilide derivatives with Diels–Alder-type (**5**) and cyclobutane-type (**4**) cyclization systems, respectively. The occurrence of compounds **2** to **9** in a fresh *A. acutiloba* sample was confirmed.

**Keywords**——tokinolide A; tokinolide B; angeloylsenkyunolide F; phthalide; *Angelica acutiloba*; Umbelliferae

Toki is the dried root of an Umbelliferae plant, *Angelica acutiloba*, which is used quite frequently in the prescriptions of Chinese traditional medicine. Its pharmacological actions are not fully established but in many cases it has been used together with senkyu, the rhizome of another Umbelliferae plant, *Cnidium officinale*, for the treatment of obstetrical and gynecological disorders. Volatile alkylphthalide derivatives are common components of *A. acutiloba* and *C. officinale*, and ligustilide (**1**) is the predominant compound of the phthalide fraction of the two plants. Recently we reported that prolonged storage of *C. officinale* rhizome causes formation and accumulation of a variety of oxygenated ligustilide derivatives.[1] In view of the importance of toki in traditional Chinese medicine, we subsequently studied its phthalide derivatives.

The crude lipid of *A. acutiloba* was subjected to solvent fractionation (hexane–methanol–water) to remove the bulk of the triglycerides. Repeated flash chromatography of the methanol-soluble fraction afforded compounds **2**—**9**, including three new compounds (**3**—**5**). All of them were found to be derivatives of ligustilide (**1**), but were isolated in small amounts. The content of **1** in *A. acutiloba* is known to be less than one-tenth of that in *C. officinale*,[2] whose large phthalide content is rather exceptional in Umbelliferae plants.

Compound **2**, mp 113—115 °C, was an optically inactive dimeric derivative of ligustilide (**1**). Its mass spectrum (MS) showed the molecular ion ($M^+$) at *m/z* 380 but the remaining ions were virtually the same as those of **1**.[3] This is a common feature of the ligustilide dimers reported previously from a variety of Umbelliferae plants.[4] Its proton nuclear magnetic resonance ($^1$H-NMR) spectrum showed signals of olefinic protons of two butylidene side chains at $\delta$ 5.00 (1H, t, $J$=7.8 Hz) and 5.07 (1H, t, $J$=7.8 Hz) and the signal of an olefinic proton of an $\alpha,\beta$-unsaturated-$\gamma$-lactone at $\delta$ 7.35 (1H, d, $J$=6.4 Hz). These and other spectral properties (Experimental) were identical with those reported for a ligustilide dimer, levistolide A, which was isolated from the Umbelliferae plants *Ligusticum wallichii*[4a] and *Levisticum*

*officinale*.[4b]

Compound **3**, $[\alpha]_D$ +26°, $C_{17}H_{20}O_4$, was a viscous oil which showed, on a thin-layer chromatography (TLC) plate, a bright blue fluorescence under a 254 nm ultraviolet (UV) lamp. This is a characteristic of the cross-conjugated triunsaturated-γ-lactone system found in **1** and senkyunolide F (**7**), and the presence of the senkyunolide F moiety was indicated by the $^1$H-NMR spectrum. It showed the signals of three olefinic protons at δ 6.29 (dt, $J$=9.8, 1.8 Hz, 7-H), 6.06 (dt, $J$=9.8, 4.0 Hz, 6-H), and at δ 5.15 (d, $J$=8.0 Hz, 10-H). The olefin proton at δ 5.15 was found to be coupled with a methine at δ 5.77 (ddd, $J$=8.0, 7.0, 6.2 Hz), which is assignable to 11-H. Other signals coincided with those of angelic acid (δ 1.91, 3H, quint. $J$=1.5 Hz; δ 2.00, 3H, dq, $J$=7.3, 1.5 Hz; δ 6.09, qq, $J$=7.3, 1.5 Hz). Compound **3** was thus shown to be 11-angeloylsenkyunolide F. It was quite labile to basic or acidic hydrolysis, giving decomposition products, and the attempted determination of the stereochemistry at C-11 was unsuccessful.

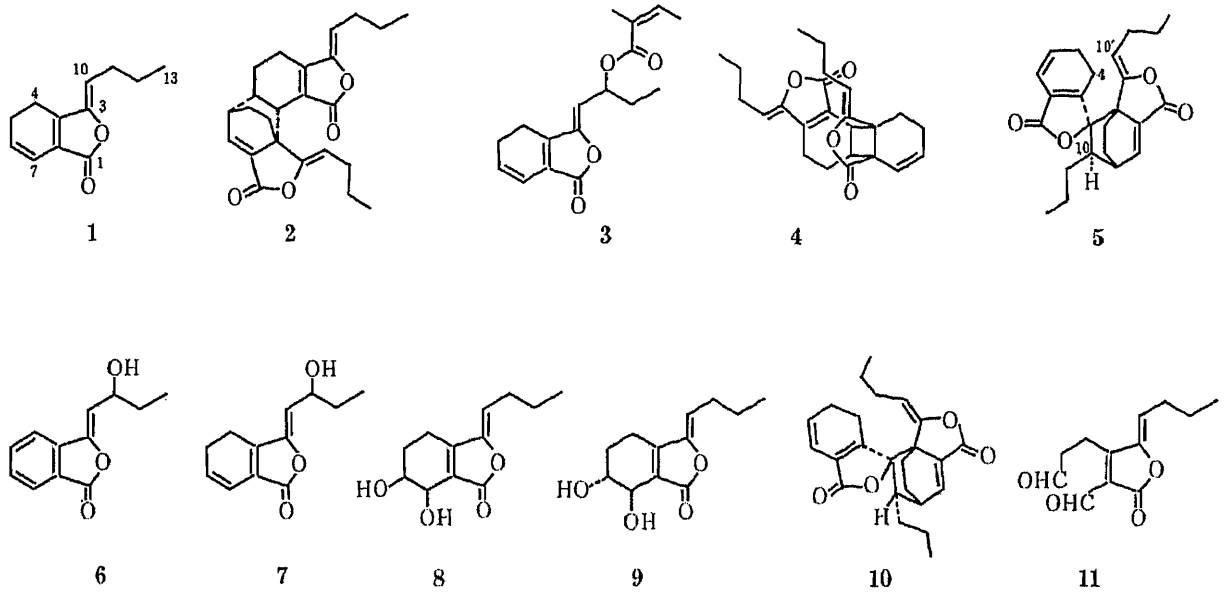


Chart 1

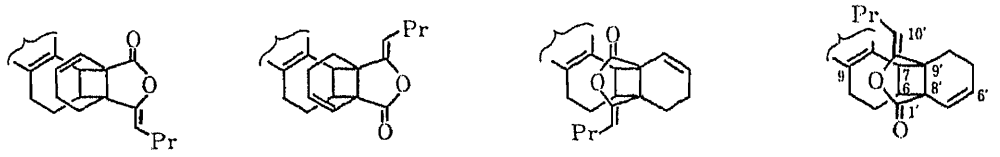


Chart 2

Tokinolide A (**4**) and tokinolide B (**5**), $C_{24}H_{28}O_4$, were ligustilide dimers and were optically inactive. Their mass spectra were quite similar to that of levistolide A (**2**). They showed the molecular ions at $m/z$ 380 and other ions at $m/z$ 190, 161 and 148 which were formed by secondary fragmentation of the ligustilide moieties. Unlike **2**, tokinolide A is not the Diels–Alder-type dimer, as indicated by the lack of olefin protons due to the α,β-unsaturated-γ-lactone moiety. The $^1$H-NMR spectrum showed the signals of the olefinic protons of two butylidene side chains at δ 4.66 (1H, dd, $J$=8.3, 7.3 Hz) and 5.21 (1H, t, $J$=7.8 Hz), and two olefinic protons of an isolated double bond at δ 6.00 (1H, d, $J$=9.8 Hz) and 6.11 (1H, dt, $J$=9.8, 4.0 Hz). These signals and the UV absorption of **4** at 276 nm (ε, 18000),

which is similar to that of 6,7-dihydroligustilide (273 nm, ε, 17800),[5] indicated that compound **4** is a dimeric ligustilide forming a cyclobutane ring at C-6 and C-7 of one ligustilide molecule with C-8′ and C-9′ of the other. The geometries of the two butylidene side chains were shown to be *Z*, as exemplified by the high-field chemical shifts of the olefin protons of the enol-γ-lactone (δ 4.66) and conjugated enol-γ-lactone moieties (δ 5.21). These protons on the *E*-side chain suffer significant deshielding from the vicinal oxygen atoms (O-2, O-2′); the signals appears at δ 5.38 in compound **10** (*vide infra*), and about δ 5.8 in the *E*-isomers of **8** and **9**.[1] Since tokinolide A is optically inactive, it could be formulated as one of the four racemic pairs shown in Chart 2. Of these, the structures A and B are unreasonable since there would be severe steric repulsion between the two bulky cyclohexene rings. The nuclear Overhauser effect (NOE) differential spectrum showed that there was NOE between the protons at δ 6.11 (6′-H) and 3.23 (1H, d, $J$=9.3 Hz, 7-H). It indicated the proximity of these two protons and narrowed the choice of structure of **4** to C or D. The non-decoupling carbon-13 NMR ($^{13}$C-NMR) spectrum indicated that the unconjugated lactonic carbonyl carbon (C-1′, 175.5 ppm), which appears at lower field than the conjugated lactonic carbonyl (169.5 ppm), is coupled with one proton with a coupling constant of 4.9 Hz. This is a typical value of the long-range coupling constants between two atoms separated by two bonds, or separated by three bonds with an antiparallel system.[6] The long-range coupling constants of those separated by four bonds are generally negligible or less than 1.5 Hz. Irradiation of 7-H (δ 3.23, d, $J$=9.3 Hz) had no influence on the 1′ carbon signal, but irradiation of 6-H (δ 2.90, ddd, $J$=9.3, 6.8, 4.4 Hz) changed the 1′-carbon signal into a sharp singlet indicating the presence of three bonds between them. The structure of tokinolide A was thus shown to be **4**, a new type of dimeric ligustilide having a cyclobutane ring.

Tokinolide B (**5**) is a Diels–Alder-type ligustilide dimer like compound **2**, and its $^1$H-NMR spectrum showed the signal of an olefinic proton of a conjugated lactone group at δ 7.53 (1H, d, $J$=6.6 Hz). Other $^1$H-NMR signals were quite similar to those of the known compound angeolide (**10**), which was isolated from an Umbelliferae plant, *A. glauca*, by Banerjee *et al.*,[4c] and indicated that the butylidene side chain of one ligustilide molecule is included as the dienophile. The major spectral differences between compounds **5** and **10** were the chemical shifts of the olefin proton at C-10′ of the enol-γ-lactone moiety and the methine proton at C-10. The chemical shifts of these signals of **10** were reported to be δ 5.38 (dd, $J$= 9.5, 7.0 Hz, 10′-H) and 2.82 (m, 10-H) respectively. In contrast, tokinolide B showed these signals at δ 4.62 (dd, $J$=8.8, 6.8 Hz) and 1.66 (m) respectively. This indicates that the side chain of **5** takes the *Z*-form, unlike that of **10**, and the C-10′ proton is unaffected by the neighboring lactonic oxygen atom (O-2′). The unusually deshielded nature of 10-H (δ 2.82) of **10** is due to the deshielding effect of the lactonic oxygen (O-2) of the other ligustilide moiety. The marked up-field shift of this signal in tokinolide B shows the absence of this effect on 10-H. These observations indicate that tokinolide B (**5**) is a C-10 epimer of angeolide (**10**), and the geometry of its side chain is 3′(10′)-*Z*. From the two-dimensional $^1$H-NMR spectrum, the signal of one of the methylene protons at C-4 was found to appear at δ 1.30, which is markedly high for an allylic proton. This is due to the influence of the 1′ carbonyl group, which a Dreiding model indicated to be sterically very close, including C-4 in its shielding region. From these results, tokinolide B was shown to be the dimeric compound **5**, which is composed of two 3(10)-*Z* ligustilide molecules, in contrast to angeolide (**10**) which is composed of two 3(10)-*E* ligustilide molecules.[4c]

Compounds **6** to **9** were identified as senkyunolide E, senkunolide F, senkyunolide H and senkyunolide I, respectively, by direct comparison of their infrared (IR), UV, MS and $^1$H-NMR data with those of authentic samples previously isolated from *C. officinale*.[1]

Except for **3**, the compounds found in the present study were optically inactive and are considered to be racemic mixtures. However, high-performance liquid chromatographic

(HPLC) examination indicated the presence of these compounds in the fresh *A. acutiloba* extract. Their amounts were mostly less than ten mg in 1 kg of sample but there were no marked differences between the fresh samples and samples which has been dried and kept for two months, except that compounds **6** and **7**, whose contents were negligible in the fresh samples, increased to 3—5 mg/kg (**6**) and 15—30 mg/kg (**7**) in the stored samples. The contents of angeloylsenkyunolide F (**3**) and senkyunolide I (**9**) were relatively high; 397 mg of **3** and 124 mg of **9** were isolated from 4.5 kg of *A. acutiloba*. This high content of optically active angeloylsenkyunolide F (**3**), compared with other optically inactive hydroxyphthalides (**6**—**9**), suggests that the formation process of **3** in *A. acutiloba* is different from that of **6** to **9**. Also, our previous assumption that the hydroxyphthalides are derived entirely by autoxidation during the preparation and storage of the crude drug, might not be correct.

The contents of the ligustilide dimers (**2**, **4**, **5**) were found to be almost the same between the fresh and the dried and aged materials, and these compounds were considered to be original components of the plant. This is not unusual, since the hitherto known ligustilide dimers found in Umbelliferae plants are invariably racemic and in some cases are quite abundant.[4c,d] Neither the heating of **1** in benzene, toluene, or xylene nor the prolonged storage of **1** (six months) at room temperature caused the formation of these ligustilide dimers. Most of the ligustilide fraction remained unchanged while some was partly oxidized, giving butylidenephthalide.[3] Only the formation of a small amount of dialdehyde (**11**) by autoxidation was confirmed when **1** was refluxed in benzene, toluene, or xylene for 3 h.

## Experimental

Melting points were determined on a Kofler hot stage and are uncorrected. Optical rotations were determined on a JASCO DIP-4 digital polarimeter. $^1$H-NMR spectra were determined on a JEOL JNM GX-270 spectrometer at 270 MHz in $CDCl_3$ solution with TMS as an internal standard. MS were determined on JEOL JMS-D300 (EI-MS) and JEOL JMS-O1SG-2 (FD-MS) spectrometers. IR spectra were taken on a JASCO A-102 spectrometer. Column chromatography was carried out by the flash chromatography method. HPLC was carried out using Senshu Pak silica 1151N (150×4.8 mm i.d.) with 5% ethyl acetate in hexane.

**Fractionation of *A. acutiloba* Extract**——Commercial roots of *A. acutiloba* were used as the source material. The dried and pulverized material (4.5 kg) was extracted thoroughly with hexane–$Et_2O$ (2 : 1) and $CHCl_3$–MeOH (1 : 1). The $CHCl_3$–MeOH extract (450 g) was partitioned with a solvent mixture of $CHCl_3$–MeOH–$H_2O$ (8 : 4 : 3) and separated into upper (327 g) and lower (96 g) extracts. The lower extract was combined with the hexane–$Et_2O$ extract (58 g), partitioned with a solvent mixture of hexane–MeOH–$H_2O$ (20 : 10 : 2), and separated into upper (110.6 g) and lower (37.1 g) extracts. The lower extract was submitted to flash chromatography over a column of silica gel and eluted with mixtures of EtOAc–hexane (2 : 8, fraction 1, 13.2 g), EtOAc–hexane (1 : 1, fraction 2, 7.0 g) and MeOH–$CHCl_3$ (1 : 9) and MeOH (fraction 3, 20.2 g). Repeated flash chromatography of fractions 1 and 2 with $Et_2O$–$CHCl_3$ and EtOAc–hexane gave **3** (397 mg), **4** (27 mg) and **5** (31 mg) from fraction 1, and **2** (53 mg), **6** (9 mg) and **7** (35 mg) from fraction 2. The *Rf*'s of **2**—**7** on silica gel TLC plate with EtOAc–hexane (3 : 7) were 0.67 (**3**), 0.64 (**4**), 0.59 (**5**), 0.37 (**2**), 0.23 (**6**), and 0.21 (**7**). Flash chromatography of fraction 3 with 3.3% MeOH in $CHCl_3$ afforded **8** (less than 1 mg) and **9** (124 mg). The *Rf*'s of **8** and **9** on silica gel TLC plate with 5% MeOH in $CHCl_3$ were 0.35 (**8**) and 0.27 (**9**).

**Levistolide A (2)**——mp 113—115 °C, $[\alpha]_D$ 0° ($c$=0.4, $CHCl_3$). $^1$H-NMR $\delta$: 0.92 (6H, t, $J$=7.3 Hz), 2.55 (1H, br t, $J$=8.3, 7.3 Hz), 2.98 (1H, m), 3.25 (1H, d, $J$=8.8 Hz), 5.00 (1H, t, $J$=7.8 Hz), 5.07 (1H, t, $J$=7.8 Hz), 7.35 (1H, d, $J$=6.4 Hz). UV $\lambda_{max}^{EtOH}$ nm ($\varepsilon$): 275 (12000), 227 (8000). IR $\nu_{max}^{Nujol}$ cm$^{-1}$: 1730, 1630. MS *m/z*: 380, 191, 190, 161, 148.

**Angeloylsenkyunolide F (3)**——Oil, $[\alpha]_D$ +26° ($c$=0.70, $CHCl_3$). $^1$H-NMR $\delta$: 0.98 (3H, t, $J$=7.3 Hz, 13-$H_3$), 1.91 (3H, quint, $J$=1.5 Hz), 2.00 (3H, dq, $J$=7.3, 1.5 Hz), 5.15 (1H, d, $J$=8.0 Hz, 10-H), 5.77 (1H, ddd, $J$=8.1, 7.0, 6.2 Hz, 11-H), 6.06 (1H, dt, $J$=9.9, 4.0 Hz, 6-H), 6.09 (1H, qq, $J$=7.3, 1.5 Hz), 6.29 (1H, dt, $J$=9.8, 1.8 Hz, 7-H). UV $\lambda_{max}^{EtOH}$ nm ($\varepsilon$): 320 (9900), 284 (9000), 270 (10700), 261 (9900), 215 (21700). IR $\nu_{max}^{Nujol}$ cm$^{-1}$: 1770, 1715. MS *m/z*: 288, 231, 205, 189. High-resolution MS: Found 288.1367. Calcd for $C_{17}H_{20}O_4$ ($M^+$) 288.1361.

**Tokinolide A (4)**——Oil, $[\alpha]_D$ 0° ($c$=0.6, $CHCl_3$). $^1$H-NMR $\delta$: 0.80 (3H, t, $J$=7.3 Hz), 0.94 (3H, t, $J$=7.3 Hz), 2.39 (1H, ddd, $J$=18.3, 6.2, 3.5 Hz, 4-$H_a$), 2.56 (1H, ddd, $J$=18.3, 9.3, 5.6 Hz, 4-$H_b$), 2.90 (1H, ddd, $J$=9.3, 6.8, 4.4 Hz, 6-H), 3.23 (1H, d, $J$=9.3 Hz, 7-H), 4.66 (1H, dd, $J$=8.3, 7.3 Hz, 10′-H), 5.21 (1H, t, $J$=7.8 Hz, 10-H), 6.00 (1H, d, $J$=9.8 Hz, 7′-H), 6.11 (1H, br dt, $J$=9.8, 4.0 Hz, 6′-H). UV $\lambda_{max}^{EtOH}$ nm ($\varepsilon$): 276 (18000). IR $\nu_{max}^{Nujol}$ cm$^{-1}$: 1760, 1700. MS *m/z*: 380, 191, 190, 161, 148. High-resolution MS: Found 380.1996. Calcd for $C_{24}H_{28}O_4$ 380.1987.

**Tokinolide B (5)**——Oil, $[\alpha]_D$ 0° ($c$=0.6, $CHCl_3$). $^1$H-NMR $\delta$: 0.82 (3H, t, $J$=7.3 Hz), 0.88 (3H, t, $J$=7.3 Hz), 1.66 (1H, m, 10-H), 2.07 (1H, dt, $J$=18.1, 10.3 Hz), 2.26—2.30 (2H, m), 2.49 (1H, t, $J$=9.5 Hz), 3.10 (1H, m, 6′-H),

4.62 (1H, dd, $J$=8.8, 6.8 Hz, 10′-H), 5.92 (1H, dt, $J$=9.5, 4.0 Hz, 6-H), 6.17 (1H, d, $J$=6.6 Hz, 7-H), 7.53 (1H, d, $J$=6.6 Hz, 7′-H). UV $\lambda_{max}^{EtOH}$ nm ($\varepsilon$): 280 (6100). IR $\nu_{max}^{Nujol}$ cm$^{-1}$: 1775, 1755, 1695. MS $m/z$: 380, 191, 190, 161. High-resolution MS: Found 380.1990. Calcd for $C_{24}H_{28}O_4$ 380.1987.

**Senkyunolide E (6)**——Oil, $[\alpha]_D$ 0° ($c$=0.4, $CHCl_3$). $^1$H-NMR $\delta$: 1.00 (3H, t, $J$=7.1 Hz), 4.87 (1H, dt, $J$=8.3, 6.5 Hz), 5.74 (1H, d, $J$=8.3 Hz), 7.50—8.00 (4H, m). UV $\lambda_{max}^{EtOH}$ nm ($\varepsilon$): 235 (11000), 259 (11000), 268 (9000). IR $\nu_{max}^{Nujol}$ cm$^{-1}$: 3400, 1785, 1685, 1610. MS $m/z$: 204 ($M^+$), 186, 175, 147, 129.

**Senkyunolide F (7)**——Oil, $[\alpha]_D$ 0° ($c$=0.6, $CHCl_3$). $^1$H-NMR $\delta$: 0.97 (3H, t, $J$=7.3 Hz), 4.74 (1H, dt, $J$=8.3, 6.5 Hz), 5.22 (1H, d, $J$=8.3 Hz), 6.06 (1H, dt, $J$=9.8, 3.9 Hz), 6.30 (1H, d, $J$=9.8 Hz). UV $\lambda_{max}^{EtOH}$ nm ($\varepsilon$): 270 (4500), 282 (4300), 296 (sh, 4000), 321 (4400). IR $\nu_{max}^{Nujol}$ cm$^{-1}$: 3400, 1770, 1610. MS $m/z$: 206 ($M^+$), 188, 177, 149.

**Senkyunolide H**——Oil. MS $m/z$: 224 ($M^+$), 180, 175, 151.

**Senkyunolide I**——Oil, $[\alpha]_D$ 0° ($c$=1.1, $CHCl_3$). $^1$H-NMR $\delta$: 0.95 (3H, t, $J$=6.8 Hz), 3.95 (1H, ddd, $J$=9.5, 6.5, 3.5 Hz), 4.50 (1H, d, $J$=6.5 Hz), 5.29 (1H, t, $J$=7.8 Hz). UV $\lambda_{max}^{EtOH}$ nm ($\varepsilon$): 274 (14600). IR $\nu_{max}^{Nujol}$ cm$^{-1}$: 3400, 1740, 1685, 1640. MS $m/z$: 224 ($M^+$), 206, 180, 165, 151, 138.

**Pyrolysis of Ligustilide**——A solution of 300 mg of **1** in 2 ml of xylene was refluxed for 3 h. TLC (ethyl acetate : hexane = 3 : 17) examination of the mixture showed the formation of small amounts of more polar products which were different from the ligustilide dimers **2**, **4**, and **5**. Heating of **1** in benzene and toluene gave similar results. The mixture obtained by heating in xylene was worked up as usual and separated over a column of silica gel with ethyl acetate–hexane (3 : 17). The most polar product (**11**, 27 mg) was purified. Oil. $^1$H-NMR $\delta$: 0.99 (3H, t, $J$=7.3 Hz, 13-$H_3$), 1.57 (2H, dt, $J$=7.8, 7.1 Hz, 12-$H_2$), 2.49 (2H, dt, $J$=7.8, 7.3 Hz, 11-$H_2$), 2.84 (2H, m), 3.12 (2H, m), 5.99 (1H, t, $J$=8.1 Hz, 10-H), 9.80 (1H, br s, 6-H), 10.0 (1H, s, 7-H). MS $m/z$: 222 ($M^+$). IR $\nu_{max}^{Nujol}$ cm$^{-1}$: 2710, 1760, 1720, 1680, 1650, 1580.

## References


1) Part XV: M. Kobayashi, M. Fujita, and H. Mitsuhashi, *Chem. Pharm. Bull.*, **35**, 1427 (1987).
2) H. Mitsuhashi, T. Muramatsu, U. Nagai, T. Nakano, and K. Ueno, *Chem. Pharm. Bull.*, **11**, 1317 (1963).
3) T. Yamagishi and H. Kaneshima, *Yakugaku Zasshi*, **97**, 237 (1977).
4) *a*) M. Kaouadji, H. Reutenauer, A. J. Chulia, and A. Marsura, *Tetrahedron Lett.*, **24**, 4677 (1983); *b*) M. Cichy, V. Wray, and G. Hofle, *Justus Liebigs Ann. Chem.*, **1984**, 397; *c*) S. K. Banerjee, B. D. Gupta, W. S. Sheldric, and G. Hofle, *ibid.*, **1982**, 699; *d*) *Idem*, *ibid.*, **1984**, 888; *e*) M. Kaouadji, F. De Pachtere, C. Pouget, A. J. Chulia, and S. Lavaitte, *J. Natural Products*, **49**, 872 (1986).
5) H. Mitsuhashi and U. Nagai, *Tetrahedron*, **19**, 1277 (1963).
6) J. L. Marshall, D. E. Miller, S. A. Conn, R. Seiwell, and A. M. Ihrig, *Accounts Chem. Res.*, **7**, 333 (1974).

[Chem. Pharm. Bull. 35(11)4465—4472(1987)]

# Studies of the Selective O-Alkylation and Dealkylation of Flavonoids. IX.[1] A New Method for Synthesizing 3,5-Dihydroxy-7,8-dimethoxyflavones from 3-Hydroxy-5,7,8-trimethoxyflavones

TOKUNARU HORIE,* MASAO TSUKAYAMA, YASUHIKO KAWAMURA, and SHIGEO YAMAMOTO

*Department of Applied Chemistry, Faculty of Engineering, Tokushima University, Minamijosanjima-cho, Tokushima 770, Japan*

(Received May 9, 1987)

2-Hydroxy-3,4,6-trimethoxy-ω-(*p*-methoxybenzoyloxy)acetophenone was prepared from 2,3,4,6-tetramethoxyacetophenone *via* the corresponding ω-bromoacetophenone. Cyclization of the acetophenone with *p*-methoxybenzoic anhydride by application of the Allan–Robinson reaction afforded 3-hydroxy-4′,5,7,8-tetramethoxyflavone along with 2-(α-hydroxy-4-methoxybenzylidene)-4,6,7-trimethoxycoumaranone. The 5-methoxy group in the tosylate or mesylate of the 3-hydroxyflavone was selectively cleaved with anhydrous aluminum bromide in acetonitrile to give the corresponding 5-hydroxyflavone, which was converted into 3,5-dihydroxy-4′,7,8-trimethoxyflavone with anhydrous potassium carbonate in methanol. 3,3′,4′,5-Tetrahydroxy-7,8-dimethoxyflavone was also synthesized by a similar method. The demethylation of the 5-methoxy group in flavones with a 3-hydroxy group is applicable to the synthesis of 3,5-dihydroxyflavones.

**Keywords**——Allan–Robinson reaction; ω-aroyloxyacetophenone; 3-hydroxy-5,7,8-trimethoxyflavone; aurone; selective demethylation; 3-sulfonyloxy-5,7,8-trimethoxyflavone; 3,5-dihydroxy-7,8-dimethoxyflavone; tambulin

We have been studying selective O-alkylation and dealkylation of flavonoids to establish new convenient methods for synthesizing polyhydroxyflavones.[1] Concurrently, the inhibitory activities of these flavones against two enzyme systems were studied. It was found that axillarin[2] (3′,4′,5,7-tetrahydroxy-3,6-dimethoxyflavone) and LARI 4[3] (3′,4′-dihydroxy-5,6,7,8-tetramethoxyflavone) strongly inhibited lens aldose reductase, which is implicated in the pathogenesis of sugar cataract ($IC_{50}$, $10^{-8}$ M), and that cirsiliol[4,5] (3′,4′,5-trihydroxy-6,7-dimethoxyflavone) was a potent inhibitor of arachidonate 5-lipoxygenase, which initiates the biosynthesis of leukotrienes with the activity of slow reacting substance of anaphylaxis ($IC_{50}$, $10^{-7}$ M). In addition, the chemical modification of the latter flavone, cirsiliol, with lipophilic alkyl groups enhanced the activity about fivefold.[6] The results show that the activities are influenced enormously by the nature of the substituents in flavones. The chemical–biological relationships of 3-hydroxyflavones are of great interest,[7] but most of the biological studies on 3-hydroxyflavones have been limited to the natural flavones such as quercetin and kaempferol, which are obtained easily from natural sources,[7,8] because the synthesis of 3-hydroxyflavones is much more difficult than that of flavones with no hydroxy group at the 3-position. Further biological studies would be made easier if convenient methods for the synthesis of 3-hydroxyflavones were available.

From these viewpoints, we studied the Allan–Robinson reaction[9] of ω-aroyloxyacetophenones and the selective demethylation of the resultant 3-hydroxy-5,7,8-trimethoxyflavones (**1**) in order to establish a method for synthesizing 3,5-dihydroxy-7,8-dimethoxyflavones (**2**).

## Results and Discussion

### Synthesis of 3-Hydroxy-5,7,8-trimethoxyflavones (1)

3-Hydroxy-5,7,8-trimethoxyflavones (**1**) were synthesized from 2,3,4,6-tetramethoxyacetophenone (**3**) as shown in Chart 1. Bromination of **3** with cupric bromide[10] in a large amount of chloroform–ethyl acetate gave the $\omega$-bromoacetophenone (**4**) in a favorable yield. In this reaction, decreasing the amount of the solvent remarkably reduced the yield of **4**, because the 2-methoxy group in **3** or **4** was cleaved by hydrogen bromide which was formed during the reaction. The condensation[11] of crude **4** with potassium *p*-methoxybenzoate in *N*,*N*-dimethylformamide (DMF) gave $\omega$-(*p*-methoxybenzoyloxy)acetophenone (**5**). The 2-methoxy group in **5** was quantitatively cleaved by the use of anhydrous aluminum chloride to give the 2-hydroxyacetophenone (**6**). Cyclization of **6** with *p*-methoxybenzoic anhydride and potassium *p*-methoxybenzoate by application of the Allan–Robinson reaction afforded the desired 3-hydroxyflavone (**1a**)[12] in 19% yield. The proton nuclear magnetic resonance ($^1$H-NMR) spectrum exhibits a singlet at $\delta$ 6.40 due to an aromatic proton in the A ring and three singlets due to four methoxy groups (Table I). In the ultraviolet (UV) spectrum of **1a** in ethanol, band I (373 nm) shifts to 433 nm in the presence of aluminum chloride and its intensity is greater than that in ethanol (Table II).

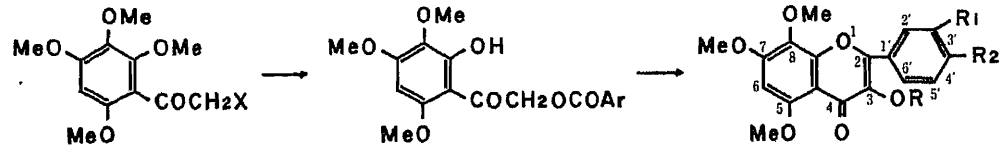


**3**: X=H
**4**: X=Br
**5**: X=OCOC$_6$H$_4$OMe(*p*)
**8**: X=OCOC$_6$H$_4$NO$_2$(*p*)

**6**: Ar=C$_6$H$_4$OMe(*p*)
**9**: Ar=C$_6$H$_4$NO$_2$(*p*)

**1a—c**: R=H
**7**: R=COC$_6$H$_3$(OCH$_2$Ph)$_2$(3,4)
R$_1$=R$_2$=OCH$_2$Ph

**a**: R$_1$=H, R$_2$=OMe **b**: R$_1$=OMe, R$_2$=OCH$_2$Ph **c**: R$_1$=R$_2$=OCH$_2$Ph

Chart 1

4′-Benzyloxy-3-hydroxy-3′,5,7,8-tetramethoxyflavone (**1b**) was also synthesized from **6** by a similar method in 22% yield. On the other hand, the condensation of **6** with 3,4-bis(benzyloxy)benzoic anhydride and potassium 3,4-bis(benzyloxy)benzoate gave 3′,4′-bis(benzyloxy)-3-[3,4-bis(benzyloxy)benzoyloxy]-5,7,8-trimethoxyflavone (**7**), which was derived from the *p*-methoxybenzoate of the 3-hydroxyflavone (**1c**) by ester exchange with 3,4-bis(benzyloxy)benzoic anhydride. Compound **7** was relatively stable in basic media and was hardly hydrolyzed with potassium hydroxide in methanol, but was easily hydrolyzed with sodium methoxide in pyridine–methanol to give 3′,4′-bis(benzyloxy)-3-hydroxy-5,7,8-trimethoxyflavone (**1c**) in 32% yield based on **6**. The results suggest that the yields of 3-hydroxyflavones depend on the stability of the flavones under the conditions used.

Generally, the yields of flavones in the Allan–Robinson reaction of $\omega$-aroyloxyacetophenones are apparently lower than those of $\omega$-methoxyacetophenones.[13] In order to find the reason for this, the Allan–Robinson reaction of **6** with *p*-methoxybenzoic anhydride was reexamined and it was found that a compound A (mp 157—159 °C) was formed along with **1a**. The yield of A (3.5%) in the condensation of **6** was apparently lower than that of **1a** (19%). However, in the condensation of **9**, in which the aroyloxy group carries a nitro group with a strongly electron-attracting character, the formation of **1a** was enormously suppressed, and A and **1a** were isolated in 7.5 and 0.5% yields, respectively. The UV spectrum of A exhibits two absorption maxima at 328 and 404 nm, but a large bathochromic shift of the latter maximum (band I) upon the addition of aluminum chloride was not observed in contrast with the case of

**1a** (see **10** in Table II). The results suggest that A is an aurone derivative. Horowitz and Gentili[14] have already reported that 4′-benzyloxy-6-hydroxy-3′,4,7-trimethoxybenzalcoumaranone is formed in the Allan–Robinson reaction of the corresponding ω-benzoyloxyacetophenone. However, compound A showed a positive color reaction with ferric chloride. In the $^1$H-NMR spectrum of A, no benzylidene methine proton signal was detected, and all of the proton signals corresponded to those of **1a**, as shown in Table I. The results suggest that A is a new aurone derivative, 2-(α-hydroxy-4-methoxybenzylidene)-4,6,7-trimethoxycoumaranone (**10**), which is the enolate of a 2-benzoylcoumaranone derivative.[15] The mass spectrum (MS) of A does not exhibit the characteristic fragmentation pattern of the 3-hydroxyflavone (**1a**). The base peak of A shows M − 16 as *m/z*. Fragmentation patterns are considered to be as shown in Chart 2, and are consistent with the structure of **10**.

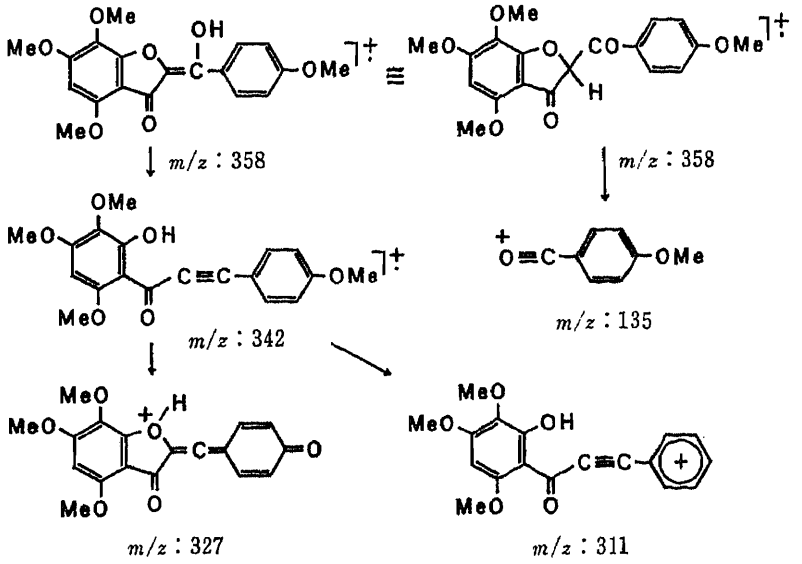


Chart 2

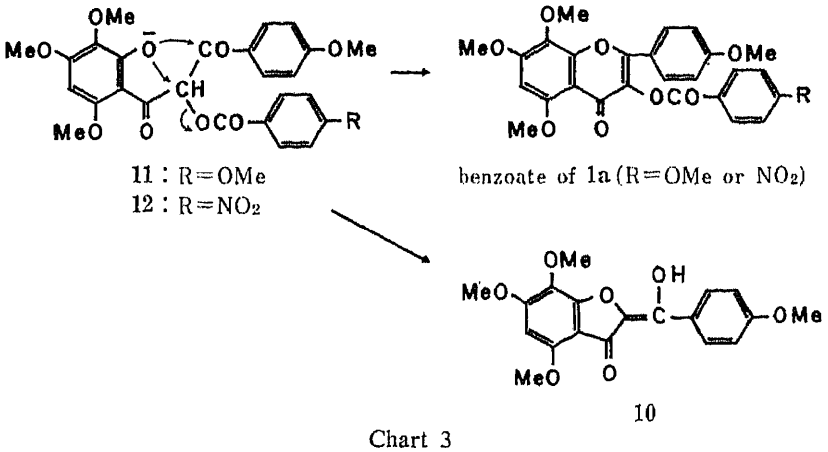


Chart 3

In the Allan–Robinson reaction, the cyclization of 2-hydroxyacetophenones into flavones has been considered to proceed *via* the diketone intermediate.[9] This suggests that the aurone (**10**) is also formed from the intermediates (**11** and **12**), as shown in Chart 3. It seems clear that the formation of the aurone (**10**) would be accelerated by the electron-attracting character of the ω-aroyloxy group. This is supported by the fact that the Allan–Robinson reaction of the ω-(*p*-nitrobenzoyloxy)acetophenone (**9**) gives the aurone (**10**) as a main

product. The stability of the aurone (**10**) seems to be low under the conditions used, since the yield is not greatly increased.

The results show that the low yields of 3-hydroxyflavones in the Allan–Robinson reaction of ω-aroyloxyacetophenones are ascribable to the concomitant formation of aurones such as **10** owing to the influence of the aroyloxy group. Therefore, we looked for a more favorable method for synthesizing 3-hydroxyflavones; the results will be reported in the next paper.

**Selective Demethylation of the 5-Methoxy Group in 3-Hydroxy-5,7,8-trimethoxyflavones (1)**

3,5-Dihydroxy-7,8-dimethoxyflavone[16] and tambulin[17] (3,5-dihydroxy-4′,7,8-trimethoxyflavone, **2a**) were synthesized from the corresponding dimethyl ethers by demethylation with anhydrous aluminum chloride in benzene or nitrobenzene, but the yields were low because of the difficulty of the selective demethylation of 3- and 5-methoxy groups in 3,5,7,8-tetramethoxyflavones. Generally, it is not possible to cleave selectively the 5-methoxy group in a flavone with a free 3-hydroxy group and a methoxy group at the 8-position.[9] In the synthesis of prudomestin (3,5,7-trihydroxy-4′,8-dimethoxyflavone) by the demethylation of 3,7-dihydroxy-4′,5,8-trimethoxyflavone, Krishnamurti *et al.*[18] had examined the demethylation of the diacetate and dibenzoate in order to eliminate the influence of the 3-hydroxy group, but the experiment did not succeed. Thus, they bypassed this difficulty by the oxidative demethylation of the dibenzyl ether to the 5,8-quinone. Therefore, we examined the synthesis of 3,5-dihydroxy-7,8-dimethoxyflavones (**2**) from 3-hydroxy-5,7,8-trimethoxyflavones (**1**) *via* the corresponding sulfonates as shown in Chart 4.

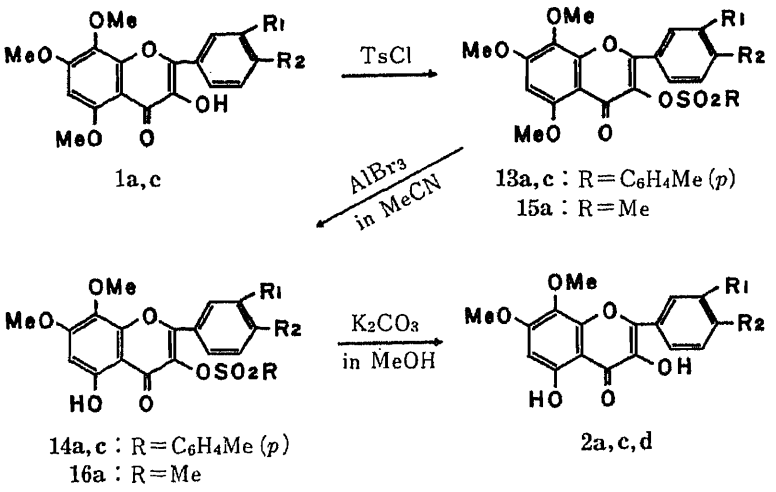


a : $R_1$=H, $R_2$=OMe c : $R_1$=$R_2$=$OCH_2Ph$ d : $R_1$=$R_2$=OH

Chart 4

The 5-methoxy group in the tosylate (**13a**) of **1a** was quantitatively cleaved with anhydrous aluminum bromide in acetonitrile[6] to give the 5-hydroxyflavone (**14a**). The $^1$H-NMR spectrum of **14a** exhibits the presence of a chelated hydroxy group, and band I (355i nm) in its UV spectrum shifted bathochromically to 416 nm in the presence of aluminum chloride (Tables I and II). The tosyloxy group in **14a** is stable in acidic media but sensitive to basic media, and was smoothly hydrolyzed with potassium carbonate in methanol to give the desired 3,5-dihydroxyflavone (**2a**), which was identical with tambulin.[17] In the selective demethylation, a mesyl group was usable as a protecting group and **2a** was also synthesized from the mesylate (**15a**) of **1a** *via* the 5-hydroxyflavone (**16a**) under similar conditions.

The flavone (**2c**) was obtained from the tosylate (**13c**) of **1c** by a similar method, but the

TABLE I. $^1$H-NMR Spectral Data for 3,5,7,8-Tetraoxygenated Flavones and the Aurone (**10**)[a]

| Compd. | Solvent | Arom. H | | | | | OMe | 5-OH | Other H |
|---|---|---|---|---|---|---|---|---|---|
| | | $C_6$-H | $C_3$-H | $C_5$-H | $C_2$-H | $C_6$-H | | | |
| **1a** | $CDCl_3$ | 6.40 s | 7.00 d (2H) | | 8.20 d (2H) | | 3.86 s (3H)<br>3.94 s (3H)<br>3.99 s (6H) | — | — |
| **1b** | $CDCl_3$ | 6.38 s | — | 6.98 d | 7.88 s | 7.80 dd | 3.91 s (3H)<br>3.97 s (9H) | — | 5.21 s (2H)<br>7.2—7.5 m (5H) |
| **1c** | $CDCl_3$ | 6.39 s | — | 7.03 d | 7.99 d′ | 7.86 dd | 3.88 s (3H)<br>3.97 s (6H) | — | 5.24 s (4H)<br>7.2—7.6 m (10H) |
| **2a** | DMSO | 6.50 s | 7.07 d (2H) | | 8.10 d (2H) | | 3.80 s (3H)<br>3.82 s (3H)<br>3.87 s (3H) | 12.16 s | —<br>— |
| **2c** | DMSO | 6.53 s | — | c) | 7.89 s | 7.81 dd | 3.79 s (3H)<br>3.89 s (3H) | 12.20 s | 5.17 s (2H)<br>5.23 s (2H)<br>7.1—7.6 m (11H) |
| **2d** | DMSO | 6.53 s | — | 6.91 d | 7.71 d′ | 7.63 dd | 3.84 s (3H)<br>3.90 s (3H) | 12.30 s | — |
| **10** | $CDCl_3$ | 6.27 s[b] | 6.99 d (2H) | | 8.28 d (2H) | | 3.87 s (3H)<br>3.95 s (6H)<br>4.00 s (3H) | — | — |
| **13a** | $CDCl_3$ | 6.39 s | 6.83 d (2H) | | 7.83 d (2H) | | 3.82 s (3H)<br>3.86 s (3H)<br>3.91 s (3H)<br>3.95 s (3H) | — | 2.38 s (3H)<br>7.15 d (2H)<br>7.79 d (2H) |
| **13c** | $CDCl_3$ | 6.38 s | — | 6.90 d | c) | c) | 3.82 s (3H)<br>3.90 s (3H)<br>3.95 s (3H) | — | 2.35 s (3H)<br>5.08 s (2H)<br>5.18 s (2H)<br>7.1—7.7 m (16H) |
| **14a** | $CDCl_3$ | 6.41 s | 6.85 d (2H) | | 7.87 d (2H) | | 3.86 s (6H)<br>3.93 s (3H) | 11.98 s | 2.40 s (3H)<br>7.17 d (2H)<br>7.74 d (2H) |
| **15a** | $CDCl_3$ | 6.43 s | 7.03 d (2H) | | 8.12 d (2H) | | 3.87 s (3H)<br>3.90 s (3H)<br>3.98 s (6H) | — | 3.64 s (3H) |
| **16a** | $CDCl_3$ | 6.60 s | 7.10 d (2H) | | 7.94 d (2H) | | 3.78 s (3H)<br>3.82 s (3H)<br>3.90 s (3H) | 11.79 s | 3.50 s (3H) |

*a*) s, singlet; d, doublet ($J$=8.5 Hz); d′, doublet ($J$=2.5 Hz); dd, double doublet ($J$=8.5, 2.5 Hz); m, multiplet. *b*) This is the signal of $C_5$-H in the benzylidene coumaranone. *c*) The signal overlapped with those of the benzyl aromatic protons.

yield (60%) was lower than that of **2a** because of partial cleavage of the benzyloxy groups in **13c** or **14c** under the demethylating conditions. Hydrogenolysis of **2c** with palladium on charcoal gave quantitatively the desired 3,3′,4′,5-tetrahydroxy-7,8-dimethoxyflavone (**2d**).

The results show that selective demethylation of the 5-methoxy group in 3-hydroxyflavone derivatives is possible provided that the 3-hydroxy group is protected with a sulfonyl group, which is removable by hydrolysis under mild basic conditions. This demethylating method should be applicable to the synthesis of various 3,5-dihydroxyflavones.

The $^1$H-NMR and UV spectral data for the flavones obtained here (Tables I and II) fully supported the assigned structures.

## Experimental

All melting points were determined in glass capillaries and are uncorrected. $^1$H-NMR spectra were recorded with

TABLE II. UV Spectral Data for 3,5,7,8-Tetraoxygenated Flavones and the Aurone (10)[a]

| Compd. | | $\lambda_{max}$ nm (log ε) | | | |
|---|---|---|---|---|---|
| **1a** | EtOH | | 269 (4.31) | 312 (4.03) | 373 (4.34) |
| | EtOH–$AlCl_3$ | 263 (4.33) | | 344 (3.75) | 433 (4.39) |
| **1b** | EtOH | 257 (4.27) | 270 sh (4.23) | 327 (3.97) | 376 (4.16) |
| | EtOH–$AlCl_3$ | 267 (4.40) | | | 435 (4.25) |
| **1c** | EtOH | 256 (4.42) | 267 i (4.25) | | 375 (4.39) |
| | EtOH–$AlCl_3$ | 266 (4.49) | | 352 (3.74) | 437 (4.49) |
| **2a** | EtOH | 254 (4.20) | 273 (4.32) | 325 (4.13) | 380 (4.25) |
| | EtOH–$AlCl_3$ | 271 (4.30) | | 354 (4.17) | 440 (4.26) |
| **2c** | EtOH | 258 (4.39) | 273 i (4.23) | 335 (4.09) | 384 (4.28) |
| | EtOH–$AlCl_3$ | 268 (4.40) | | 362 (4.10) | 444 (4.35) |
| **2d** | EtOH | 260 (4.36) | 273 i (4.16) | | 388 (4.32) |
| | EtOH–$AlCl_3$ | 271 (4.40) | | 370 (3.95) | 449 (4.38) |
| **14a** | EtOH | 275 (4.42) | 302 (4.19) | 325 (4.20) | 355 i (4.05) |
| | EtOH–$AlCl_3$ | 289 (4.35) | 316 (4.27) | 347 (4.18) | 416 (3.86) |
| **16a** | EtOH | 274 (4.37) | 307 sh (4.22) | 323 (4.25) | 355 i (4.09) |
| | EtOH–$AlCl_3$ | 284 (4.30) | 314 (4.27) | 344 (4.24) | 412 (3.80) |
| **10** | EtOH | 246 (4.09) | | 328 (4.15) | 404 (4.49) |
| | EtOH–$AlCl_3$ | 247 (4.05) | | 333 (4.16) | 409 (4.48) |

*a*) sh, shoulder; i, inflection point.

a Hitachi R-24 spectrometer (60 MHz), using tetramethylsilane as an internal standard, and chemical shifts are given in δ values. UV spectra were taken on a Hitachi 124 spectrophotometer. Elemental analyses were performed with a Yanaco CHN corder, model MT-2.

**2,3,4,6-Tetramethoxy-ω-(*p*-methoxybenzoyloxy)acetophenone (5)**——2,3,4,6-Tetramethoxyacetophenone (**3**) (bp 156 °C/0.7 mmHg) (5 g), which was prepared by the methylation of 2-hydroxy-3,4,6-trimethoxyacetophenone[19] with dimethyl sulfate, in $CHCl_3$–EtOAc (1 : 1, 400 ml) was stirred in the presence of $CuBr_2$ (10 g) at 40—50 °C for 2.5 h, and then $H_2O$ was added to the mixture. After removal of CuBr by filtration, the organic layer was washed with $H_2O$ and dried with anhydrous $Na_2SO_4$. Evaporation of the solvent gave crude oily ω-bromo-2,3,4,6-tetramethoxyacetophenone (**4**). The pure material was obtained by column chromatography on silica gel with $CHCl_3$. $^1$H-NMR ($CDCl_3$) δ: 3.80, 3.90 (each 6H, s, each 2×OMe), 4.34 (2H, s, $CH_2$), 6.27 (1H, s, $C_5$-H).

A mixture of crude **4** and potassium *p*-methoxybenzoate (6 g) in DMF (20 ml) was heated at 150—160 °C for 2 h, and then $H_2O$ was added to the mixture. The precipitate was recrystallized from EtOAc to give **5** (4.2 g, 52%) as colorless prisms, mp 135—137 °C. $^1$H-NMR ($CDCl_3$) δ: 3.80 (6H, s, 2×OMe), 3.85, 3.89, 3.93 (each 3H, s, OMe), 5.20 (2H, s, $CH_2$), 6.27 (1H, s, $C_5$-H), 6.90, 8.04 (each 2H, d, $J$=8.5 Hz, arom. H). *Anal.* Calcd for $C_{20}H_{22}O_8$: C, 61.53; H, 5.68. Found: C, 61.45; H, 5.57.

**2,3,4,6-Tetramethoxy-ω-(*p*-nitrobenzoyloxy)acetophenone (8)**——The acetophenone (**8**) was synthesized from **4** (derived from 5 g of **3**) with potassium *p*-nitrobenzoate (6.4 g) by a method similar to that described for **5**: mp 159—160 °C (colorless prisms from EtOAc), yield 3.0 g (36%). *Anal.* Calcd for $C_{19}H_{19}NO_9$: C, 56.29; H, 4.72; N, 3.46. Found: C, 56.32; H, 5.02; N, 3.57.

**2-Hydroxy-3,4,6-trimethoxy-ω-(*p*-methoxybenzoyloxy)acetophenone (6)**——Compound **5** (12 g) was dissolved in a solution of anhydrous $AlCl_3$ (23.7 g) in dry MeCN (180 ml), and the mixture was heated at 60 °C for 2 h. The mixture was poured into 2—3% HCl and warmed at 50—60 °C for 10 min, then the organic solvent was evaporated off under reduced pressure. The precipitate was recrystallized from $CHCl_3$–EtOAc to give **6** (10.4 g, 90%) as pale yellow prisms, mp 151—152 °C. $^1$H-NMR ($CDCl_3$) δ: 3.80, 3.86 (each 3H, s, OMe), 3.93 (6H, s, 2×OMe), 5.40 (2H, s, $CH_2$), 5.99 (1H, s, $C_5$-H), 6.90, 8.06 (each 2H, d, $J$=8.5 Hz, arom. H), 13.17 (1H, s, OH). *Anal.* Calcd for $C_{19}H_{20}O_8$: C, 60.63; H, 5.36. Found: C, 60.54; H, 5.20.

**2-Hydroxy-3,4,6-trimethoxy-ω-(*p*-nitrobenzoyloxy)acetophenone (9)**——The acetophenone (**9**) was synthesized from **8** (2.7 g) by demethylation as described for **6**: mp 173—174 °C (colorless needles from $CHCl_3$–EtOAc), yield 2.35 g (90%). $^1$H-NMR ($CDCl_3$) δ: 3.78 (3H, s, OMe), 3.94 (6H, s, 2×OMe), 5.45 (2H, s, $CH_2$), 5.99 (1H, s, $C_5$-H), 8.26 (4H, s, arom. H), 12.93 (1H, s, OH). *Anal.* Calcd for $C_{18}H_{17}NO_9$: C, 55.24; H, 4.38; N, 3.58. Found: C, 55.14; H, 4.44; N, 3.69.

**3-Hydroxy-4′-5,7,8-tetramethoxyflavone (1a)**——Method A: A mixture of **6** (1.0 g), *p*-methoxybenzoic anhydride (3.5 g), and potassium *p*-methoxybenzoate (2.0 g) was heated at 170—180 °C for 7—8 h under reduced pressure. The

mixture was dissolved in $Me_2CO$–MeOH–$H_2O$ (10 : 5 : 3), then an aqueous solution of KOH (2.5 g) was added to the solution and the whole was refluxed gently for 15—20 min. The solvent was removed under reduced pressure, and the residue was acidified with HCl then extracted with EtOAc. The extract was washed with an aqueous solution of $Na_2CO_3$, and the solvent was evaporated off. The residue was triturated with $Et_2O$–$CHCl_3$ and the precipitate was recrystallized from MeOH to give **1a** (180 mg, 19%) as yellow prisms, mp 198—200 °C (lit.[12] mp 198—200 °C). *Anal.* Calcd for $C_{19}H_{18}O_7$: C, 63.68; H, 5.06. Found: C, 63.58; H, 4.99.

The aurone (**10**) was separated from the mother liquor of **1a** by column chromatography on silica gel with $CHCl_3$–EtOAc (5 : 1): mp 157—159 °C (yellow needles from EtOAc), yield 34 mg (3.6%). MS *m/z* (rel. intensity): 358 (48, $M^+$), 342 (100), 327 (40), 313 (16), 311 (22), 235 (10), 135 (30). *Anal.* Calcd for $C_{19}H_{18}O_7$: C, 63.68; H, 5.06. Found: C, 63.42; H, 5.09.

Method B: A mixture of **9** (2.3 g), *p*-methoxybenzoic anhydride (5.1 g), and potassium *p*-methoxybenzoate (4.5 g) was heated at 160—170 °C for 6 h under reduced pressure. The mixture was treated by the method described above to give a phenolic material. This was recrystallized from EtOAc to give **10**. From the mother liquor, **1a** was obtained (10 mg, 0.5%) along with **10** by column chromatography on silica gel with $CHCl_3$. The total yield of **10** was 161 mg (7.5%).

**4′-Benzyloxy-3-hydroxy-3′,5,7,8-tetramethoxyflavone (1b)**——A mixture of **6** (2.0 g), 4-benzyloxy-3-methoxybenzoic anhydride (8.0 g), and potassium 4-benzyloxy-3-methoxybenzoate (2.4 g) was heated at 170—180 °C for 8 h. The mixture was treated by method A to give **1b** (550 mg, 22%) as yellow needles from $CHCl_3$–MeOH, mp 181—183 °C. *Anal.* Calcd for $C_{26}H_{24}O_8$: C, 67.23; H, 5.21. Found: C, 67.00; H, 5.18.

**3′,4′-Bis(benzyloxy)-3-hydroxy-5,7,8-trimethoxyflavone (1c)**——A mixture of **6** (1.0 g), 3,4-bis(benzyloxy)benzoic anhydride (5.2 g), and potassium 3,4-bis(benzyloxy)benzoate (4.0 g) was heated at 160—170 °C for 8 h under reduced pressure. The mixture was dissolved in $Me_2CO$–MeOH–$H_2O$, then an aqueous solution of $K_2CO_3$ (2.9 g) was added and the mixture was refluxed for 15 min. The organic solvent was evaporated off under reduced pressure and the remaining solution was allowed to stand in a refrigerator overnight. The precipitate (**7**) was collected by filtration and washed with MeOH: mp 176—178 °C. $^1$H-NMR ($CDCl_3$) $\delta$: 3.86, 3.90, 3.95 (each 3H, s, OMe), 4.95, 5.19 (each 2H, s, $OCH_2Ph$), 5.15 (4H, s, $2\times OCH_2Ph$), 6.40 (1H, s, $C_6$-H), 6.94 (1H, d, $J$=8.5 Hz, $C_5$-H).

NaOMe–MeOH (about 28%, 1 ml) was added to a solution of **7** in pyridine–MeOH (1 : 1, 30 ml), and the mixture was heated with stirring at 60 °C for 10 min, then poured into ice-HCl and extracted with $CHCl_3$. The extract was chromatographed on silica gel with $CHCl_3$ and then recrystallized from EtOAc to give **1c** (460 mg, 32%) as pale yellow needles, mp 164—165 °C. *Anal.* Calcd for $C_{32}H_{28}O_8$: C, 71.10; H, 5.22. Found: C, 71.07; H, 5.27.

**4′,5,7,8-Tetramethoxy-3-tosyloxyflavone (13a)**——A mixture of **1a** (300 mg), *p*-toluenesulfonyl chloride (190 mg), and anhydrous $K_2CO_3$ (1.2 g) in $Me_2CO$ (50 ml) was refluxed with stirring for 2 h. The mixture was poured into $H_2O$ and extracted with EtOAc. The solvent was evaporated off and the residue was recrystallized from EtOAc to give **13a** (380 mg, 89%) as colorless needles, mp 162—163 °C. *Anal.* Calcd for $C_{26}H_{24}O_9S$: C, 60.93; H, 4.72. Found: C, 60.75; H, 4.64.

**3′,4′-Bis(benzyloxy)-5,7,8-trimethoxy-3-tosyloxyflavone (13c)**——A mixture of **1c** (300 mg) and *p*-toluenesulfonyl chloride (130 mg) in $Me_2CO$ was treated by the same method as described for **13a**: mp 87—89 °C (pale yellow needles from EtOAc), yield 340 mg (88%). *Anal.* Calcd for $C_{39}H_{34}O_{10}S$: C, 67.42; H, 4.93. Found: C, 67.16; H, 4.84.

**4′-5,7,8-Tetramethoxy-3-mesyloxyflavone (15a)**——A mixture of **1a** (250 mg) and methanesulfonyl chloride (0.26 ml) in pyridine (3.6 ml) was allowed to stand overnight. The mixture was poured into ice-HCl and the precipitate was recrystallized from EtOAc to give **15a** (220 mg, 80%) as pale yellow needles, mp 191—192 °C. *Anal.* Calcd for $C_{20}H_{20}O_9S$: C, 55.05; H, 4.62. Found: C, 54.82; H, 4.51.

**5-Hydroxy-4′,7,8-trimethoxy-3-tosyloxyflavone (14a)**——Compound **13a** (330 mg) was dissolved in MeCN (15 ml) containing anhydrous $AlBr_3$ (1.5 g) and heated at 50 °C for 1 h. The mixture was poured into 2% HCl and heated at 50—60 °C for 20 min. The MeCN was evaporated under reduced pressure, and the crystals that separated were recrystallized from $CHCl_3$–MeOH to give **14a** (315 mg, 98%) as pale yellow needles, mp 203—205 °C. *Anal.* Calcd for $C_{25}H_{22}O_9S$: C, 60.24; H, 4.45. Found: C, 59.96; H, 4.26.

**5-Hydroxy-4′,7,8-trimethoxy-3-mesyloxyflavone (16a)**——Compound **15a** (150 mg) was dissolved in MeCN (10 ml) containing anhydrous $AlBr_3$ (1.0 g) and heated at 50 °C for 1 h. The mixture was treated by a method similar to that described for **14a** to give **16a** (130 mg, 90%) as yellow needles from EtOAc, mp 193—195 °C. *Anal.* Calcd for $C_{19}H_{18}O_9S$: C, 54.03; H, 4.30. Found: C, 54.01; H, 4.12.

**3,5-Dihydroxy-4′,7,8-trimethoxyflavone (Tambulin) (2a)**——A mixture of **14a** (270 mg) and anhydrous $K_2CO_3$ (4.0 g) in MeOH (70 ml) was refluxed with stirring for 1 h and acidified with diluted HCl. The MeOH was evaporated off and the crystals that separated were recrystallized from $CHCl_3$–MeOH to give **2a** (150 mg, 80%) as yellow needles, mp 206—207 °C (lit.[17] 204—205 °C). *Anal.* Calcd for $C_{18}H_{16}O_7$: C, 62.79; H, 4.68. Found: C, 62.84; H, 4.57.

The mesylate (**16a**) (30 mg) was hydrolyzed with $K_2CO_3$ by a method similar to that described above to give **2a** (19 mg, 78%).

**3′,4′-Bis(benzyloxy)-3,5-dihydroxy-7,8-dimethoxyflavone (2c)**——Compound **13c** (320 mg) was dissolved in MeCN (25 ml) containing anhydrous $AlBr_3$ (1.3 g) and heated at 40 °C for 1 h. The mixture was poured into 2% HCl and heated at 50—60 °C for 30 min. The MeCN was evaporated off under reduced pressure, then the mixture was

extracted with EtOAc and the extract was chromatographed on silica gel with chloroform to give **14c** as a yellow semisolid. A mixture of **14c** and anhydrous $K_2CO_3$ (1.5 g) in MeOH–$Me_2CO$ (2 : 1, 20 ml) was refluxed with stirring for 1.5 h. The mixture was acidified with dilute HCl and the organic solvent was evaporated off. The crystals that separated were recrystallized from EtOAc to give **2c** (145 mg, 60%) as yellow needles, mp 208—209 °C. *Anal.* Calcd for $C_{31}H_{26}O_8$: C, 70.71; H, 4.98. Found: C, 70.89; H, 5.11.

**3,3',4'-5-Tetrahydroxy-7,8-dimethoxyflavone (2d)**——Compound **2c** (145 mg) was hydrogenated over Pd–C (10%, 60 mg) in EtOAc–MeOH (1 : 1, 80 ml) till the uptake of $H_2$ ceased. After removal of the catalyst by filtration, the solvent was evaporated off and the residue was recrystallized from EtOAc–MeOH to give **2d** (78 mg, 82%) as yellow needles, mp 280—282 °C. *Anal.* Calcd for $C_{17}H_{14}O_8$: C, 58.96; H, 4.08. Found: C, 58.70; H, 3.98.

## References and Notes


1) Part VIII of this series: T. Horie, M. Tsukayama, H. Kourai, Y. Nakayama, and M. Nakayama, *Chem. Pharm. Bull.*, **34**, 30 (1986).
2) J. Okuda, I. Miwa, K. Inagaki, T. Horie, and M. Nakayama, *Biochem. Pharmacol.*, **31**, 3807 (1982).
3) J. Okuda, I. Miwa, K. Inagaki, T. Horie, and M. Nakayama, *Chem. Pharm. Bull.*, **32**, 767 (1984).
4) T. Yoshimoto, M. Furukawa, S. Yamamoto, T. Horie, and S. Watanabe-Kohno, *Biochem. Biophys. Res. Commun.*, **116**, 612 (1983).
5) S. Yamamoto, T. Yoshimoto, M. Furukawa, T. Horie, and S. Watanabe-Kohno, *J. Allergy Clin. Immunol.*, **74**, 349 (1984).
6) T. Horie, M. Tsukayama, H. Kourai, C. Yokoyama, M. Furukawa, T. Yoshimoto, S. Yamamoto, S. Watanabe-Kohno, and K. Ohata, *J. Med. Chem.*, **29**, 2256 (1986).
7) E. L. Wheeler and D. L. Berry, *Carcinogenesis*, **7**, 33 (1986).
8) L. A. Griffiths, "The Flavonoids, Advances in Research," ed. by J. B. Harborne and T. J. Mabry, Chapman and Hall, London, 1982, pp. 700—702.
9) H. Wagner and L. Farkas, "The Flavonoids," ed. by J. B. Harborne, T. S. Mabry, and H. Mabry, Chapman and Hall, London, 1975, pp. 141—146, pp. 155—158.
10) M. L. Malik and S. K. Grover, *Indian J. Chem.*, **14B**, 513 (1976).
11) T. Horie, H. Kourai, H. Osaka, and M. Nakayama, *Bull. Chem. Soc. Jpn.*, **55**, 2933 (1982).
12) N. Narashimhachari and T. R. Seshadri, *Proc. Indian Acad. Sci.*, **30A**, 216 (1949).
13) For example: Reference 9 *vs.* L. Farkas and M. Nógrádi, *Acta Chimica Acad. Sci. Hungaricae Tomus*, **58**, 93 (1968).
14) R. M. Horowitz and B. Gentili, *J. Org. Chem.*, **26**, 2899 (1961).
15) *a*) W. E. Fitzmaurice, W. I. O'Sullivan, E. M. Philbin, T. S. Wheeler, and T. A. Geissman, *Chem. Ind.* (London), **1955**, 652 [*Chem. Abstr.*, **50**, 7748 (1956)]; *b*) T. H. Minton and H. Stephen, *J. Chem. Soc.*, **121**, 1598 (1922); *c*) K. V. Auwers, *Chem. Ber.*, **49**, 809 (1916).
16) H. Wagner, G. Maurer, L. Farkas, R. Hänsel, and D. Ohlendorf, *Chem. Ber.*, **104**, 2381 (1971).
17) *a*) K. J. Balakrishna and T. R. Seshadri, *Proc. Indian Acad. Sci.*, **26A**, 296 (1947); *b*) A. Chatterjee, D. Malakar, and D. Ganguly, *Indian J. Chem.*, **14B**, 233 (1976).
18) M. Krishnamurti, T. R. Seshadri, and P. R. Shankaran, *Tetrahedron*, **22**, 941 (1966).
19) W. Baker, *J. Chem. Soc.*, **1941**, 662.

[Chem. Pharm. Bull. 35(11)4473—4481(1987)]

# Thioalkoxytributyl- and Thioalkoxytriphenylphosphonium Salts: Preparation and Application to the Synthesis of Thiolesters and Unsymmetrical Sulfides

HIDENOBU OHMORI,* HATSUO MAEDA, KOHICHI KONOMOTO, KIYOSHI SAKAI, and MASAICHIRO MASUI

*Faculty of Pharmaceutical Sciences, Osaka University, 1-6 Yamadaoka, Suita, Osaka 565, Japan*

(Received May 19, 1987)

Thioalkoxyphosphonium salts, $Ph_3P^+SR\ ClO_4^-$ (**3**) and $Bu_3P^+SR\ X^-$ (X = $ClO_4$ and $BF_4$) (**5**), have been prepared from the corresponding tertiary phosphines and disulfides by simple procedures, which involve (i) constant current electrolysis in acetonitrile in the presence of either $HClO_4$ (for **3**) or PhCOOH and LiX (for **5**), and (ii) stirring an equimolar mixture of a phosphine, a disulfide, PhCOOH, and LiX in acetonitrile at ambient temperature. For the preparation of **3**, which have been reported as useful reagents for the synthesis of unsymmetrical disulfides, the electrochemical method is recommended, while for **5** the latter non-electrochemical procedure gave better results. Reactions of the phosphonium salts **5** with carboxylic acids and primary alcohols in benzene at ambient temperature gave thiolesters and unsymmetrical sulfides, respectively, in fair to excellent yields.

**Keywords**——triphenylphosphine; tributylphosphine; disulfide; thioalkoxyphosphonium salt; thiolester; unsymmetrical sulfide

Previously we reported that thioalkoxytriphenylphosphonium perchlorates [$Ph_3P^+SR\ ClO_4^-$] (**3**), prepared electrochemically from $Ph_3P$ (**1**) and RSSR (**2**), are useful reagents for the synthesis of unsymmetrical disulfides.[1] Although a phosphonium ion of type [$Ph_3P^+SPh\ PhS^-$] has been suggested as the primary intermediate in the preparation of thiolesters from **1**, **2** (R = Ph), and carboxylic acids,[2] attempts to prepare thiolesters from **3** (R = alkyl) and carboxylic acids were unsuccessful: with **3** (R = Ph), thiolester formation was actually effected.[3] On the other hand, thiomethoxytributylphosphonium salts [$Bu_3P^+SMe\ X^-$ (X = $BF_4$, $OSO_2CF_3$, and $OSO_2C_6H_4Me$-*p*)] have recently been shown to react with carboxylic acids and primary alcohols to give the corresponding thiolesters and unsymmetrical sulfides, respectively.[4] However, thioalkoxyphosphonium salts are usually obtained by the reaction of phosphine sulfides with alkylating agents such as $R_3OBF_4$, $ROSO_2CF_3$, and $ROSO_2C_6H_4Me$-*p*; and, as far as we are aware, most of the phosphonium salts synthesized by this method are limited to the methylthio and ethylthio derivatives.[4,5] Since the electrochemical oxidation of **1** in the presence of **2** has been suggested to afford **3** with various alkyl groups,[6] thioalkoxytributylphosphonium salts [$Bu_3P^+SR\ X^-$] (**5**) were also expected to be prepared electrochemically from $Bu_3P$ (**4**) and **2**. This paper reports the preparation of **5** (X = $ClO_4$ and $BF_4$) along with a modification of the electrochemical method for **3**. Further, the reactions of **5** with carboxylic acids and alcohols were examined. Unexpectedly, the phosphonium salts **3** and **5** were also obtained without electrolysis from the disulfides **2** and the phosphines **1** and **4**, respectively.

## Results and Discussion

### Improved Electrochemical Preparation of the Phosphonium Salts 3

Our earlier method for **3** involved rather troublesome controlled potential electrolysis (CPE) in a divided electrolysis cell.[6] Constant current electrolysis (CCE) in an undivided cell, if possible, will be more practical for synthetic purposes.[7]

CCE of a mixture of the phosphine **1**, a disulfide **2**, and $HClO_4$[8] (amount, 1:2:2) in MeCN was found to give **3** in yields comparable to or better than those attained[6] by the CPE. The results are summarized in Table I. In addition to the greater ease of operations, the CCE method allows the preparation of larger amounts of **3** with even improved yields [see Table I, for **3** (R = Me and Ph)]. Perchloric acid is employed not only as the supporting electrolyte but also as a proton source, which will be reduced preferentially at the cathode to prevent the reduction of **3** once formed at the anode.[9] When the acid was replaced by $NaClO_4$, the

Table I. Preparation of $Ph_3P^+SR\ ClO_4^-$ (3) by CCE[a]

| R | Yield (%)[b,c] of 3 | R | Yield (%)[b,c] of 3 |
|---|---|---|---|
| Me | 77 (88)[d] | *sec*-Bu | 53 |
| Et | 68 | *tert*-Bu | [e] |
| Pr | 67 | Ph | 63 (94)[d] |
| Bu | 67 | $PhCH_2$ | 48 |

*a*) In MeCN (40 ml) containing **1** (2 mmol), **2** (4 mmol), and $HClO_4$ (4 mmol) unless otherwise noted. *b*) Isolated yield after recrystallization. *c*) $Ph_3PO$ was formed as the major by-product. *d*) In MeCN (150 ml) containing **1** (50 mmol), **2** (100 mmol), and $HClO_4$ (100 ml). *e*) $Ph_3PS$ (65%) and $Ph_3PO$ (28%) were obtained together with MeCONH-*tert*-Bu (yield, not determined).

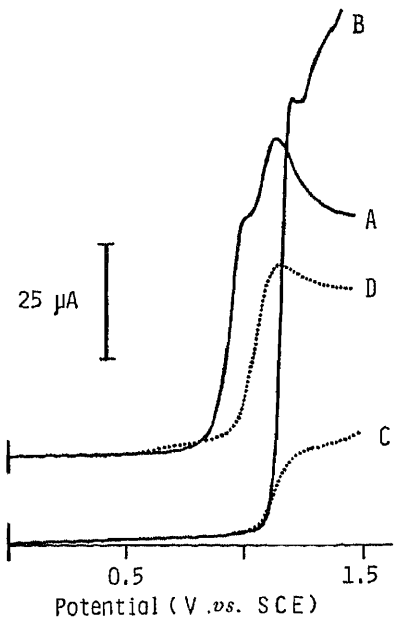


Fig. 1. Cyclic Voltammograms of **1** and **2** in MeCN (0.1 M $NaClO_4$)

A, **1** (5.0 mM); B, **2** (R = Me) (4.9 mM); C, **1** (5.0 mM) + $HClO_4$ (10 mM); D, $Ph_3PH^+ClO_4$ (5.0 mM): at 25 °C; glassy carbon anode (area = 0.071 $cm^2$); voltage sweep rate, 50 mV/s.

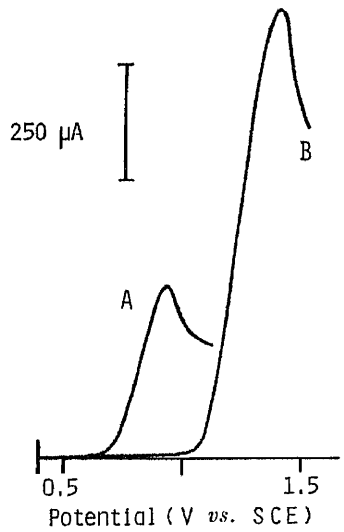


Fig. 2. Cyclic Voltammograms of **4** and **2** in MeCN

A, **4** (63 mM) and $LiClO_4$ (250 mM); B, A + [2(R = Me) (125 mM) and PhCOOH (63 mM)]: at 25 °C; glassy carbon anode (area = 0.071 $cm^2$); voltage sweep rate, 50 mV/s.

supporting electrolyte in the CPE method,[6] the yield of **3** (R=Me) decreased to 28%.[10]

The phosphonium salt **3** (R=*tert*-Bu) was not obtained by either of the methods, CPE and CCE. In the latter electrolysis, $Ph_3PS$ was the major product and formation of MeCONH–*tert*-Bu was recognized [see Table I, footnote *e*)]. On the other hand, $Ph_3PO$ accounted for most of the by-products in the preparation of **3** (R=Me). These results suggest that **3** (R=*tert*-Bu) is formed in the electrolysis solution but decomposes rapidly by an $S_N1$-type mechanism. Reaction of the resulting *tert*-butyl cation with MeCN followed by hydrolysis will give the acetamide.[8] Electrochemical acetamidation is well known when a carbenium ion is generated in MeCN.[11]

Figure 1 shows the cyclic voltammograms of **1** and **2** (R=Me) in MeCN. Based on the observation that **1** is oxidized at a potential less positive than **2** (see Fig. 1, curves A and B), together with coulometric results,[12] the process of formation of **3** in the CPE method has been suggested to be as described in Eq. 2 (Chart 1), where the radical cation from **1** initially formed at the electrode attacks the disulfide. In the presence of $HClO_4$, however, the voltammetric oxidation potential of **1** and **2** are close to each other (Fig. 1, curves B and C).[13] Thus, an alternative process involving the attack of **1** on the radical cation generated from **2** (Eqs. 1 and 3) may take place concurrently with that represented by Eqs. 1 and 2.

$$\underset{\mathbf{1}}{Ph_3P} + HClO_4 \rightleftharpoons Ph_3PH^+ClO_4^- \qquad (1)$$

$$\mathbf{1} \xrightarrow{-e} Ph_3P^{+\cdot} \xrightarrow{+2} [Ph_3P\text{-}S(R)\text{-}SR]^{+\cdot} \xrightarrow[+1]{-e} 2Ph_3P^+SR \qquad (2)$$

$$\underset{\mathbf{2}}{RSSR} \xrightarrow{-e} [RSSR]^{+\cdot} \xrightarrow{+1} [Ph_3P\text{-}S(R)\text{-}SR]^{+\cdot} \xrightarrow[+1]{-e} 2Ph_3P^+SR \qquad (3)$$

Chart 1

**Electrochemical Preparation of the Phosphonium Salts 5**

When a mixture of the phosphine **4** and a disulfide **2** was electrolyzed similarly with excess $HClO_4$ as the proton source, the yield of **5** seldom exceeded 50%[14] and in some cases **4** was recovered from the electrolysis solution as the hydroperchlorate. These results can be explained as follows. Since **4** is a stronger base ($pK_a=8.43$) than **1** ($pK_a=2.73$),[15] the protonation equilibrium in the presence of $HClO_4$ must lie far to the right (*cf.* Eq. 1), and only a small amount of **4** will be present in the unprotonated form, as evidenced by the observation that the voltammetric oxidation peak of **4** in MeCN (Fig. 2) disappeared completely on addition of the acid. Consequently, if the formation of **5** proceeds by a mechanism similar to that in Eq. 3, the attack of **4** on the disulfide radical cation (the 2nd step) will be slower than in the case of **3** and the possibility of side reactions of the radical cation will be enhanced. The major part of the latter reactions would be caused by water, which is added unavoidably to the medium along with $HClO_4$.[8]

The yield of **5** increased when $HClO_4$ was replaced by $LiClO_4$ and PhCOOH, though the voltammetric peak of **4** was again absent in the solution employed for the electrolysis (Fig. 2, curve B). Table II lists the best results among those obtained on CCE in MeCN under various electrolysis conditions, where the electrolysis solution was composed of **4**, **2**, PhCOOH, $LiClO_4$, and suspended alumina. When **4** was added to a solution of PhCOOH and $LiClO_4$ in MeCN, a large portion of PhCOOH was separated out as PhCOOLi, indicating that the electrolysis had been conducted in a nominally anhydrous solution of $HClO_4$ in MeCN saturated with PhCOOLi. PhCOOH can be replaced by other organic acids with similar acidity, but the yield of **5** was not improved. The presence of PhCOOLi (or a lithium salt of an

TABLE II. Preparation of $Bu_3P^+SR\ ClO_4^-$ (5) by CCE[a]

| R | Electrolysis Current (mA) | Time[b] (min) | Yield (%)[c] of 5 | R | Electrolysis Current (mA) | Time[b] (min) | Yield (%)[c] of 5 |
|---|---|---|---|---|---|---|---|
| Me | 400 | 30 | 57 | *sec*-Bu | 100 | 120 | — |
| Et | 200 | 60 | 38 | *tert*-Bu | 100 | 120 | [d] |
| Pr | 100 | 120 | 29 | Ph | 100 | 120 | 35 (50)[e] |
| Bu | 100 | 120 | 25 | $PhCH_2$ | 100 | 120 | 51 |

*a*) In MeCN (40 ml) containing **4** (7.5 mmol), **2** (15 mmol), PhCOOH (7.5 mmol), $LiClO_4$ (30 mmol), and $Al_2O_3$ (0.2 g). *b*) Time required to consume 1 F per mole of **4**. *c*) Isolated yield after recrystallization. *d*) $Bu_3PS$ was obtained in 81% yield. *e*) In the presence of PhSH (12 mmol) in addition to the materials listed in *a*).

TABLE III. Preparation of $Ph_3P^+SR\ ClO_4^-$ (3) and $Bu_3P^+SR\ X^-$ (5) by the Non-electrochemical Procedure[a]

| R | Yield (%)[b] of 3 | Yield (%)[b] of 5 (X = $ClO_4$) | 5 (X = $BF_4$) | R | Yield (%)[b] of 3 | Yield (%)[b] of 5 (X = $ClO_4$) | 5 (X = $BF_4$) |
|---|---|---|---|---|---|---|---|
| Me | 78 | 69 | 72 | *sec*-Bu | 11 | 0 | 0 |
| Et | 54 | 68 | 50 | *tert*-Bu | 0 | 0 | 0 |
| Pr | 50 | 64 | 39 | Ph | 54 | 3[c] | 0 |
| Bu | 55 | 48 | 9 | $PhCH_2$ | 0 | 75 | 63 |

*a*) For **3**, in MeCN (10 ml) containing 5 mmol each of **1**, **2**, PhCOOH, and $LiClO_4$, and $Al_2O_3$ (0.2 g). For **5**, in MeCN (20 ml) containing 12.5 mmol each of **4**, **2**, PhCOOH, and LiX, and $Al_2O_3$ (0.2 g). *b*) Isolated yield after recrystallization. *c*) PhCOSPh was formed as the major product (yield not determined).

organic acid) seems indispensable, though the amount dissolved in the reaction medium in equilibrium with the deposited salt must be small. Thus, **5** was not obtained on CCE of a mixture of $Bu_3PH^+ClO_4^-$, **2**, $LiClO_4$, and suspended alumina in MeCN. The role of PhCOOLi or $PhCOO^-$ in the medium may be to assist the deprotonation of $Bu_3PH^+$ formed from **4** and the $HClO_4$. Use of $NaClO_4$ as the supporting electrolyte was less effective. Electrolysis at lower temperatures gave poor results.

**Preparation of 5 by Non-electrochemical Reaction**

When the electrolysis solution (see above) was simply allowed to stand as a control experiment, formation of **5** was hardly recognized within the time required for the electrolysis. After a longer period (*ca.* 10 h), however, **5** was produced in a yield higher than those attained in the CCE except for **5** (R = Ph). The following conditions were found to be preferable for the preparation of **5**: stirring an equimolar mixture of **2**, **4**, PhCOOH, and $LiClO_4$ or $LiBF_4$ in MeCN with suspended alumina for 12 h at ambient temperature. Typical results are summarized in Table III.

Although the present results alone do not allow us to elucidate the mechanism of the formation of **5** by the non-electrochemical procedure, the process described in Chart 2 can be proposed in the light of various studies reported on the reactions between tertiary phosphines and disulfides.[16] In the reduction of disulfides with phosphines and water to give thiols and phosphine oxides, protonation of the thiolate anion by an acid (*cf.* Eq. 6) has been suggested to suppress the dissociation of the initially formed phosphonium ion back to the starting materials (*cf.* Eq. 5).[17]

The low yield of **5** (R = Ph) can be ascribed to its reaction with PhCOOLi or $PhCOO^-$, which remains in the medium as described above: PhCOSPh was formed as a by-product. In the CCE, **5** (R = Ph) was obtained in a fair yield (Table II), probably because the reaction time

$$Bu_3P + LiClO_4 + PhCOOH \rightleftharpoons Bu_3PH^+ClO_4^- + PhCOOLi + PhCOOLi \quad (4)$$
**4** (deposited) (in solution)

$$RSSR + 4 \rightleftharpoons [Bu_3P^+SR\ RS^-] \quad (5)$$
**2**

$$[Bu_3P^+SR\ RS^-] + Bu_3PH^+ClO_4^- \longrightarrow Bu_3P^+SR\ ClO_4^- + RSH + 4 \quad (6)$$

Chart 2

is shorter than in the non-electrochemical procedure. The reason for the failure to obtain **5** (R=*sec*-Bu and *tert*-Bu) may be similar to that given for **3** (R=*tert*-Bu), but some contribution of other unknown causes cannot be ruled out.

The non-electrochemical procedure was also applied to the preparation of **3**, and the results are included in Table III.

## Reactions of the Phosphonium Salts 5

As reported for **5** (R=Me; X=$OSO_2C_6H_4Me$-*p*, $OSO_2CF_3$, and $BF_4$),[4] the reactions of **5** prepared in the present study with carboxylic acids and alcohols were examined. When an equimolar mixture of **5**, a simple carboxylic acid or a primary alcohol, and a base in benzene

TABLE IV. Reaction of $Bu_3P^+SR\ ClO_4^-$ (**5**) with R'COOH[a]

| R in 5 | R' | Base | Yield (%)[b] of R'COSR | bp (°C)/Torr [lit.] | $^1$H-NMR $\delta$ ($CDCl_3$, $J$=Hz) [IR $\nu$ cm$^{-1}$][c] |
|---|---|---|---|---|---|
| Me | Ph | DMAP | 61 | 79/2 | 2.47 (3H, s), 7.2—8.1 (5H, m) [1660, |
| | | DBU | 98 | [124/15][d] | 1595, 1580][e] |
| Me | $Me(CH_2)_5$ | DMAP | 72 | 82/13 | 0.7—1.1 (3H, m), 1.2—2.0 (8H, m), 2.30 |
| | | DBU | 79 | | (3H, s), 2.62 (2H, t, $J$=8) [1690] |
| Me | $Me(CH_2)_4CH=CH$ | DMAP | 39 | 82/3 | 0.8—1.0 (3H, m), 1.0—1.7 (6H, m), 2.0— |
| | | DBU | 12[f] | | 2.4 (2H, m), 2.36 (3H, s), 6.1—6.2 (1H, |
| | | | | | m), 6.8—7.1 (1H, m) [1680, 1630] |
| Et | Ph | DMAP | 60 | 80/3 | 1.32 (3H, t, $J$=8), 3.05 (2H, q, $J$=8), |
| | | DBU | 72 | [58/0.25][g] | 7.2—8.1 (5H, m) [1660, 1595, 1580] |
| Pr | Ph | DMAP | 60 | 123/9 | 1.05 (3H, t, $J$=7), 1.4—2.1 (2H, m), 3.05 |
| | | DBU | 70 | [164—170/47][h] | (2H, t, $J$=7), 7.2—8.2 (5H, m) [1660, |
| | | | | | 1600, 1580] |
| Bu | Ph | DMAP | 74 | 106—109/3 | 0.7—1.1 (3H, m), 1.2—2.0 (4H, m), 2.9— |
| | | DBU | 64 | [125/5][i] | 3.3 (2H, m), 7.2—8.2 (5H, m) [1665, |
| | | | | | 1600, 1580] |
| Bu | $Me(CH_2)_5$ | DMAP | 66 | 101—110/25 | 0.7—1.1 (6H, m), 1.1—1.9 (12H, m), 2.52 |
| | | DBU | 83 | | (2H, t, $J$=7), 2.85 (2H, t, $J$=7) [1690] |
| Ph | Ph | DMAP | 61 | 53—54[j] | 7.1—8.1 (10H, m) [1670, 1580][e] |
| | | DBU | 85 | [55—56][k] | |
| Ph | $Me(CH_2)_5$ | DMAP | 90 | 131—137/3 | 0.7—1.1 (3H, m), 1.2—1.9 (8H, m), 2.62 |
| | | DBU | 72 | | (2H, t, $J$=7), 7.3—7.7 (5H, m) [1710, |
| | | | | | 1585] |
| $PhCH_2$ | Ph | DMAP | 84 | 34.5—35.5[j] | 4.29 (2H, s), 7.1—8.1 (10H, m) [1660, |
| | | DBU | 62 | [36—38][l] | 1600, 1580, 1500] |

*a*) The salt **5**, R'COOH, and the base (5 mmol apiece) in benzene (5 ml) were stirred for 12 h at ambient temperature. *b*) Isolated yield. *c*) The IR spectra were obtained with the neat liquid unless otherwise stated. *d*) R. Mayer, S. Scheithauer, and D. Kunz, *Chem. Ber.*, **99**, 1393 (1966). *e*) Obtained in Nujol. *f*) Mixture of $Me(CH_2)_4CH=CHCOSMe$ and $Me(CH_2)_4CH(SMe)CH_2COSMe$. *g*) G. A. Olah, M. R. Bruce, and F. L. Clouet, *J. Org. Chem.*, **49**, 438 (1981). *h*) W. R. Vaugham and J. B. Baumann, *J. Org. Chem.*, **27**, 739 (1962). *i*) S. Yamada, Y. Yokoyama, and T. Shioiri, *J. Org. Chem.*, **39**, 3302 (1974). *j*) mp (°C). *k*) T. Inamoto, M. Kodera, and M. Yokoyama, *Synthesis*, **1982**, 134. *l*) W. Hieber and D. von Pigenot, *Chem. Ber.*, **89**, 193 (1956).

TABLE V. Reaction of $Bu_3P^+SR\ X^-$ (5) with R''OH[a]

| 5 R | 5 X | R'' | Yield (%)[b] of RSR'' | bp (°C)/Torr [lit.] | $^1$H-NMR $\delta$ ($CDCl_3$, $J$=Hz) |
|---|---|---|---|---|---|
| Me | $ClO_4$ | $PhCH_2$ | 72[c] (92)[c,d] | 95—98/25 | 2.00 (3H, s), 3.69 (2H, s), 7.1—7.4 (5H, |
| | $BF_4$ | | 92[c] | [94—96/18][e] | m) |
| Me | $ClO_4$ | $Me(CH_2)_7$ | 55 | 75/35 | 0.5—1.1 (3H, m), 1.0—1.8 (12H, m), |
| | $BF_4$ | | 35 | [97/16][f] | 2.07 (3H, s), 2.50 (2H, t, $J$=7) |
| Me | $ClO_4$ | $Me(CH_2)_2CH=CHCH_2$ | 32 | 63—64/25 | 0.7—1.1 (3H, m), 1.1—1.2 (4H, m), |
| | $BF_4$ | | 33 | | 2.00 (3H, s), 3.04 (2H, d, $J$=6), 5.1— |
| | | | | | 5.8 (2H, m) |
| Me | $ClO_4$ | $Me(CH_2)_5CHMe$ | 10 | 94—98/15 | 0.8—1.1 (3H, m), 1.2—1.8 (13H, m), |
| | $BF_4$ | | 7 | [84—85.5/10][g] | 2.05 (3H, s), 2.4—3.0 (1H, m) |
| Me | $ClO_4$ | $MeCH_2CMe_2$ | 0 | | |
| Et | $ClO_4$ | $PhCH_2$ | 54 | 98/13 | 1.19 (3H, t, $J$=7), 2.40 (2H, q, $J$=7), |
| | | | | [68/4][h] | 3.68 (2H, s), 7.1—7.4 (5H, m) |
| Pr | $ClO_4$ | $PhCH_2$ | 68 | 99—103/10 | 0.91 (3H, t, $J$=7), 1.2—1.9 (2H, m), |
| | | | | [83—84/6][i] | 2.36 (2H, t, $J$=7), 3.64 (2H, s), 7.1— |
| | | | | | 7.4 (5H, m) |
| Bu | $ClO_4$ | $PhCH_2$ | 55 | 101—104/14 | 0.7—1.0 (3H, m), 1.1—1.8 (4H, m), |
| | | | | [102—104/2][i] | 2.38 (2H, t, $J$=7), 3.65 (2H, s), 7.1— |
| | | | | | 7.4 (5H, m) |
| Ph | $ClO_4$ | $Me(CH_2)_2CH=CHCH_2$ | 69 (85)[d] | 102—106/2 | 0.6—1.0 (3H, m), 1.0—2.2 (4H, m), |
| | | | | | 3.4—3.6 (2H, m), 5.3—5.6 (2H, m), |
| | | | | | 7.0—7.6 (5H, m) |
| $PhCH_2$ | $ClO_4$ | $PhCH_2$ | 48 | 47—48[j] | 3.39 (4H, s), 7.2—7.5 (10H, m) |
| | | | | [47—49][j,k] | |

*a*) The phosphonium salt **5**, R''OH, and DBU (10 mmol each) in benzene (10 ml) were stirred for 48 h at ambient temperature. *b*) Isolated yield. *c*) Determined by gas chromatography [PEG-20M (10%) as packing]. *d*) In $CH_2Cl_2$. *e*) T. Ichikawa, H. Owatari, and T. Kato, *J. Org. Chem.*, **35**, 344 (1970). *f*) I. Degani, R. Fochi, and V. Regondi, *Synthesis*, **1983**, 630. *g*) H. Matsuyama, H. Minato, and M. Kobayashi, *Bull. Chem. Soc. Jpn.*, **48**, 3287 (1975). *h*) M. Furukawa, T. Suda, and S. Hayashi, *Synthesis*, **1974**, 282. *i*) T. Kubota, S. Miyashita, T. Kitazume, and N. Ishikawa, *J. Org. Chem.*, **45**, 5052 (1980). *j*) mp (°C). *k*) R. S. Davidson, *J. Chem. Soc.* (*C*), **1967**, 2131.

was stirred at ambient temperature, the corresponding thiolester or unsymmetrical sulfide, respectively, was obtained in fair to excellent yield. As the base, 4-(dimethylamino)pyridine (DMAP) and/or 1,8-diazabicyclo[5.4.0]undec-7-ene (DBU) were found to afford favorable results. Reactions of **5** with unsaturated acids or with secondary and tertiary alcohols gave poor yields of the expected products. Typical results are collected in Tables IV and V.

As described so far, the phosphonium salts **3** and **5** can be prepared from disulfides **2** and the phosphines **1** and **4**, respectively, either by the CCE method or by the non-electrochemical reaction, both in one step without the use of any special or unstable reagents: the yields of the phosphonium salts are comparable to or a little lower than those (usually >70%) reported in the alkylation of phosphine sulfides.[4,5] For the preparation of **3**, which is a useful reagent for the synthesis of unsymmetrical disulfides,[1] the CCE method is recommended, because it requires no extra reagent other than $HClO_4$ and the yield of **3** was always better than that attained by the non-electrochemical reaction: in the work-up, remaining $HClO_4$ can be removed easily (see Experimental). On the other hand, the non-electrochemical procedure is obviously superior to its electrochemical counterpart for the preparation of **5** with primary thioalkoxy groups.

Several methods have been developed to obtain thiolesters[18] and unsymmetrical sulfides[19] starting from carboxylic acids or their activated forms and from alcohols or alkyl halides, respectively. As mentioned by Haynes and Indorato,[4] however, the present methods

with the phosphonium salts **5** at least by-pass the inconvenience of using thiols or their metal salts. The phosphonium salts **5** as well as **3** are stable and can be stored over a long period simply in a stoppered bottle.

## Experimental

All melting points are uncorrected. Infrared (IR) and nuclear magnetic resonance ($^1$H-NMR) spectra were measured with Nippon Bunko A202 and Hitachi R-20 spectrometers, respectively. Cyclic voltammetry was carried out essentially as described previously.[20] CCE was performed using a conventional DC power supply (50 V-2 A).

**Materials**——The phosphine **1** was recrystallized from hexane, and **4** was distilled under reduced pressure. $LiClO_4$ was recrystallized from 95% ethanol and stored over $P_2O_5$ under reduced pressure. Commercially available

TABLE VI. Physical and $^1$H-NMR Spectral Data for $Ph_3P^+SR\ ClO_4^-$ (**3**) and $Bu_3P^+SR\ X^-$ (**5**)[a]

| Compd. | Formula and mp (°C) | Analysis (%) Calcd (Found) C | H | $^1$H-NMR $\delta$ ($CDCl_3$, $J$=Hz) |
|---|---|---|---|---|
| **3** (R=Me) | $C_{19}H_{18}ClO_4PS$ | 55.82 | 4.44 | 2.47 (3H, d, $J_{PH}$=15), 7.4—8.0 (15H, m) |
| | 139—140 | (55.54 | 4.35) | |
| **3** (R=Et) | $C_{20}H_{20}ClO_4PS$ | 56.81 | 4.77 | 1.35 (3H, t, $J_{HH}$=7.5), 2.98 (2H, dq, $J_{HH}$=7.5, $J_{PH}$=11), |
| | 191—192 | (56.63 | 4.64) | 7.4—8.0 (15H, m) |
| **3** (R=Pr) | $C_{21}H_{22}ClO_4PS$ | 57.73 | 5.08 | 0.94 (3H, t, $J_{HH}$=7), 1.68 (2H, tq, $J_{HH}$=7, 7), 2.98 (2H, dt, |
| | 169—170 | (57.67 | 5.09) | $J_{HH}$=7, $J_{PH}$=11), 7.5—8.1 (15H, m) |
| **3** (R=Bu) | $C_{22}H_{24}ClO_4PS$ | 58.60 | 5.36 | 0.80 (3H, t, $J_{HH}$=7), 1.0—2.0 (4H, m), 2.93 (2H, dt, $J_{HH}$=7, |
| | 140—141 | (58.47 | 5.31) | $J_{PH}$=11), 7.4—8.1 (15H, m) |
| **3** (R=*sec*-Bu) | $C_{22}H_{24}ClO_4PS$ | 58.60 | 5.36 | 0.91 (3H, t, $J_{HH}$=7), 1.31 (3H, d, $J_{HH}$=7), 1.62 (2H, dq, |
| | 103—104 | (58.51 | 5.32) | $J_{HH}$=7, 7), 2.87—3.67 (1H, m), 7.5—8.1 (15H, m) |
| **3** (R=Ph) | $C_{24}H_{20}ClO_4PS$ | 61.21 | 4.28 | 7.8—8.0 (20H, m) |
| | 172—173 | (61.41 | 4.26) | |
| **3** (R=$PhCH_2$) | $C_{25}H_{22}ClO_4PS$ | 61.92 | 4.57 | 4.12 (2H, d, $J_{PH}$=11), 7.0—7.3 (5H, m), 7.4—8.1 (15H, m) |
| | 141—142 | (61.81 | 4.40) | |
| **5** (R=Me, | $C_{13}H_{30}ClO_4PS$ | 44.76 | 8.67 | 0.7—1.2 (9H, m), 1.3—1.8 (12H, m), 2.3—2.9 (6H, m), 2.50 |
| X=$ClO_4$) | 60—61 | (44.61 | 8.95) | (3H, d, $J_{PH}$=13) |
| **5** (R=Me, | $C_{13}H_{30}BF_4PS$ | 46.44 | 8.99 | 0.8—1.2 (9H, m), 1.3—1.9 (12H, m), 2.2—2.8 (6H, m), 2.48 |
| X=$BF_4$) | 52—53 | (46.26 | 9.21) | (3H, d, $J_{PH}$=13) |
| **5** (R=Et, | $C_{14}H_{32}ClO_4PS$ | 46.34 | 8.89 | 0.7—1.2 (9H, m), 1.3—1.8 (15H, m), 2.3—2.9 (6H, m), 3.10 |
| X=$ClO_4$) | 75—76 | (46.24 | 9.11) | (2H, dq, $J_{HH}$=7, $J_{PH}$=10) |
| **5** (R=Et, | $C_{14}H_{32}BF_4PS$ | 48.01 | 9.21 | 0.8—1.2 (9H, m), 1.3—1.9 (15H, m), 2.1—2.8 (6H, m), 3.03 |
| X=$BF_4$) | 42—43 | (47.96 | 9.56) | (2H, dq, $J_{HH}$=8, $J_{PH}$=10) |
| **5** (R=Pr, | $C_{15}H_{34}ClO_4PS$ | 47.80 | 9.09 | 0.7—1.2 (12H, m), 1.3—2.1 (14H, m), 2.3—2.9 (6H, m), |
| X=$ClO_4$) | 61—62 | (47.56 | 9.26) | 3.03 (2H, dt, $J_{HH}$=7, $J_{PH}$=9) |
| **5** (R=Pr, | $C_{15}H_{34}BF_4PS$ | 49.46 | 9.41 | 0.8—1.3 (12H, m), 1.3—2.1 (14H, m), 2.1—2.7 (6H, m), |
| X=$BF_4$) | 62—63 | (49.60 | 9.66) | 3.04 (2H, dt, $J_{HH}$=8, $J_{PH}$=10) |
| **5** (R=Bu, | $C_{16}H_{36}ClO_4PS$ | 49.16 | 9.28 | 0.7—1.2 (12H, m), 1.3—2.0 (16H, m), 2.3—2.8 (6H, m), |
| X=$ClO_4$) | 56—57 | (48.92 | 9.50) | 3.05 (2H, dt, $J_{HH}$=7, $J_{PH}$=10) |
| **5** (R=Bu, | $C_{16}H_{36}BF_4PS$ | 50.80 | 9.59 | 0.8—1.2 (12H, m), 1.2—1.9 (16H, m), 2.2—2.8 (6H, m), |
| X=$BF_4$) | 57—58 | (50.82 | 9.88) | 3.05 (2H, dt, $J_{HH}$=8, $J_{PH}$=9) |
| **5** (R=Ph, | $C_{18}H_{32}ClO_4PS$ | 52.61 | 7.85 | 0.7—1.2 (9H, m), 1.2—2.0 (12H, m), 2.2—2.7 (6H, m), |
| X=$ClO_4$) | 56—57 | (52.38 | 8.02) | 7.3—7.8 (5H, m) |
| **5** (R=$PhCH_2$, | $C_{19}H_{34}ClO_4PS$ | 53.70 | 8.06 | 0.7—1.2 (9H, m), 1.3—2.0 (12H, m), 2.3—2.8 (6H, m), 4.25 |
| X=$ClO_4$) | 88—89 | (53.54 | 8.21) | (2H, d, $J_{PH}$=11), 7.1—7.6 (5H, m) |
| **5** (R=$PhCH_2$, | $C_{19}H_{34}BF_4PS$ | 55.35 | 8.31 | 0.8—1.2 (9H, m), 1.3—1.9 (12H, m), 2.2—2.8 (6H, m), 4.20 |
| X=$BF_4$) | 86—87 | (55.49 | 8.61) | (2H, d, $J_{PH}$=10), 7.1—7.5 (5H, m) |

*a*) IR spectra of the phosphonium salts with $ClO_4^-$ showed characteristic absorption at around 1100 $cm^{-1}$, and those with $BF_4^-$ at around 1050 $cm^{-1}$.

anhydrous $LiBF_4$ was used without further purification. MeCN was purified by the method of Kiesele.[21] Other chemicals were obtained from commercial sources and were purified, if necessary, by distillation or recrystallization.

**General Procedure for the Electrochemical Preparation of 3**——A 50 ml sample tube (diameter, 3.5 cm; height, 7.5 cm) was used as the electrolysis cell, which was equipped with a graphite plate anode (1 × 10 cm) and a platinum foil cathode (1 × 10 cm)[22] through a silicon stopper. A solution of **1** (2 mmol), **2** (4 mmol), and 70% $HClO_4$ (4 mmol as $HClO_4$) in MeCN (40 ml) was placed in the cell: caution, $HClO_4$ should be added slowly to the mixture of **1** and **2** in MeCN with stirring. The system was subjected to CCE (50 mA; current density, *ca.* 6 mA/cm$^2$) at ambient temperature until 1 F per mol of **1** (193 C, *ca.* 65 min) had been consumed. The electrolyzed solution was concentrated to *ca.* 2 ml under reduced pressure at below 30 °C. Ether (100 ml) was added to the residue. The phosphonium salt **3** that separated out (as colorless crystals) was filtered off, washed with ether and AcOEt, and recrystallized from MeCOEt and AcOEt. The physical and spectroscopic data for **3** are summarized in Table VI. CCE with a larger amount of **1** was carried out in a 200 ml beaker (diameter, 5.5 cm; height, 10 cm): a graphite plate of 3 × 10 cm was used as the anode. A mixture of **1** (50 mmol), **2** (100 mmol), and 70% $HClO_4$ (100 mmol) in MeCN (150 ml) was subjected to CCE (70 mA; current density, *ca.* 2 mA/cm$^2$) as described above (*ca.* 20 h): at the beginning of electrolysis, it is not necessary to dissolve **1** completely in the medium.

**General Procedure for the Electrochemical Preparation of 5**——A mixture of **4** (7.5 mmol), **2** (15 mmol), PhCOOH (7.5 mmol), $LiClO_4$ (30 mmol) and $Al_2O_3$ (0.2 g) in MeCN (40 ml) was subjected to CCE in a 50 ml sample tube (see above) under the conditions cited in Table II until 1 F per mol of **4** had been consumed. The electrolyzed solution, after deposited PhCOOLi and $Al_2O_3$ had been removed by filtration, was concentrated to *ca.* 2 ml under reduced pressure. Water (40 ml) was added to the residue and the mixture was extracted with $CHCl_3$ (5 × 20 ml). The extracts were dried over anhydrous $MgSO_4$ and concentrated to *ca.* 2 ml. When ether (200 ml) was added to the residue, the phosphonium salt **5** separated out as colorless crystals, which were filtered off, washed with ether, and recrystallized from AcOEt and ether. The physical and spectroscopic data for **5** are given in Table VI.

**General Procedure for the Non-electrochemical Preparation of 5**——A mixture of **4** (12.5 mmol), **2** (12.5 mmol), PhCOOH (12.5 mmol), $LiClO_4$ or $LiBF_4$ (12.5 mmol), and $Al_2O_3$ (0.2 g) in MeCN (20 ml) was stirred at ambient temperature for 12 h. Work-up of the reaction mixture as described above gave the phosphonium salt **5**. The preparation of **3** was performed by essentially the same procedure.

**Reaction of 5 with Carboxylic Acids**——Essentially the same procedure as reported by Haynes and Indorato[4] was employed. Thus, the phosphonium salt **5** (5 mmol) was added in one portion to a solution of a carboxylic acid (5 mmol) and a base (DBU or DMAP) (5 mmol) in benzene (5 ml),[23] and the resulting mixture was stirred at ambient temperature for 24 h. Insoluble material in the reaction mixture was filtered off, and the filtrate was evaporated under reduced pressure. The residue was then subjected to column chromatography on silica gel [hexane–AcOEt (20 : 1)] to give the expected thiolester, which was purified by vacuum distillation.

**Reaction of 5 with Alcohols**——Compound **5** (10 mmol) was added in one portion to a solution of an alcohol (10 mmol) and DBU (10 mmol) in benzene or $CH_2Cl_2$ (10 ml). The mixture was stirred at ambient temperature for 48 h, and then filtered. The filtrate was evaporated under reduced pressure, and the residue was subjected to column chromatography on silica gel [hexane–AcOEt (40 : 1)] to give the expected unsymmetrical sulfide.

**Acknowledgement** This work was supported in part by a Grant-in-Aid for Scientific Research (60570987) from the Ministry of Education, Science and Culture.

## References and Notes

1) M. Masui, Y. Mizuki, K. Sakai, C. Ueda, and H. Ohmori, *J. Chem. Soc., Chem. Commun.*, **1984**, 843.
2) T. Endo, S. Ikenaga, and T. Mukaiyama, *Bull. Chem. Soc. Jpn.*, **43**, 2632 (1970).
3) H. Ohmori, H. Maeda, K. Sakai, and M. Masui, unpublished results.
4) R. K. Haynes and C. Indorato, *Aust. J. Chem.*, **37**, 1183 (1984).
5) A. Hantsch and H. Hibbert, *Ber.*, **40**, 1508 (1907); L. Horner and H. Winker, *Tetrahedron Lett.*, **1964**, 175; C. Glidewell and E. J. Leslie, *J. Chem. Soc., Dalton Trans.*, **1977**, 527; J. Omelanczuk and M. Mikołajczyk, *J. Am. Chem. Soc.*, **101**, 7292 (1979), and *Tetrahedron Lett.*, **1984**, 2493; D. H. R. Barton, D. P. Manly, and D. A. Widdowson, *J. Chem. Soc., Perkin Trans. 1*, **1975**, 1568; L. Horner and M. Jordan, *Phosphorus and Sulfur*, **8**, 209 and 215 (1980).
6) H. Ohmori, S. Nakai, M. Sekiguchi, and M. Masui, *Chem. Pharm. Bull.*, **28**, 910 (1980).
7) Preparation of **3** by CCE has been briefly mentioned (ref. 1).
8) Since 70% $HClO_4$ obtained from a commercial source was used without any treatment, the reaction medium inevitably contained a small amount of water.
9) Cathodic reduction of **3** in MeCN was found to give **1** and **2**.
10) Higher yields of **5** were observed when water was deliberately added to the medium along with $NaClO_4$. However, it was rather difficult to find the optimum amount of water required in each experiment.
11) S. Torii, "Electroorganic Synthesis (Part 1: Oxidations)," Kodansha, Tokyo, and VCH, Weinheim, 1985, pp.

57—58, 61—62, 85—86, 125, 223—224, and 310—313.
12) In the CPE method, the amount of electricity required for the formation of **3** has been found to be 1 F per mol of **1**.
13) The voltammetric peak of **1** in the presence of $HClO_4$ may be ascribed to the oxidation of $Ph_3PH^+$ to $Ph_3P^{+\cdot}$ and $H^+$, though further studies are required to elucidate the exact nature of the electrode process.
14) The yield of **5** was improved a little on CCE at 0 °C.
15) C. A. Steuli, *Anal. Chem.*, **32**, 985 (1960).
16) T. Mukaiyama and H. Takei, "Topics in Phosphorus Chemistry," Vol. 8, ed. by E. J. Griffith and M. Grayson, John Wiley and Sons, Inc., New York, 1976, pp. 587—645.
17) Ref. 16, pp. 620—621.
18) E. Haslam, *Tetrahedron*, **36**, 2409 (1980); H.-J. Liu and S. I. Sabesan, *Can. J. Chem.*, **58**, 2645 (1980); S. Kim and S. Yang, *Chem. Lett.*, **1981**, 133; Y. Kawanami, Y. Dainobu, J. Inanaga, T. Katsuki, and M. Yamaguchi, *Bull. Chem. Soc. Jpn.*, **54**, 943 (1981); T. Inamoto, M. Kodera, and M. Yokoyama, *Synthesis*, **1982**, 134; K. Soai, H. Hayashi, and A. Ookawa, *J. Chem. Res.*, **1983**, 20; and references cited therein.
19) N. Ono, H. Miyake, T. Sato, and A. Kaji, *Synthesis*, **1980**, 952; J. T. B. Ferreira, J. V. Comasseto, and A. J. Braga, *Synth. Commun.*, **12**, 595 (1982); W. Ando, T. Furuhata, H. Tsumaki, and A. Sekiguchi, *ibid.*, **12**, 627 (1982); M. Yamato, Y. Takeuchi, K. Hattori, and K. Hashigaki, *Synthesis*, **1982**, 1014; I. Degani, R. Fochi, and V. Regondi, *ibid.*, **1983**, 630; J. C. Sih and D. R. Graber, *J. Org. Chem.*, **48**, 3842 (1983); F. A. Luzzio, *Synth. Commun.*, **14**, 209 (1984); and references cited therein.
20) H. Ohmori, A. Matsumoto, and M. Masui, *J. Chem. Soc., Perkin Trans. 2*, **1980**, 347.
21) H. Kiesele, *Anal. Chem.*, **52**, 2230 (1980).
22) A stainless steel plate or a graphite plate can also be used as the cathode.
23) The mixture was warmed, if necessary, to obtain a clear solution.

[Chem. Pharm. Bull. 35(11)4482—4493(1987)]

# Purines. XXIX.[1] Syntheses of 9-Alkyl-2-deuterio-$N^6$-methoxyadenines and 2-Deuterio-$N^6$,9-dimethyladenine: Tautomerism in 9-Substituted $N^6$-Alkoxyadenines

TOZO FUJII,* TOHRU SAITO, TAISUKE ITAYA, KYOKO KIZU, YUKINARI KUMAZAWA, and SATOSHI NAKAJIMA

*Faculty of Pharmaceutical Sciences, Kanazawa University, Takara-machi, Kanazawa 920, Japan*

(Received May 26, 1987)

Cyclizations of the alkoxyamidines **7a**, **i** with formic acid gave $N^6$-methoxy-9-methyladenine (**8a**) and 9-benzyl-$N^6$-methoxyadenine (**8i**). Replacement of formic acid by formic-*d* acid-*d* in these cyclizations afforded the 2-deuterated species **13a** and **13i**. A similar cyclization of **22**, obtained from **21** by alkaline hydrolysis, with formic-*d* acid-*d* yielded 2-deuterio-$N^6$-methoxy-1,9-dimethyladenine (**24**). The $N^6$-methyl isomer **19** was prepared from **13a** by treatment with NaH and MeI. Comparison of the proton nuclear magnetic resonance ($^1$H-NMR) spectrum of **8a** in $Me_2SO$-$d_6$ with that of **13a** revealed that **8a** exists as an equilibrated 1 : 3.5 mixture of the amino (type **14** or **15**) and the imino (type **16** or **17**) forms. The deuterated species **19** and **24** were utilized for interpretation of the $^1$H-NMR spectra of the amino-form model **18** and the imino-form model **23**. The existence of amino–imino tautomerism in **8a** was also supported by ultraviolet and infrared spectroscopic evidence. Such tautomerism, with a preference for the imino form, in $Me_2SO$-$d_6$ was found to be common to 13 other 9-substituted $N^6$-alkoxyadenines (type **8**) including adenosine analogues. On the other hand, comparison of the $^1$H-NMR spectra of **11**, $N^6$,9-dimethyladenine (**12**), and $N^6$,$N^6$,9-trimethyladenine (**36**) indicated that **12** exists solely in the amino form in $CDCl_3$ or $Me_2SO$-$d_6$.

**Keywords**——$N^6$-alkoxy-9-alkyladenine; $N^6$-alkoxyadenosine; 9-alkyl-2-deuterio-$N^6$-methoxyadenine; 2-deuterio-$N^6$,9-dimethyladenine; amino–imino tautomerism; $^1$H-NMR; UV; IR

An alkoxy group at the $N^6$-position of adenine (**1**: $R^1$ = H) and substituted adenines has been found of considerable synthetic utility because of its unique directivity in alkylation and substantial removability under hydrogenolytic conditions.[2,3] The synthesis of 7,9-dialkyladeninium salts by us[2a,c-e] from $N^6$-alkoxy-9-alkyladenines (type **8**) is a representative of such synthetic utility, culminating in the elegant syntheses of agelasine B, a sea sponge bicyclic diterpene with the 9-methyl-7-adeninylium moiety, and analogues by Tokoroyama's group.[4] In 1966, we synthesized the $N^6$-alkoxyadenines **8** for the first time[5] and found that unambiguous assignments of the NH and the purine-ring proton signals in their nuclear magnetic resonance (NMR) spectra were difficult in many cases because of the complexity or dullness of the low-field signals. In order to interpret these spectra, we synthesized several 2-deuterated species and measured their $^1$H-NMR spectra in the present study.

The synthesis of the 2-deuterated species **13a** and **13i** was planned on the basis of our knowledge[3] concerning fission and reclosure of the adenine ring, employing an alkoxy group at the 1-position, and of our recent success[6] in synthesizing 9-substituted 2-deuterioadenines (type **5**) from 9-substituted adenines (type **1**) through the intermediates **2**, **3**, **4**, **7**, and **6** (Chart 1). Thus, the monocycle **7a**[5b] was treated with formic-*d* acid-*d* (of over 99% isotopic purity) in boiling MeCN for 6 h, giving **13a** in 52% yield. The 1-benzyl analogue **7i**[6] was likewise cyclized to produce **13i** in 63% yield. This cyclization of the 5-aminoimidazole-4-

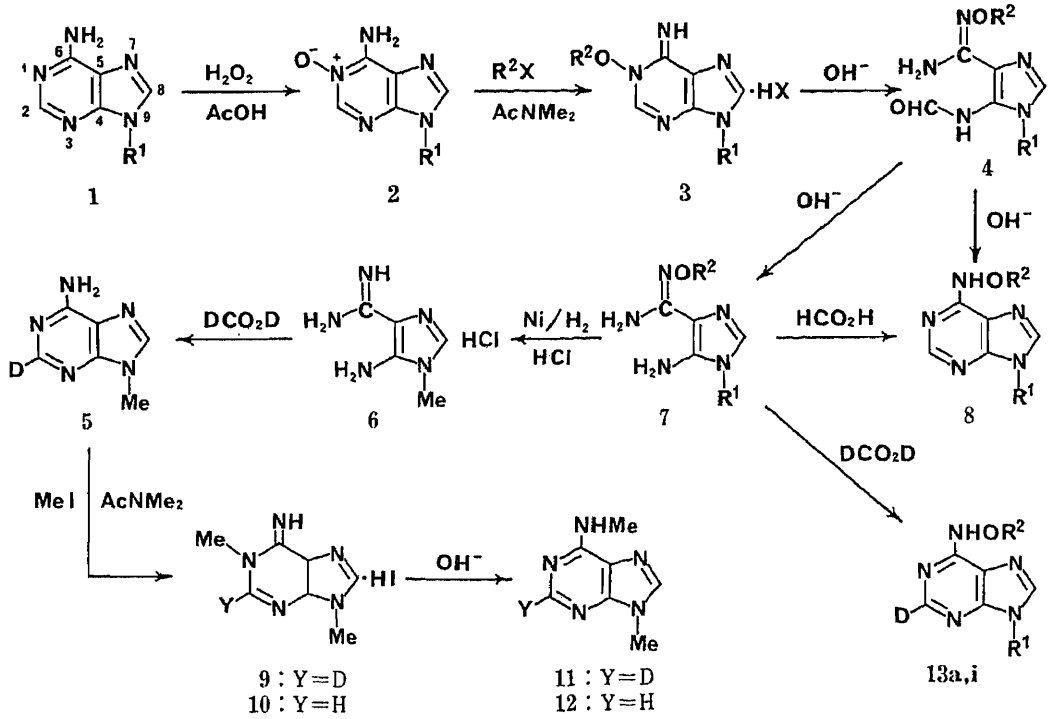

a : $R^1$=Me; $R^2$=Me b : $R^1$=Me; $R^2$=Et c : $R^1$=Me; $R^2$=$PhCH_2$

d : $R^1$=Me; $R^2$=MeO- 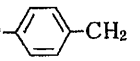 -$CH_2$ e : $R^1$=Me; $R^2$= 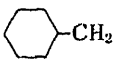 -$CH_2$

f : $R^1$=Et; $R^2$=Me g : $R^1$=Et; $R^2$=Et h : $R^1$=Et; $R^2$=$PhCH_2$

i : $R^1$=$PhCH_2$; $R^2$=Me j : $R^1$=$PhCH_2$; $R^2$=Et k : $R^1$=$PhCH_2$; $R^2$=$PhCH_2$

Chart 1

carboxamidines **7a, i** by incorporation of a $C_1$ unit in the form of a formic acid was analogous to that[7] employed for the preparation of adenine-*2*-$^{14}C$, and the correctness of the synthetic outcome was supported by parallel cyclizations of **7a** and **7i** with unlabeled formic acid, which afforded the known and new $N^6$-methoxyadenines **8a**[5a,b] and **8i** in 50% and 80% yields, respectively. The benzyl analogue **8i** was identical with a sample prepared from **3i** (X=I) through **4i** according to the previously reported procedure.[5b] Judged from $^1$H-NMR and mass spectral data, the 2-deuterated species **13a** and **13i** thus obtained had a deuterium content at the 2-position equal in order of magnitude to that of the formic-*d* acid-*d* used, but were contaminated with the 2,8-dideuterated species to the extent of *ca.* 16% and *ca.* 50%, respectively. The formation of the 2,8-dideuterated species is most likely due to isotopic exchange of C(8)-H of **13** already produced or of C(2)-H of **7** with formic-*d* acid-*d* (and/or HDO) during the cyclization reaction. It is well known that adenine (**1**: $R^1$=H) and 9-substituted adenines including adenosine undergo hydrogen exchange at C(8) much faster than at C(2).[6]

The synthesis of **11** started with 2-deuterio-9-methyladenine (**5**)[6] because that of the unlabeled species **12** from **10**, obtainable from **1** ($R^1$=Me) by methylation, had already been reported.[8] Thus, methylation of **5** with MeI in $AcNMe_2$ at 60 °C for 2 h gave the 1-methylated product **9** in 78% yield. Dimroth rearrangement of **9** was effected in boiling 0.2 N aqueous NaOH for 15 min, furnishing the desired $N^6$,9-dimethyl isomer **11** in 72% yield. The deuterium content in **9** and **11** was as high as that in the starting material **5**.

Figure 1 illustrates the complexity of the low-field signals in the $^1$H-NMR spectrum of **8a**

in $Me_2SO$-$d_6$. The moisture and acidic impurities in the solvent tend to cause these signals to become dull. Comparison of this spectrum with that of **13a** made possible the assignments of the NH, C(2)-H, and C(8)-H proton signals. Two sets of signals observed for the C(2)-H, C(8)-H, and NH protons, all with identical ratios (1 : 3.5) of relative integral intensities, were suggestive of the presence of both the $N^6$-amino (type **14** and/or **15**) and $N^6$-imino (type **16** and/or **17**) tautomers. The N(9)-Me protons also appeared as a set of two singlets at $\delta$ 3.77 and 3.63 with the area ratio of 1 : 3.5; but the $N^6$-OMe protons, only as a three-proton singlet at $\delta$ 3.75.

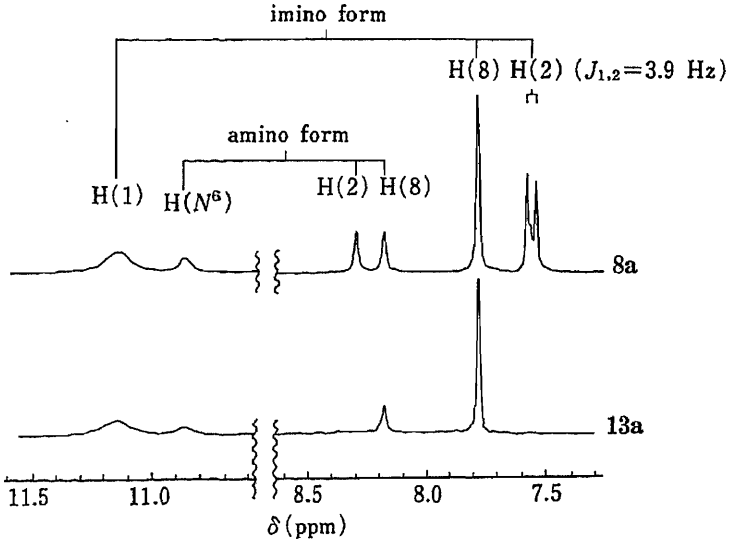


Fig. 1. The $^1$H-NMR Spectra of $N^6$-Methoxy-9-methyladenine (**8a**) and the C(2)-D Labeled Species **13a** in $Me_2SO$-$d_6$

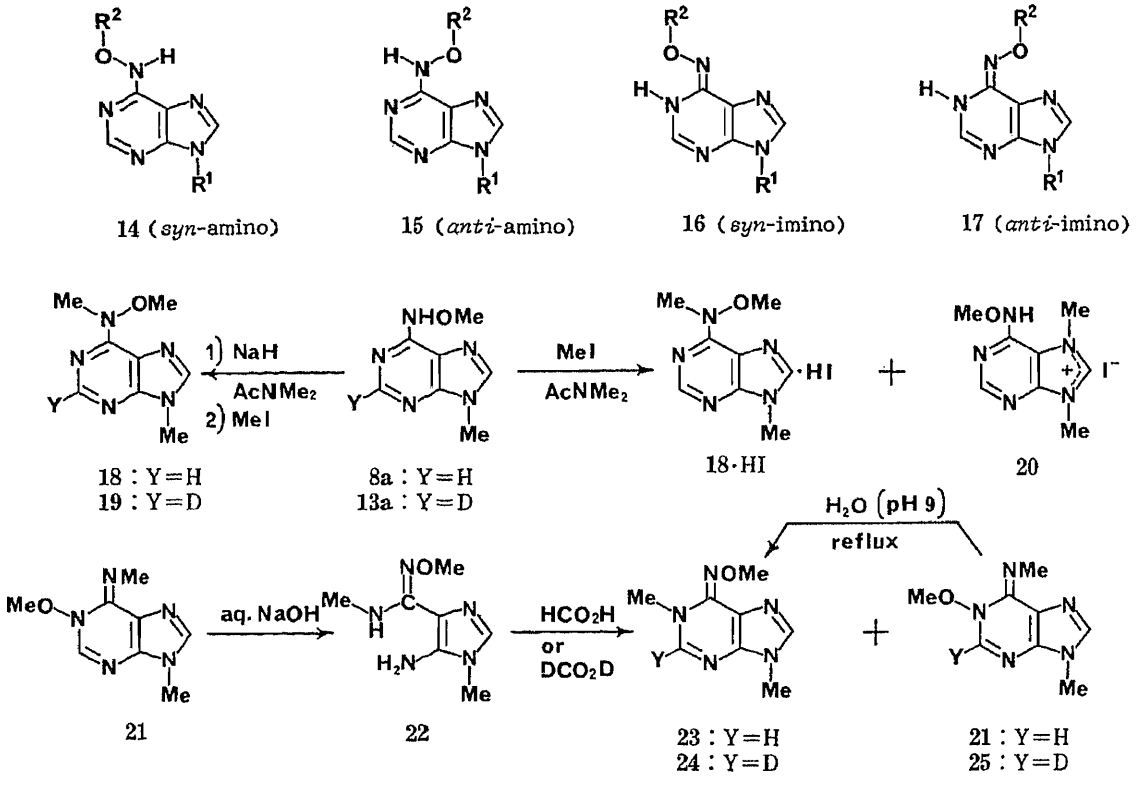


Chart 2

For further help in the assignments of the ring proton signals, the amino-form models **18** and **19** and the imino-form models **23** and **24** were prepared as shown in Chart 2. Methylation of **8a** with MeI in $AcNMe_2$ is known to give the $N^6$-methylated product **18**·HI, but in low yield (24%); the major product is the N(7)-methylated isomer **20** (59%).[2a,c] In order to increase the nucleophilicity at the $N^6$-position, **8a** was first treated with NaH in $AcNMe_2$, and the anion generated *in situ* was methylated with MeI at room temperature for 26 h. As expected, this procedure improved the yield of the $N^6$-methylated product **18** to 84%. A similar methylation of the deuterated species **13a** afforded **19** in 55% yield. The synthesis of **24** was first tested in the unlabeled series. Hydrolysis of the 1-methoxy isomer **21**[9] in boiling aqueous NaOH for 15 min produced the monocycle **22** in 67% yield. Treatment of **22** with formic acid in boiling MeCN for 5.5 h furnished the $N^6$-methoxy isomer **23**[9] (31% yield) together with a little by-product presumed to be the 1-methoxy isomer **21**,[9] which was converted into **23** in 6% overall yield (from **22**) under known Dimroth rearrangement conditions.[9] A parallel cyclization of **22** with formic-*d* acid-*d* provided the deuterated species **24** (20% yield) and a small amount of a by-product presumed to be **25**. However, this sample of **24** was found to contain the 2,8-dideuterated species to the extent of *ca.* 50%. This suggested that isotopic exchange of C(8)-H had occurred during cyclization, as in the cases of **13a** and **13i**.

Comparison of the $^1$H-NMR spectral data for **18**, **19**, **23**, and **24** revealed that the ring protons of the amino-form model **18** resonated in the $\delta$ 8.4—8.2 region and that the C(2)-H proton was less shielded than the C(8)-H proton. In contrast to this, those protons of the imino-form model **23** resonated in the $\delta$ 7.9—7.7 region,[9] and the C(2)-H proton was more shielded than the C(8)-H proton. These results supported the correctness of the assignments made in Fig. 1 for the most likely tautomeric forms of **8a**. The existence of the imino form [with the proton on N(1)] in **8a** was further corroborated by the observation of coupling ($J$= 3.9 Hz) between C(2)-H and N(1)-H. For an alternative interpretation of this coupling, the N(3)-H isomer (type **26** and/or **27**) may be equally considered. However, this was disproved by the following ultraviolet (UV) spectroscopic approach.

Figure 2 shows the UV spectra of the neutral species of **8a** (p$K_a$ 3.06 and 11.26),[5b] **18** (p$K_a$ 3.75), **23** (p$K_a$ 4.09), and **28**[2b] (p$K_a$ 5.09) in $H_2O$ at pH 7.41. The curve for **8a** bears no

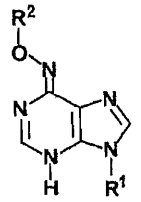


26 (*syn*-imino)

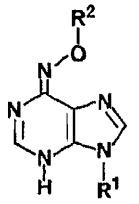


27 (*anti*-imino)

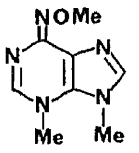


28

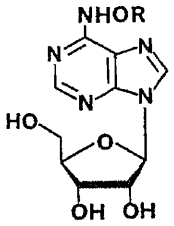


29 : R=Me
30 : R=Et
31 : R=PhCH$_2$

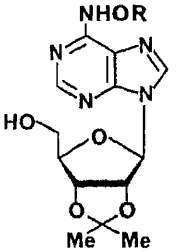


32 : R=Me
33 : R=Et
34 : R=PhCH$_2$

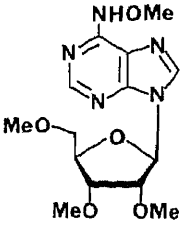


35

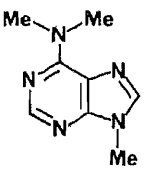


36

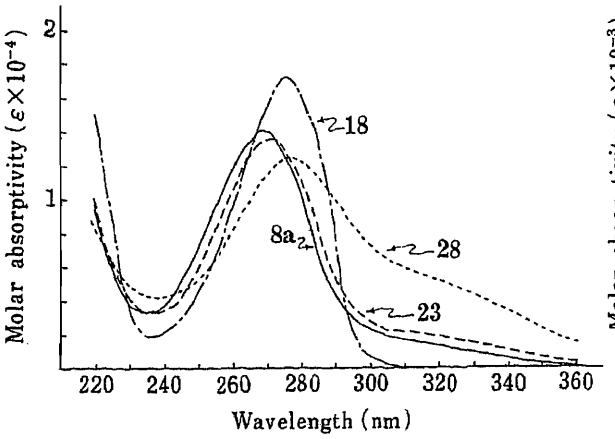


Fig. 2. UV Spectra of the $N^6$-Methoxyadenine Derivatives **8a**, **18**, **23**, and **28** in 0.005 M Aqueous $KH_2PO_4$–$Na_2HPO_4$ at pH 7.41 and 25 °C

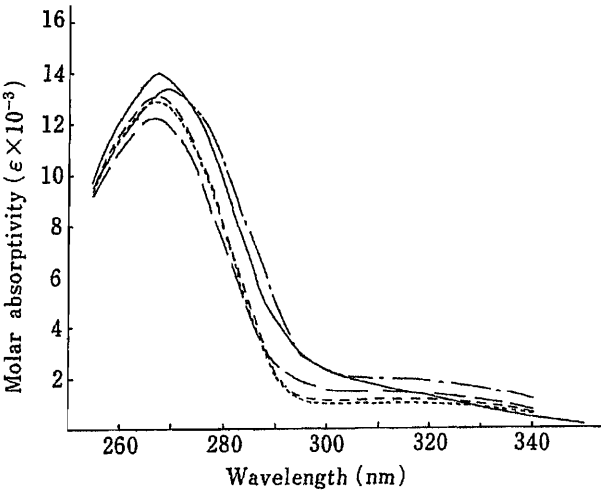


Fig. 3. Effect of Solvent on the UV Spectrum of **8a**

——, in $H_2O$; — · —, in $Me_2SO$; — —, in MeCN; – – –, in tetrahydrofuran; ------, in 1,4-dioxane.

similarity to that for the amino-form model **18** nor to that for the isomeric imino-form [N(3)-H] model **28**, but is closely similar to that for the imino-form [N(1)-H] model **23**. Characteristic is the long-wavelength absorption [$\lambda_{shoulder}$ 312 nm ($\varepsilon$ 2200)] observed for the imino-form model **23**; this absorption may be used as a measure of the population of the imino form in **8a**. Thus, the similarity between the UV curves of **8a** and **23** indicates that **8a** exists in $H_2O$ as an equilibrated mixture of the amino form (type **14** and/or **15**) and the imino form (type **16** and/or **17**), in which the latter is predominant. Figure 3 shows the UV spectra of **8a** in various solvents. It may be seen that the absorption intensity in the 312 nm region tends to increase with increase of the dielectric constant of a solvent. Obviously, solvent polarity exercises a considerable effect on the population of the tautomers, in favor of the imino form in polar solvents.

The existence of amino–imino tautomerism in **8a** was also demonstrated by infrared (IR) spectroscopy. It may be seen from Fig. 4 that in $CHCl_3$ solution the amino-form model **18** showed a strong absorption band at 1585 $cm^{-1}$ arising from the ring stretching vibration [Fig. 4(A)]. On the other hand, the imino-form model **23** exhibited a strong band at 1653 $cm^{-1}$ besides a weak one at 1603 $cm^{-1}$ [Fig. 4(B)]. The two strong absorption bands observed for **8a** at 1666 and 1602 $cm^{-1}$ [Fig. 4(C)] may thus be regarded as a reflection of the presence of both the amino and the imino forms in $CHCl_3$, with a slight preference for the former. A similar result was also obtained with the 9-benzyl analogue **8i** [Fig. 4(D)].

The above results clearly demonstrate the existence of amino–imino equilibrium of **8a** and of **8i** in solution. They are in general agreement with those obtained for $N^6$-methoxyadenosine (**29**) by Morozov *et al.*[10] through a UV spectroscopic and quantum chemical approach, for a synthetic matrix containing **29** by Singer and Spengler[11] through a biochemical approach, and for $N^6$-methoxy-2′,3′,5′-tri-*O*-methyladenosine (**35**) by Shugar and co-workers through $^1$H- and $^{13}$C-NMR spectroscopic[12] and UV and IR spectroscopic[13] approaches. As regards the problem of conformation or configuration of the exocyclic $N^6$-OMe group, the orientation of the OMe group may be *syn* or *anti* with respect to the ring N(1), as represented by formulas **14**—**17** in Chart 2. There are no data available for solving this problem in the present study, but the *syn* forms **14** and **16** are favored on the basis of previous discussions reported in the literature.[10,12–14] However, the $^1$H-NMR spectrum of **8a**

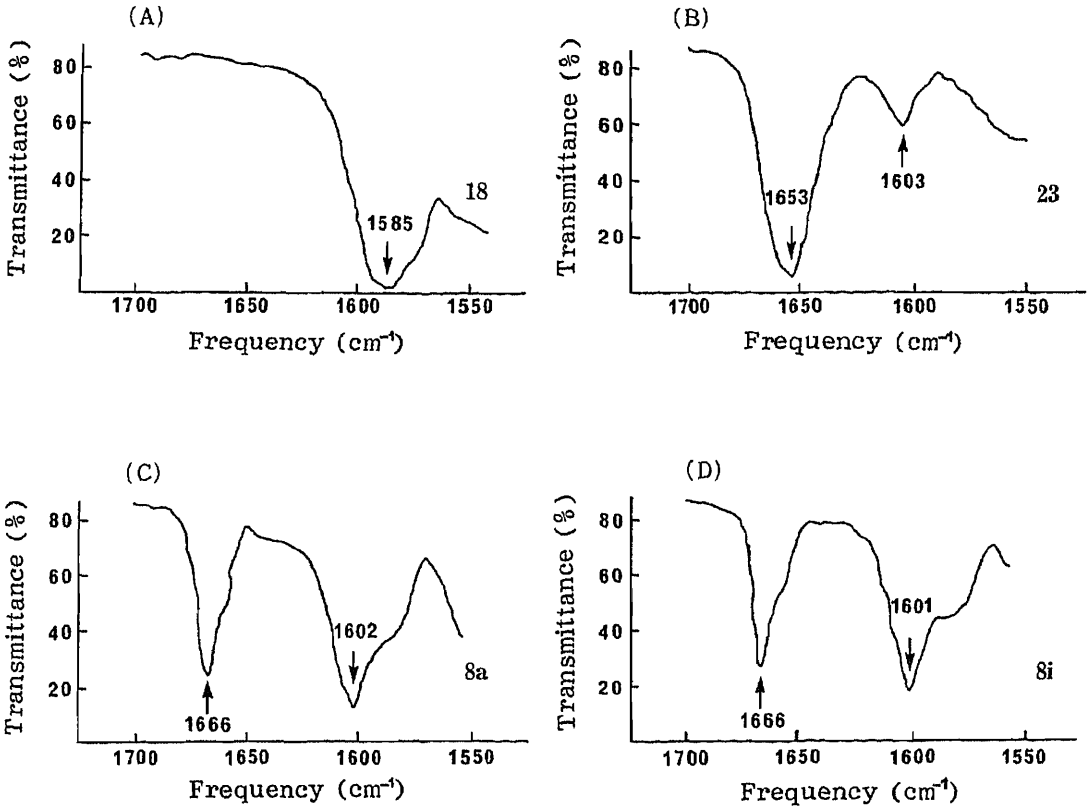


Fig. 4. The Ring Stretching Frequencies of the $N^6$-Methoxyadenine Derivatives **8a**, **8i**, **18**, and **23** in $CHCl_3$

(A), $2.6\times10^{-3}$M solution; (B), $2.6\times10^{-3}$M solution; (C), $2.5\times10^{-3}$M solution; (D), $1.95\times10^{-3}$M solution.

in $Me_2SO$-$d_6$ (Fig. 1) revealed a small, partially overlapping peak at $\delta$ 7.56 in the imino-form C(2)-H region. This is suggestive of the presence of a minor isomer, the *anti*-imino form (type **17**). The "pure" uncharged *syn*-imino form (type **16**) of **35** in the solid state has recently been confirmed by Shugar's group[15] by means of X-ray analysis. The same approach by us to a single crystal of the 9-benzyl analogue **8i** has also confirmed such *syn*-imino geometry (type **16**) it has.[16]

We next checked the populations in $Me_2SO$-$d_6$ of the two tautomeric forms of 16 other species of 9-substituted $N^6$-alkoxyadenines (**8b**—**k**, **29**—**34**), which were available in our laboratory, from the $^1$H-NMR signal intensities as in the case of **8a**. Tables I and II list the $^1$H-NMR spectral data and results, together with those for **8a**. For assignments of the C(2)-H and C(8)-H proton signals of the benzyl analogue **8i**, its spectrum was compared with that of the 2-deuterated species **13i**. This permitted differentiation between the two purine-ring protons in the imino form, but not in the amino form, because the amino-form C(8)-H signal of **13i** was so dull that it spread over the region where the amino-form C(2)-H of **8i** also resonated. However, we have recently found that in a series of 9-substituted adenines (which exist in the amino form) the influence of a 9-substituent on chemical shift was little for the C(2)-H proton, whereas it was rather great for the C(8)-H proton: electron-withdrawing groups (relative to a simple alkyl group), such as the benzyl and $\beta$-D-ribofuranosyl groups, tend to deshield the C(8)-H proton.[6] On the basis of this finding as well as the chemical shifts definitely assigned for the amino-form ring protons ($\delta$ 8.30 [H(2)] and 8.18 [H(8)]) of **8a**, two singlets at $\delta$ 8.30 and 8.35 observed for the benzyl analogue **8i** were assignable to the amino-form C(2)-H and C(8)-H protons, respectively. The purine-ring proton signals of the other

TABLE I. $^1$H-NMR Data and Populations of the Amino and Imino Tautomers of $N^6$-Alkoxy-9-alkyladenines in $Me_2SO$-$d_6$ at 25 °C

| Compound | | | | Chemical shift ($\delta$)[a] | | | | | | Population A : I[b] |
|---|---|---|---|---|---|---|---|---|---|---|
| No. | $R^1$ | $R^2$ | Tautomeric form[b] | NH | C(2)-H | C(8)-H | N(9)-Me or N(9)-$CH_2$ | $N^6$-OMe or $N^6$-$OCH_2$ | Other protons | |
| **8a** | Me | Me | A | 10.87 (br) | 8.30 (s) | 8.18 (s) | 3.77 (s) | 3.75 (s) | | 1 : 3.5 |
| | | | I | 11.14 (br) | 7.56 (d)[c] | 7.78 (s) | 3.63 (s) | 3.75 (s) | | |
| **8b** | Me | Et | A | 10.78 (br) | 8.29 (s) | 8.17 (s) | 3.74 (s) | 3.99 (q)[d] | 1.24 (t, $OCH_2\underline{Me}$)[d] | 1 : 3 |
| | | | I | 11.05 (br) | 7.56 (d)[e] | 7.77 (s) | 3.63 (s) | 3.99 (q)[d] | 1.24 (t, $OCH_2\underline{Me}$)[d] | |
| **8c** | Me | $PhCH_2$ | —[f] | 11.18 (br) | 7.60 (br) | 7.78 (br) | 3.64 (s) | 5.02 (s) | 7.36 ($OCH_2\underline{Ph}$) | —[f] |
| **8d** | Me | $ArCH_2$ | A | 10.8 (br) | 8.32 (s) | 8.21 (s) | 3.76 (s) | 4.93 (s) | 3.74 (s, OMe)[g] | 1 : 5 |
| | | | I | 11.12 (br) | 7.56 (d)[e] | 7.77 (s) | 3.63 (s) | 4.93 (s) | 3.74 (s, OMe)[g] | |
| **8e** | Me | $C_7H_{13}$ | A | 10.8 (br) | 8.28 (s) | 8.16 (s) | 3.74 (s) | 3.73 (m) | 0.7—2.0 ($OCH_2C_6\underline{H}_{11}$) | 1 : 4 |
| | | | I | 10.97 (br) | 7.56 (d)[e] | 7.77 (s) | 3.63 (s) | 3.73 (m) | 0.7—2.0 ($OCH_2C_6\underline{H}_{11}$) | |
| **8f** | Et | Me | A | 10.87 (br) | 8.29 (s) | 8.25 (s) | 3.9—4.4 (m) | 3.75 (s) | 1.35 (t, $NCH_2\underline{Me}$)[h] | 1 : 3.5 |
| | | | I | 11.14 (br) | 7.55 (d)[e] | 7.84 (s) | 3.9—4.4 (m) | 3.75 (s) | 1.35 (t, $NCH_2\underline{Me}$)[h] | |
| **8g** | Et | Et | A | 10.79 (br) | 8.28 (s) | 8.24 (s) | 3.8—4.4 (m) | 3.8—4.4 (m) | 1.35 (t, $NCH_2\underline{Me}$),[i] 1.24 (t, $OCH_2\underline{Me}$)[i] | 1 : 3 |
| | | | I | 11.05 (br) | 7.55 (d)[e] | 7.83 (s) | 3.8—4.4 (m) | 3.8—4.4 (m) | 1.35 (t, $NCH_2\underline{Me}$),[i] 1.24 (t, $OCH_2\underline{Me}$)[i] | |
| **8h** | Et | $PhCH_2$ | A | 10.92 (br) | 8.32 (s) | 8.28 (s) | 4.20 (q)[j] | 5.02 (s) | 1.4 (Me), 7.36 (Ph) | 1 : 5 |
| | | | I | 11.20 (br) | 7.58 (d)[e] | 7.83 (s) | 4.06 (q)[j] | 5.02 (s) | 1.34 (t, Me),[j] 7.36 (Ph) | |
| **8i** | $PhCH_2$ | Me | A | 10.93 (br) | 8.30 (s) | 8.35 (s) | 5.40 (s) | 3.77 (s) | 7.30 ($NCH_2\underline{Ph}$) | 1 : 3.5 |
| | | | I | 11.18 (br) | 7.56 (d)[e] | 7.94 (s) | 5.27 (s) | 3.74 (s) | 7.30 ($NCH_2\underline{Ph}$) | |
| **8j** | $PhCH_2$ | Et | —[f] | 11.07 (br) | 7.62 (br) | 8.01 (br) | 5.30 (s) | 3.99 (q)[i] | 7.31 (Ph), 1.24 (t, Me)[i] | —[f] |
| **8k** | $PhCH_2$ | $PhCH_2$ | A | 11.21 (br) | 8.35 (br) | 8.35 (br) | 5.39 (s) | 5.02 (s) | 7.3 (m, Ph's) | 1 : 4 |
| | | | I | 11.21 (br) | 7.60[k] | 7.94 (s) | 5.27 (s) | 5.02 (s) | 7.3 (m, Ph's) | |

*a*) In ppm downfield from internal $Me_4Si$. Compounds **8a**, **b**, **f**—**j** were measured at 0.05 M concentration; **8c**, at 0.03 M; **8d**, at 0.004 M; **8e**, at 0.015 M; **8k**, at 0.025 M. The letter(s) in parentheses designate(s) the multiplicity or shape or assignment of the signal; the abbreviations are given in Experimental. *b*) The letter A stands for the amino form; I, the imino form. *c*) With $J$ = 3.9 Hz. This signal was partially overlaid with a small, unidentified signal. *d*) With $J$ = 7.1 Hz. *e*) With $J$ = 3.7 Hz. The signal was partially overlaid with a small, unidentified signal. *f*) Undetermined because of difficulty in spectral identification of the tautomers. *g*) The phenyl ring proton signals appeared at $\delta$ 7.35 [2H, m, H(2') and H(6')] and 6.9 [2H, m, H(3') and H(5')]. *h*) With $J$ = 7.2 Hz. *i*) With $J$ = 7.0 Hz. *j*) With $J$ = 7.3 Hz. *k*) Overlapped with the phenyl proton signals.

TABLE II. $^1$H-NMR Data and Populations of the Amino and Imino Tautomers of $N^6$-Alkoxyadenosines in $Me_2SO$-$d_6$ at 25°C

| Nucleoside | | | Chemical shift ($\delta$)[a,b] | | | | | | Population |
|---|---|---|---|---|---|---|---|---|---|
| No. | R | Tautomeric form[a] | NH | C(2)-H | C(8)-H | C(1')-H | $N^6$-OMe or $N^6$-$OCH_2$ | Other protons[c] | A : I[a] |
| **29** | Me | —[d] | 11.25 (br) | 7.66 (br) | 8.17 (br) | 5.79 (d)[e] | 3.76 (s) | | —[d] |
| **30** | Et | A | 10.94 (br) | 8.29 (s) | 8.45 (s) | 5.92 (d)[f] | 4.00 (q)[g] | 1.24 (t, $OCH_2\underline{Me}$)[g] | 1 : 2.5 |
| | | I | 11.15 (br) | 7.57[h] | 8.08 (s) | 5.75 (d)[i] | 4.00 (q)[g] | 1.24 (t, $OCH_2\underline{Me}$)[g] | |
| **31** | $PhCH_2$ | A | 11.07 (br) | 8.34 (s) | 8.49 (s) | 5.95 (d)[j] | 5.03 (s) | 7.38 ($OCH_2\underline{Ph}$) | 1 : 3.8 |
| | | I | 11.30 (br) | 7.61[h] | 8.08 (s) | 5.75 (d)[i] | 5.03 (s) | 7.38 ($OCH_2\underline{Ph}$) | |
| **32** | Me | A | 11.05 (br) | 8.34 (s) | 8.42 (s) | 6.14 (br) | 3.76 (s) | | 1 : 2.6 |
| | | I | 11.29 (br) | 7.60[h] | 8.07 (s) | 6.01 (br) | 3.76 (s) | | |
| **33** | Et | A | 10.94 (br) | 8.31 (s) | 8.43 (s) | 6.14 (br) | 4.00 (q)[g] | 1.24 (t, $OCH_2\underline{Me}$)[g] | 1 : 2.5 |
| | | I | 11.17 (br) | 7.60[h] | 8.07 (s) | 6.00 (br) | 4.00 (q)[g] | 1.24 (t, $OCH_2\underline{Me}$)[g] | |
| **34**[m] | $PhCH_2$ | A | 11.06 (br) | 8.36 (s) | 8.47 (s) | 6.18 (d)[k] | 5.03 (s) | 7.31 ($OCH_2\underline{Ph}$) | 1 : 4 |
| | | I | 11.32 (br) | 7.62[h] | 8.06 (s) | 5.99 (d)[l] | 5.03 (s) | 7.31 ($OCH_2\underline{Ph}$) | |

*a*) The symbols and abbreviations are as defined in Table I. *b*) Unless otherwise noted, 0.05 M solutions of the nucleoside analogues were used. *c*) Those of the sugar moiety are not included. *d*) Undetermined because of difficulty in spectral identification of the tautomers. *e*) With $J$=5.6 Hz. *f*) With $J$=5.4 Hz. *g*) With $J$=7.0 Hz. *h*) Unresolved peak. *i*) With $J$=5.9 Hz. *j*) With $J$=6.3 Hz. *k*) With $J$=2.7 Hz. *l*) With $J$=2.9 Hz. *m*) Measured at 0.025 M concentration.

TABLE III. $^1$H-NMR Data for $N^6$,9-Dimethyladenine (**12**), 2-Deuterio-$N^6$,9-dimethyladenine (**11**), and $N^6$,$N^6$,9-Trimethyladenine (**36**)

| Compound | Solvent | Chemical shift ($\delta$)[a] | | | | |
|---|---|---|---|---|---|---|
| | | C(2)-H | C(8)-H | $N^6$-H | N(9)-Me | $N^6$-Me |
| **11** | $CDCl_3$ | — | 7.71 (s) | 5.84 (br) | 3.83 (s) | 3.22 (d)[b] |
| | $Me_2SO$-$d_6$ | — | 8.07 (s) | 7.61 (br) | 3.72 (s) | 2.98 (s, br)[c] |
| **12** | $CDCl_3$ | 8.44 (s) | 7.71 (s) | 5.82 (br) | 3.83 (s) | 3.22 (d)[b] |
| | $Me_2SO$-$d_6$ | 8.22 (s) | 8.07 (s) | 7.61 (br) | 3.72 (s) | 2.98 (s, br)[c] |
| **36** | $CDCl_3$ | 8.37 (s)[d] | 7.70 (s)[d] | — | 3.81 (s) | 3.54 (s) |
| | $Me_2SO$-$d_6$ | 8.22 (s)[d] | 8.10 (s)[d] | — | 3.72 (s) | 3.45 (s) |

*a*) Measured for a 0.05 M solution at 25°C. The symbol and abbreviations are as defined in Table I. *b*) With $J$=5 Hz. *c*) Turned into a sharp singlet on addition of $D_2O$. *d*) Tentatively assigned on the assumption that the chemical shifts for the corresponding protons in **36** and **12** are similar.

$N^6$-alkoxy compounds were tentatively assigned in a similar manner. In the cases of **8c**, **8j**, and **29**, the C(2)-H and C(8)-H proton signals appeared in the imino-form region, but they were so broad that unambiguous assignments were not possible. It may be seen from Tables I and II that in $Me_2SO$-$d_6$ the imino form was much more favored than the amino form in all the 14 cases where tautomerism was clearly found to exist. This is in general agreement with what Shugar's group[12b,13] found for **35** in $Me_2SO$-$d_6$. The observed preference of the imino form over the amino form may be a reflection of possible stabilization of **16** through intramolecular hydrogen bonding between N(1)-H and $N^6$-O.[15]

In contrast to the above $N^6$-alkoxy derivatives, $N^6$-monoalkyladenines substituted or unsubstituted at the 9-position have been known to exist exclusively in the amino form in both the solid state and solution.[17] Table III lists the $^1$H-NMR spectral data for **11**, **12**, and the fixed amino-form model **36**. In $CDCl_3$, the $N^6$-Me protons of **12** resonated at $\delta$ 3.22 as a three-proton doublet ($J$=5 Hz), indicating the presence of one hydrogen atom at the exocyclic

nitrogen. Comparison of this spectrum with that of the 2-deuterated species **11** permitted unequivocal assignments of the purine-ring proton signals, and the results were in agreement with those reported by Engel and von Hippel[17c] for **12**. In the spectrum of **12** in $Me_2SO$-$d_6$, the dull singlet ($N^6$-Me) at $\delta$ 2.98 turned into a sharp singlet on addition of $D_2O$, and the two ring-protons resonated in the same region as did those of the amino-form model **36**. Therefore, it is most likely that **12** exists in the amino form also in $Me_2SO$-$d_6$.

In summary, the above results demonstrate the usefulness of our strategy of "fission and reclosure of the adenine ring" for the synthesis of 2-deuterioadenine derivatives. The use of the 2-deuterated species **11**, **13a**, **13i**, **19**, and **24** in the $^1$H-NMR spectroscopic study has been a great help in interpretation of the purine-ring proton signals, and the $^1$H-NMR, UV, and IR spectroscopic approaches have shown that amino–imino tautomerism is common to 9-substituted $N^6$-alkoxyadenines (type **8**) in solution. Interestingly, this generality also covers $N^6$-alkoxyadenosines (**30**—**34**) themselves, analogues of promutagenic $N^6$-methoxyadenosine (**29**) that is producible by interaction between the mutagen methoxyamine and adenosine.[11,18]

## Experimental

**General Notes**——All melting points were taken on a Yamato MP-1 capillary melting point apparatus and are corrected. Spectra reported herein were recorded on a Hitachi 320 UV spectrophotometer, a JASCO A-202 IR spectrophotometer, a Hitachi M-80 or a JEOL JMS-01SG mass spectrometer, or a JEOL JNM-FX-100 NMR spectrometer at 25 °C with $Me_4Si$ as an internal standard. A 5-mm solution cell fitted with KBr windows was used for the measurements of solution IR spectra. Acid dissociation constants at 20 °C and ionic strength 0.10 were determined in a manner similar to that described previously.[5e] Elemental analyses were performed by Mr. Y. Itatani and his associates at Kanazawa University. The following abbreviations are used: br = broad, d = doublet, m = multiplet, q = quartet, s = singlet, t = triplet.

**Materials**——The known compounds selected for the spectroscopic studies were taken from stocks which had been prepared according to published procedures: **8a**[5b]; **8b**[5b]; **8c**[5e]; **8d**[5f]; **8e**[5f]; **8f**[19]; **8g**[5b]; **8h**[5d]; **8j**[5d]; **8k**[5b]; **12**[8]; **18**[2e]; **23**[9]; **28**·$HClO_4$[2b,20]; **29**[5d]; **30**[5d]; **31**[5d]; **32**[5d]; **33**[5d]; **34**[5d]; **36**.[21] A few of these were alternatively synthesized *via* new routes in the present study, and other compounds were obtained as described below.

**$N^6$-Methoxy-9-methyladenine (8a)**——A solution of **7a**[5b] (846 mg, 5 mmol) and formic acid (of more than 98% purity) (1.70 ml, 45 mmol) in MeCN (16 ml) was heated under reflux for 6 h. After cooling, the reaction mixture was kept in a refrigerator overnight. The precipitate that resulted was filtered off, washed with a little MeCN, dried, and dissolved in $H_2O$ (8 ml). The aqueous solution was passed through a column packed with Amberlite IRA-402 ($HCO_3^-$) (3 ml), and the column was eluted with $H_2O$ (150 ml). The combined eluates were concentrated *in vacuo* to leave, after drying, **8a** (270 mg, 30%) as a slightly brownish solid, mp 244—245 °C (dec.) [lit.[5b] mp 239 °C (dec.)]. This sample was identical [by comparison of the IR spectrum and thin-layer chromatographic (TLC) mobility] with authentic **8a**.[5b]

The filtrate and washings, obtained when the product was isolated from the reaction mixture, were combined and concentrated *in vacuo*. The residue was dissolved in $H_2O$ (7 ml), and the aqueous solution was treated with Amberlite IRA-402 ($HCO_3^-$) (4 ml) in the same way as described above. The resulting aqueous eluate (*ca.* 150 ml) was concentrated to a volume of *ca.* 40 ml, heated under reflux for 3 h, and concentrated to dryness *in vacuo*. The residue was recrystallized from $H_2O$ to give a second crop (178 mg, 20%), which raised the yield of **8a** to 50%.

**9-Benzyl-$N^6$-methoxyadenine (8i)**——i) By Dimroth Rearrangement of **3i** (X = I): A solution of **3i** (X = I)[22] (7.66 g, 20 mmol) in 0.5 M phosphate buffer (pH 6.5) (150 ml) was heated under reflux for 4 h. After cooling, the precipitate that resulted was filtered off, washed with $H_2O$, and dried to give **8i** (4.16 g, 82%), mp 222—223 °C (dec.). Recrystallization from EtOH provided an analytical sample as colorless prisms, mp 224—225 °C (dec.); UV $\lambda_{max}^{95\%\,aq.\,EtOH}$ 269 nm ($\varepsilon$ 14100); $\lambda_{max}^{H_2O}$ (pH 1) 268.5 (15300); $\lambda_{max}^{H_2O}$ (pH 7) 268.5 (15400); $\lambda_{max}^{H_2O}$ (pH 13) 285 (12000); IR $\nu_{max}^{CHCl_3}$ [Fig. 4(D)]; $^1$H-NMR ($Me_2SO$-$d_6$) (Table I). *Anal.* Calcd for $C_{13}H_{13}N_5O$: C, 61.17; H, 5.13; N, 27.43. Found: C, 61.38; H, 5.15; N, 27.65.

ii) By Cyclization of **7i** with Formic Acid: A solution of **7i**[6] (491 mg, 2 mmol) and formic acid (of over 98% purity) (0.67 ml, 18 mmol) in MeCN (7 ml) was heated under reflux for 6 h. The reaction mixture was concentrated *in vacuo*, and the residue was triturated with EtOH (2 ml) under cooling. The crystals that resulted were filtered off, washed with a little EtOH, and dried to give **8i** (379 mg, 74%), mp 224—225 °C (dec.), which was identical (by comparison of the IR spectrum and TLC mobility) with a sample prepared by method (i). The filtrate and washings were combined and concentrated *in vacuo*, and the residue was heated in 0.5 M phosphate buffer (pH 6.5) (10 ml) under reflux for 4 h. On cooling, the reaction mixture deposited pale brownish crystals, which were filtered off,

washed with a little $H_2O$, dried, and recrystallized from EtOH (2 ml) to afford a second crop (32 mg, 6%) of **8i**. The total yield was 411 mg (80%).

**1,9-Dimethyladenine-2-*d* Hydriodide (9)**——A mixture of 9-methyladenine-2-*d* (**5**)[6] (451 mg, 3 mmol) and MeI (2.13 g, 15 mmol) in $AcNMe_2$ (15 ml) was stirred at 60 °C for 2 h. The precipitate that resulted was filtered off, washed with a little EtOH, and dried to give **9** (534 mg, 61%). The filtrate was concentrated *in vacuo* and the residue was triturated with ether (20 ml). The resulting insoluble solid was separated from the ethereal layer by decantation and recrystallized from MeOH (15 ml) to provide a second crop (147 mg, 17%) of **9**. The total yield was 681 mg (78%). Recrystallization of the crude **9** from MeOH yielded an analytical sample as colorless prisms, mp 298—299 °C (dec.); UV $\lambda_{max}^{95\%\,aq.\,EtOH}$ 259 nm ($\varepsilon$ 11600); $\lambda_{max}^{H_2O}$ (pH 1) 260 (12300); $\lambda_{max}^{H_2O}$ (pH 7) 259 (12300); $\lambda_{max}^{H_2O}$ (pH 13) 260 (13200); $^1$H-NMR ($Me_2SO$-$d_6$) $\delta$: 3.80 [3H, s, N(1)-Me], 3.83 [3H, s, N(9)-Me],[23] 8.47 [1H, s, H(8)], 9.1 and 9.7 (1H each, br, NH's).[24] *Anal.* Calcd for $C_7H_9DIN_5$ (by $H_2O$/HDO gas volume analysis): C, 28.78; H, 3.45; N, 23.98. Found: C, 28.99; H, 3.57; N, 24.22.

***N*$^6$,9-Dimethyladenine-2-*d* (11)**——A mixture of **9** (380 mg, 1.3 mmol) and 0.2 N aqueous NaOH (13 ml) was heated under reflux for 15 min. After cooling, the reaction mixture was neutralized with 10% aqueous HCl and concentrated *in vacuo*. The residue was dried and extracted with hot benzene. The benzene extracts were filtered while hot, and the filtrate was concentrated to a volume of *ca.* 20 ml. The crystals that resulted were filtered off to give **11** (155 mg, 72%), mp 184 °C. Recrystallization from benzene furnished an analytical sample as colorless scales, mp 184—185 °C; MS *m/z*: 165 ($M^+ + 1$) [$d_2$ (0%)], 164 ($M^+$) [$d_1$ (>99%)][25]; UV $\lambda_{max}^{95\%\,aq.\,EtOH}$ 267 nm ($\varepsilon$ 15300); $\lambda_{max}^{H_2O}$ (pH 1) 263 (16700); $\lambda_{max}^{H_2O}$ (pH 7) 267 (15700); $\lambda_{max}^{H_2O}$ (pH 13) 267 (15900); $^1$H-NMR (Table III). *Anal.* Calcd for $C_7H_8DN_5$ (by $H_2O$/HDO gas volume analysis): C, 51.21; H, 5.52; N, 42.65. Found: C, 51.36; H, 5.55; N, 42.67.

***N*$^6$-Methoxy-9-methyladenine-2-*d* (13a)**——A solution of **7a**[5b] (846 mg, 5 mmol) and formic-*d* acid-*d* (of over 99% isotopic purity) (1.70 ml, 45 mmol) in MeCN (16 ml) was heated under reflux for 6 h. On cooling, the reaction mixture deposited crystals, and it was worked up in a manner similar to that described above for **8a**, giving **13a** (469 mg, 52%) as a colorless solid, mp 243—244 °C (dec.). Recrystallizations from $H_2O$ and from MeOH yielded slightly purplish, fine crystals, mp 244—245 °C (dec.); MS *m/z*: 181 [$d_2$ (16%)], 180 [$d_1$ (84%)][25]; UV $\lambda_{max}^{95\%\,aq.\,EtOH}$ 269 nm ($\varepsilon$ 13200); $\lambda_{max}^{H_2O}$ (pH 1) 270 (12600); $\lambda_{max}^{H_2O}$ (pH 7) 269 (13100); $\lambda_{max}^{H_2O}$ (pH 13) 286 (10500); $^1$H-NMR ($Me_2SO$-$d_6$) $\delta$: 3.63 [2.3H, s, N(9)-Me (imino form)], 3.75 (3H, s, OMe), 3.77 [0.7H, s, N(9)-Me (amino form)], other protons (Fig. 1). The mass and $^1$H-NMR spectra indicated that this sample was most likely contaminated with the 2,8-dideuterated species to the extent of 16%.

**9-Benzyl-*N*$^6$-methoxyadenine-2-*d* (13i)**——A solution of **7i**[6] (491 mg, 2 mmol) and formic-*d* acid-*d* (of over 99% isotopic purity) (865 mg, 18 mmol) in MeCN (7 ml) was heated under reflux for 6 h. The reaction mixture was worked up as described above for **8i** under item (ii), yielding a first crop (275 mg, 54%) and a second crop (47 mg, 9%) of **13i**. Recrystallization of the first crop of **13i** from EtOH gave colorless scales, mp 223—224 °C (dec.); MS *m/z*: 257 [$d_2$ (53%)], 256 [$d_1$ (47%)][25]; UV $\lambda_{max}^{95\%\,aq.\,EtOH}$ 270 nm ($\varepsilon$ 14400); $\lambda_{max}^{H_2O}$ (pH 1) 269 (16300); $\lambda_{max}^{H_2O}$ (pH 7) 269 (16100); $\lambda_{max}^{H_2O}$ (pH 13) 286 (12700); $^1$H-NMR ($Me_2SO$-$d_6$) $\delta$: 3.76 (3H, s, OMe), 5.29 [2H, s, N(9)-$CH_2$], 7.31 (5H, s, Ph), 7.96 (br) and 8.0—8.4 (br) [0.5H, H(8)], 11.18 (br, NH). Judged from the mass and $^1$H-NMR spectral data, this sample was a 1 : 1 mixture of **13i** and the 2,8-dideuterated species.

***N*$^6$-Methoxy-*N*$^6$,9-dimethyladenine (18)**——An oil dispersion (66 mg) containing 60% NaH (1.65 mmol) was added to a stirred suspension of **8a**[5b] (269 mg, 1.5 mmol) in $AcNMe_2$ (2.5 ml). After addition of a solution of MeI (241 mg, 1.7 mmol) in $AcNMe_2$ (0.8 ml), the mixture was stirred at 27—30 °C for 26 h and then concentrated to dryness *in vacuo*. The residue was chromatographed on alumina (43 g), and fractions eluted with $CH_2Cl_2$ gave **18** (243 mg, 84%), mp 92.5—94 °C. Recrystallization from hexane afforded a pure sample as colorless prisms, mp 95—96 °C (lit.[2c] mp 95—96 °C); $pK_a$ 3.75 (at 20 °C); UV $\lambda_{max}^{H_2O}$ (pH 7.41) (Fig. 2); IR $\nu_{max}^{CHCl_3}$ [Fig. 4(A)]; $^1$H-NMR ($Me_2SO$-$d_6$) $\delta$: 3.50, 3.77, and 3.86 (3H each, s, NMe's and OMe), 8.24 [1H, s, H(8)], 8.38 [1H, s, H(2)]. This sample was identical (by mixture melting point test and comparison of the IR spectrum and TLC mobility) with authentic **18**.[2c]

***N*$^6$-Methoxy-*N*$^6$,9-dimethyladenine-2-*d* (19)**——A sample (180 mg, 1 mmol) of the 2-deuterated species **13a**, which contained some of the 2,8-dideuterated species, was methylated as described above for **18**. The crude product (106 mg, 55%) was recrystallized from hexane to give **19** as colorless prisms, mp 93.5—94.5 °C; MS *m/z*: 195 [$d_2$ (62%)], 194 [$d_1$ (38%)][25]; $^1$H-NMR ($Me_2SO$-$d_6$) $\delta$: 3.50, 3.77, and 3.86 (3H each, s, NMe's and OMe), 8.24 [0.4H, s, H(8)].

**5-Amino-*N*′-methoxy-*N*,1-dimethylimidazole-4-carboxamidine (22)**——Compound **21**·HI[9] (733 mg, 2.3 mmol) was added to a solution of NaOH (649 mg, 15 mmol) in $H_2O$ (13 ml), and the mixture was heated under reflux for 15 min. After cooling, the reaction mixture was neutralized with 10% aqueous HCl, then made slightly alkaline (pH 8—9) with saturated aqueous $NaHCO_3$, and concentrated to dryness *in vacuo*. The residue, after being dried, was extracted with hot benzene, and the benzene extracts were concentrated *in vacuo* to leave a yellowish brown oil (349 mg). Column chromatographic purification [silica gel, $CHCl_3$–EtOH (6 : 1, v/v)] of the oil furnished **22** (279 mg, 67%) as a brownish oil, $^1$H-NMR ($Me_2SO$-$d_6$) $\delta$: 2.96 (3H, unresolved m, NHMe), 3.39 [3H, s, N(1)-Me], 3.62 (3H, s, OMe), 5.28 (2H, br, $NH_2$), 5.5—5.7 (1H, br, NHMe), 7.10 [1H, s, H(2)].

***N*$^6$-Methoxy-1,9-dimethyladenine (23)**——A solution of **22** (91.6 mg, 0.5 mmol) and formic acid (of over 98% purity) (0.17 ml, 4.5 mmol) in MeCN (1.6 ml) was heated under reflux for 5.5 h. The reaction mixture was

concentrated to dryness *in vacuo*, and the residue was chromatographed on a silica gel column. Fractions eluted with $CHCl_3$–EtOH (10 : 1, v/v) were concentrated *in vacuo* to leave a yellow jelly, which was dissolved in $H_2O$ (2 ml). The aqueous solution was passed through a column of Amberlite IRA-402 ($HCO_3^-$) (1 ml), and the column was eluted with $H_2O$ (40 ml). Concentration of the eluates and drying of the resulting residue furnished **23** (30 mg, 31%) as a yellowish solid. Recrystallization from benzene yielded a pure sample, mp 174—179.5 °C (lit.[9] mp 182—183 °C); MS *m/z*: 193 ($M^+$); p$K_a$ 4.09 (at 20 °C); $^1$H-NMR ($CDCl_3$) $\delta$: 3.37, 3.69, and 3.95 (3H each, s, NMe's and OMe), 7.48 [1H, s, H(2)], 7.59 [1H, s, H(8)]. This sample was identical (by comparison of the IR spectrum and TLC mobility) with authentic **23**.[9]

On the other hand, fractions eluted with MeOH in the above silica gel column chromatography gave a mixture containing a material presumed to be **21**. The mixture was treated with Amberlite IRA-402 ($HCO_3^-$) (2 ml) as described above for **23**, and the resulting aqueous eluates were concentrated to a volume of *ca.* 3 ml. This solution was made alkaline (pH 9) with conc. aqueous $NH_3$, heated under reflux for 3 h, and concentrated *in vacuo*. The residue, after being dried, was purified by column chromatography [silica gel, $CHCl_3$–EtOH (10 : 1, v/v)] to provide a second crop (6 mg, 6%) of **23**. The total yield was 36 mg (37%).

**$N^6$-Methoxy-1,9-dimethyladenine-2-*d* (24)**——A solution of **22** (166 mg, 0.9 mmol) and formic-*d* acid-*d* (of over 99% isotopic purity) (0.31 ml, 8.2 mmol) in MeCN (3 ml) was heated under reflux for 3 h. The reaction mixture was worked up in a manner similar to that described above for **23**, giving crude **24** (35 mg, 20%) as a yellow solid. Recrystallization from benzene afforded colorless fine crystals, mp 178.5—181.5 °C; $^1$H-NMR ($CDCl_3$) $\delta$: 3.37, 3.69, and 3.96 (3H each, s, NMe's and OMe), 7.59 [0.5H, s, H(8)]. The $^1$H-NMR spectrum indicated that this sample was contaminated with the 2,8-dideuterated species to the extent of *ca.* 50%.

**Acknowledgment** We are pleased to acknowledge the support of this work by a grant from the Japan Research Foundation for Optically Active Compounds.

## References and Notes

1) Paper XXVIII in this series, T. Fujii, T. Saito, I. Inoue, Y. Kumazawa, and N. J. Leonard, *Chem. Pharm. Bull.*, **34**, 1821 (1986).
2) *a*) T. Fujii, F. Tanaka, K. Mohri, T. Itaya, and T. Saito, *Tetrahedron Lett.*, **1973**, 4873; *b*) T. Fujii, T. Itaya, K. Mohri, and T. Saito, *J. Chem. Soc., Chem. Commun.*, **1973**, 917; *c*) T. Fujii, T. Saito, T. Sakuma, M. Minami, and I. Inoue, *Heterocycles*, **16**, 215 (1981); *d*) T. Fujii and T. Saito, *ibid.*, **17**, 117 (1982); *e*) T. Fujii, T. Itaya, F. Tanaka, T. Saito, K. Mohri, and K. Yamamoto, *Chem. Pharm. Bull.*, **31**, 3149 (1983); *f*) T. Fujii, T. Saito, and T. Nakasaka, *ibid.*, **31**, 3521 (1983); *g*) T. Fujii, T. Saito, and T. Muramoto, *ibid.*, **31**, 4270 (1983).
3) For a review, see T. Fujii, T. Itaya, and T. Saito, *Yuki Gosei Kagaku Kyokai Shi*, **41**, 1193 (1983).
4) H. Iio, K. Asao, and T. Tokoroyama, *J. Chem. Soc., Chem. Commun.*, **1985**, 774.
5) *a*) T. Fujii, T. Itaya, C. C. Wu, and S. Yamada, *Chem. Ind.* (London), **1966**, 1967; *b*) T. Fujii, T. Itaya, C. C. Wu, and F. Tanaka, *Tetrahedron*, **27**, 2415 (1971); *c*) T. Fujii, T. Sato, and T. Itaya, *Chem. Pharm. Bull.*, **19**, 1731 (1971); *d*) T. Fujii, C. C. Wu, T. Itaya, S. Moro, and T. Saito, *ibid.*, **21**, 1676 (1973); *e*) T. Itaya, T. Saito, S. Kawakatsu, and T. Fujii, *ibid.*, **23**, 2643 (1975); *f*) T. Fujii, T. Itaya, T. Saito, and S. Kawakatsu, *ibid.*, **32**, 4842 (1984).
6) T. Fujii, T. Saito, K. Kizu, H. Hayashibara, Y. Kumazawa, and S. Nakajima, *Heterocycles*, **24**, 2449 (1986).
7) A. R. P. Paterson and S. H. Zbarsky, *J. Am. Chem. Soc.*, **75**, 5753 (1953).
8) T. Itaya, F. Tanaka, and T. Fujii, *Tetrahedron*, **28**, 535 (1972).
9) T. Fujii, F. Tanaka, K. Mohri, and T. Itaya, *Chem. Pharm. Bull.*, **22**, 2211 (1974).
10) Yu. V. Morozov, F. A. Savin, V. O. Chekhov, E. I. Budowsky, and D. Yu. Yakovlev, *J. Photochem.*, **20**, 229 (1982).
11) B. Singer and S. Spengler, *FEBS Lett.*, **139**, 69 (1982).
12) *a*) B. Kierdaszuk, R. Stolarski, and D. Shugar, *FEBS Lett.*, **158**, 128 (1983); *b*) R. Stolarski, B. Kierdaszuk, C-E. Hagberg, and D. Shugar, *Biochemistry*, **23**, 2906 (1984).
13) B. Kierdaszuk, R. Stolarski, and D. Shugar, *Acta Biochim. Pol.*, **31**, 49 (1984).
14) D. Shugar, C. P. Huber, and G. I. Birnbaum, *Biochim. Biophys. Acta*, **447**, 274 (1976).
15) G. I. Birnbaum, B. Kierdaszuk, and D. Shugar, *Nucleic Acids Res.*, **12**, 2447 (1984).
16) T. Date, personal communication.
17) See, for example, *a*) C. E. Bugg and U. Thewalt, *Biochem. Biophys. Res. Commun.*, **46**, 779 (1972); *b*) H. Sternglanz and C. E. Bugg, *Science*, **182**, 833 (1973); *c*) J. D. Engel and P. H. von Hippel, *Biochemistry*, **13**, 4143 (1974); *d*) T. Fujii and T. Nishitani, *Chem. Pharm. Bull.*, **21**, 2349 (1973); *e*) T. Fujii and T. Saito, *ibid.*, **33**, 3635 (1985); *f*) T. Fujii, T. Saito, and N. Terahara, *ibid.*, **34**, 1094 (1986); *g*) G. Surico, A. Evidente, N. S. Iacobellis, and G. Randazzo, *Phytochemistry*, **24**, 1499 (1985); *h*) T. Itaya, T. Fujii, A. Evidente, G. Randazzo, G. Surico, and N. S. Iacobellis, *Tetrahedron Lett.*, **27**, 6349 (1986).
18) For a review, see E. I. Budowsky, *Prog. Nucleic Acid Res. Mol. Biol.*, **16**, 125 (1976).

19) T. Fujii, T. Itaya, T. Saito, and M. Kawanishi, *Chem. Pharm. Bull.*, **26**, 1929 (1978).
20) T. Fujii, T. Saito, and M. Kawanishi, *Tetrahedron Lett.*, **1978**, 5007.
21) T. Itaya, H. Matsumoto, and K. Ogawa, *Chem. Pharm. Bull.*, **28**, 1920 (1980).
22) T. Fujii, C. C. Wu, and T. Itaya, *Chem. Pharm. Bull.*, **19**, 1368 (1971).
23) The assignments for the two *N*-Me proton signals were based on a nuclear Overhauser effect observed between the C(8)-H signal and this signal.
24) On the basis of these data, the $^1$H-NMR spectrum of 1,9-dimethyladenine perchlorate (**10**: $HClO_4$ for HI),[8] the unlabeled species, in $Me_2SO$-$d_6$ [$\delta$: 3.80 [3H, s, N(1)-Me], 3.83 [3H, s, N(9)-Me], 8.47 [1H, s, H(8)], 8.68 [1H, s, H(2)], 9.1 and 9.8 (1H each, br, NH's)] now became interpretable.
25) For the method used for determining the extent of deuterium incorporation, see J. B. Lambert, H. F. Shurvel, L. Verbit, R. G. Cooks, and G. H. Stout, "Organic Structural Analysis," Macmillan, New York, 1976, pp. 446—448.

[Chem. Pharm. Bull. 35(11)4494—4497(1987)]

# Nucleosides. CXLIII. Synthesis of 5′-Deoxy-5′-substituted-2,2′-anhydro-1-(β-D-arabinofuranosyl)uracils. A New 2,5′- to 2,2′-Anhydronucleoside Transformation. Studies Directed toward the Synthesis of 2′-Deoxy-2′-substituted *arabino* Nucleosides. (4)[1]

KRZYSZTOF W. PANKIEWICZ and KYOICHI A. WATANABE*

*Sloan-Kettering Institute for Cancer Research, Memorial Sloan-Kettering Cancer Center, Sloan-Kettering Division, Graduate School of Medical Sciences, Cornell University, New York, NY 10021, U.S.A.*

(Received June 22, 1987)

Treatment of 2,5′-anhydro-3′-*O*-acetyl-2′-*O*-triflyluridine with a nucleophile such as NaOAc, $NaN_3$, LiCl or LiBr, did not afford the 2′-substituted 2,5′-anhydro-arabinosyluracil, but gave 2,2′-anhydro-1-(5-substituted-β-D-arabinofuranosyl)uracil instead.

**Keywords**——nucleoside; anhydronucleoside; 2,5′-anhydrouracilnucleoside; 2,2′-anhydrouracilnucleoside; 2,5′-anhydro-3′-*O*-acetyl-2′-*O*-triflyluridine; 5′-substituted-2,2′-anhydroabinosyluracil; new transformation

The two pyrimidine nucleosides, 1-(2-deoxy-2-fluoro-β-D-arabinofuranosyl)-5-iodocytosine and -thymine (2′-F-5-iodo-ara-C or FIAC and 2′-F-5-methyl-ara-U or FMAU), developed in our laboratory[2] have shown potent *in vitro* and *in vivo* activity against herpes simplex viruses types 1 and 2 (HSV-1 and -2) and varicella zoster virus (VZV).[3-5] Both compounds inhibited human cytomegalovirus (HCMV)[6-8] *in vitro* as well as Epstein-Barr virus (EBV).[9] FIAC has demonstrated clinical efficacy against VZV in both phase I[10] and phase II[11] clinical trials. More recently, the triphosphates of FIAC and FMAU have been shown[12] to be the most potent inhibitors of deoxyribonucleic acid (DNA) polymerases from woodchuck hepatitis virus (WHV) and human hepatitis B virus *in vitro*. *In vivo*, both were active against chronic active hepatitis in the woodchuck, with FMAU giving immediate and long-lasting inhibition of WHV replication.

These nucleosides were synthesized by condensation of 3,5-di-*O*-acyl-2-deoxy-2-fluoro-D-arabinofuranosyl bromide and pyrimidine base.[2,12] Introduction of a substituent to the 2′-"up" position of a preformed pyrimidine *N*-nucleoside by nucleophilic reaction has not been achieved due to close proximity of the 2-carbonyl group to the 2′-position. Thus, treatment of a uridine derivative bearing a leaving group at the 2′-position with a nucleophile results in the formation of the *arabino* nucleoside or 2′-substituted *ribo* nucleoside *via* the anhydronucleoside intermediate, depending upon the nature of the nucleophile and reaction conditions.

In this report, we describe our attempts to convert uridine into a 2′-substituted-2′-deoxyarabinosyluracil, and our discovery of anhydronucleoside interconversion. In this investigation, we chose 2,5′-anhydrouridine (**1**)[13] as the starting material. Treatment of **1** with *n*-$Bu_2SnO$ in MeOH afforded the 2′,3′-*O*-stannylene derivative which was, without purification, directly acetylated[14] with $Ac_2O$ in dimethylformamide (DMF) to give the 3′-acetate **2** in 84% yield after crystallization from EtOH. Triflylation of **2** with triflyl chloride in methylene chloride containing 4-dimethylaminopyridine (DMAP) and triethylamine afforded

3′-*O*-acetyl-2,5′-anhydro-1-*O*-triflyluridine (**3**) in high yield as colorless crystals. In this nucleoside **3**, we hoped that intramolecular nucleophilic reaction by O2 could be prevented during the displacement that would occur at C2′, since O2 is tied up with C5′.

Reaction of **3** with sodium acetate in DMF at 50—60 °C afforded two products in approximately equal amounts. The less polar compound was identical with 2,2′-anhydro-(3,5-di-*O*-acetyl-β-D-arabinofuranosyl)uracil (**4a**).[15] The proton nuclear magnetic resonance ($^1$H-NMR) spectrum of the more polar product was very similar to that of **4a** except that one acetyl signal at $\delta$ 1.90 was absent, but a signal characteristic of a formyl proton was present at $\delta$ 7.99. This product is assigned to the 5′-*O*-formyl derivative **4b**. Deformylation of **4b** according to Smrt[16] gave 2,2′-anhydro-1-(3-*O*-acetyl-β-D-arabinofuranosyl)uracil (**4c**). These results show that the intermolecular nucleophilic reaction occurred first on the C5′ position, liberating 2-oxide, which then attacked C2′, resulting in the formation of the 2,2′-anhydro nucleoside linkage. The formation of **4a** from **3** indicates that the 2,5′-anhydro linkage in **3** is less stable than the 4,5′-anhydro bond of the C-nucleoside 4,5′-anhydro-pseudouridine, and the 2′-triflate group in **3** is less reactive than that in the C-nucleoside, since it had already been demonstrated[17] that 4,5′-anhydro-3′-*O*-acetyl-2′-*O*-triflyl-1-methyl-pseudouridine (a C-nucleoside structurally very similar to **3**) could be directly converted into various 2′-substituted 2′-arabinosyl C-nucleosides by nucleophilic reactions.

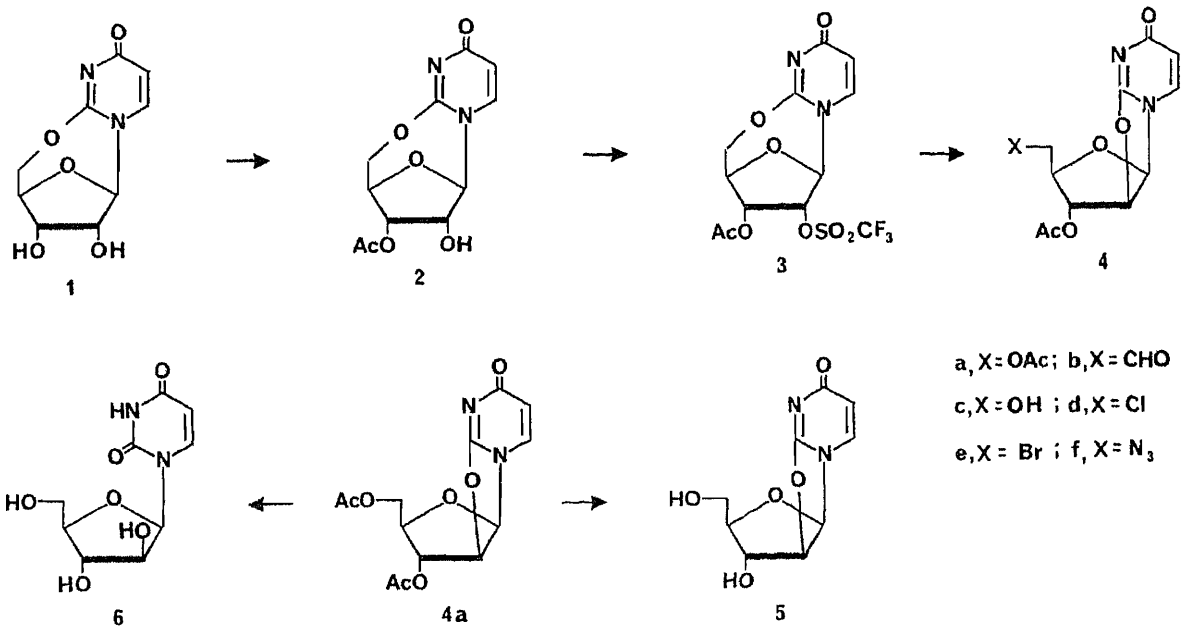


Chart 1

When **3** was treated with NaOAc in hexamethylphosphoric triamide (HMPA) at room temperature, the diacetate **4a** was the exclusive product. We also treated **3** with better nucleophilic reagents than NaOAc, *i.e.*, sodium azide, lithium bromide, sodium chloride, in HMPA at room temperature. In all cases, we obtained the 5′-substituted 5′-deoxy-3′-*O*-acetyl derivatives (**4d**—**f**) of 2,2′-anhydro-1-(β-D-arabinofuranosyl)uracil in high yield.

## Experimental

Melting points were determined on a Thomas-Hoover capillary apparatus and are uncorrected. Column chromatography was performed on Silica gel G60 (70—230 mesh, ASTM, Merck). Thin-layer chromatography was performed on Analtech Uniplates with short-wavelength UV light for visualization. Elemental analyses were performed by M.H.W. Laboratories, Phoenix, AZ, or Spang Microanalytical Laboratory, Eagle Harbor, MI. $^1$H-

NMR spectra were recorded on a JEOL FX90Q spectrometer with $Me_4Si$ as the internal standard. Chemical shifts are reported in ppm ($\delta$) and signals are described as a (singlet), d (doublet), t (triplet), q (quartet), m (multiplet), dd (double doublet), dt (double triplet), br s (broad singlet). Values given for coupling constants are first order.

**3'-*O*-Acetyl-2,5'-anhydrouridine (2)**——A suspension of 2,5'-anhydrouridine[13] (6.5 g, 28.8 mmol) and *n*-$Bu_2SnO$ (7.2 g, 28.8 mmol) in MeOH (500 ml) was heated under reflux until a clear solution was obtained (~30 min). The solution was concentrated *in vacuo*, and residue was dissolved in DMF (300 ml). $Ac_2O$ (29 ml) was added to the solution, and the mixture was kept overnight at ~4 °C, and then concentrated *in vacuo*. The residue was triturated with EtOH to give a solid which was crystallized from EtOH to afford 6.5 g (84%) of **2**, mp 210—211 °C. $^1$H-NMR (DMSO-$d_6$) $\delta$: 2.09 (s, 3H, Ac), 4.15 (d, 1H, H-5', $J_{5',5''}$=12.8 Hz), 4.23—4.63 (m, 3H, H-2',4',5'), 5.40 (d, 1H, H-3', $J_{2',3'}$=6.4 Hz), 5.61 (s, 1H, H-1'), 5.99 (m, 2H, H-5, 2'-OH, $J_{5,6}$=7.6 Hz), 7.98 (d, 1H, H-6). *Anal.* Calcd for $C_{11}H_{12}N_2O_6$: C, 49.25; H, 4.51; N, 10.44. Found: C, 49.49; H, 4.79; N, 10.15.

**3'-*O*-Acetyl-2,5'-anhydro-2'-*O*-triflyluridine (3)**——To a suspension of **2** (6.1 g; 22.8 mmol), DMAP (2.8 g, 22.8 mmol) and $Et_3N$ (6.4 ml, 45.5 mmol) in $CH_2Cl_2$ (700 ml) was added dropwise a solution of triflyl chloride (4.8 ml, 45.5 mmol) in $CH_2Cl_2$ (20 ml) while stirring. The mixture became clear and then precipitation occurred. Stirring was continued and then crystals were collected by filtration and washed with $CH_2Cl_2$ (50 ml) to give **3** (7.8 g, 85%), mp 155—157 °C (dec.). $^1$H-NMR (DMSO-$d_6$) $\delta$: 2.13 (s, 3H, Ac), 4.25 (d, 1H, H-5', $J_{5',5''}$=13.0 Hz), 4.62 (d, 1H, H-5''), 4.92 (s, 1H, H-4'), 5.70 (d, 1H, H-3', $J_{2',3'}$=6.4 Hz), 6.00 (d, 1H, H-5, $J_{5,6}$=7.3 Hz), 6.19 (d, 1H, H-2'), 6.44 (s, 1H, H-1'), 7.95 (d, 1H, H-6). *Anal.* Calcd for $C_{12}H_{11}F_3N_2O_8S$: C, 36.00; H, 2.77; N, 7.00; S, 8.01. Found: C, 35.85; H, 2.89; N, 6.88; S, 8.03.

**Reaction of 3 with NaOAc in DMF**——To a solution of **3** (400 mg, 1 mmol) in DMF (10 ml) was added NaOAc (410 mg, 5 mmol), and the mixture was stirred overnight at 50—60 °C. After concentration of the mixture *in vacuo*, the residue was chromatographed on a silica gel column using $CHCl_3$–EtOH (9 : 1, v/v) followed by $CHCl_3$–EtOH (5 : 1, v/v).

Two nucleosidic fractions were obtained. From the less polar fraction, 2,2'-anhydro-1-(3-*O*-acetyl-5-*O*-formyl-β-D-arabinofuranosyl)uracil (**4b**) (100 mg, 33.8%) was obtained after concentration, mp 187—189 °C. $^1$H-NMR (DMSO-$d_6$) $\delta$: 2.11 (s, 3H, Ac), 4.13 (d, 2H, H-5',5''), 4.60 (m, 1H, H-4'), 5.34 (d, 1H, H-3', $J_{3',4'}$=1.5 Hz), 5.52 (d, 1H, H-2', $J_{1',2'}$=5.8 Hz), 5.88 (d, 1H, H-5, $J_{5,6}$=7.6 Hz), 6.40 (d, 1H, H-1'), 7.87 (d, 1H, H-6), 7.99 (s, 1H, CHO). *Anal.* Calcd for $C_{12}H_{12}N_2O_6$: C, 48.65; H, 4.08; N, 9.45. Found: C, 48.45; H, 4.22; N, 9.19.

From the second fraction, 120 mg of 2,2'-anhydro-1-(3,5-di-*O*-acetyl-β-D-arabinofuranosyl)uracil (**4a**) was obtained (38.7%), mp 178—180 °C. $^1$H-NMR (DMSO-$d_6$) $\delta$: 1.90 (s, 3H, Ac), 2.11 (s, 3H, Ac), 3.95 (dd, 1H, H-5', $J_{5',5''}$=12.5, $J_{4',5'}$=4.9 Hz), 4.13 (dd, 1H, H-5'', $J_{5',5''}$=12.5, $J_{4',5''}$=4.0 Hz), 4.58 (m, 1H, H-4'), 5.31 (d, 1H, H-3', $J_{3',4'}$=2.1 Hz), 5.52 (d, 1H, H-2', $J_{1',2'}$=5.8 Hz), 5.88 (d, 1H, H-5, $J_{5,6}$=7.6 Hz), 6.39 (d, 1H, H-1'), 7.88 (d, 1H, H-6). *Anal.* Calcd for $C_{13}H_{14}N_2O_7$: C, 50.32; H, 4.55; N, 9.03. Found: C, 50.14; H, 4.55; N, 8.83.

**2,2'-Anhydro-1-(3-*O*-acetyl-β-D-arabinofuranosyl)uracil (4c)**——A mixture of **4b** (100 mg, 0.34 mmol), MeOH (2 ml), tetrahydrofuran (THF) (1 ml) and $Et_3N$ (303 mg, 3 mmol) was stirred at room temperature for 30 min, and then concentrated *in vacuo*. The residue was chromatographed on a silica gel column using $CHCl_3$–EtOH (5 : 1, v/v) to give **4c** (69 mg, 78%), mp 190—195 °C. $^1$H-NMR (DMSO-$d_6$) $\delta$: 2.11 (s, 3H, Ac), 3.28 (dd, 1H, H-5', $J_{5',5''}$=12.0, $J_{4',5'}$=5.5 Hz), 3.39 (dd, 1H, H-5'', $J_{5',5''}$=12.0, $J_{4',5''}$=4.2 Hz), 4.34 (m, 1H, H-4'), 5.11 (t, 1H, OH), 5.34 (s, 1H, H-3'), 5.46 (d, 1H, H-2', $J_{2',2'}$=5.8 Hz), 5.84 (d, 1H, H-5, $J_{5,6}$=7.6 Hz), 6.34 (d, 1H, H-1'), 7.82 (d, 1H, H-6). *Anal.* Calcd for $C_{11}H_{12}N_2O_6$: C, 49.25; H, 4.51; N, 10.44. Found: C, 49.12; H, 4.62; N, 10.27.

**2,2'-Anhydro-1-(β-D-arabinofuranosyl)uracil (5)**——A mixture of **4a** (100 mg, 0.32 mmol), $Et_3N$ (10 ml) and MeOH (20 ml) was stirred for 4 h at room temperature, and was then concentrated *in vacuo*. Upon trituration of the residue with EtOH, crystalline **5** (50 mg, 68%) was obtained, mp 239—240 °C, unchanged upon admixture of an authentic sample.[18]

**1-(β-D-Arabinofuranosyl)uracil (6)**——Compound **4a** (310 mg, 1 mmol) was dissolved in 2 N NaOH (20 ml). After being kept at room temperature for 4 h, the mixture was neutralized with 1 N HCl, and concentrated *in vacuo*. The residue was taken up in pyridine and the suspension filtered from inorganic salt. The filtrate was concentrated *in vacuo*, and the residue crystallized from EtOH to give **6** (166 mg, 68%), mp 209—211 °C. The mixture's melting point with an authentic sample[19] was undepressed.

**Acetylation of 5**——A mixture of **5** (226 mg, 1 mmol), $Ac_2O$ (1 ml) in pyridine (5 ml) was stirred at room temperature for 2 h, and then diluted with EtOH (5 ml). After concentration of the mixture *in vacuo*, the residue was crystallized from EtOH to give **4a** (300 mg, 97%), mp 178—180 °C, undepressed upon admixture with an authentic sample.[15]

**2,2'-Anhydro-1-(3-*O*-acetyl-5-substituted-β-D-arabinofuranosyl)uracils (4a, d—f)**——A mixture of **3** (400 mg, 1 mmol) and NaOAc, LiCl, LiBr, or $NaN_3$ (5—10 mmol) in HMPA (10 ml) was stirred at room temperature for 2—3 d. After concentration of the mixture *in vacuo*, the residue was now chromatographed on a silica gel column using $CHCl_3$–EtOH (5 : 1, v/v) or $Me_2CO$–$CHCl_3$ (3 : 1, v/v) as the eluent to give: **4a** (263 mg, 85%), mp 178—180 °C. **4d** (264 mg, 92%), mp 222—225 °C, $^1$H-NMR (DMSO-$d_6$) $\delta$: 2.11 (s, 3H, Ac), 3.59 (dd, 1H, H-5', $J_{5',5''}$=12.2, $J_{4',5'}$=4.9 Hz), 3.72 (dd, 1H, H-5'', $J_{5',5''}$=12.2, $J_{4',5''}$=5.2 Hz), 4.55 (m, 1H, H-4'), 5.31 (d, 1H, H-3', $J_{3',4'}$=3.0 Hz), 5.53 (d, 1H, H-2', $J_{1',2'}$=5.8 Hz), 5.90 (d, 1H, H-5, $J_{5,6}$=7.3 Hz), 6.40 (d, 1H, H-1'), 7.9 (d, 1H, H-6). *Anal.* Calcd for

$C_{11}H_{11}ClN_2O_5$: C, 46.09; H, 3.87; Cl, 12.36; N, 9.77. Found: C, 45.83; H, 4.00; Cl, 12.21; N, 9.68. **4e** (172 mg, 52%), glass. $^1$H-NMR (DMSO-$d_6$) $\delta$: 2.11 (s, 3H, Ac), 3.40 (dd, 1H, H-5′, $J_{5',5''}=11.3$, $J_{4',5'}=5.2$ Hz), 3.58 (dd, 1H, H-5″, $J_{5',5''}=11.3$, $J_{4',5''}=6.7$ Hz), 4.52 (m, 1H, H-4′), 5.32 (d, 1H, H-3′, $J_{3',4'}=2.5$ Hz), 5.53 (d, 1H, H-2′, $J_{1',2'}=5.8$ Hz), 5.90 (d, 1H, H-5, $J_{5,6}=7.3$ Hz), 6.40 (d, 1H, H-1′), 7.93 (d, 1H, H-6). *Anal.* Calcd for $C_{11}H_{11}BrN_2O_5$: C, 39.90; H, 3.35; Br, 24.13; N, 8.46. Found: C, 39.72; H, 3.40; Br, 24.11; N, 8.28. **4f** (200 mg, 69%), mp 160—163 °C. $^1$H-NMR (DMSO-$d_6$) $\delta$: 2.11 (s, 3H, Ac), 3.34 (dd, 1H, H-5′, $J_{5',5''}=13.5$, $J_{4',5'}=4.3$ Hz), 3.55 (dd, 1H, H-5″, $J_{5',5''}=13.5$, $J_{4',5''}=6.0$ Hz), 4.50 (m, 1H, H-4′), 5.26 (d, 1H, H-3′, $J_{3',4'}=2.4$ Hz), 5.52 (d, 1H, H-2′, $J_{1',2'}=5.8$ Hz), 5.94 (d, 1H, H-5, $J_{5,6}=7.6$ Hz), 6.41 (d, 1H, H-1′), 7.90 (d, 1H, H-6). *Anal.* Calcd for $C_{11}H_{11}N_5O_5 \cdot 1/3H_2O$: C, 43.28; H, 3.83; N, 22.95. Found: C, 42.94; H, 3.73; N, 22.77.

**Acknowledgement** This investigation was supported in part by funds from the National Cancer Institute, National Institutes of Health, U. S. Department of Health and Human Services (Grants No. CA-08748 and CA-33907).

## References

1) Relevant papers of this series: K. W. Pankiewicz, K. A. Watanabe, H. Takayanagi, T. Itoh and H. Ogura, *J. Heterocycl. Chem.*, **22**, 1703 (1985); K. W. Pankiewicz and K. A. Watanabe, *Nucleosides Nucleotides*, **4**, 613 (1985); also reference 17.
2) K. A. Watanabe, U. Reichman, H. Hirota, C. Lopez and J. J. Fox, *J. Med. Chem.*, **22**, 21 (1979).
3) J. J. Fox, C. Lopez and K. A. Watanabe, "Medicinal Chemistry Advances," F. G. de las Heras and S. Vega, Eds., Pergamon Press, New York, 1981, p. 27.
4) R. F. Schinazi, J. Peters, M. K. Sokol and A. J. Nahmias, *Antimicrob. Agents Chemother.*, **24**, 95 (1983).
5) R. F. Schinazi, J. J. Fox, K. A. Watanabe and A. J. Nahmias, *Antimicrob. Agents Chemother.*, **29**, 77 (1986).
6) C. Lopez, K. A. Watanabe and J. J. Fox, *Antimicrob. Agents Chemother.*, **17**, 803 (1980).
7) J. M. Colacino and C. Lopez, *Antimicrob. Agents Chemother.*, **28**, 252 (1985).
8) E-C. Mar, P. C. Patel, Y-C. Cheng, J. J. Fox, K. A. Watanabe and E-S. Huang, *J. Gen. Virol.*, **65**, 47 (1984).
9) J-C. Lin, M. C. Smith, Y-C. Cheng and J. S. Pagano, *Science*, **221**, 579 (1983).
10) C. W. Young, R. Schneider, B. Leyland-Jones, D. Armstrong, T. C. Tan, C. Lopez, K. A. Watanabe, J. J. Fox and F. S. Philips, *Cancer Res.*, **43**, 5006 (1983).
11) B. Leyland-Jones, H. Donnelly and P. Myskowski, *AFCR Publications Clin. Res.*, **31**, 369A (1983).
12) C. H. Tann, P. R. Brodfuehrer, S. P. Brundidge, C. Sapino and H. G. Howell, *J. Org. Chem.*, **50**, 3644 (1985).
13) S. Shibuya, A. Kuminaka and H. Yoshino, *Chem. Pharm. Bull.*, **22**, 719 (1974); K. A. Watanabe, C-K. Chu, U. Reichman and J. J. Fox, "Nucleic Acid Chemistry," Part 1, L. B. Townsend and R. S. Tipson, Eds., Wiley-Interscience, New York, 1978, p. 343.
14) D. Wagner, J. P. H. Verheyden and J. G. Moffatt, *J. Org. Chem.*, **39**, 24 (1974).
15) D. M. Brown, D. B. Parihar and G. R. Todd, *J. Chem. Soc.*, **1958**, 4242.
16) J. Smrt, *Collection Czechoslovak Chem. Commun.*, **47**, 2157 (1982).
17) K. W. Pankiewicz, J-H. Kim and K. A. Watanabe, *J. Org. Chem.*, **50**, 3319 (1985).
18) U. Reichman, C-K. Chu, D. H. Hollenberg, K. A. Watanabe and J. J. Fox, *Synthesis*, **1976**, 533.
19) D. M. Brown, D. B. Parihar, C. B. Reese and A. R. Todd, *J. Chem. Soc.*, **1956**, 2388; J. F. Codington, R. Fecher and J. J. Fox, *J. Am. Chem. Soc.*, **82**, 2794 (1960).

[Chem. Pharm. Bull. 35(11)4498—4502(1987)]

# Nucleosides. CXLIV. Some Reactions of 2′-*O*-Triflyl-2,3′-anhydroxylosyluracil with Nucleophilic Reagents. Synthesis of 2′-Chloro-2′,3′-dideoxyuridinene. Studies Directed toward the Synthesis of 2′-Deoxy-2′-substituted *arabino* Nucleosides. (5)[1]

KRZYSZTOF W. PANKIEWICZ and KYOICHI A. WATANABE*

*Sloan-Kettering Institute for Cancer Research, Memorial Sloan-Kettering Cancer Center, Sloan-Kettering Division, Graduate School of Medical Sciences, Cornell University, New York, NY 10021, U.S.A.*

(Received June 22, 1987)

Treatment of 2,3′-anhydro-1-(5-*O*-acetyl-2-*O*-triflyl-β-D-xylofuranosyl)uracil with LiCl in hexamethylphosphoric triamide afforded the 2′-"up" chloride of the anhydronucleoside, *i.e.*, the 2′-triflate group was directly displaced by the chloride nucleophile. All attempts to hydrolyze the 2,3′-anhydro linkage resulted in the formation of 2′-chloro-2′,3′-didehydro-dideoxynucleoside.

**Keywords**——nucleoside; anhydronucleoside; reaction mechanism; 2,3′-anhydro-1-(2-*O*-triflyl-β-D-xylofuranosyl)uracil; 2,3′-anhydro-1-(2-chloro-2-deoxy-β-D-lyxofuranosyl)uracil; 1-(2-chloro-2,3-didehydro-2,3-dideoxy-β-D-glyceropento-2-enofuranosyl)uracil; 2′-chloro-2′,3′-dideoxyuridinene

In the preceding report,[1] we described that our attempts to displace the 2′-triflate group of 2,5′-anhydro-3′-*O*-acetyl-2′-*O*-triflyluridine with various nucleophiles resulted in the formation of 5′-substituted-2,2′-anhydro-3′-*O*-acetyl-β-D-arabinosyluracils instead of 2′-substituted-2,5′-anhydroarabinosyluracils, due mainly to instability of the 2,5′-anhydro-linkage. Now it became interesting to investigate the course of reaction of a 2′-*O*-triflyl-2,3′-anhydro-xylosyluracil with nucleophilic reagents for two reasons: if the 2,3′-anhydrolinkage was more reactive than the 2′-triflate group, the initial product would be 3′-substituted uridine which would be further converted into a 3′-substituted-2,2′-anhydro-arabinosyluracil, whereas if the 2′-position was more susceptible to nucleophilic attack than the 3′-position, the reaction would lead to the formation of 2′-substituted-2,3′-anhydro-lyxosyluracil which may then be converted into a 2′-substituted-arabinofuranosyluracil.

Our starting material for the present investigation, *i.e.*, 5′-*O*-protected-2,3′-anhydro-1-(β-D-xylofuranosyl)uracil (**4**) (Chart 1) was prepared from 3′-*O*-mesyl-2′,5′-di-*O*-trityluridine (**1**).[2,3] Treatment of **1** with 1,8-diazabicyclo[5.4.0]undec-7-ene (DBU) in *N*.*N*-dimethylformamide (DMF) afforded the 2,3′-anhydronucleoside **2** in 91% yield. The 5′-*O*-trityl group of **2** was selectively removed in 80% acetic acid to give 2,3′-anhydro-1-(2′-*O*-trityl-β-D-xylofuranosyl)uracil (**3a**) which was acylated with acetic anhydride or benzoyl chloride in pyridine to give **3b** and **3c**, respectively. De-*O*-tritylation of **3b** and **3c** with 10% trifluoroacetic acid in chloroform (v/v) afforded the corresponding 5′-*O*-protected 2,3′-anhydroxylosyluracils **4b** and **4c**. Compound **4b** was hydrolyzed in 80% acetic acid to 1-(5-*O*-acetyl-β-D-xylofuranosyl)uracil (**8b**) which was further converted into the known compound 1-(β-D-xylofuranosyl)uracil.[4] Tritylation of 2,3′-anhydro-1-(β-D-xylofuranosyl)uracil (**4a**)[2] with trityl chloride in pyridine gave 5′-*O*-trityl-2,3′-anhydroxylosyluracil **4d**. Treatment of **4b—d** with triflyl chloride in methylene chloride in the presence of *p*-dimethylaminopyridine (DMAP) and triethylamine afforded the corresponding 2′-*O*-triflyl derivatives **5b—d** in high

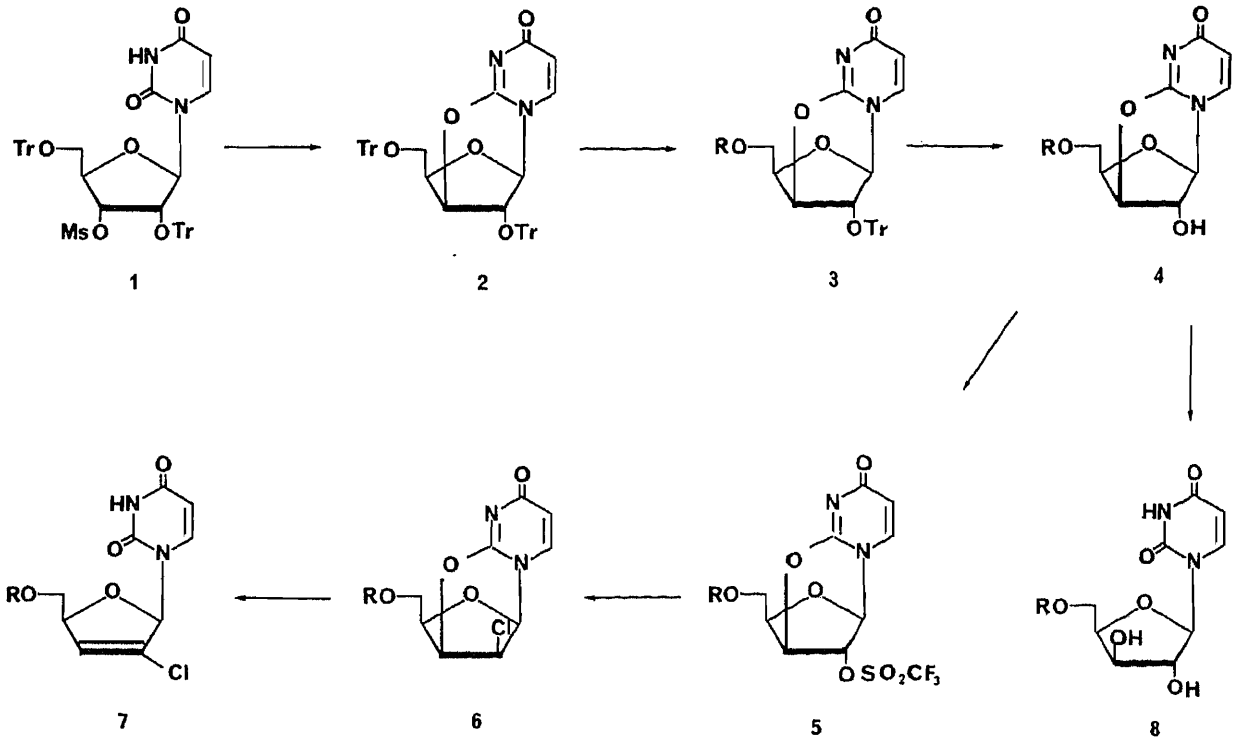


Chart 1

yield.[5]

Reaction of **5b** and **5c** with lithium chloride in hexamethylphosphoric triamide (HMPA) at 100 °C afforded the corresponding 2′-chloro-2′-deoxy-2,3′-anhydrolyxosyluracils **6b** and **6c** as major products. The ultraviolet (UV) spectra of these products are typical for those of 2,3′-anhydronucleosides.[2,4,6] Compound **6b** was not identical to the known 2,2′-anhydro-1-(5′-*O*-acetyl-3′-chloro-3′-deoxy-β-D-arabinofuranosyl)uracil.[7] Apparently, the 2′-triflate was directly displaced by chloride. Our attempts to open the 2,3′-anhydro linkage of **6b** and **6c** in base resulted in the formation of 2′-chloro-2′,3′-dideoxy-2′,3′-didehydrouridine (2′-chloro-uridinene) (**7a**). Compound **7a** was analyzed correctly for $C_9H_9ClN_2O_4$ and showed one each of olefinic proton, and dissociable NH signals. The relatively large $J_{1',3'}$ and small $J_{1',4'}$ values (each 1.5 Hz) are consistent with the β-2-enofuranosyl structure.[8,9] The formation of **7** from **6** clearly established the *lyxo* structure for **6**, since proton and oxide must have been removed from C-2′ and C-3′, respectively, by a *trans* elimination mechanism. Formation of 2′,3′-dideoxy-2′,3′-didehydronucleosides from 2,3′-anhydro-2′-deoxynucleosides by a similar mechanism has been reported by Horwitz *et al.*[10] Acid catalyzed solvolysis[11] of **6b** with sodium benzoate and benzoic acid in DMF led to the formation of the olefins **7b** and no 2′-chloro-arabinosyluracil was obtained.

## Experimental

**2,3′-Anhydro-1-(2,5-di-*O*-trityl-β-D-xylofuranosyl)uracil (2)**——To a solution of 3′-*O*-mesyl-2′,5′-di-*O*-trityluridine[2] (**1**, 18.75 g, 23 mmol) in DMF (150 ml) was added 1,8-diazabicyclo[5.4.0]undec-7-ene (DBU) (4 ml), and the mixture was heated at 100 °C for 3 h. A second charge of DBU (4 ml) was added, and heating continued for three more hours. The mixture was concentrated *in vacuo*, and the residue chromatographed on a silica gel column to give **2** (15 g, 91%), mp 224—225 °C. $^1$H-NMR (DMSO-$d_6$) δ: 3.17 (m, 2H, H-5′,5″), 4.36—4.56 (m, 3H, H-2′,3′,4′), 4.88 (s, 1H, H-1′), 5.74 (d, 1H, H-5, $J_{5,6}$=7.3 Hz), 7.15—7.42 (m, 31H, H-6 and Tr). The melting point was undepressed

upon admixture with an authentic sample.[2)]

**2,3'-Anhydro-1-(2-*O*-trityl-β-D-xylofuranosyl)uracil (3a)**——A solution of **2** (2.8 g, 3.9 mmol) in 80% HOAc (150 ml) was stirred overnight at room temperature, and then concentrated *in vacuo*. Traces of HOAc were azeotropically removed with toluene and EtOH. Upon trituration of the residue with EtOH, **3a** crystallized (1.7 g, 92%), mp 284—285 °C. $^1$H-NMR (DMSO-$d_6$) δ: 3.50 (t, 2H, H-5',5'', changed to d upon addition of $D_2O$), 4.37—4.59 (m, 3H, H-2',3',4'), 4.90 (s, 1H, H-1'), 5.07 (t, 1H, OH), 5.68 (d, 1H, H-5, $J_{5,6}$=7.3 Hz), 7.15 (d, 1H, H-6), 7.33—7.44 (m, 15H, Tr). *Anal.* Calcd for $C_{28}H_{24}N_2O_5$: C, 71.78; H, 5.16; N, 5.98. Found: C, 71.71; H, 5.21; N, 5.81.

**2,3'-Anhydro-1-(5-*O*-acetyl-2-*O*-trityl-β-D-xylofuranosyl)uracil (3b)**——A mixture of **3a** (4.68 g, 10 mmol) and $Ac_2O$ (10 ml) in pyridine (70 ml) was stirred at room temperature for 3 h, and then the reaction quenched by dilution with EtOH (20 ml). The mixture was concentrated *in vacuo*, the residue dissolved in $CHCl_3$ (500 ml) and the solution washed with water (3 × 200 ml), dried ($Na_2SO_4$), and concentrated to *ca.* 100 ml. EtOH (300 ml) was added, and the mixture concentrated until crystals started to precipitate. The mixture was kept at *ca.* 4 °C overnight, and then the crystalline product **3b** was collected by filtration (5.0 g, 98%), mp 110—115 °C. $^1$H-NMR (DMSO-$d_6$) δ: 1.91 (s, 3H, Ac), 4.14—4.27 (m, 2H, H-5',5''), 4.42 (s, 1H, H-2'), 4.59—4.72 (m, 2H, H-3',4'), 4.95 (s, 1H, H-1'), 5.69 (d, 1H, H-5, $J_{5,6}$=7.6 Hz), 7.12 (d, 1H, H-6), 7.33—7.44 (m, 15H, Tr). *Anal.* Calcd for $C_{30}H_{25}N_2O_6 \cdot 1/2H_2O$: C, 69.49; H, 5.25; N, 5.40. Found: C, 69.39; H, 5.33; N, 5.25.

By following the same procedure but using BzCl instead of $Ac_2O$, 2,3-anhydro-1-(5-*O*-benzoyl-2-*O*-trityl-β-D-xylofuranosyl)uracil (**3c**) was obtained (5.16 g, 90%), mp 158—160 °C. $^1$H-NMR (DMSO-$d_6$) δ: 4.42 (m, 3H, H-2',5',5''), 4.69 (m, 1H, H-4'), 4.88—5.00 (m, 2H, H-1',3'), 5.67 (d, 1H, H-5, $J_{5,6}$=7.3 Hz), 7.09—7.94 (m, 21H, Tr, Bz, H-6). *Anal.* Calcd for $C_{35}H_{28}N_2O_6 \cdot 3/2H_2O$: C, 70.10; H, 5.20; N, 4.67. Found: C, 70.22; H, 5.05; N, 4.48. The presence of $H_2O$ was shown in $^1$H-NMR at δ 3.32.

**2,3'-Anhydro-1-(5-*O*-acetyl-β-D-xylofuranosyl)uracil (4b)**——Compound **3b** (510 mg, 1.0 mmol) was dissolved in 10% $CF_3CO_2H/CHCl_3$ (6 ml). After 5 min at room temperature, the mixture was diluted with benzene (50 ml) and then concentrated *in vacuo*. The residue was triturated with $Et_2O$, and the solid crystallized from EtOH–$Et_2O$ to give **4b** (250 mg, 93%), mp 204—205 °C. $^1$H-NMR (DMSO-$d_6$) δ: 1.92 (s, 3H, Ac), 4.20 (dd, 1H, H-5', $J_{5',5''}$=12.2, $J_{4',5'}$=5.5 Hz), 4.35 (dd, 1H, H-5'', $J_{4',5''}$=4.5 Hz), 4.63 (m, 1H, H-4'), 4.76 (s, 1H, H-2'), 5.03 (br s, 1H, H-3'), 5.65 (s, 1H, H-1'), 5.85 (d, 1H, H-5, $J_{5,6}$=7.3 Hz), 6.45 (d, 1H, OH), 7.67 (d, 1H, H-6). *Anal.* Calcd for $C_{11}H_{12}N_2O_6$: C, 49.25; H, 4.51; N, 10.44. Found: C, 49.35; H, 4.72; N, 10.17.

In a similar manner, **3c** (600 mg, 1.05 mmol) was converted into 2,3'-anhydro-1-(5-*O*-benzoyl-β-D-xylofuranosyl)uracil (**4c**) (300 mg, 83%), mp 227—230 °C. $^1$H-NMR (DMSO-$d_6$) δ: 422 (dd, 1H, H-5', $J_{5',5''}$=11.6, $J_{4',5'}$=7.4 Hz), 4.49 (dd, 1H, H-5'', $J_{4',5''}$=4.0 Hz), 4.70—4.80 (m, 2H, H-2',4'), 5.13 (s, 1H, H-3'), 5.68 (s, 1H, H-1'), 5.80 (d, 1H, H-5, $J_{5,6}$=7.4 Hz), 7.42—7.95 (m, 6H, H-6 and Bz). *Anal.* Calcd for $C_{16}H_{14}N_2O_6$: C, 58.18; H, 4.27; N, 8.48. Found: C, 58.46; H, 4.58; N, 8.22.

**2,3'-Anhydro-1-(5-*O*-trityl-β-D-xylofuranosyl)uracil (4d)**——A mixture of **4a**[2)] (1.13 g, 5 mmol) and TrCl (1.6 g, 6 mmol) in pyridine (75 ml) was heated at 70 °C for 5 h. The reaction was quenched by dilution with EtOH (5 ml), and the mixture concentrated *in vacuo*. The residue was chromatographed on a silica gel column using $CHCl_3$–EtOH (6:1, v/v) as the eluent to give **4d** (1.6 g, 69%), mp 240—245 °C (dec). $^1$H-NMR (DMSO-$d_6$) δ: 3.18 (d, 2H, H-5',5''), 4.61—4.74 (m, 2H, H-2',4'), 5.01 (s, 1H, H-3'), 5.67 (s, 1H, H-1'), 5.85 (d, 1H, H-5, $J_{5,6}$=7.3 Hz), 6.43 (d, 1H, OH), 7.34 (m, 15H, Tr), 7.69 (d, 1H, H-6). *Anal.* Calcd for $C_{28}H_{24}N_2O_5 \cdot 1/2H_2O$: C, 70.43; H, 5.28; N, 5.86. Found: C, 70.51; H, 5.48; N, 5.72. A small amount of $H_2O$ in the analytical sample was detected by $^1$H-NMR.

**1-(5-*O*-Acetyl-β-D-xylofuranosyl)uracil (8b)**——Compound **4b** (255 mg, 0.5 mmol) was dissolved in 80% HOAc (10 ml), and the solution heated at 100 °C for 2 h. After evaporation of the solvent, the residue was chromatographed on a silica gel column ($CHCl_3$–EtOH 9:1, v/v) to give **8b** (112 mg, 79%), mp 141—143 °C. $^1$H-NMR (DMSO-$d_6$) δ: 2.04 (s, 3H, Ac), 3.97 (m, 2H, H-5',5''), 4.29 (m, 3H, H-2',3',4'), 5.68 (d, 1H, H-5, $J_{5,6}$=8.2 Hz), 5.60 (d, 1H, OH), 5.68 (s, 1H, H-1'), 5.85 (d, 1H, OH), 7.74 (d, 1H, H-6). *Anal.* Calcd for $C_{11}H_{14}N_2O_7$: C, 46.16; H, 4.93; N, 9.78. Found: C, 45.96; H, 4.95; N, 9.62.

**Triflation of 4b—d**——To a stirred suspension of **4** (1 mmol), DMAP (122 mg, 1 mmol) and $Et_3N$ (202 mg, 2 mmol) in $CH_2Cl_2$ (20 ml) was added dropwise a solution of TflCl (236 mg, 2 mmol) in $CH_2Cl_2$ (5 ml). The suspension dissolved and from the clear solution, crystalline product precipitated out. Crystals were collected by filtration and washed with $CH_2Cl_2$ to give: 2,3'-Anhydro-1-(5-*O*-acetyl-2-*O*-triflyl-1-β-D-xylofuranosyl)uracil (**5b**) (384 mg, 96%), mp 205—207 °C (dec.). $^1$H-NMR (DMSO-$d_6$) δ: 1.88 (s, 3H, Ac), 4.28 (dd, 1H, H-5', $J_{5',5''}$=12.5, $J_{4',5'}$=4.8 Hz), 4.43 (dd, 1H, H-5'', $J_{4',5''}$=4.8 Hz), 4.71 (m, 1H, H-4'), 5.67 (s, 1H, H-3'), 5.93 (d, 1H, H-5, $J_{5,6}$=7.6 Hz), 6.33 (s, 1H, H-2'), 6.57 (s, 1H, H-1'), 7.71 (d, 1H, H-6). *Anal.* Calcd for $C_{12}H_{11}F_3N_2O_8S$: C, 36.00; H, 2.77; N, 7.00; S, 8.01. Found: C, 35.92; H, 2.80; N, 6.98; S, 8.23. 2,3'-Anhydro-1-(5-*O*-benzoyl-2-*O*-triflyl-1-β-D-xylofuranosyl)uracil (**5c**) (356 mg, 77%), mp 210—211 °C (dec.). $^1$H-NMR (DMSO-$d_6$) δ: 4.52 (dd, 1H, H-5', $J_{5',5''}$=11.9, $J_{4',5'}$=6.1 Hz), 4.62 (dd, 1H, H-5'', $J_{4',5''}$=4.9 Hz), 4.89 (m, 1H, H-4'), 5.75—5.90 (m, 2H, H-3',5), 6.39 (s, 1H, H-1'), 6.65 (s, 1H, H-2'), 7.48—8.25 (m, 6H, Bz and H-6). *Anal.* Calcd for $C_{17}H_{13}F_3N_2O_8S$: C, 44.16; H, 2.83; N, 6.06; S, 6.93. Found: C, 44.27; H, 2.88; N, 6.03; S. 6.90. 2,3'-Anhydro-1-(2-*O*-triflyl-5-*O*-trityl-1-β-D-xylofuranosyl)uracil (**5d**) was obtained in crystalline form after chromatographic purification on a silica gel column using $CHCl_3$–EtOH (95:5, v/v) as the eluent (480 mg, 80%), mp 193—194 °C (dec.). $^1$H-NMR (DMSO-$d_6$) δ: 3.21 (d,

2H, H-5′,5″), 4.67 (m, 1H, H-4′), 5.67 (m, 1H, H-3′), 5.88 (d, 1H, H-5, $H_{5,6}$ = 7.3 Hz), 6.36 (s, 1H, H-1′), 6.57 (s, 1H, H-2′), 7.32 (m, 15H, Tr), 7.73 (d, 1H, H-6). *Anal.* Calcd for $C_{29}H_{23}F_3N_2O_7S$: C, 58.00; H, 3.86; N, 4.66; S, 5.34. Found: C, 58.28; H, 4.01; N, 4.47; S, 5.28.

**2,3′-Anhydro-1-(5-*O*-acetyl-2-chloro-2-deoxy-β-D-lyxofuranosyl)uracil (6b)**——A mixture of **5b** (400 mg, 1 mmol) and LiCl (430 mg, 10 mmol) in HMPA (10 ml) was heated at 110 °C for 36 h. The reaction was quenched by addition of water (100 ml), and the mixture was extracted with EtOAc (3 × 100 ml). The organic extracts were combined, dried ($Na_2SO_4$), evaporated *in vacuo*, and the residue triturated with pyridine (20 ml) and filtered. The filtrate was condensed *in vacuo*, and the residue chromatographed on a silica gel column using $CHCl_3$–$Me_2CO$ (2 : 1, v/v) followed by $CHCl_3$–$Me_2CO$ (1 : 1, v/v). Compound **6b** was crystallized from EtOH–$Et_2O$ (177 mg, 63%), mp 205—207 °C. $^1$H-NMR (DMSO-$d_6$) $\delta$: 1.91 (s, 3H, Ac), 4.20 (dd, 1H, H-5′, $J_{5',5''}$ = 12.2, $J_{4',5'}$ = 5.3 Hz), 4.32 (dd, 1H, H-5″, $J_{4',5''}$ = 4.5 Hz), 4.62 (m, 1H, H-4′), 5.31—5.34 (m, 2H, H-2′,3′), 5.94 (d, 1H, H-5, $J_{5,6}$ = 7.4 Hz), 6.04 (d, 1H, H-1′, $J_{1',2'}$ = 4.1 Hz), 7.74 (d, 1H, H-6). *Anal.* Calcd for $C_{11}H_{11}ClN_2O_5$: C, 46.09; H, 3.87; Cl, 12.36; N, 9.72. Found: C, 46.05; H, 3.81; Cl, 12.35; N, 9.69.

In a similar manner, **5c** (1.0 g, 2.16 mmol) was converted into 2,3′-anhydro-1-(5-*O*-benzoyl-2-chloro-2-deoxy-β-D-lyxofuranosyl)uracil (**6c**) (350 mg, 48%), mp 203—205 °C. $^1$H-NMR (DMSO-$d_6$) $\delta$: 4.45 (dd, 1H, H-5′, $J_{5',5''}$ = 11.9, $J_{4',5'}$ = 6.6 Hz), 4.52 (dd, 1H, H-5″, $J_{4',5''}$ = 6.1 Hz), 4.77 (m, 1H, H-4′), 5.33—5.50 (m, 2H, H-2′,3′), 5.86 (d, 1H, H-5, $J_{5,6}$ = 7.3 Hz), 6.08 (d, 1H, H-1′, $J_{1',2'}$ = 3.8 Hz), 7.41—7.94 (m, 6H, Bz and H-6). *Anal.* Calcd for $C_{16}H_{13}ClN_2 \cdot 1/2H_2O$: C, 53.72; H, 3.94; Cl, 9.91; N, 7.83. Found: C, 53.87; H, 3.92; Cl, 9.83; N, 7.83.

**5′-*O*-Acetyl-2′-chloro-2′,3′-didehydro-2′,3′-dideoxyuridine (5′-*O*-Acetyl-2′-chlorouridinene) (7b)**——A mixture of **6b** (143 mg, 0.5 mmol), NaOBz (288 mg, 2 mmol) and HOBz (122 mg, 1 mmol) in DMF (15 ml) was heated under reflux with stirring for 5 h, and then partitioned between EtOAc and $H_2O$ (100 ml each). The organic layer was washed with $H_2O$, dried ($Na_2SO_4$), concentrated *in vacuo* and the residue crystallized from EtOH to give **7b** (110 mg, 77%), mp 215—217 °C. $^1$H-NMR (DMSO-$d_6$) $\delta$: 2.05 (s, 3H, Ac), 4.21 (d, 2H, H-5′,5″), 5.08 (m, 1H, H-4′), 5.79 (d, 1H, H-5, $J_{5,6}$ = 7.9 Hz), 6.88 (t, H-1′, $J_{1',3'} = J_{1',4'}$ = 1.8 Hz). 6.77 (dd, 1H, H-3′, $J_{1',3'}$ = 1.8, $J_{3',4'}$ = 3.3 Hz), 7.51 (d, 1H, H-6), 11.54 (s, 1H, NH). *Anal.* Calcd for $C_{11}H_{11}ClN_2O_5$: C. 46.09; H, 3.87; N, 9.77. Found: C, 46.07; H, 3.82; N, 9.69.

**2′-Chloro-2′,3′-didehydro-2′,3′-dideoxyuridine (2′-Chlorouridinene) (7a)**——Compound **6b** (100 mg, 0.04 mmol) was dissolved in 1 N NaOH (3 ml). After 1 h at room temperature, the solution was neutralized with 1 N HCl and then concentrated *in vacuo*. The residue was triturated with EtOH (3 × 5 ml) and insoluble solid was removed by filtration. The combined filtrates were concentrated, and the residue crystallized from EtOH to give **7a** (65 mg, 65%), mp 155—157 °C. $^1$H-NMR (DMSO-$d_6$) $\delta$: 3.62 (m, 2H, H-5′,5″), 4.88 (m, 1H, H-4′), 5.15 (t, 1H, OH), 5.70 (d, 1H, H-5, $J_{5,6}$ = 7.9 Hz), 6.60 (t, 1H, H-1′, $J_{1',3'} = J_{1',4'}$ = 1.5 Hz), 6.75 (dd, 1H, H-3′, $J_{1',3'}$ = 1.5, $J_{3',4'}$ = 3.3 Hz), 7.84 (d, 1H, H-6), 11.47 (s, 1H, NH). *Anal.* Calcd for $C_9H_9ClN_2O_4$: C, 44.19; H, 5.71; Cl, 14.49; N, 11.45. Found: C, 44.19; H, 3.82; Cl, 14.50; N, 11.33.

**2′-*O*-*tert*-Butyldimethylsilyl-5′-*O*-dimethoxytrityl-3′-*O*-mesyluridine**——To a solution of 2′-*O*-*tert*-butyldimethylsilyl-5′-*O*-dimethoxytrityluridine[3] (1.3 g, 2 mmol) in pyridine (10 ml) was added MsCl (192 μl, 4.5 mmol), and the mixture kept at *ca.* 4 °C for 20 h, and then at room temperature for 8 h. The reaction was quenched by addition of MeOH (10 ml), and the mixture concentrated *in vacuo*. The residue was dissolved in $CH_2Cl_2$ (100 ml), and the solution washed with water, dried ($Na_2SO_4$), concentrated *in vacuo*, and the residue chromatographed on a silica gel column ($Et_2O$–hexane, 2 : 1) to give the title compound (1.26 g, 87%) as a foam. $^1$H-NMR (DMSO-$d_6$) $\delta$: 0.03 (s, 3H, SiMe), 0.08 (s, 3H, SiMe), 0.83 (s, 9H, *tert*-Bu), 3.16 (s, 3H, Ms), 3.43 (m, 2H, H-5′,5″), 3.75 (s, 6H, OMe), 4.30 (m, 1H, H-4′), 4.56 (t, 1H, H-2′, $J_{1',2'} = J_{2',3'}$ = 5.7 Hz), 5.01 (m, 1H, H-3′), 5.45 (d, 1H, H-5, $J_{5,6}$ = 8.0 Hz), 5.77 (d, 1H, H-1′), 6.90—7.35 (14H, Tr), 7.70 (d, 1H, H-6), 11.5 (s, 1H, NH). *Anal.* Calcd for $C_{37}H_{46}N_2O_{10}SSi$: C, 60.14; H, 6.27; N, 3.79. Found: C, 60.28; H, 6.08; N, 3.60.

**2,3′-Anhydro-1-(2-*O*-*tert*-butyldimethylsilyl-5-*O*-dimethoxytrityl-β-D-xylofuranosyl)uracil**——The 3′-*O*-mesylate (738 mg, 1 mmol) as prepared above, was dissolved in MeCN (15 ml). DBU 228 mg, 1.5 mmol) was added to the solution, and the mixture was heated under reflux for 8 h. After concentration of the mixture *in vacuo*, the residue was chromatographed on a silica gel column using $CHCl_3$–EtOH (39 : 1, v/v) as the eluent to give the title compound (30 mg, 4.7%) as a foam. $^1$H-NMR (DMSO-$d_6$) $\delta$: 0.17 (s, 3H, Me), 0.18 (s, 3H, Me), 0.88 (s, 9H, *tert*-Bu), 3.17 (m, 2H, H-5′,5″), 3.72 (s, 6H, OMe), 4.43 (m, 1H, H-4′), 5.00 (s, 2H, H-2′,3′), 5.71 (s, 1H, H-1′), 5.83 (d, 1H, H-5, $J_{5,6}$ = 7.4 Hz), 6.84—7.34 (m, 13H, aromatic), 7.70 (d, 1H, H-6). *Anal.* Calcd for $C_{36}H_{42}N_2O_7Si$: C, 67.26; H, 6.58; N, 4.36. Found: C, 67.52; H, 6.29; N, 4.29.

A significant amount (500 mg, 68%) of the starting material was recovered from the column.

**2,3′-Anhydro-1-(2-*O*-mesyl-5-*O*-trityl-β-D-xylofuranosyl)uracil**——To a solution of **4d** (234 mg, 0.5 mmol) in tetrahydrofuran (THF) (20 ml) was added NaH (70 mg, 50% in oil), then MsCl in THF (75 mg, 0.65 mmol in 5 ml). The mixture was stirred at room temperature, concentrated *in vacuo*. The residue was dissolved in $CHCl_3$, (50 ml), washed (water), dried ($Na_2SO_4$), concentrated, and the residue chromatographed on a silica gel column ($CHCl_3$–EtOH 9 : 1, v/v) to give 2,3′-anhydro-1-(2-*O*-mesyl-5-*O*-trityl-β-D-xylofuranosyl)uracil (165 mg, 60%), mp 150—152 °C. $^1$H-NMR (DMSO-$d_6$) $\delta$: 3.19 (m, 2H, H-5′,5″), 3.32 (s, 3H, Ms), 4.61 (m, 1H, H-4′), 5.45 (brs, 1H, H-3′), 5.86 (d, 1H, H-5, $J_{5,6}$ = 7.3 Hz), 5.93 (s, 1H, H-1′), 6.14 (s, 1H, H-2′), 7.32 (m, 15H, Tr), 7.75 (d, 1H, H-6). *Anal.* Calcd

for $C_{29}H_{26}N_2O_7S \cdot 2H_2O$: C, 59.78; H, 5.19; N, 4.80; S, 5.50. Found: C, 59.78; H, 4.96; N, 4.69; S, 5.33.

In a similar manner, 2,3′-anhydro-*tert*-(2-*O*-tosyl-5-*O*-trityl-β-D-xylofuranosyl)uracil was prepared (320 mg, 51%) mp 133—135 °C. $^1$H-NMR (DMSO-$d_6$) $\delta$: 2.44 (s, 3H, MePh), 3.15 (d, 2H, H-5′,5″), 4.54 (m, 1H, H-4′), 5.22 (br s, 1H, H-3′), 5.83 (d, 1H, H-5, $J_{5,6}$ = 7.4 Hz), 5.88 (s, 1H, H-1′), 6.03 (s, 1H, H-2′), 7.30 (m, 15H, Tr), 7.54—7.69 (d, 2H, MePh), 7.69 (d, 1H, H-6), 7.45 (d, 2H, MePh). *Anal.* Calcd for $C_{35}H_{30}N_2O_7 \cdot H_2O$: C, 65.62; H, 5.03; N, 4.37; S, 5.00. Found: C, 65.97; H, 5.03; N, 4.26; S. 5.03.

**Acknowledgement** This investigation was supported in part by funds from the National Cancer Institute, National Institutes of Health, U.S. Department of Health and Human Services (Grants CA-08748 and CA-44083).

## References

1) Nucleosides 143 (preceding paper).
2) N. C. Young and J. J. Fox, *J. Am. Chem. Soc.*, **83**, 3060 (1961).
3) 2′-*O*-Dimethyl-*tert*-butylsilyl-5′-*O*-dimethoxytrityluridine [G. H. Hakimelachi, Z. A. Proba and K. K. Ogilvie, *Can. J. Chem.*, **60**, 1106 (1982)] could be quantitatively mesylated. Treatment of the 3′-mesylate with DBU, however, afforded the desired 2,3′-anhydroxylosyluracil in only 5% yield. 2′-*O*-Desilylation prior to DBU treatment did not improve the yield of 2,3′-anhydronucleoside.
4) J. F. Codington, R. Fecher and J. J. Fox, *J. Am. Chem. Soc.*, **82**, 2794 (1960).
5) No sulfonylation products were obtained when **4h—d** were treated with MsCl, TsCl or TfiCl in pyridine. Compound **4d** could be mesylated or tosylated in THF in the presence of NaH, but triflation under these conditions yielded an intractable mixture.
6) R. Fecher, J. F. Codington and J. J. Fox, *J. Am. Chem. Soc.*, **83**, 1889 (1961).
7) T. Naito, M. Hirota, Y. Nakai, T. Kobayashi and M. Kanao, *Chem. Pharm. Bull.*, **13**, 1258 (1965).
8) R. U. Lemieux, K. A. Watanabe and A. A. Pavia, *Can. J. Chem.*, **47**, 4413 (1969).
9) A. Matsuda, C. K. Chu, U. Reichman, K. Pankiewicz, K. A. Watanabe and J. J. Fox, *J. Org. Chem.*, **46**, 3603 (1981).
10) J. P. Horwitz, J. Chua, I. L. Klundt, M. A. DaRooge and M. Noel, *J. Am. Chem. Soc.*, **86**, 1896 (1964); J. P. Horwitz, J. Chua, M. A. DaRooge, M. Noel and I. L. Klundt, *J. Org. Chem.*, **31**, 205 (1966).
11) J. J. Fox and N. C. Miller, *J. Org. Chem.*, **28**, 936 (1963).

[Chem. Pharm. Bull. 35(11)4503—4509(1987)]

# Effect of Catechol on the Photo-Induced Activation of Bleomycin

HIROMASA MORI

*Laboratory of Theoretical and Molecular Biology, Faculty of Pharmaceutical Sciences, Kumamoto University, Ohe-Honmachi 5-1, Kumamoto 862, Japan*

(Received May 16, 1986)

Bleomycin decreases the melting temperature ($T_m$) of deoxyribonucleic acid (DNA) determined by the optical density and viscosity methods and breaks the DNA strand in the presence of 1,2-benzenediol (catechol). The effect of bleomycin in the presence of catechol is markedly in acidic solution. However, in contrast with the case of sulfhydryl compounds such as 2-hydroxy-1-ethanethiol (2-mercaptoethanol), catechol inhibits the interaction of ultraviolet (UV)-irradiated bleomycin with DNA. These results show that catechol has two functions, *i.e.*, increasing the activity of non-irradiated bleomycin and inhibiting that of UV-irradiated bleomycin. Moreover, it was demonstrated that irradiation is not effective for enhancing the antibacterial activity of bleomycin.

**Keywords**——bleomycin; catechol; sulfhydryl compound; UV irradiation; DNA melting temperature; DNA strand breakage; fluorescence; antibacterial activity

## Introduction

Bleomycin, an antitumor antibiotic isolated from *Streptomyces verticillus*,[1] can interact directly with double-helical deoxyribonucleic acid (DNA) *in vitro*. It is well known that bleomycin decreases the melting temperature ($T_m$) of DNA,[2] releases free bases from DNA[3-7] and breaks the DNA strand(s)[8-10] in the presence of a reducing agent or ferrous ions, and that these abilities of bleomycin are enhanced by ultraviolet (UV) irradiation.[11,12] Recently, it has been shown that the activities of bleomycin for decreasing $T_m$ of DNA and breaking the DNA strand were also enhanced by UV pre-irradiation of bleomycin solution in the presence of sulfhydryl compounds.[13] When UV pre-irradiation was carried out in 48 $\mu$M bleomycin solution at pH 7.4, the maximum activity was obtained at a short irradiation time, *e.g.*, about 10 min. Such an irradiation dose causing the greatest enhancement of the DNA $T_m$-decreasing ability and the strand breakage activity was in agreement with that causing the greatest quenching at 350 nm in the transition of the fluorescence maximum from 350 to 400 nm.[13] Although it has been reported that a photo-induced change occurs at the bithiazole moiety,[11-14] the mechanism of this activation has not been made clear.

It would be of interest to verify whether the enhancement of the activities of bleomycin by irradiation is a common feature *in vitro* and *in vivo* or not. In this study, the interactions of UV-irradiated and non-irradiated bleomycin with DNA were investigated by measuring $T_m$ and the strand breakage of DNA in the presence of 1,2-benzenediol (catechol) for comparison with the case of sulfhydryl compounds. The photo-induced change of the antibacterial activity of bleomycin was also examined.

### Materials and Methods

**Materials**——Bleomycin was obtained from Nippon Kayaku Co. Highly polymerized salmon sperm DNA and 3,8-diamino-5-ethyl-6-phenylphenanthridinium bromide (ethidium bromide) were obtained from Sigma Co. and

catechol, 2-hydroxy-1-ethanethiol (2-mercaptoethanol), DL-*threo*-1,4-dimercapto-2,3-butanediol (dithiothreitol) and other reagents from Wako Pure Chemical Industries Co. So-called reversible DNA, salmon sperm DNA treated with $HNO_2$, was prepared by the method of Geiduschek.[15] Reversible DNA having 90% reversibility was used to test the strand breakage of DNA caused by bleomycin. The materials for assaying the antibacterial activity were obtained from Eiken Chemical Co.

**Preparation of UV-Irradiated Bleomycin for Spectrophotometric Analyses and for Action on DNA**——A solution (3 ml) of 48 or 480 $\mu$M bleomycin in 50 mM tris(hydroxymethyl)aminomethane (Tris)–HCl buffer of pH 3.0, 7.4 or 10.6 in a cuvette was irradiated through a mercury lamp (15 W) at a distance of 23 cm. Under these conditions, the irradiation dose was estimated to be 35 erg/mm$^2$/s. Bleomycin solutions (48 $\mu$M) irradiated under pH 3.0 and 10.6 were neutralized to pH 7.4 by adding 1 N NaOH or 1 N HCl. UV absorption and fluorescence spectra were measured with a Hitachi EPS-3T spectrophotometer and an MPF-3 fluorescence spectrometer, respectively.

**Examination of Thermal Melting Curves of DNA Treated with Bleomycin by Using Optical Density and Viscosity Methods**——For measurements of optical density, the following reaction mixture was prepared; 50 $\mu$g/ml salmon sperm DNA ($A_{260}=0.6$), 40 $\mu$M UV-irradiated or non-irradiated bleomycin (in the preparation of the UV-irradiated solution, the bleomycin concentration fell from an initial value of 48 to 40 $\mu$M) and 1 mM catechol or 1 mM 2-mercaptoethanol in 50 mM Tris–HCl and 1 mM KCl buffer of pH 7.4. In the absence of a reducing agent, the reaction mixture contained 400 $\mu$M UV-irradiated or non-irradiated bleomycin (in the preparation of the UV-irradiated solution, the bleomycin concentration fell from an initial value of 480 to 400 $\mu$M) in place of 40 $\mu$M bleomycin in the above-mentioned reaction mixture.

These reaction mixtures were incubated at 37 °C for 2 h, and the optical density of each reaction mixture in a cuvette (1 cm light path) with a stopper was measured at 260 nm to obtain the thermal melting curve in the temperature range from 37 to 95 °C; the temperature was raised by one degree every 2 min.[13] The parameter, $T_m$, characterizing the melting transition corresponds to the temperature at which the rise in $A_{260}$ was half complete.

In the viscosity method, 100 $\mu$g/ml salmon sperm DNA ($A_{260}=1.2$) was added instead of 50 $\mu$g/ml DNA used for measuring the optical density. A reaction mixture incubated at 37 °C for 2 h (2 ml) was placed in an Ostwald-type capillary viscometer and the relative viscosity was measured to analyze the thermal melting curve in the temperature range from 37 to 95 °C; the temperature was raised by one degree every 3 min.[13] The relative viscosity was obtained by using the following equation:

$$\text{relative viscosity}=\frac{\text{flow time (s) of reaction mixture}}{\text{flow time (s) of blank solution}}$$

The parameter, $T_m$, characterizing the melting transition corresponds to the temperature at which the decrease in relative viscosity was half complete.

**Examination of DNA Strand Breakage Caused by Bleomycin**——The effect of pH on the DNA strand breakage activity of bleomycin in the presence of catechol or dithiothreitol was examined by using the method of Morgan and Pulleyblank.[16] The reaction mixture was prepared in the same way as that for measurement of optical density. Reversible DNA at a concentration of $A_{260}=1.0$ was used instead of 50 $\mu$g/ml salmon sperm DNA. The pH of the reaction mixtures was adjusted to various values and then the mixtures were incubated at 37 °C for 3.5 h, denatured in boiling water for 3 min and quenched immediately in ice. Finally, 500 $\mu$g/ml ethidium bromide, dissolved in a solution of 20 mM $K_2HPO_4$ and 200 $\mu$M ethylenediaminetetraacetic acid (EDTA) adjusted to pH 11.5, was immediately added to each reaction mixture. The fluorescence intensity of the final solution of pH 11.3 was measured at 590 nm, with excitation at 525 nm.[13,16] Reversibility (%) was estimated by using the following equation:

$$\text{reversibility (\%)}=\frac{\text{fluorescence intensity of the reaction mixture treated with bleomycin}}{\text{fluorescence intensity of the reaction mixture not treated with bleomycin}}$$

**Assay of Antibacterial Activity of Bleomycin**——The effect of UV irradiation on the antibacterial activity of bleomycin was tested by using the cylinder assay. Three milliliters of 480 $\mu$M bleomycin solution (pH 7.4) for assaying the antibacterial activity was irradiated with UV light for 60 min and diluted with 50 mM Tris–HCl buffer of pH 7.4 to give the concentrations shown in Fig. 7. A suspension (1 ml) of *Escherichia coli* (K-12) having the optical density of 0.24 was seeded in 50 ml of medium containing 1.5% agar and was divided into 2.5 ml test tubes. These test tubes were stored overnight at 5 °C, then a bleomycin solution (0.4 ml) was gently laid on the agar layer in the test tube and it was incubated at 37 °C for 20 h. The length of the inhibitory zone of each test tube was measured.

## Results

Table I shows the DNA $T_m$-decreasing ability of bleomycin in the presence of catechol or 2-mercaptoethanol obtained by the optical density method. Bleomycin decreased $T_m$ of DNA at pH 7.4 in the presence of 1 mM catechol more effectively than in the presence of 1 mM 2-mercaptoethanol. Moreover, bleomycin also decreased $T_m$ in the presence of other poly-

TABLE I. Effects of Reducing Agents on $T_m$ of DNA Treated with 40 μM Bleomycin

| Reducing agent | $T_m$ of DNA (°C) |
|---|---|
| Reducing agent-free | 80 |
| 1 mM Catechol | 65 |
| 1 mM 2-Mercaptoethanol | 74 |

Each reaction mixture, containing 50 μg/ml salmon sperm DNA, 40 μM bleomycin with 1 mM catechol or 1 mM 2-mercaptoethanol in 50 mM Tris-HCl and 1 mM KCl buffer of pH 7.4, was incubated at 37°C for 2 h and $T_m$ was measured in terms of optical density.

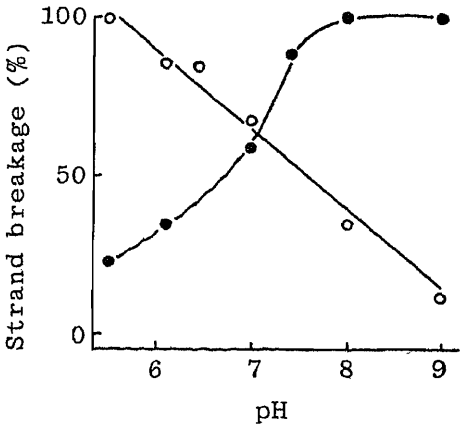


Fig. 1. Plot of DNA Strand Breakage Activity *versus* pH Value for Bleomycin in the Presence of Catechol or Dithiothreitol

The reaction mixture contained reversible DNA at a concentration of $A_{260}=1.0$, 40 μM bleomycin and 1 mM catechol or 1 mM dithiothreitol in 50 mM Tris-HCl and 1 mM KCl buffer of various pH values.
—○—, 1 mM catechol; ---●---, 1 mM dithiothreitol.

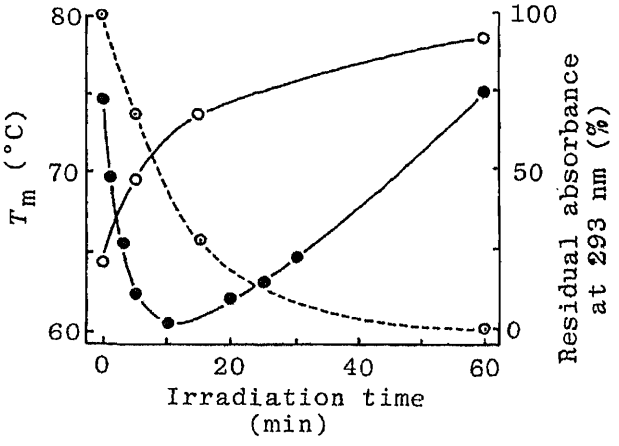


Fig. 2. Effect of UV Irradiation Time of Bleomycin on $T_m$ of DNA in the Presence of Catechol or 2-Mercaptoethanol, Measured in Terms of Optical Density, and Decrease in UV Absorbance of UV-Irradiated Bleomycin

The reaction mixture contained 50 μg/ml salmon sperm DNA, 40 μM UV-irradiated or non-irradiated bleomycin and 1 mM catechol or 1 mM 2-mercaptoethanol in 50 mM Tris-HCl and 1 mM KCl buffer of pH 7.4.
Left and right scales represent $T_m$ in the presence of catechol (—○—) or 2-mercaptoethanol (---●---) and the residual absorbance (%) of UV-irradiated bleomycin at 293 nm (---⊙---), respectively.

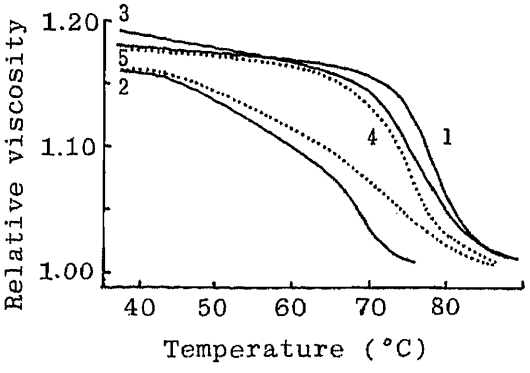


Fig. 3. Thermal Melting Curves of DNA Treated with UV-Irradiated Bleomycin in the Presence of Catechol or 2-Mercaptoethanol, Measured in Terms of Viscosity

The reaction mixture contained 100 μg/ml salmon sperm DNA, 400 μM UV-irradiated or non-irradiated bleomycin and 100 μM catechol or 100 μM 2-mercaptoethanol in 50 mM Tris-HCl and 1 mM KCl buffer of pH 7.4.
(1) DNA, (2) DNA+non-irradiated bleomycin+catechol, (3) DNA+UV-irradiated bleomycin for 60 min+catechol, (4) DNA+non-irradiated bleomycin+2-mercaptoethanol and (5) DNA+UV-irradiated bleomycin for 60 min+2-mercaptoethanol.

phenols such as 1,3-benzenediol (resorcinol), 1,3,5-benzenetriol (phloroglucinol) and 1,2,3-benzenetriol (pyrogallol). Figure 1 shows that bleomycin also broke the DNA strands in the presence of catechol and that this activity decreased linearly with increase in pH value. On the other hand, bleomycin in the presence of dithiothreitol showed different features of DNA strand breakage; the breakage was especially enhanced in the pH range higher than pH 7.5 as compared with that with catechol.

Figure 2 shows the change of the DNA $T_m$-decreasing ability of bleomycin, treated with UV irradiation, in the presence of catechol or 2-mercaptoethanol, obtained in terms of optical density. The $T_m$ of DNA in the presence of catechol gradually increased with increasing irradiation time, whereas the DNA $T_m$-decreasing ability in the presence of 2-mercaptoethanol was enhanced by irradiation and became maximum after irradiation for about 10 min, when about 50% decrease of the residual absorbance at 293 nm and the greatest quenching of the fluorescence maximum at 350 nm were seen.[13] As shown in Fig. 3, the inhibition by catechol was also observed in terms of viscosity. Although non-irradiated bleomycin remarkably decreased the relative viscosity of DNA at low temperature in the presence of 100 $\mu$M catechol (solid line 2), the activity of UV-irradiated bleomycin was hampered in the presence of catechol (solid line 3). In the case of 2-mercaptoethanol, the relative viscosity of DNA treated with bleomycin was enhanced by UV irradiation (dotted lines 4 and 5).

Figure 4 shows the effect of UV irradiation on the DNA $T_m$-decreasing ability of bleomycin in the absence of a reducing agent, obtained by using the optical density method, and the change of absorbance of bleomycin at 293 nm on UV irradiation. Although $T_m$ of DNA treated with or without non-irradiated bleomycin was 80 °C, $T_m$ of DNA treated with UV-irradiated bleomycin decreased at irradiation times of less than 60 min, then increased at 5 h. The absorbance of bleomycin at 293 nm also decreased with irradiation time. Decreases of 10 °C in $T_m$ and of about 50% in absorbance at 293 nm were observed after irradiation for 60 min. These findings agree with those in the presence of 2-mercaptoethanol, presented in the previous report.[13] The thermal melting curves of DNA treated with 400 $\mu$M UV-irradiated or non-irradiated bleomycin, obtained by using the viscosity method, are shown in Fig. 5. Although non-irradiated bleomycin did not affect the relative viscosity of DNA at these temperatures, the addition of UV-irradiated bleomycin markedly diminished the relative viscosity at 37 °C and resulted in loss of the typical melting pattern of DNA in the range of 37 to 95 °C.

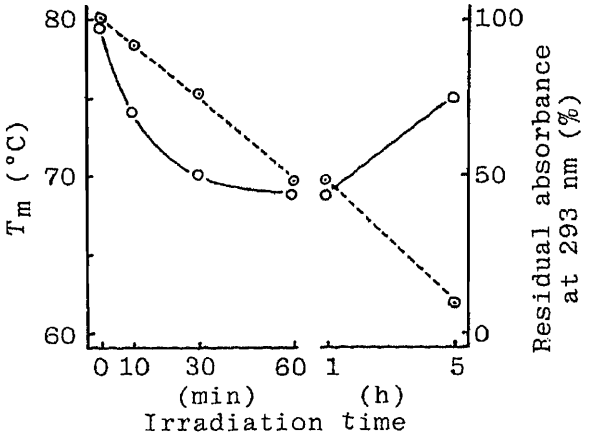


Fig. 4. Effect of UV Irradiation Time of Bleomycin on $T_m$ of DNA in the Absence of a Reducing Agent, Measured in Terms of Optical Density, and Decrease in UV Absorbance of UV-Irradiated Bleomycin

The reaction mixture contained 50 $\mu$g/ml salmon sperm DNA and 400 $\mu$M UV-irradiated or non-irradiated bleomycin in 50 mM Tris-HCl and 1 mM KCl buffer of pH 7.4.

Left and right scales represent $T_m$ (—○—) and the residual absorbance (%) of UV-irradiated bleomycin at 293 nm (---○---), respectively.

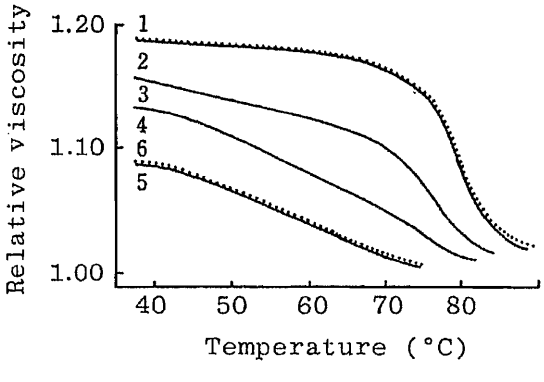


Fig. 5. Thermal Melting Curves of DNA Treated with UV-Irradiated Bleomycin in the Absence of a Reducing Agent, Measured in Terms of Viscosity

The reaction mixture contained 100 $\mu$g/ml salmon sperm DNA and 400 $\mu$M UV-irradiated or non-irradiated bleomycin in 50 mM Tris-HCl and 1 mM KCl buffer of pH 7.4.

(1) DNA, (2) DNA + non-irradiated bleomycin, (3) DNA + UV-irradiated bleomycin for 5 min, (4) DNA + UV-irradiated bleomycin for 10 min, (5) DNA + UV-irradiated bleomycin for 20 min and (6) DNA + UV-irradiated bleomycin for 60 min.

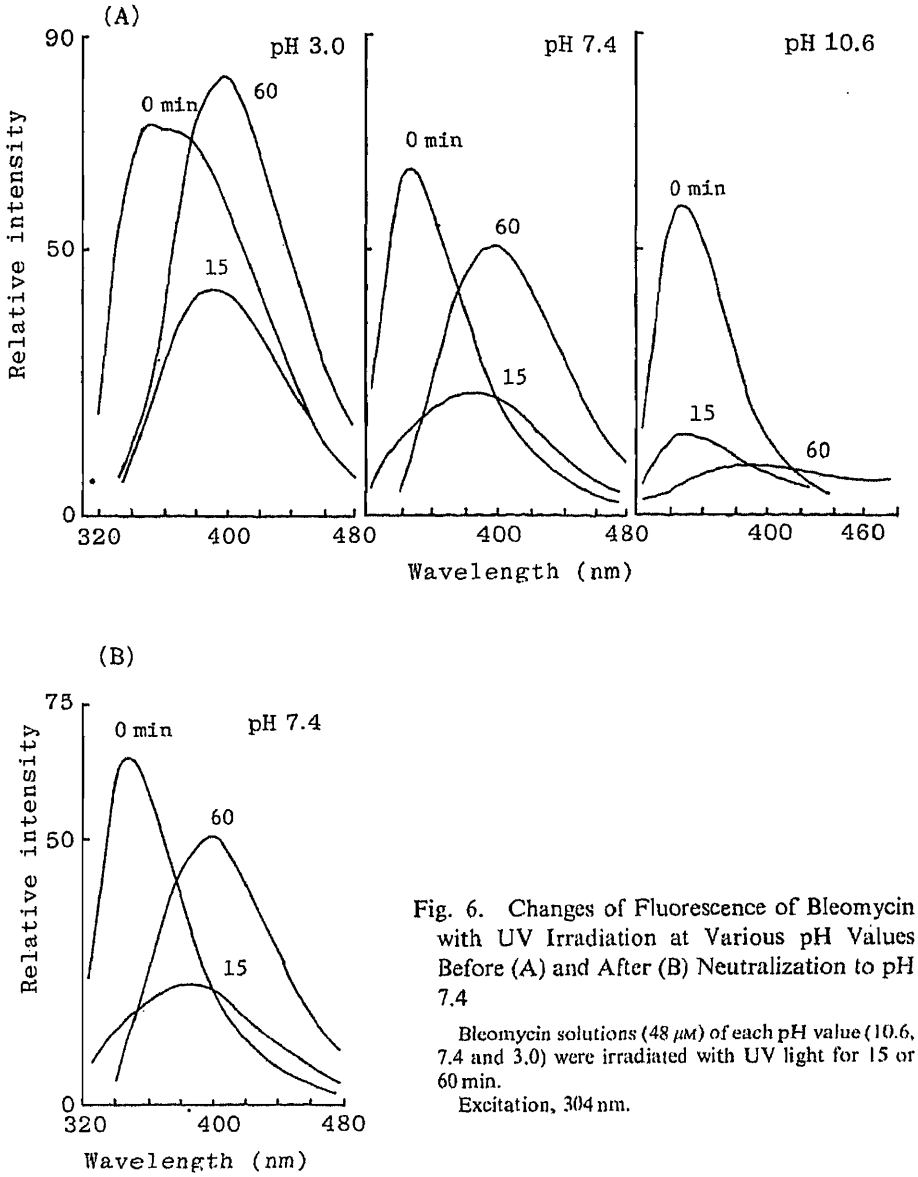


Fig. 6. Changes of Fluorescence of Bleomycin with UV Irradiation at Various pH Values Before (A) and After (B) Neutralization to pH 7.4

Bleomycin solutions (48 $\mu$M) of each pH value (10.6, 7.4 and 3.0) were irradiated with UV light for 15 or 60 min.
Excitation, 304 nm.

The effect of bleomycin, irradiated with UV light for 15 min at pH 3.0, 7.4 and 10.6 and then neutralized to pH 7.4, on $T_m$ of DNA obtained by using the optical density method is summarized in Table II. The DNA $T_m$-decreasing ability of 40 $\mu$M bleomycin in the presence of 2-mercaptoethanol was enhanced in order of pH 10.6, 7.4 and 3.0. The features of quenching of the fluorescence of bleomycin by UV irradiation differed depending on the pH values as shown in Fig. 6. However, as the solutions of pH 10.6 and 3.0 were neutralized to pH 7.4 under reducing agent-free conditions, these different fluorescence spectra became similar to that at pH 7.4.

Figure 7 shows the dose dependence of the antibacterial activity of UV-irradiated and non-irradiated bleomycin obtained by using the cylinder assay. The bleomycin solution (480 $\mu$M) was irradiated for 60 min, which caused the greatest enhancement of the *in vitro* activity. Inhibition of the growth of *Escherichia coli* was not linearly dependent on the concentration of UV-irradiated bleomycin (solid line), whereas it was in the case of non-irradiated bleomycin (dotted line). Moreover, the lengths of the inhibitory zone of UV-irradiated bleomycin were shorter than in the case of non-irradiated bleomycin.

TABLE II. Effects of Bleomycin Irradiated at Various pH Values on $T_m$ of DNA in the Presence of 2-Mercaptoethanol

| pH (during irradiation) | $T_m$ of DNA (°C) |
|---|---|
| 3.0 | 56 |
| 7.4 (non-irradiation) | 74 |
| 7.4 | 65 |
| 10.6 | 71 |

Bleomycin solutions (48 μM) of pH 3.0, 7.4 and 10.6 were pre-irradiated for 15 min and neutralized to pH 7.4 by adding 1 N NaOH or 1 N HCl. Each reaction mixture contained 50 μg/ml salmon sperm DNA, 40 μM bleomycin with or without UV irradiation and 1 mM 2-mercaptoethanol in 50 mM Tris–HCl and 1 mM KCl buffer of pH 7.4.

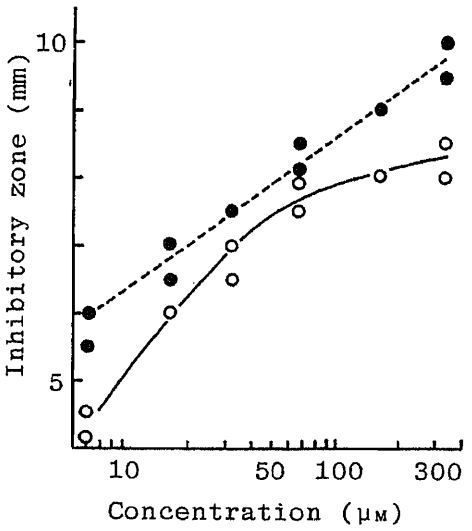


Fig. 7. Change of Antibacterial Activity of Bleomycin towards *Escherichia coli* during UV Irradiation, Determined by Cylinder Assay

Bleomycin solutions (480 μM) with or without UV irradiation for 60 min were diluted to the indicated concentration and the antibacterial activity of bleomycin was assayed by means of the cylinder assay. —●—, non-irradiated bleomycin; —○—, UV-irradiated bleomycin.

## Discussion

It is well known that bleomycin decreases $T_m$ of DNA and breaks the DNA strand(s) in the presence of 2-mercaptoethanol, dithiothreitol, hydrogen peroxide or ascorbic acid. In addition to these reagents, it was found out that similar effects occur in the presence of catechol (Table I and Fig. 1). The observation that the optimal pH range for strand breakage by bleomycin in the presence of catechol (below pH 6.0) differed from that in the presence of dithiothreitol (above pH 7.5) suggests that the activity of bleomycin to break the DNA strand is mediated by the reducing power of these reagents. That is, bleomycin is active in the pH range from pH 5 to 9 which was employed in this experiment. The present result is consistent with the previous report.[17]

Catechol inhibited the DNA $T_m$-decreasing ability of bleomycin activated by UV irradiation, whereas the activity of bleomycin for decreasing $T_m$ without a reducing agent or with 2-mercaptoethanol was remarkably enhanced by UV irradiation (Figs. 2—5). Therefore, it is presumed that catechol has two functions, *i.e.*, increasing the activity of non-irradiated bleomycin in the same manner as other reducing agents, and inhibiting that of photochemically activated bleomycin. The activity of bleomycin to break the DNA strand in the presence of catechol was lost with increase of pH (Fig. 1). Further, the enhancement of the activity of bleomycin by UV irradiation was weak in alkaline solution (Table II). These observations suggest that inhibition by catechol may be caused by the formation of a quinoid form due to the liberation of protons (oxidized form). It has been proposed that Fe(II)·bleomycin changes an active Fe complex.[18] Therefore, it is presumed that a quinoid form of catechol may specifically inhibit the formation of active Fe·bleomycin or the activated site formed by the photo-induced change. However, the mechanism of this inactivation remains unclear.

It has been reported that the activities of bleomycin to break the DNA strand, to release free bases from DNA and to decrease $T_m$ of DNA were enhanced by UV irradiation.[11-13] The photo-induced activation is accompanied with change of the fluorescence maximum from

350 to 400 nm due to the alteration of the bithiazole rings in the bleomycin molecule.[12,13] Recently, it was shown that 2,4′-bithiazole in the bleomycin molecule and a model compound were photo-transformed to 4,4′-bithiazole by UV irradiation.[14] Hence, it is conceivable that the photo-induced change of the bithiazole moiety may cause the enhancement of interaction between bleomycin and DNA. On the other hand, it is well known that bleomycin can be classified into two functional parts. That is, the bithiazole rings of the C-terminal intercalate into the base stacking of DNA, and the other part, the active site of the N-terminal, is able to break the DNA strand.[19-22] Therefore, it is reasonable to consider that the function of the bithiazole rings might be enhanced by UV irradiation. In addition, it was noticed that although the alteration of fluorescence due to UV irradiation differed at pH 10.6, 7.4 and 3.0 and all the spectra became similar on neutralization to pH 7.4, the DNA $T_m$-decreasing ability of bleomycin irradiated at each pH was enhanced in order of pH 10.6, 7.4 and 3.0 (Table II and Fig. 6). These findings seem to show that the photo-induced change for activating bleomycin might also be caused at the other site.

As bleomycin is photo-sensitive, a change of *in vivo* activity of bleomycin on UV irradiation would be expected. As shown in Fig. 7, the antibacterial activity of bleomycin towards *Escherichia coli* declined upon UV irradiation. As it has been reported that an enhancement of the permeability of the cellular membrane, induced by dibucaine, affected the activity of bleomycin on cell growth,[23] the decline of the antibacterial activity of bleomycin caused by UV irradiation may be a result of decreased permeability through the cellular membrane or due to an inhibitor such as catechol in the cell. However, the mechanism of photo-induced inactivation remains unclear. The present results show that bleomycin should be used under 'dark' conditions for maintenance of the antibacterial activity.

In conclusion, although bleomycin decreases $T_m$ of DNA and breaks the DNA strand in the presence of catechol, the activity of photochemically activated bleomycin is inhibited by catechol. Further, the antibacterial activity of bleomycin is lessened by UV irradiation. These results suggest that, as UV irradiation may reduce the activity of bleomycin, precautions against exposure to light may be necessary during bleomycin treatment.

## References


1) H. Umezawa, K. Maeda, T. Takita and Y. Ohkami, *J. Antibiot., Ser. A*, **19**, 200 (1966).
2) K. Nagai, H. Suzuki, N. Tanaka and H. Umezawa, *J. Antibiot.*, **22**, 569 (1969).
3) W. E. G. Müller, Z. Yamazaki, H.-J. Breter and R. K. Zahn, *Eur. J. Biochem.*, **31**, 518 (1972).
4) C. W. Haidle, K. K. Weiss and M. T. Kuo, *Molec. Pharmacol.*, **8**, 531 (1972).
5) M. T. Kuo and C. W. Haidle, *Biochim. Biophys. Acta*, **335**, 109 (1973).
6) J. M. C. Gutteridge, *FEBS Lett.*, **105**, 278 (1979).
7) R. M. Burger, A. R. Berkowitz, J. Peisach and S. B. Horwitz, *J. Biol. Chem.*, **255**, 11832 (1980).
8) H. Suzuki, K. Nagai, H. Yamaki, N. Tanaka and H. Umezawa, *J. Antibiot.*, **22**, 446 (1969).
9) C. W. Haidle, *Mol. Pharmacol.*, **7**, 645 (1971).
10) E. A. Sausville, J. Peisach and S. B. Horwitz, *Biochem. Biophys. Res. Commun.*, **73**, 814 (1976).
11) K. T. Douglas, N. Thakrar, S. J. Minter, R. W. Davies and C. Scazzochio, *Cancer Lett.*, **16**, 339 (1982).
12) J. Kakinuma, M. Tanabe and H. Orii, *Photobiochem. Photobiophys.*, **7**, 183 (1984).
13) H. Mori, *Chem. Pharm. Bull.*, **33**, 4030 (1985).
14) T. Morii, T. Matsuura, I. Saito, T. Suzuki, J. Kuwahara and Y. Sugiura, *J. Am. Chem. Soc.*, **108**, 7089 (1986).
15) E. P. Geiduschek, *Proc. Natl. Acad. Sci. U.S.A.*, **47**, 950 (1961).
16) A. R. Morgan and D. E. Pulleyblank, *Biochem. Biophys. Res. Commun.*, **61**, 396 (1974).
17) E. A. Sausville, R. W. Stein, J. Peisach and S. B. Horwitz, *Biochemistry*, **17**, 2746 (1978).
18) S. M. Hecht, *Acc. Chem. Res.*, **19**, 383 (1986).
19) H. Murakami, H. Mori and S. Taira, *J. Theor. Biol.*, **42**, 443 (1973).
20) H. Murakami, H. Mori and S. Taira, *J. Theor. Biol.*, **59**, 1 (1976).
21) M. Takeshita, A. P. Grollman, E. Ohtsubo and H. Ohtsubo, *Proc. Natl. Acad. Sci. U.S.A.*, **75**, 5983 (1978).
22) L. F. Povirk, M. Hogan and N. Dattagupta, *Biochemistry*, **18**, 96 (1979).
23) D. E. Berry, R. E. Kilkuskie and S. M. Hecht, *Biochemistry*, **24**, 3214 (1985).

[Chem. Pharm. Bull.
35(11)4510—4516(1987)]

# Studies on Structure–Activity Relationships of Prostacyclin Analogs Based on Molecular Mechanics and Molecular Orbital Methods

SHUICHI MIYAMOTO* and MASAFUMI YOSHIMOTO

*Chemical Research Laboratories, Sankyo Co., Ltd., 2–58, 1-chome, Hiromachi, Shinagawa-ku, Tokyo 140, Japan*

(Received February 10, 1987)

Some analogs of isocarbacyclin were found to be potent inhibitors of platelet aggregation. Molecular mechanics and molecular orbital calculations on model compounds of prostacyclin and isocarbacyclin analogs were undertaken in an attempt to elucidate structure–activity relationships. It was found that the net atomic charges of the $\pi$-electron systems could be correlated with the platelet aggregation-inhibitory potency. The $\pi$-electron systems are considered to play an essential role directly in binding with the receptor by electronic interaction and a significant role indirectly in regulating the orientation of the $\alpha$-chain.

**Keywords**——prostacyclin; isocarbacyclin; carbacyclin; structure–activity relationship; $\pi$-electron system; conformational analysis; molecular mechanics; MM2′; quantum mechanics; MNDO

Prostacyclin ($PGI_2$) (**1**) (Chart 1) is a potent, naturally occurring inhibitor of platelet aggregation as well as a very effective vasodilator.[1] From a pharmacotherapeutic point of view, however, $PGI_2$ is an unfavorable candidate for drug development; due to the presence of an enol-ether group that is susceptible to hydrolysis, $PGI_2$ has a very short half-life under physiological conditions.[2] Therefore, a variety of its analogs have been prepared in attempts to reduce this instability.[3]

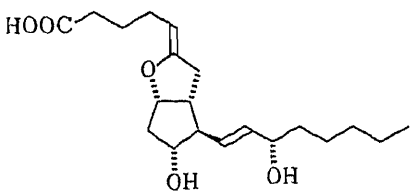


prostacyclin ($PGI_2$) (1)

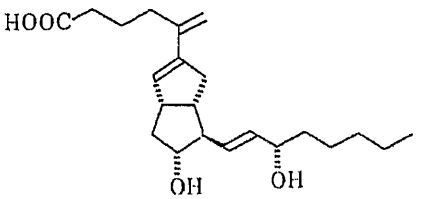


5-methyleneisocarbacyclin (2)

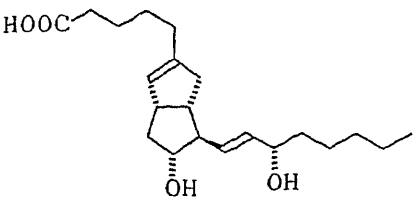


isocarbacyclin (3)

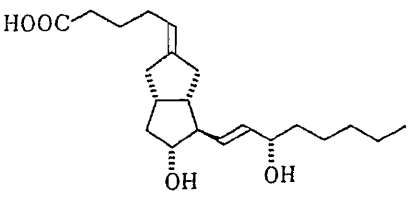


carbacyclin (4)

Chart 1

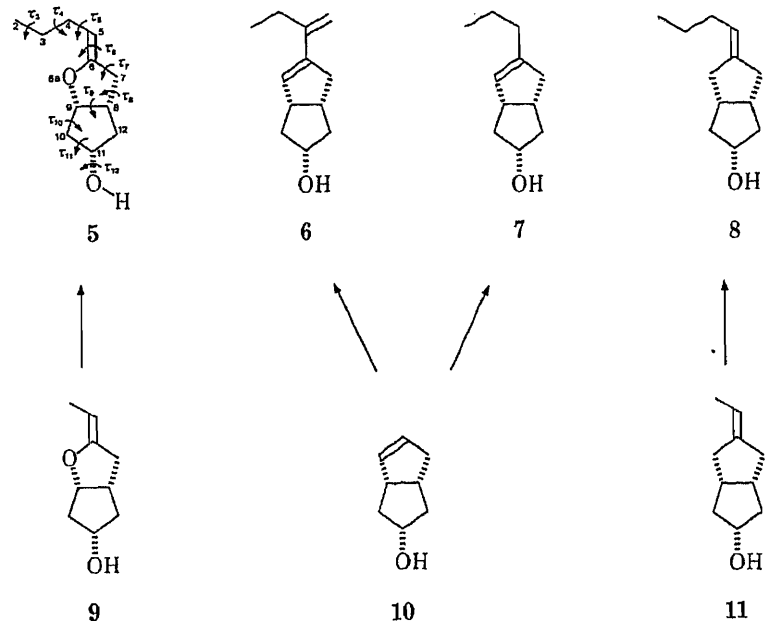

Fig. 1. Scheme to Build up the Model Compounds with Their Substructures, Showing Atom Numbering and Torsional Angles

Torsional angle definitions are as follows: $\tau_3$: H–C2–C3–C4, $\tau_4$: C2–C3–C4–C5, $\tau_5$: C3–C4–C5–C6, $\tau_6$: C4–C5–C6–C7, $\tau_7$: C5–C6–C7–C8, $\tau_8$: C6–C7–C8–C9, $\tau_9$: C7–C8–C9–C6a, $\tau_{10}$: C8–C9–C10–C11, $\tau_{11}$: C9–C10–C11–O, $\tau_{12}$: C10–C11–O–H. $\tau$: A–B–C–D is the angle between the planes A–B–C and B–C–D, with the eclipse form being defined as 0°. Looking along A–B–C–D, a clockwise rotation of the plane B–C–D is considered positive.

Synthetic studies of chemically stable derivatives with functional groups which are considered to be bioisosters of or pharmacologically similar to the eno-ether group have proceeded in our laboratories. Recently, isocarbacyclin analogs (**2**,**3**) (Chart 1) were found to be potent inhibitors of platelet aggregation.[4] The relative potencies of prostacyclin (**1**), 5-methyleneisocarbacyclin (**2**), isocarbacyclin (**3**) and carbacyclin (**4**) are 10, 9, 3 and 1, respectively. We have elucidated the stable conformations and electronic properties of these compounds using molecular mechanics and molecular orbital methods in an attempt to find a structure–activity relationship.

Molecules such as **2** and **3** consist of too many atoms for molecular mechanics or molecular orbital calculations on the whole molecule to be feasible in view of the excessive computing time involved. These compounds also have so many rotatable bonds that an extremely large number of initial structures would have to be taken into account. It seemed to be reasonable for practical analyses to employ model compounds instead of the whole molecules. Since **1**, **2**, **3** and **4** have an identical $\omega$-chain structure, we decided to omit it. There are also some similarities between the $\alpha$-chains of these molecules. The carboxyl moieties, therefore, were excluded from the calculations. As a result, model compounds **5**, **6**, **7** and **8** (Fig. 1) were selected for analysis. Atom numbering and definition of dihedral angles are shown in Fig. 1 using **5** as an example. The same notations are employed for the other model compounds.

## Methods

A model builder program MBCS[5] with a conformational search capability was used in order to generate the coordinates of a series of conformers, which were employed as the starting structures for geometry optimizations. Energy minimizations were performed using the molecular mechanics program MM2'[6] because of its relatively short

computation time. The same approach as used previously[5] was adopted to facilitate calculations. Specifically, stable conformations of the ring structures **10** and **11** were used as basic skeletons for construction of the starting geometries of **7** to **8** as shown in Fig. 1. Since stable three-dimensional (3-D) structures of **5**, **6**, **9** and **10** had been elucidated earlier,[5] only those of **7**, **8** and **11** were examined this time. After stable conformations were obtained, electrostatic properties were calculated using the semiempirical molecular orbital method called modified neglect of diatomic overlap (MNDO).[7]

## Results and Discussion

### Stable Conformations

**Analysis of 7**——Based on the most stable conformer of **10**,[5] starting conformations of **7** were built with the MBCS program by increasing $\tau_6$ by 30°, changing $\tau_5$ to −60, 60 and 180°, and setting $\tau_4$ to 60°. This last value was defined as the torsional angle involving one of the three hydrogens at C3 instead of C2. Geometry optimizations with MM2′ were carried out on the 24 starting structures to afford **9** independent stable conformers (Table I). Both $\tau_6$ and $\tau_5$ of the stable conformers with $\Delta E$ (difference from the lowest energy) less than 1.0 kcal/mol have a preference for −60, 60 and 180°.

**Analysis of 11**——$\tau_{10}$ and $\tau_{12}$ of the initial structures of **11** were set to 25 and −60°, respectively, referring to the most stable conformation of **9**[5] which seemed to have some similarities to **11**. On the other hand, $\tau_8$ and $\tau_9$ were changed to −30, 0 and 30°, and $\tau_5$ and $\tau_6$ were set to 0[8] and 180°, respectively. $\tau_5$ was defined using one of the three hydrogens at C4 instead of the removed C3. As the coordinates of C5 and C12 were determined uniquely by the above assignments, $\tau_7$ and $\tau_{11}$ did not need to be specified.

After energy minimizations were performed on the 5 starting conformers generated, 4 independent stable conformers were obtained (Table II), these conformers having almost constant values for $\tau_5$ and $\tau_6$, *i.e.*, $-5<\tau_5<5°$ and $179<\tau_6<181°$. In the lowest energy conformer of **11**, one five-membered ring consisting of C6-C7-C8-C9-C6a has an envelope conformation with C6 under the plane (when C8, C9 and C6a are on the plane).

**Analysis of 8**——Using the most stable conformer 11-1, initial conformations of **8** were built by increasing $\tau_5$ by 30°, changing $\tau_4$ to −60, 60 and 180°, and setting $\tau_3$ to 60°. The resulting structures were subjected to geometry optimizations to find that the stable conformations of **8** can be divided into two major classes with respect to the value of $\tau_5$. One class includes conformations with $\tau_5 = 77—146°$ (the conformation is called C3-up because C3 comes over the plane when C4, C5 and C6 are on the plane) and the other class contains

Table I. Relative Energies and Torsional Angles of **7** with the Minimum Energies

| Conformer No. | $\Delta E^{a)}$ (kcal/mol) | Torsional angles (°) | | |
|---|---|---|---|---|
| | | $\tau_4$ | $\tau_5$ | $\tau_6$ |
| 7-1 | 0 | 60 | −179 | 180 |
| 7-2 | 0.1 | 58 | 58 | 65 |
| 7-3 | 0.2 | 60 | 177 | 68 |
| 7-4 | 0.2 | 61 | −178 | −63 |
| 7-5 | 0.4 | 62 | −60 | −62 |
| 7-6 | 0.9 | 62 | −64 | 162 |
| 7-7 | 1.0 | 59 | 67 | −165 |
| 7-8 | 1.3 | 64 | −60 | 108 |
| 7-9 | 1.7 | 53 | 62 | −98 |

*a*) Difference from the lowest energy.

Table II. Relative Energies and Torsional Angles of **11** with the Minimum Energies

| Conformer No. | $\Delta E^{a)}$ (kcal/mol) | Torsional angles (°) | | | | | |
|---|---|---|---|---|---|---|---|
| | | $\tau_7$ | $\tau_8$ | $\tau_9$ | $\tau_{10}$ | $\tau_{11}$ | $\tau_{12}$ |
| 11-1 | 0 | −140 | −24 | 3 | 24 | −161 | −69 |
| 11-2 | 0.5 | 140 | 29 | −10 | 32 | −163 | −69 |
| 11-3 | 1.0 | 162 | 32 | −36 | 37 | −145 | −64 |
| 11-4 | 1.4 | −153 | −5 | −17 | −6 | −92 | −71 |

*a*) Difference from the lowest energy.

those with $\tau_5 = -91$——$114°$ (C3-down). In each class $\tau_4$ has a preference for $-60$, 60, and $180°$ as expected, as a result of which there emerge six groups of stable structures of **8**. The most stable conformations of each group are described in Table III. The largest factor favoring C3-up or C3-down conformations seems to be the steric repulsion between the methylene group at C3 and the hydrogens at C6a or the hydrogen at C5. The data in Table III indicates that C3-down conformers (8-1, 8-2 and 8-3) are a little more stable than C3-up ones (8-4, 8-5 and 8-6). This feature of the C3 position is similar to that of **5**.[5]

In the process in which the stable conformations of **7** and **8** were determined, only the most stable conformations of substructures (**10** and **11**, respectively) were taken into account. The conformers listed in Tables I and III, therefore, do not necessarily represent all of the stable 3-D structures of **7** and **8**, but most of them. Although it would be more sophisticated to perform calculations based on several stable conformations of the substructures, it takes too much computation time. In the current state of energy calculation studies, the pragmatic strategy employed here was assumed to be reasonable for the present purpose.

## Electronic Properties

Electronic properties were calculated on the most stable conformers of **5**,[5] **6**,[5] **7** and **8** (conformers 5-1, 6-1, 7-1 and 8-1, respectively) by optimizing the geometries of only hydrogens with the MNDO program. Net atomic charges thus obtained are given in Fig. 2. The most negatively charged atom is the oxygen atom attached to C11 in all four molecules. Most atoms forming the $\pi$-electron systems located around the 5 and 6 positions had negative charges in each compound. All of the highest occupied molecular orbitals (HOMO) and the lowest unoccupied molecular orbitals (LUMO) were essentially $\pi$-orbitals, centered on the

TABLE III. Relative Energies and Torsional Angles of **8** with the Minimum Energies

| Conformer No. | $\Delta E^{a)}$ (kcal/mol) | Torsional angles (°) | | | | Position[b] of C3 |
|---|---|---|---|---|---|---|
| | | $\tau_3$ | $\tau_4$ | $\tau_5$ | $\tau_6$ | |
| 8-1 | 0 | 58 | 62 | −114 | 180 | Down |
| 8-2 | 0.1 | 60 | 180 | −95 | 179 | Down |
| 8-3 | 0.6 | 64 | −61 | −93 | 178 | Down |
| 8-4 | 0.7 | 60 | 180 | 121 | 180 | Up |
| 8-5 | 0.8 | 63 | −64 | 102 | −179 | Up |
| 8-6 | 1.3 | 57 | 63 | 91 | −179 | Up |

*a*) Difference from the lowest energy. *b*) The expression "up" indicates that C3 comes over the plane when C4, C5 and C6 are on the plane, whereas "down" indicates that C3 is located under the plane.

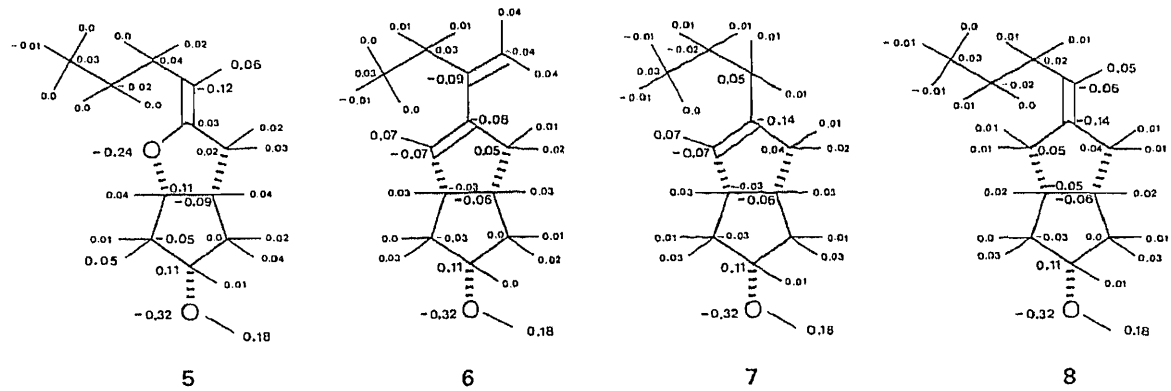


Fig. 2. Net Atomic Charges of Conformers 5-1, 6-1, 7-1 and 8-1

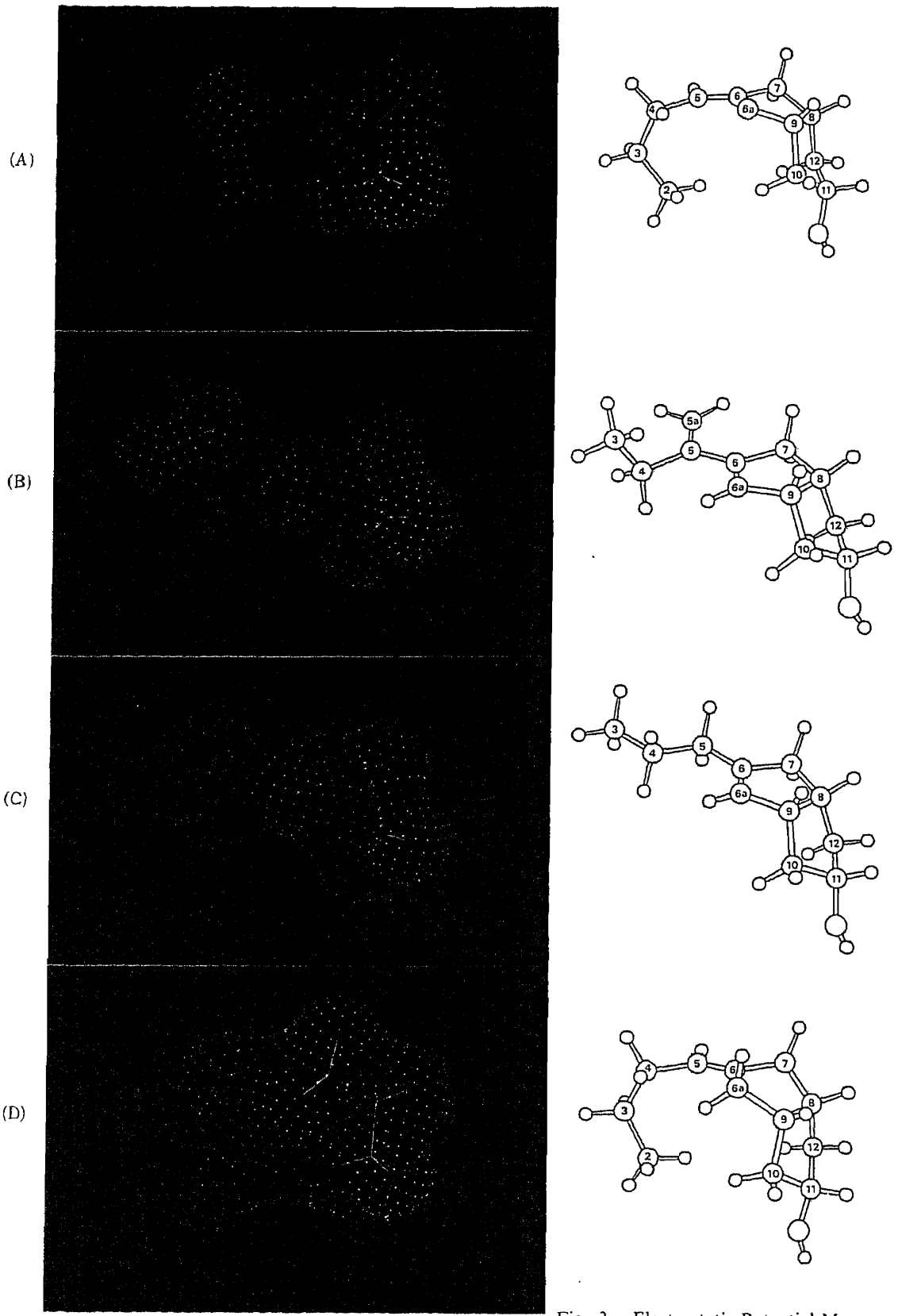


Fig. 3. Electrostatic Potential Maps

(A) Conformer 5-1; (B) conformer 6-1; (C) conformer 7-1; (D) conformer 8-1.

Electrostatic potential (EP) levels: red, $EP < -4.2$ (kcal/mol); orange, $-4.2 < EP < -3.0$ (kcal/mol); yellow, $-3.0 < EP < -1.8$ (kcal/mol); green-yellow, $-1.8 < EP < -0.6$ (kcal/mol); green $-0.6 < EP < 0.6$ (kcal/mol); green-blue, $0.6 < EP < 1.8$ (kcal/mol); light blue $1.8 < EP < 3.0$ (kcal/mol); green-blue, $0.6 < EP < 1.8$ (kcal/mol); light blue $1.8 < EP < 3.0$ (kcal/mol); blue, $3.0 < EP < 4.2$ (kcal/mol); dark blue, $4.2 < EP$ (kcal/mol).

TABLE IV. Electronic Properties and Relative Inhibitory Potency on Human Platelet Aggregation

| Model compound | | | | | Corresponding compound | |
|---|---|---|---|---|---|---|
| No. | Net atomic charge | | HOMO (eV) | LUMO (eV) | No. | Relative[b] potency |
| | 6a | $\sum 5+6+6a$[a] | | | | |
| **5** | −0.24 | −0.32 | −9.2 | 0.9 | **1** | 10 |
| **6** | −0.07 | −0.24 | −9.0 | 0.2 | **2** | 9 |
| **7** | −0.07 | −0.16 | −9.7 | 0.8 | **3** | 3 |
| **8** | 0.05 | −0.15 | −9.7 | 0.9 | **4** | 1 |

*a*) The sum of net atomic charges at positions 5, 6 and 6a. *b*) Relative inhibitory potency on human platelet aggregation of **2**, **3** and **4** when that of **1** is set to 10.

junction of the bicyclic ring with the α-chain. The energies of HOMO and LUMO are given in Table IV. The nature and energy of HOMO and LUMO of the four compounds do not vary in any consistent or significant manner.

**Structure–Activity Relationships**

The main differences between the stable 3-D structures of **5**, **6**, **7** and **8** are the orientation of the α-chain, that is, the values of torsional angles $\tau_5$ and $\tau_6$. In **5**,[5] **6**[5] and **8** (Table III), $\tau_5$ has a preference for about $\pm 100°$ and $\tau_6$ has one for around 180°. On the other hand, each of $\tau_5$ and $\tau_6$ of **7** has a preference for −60, 180 and 60° (Table I). In other words, **7** is more flexible than **5**, **6** and **8**, and the pattern of favorable $\tau_5$ value for **7** is quite different from those of **5**, **6** and **8**. The sum of net atomic charges at positions 5, 6 and 6a, changes gradually from a large negative value to a small negative value (−0.32, −0.24, −0.16, −0.15, respectively). As mentioned before, the relative inhibitory potencies on human platelet aggregation of **1**, **2**, **3** and **4**, corresponding to **5**, **6**, **7** and **8**, respectively, are 10, 9, 3 and 1.

From the above observations, it can be said that the more negative the sum of net atomic charges at positions 5, 6 and 6a of a molecule is, the more potent the molecule is as an inhibitor of platelet aggregation (Table IV). This relationship can be well understood by the use of electrostatic potential maps. Figure 3 shows those maps on the molecular surface for models **5**, **6**, **7** and **8** using the GREEN system.[9] Every molecule has a strong negative potential due to the hydroxyl group at position 11. The π-electron system also produces a negative potential at the upper part of the molecules. The intensity of the negative potential varies with the type of π-electron system. The color of the surface due to the π-electron system changes from red to green-yellow and from wide to narrow, as the platelet aggregation-inhibitory potency varies from strong to weak.

Another correlation might be possible between the net atomic charge of the carbon or oxygen atom at position 6a and the inhibitory activity. Compound **3** is a weaker inhibitor than **2**, though the corresponding models, **7** and **6**, have the same net atomic charges at position 6a. The reason seems to be that the α-chain of **7** is more flexible than that of **6** and that the preference of $\tau_5$ value of **7** is quite different from those of **6** and **5**.

From the present and earlier analyses, the π-electron systems are considered to play an essential role directly in binding with the receptor through electronic interactions and a significant role indirectly in fixing the C3 and C4 positions, that is, in regulating the orientation of the α-chain.

**Acknowledgement** We wish to thank Drs. E. Osawa of Hokkaido University, O. Kikuchi of Tsukuba University and K. Kojima in Sankyo Co., Ltd. for helpful discussions.

## References


1) S. Moncada, R. Gryglewski, S. Bunting and J. R. Vane, *Nature* (London), **263**, 663 (1976); S. Moncada and J. R. Vane, "Advances in Prostaglandin and Thromboxane Research," Vol. 6, ed. by B. Samuelsson, P. W. Ramwell and R. Paoletti, Raven Press, New York, 1980, pp. 43—60.
2) M. J. Cho and M. A. Allen, *Prostaglandins*, **15**, 943 (1978); Y. Chiang, A. J. Kresge and M. J. Cho, *J. Chem. Soc., Chem. Commun.*, **1979**, 129.
3) P. A. Aristoff, "Advances in Prostaglandin, Thromboxane and Leukotriene Research," Vol. 14, ed. by J. E. Pike and D. R. Morton, 1985, p. 309; R. C. Nickolson, M. H. Town and H. Vorbrunggen, *Med. Research Rev.*, **5**, 1 (1985).
4) S. Amemiya, K. Koyama, S. Saito and K. Kojima, *Chem. Pharm. Bull.*, **34**, 4403 (1986).
5) S. Miyamoto, M. Yoshimoto and K. Kojima, *Chem. Pharm. Bull.*, **35**, 1443 (1987).
6) C. Jaime and E. Osawa, *Tetrahedron*, **39**, 2769 (1983).
7) W. Thiel, *QCPE*, **11**, 353 (1978).
8) N. L. Allinger and J. T. Sprangue, *J. Am. Chem. Soc.*, **94**, 5734 (1972).
9) A. Itai and N. Tomioka, Abstracts of Papers, The 12th Symposium of Structure–Activity Relationships, Osaka, November 1984, p. 285.

[Chem. Pharm. Bull. 35(11)4517—4523(1987)]

# Lipid A and Related Compounds. XV.[1] Efficient Synthesis of Novel Analogs of Glucosamine-4-phosphate, the Nonreducing Sugar Moiety of Lipid A

SHIN-ICHI NAKAMOTO, TOSHIO TAKAHASHI, KIYOSHI IKEDA, and KAZUO ACHIWA*

*School of Pharmaceutical Science, University of Shizuoka, Oshika 2-2-1, Shizuoka 422, Japan*

(Received April 30, 1987)

An efficient method for the synthesis of monosaccharide analogs of the nonreducing sugar moiety of lipid A is described. A brief analysis of their biological activities is also presented.

**Keywords**——lipid A analog; glucosamine derivative; 4-phosphorylated monosaccharide; antitumor activity; lethal toxicity; mitogenic activity

Lipid A is of considerable biological and pharmacological interest, because it is responsible for the expression of many biological activities[2] of the lipopolysaccharide (LPS) of gram-negative bacteria, *e.g.* endotoxicity, adjuvanticity, antitumor activity and so on. Recent chemical analysis revealed that lipid A is composed of two structural parts, D-glucosamine-1-phosphate (reducing sugar part) and D-glucosamine-4-phosphate (nonreducing sugar part) substituted by ester and amide-bound fatty acid,[3] as shown in Chart 1. Although Shiba *et al.*[4] and our group[1a,d] have established synthetic routes for the reducing sugar part lipid A (lipid X and lipid Y), no general method for the synthesis of the nonreducing sugar part has been developed.

In a recent communication,[1b] we reported a novel synthesis of the corresponding D-glucosamine-4-phosphate as the nonreducing sugar part to clarify which moiety is more

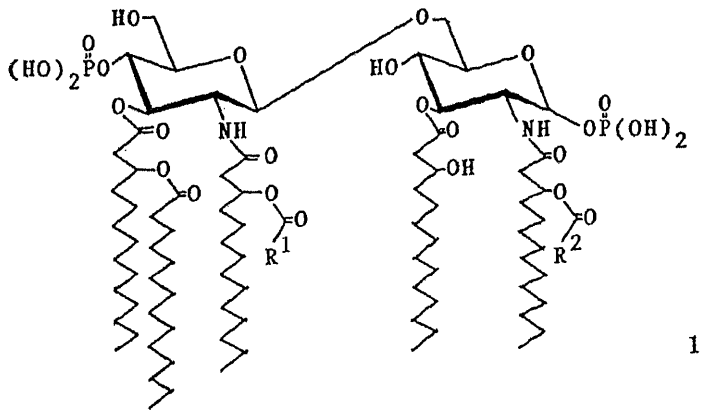

1

←nonreducing sugar part→ ←reducing sugar part→

**1a**: $R^1=CH_3(CH_2)_{10}$, $R^2=H$ (*Escherichia coli*)

**1b**: $R^1=CH_3(CH_2)_{10}$, $R^2=CH_3(CH_2)_{14}$ (*Salmonella minnesota*)

**1c**: $R^1=CH_3(CH_2)_{12}$, $R^2=H$ or $CH_3(CH_2)_{14}$ (*Proteus mirabilis*)

Chart 1

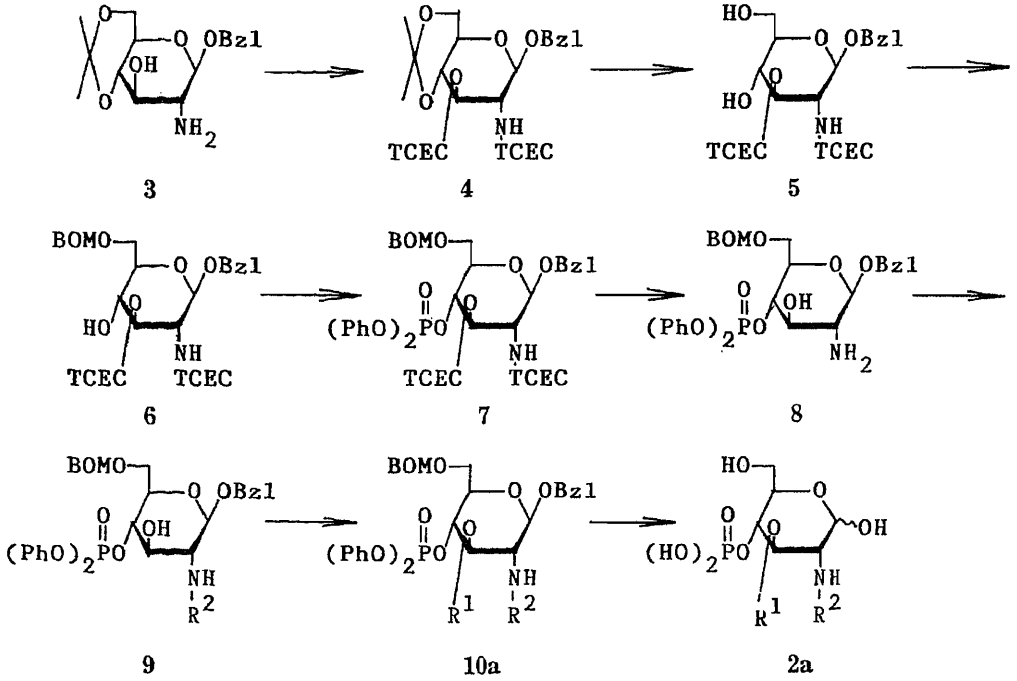

TCEC = $CCl_3CH_2OCO$–, BOM = $C_6H_5CH_2OCH_2$–, Bzl = $C_6H_5CH_2$–
**10a, 2a**: $R^1 = C_{14}$–O–$C_{14}$, $R^2 = C_{14}$–O–$C_{12}$
**10b, 2b**: $R^1 = C_{14}$–O–$C_{12}$, $R^2 = C_{14}$–O–$C_{12}$
**10c, 2c**: $R^1 = C_{14}$–O–$C_{14}$, $R^2 = C_{14}$–O–$C_{14}$
**10d, 2d**: $R^1 = C_{14}$–O–$C_{16}$, $R^2 = C_{14}$–O–$C_{16}$
$C_{14}$–O–$C_{12}$: (*R*)-3-dodecanoyloxytetradecanoyl $C_{14}$–O–$C_{14}$: (*R*)-3-tetradecanoyloxytetradecanoyl $C_{14}$–O–$C_{16}$:(*R*)-3-hexadecanoyloxytetradecanoyl

Chart 2

important for the expression of these biological activities of lipid A. Our strategy included the introduction of optically active fatty acid moieties at the desired positions in the final stage. Thus, the monosaccharide 4-phosphate (**8**) bearing one unsubstituted amino group and one free hydroxyl group at the C-2 and C-3 positions of glucosamine skeleton, respectively, was exploited as the common intermediate. Efficient conversion of **8** into several 4-phosphorylated monosaccharides (**2a—d**) substituted with suitable fatty acid groups was found to proceed smoothly. This paper describes these results in detail, as summarized in Chart 2.

Synthesis of the key compound (**8**) was carried out as follows. A synthetic intermediate (**3**) employed in the previous work[1d] was used as the starting material. The diacylate (**4**) was readily prepared in 96% yield by reacting the free amino and hydroxyl groups of **3** with 2,2,2-trichloroethoxycarbonyl chloride (TCEC-Cl) and pyridine in the presence of a catalytic amount of 4-dimethylaminopyridine (DMAP)[5] at room temperature for 2 h. The infrared (IR) spectrum of **4** showed absorption bands at 1770 and 1745 $cm^{-1}$ (>C=O). The nuclear magnetic resonance ($^1$H-NMR) spectrum of **4** showed signals of the methylene protons of the TCEC groups at 4.64 and 4.75 ppm. Removal of the isopropylidene group of **4** was accomplished by hydrolysis with aqueous 90% acetic acid at 90 °C for 15 min to give the diol (**5**) in 99% yield. The primary hydroxyl group of **5** was selectively protected with benzyloxymethyl chloride (BOM-Cl) and tetramethylurea in dichloromethane at room temperature for 16 h to afford the 6-*O*-benzyloxymethyl ether (**6**) in 86% yield. Subsequent phosphorylation of **6** was carried out with diphenyl phosphorochloridate, pyridine and DMAP in benzene[6] at room temperature for 2 h to give the diphenylphosphate (**7**) in 87% yield. Deprotection of the TCEC groups of **7** was accomplished by treatment with excess zinc

powder in acetic acid at room temperature for 5 h to afford the key common intermediate (**8**) in 90% yield. The structure of **8** was confirmed by disappearance of the methylene protons of the TCEC groups in the $^1$H-NMR spectrum and that of the carbonyl absorption in the IR spectrum.

Acylation of this key compound (**8**) with the desired acyl groups proceeded smoothly. The amino-hydroxy compound (**8**) was first acylated at the amino group with (*R*)-3-dodecanoyloxytetradecanoic acid in the presence of 1,3-dicyclohexylcarbodiimide (DCC) in dichloromethane at 5 °C to give the monoacylate (**9**) in 49% yield. The remaining hydroxyl group of **9** was acylated with (*R*)-3-tetradecanoyloxytetradecanoic acid and DCC containing a catalytic amount of DMAP in dichloromethane to give the diacylate (**10a**) in 70% yield. The protective benzyl and phenyl groups of **10a** were removed stepwise by hydrogenolysis catalyzed by 10% Pd-on-carbon at 45 °C for 5 h and then $PtO_2$ at room temperature for 16 h in methanol[7] to yield **2a** in 56% yield after purification on a silica gel column (chloroform : methanol = 10 : 1) followed by lyophilization from dioxane.

Similarly, the diacylates (**10a—d**) were obtained by simultaneous acylation of the amino and hydroxyl groups of **8** with the corresponding fatty acids in the presence of DCC and DMAP in dichloromethane at room temperature in 62% (**10b**), 40% (**10c**), and 52% (**10d**) yields, respectively. The monosaccharide analogs, nonreducing moieties of lipid A (**2b—d**), were also obtained by hydrogenolysis as described for **2a**, in 47% (**2b**), 42% (**2c**), and 31% (**2d**) yields, respectively. These compounds (**2a—d**) showed the characteristic blue color with the phosphate-specific spray reagent.[8]

Compound **10a** was also prepared by acylation in the early stage from intermediate **3** as shown in Chart 3.

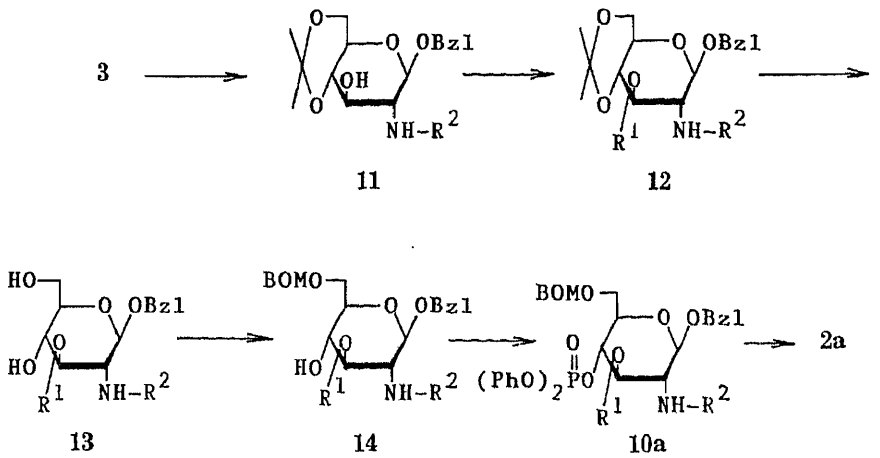


BOM: $C_6H_5CH_2OCH_2$–, Bzl: $C_6H_5CH_2$–
**10a, 2a**: $R^1 = C_{14}$–O–$C_{14}$, $R^2 = C_{14}$–O–$C_{12}$

Chart 3

The diacylate (**12**) was obtained under the same experimental conditions as above (**8**→**10a**). At first, the amino-hydroxy compound (**3**) was acylated at the amino group with (*R*)-3-dodecanoyloxytetradecanoic acid and DCC in dichloromethane at 0—5 °C to give the monoacylate (**11**) in 51% yield and an additional by-product (**11'**) was separated from this reaction mixture in 21% yield. The formation of this side product may be attributed to the acylation of **3** with the active acid anhydride (A) which was formed by intramolecular rearrangement of the DCC additive as shown in Chart 4.

The hydroxy group of **11** was acylated with (*R*)-3-dodecanoyloxytetradecanoic acid, DCC and DMAP in dichloromethane to afford the diacylate (**12**) in 91% yield. Deprotection

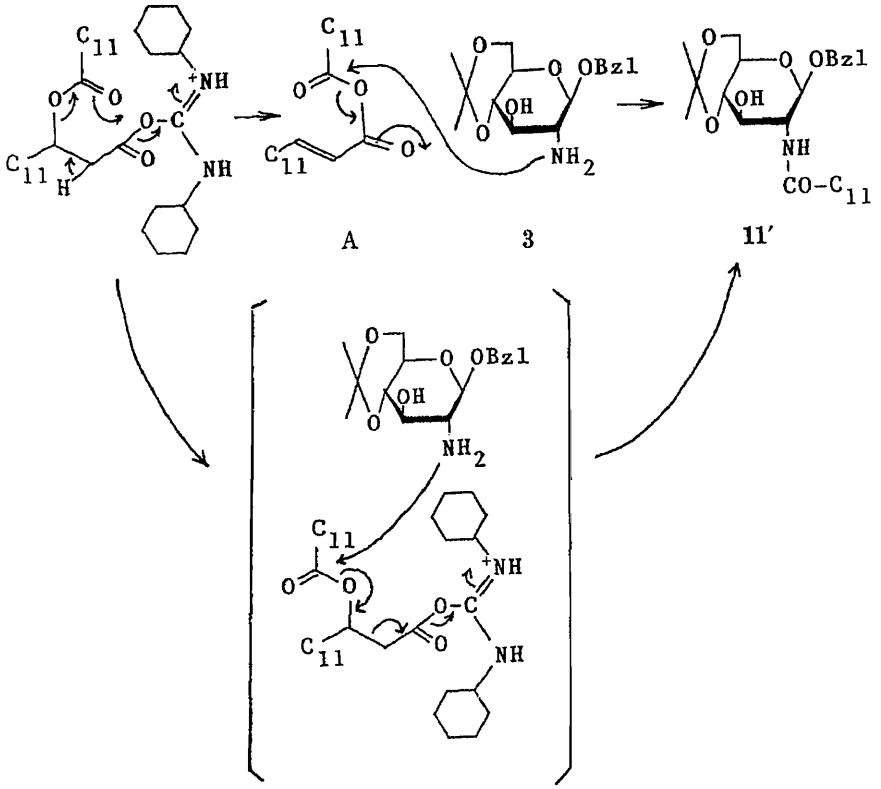


Chart 4

of the isopropylidene group of **12** was accomplished by hydrolysis with aqueous 90% acetic acid at 80 °C for 40 min to yield the diol (**13**) in 84% yield. Subsequently, selective benzyloxymethylation of the hydroxyl group at the C-6 position of **13** afforded the benzyloxymethyl ether (**14**) in 92% yield. The 4-hydroxyl group of **14** was phosphorylated with diphenyl phosphorochloridate, pyridine, and DMAP to give the 4-*O*-phosphate in 85% yield; it was indistinguishable from an authentic sample (**10a**).

The structures of all compounds were characterized by $^1$H-NMR and IR spectroscopies, as well as elemental analyses.

The biological effects (antitumor activity, lethal toxicity, and mitogenicity) of four synthetic monosaccharide analogs (**2a**—**d**) of lipid A were tested.[1h] Although the antitumor activities of 4-*O*-phosphorylglucosamines (**2a**—**d**) were weaker than that of the natural lipopolysaccharide, the activities of **2b** and **2c** were significant, whereas **2a** and **2d** were less effective. The synthetic compounds (**2a**—**d**) exhibited lethal toxicity, and had little or no mitogenic activity.

## Experimental

All melting points were determined with a micro-melting point apparatus (Yanagimoto) and are uncorrected. Optical rotations were measured on a JASCO DIP-140 digital polarimeter. IR spectra were measured on a JASCO A-202 infrared spectrophotometer. $^1$H-NMR spectra were recorded on a JEOL JNM-FX90Q (90 MHz) FT-NMR spectrometer with tetramethylsilane (TMS) as an internal standard. Chemical shifts were recorded in values ($\delta$) downfield from TMS and the abbreviations of signal patterns are as follows: s, singlet; d, doublet; t, triplet; q, quartet; m, multiplet; br, broad. Thin layer chromatography (TLC) was performed on silica gel (Kiesel 60$F_{254}$ on aluminium sheets, Merck). All compounds were located by spraying with sulfuric acid and heating on a hot plate. Phosphorus-containing compounds were detected by spraying with phosphate-specific spray reagent. Column chromatography was performed on silica gel (Kiesel gel 60, 70—230 mesh, Merck). Evaporations were carried out under reduced pressure at 35 °C.

**Benzyl 2-Deoxy-4,6-*O*-isopropylidene-2-[(2,2,2-trichloroethoxycarbonyl)amino]-3-*O*-(2,2,2-trichloroethoxycarbonyl)-β-D-glucopyranoside (4)**——TCEC-Cl (3.18 g, 15 mmol) was added dropwise to a solution of benzyl 2-amino-2-deoxy-4,6-*O*-isopropylidene-β-D-glucopyranoside (**3**) (0.464 g, 1.50 mmol) in dry pyridine (12.6 ml) at 0 °C with stirring. The mixture was warmed at room temperature and stirred for 20 h, the reaction being monitored by TLC (chloroform : isopropyl ether = 10 : 1). After complete disappearance of the starting material, *n*-hexane was added, the insoluble residue was filtered off and the filtrate was concentrated to dryness. The residue was purified on a column (25 g) of silica gel (chloroform : isopropyl ether = 20 : 1) to give **4** (0.950 g, 96%), mp 65—68 °C. $[\alpha]_D^{18}$ −32.5° ($c$ = 1.20, $CHCl_3$). IR (KBr): 3392, 1770, 1745, 1541, 1283, 858, 822, 739 $cm^{-1}$. $^1$H-NMR ($CDCl_3$) $\delta$: 1.30, 1.42 (each 3H, s, $Me_2C$), 4.64, 4.75 (each 2H, br s, $CH_2CCl_3 \times 2$), 7.22 (5H, s, Ph). *Anal.* Calcd for $C_{22}H_{25}Cl_6NO_9$: C, 40.02; H, 3.83; N, 2.12. Found: C, 39.48; H, 3.68; N, 2.02.

**Benzyl 2-Deoxy-2-[(2,2,2-trichloroethoxycarbonyl)amino]-3-*O*-(2,2,2-trichloroethoxycarbonyl)-β-D-glucopyranoside (5)**——A solution of **4** (0.860 g, 1.30 mmol) in aqueous 90% acetic acid was stirred at 85—90 °C for 15 min. The mixture was concentrated to dryness. The residue was purified on a column (25 g) of silica gel (chloroform : methanol = 20 : 1) to give **5** (0.80 g, 99%), mp 102—103 °C. $[\alpha]_D^{18}$ −26.2° ($c$ = 1.20, $CHCl_3$). IR (KBr): 3350, 1762, 1720, 1548, 1382, 1290, 820, 738 $cm^{-1}$. $^1$H-NMR ($CDCl_3$) $\delta$: 4.64, 4.75 (each 2H, br s, $CH_2CCl_3 \times 2$), 7.23 (5H, s, Ph). *Anal.* Calcd for $C_{19}H_{21}Cl_6NO_9$: C, 36.80; H, 3.41; N, 2.26. Found: C, 36.85; H, 3.31; N, 2.18.

**Benzyl 6-*O*-Benzyloxymethyl-2-deoxy-2-[(2,2,2-trichloroethoxycarbonyl)amino]-3-*O*-(2,2,2-trichloroethoxycarbonyl)-β-D-glucopyranoside (6)**——A mixture of **5** (4.63 g, 7.5 mmol) and Molecular Sieves 4A (1.0 g) in dichloromethane (100 ml) was stirred for 30 min. After addition of tetramethylurea (4.35 g, 37.5 mmol) to the mixture, benzyloxymethyl chloride (7.04 g, 45 mmol) was added dropwise at room temperature over a period of 60 min. After 5 h, when TLC (chloroform : isopropyl ether = 10 : 3) showed the reaction to be complete, the insoluble material was filtered off and the filtrate was washed with saturated aqueous sodium hydrogen carbonate (50 ml) and water (25 ml), then dried ($MgSO_4$). After removal of the solvent, the residual syrup was purified on a column (200 g) of silica gel (chloroform : isopropyl ether = 50 : 1) to give **6** (3.72 g, 86%), amorphous. $[\alpha]_D^{23}$ −24.2° ($c$ = 0.82, $CHCl_3$). IR (KBr): 3400, 1768, 1538, 1382, 1283, 1258, 821, 738 $cm^{-1}$. $^1$H-NMR ($CDCl_3$) $\delta$: 4.6—4.7 (6H, m, $NCO_2CH_2CCl_3$, $OCH_2OCH_2Ph$), 4.71 (2H, br s, $OCO_2CH_2CCl_3$), 7.23 (10H, s, Ph × 2). *Anal.* Calcd for $C_{27}H_{29}Cl_6NO_{10}$: C, 43.81; H, 3.95; N, 1.89. Found: C, 43.97; H, 3.98; N, 1.84.

**Benzyl 6-*O*-Benzyloxymethyl-4-*O*-diphenylphosphono-2-[(2,2,2-trichloroethoxycarbonyl)amino]-3-*O*-(2,2,2-trichloroethoxycarbonyl)-β-D-glucopyranoside (7)**——Diphenyl phosphorochloridate (1.34 g, 5 mmol) was added to a mixture of **6** (0.74 g, 1.0 mmol), pyridine (0.40 g, 5 mmol), DMAP (0.61 g, 5 mmol) and Molecular Sieves 4A (0.5 g) in benzene (5 ml) at 0 °C under nitrogen. The reaction mixture was warmed at room temperature and stirred for 2 h. A small amount of water was added to the cooled reaction mixture and the whole was diluted with benzene. The organic phase was successively washed with saturated aqueous sodium hydrogen carbonate and water, and dried ($MgSO_4$). The solvent was evaporated off to give the crude product, which was purified on column (25 g) of silica gel (chloroform : isopropyl ether = 50 : 1) to give **7** (0.85 g, 87%), mp 119—120 °C. $[\alpha]_D^{23}$ −8.57° ($c$ = 0.98, $CHCl_3$). IR (KBr): 3300, 1764, 1545, 1280, 1248, 1020, 952, 812, 731 $cm^{-1}$. *Anal.* Calcd for $C_{39}H_{38}Cl_6NO_{13}P$: C, 48.81; H, 3.95; N, 1.44. Found: C, 48.54; H, 3.93; N, 1.37.

**Benzyl 2-Amino-6-*O*-benzyloxymethyl-2-deoxy-4-*O*-diphenylphosphono-β-D-glucopyranoside (8)**——Zinc powder (2.40 g, 36.7 mmol) was added to a solution of **7** (1.85 g, 1.90 mmol) in acetic acid (18.5 ml) and the mixture was stirred at 25 °C for 5 h, after which time TLC (chloroform : methanol = 10 : 1) showed the reaction to be complete. The mixture was concentrated to dryness, then removal of acetic acid was performed by co-distillation with toluene under reduced pressure. The residual syrup was purified on a column (50 g) of silica gel (chloroform : methanol = 100 : 3) to give the key common intermediate (**8**) (1.06 g, 90%), mp 40—45 °C. $[\alpha]_D^{21}$ +9.47° ($c$ = 1.14, $CHCl_3$). IR (KBr): 3300, 1592, 1276, 1190, 1030, 955, 751 $cm^{-1}$. $^1$H-NMR ($CDCl_3$) $\delta$: 4.5—4.6 (4H, m, $OCH_2O$, $CH_2Ph$), 7.1—7.2 (20H, m, Ph × 4). *Anal.* Calcd for $C_{33}H_{36}NO_9P \cdot 3H_2O$: C, 58.66; H, 6.27; N, 2.07. Found: C, 58.38; H, 5.99; N, 1.84.

**Benzyl 6-*O*-Benzyloxymethyl-2-deoxy-4-*O*-diphenylphosphono-2-[(*R*)-3-dodecanoyloxytetradecanamido]-β-D-glucopyranoside (9)**——Dicyclohexylcarbodiimide (0.070 g, 0.34 mmol) was added to a stirred solution of **8** (0.124 g, 0.20 mmol) and (*R*)-3-dodecanoyloxytetradecanoic acid (0.120 g, 0.28 mmol) in dry dichloromethane (2 ml) at 0 °C under nitrogen. The mixture was stirred for 2 h at room temperature. The resulting suspension was filtered and the filtrate was concentrated to dryness. The residue was purified on a column (10 g) of silica gel (chloroform : isopropyl ether = 50 : 1) to give **9** (0.100 g, 48%), mp 97—99 °C. $[\alpha]_D^{23}$ −13.1° ($c$ = 0.61, $CHCl_3$). IR (KBr): 3380, 3330, 2930, 1720, 1652, 1562, 1288, 1194, 1035, 941, 695 $cm^{-1}$. *Anal.* Calcd for $C_{59}H_{83}NO_{12}P$: C, 68.85; H, 8.13; N, 1.36. Found: C, 68.64; H, 8.08; N, 1.34.

**Benzyl 6-*O*-Benzyloxymethyl-2-deoxy-4-*O*-diphenylphosphono-2-[(*R*)-3-dodecanoyloxytetradecanamido]-3-*O*-[(*R*)-3-tetradecanoyloxytetradecanoyl]-β-D-glucopyranoside (10a)**——i) From **9**: DCC (0.155 g, 0.75 mmol) was added to a stirred solution of **9** (0.310 g, 0.30 mmol), (*R*)-3-tetradecanoyloxytetradecanoic acid (0.340 g, 0.75 mmol), and DMAP (0.024 g, 0.20 mmol) in dry dichloromethane (2.5 ml) at 0 °C under nitrogen. The mixture was stirred for 1 h at 5 °C, then at room temperature for 2 h. The resulting suspension was filtered and the filtrate was concentrated to dryness. The residue was purified on a column (10 g) of silica gel (chloroform : isopropyl ether = 50 : 1) to afford **10a**

(0.310 g, 70%), mp 71—73 °C. $[\alpha]_D^{25}$ −8.94° ($c$=0.94, $CHCl_3$). IR (KBr): 3380, 2930, 1729, 1498, 1288, 1200, 1112, 1040, 954, 756, 697 $cm^{-1}$. $^1$H-NMR ($CDCl_3$) $\delta$: 0.88 [12H, t, $J$=5.6 Hz, $-CH-(CH_2)_{10}C\underline{H}_3\times2$, $-CO(CH_2)_{10}C\underline{H}_3$, $-CO(CH_2)_{12}C\underline{H}_3$], 1.25 [80H, brs, $-CH(C\underline{H}_2)_{10}CH_3\times2$, $-COCH_2(C\underline{H}_2)_9CH_3$, $-COCH_2(C\underline{H}_2)_{11}CH_3$], 2.1—2.5 (8H, m, $COCH_2\times4$), 6.12 (1H, brd, $J$=6.6 Hz, NH), 7.13—7.22 (20H, m, Ph×4). *Anal.* Calcd for $C_{87}H_{136}NO_{15}P$: C, 71.23; H, 9.34; N, 0.95. Found: C, 71.42; H, 9.60; N, 0.91.

ii) From **14**: Diphenyl phosphorochloridate (0.128 g, 0.475 mmol) was added to a stirred solution of **14** (0.117 g, 0.095 mmol), pyridine (0.036 g, 0.475 mmol), and 4-dimethylaminopyridine (0.058 g, 0.475 mmol) in benzene (2 ml) at 0 °C under nitrogen. The mixture was warmed at room temperature and stirred for 2 h. The reaction mixture was filtered, and the filtrate was washed with water and dried ($MgSO_4$). After removal of the solvent, the residue was purified on a column (5 g) of silica gel (chloroform : isopropyl ether=40 : 1) to give **10a** (0.118 g, 85%), mp 70—73 °C. $[\alpha]_D^{22}$ −9.04° ($c$=1.02, $CHCl_3$). *Anal.* Calcd for $C_{87}H_{136}NO_{15}P$: C, 71.23; H, 9.34; N, 0.95. Found: C, 71.23; H, 9.49; N, 0.92.

**Benzyl 6-*O*-Benzyloxymethyl-2-deoxy-4-*O*-diphenylphosphono-2-[(*R*)-3-dodecanoyloxytetradecanamido]-3-*O*-[(*R*)-3-dodecanoyloxytetradecanoyl]-β-D-glucopyranoside (10b)**——Treatment of **8** (0.124 g, 0.20 mmol) as described for **10a** gave **10b** (0.178 g, 62%), mp 40—45 °C. $[\alpha]_D$ −15.8° ($c$=0.96, $CHCl_3$).

**Benzyl 6-*O*-Benzyloxymethyl-2-deoxy-4-*O*-diphenylphosphono-2-[(*R*)-3-tetradecanoyloxytetradecanamido]-3-*O*-[(*R*)-3-tetradecanoyl]-β-D-glucopyranoside (10c)**——Treatment of **8** (0.124 g, 0.20 mmol) as described for **10a** gave **10c** (0.120 g, 40%), mp 62—64 °C. $[\alpha]_D^{21}$ −9.75° ($c$=0.80, $CHCl_3$).

**Benzyl 6-*O*-Benzyloxymethyl-2-deoxy-4-*O*-diphenylphosphono-2-[(*R*)-3-hexadecanoyloxytetradecanamido]-3-*O*-[(*R*)-3-hexadecanoyloxytetradecanoyl]-β-D-glucopyranoside (10d)**——Treatment of **8** (0.124 g, 0.20 mmol) as described for **10a** gave **10d** (0.160 g, 52%), mp 60—63 °C. $[\alpha]_D^{20}$ −11.5° ($c$=1.00, $CHCl_3$).

**2-Deoxy-2-[(*R*)-3-dodecanoyloxytetradecanamido]-4-phosphono-3-*O*-[(*R*)-3-tetradecanoyloxytetradecanoyl]-D-glucopyranose (2a)**——A solution of **10a** (0.147 g, 0.10 mmol) in methanol (4 ml) was hydrogenated in the presence of 10% Pd-on-carbon at 40—45 °C under slight pressure, the reaction being monitored by TLC (chloroform : methanol=10 : 1, $Rf$=0.6). The catalyst was filtered off and Adams platinum catalyst (0.040 g) was added to the filtrate. Hydrogenolysis was continued at room temperature for 20 h, when TLC (chloroform : methanol=10 : 3, $Rf$=0.2) showed the reaction to be complete. The catalyst was filtered off and the filtrate was concentrated to dryness. The residue was purified on a column (10 g) of silica gel (chloroform : methanol=10 : 1) followed by lyophilization from dioxane to obtain the desired compound (**2a**) (0.062 g, 56%), mp 166—168 °C. $[\alpha]_D$ +33.5° ($c$=0.40, $CHCl_3$). IR (KBr): 3440, 2930, 1737, 1654, 1471, 1184, 1056 $cm^{-1}$. *Anal.* Calcd for $C_{60}H_{114}NO_4P\cdot2H_2O$: C, 63.24; H, 10.35; N, 1.23. Found: C, 63.21; H, 10.25; N, 1.21.

**2-Deoxy-2-[(*R*)-3-dodecanoyloxytetradecanamido]-3-*O*-[(*R*)-3-dodecanoyloxytetradecanoyl]-4-*O*-phosphono-D-glucopyranose (2b)**——Treatment of **10b** (0.144 g, 0.10 mmol) as described for **2a** gave **2b** (0.051 g, 47%), amorphous. $[\alpha]_D^{25}$ +11.0° ($c$=0.80, $CHCl_3$). *Anal.* Calcd for $C_{58}H_{110}NO_{14}P\cdot4H_2O$; C, 60.71; H, 10.27; N, 1.22. Found: C, 60.58; H, 10.01; N, 1.14.

**2-Deoxy-4-*O*-phosphono-2-[(*R*)-3-tetradecanoyloxytetradecanamido]-3-*O*-[(*R*)-tetradecanoyloxytetradecanoyl]-D-glucopyranose (2c)**——Treatment of **10c** (0.070 g, 0.047 mmol) as described for **2a** gave **2c** (0.022 g, 42%), mp 155—157 °C. $[\alpha]_D^{24}$ +10.5° ($c$=0.40, $CHCl_3$). *Anal.* Calcd for $C_{62}H_{118}NO_{14}P\cdot H_2O$: C, 64.89; H, 10.28; N, 1.22. Found: C, 64.88; H, 10.29; N, 1.17.

**2-Deoxy-2-[(*R*)-3-hexadecanoyloxytetradecanamido]-3-*O*-[(*R*)-3-tetradecanoyloxytetradecanoyl]-4-*O*-phosphono-D-glucopyranose (2d)**——Treatment of **10d** (0.058 g, 0.037 mmol) as described for **2a** gave **2d** (0.014 g, 31%), mp 157—159 °C. $[\alpha]_D^{24}$ +19.4° ($c$=1.24, $CHCl_3$). *Anal.* Calcd for $C_{66}H_{126}NO_{14}P\cdot2H_2O$: C, 64.72; H, 10.70; N, 1.14. Found: C, 64.92; H, 10.50; N, 1.07.

**Benzyl 2-Deoxy-4,6-*O*-isopropylidene-2-[(*R*)-3-dodecanoyloxytetradecanamido]-β-D-glucopyranoside (11)**——DCC (1.03 g, 5 mmol) was added to a stirred solution of **3** (1.24 g, 4 mmol) and (*R*)-3-dodecanoyloxytetradecanoic acid (2.13 g, 5 mmol) in dry dichloromethane (10 ml) at 0 °C under nitrogen. The mixture was warmed at room temperature and stirred for 4 h. The resulting suspension was filtered and the filtrate was washed with water and dried ($MgSO_4$). After removal of the solvent, the residue was purified on a column (50 g) of silica gel (chloroform : isopropyl ether=20 : 1) to give **11** (1.45 g, 51%) and a by-product (**11'**) (0.41 g, 21%).

Data for **11**: mp 61—62 °C. $[\alpha]_D^{24}$ −48.3° ($c$=0.82, $CHCl_3$). IR (KBr): 3380, 2930, 1728, 1664, 1535, 1104, 858, 700 $cm^{-1}$. $^1$H-NMR ($CDCl_3$) $\delta$: 0.89 [6H, t, $J$=5.5 Hz, $-CH(CH_2)_{10}C\underline{H}_3$, $-CO(CH_2)_{10}C\underline{H}_3$], 1.25 [38H, brs, $-CH(C\underline{H}_2)_{10}CH_3$, $-COCH_2(C\underline{H}_2)_9CH_3$], 1.42, 1.50 (each 3H, s, $Me_2C$), 2.1—2.5 (4H, m, $COCH_2\times2$), 4.50, 4.85 (each 1H, d, $J$=11.4 Hz, $CH_2Ph$), 6.11 (1H, brd, $J$=5.4 Hz, NH). *Anal.* Calcd for $C_{42}H_{71}NO_8\cdot H_2O$: C, 68.54; H, 10.00; N, 1.90. Found: C, 68.17; H, 9.95; N, 1.94.

Data for **11'**: mp 114—116 °C. $[\alpha]_D^{23}$ −65.7° ($c$=0.84, $CHCl_3$). IR (KBr): 3300, 2930, 1649, 1554, 1378, 1086, 859, 730 $cm^{-1}$. $^1$H-NMR ($CDCl_3$) $\delta$: 0.86 [3H, t, $J$=5.6 Hz, $-CO(CH_2)_{10}C\underline{H}_3$], 1.25 [18H, brs, $-COCH_2(CH_2)_9CH_3$], 1.28, 1.37 (each 3H, s, $Me_2C$), 1.9—2.3 (2H, m, $COCH_2$), 4.42, 4.78 (each 1H, d, $J$=11.4 Hz, $CH_2Ph$), 4.56 (1H, d, $J$=7.8 Hz, H-1), 5.88 (1H, brd, $J$=5.4 Hz, NH), 7.26 (5H, s, Ph). *Anal.* Calcd for $C_{28}H_{45}NO_6$: C, 68.40; H, 9.23; N, 2.85. Found: C, 68.13; H, 9.22; N, 2.81.

**Benzyl 2-Deoxy-2-[(*R*)-3-dodecanoyloxytetradecanamido]-4,6-*O*-isopropylidene-3-*O*-[(*R*)-3-tetradecanoyloxy-**

**tetradecanoyl]-β-D-glucopyranoside (12)**——DCC (0.530 g, 2.44 mmol) was added to a stirred solution of **11** (1.40 g, 1.95 mmol), (*R*)-3-tetradecanoyloxytetradecanoic acid (1.11 g, 2.44 mmol), and DMAP (0.030 g, 0.244 mmol) in dichloromethane (10 ml) at 0 °C under nitrogen. The mixture was stirred at 10 °C for 2 h. The reaction suspension was filtered and the filtrate was washed with water and dried ($MgSO_4$). After removal of the solvent, the residue was purified on a column (50 g) of silica gel (chloroform : isopropyl ether = 20 : 1) to give **12** (2.05 g, 91%), mp 51—54 °C. $[\alpha]_D^{23}$ −23.4° (*c* = 0.32, $CHCl_3$). IR(KBr): 3330, 2925, 1737, 1658, 1180, 1093, 859, 733 $cm^{-1}$. $^1$H-NMR ($CDCl_3$) δ: 0.91 [12H, t, *J* = 5.4 Hz, $-CH(CH_2)_{10}CH_3 \times 2$, $-CO(CH_2)_{10}CH_3$, $-CO(CH_2)_{12}CH_3$], 1.24 [80H, brs, $-CH(CH_2)_{10}CH_3 \times 2$, $-COCH_2(CH_2)_9CH_3$, $-COCH_2(CH_2)_{11}CH_3$], 1.45, 1.55 (each 3H, s, $Me_2C$), 2.1—2.5 (8H, m, $COCH_2 \times 4$), 5.92 (1H, d, *J* = 9.0 Hz, NH), 7.22 (5H, s, Ph). *Anal.* Calcd for $C_{70}H_{123}NO_{11}$: C, 72.81; H, 10.74; N, 1.21. Found: C, 72.56; H, 10.73; N, 1.21.

**Benzyl 2-Deoxy-2-[(*R*)-3-dodecanoyloxytetradecanamido]-3-*O*-[(*R*)-3-tetradecanoyloxytetradecanoyl]-β-D-glucopyranoside (13)**——A solution of **12** (1.83 g, 1.59 mmol) in 90% acetic acid (40 ml) was stirred at 80 °C for 40 min. The reaction mixture was evaporated to dryness after confirmation of complete of the reaction by TLC (chloroform : methanol = 10 : 1). The residue was purified on a column (15 g) of silica gel (chloroform : methanol = 20 : 1) to yield **13** (1.48 g, 84%), mp 103—105 °C. $[\alpha]_D^{23}$ −17.8° (*c* = 0.82, $CHCl_3$). IR (KBr): 3300, 2925, 1735, 1661, 1553, 1468, 1174, 1082, 731 $cm^{-1}$. $^1$H-NMR ($CDCl_3$) δ: 0.88 [12H, t, *J* = 5.4 Hz, $-CH(CH_2)_{10}CH_3 \times 2$, $CO(CH_2)_{10}CH_3$, $-CO(CH_2)_{12}CH_3$], 1.35 [80H, brs, $-CH(CH_2)_{10}CH_3 \times 2$, $-COCH_2(CH_2)_9CH_3$, $-COCH_2(CH_2)_{11}CH_3$], 2.1—2.7 (8H, m, $COCH_2 \times 4$), 6.15 (1H, brd, *J* = 7.8 Hz, NH), 7.23 (5H, s, Ph). *Anal.* Calcd for $C_{67}H_{119}NO_{11}$: C, 72.19; H, 10.76; N, 1.26. Found: C, 71.89; H, 10.77; N, 1.35.

**Benzyl 6-*O*-Benzyloxymethyl-2-deoxy-2-[(*R*)-dodecanoyloxytetradecanamido]-3-*O*-[(*R*)-3-tetradecanoyloxytetradecanoyl]-β-D-glucopyranoside (14)**——Benzyloxymethyl chloride (0.173 g, 0.87 mmol) was added to a stirred solution of **13** (0.163 g, 0.146 mmol) and tetramethylurea (0.085 g, 0.73 mmol) in dry dichloromethane (2.2 ml) at 0 °C under nitrogen. The mixture was warmed at room temperature and stirred for 16 h. The reaction mixture was washed with brine, dried ($MgSO_4$), and concentrated to dryness. The residue was purified on a column (10 g) of silica gel (chloroform : isopropyl ether = 20 : 1) to give **14** (0.166 g, 92%), mp 65—68 °C. $[\alpha]_D^{16}$ −21.0° (*c* = 0.92, $CHCl_3$). IR (KBr): 2930, 1732, 1660, 1039 $cm^{-1}$. $^1$H-NMR ($CDCl_3$) δ: 0.88 [12H, t, *J* = 5.6 Hz, $-CH(CH_2)_{10}CH_3 \times 2$, $-CO(CH_2)_{10}CH_3$, $-CO(CH_2)_{12}CH_3$], 1.24 [80H, brs, $-CH(CH_2)_{10}CH_3$, $-COCH_2(CH_2)_9CH_3$, $-COCH_2(CH_2)_{11}CH_3$], 2.0—2.5 (8H, m, $COCH_2 \times 4$), 5.90 (1H, brd, *J* = 6.1 Hz, NH), 7.20, 7.24 (each 5H, s, Ph), *Anal.* Calcd for $C_{75}H_{127}NO_{12}$: C, 72.65; H, 10.37; N, 1.13. Found: C, 72.65; H, 10.35; N, 1.11.

**Acknowledgment** The authors are indebted to Dr. K. Narita and the staff of the Analysis Center of this college for microanalysis. This work was supported in part by a Grant-in-Aid from Tokyo Biochemical Research Foundation.

## References

1) *a*) T. Takahashi, C. Shimizu, S. Nakamoto, K. Ikeda, and K. Achiwa, *Chem. Pharm. Bull.*, **33**, 1760 (1985); *b*) S. Nakamoto, T. Takahashi, K. Ikeda, and K. Achiwa, *ibid.*, **33**, 4098 (1985); *c*) T. Shimizu, S. Akiyama, T. Masuzawa, Y. Yanagihara, S. Nakamoto, T. Takahashi, K. Ikeda, and K. Achiwa, *ibid.*, **33**, 4621 (1985); *d*) K. Ikeda, S. Nakamoto, T. Takahashi, and K. Achiwa, *Carbohydr. Res.*, **145**, C5 (1986); *e*) T. Takahashi, S. Nakamoto, K. Ikeda, and K. Achiwa, *Tetrahedron Lett.*, **27**, 1819 (1986); *f*) S. Nakamoto and K. Achiwa, *Chem. Pharm. Bull.*, **34**, 2302 (1986); *g*) T. Shimizu, S. Akiyama, T. Masuzawa, Y. Yanagihara, S. Nakamoto, and K. Achiwa, *ibid.*, **34**, 2310 (1986); *h*) T. Shimizu, S. Akiyama, T. Masuzawa, Y. Yanagihara, S. Nakamoto, T. Takahashi, K. Ikeda, and K. Achiwa, *ibid.*, **34**, 5169 (1986); *i*) T. Shimizu, S. Akiyama, T. Masuzawa, Y. Yanagihara, S. Nakamoto, and K. Achiwa, *ibid.*, **35**, 873 (1987); *j*) K. Ikeda, T. Takahashi, H. Kondo, and K. Achiwa, *ibid.*, **35**, 1311 (1987); *k*) K. Ikeda, T. Takahashi, C. Shimizu, S. Nakamoto, and K. Achiwa, *ibid.*, **35**, 1383 (1987); *l*) T. Shimizu, S. Akiyama, T. Masuzawa, Y. Yanagihara, K. Ikeda, T. Takahashi, H. Kondo, and K. Achiwa, *Microbiol. Immunol.*, **31**, 381 (1987); *m*) T. Shimizu, S. Akiyama, T. Masuzawa, Y. Yanagihara, S. Nakamoto, and K. Achiwa, *Infection and Immunology*, **55**, 2287 (1987); *n*) K. Ikeda, S. Nakamoto, T. Takahashi, and K. Achiwa, *Chem. Pharm. Bull.*, **35**, 4436 (1987).
2) O. Westphal and O. Luderitz, *Angew. Chem.*, **66**, 407 (1954); O. Luderitz, C. Galanos, V. Lehmann, H. Mayer, E. T. Rietschel, and J. Weckesser, *Naturwissenschaften*, **65**, 578 (1978).
3) K. Takayama, N. Qureshi, and P. Mascagni, *J. Biol. Chem.*, **258**, 12801 (1983); M. Imoto, S. Kusumoto, T. Shiba, H. Naoki, T. Iwashita, E. Th. Rietschel, H.-W. Wollenweber, C. Galanos, and O. Luderitz, *Tetrahedron Lett.*, **24**, 4017 (1983); U. Seydel, B. Lindner, H.-W. Wollenweber, and E. T. Rietschel, *Eur. J. Biochem.*, **145**, 505 (1984).
4) S. Kusumoto, M. Yamamoto, and T. Shiba, *Tetrahedron Lett.*, **25**, 3727 (1984).
5) T. B. Windholz and D. B. R. Jonston, *Tetrahedron Lett.*, **1967**, 2555.
6) C. Diolez, M. Mondange, S. R. Sarfati, L. Szabo, and P. Szabo, *J. Chem. Soc., Perkin Trans. 1*, **1985**, 275.
7) D. Charon, M. Mondange and L. Szabo, *J. Chem. Soc., Perkin Trans. 1*, **1984**, 2291.
8) J. C. Dittmer and R. L. Lester, *J. Lipid. Res.*, **5**, 126 (1964).

[Chem. Pharm. Bull. 35(11)4524—4529(1987)]

# Studies on Chemical Constituents of Antitumor Fraction from *Periploca sepium* BGE. I

HIDEJI ITOKAWA,* JUNPING XU, and KOICHI TAKEYA

*Tokyo College of Pharmacy, Horinouchi 1432-1, Hachioji, Tokyo 192-03, Japan*

(Received March 26, 1987)

When the $CHCl_3$ extract obtained by partitioning the methanolic extract of *Periploca sepium* between $H_2O$ and $CHCl_3$ was subjected to column chromatography on silica gel, the antitumor activity against Sarcoma 180 ascites in mice was concentrated in the fraction eluted with $CHCl_3$–MeOH (10 : 1). From the antitumor fraction, eight products, S-1—S-8, were isolated. S-1 was identified as 12β-hydroxypregna-4,6,16-triene-3,20-dione (neridienone-A), obtained for the first time from Asclepiadaceous plants, by direct comparison with an authentic sample and the others were found to be steroidal glycosides. A new compound S-2A (named periplocogenin), and two known aglycones S-3A and S-5A, obtained by hydrolyzing the above glycosides with diluted acid, were respectively identified as 3β-*O*-(4′,6′-dideoxy-3′-*O*-methyl-$\Delta^{3'}$-D-2′-hexosulosyl)-$\Delta^5$-pregnene-17α,20(*S*)-diol, periplogenin, and $\Delta^5$-pregnene-3β,20(*S*)-diol from the proton and carbon-13 nuclear magnetic resonance spectral data. The structure of S-6A was identical with that of S-5A, and S-7A and S-8A were identical with S-2A.

**Keywords**——*Periploca sepium*; neridienone-A; periplocogenin; periplogenin; $\Delta^5$-pregnene-3β,20(*S*)-diol; antitumor activity

The crude drug "beiwujiapi," the root bark of *Periploca sepium* BGE. (Asclepiadaceae) is one of the famous "wujiapi" in Chinese literature and has been widely used as a tonic for at least two thousand years.[1] The presence of steroidal glycosides G, K, E, $H_1$ and $H_2$, and oligosaccharides $C_1$, $D_2$, $F_1$ and $F_2$ in this plant has been reported by Shoji *et al.*[2] In the course of screening for antineoplastic activity of crude drugs and collected plants by means of the total packed cell volume method using Sarcoma 180 ascites in mice,[3] we found that the methanolic extract of *P. sepium* exhibited significant antitumor activity. This paper deals mainly with the isolation and chemical constituents of the active fraction.

When the methanolic extract of *P. sepium* was fractionated as shown in Chart 1 with the guidance of bioassay against Sarcoma 180 ascites in mice, the antitumor activity was concentrated in the chloroform extract. Column chromatography of the chloroform extract on silica gel was carried out by eluting with benzene, benzene–$CHCl_3$ (1 : 1), $CHCl_3$, $CHCl_3$–MeOH (10 : 1) and (1 : 1) successively. In the above bioassay, only the $CHCl_3$–MeOH (10 : 1) fraction exhibited powerful antineoplastic activity (growth ratio (GR): 4.6%, +++) at the dose of 10 mg/kg/d for 5 consecutive days. When this fraction was divided into six subfractions by preparative thin layer chromatography (TLC) on silica gel using the solvent system of $CHCl_3$–MeOH (10 : 1), the antitumor activity was observed in three subfractions, each of which showed several spots. Therefore, the chemical constituents of the $CHCl_3$–MeOH (10 : 1) eluate were mainly examined. Repeated silica gel, RP-8 and RP-18 column chromatography of the active fraction gave eight compounds S-1—S-8. Except for S-1, these were steroidal glycosides, though work on S-4 is still in progress due to the difficulty of purification. After hydrolysis of S-2—S-8 with 0.05 N $H_2SO_4$ in 50% aqueous MeOH, each of the reaction mixtures was extracted with $CHCl_3$–MeOH (96 : 4). Three hydrolyzates, S-2A, S-

3A and S-5A, were obtained as crystalline products. Further, S-6A was identical with S-5A, and S-7A and S-8A were identical with S-2A. The chemical structures were established as follows.

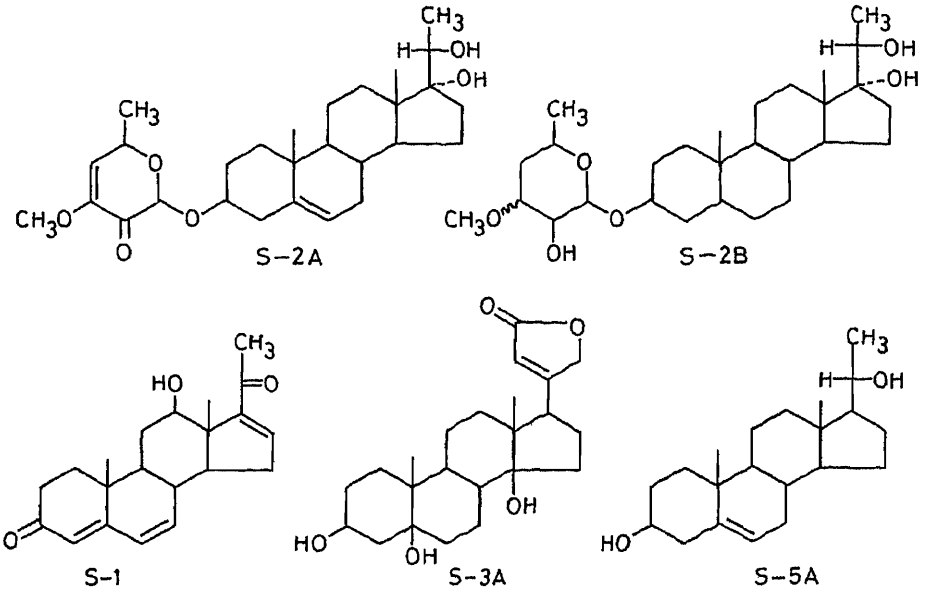


Fig. 1. Steroidal Compounds from *Periploca sepium*

TABLE I. $^{13}C$ Chemical Shifts of Pregnenes from *Periploca sepium*

| Carbon No. | S-1 | S-2A | S-3A | S-5A |
|---|---|---|---|---|
| 1, (1′) | 33.66 (t) | 37.55 (t), 97.26 (d) | 24.85 (t) | 37.33 (t) |
| 2, (2′) | 33.94 (t) | 29.37 (t), 185.90 (s) | 27.85 (t) | 31.64 (t) |
| 3, (3′) | 199.36 (s) | 78.56 (d), 147.81 (s) | 67.91 (d) | 71.82 (d) |
| 4, (4′) | 124.35 (d) | 38.52 (t), 118.49 (d) | 36.86 (t) | 42.36 (t) |
| 5, (5′) | 162.73 (s) | 140.31 (s), 68.88 (d) | 74.67 (s) | 140.85 (s) |
| 6, (6′) | 129.17 (d) | 121.96 (d), 23.00 (q) | 35.15 (t) | 121.62 (d) |
| 7 | 138.62 (d) | 31.92 (t) | 23.69 (t) | 31.93 (t) |
| 8 | 34.88 (d) | 31.83 (d) | 40.74 (d) | 31.72 (d) |
| 9 | 49.07 (d) | 49.72 (d) | 38.98 (d) | 50.19 (d) |
| 10 | 36.14 (s) | 36.73 (s) | 40.66 (s) | 36.59 (s) |
| 11 | 28.66 (t) | 20.53 (t) | 21.49 (t) | 20.86 (t) |
| 12 | 73.33 (d) | 31.07 (t) | 39.99 (t) | 38.87 (t) |
| 13 | 52.88 (s) | 45.67 (s) | 49.50 (s) | 41.69 (s) |
| 14 | 51.47 (d) | 51.41 (d) | 85.32 (s) | 58.49 (d) |
| 15 | 31.77 (t) | 23.54 (t) | 32.94 (t) | 25.68 (t) |
| 16 | 148.90 (d) | 37.65 (t) | 26.82 (t) | 24.26 (t) |
| 17 | 155.33 (s) | 85.76 (s) | 50.61 (d) | 56.65 (d) |
| 18 | 11.66 (q) | 14.01 (q) | 15.70 (q) | 12.51 (q) |
| 19 | 16.21 (q) | 19.34 (q) | 16.69 (q) | 19.44 (q) |
| 20 | 198.84 (s) | 72.35 (d) | 174.71 (s)[a] | 70.32 (d) |
| 21 | 26.75 (q) | 18.59 (q) | 73.53 (t) | 23.58 (q) |
| 22 | — | — | 117.38 (d) | — |
| 23 | — | — | 174.63 (s)[a] | — |

The measurements were made on a Bruker AM400 spectrometer in $CDCl_3$ with TMS as an internal reference and are expressed in terms of ppm. *a*) The assignments may be reversed.

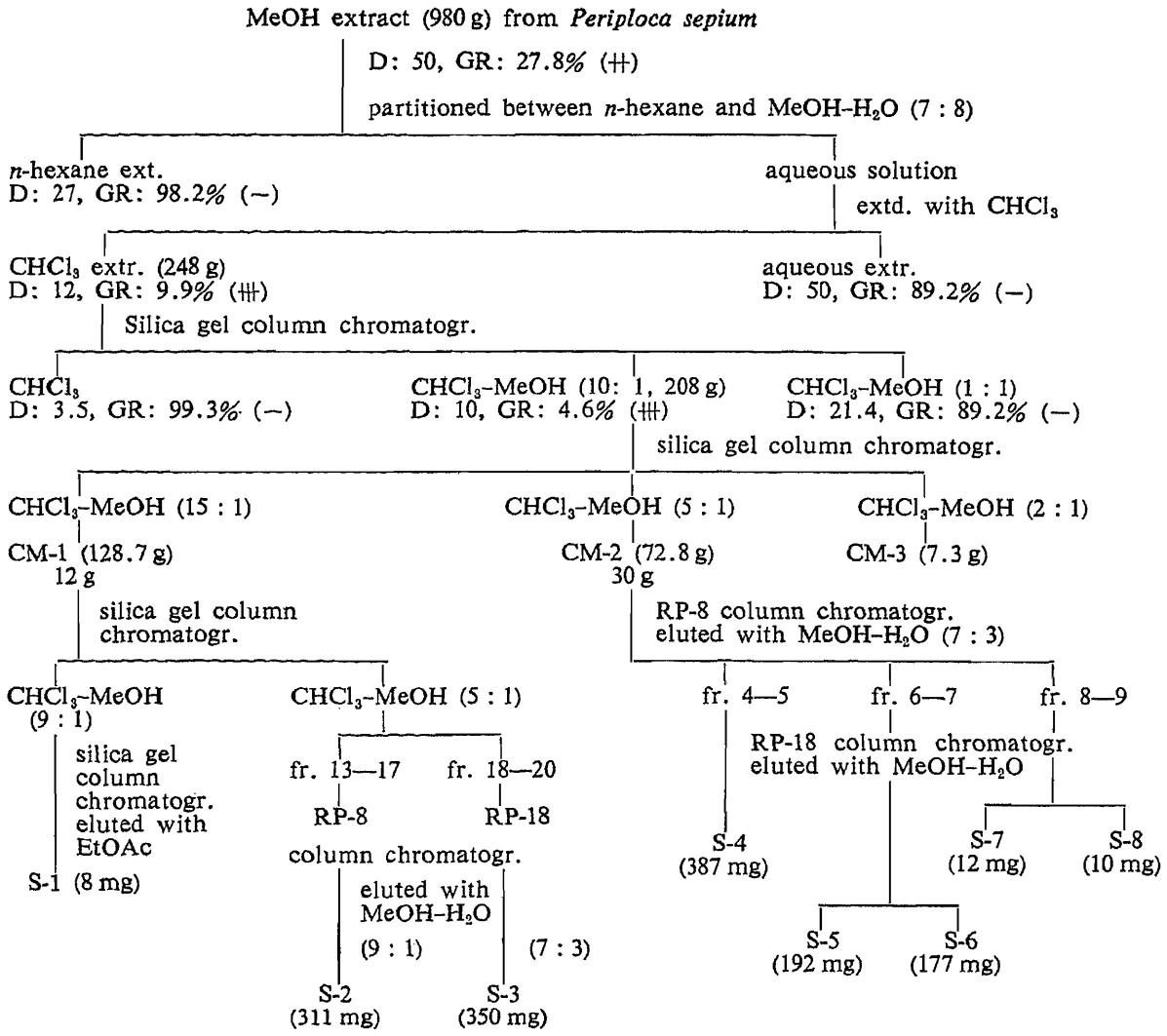


Chart 1. Procedure for Separation of S-1—S-8 from *P. sepium*

Antitumor activity was determined against Sarcoma 180 ascites in mice and the effectiveness was evaluated by the total packed cell volume method. Sarcoma 180 was implanted i.p. ($1 \times 10^6$) in ICR mice ($n=6$) on day 0.

Drugs were given daily at the indicated doses (i.p.) for 5 consecutive days (1—5 d). D means dose (mg/kg/d). GR means growth ratio; 0—10% (+++), 11—40% (++), 40—65% (+), over 66% (−).

S-1; $C_{21}H_{26}O_3$, mp 210—212 °C. This compound showed a molecular ion ($M^+$) at *m/z* 326 in the mass spectrum (MS) and appeared to have 4,6-dien-3-one and 16-en-20-one systems on the basis of the absorption bands in the ultraviolet (UV) (281 and 243 nm) and infrared (IR) (1655, 1650, 1620, and 1587 $cm^{-1}$) spectra, as well as olefinic proton signals at $\delta$ 5.70 (s), 6.13 (dd, $J=1.5$, 10 Hz); 6.17 (dd, $J=2.5$, 10 Hz) and 7.00 (dd, $J=2$, 3.4 Hz) in the proton nuclear magnetic resonance ($^1$H-NMR) spectrum. When the signal at $\delta$ 6.13 was irradiated, a nuclear Overhauser effect (NOE) could be seen (12% enhancement) at $\delta$ 5.70. On the basis of these data, S-1 was suggested to be 12$\beta$-hydroxypregna-4,6,16-triene-3,20-dione, and this was confirmed by comparing the IR, $^1$H- and $^{13}$C-NMR spectra with those of an authentic sample, neridienone-A.[4] This is the first time that this substance has been obtained from Asclepiadaceous plants.

S-2A; $C_{28}H_{42}O_6$, mp 203—206 °C. This compound was considered to contain $C_{21}$-steroidal and hexosulosyl moieties from the $^{13}$C-NMR spectrum. In the $^1$H-NMR spectrum,

the proton at C-20 of the steroidal moiety was observed as a quadruplet signal at $\delta$ 3.85 ($J$=6.4 Hz), which suggested the presence of a hydroxyl group at C-17. The methyl group at C-18 was observed as a singlet signal at $\delta$ 0.75, which was shifted upfield in comparison with those of 14$\beta$-androsteroidal compounds which are C/D-*cis*-pregnanes.[5] Since the acetonide derived from the two hydroxyl groups at C-17 and C-20 showed a cross signal between the two methyl groups at C-21 and C-18 in the H–H NOE correlated spectrum, the configuration at C-20 was deduced to be "*S*". The steroidal moiety of S-2A was therefore characterized as $\Delta^5$-pregnene-3$\beta$,17$\alpha$,20(*S*)-triol and the hexosulosyl moiety was attached to the C-3 hydroxyl group, because the carbon signal at C-3 was shifted downfield due to the glycosylation shifts.[6]

On the basis of the UV absorption maximum at 262 nm, the carbonyl group and double bond were considered to be conjugated in the hexosulosyl moiety. Since a singlet signal due to an anomeric proton at $\delta$ 5.06 was observed, the enone group was located as 3′-en-2′-one. The olefinic proton observed at $\delta$ 5.78 as a doublet ($J$=3 Hz) signal was coupled with a doublet of quartets ($J$=3 and 6.8 Hz) at $\delta$ 4.72 due to H-5′. The 3′-en-2′-one system was also suggested by the carbon signals at $\delta$ 185.90 (s, C-2′), 147.81 (s, C-3′) and 118.49 (d, C-4′), and the MS fragment peak at *m/z*: 112 (100%). In a comparison of the hexosulosyl moiety with that of affinoside O, which was isolated from *Anodendron affine* by Yamauchi *et al.*,[7] the $^1$H- and $^{13}$C-NMR chemical shifts of signals due to the hexosulosyl moieties of the two compounds were in good agreement with each other. Also, the decoupling examination of S-2B prepared by reducing S-2A with Pd–C/$H_2$ supported the above structural features. The hexosulosyl moiety of S-2A was concluded to be 4,6-dideoxy-3-*O*-methyl-$\Delta^3$-D-2-hexosulose. Therefore, S-2A was confirmed to be 3$\beta$-*O*-(4′,6′-dideoxy-3′-*O*-methyl-$\Delta^{3'}$-D-2′-hexosulosyl)-$\Delta^5$-pregnene-17$\alpha$,20(*S*)-triol, named periplocogenin.

S-3A; $C_{23}H_{34}O_5$, mp 140 °C (sinters). This compound was considered to have an unsaturated five-membered lactone from the IR absorptions (1750, 1620, 1200 cm$^{-1}$), UV absorption maximum at 218 nm ($\varepsilon$=13000), and $^1$H- and $^{13}$C-NMR spectral data, and it was identified as periplogenin, which has been isolated from *P. sepium*.[8] Its structure was also supported by signal assignments based on known chemical shift rules and distortionless enhancement by polarization transfer (DEPT) techniques in the $^{13}$C-NMR spectrum, as summarized in Table I.

S-5A; $C_{21}H_{34}O_5$, mp 174—176 °C. This compound appeared to have no UV absorption band and one double bond ($\delta$ 5.35 (1H, t, $J$=2.6 Hz), 121.62 (d) and 140.85 (s)) at C-5 of the $C_{21}$-steroidal skeleton based on the $^1$H- and $^{13}$C-NMR spectral data. The signal pattern of the $^1$H-NMR spectrum was similar to that of S-2A except for a 4′,6′-dideoxy-3′-*O*-methyl-$\Delta^{3'}$-2′-hexosulosyl moiety. However, the C-20 proton signal at $\delta$ 3.70 appeared as a doublet of quadruplets, because it was coupled with the C-21 methyl protons ($J$=6.2 Hz) and the C-17 proton ($J$=2 Hz) due to the appearance of a proton at C-17. Consequently, S-5A was deduced to be a $\Delta^5$-pregnene-3$\beta$,20-diol. The C-20 configuration was determined to be "*S*" by comparing the $^1$H-NMR spectral data with those of $\Delta^5$-pregnene-3$\beta$,20(*S*)-diol-3-

Table II. Comparison of $^1$H Chemical Shifts at C18—C21 in Pregnenes

| No. | S-5A | $\Delta^5$-Pregnene-3$\beta$,20(*S*)-diol-3-monoacetate | $\Delta^5$-Pregnene-3$\beta$,20(*R*)-diol-3-monoacetate |
|---|---|---|---|
| 18 | 0.68 | 0.68 | 0.77 |
| 19 | 1.01 | 1.02 | 1.03 |
| 20 | 3.71 | 3.72 | 3.74 |
| 21 | 1.23 | 1.25 | 1.16 |

The measurements were made on a Bruker AM400 spectrometer in $CDCl_3$ with TMS as an internal reference and are expressed in terms of ppm.

monoacetate and $\Delta^5$-pregnene-3$\beta$,20(*R*)-diol-3-monoacetate[9] as shown in Table II. From the above results, it is reasonable to conclude that S-5A is $\Delta^5$-pregnene-3$\beta$,20(*S*)-diol.

Further studies on the chemical structures and antitumor activity of these glycosides is in progress.

## Experimental

All melting points were measured with a Yanaco MP-3 apparatus and are uncorrected. IR spectra were taken with a Nihon Bunko IRA-I spectrometer, UV with a Hitachi UV-Vis 320 spectrometer, and $^1$H- and $^{13}$C-NMR with a Bruker AM400 instrument. Chemical shifts are given on the $\delta$ (ppm) scale with tetramethylsilane (TMS) as an internal standard. MS were measured with a direct probe using a Hitachi M-80 mass spectrometer.

The following solvent systems were used for silica gel, RP-8, and RP-18 TLC: solvent 1, $CHCl_3$–MeOH (10:1); solv. 2, $CHCl_3$–MeOH (5:1); solv. 3, MeOH–$H_2O$ (9:1); solv. 4, MeOH–$H_2O$ (7:3); solv. 5, MeOH–$H_2O$ (6:4). Each spot on the TLC plate was detected by spraying 10% $H_2SO_4$ and heating the plate.

**Extraction and Isolation**——The root bark of *P. sepium* used in this experiment was purchased in China. The crude drug (4 kg) was extracted with MeOH (3×30 l). The concentrated MeOH extract (980 g) was partitioned between MeOH–$H_2O$ (7:8) and *n*-hexane, and then between $H_2O$ and $CHCl_3$ three times. The $CHCl_3$ extract (248 g) was subjected to column chromatography on silica gel and eluted with $CHCl_3$, $CHCl_3$–MeOH (10:1) and (1:1) successively. The obtained $CHCl_3$–MeOH (10:1) fraction was once again subjected to silica gel column chromatography with $CHCl_3$–MeOH (15:1), (5:1) and (2:1) successively to furnish fractions CM-1 (128.71 g), CM-2 (72.77 g) and CM-3 (7.25 g), respectively. The fraction CM-1 (12 g) was separated by silica gel column chromatography with $CHCl_3$–MeOH (9:1) and (5:1) as eluents. The $CHCl_3$–MeOH (9:1) fraction was subjected to column chromatography on silica gel to give S-1 (8 mg) on elution with EtOAc. The obtained $CHCl_3$–MeOH (5:1) fraction was subjected to RP-8 and RP-18 column chromatography and eluted with MeOH–$H_2O$ (9:1) and (7:3) to furnish S-2 (311 mg) and S-3 (350 mg). Repeated RP-8 and RP-18 column chromatography of the fraction CM-2 (30 g) using the solvent systems of MeOH–$H_2O$ (7:3) and (6:4) gave S-4 (387 mg), S-5 (192 mg), S-6 (177 mg), S-7 (12 mg) and S-8 (8 mg), respectively.

S-1: Colorless prisms (from hexane–EtOAc), mp 210—212 °C, $[\alpha]_D^{20}$ +69.5° (*c*=0.05 in MeOH). MS *m/z*: 326 ($M^+$, $C_{21}H_{26}O_3$), 308 ($M^+-H_2O$), 293 ($M^+-H_2O-CH_3$), 283 ($M^+-43$), 265 ($M^+-43-H_2O$), 204 ($M^+-122$), 123 ($M^+-204+H$). $^1$H-NMR ($CDCl_3$) $\delta$: 0.96 (3H, s, 18-$CH_3$), 1.14 (3H, s, 19-$CH_3$), 2.40 (3H, s, 21-$CH_3$), 3.72 (1H, dd, *J*=5, 10 Hz, 12-H), 5.70 (1H, s, 4-H), 5.83 (1H, s, OH), 6.13 (1H, dd, *J*=1.5, 10 Hz, 6-H), 6.17 (1H, dd, *J*=2.5, 10 Hz, 7-H), 7.00 (1H, dd, *J*=2, 3.4 Hz, 16-H).

**Acid Hydrolysis of S-2, S-3 and S-5**——S-2 (25 mg), S-3 (30 mg) and S-5 (20 mg) were hydrolyzed with 0.05 N $H_2SO_4$ in 50% MeOH (6 ml) at 80 °C for 1 h respectively. Each reaction mixture was diluted with water and the MeOH was evaporated off *in vacuo* at room temperature. The aqueous residue was extracted with $CHCl_3$ (×3) and the $CHCl_3$ layer was washed with water. After removal of the solvent, the residue was purified by means of silica gel column chromatography with $CHCl_3$–MeOH (96:4) to give the aglycones S-2A, S-3A and S-5A.

S-2A: Colorless needles (from benzene–$CHCl_3$), mp 203—206 °C, $[\alpha]_D^{20}$ −51.2° (*c*=0.3 in MeOH). MS *m/z*: 474 ($M^+$, $C_{28}H_{42}O_6$). UV $\lambda_{max}^{MeOH}$ nm: 262 ($\varepsilon$=2900). IR $\nu_{max}^{CHCl_3}$ cm$^{-1}$: 3580, 1710, 1640, 1630. $^1$H-NMR ($CDCl_3$) $\delta$: 0.75 (3H, s, 18-$CH_3$), 1.01 (3H, s, 19-$CH_3$), 1.20 (3H, d, *J*=6.4 Hz, 21-$CH_3$), 1.52 (3H, d, *J*=6.8 Hz, 6′-$CH_3$), 3.67 (1H, m, 3-H), 3.85 (1H, q, *J*=6.4 Hz, 20-H), 4.72 (1H, dq, *J*=6.8, 3 Hz, 5′-H), 5.06 (1H, s, 1′-H), 5.37 (1H, t, *J*=2.6 Hz, 6-H), 5.78 (1H, d, *J*=3 Hz, 4′-H), 3.64 (3H, s, 3′-$OCH_3$).

**Pd–C/$H_2$ Reduction of S-2A**——A solution of S-2A (5 mg) in EtOH (3 ml) was catalytically reduced on a little palladium–carbon in $H_2$ for 2 h at room temperature. The reaction mixture was worked up by usual methods and subjected to silica gel column chromatography with the solvent system of $CHCl_3$–MeOH (96:4). The reduced derivative of S-2A was obtained as a solid (3.3 mg). $^1$H-NMR ($CDCl_3$) $\delta$: 0.70 (3H, s, 18-$CH_3$), 0.80 (3H, s, 19-$CH_3$), 1.17 (3H, d, *J*=6.4 Hz, 21-$CH_3$), 1.29 (3H, d, *J*=6.0 Hz, 6′-$CH_3$), 3.30 (1H, m, 3′-H), 3.40 (3H, s, $OCH_3$), 3.46 (1H, m, 5′-H), 3.70 (1H, m, 3-H), 3.80 (1H, q, *J*=6.4 Hz, 20-H), 3.95 (1H, br s, 2′-H), 4.46 (1H, d, *J*=1 Hz, 1′-H).

**Acetonide Formation from S-2A**——*p*-TsOH (5 mg) was added to a solution of S-2A (14.5 mg) in acetone (3 ml) and the whole was refluxed for 2 h. The reaction mixture was poured into $H_2O$ and then extracted with ether. The ether layer was washed with aqueous saturated $NaHCO_3$ solution, and concentrated to give the acetonide as a solid (14.2 mg). $[\alpha]_D^{20}$ −74.4° (*c*=0.3 in $CHCl_3$). $^1$H-NMR ($CDCl_3$) $\delta$: 0.84 (3H, s, 18-$CH_3$), 1.00 (3H, s, 19-$CH_3$), 1.38 (3H, d, *J*=6.7 Hz, 21-$CH_3$), 1.40 and 1.44 (3H, s,  , respectively), 1.51 (3H, d, *J*=6.8 Hz, 6′-$CH_3$), 3.63 (3H, s, 3′-$OCH_3$), 3.65 (1H, m, 3-H), 4.23 (1H, q, *J*=6.7 Hz, 20-H), 4.71 (1H, dq, *J*=2.9, 6.8 Hz, 5′-H), 5.05 (1H, s, 1′-H), 5.35 (1H, br s, 6-H), 5.79 (1H, d, *J*=2.9 Hz, 4′-H).

S-3A: Colorless powder (from $CHCl_3$), mp 138—140 °C (sinters), $[\alpha]_D^{20}$ +29.1° (*c*=0.8 in EtOH). MS *m/z*: 390 ($M^+$, $C_{23}H_{34}O_5$). UV $\lambda_{max}^{MeOH}$ nm: 218 ($\varepsilon$=13000). IR $\nu_{max}^{CHCl_3}$ cm$^{-1}$: 3500, 1750, 1620, 1200. $^1$H-NMR ($CDCl_3$) $\delta$: 0.86 (3H, s, 18-$CH_3$), 0.92 (3H, s, 19-$CH_3$), 2.76 (1H, q, *J*=5.4 Hz, 17-H), 4.15 (1H, br s, 3-H), 4.80 (1H, dd, *J*=18.1,

1.6 Hz, 21-H), 4.98 (1H, dd, $J$=18.1, 1.6 Hz, 21-H), 5.86 (1H, t, $J$=1.6 Hz, 22-H).

S-5A: Colorless needles (from MeOH), mp 174—176 °C, $[\alpha]_D^{20}$ −52.1° ($c$=0.2 in $CHCl_3$). MS $m/z$: 318 ($M^+$, $C_{21}H_{34}O_2$). $^1$H-NMR ($CDCl_3$) $\delta$: 0.68 (3H, s, 18-$CH_3$), 1.01 (3H, s, 19-$CH_3$), 1.23 (3H, d, $J$=6.2 Hz, 21-$CH_3$), 3.52 (1H, m, 3-H), 3.71 (1H, dq, $J$=6.2, 2.1 Hz, 20-H), 5.35 (1H, t, $J$=2.6 Hz, 6-H).

**Assay of Activity Against Sarcoma 180 Ascites**[10]——ICR male mice, 5 weeks old, supplied by Clea Japan Co., Ltd., were used in groups in 6 animals. Sarcoma 180 ascites, provided by the National Cancer Center Research Institute and maintained in successive generations by us, was implanted i.p. at $1 \times 10^6$ cells/body. Administration of a test drug was started at one day after the implantation and continued for five days by the i.p. route. The effectiveness was evaluated by means of the packed cell volume method[11]; growth ratio (GR%)=(packed cell volume (PCV) of test groups/PCV of control groups) × 100; GR=0—10% (+++), 10—40% (++), 40—65% (+) and over 66% (−).

**Acknowledgement** We wish to thank Prof. T. Yamauchi, Faculty of Pharmaceutical Science, Fukuoka University, for providing an authentic sample, neridienone-A, and the staff of the analytical center of Tokyo College of Pharmacy for MS measurements. Part of this research was supported by Grants-in-Aid from the Ministry of Education, Science and Culture of Japan.

## References and Notes

1) T. Namba (ed.), "The Crude Drugs in Japan, China and the Neighbouring Countries," Vol. II, Hoikusha Publishing Co., Ltd., Osaka, 1980, p. 136.
2) S. Sakuma, H. Ishizone, R. Kasai, S. Kawanishi, and J. Shoji, *Chem. Pharm. Bull.*, **19**, 52 (1971); S. Kawanishi, S. Sakuma, and J. Shoji, *ibid.*, **20**, 469 (1972); R. Kasai, S. Sakuma, S. Kawanishi, and J. Shoji, *ibid.*, **20**, 1869 (1972); H. Ishizone, S. Sakuma, S. Kawanishi, and J. Shoji, *ibid.*, **20**, 2402 (1972); S. Kawanishi, R. Kasai, S. Sakuma, and J. Shoji, *ibid.*, **25**, 2055 (1977); S. Sakuma, S. Kawanishi, and J. Shoji, *ibid.*, **28**, 163 (1980).
3) H. Itokawa, K. Watanabe, and S. Mihashi, *Shoyakugaku Zasshi*, **33**, 95 (1979); H. Itokawa, K. Watanabe, K. Mihara, and K. Takeya, *ibid.*, **36**, 145 (1982).
4) F. Abe and T. Yamauchi, *Phytochemistry*, **15**, 1745 (1976).
5) K. Tsuda (ed.), "Steroids," Asakura Publishing Co., Ltd., Tokyo, 1971, p. 16.
6) O. Tanaka, *Yakugaku Zasshi*, **105**, 323 (1985).
7) F. Abe, T. Yamauchi, T. Fujioka, and K. Mihashi, *Chem. Pharm. Bull.*, **34**, 2774 (1986).
8) S. Sakuma, S. Kawanishi, J. Shoji, and S. Shibata, *Chem. Pharm. Bull.*, **16**, 326 (1986).
9) M. Kimura, K. Hayashi, H. Narita, and H. Mitsuhashi, *Chem. Pharm. Bull.*, **30**, 3932 (1982).
10) R. G. Geran, N. J. Greenberg, M. M. MacDonald, A. M. Schumacher, and B. J. Abbott, *Cancer Chemother. Rep.*, Part 3, **3**, 1 (1972).
11) A. Hoshi and K. Kuretani, *Farmacia*, **9**, 464 (1973).

[Chem. Pharm. Bull. 35(11)4530—4536(1987)]

# Histochemistry. XI.[1] Histological and Chemical Characteristics of Bolting and Non-bolting Roots of Cultivated *Bupleurum falcatum* L.

TADATO TANI,*,[a] TADAHISA KATSUKI,[a] MICHINORI KUBO,[b] YUKO OKAZAKI,[b] and SHIGERU ARICHI[a]

*The Research Institute of Oriental Medicine, Kinki University,[a] 380, Nishiyama, Sayama, Minamikawachi, Osaka 589, Japan and Faculty of Pharmaceutical Sciences, Kinki University,[b] 3-4-1, Kowakae, Higashi-Osaka, Osaka 577, Japan*

(Received May 11, 1987)

The morphological, histological and chemical characteristics of non-bolting and bolting roots of cultivated *Bupleurum falcatum* L. were statistically compared. In external characteristics, non-bolting (rosette) roots were found to be lighter, thinner, and more flexible than bolting roots taken from plants with flower-stalks. Histologically, non-bolting roots had a smaller xylem ratio, wider phloem tissue and a tendency to contain greater concentrations of tissue-specifically stored bioactive saikosaponins than did bolting roots, which had well-developed xylem mechanical tissue. Of these two types of growing plants, higher concentrations of magnesium and phosphorus were observed in roots of non-bolting plants.

**Keywords**——Chinese crude drug; *Bupleurum falcatum*; saikosaponin; magnesium; phosphorus; HPLC; plasma spectrometer; multivariate analysis

Cultivation of medicinal plants is being done to supply the increasing demand for crude herbal drugs, some preparations of which, kampo-seizai in Japanese, are widely used in Japan in current drug therapy. The production in Japan of *Bupleurum falcatum* L. (Umbelliferae), Mishima-saiko in Japanese, one of the starting materials for the Chinese crude drug Bupleuri Radix prescribed in so-called saiko-zai, is increasing year by year.

The external characteristics of cultivated *B. falcatum* roots available on the market vary depending on the environmental conditions, whether the plant showed bolting or non-bolting growth and/or the processing methods. In the course of our histochemical investigations on crude drugs,[1] we examined how bolting pedunculate growth influenced the histological characteristics and saikosaponin and cationic compositions of *B. falcatum* roots cultivated in Nara Prefecture, an area in which medicinal plants are extensively cultivated. As shown in our previous reports,[1,2] multivariate analysis is applicable for evaluation of crude drugs. In this study, sixteen morphological, histological and chemical characteristics of non-bolting and bolting roots of cultivated *B. falcatum* were compared statistically.

## Experimental

**Materials**——One-year-old roots of *B. falcatum*, the seeds of which had been harvested in Gotemba, Shizuoka Prefecture, and sown in four productive fields (A, Tanise; B, Ono; C, Yamazaki; and D, Iosumi) in Yoshino-gun, Nara Prefecture, at the end of March in 1981, were used. Twenty to 30 roots from non-bolting (rosette) and bolting plants with flower-stalks were harvested from the same ridge in each field in November 1982. About three times more bolting plants than non-bolting plants were found in each field.

**Morphological Characteristics**——Each whole fresh root was weighed on an electric balance (ED-200, Shimadzu), and then reweighed following air-drying for 2 d; the percentage weight loss was then calculated according

to the equation (dry weight) × 100/(wet weight). The maximum diameter of each main root was measured using a caliper (Kanon) when the roots were still fresh, prior to histological examination.

The thickest part was cross-sectioned using a freezing microtome (MA-101, Komatsu Electronic) in the usual way. Thin cross-sections thus obtained were examined using a light microscope (Vanox, Olympus) equipped with a microphotographic camera (PM-10, Olympus), to determine the xylem ratio (%) [(xylem diameter) × 100/(main root diameter)] as an index of root flexibility.

Five measurements were carried out to obtain the mean and the standard deviation (mean ± S.D.) of the observed values. As shown in Table I, the data are presented in non-bolting and bolting groups, and in four histological types (I, II-NB, II-B and III), classified according to the distribution pattern of thick-walled mechanical cells in the root xylem as observed under microscopic examination.

**Cation Composition**——Five roots randomly selected from the four types were combined and pulverized in an agate mortar, then exactly 100 mg of each powder was treated with a plasma asher (ASH-302, Hitachi). Eight cationic elements in the ash, magnesium (Mg), aluminium (Al), phosphorus (P), potassium (K), calcium (Ca), iron (Fe), manganese (Mn) and strontium (Sr) were quantified by the standard addition method using an inductively coupled plasma spectrometer (ICP, Hitachi 300) under previously reported conditions.[1]

**Saikosaponins a, c and d**——Exactly 500 mg of powder prepared as above was extracted twice with hot methanol (80 ml each time). These extracts were treated with a SEP-PAK $C_{18}$ cartridge (Waters), followed by high-performance liquid chromatography (HPLC) to quantitate the biologically active saikosaponins a, c and d. Total saikosaponin content is taken as the sum of saikosaponins a, c and d. The HPLC system and detection conditions for saikosaponins were the same as reported previously.[3]

**Statistical Analysis**——Statistically significant differences between the means of sixteen variables of non-bolting and bolting groups were evaluated by the use of Student's $t$-test.

The standardized mean values ($z_i$; $i=1$—16) of the sixteen variable characteristics of the non-bolting and bolting groups were compared using the equation $z_i=(x_i-X_i)/\text{S.D.}$, where $x_i$ represents the means of the sixteen variables of each group, and $X_i$ and S.D. are the total means and standard deviation, respectively. The standardized data of two groups were analyzed by using a radar chart (Fig. 2) in which the regular hexadecagon represents the standardized total mean values. The sixteen variables determined from the three histological types I, II (II-NB and II-B) and III were also compared in a radar chart (Fig. 4).

To clarify the exact group to which each sample belonged, the eight non-bolting and seven bolting samples were also examined by discriminant analysis using Mahalanobis' generalized distance of the variables, as shown in Table II and Fig. 3.

These statistical calculations were performed using a personal computer (PC-9801 Vm2, NEC) with a multivariate analysis program written by Nippon Maikon Gakuin.

## Results and Discussion

A series of investigations on the effects of temperature, years of cultivation and geographical variations on bolting growth of *B. falcatum* cultivated in test fields has been carried out.[4] In the present study, samples collected from the same ridge in production fields possessing similar cultivation and climatic conditions consisted of both non-bolting and bolting plants. Bolting growth in one-year-old plants may be affected by genetic factors in addition to environmental conditions.

The means and S.D. values of four morphological and twelve chemical variables obtained with eight non-bolting and seven bolting samples of *B. falcatum* are shown in Table I.

Large coefficients of variation (C.V.) were found in such mean values as dry whole root weight and saikosaponins a, c, d and total saikosaponin contents. Although differences in soil conditions in the four fields could have influenced the cationic composition, the C.V. values for all, except Al and P were unexpectedly small.

There were statistically significant differences ($p<0.05$) between the means of non-bolting and bolting samples in five characteristics: dry whole root weight ($t=-2.718$), main root diameter ($t=-2.077$), xylem ratio ($t=-3.356$) and Mg ($t=1.834$) and P ($t=2.456$) contents. Although the involvement of Mg and P in the mechanism causing *B. falcatum* root bolting is not established, bolting roots are known to contain less Mg and P than non-bolting roots. Morphologically, bolting roots have been found to be bigger, thicker, and less flexible

TABLE I. Morphological and Chemical Characteristics of *B. falcatum* Roots

| | Whole root dry weight (g) (1) | Weight loss by drying (%) (2) | Main root diameter (mm) (3) | Xylem ratio (%) (4) | Mg (5) | Al (6) | P (7) | K (8) | Ca (9) | Fe (10) | Mn (11) | Sr (12) | Saikosaponin (mg/g) a (13) | c (14) | d (15) | Total (16) |
|---|---|---|---|---|---|---|---|---|---|---|---|---|---|---|---|---|
| | | | | | (mg/g) | | | | | | (μg/g) | | | | | |
| Non-bolting roots (8 samples of 40 roots) | | | | | | | | | | | | | | | | |
| | 0.99[a] | 65.5 | 7.21[a] | 59.7[a] | 1.86[a] | 0.60 | 2.47[a] | 6.93 | 2.36 | 0.23 | 60.2 | 37.0 | 0.95 | 0.46 | 0.45 | 1.85 |
| | ±0.42 | ±5.88 | ±0.42 | ±4.95 | ±0.45 | ±0.39 | ±0.79 | ±1.58 | ±0.53 | ±0.08 | ±10.4 | ±6.66 | ±0.46 | ±0.21 | ±0.30 | ±0.90 |
| Histological type I (4 samples of 20 roots) | | | | | | | | | | | | | | | | |
| | 1.02 | 66.2 | 7.31 | 58.9 | 1.73 | 0.70 | 2.30 | 6.90 | 2.16 | 0.27 | 60.1 | 35.6 | 1.02 | 0.55[b] | 0.57 | 2.14 |
| | ±0.60 | ±7.42 | ±0.48 | ±6.98 | ±0.50 | ±0.48 | ±0.70 | ±2.35 | ±0.39 | ±0.08 | ±7.67 | ±5.74 | ±0.57 | ±0.24 | ±0.39 | ±1.18 |
| Histological type II-NB (4 samples of 20 roots) | | | | | | | | | | | | | | | | |
| | 0.96 | 64.9 | 7.12 | 60.5 | 2.00 | 0.51 | 2.64 | 6.96 | 2.56 | 0.20 | 60.4 | 38.4 | 0.87 | 0.36 | 0.32 | 1.56 |
| | ±0.20 | ±4.96 | ±0.39 | ±2.51 | ±0.42 | ±0.30 | ±0.95 | ±0.54 | ±0.61 | ±0.07 | ±14.0 | ±8.11 | ±0.40 | ±0.16 | ±0.13 | ±0.53 |
| Bolting roots (7 samples of 35 roots) | | | | | | | | | | | | | | | | |
| | 1.59 | 62.9 | 7.73 | 68.3 | 1.46 | 0.57 | 1.46 | 6.75 | 2.30 | 0.25 | 50.4 | 42.1 | 0.78 | 0.31 | 0.31 | 1.40 |
| | ±0.45 | ±7.16 | ±0.55 | ±4.91 | ±0.39 | ±0.30 | ±0.79 | ±1.33 | ±0.34 | ±0.07 | ±11.2 | ±13.4 | ±0.33 | ±0.12 | ±0.12 | ±0.62 |
| Histological type II-B (4 samples of 20 roots) | | | | | | | | | | | | | | | | |
| | 1.57 | 63.3 | 7.43 | 68.9 | 1.36 | 0.57 | 1.40 | 6.53 | 2.11 | 0.24 | 42.9 | 36.5 | 0.99 | 0.35 | 0.39 | 1.73 |
| | ±0.25 | ±8.18 | ±0.61 | ±4.31 | ±0.50 | ±0.29 | ±0.89 | ±0.97 | ±0.34 | ±0.06 | ±6.38 | ±11.8 | ±0.29 | ±0.13 | ±0.22 | ±0.62 |
| Histological type III (3 samples of 15 roots) | | | | | | | | | | | | | | | | |
| | 1.63 | 62.5 | 7.72 | 67.4 | 1.60 | 0.59 | 1.55 | 7.05 | 2.55 | 0.26 | 60.4 | 47.6 | 0.51 | 0.25 | 0.20 | 0.96 |
| | ±0.71 | ±7.30 | ±0.46 | ±6.48 | ±0.16 | ±0.39 | ±0.81 | ±1.91 | ±0.08 | ±0.10 | ±6.95 | ±14.9 | ±0.14 | ±0.09 | ±0.07 | ±0.27 |
| Total (15 samples of 75 roots) | | | | | | | | | | | | | | | | |
| | 1.27 | 64.3 | 7.46 | 63.7 | 1.68 | 0.59 | 2.00 | 6.85 | 2.33 | 0.24 | 55.6 | 39.0 | 0.87 | 0.39 | 0.38 | 1.64 |
| | ±0.52 | ±9.97 | ±0.54 | ±6.48 | ±0.46 | ±0.34 | ±0.92 | ±1.42 | ±0.43 | ±0.07 | ±11.6 | ±10.2 | ±0.40 | ±0.18 | ±0.26 | ±0.79 |
| C.V. | 40.9 | 9.97 | 7.24 | 10.2 | 27.4 | 57.6 | 46.0 | 20.7 | 18.5 | 29.2 | 20.9 | 26.2 | 46.0 | 46.2 | 68.4 | 48.2 |

*a*) $p<0.05$ (non-bolting roots *vs.* bolting roots). *b*) $p<0.05$ (type I *vs.* type III).

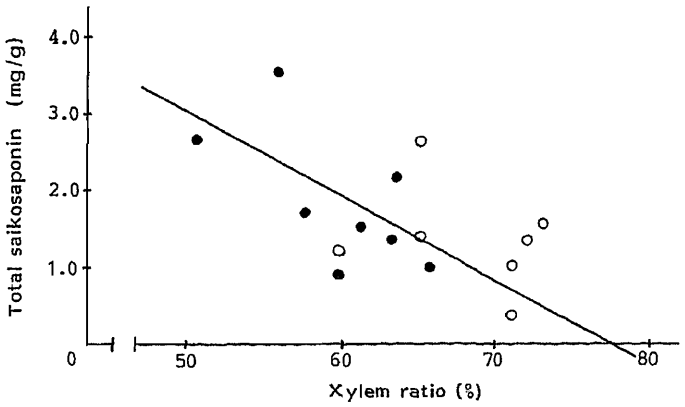


Fig. 1. Correlation between Total Saikosaponins Content and Xylem Ratio of Non-bolting and Bolting Roots of *B. falcatum*

Regression line ($y$) and correlation coefficient ($r$) of non-bolting roots.
$y=-0.118x+8.940$ ($r=-0.65$).
●, non-bolting root; ○, bolting root.

than non-bolting samples.

In thin, flexible non-bolting samples, the relationship of total saikosaponin content, one measure of a crude drug's quality, with several morphological and chemical variables was examined. The total saikosaponin content was found to have a negative correlation coefficient ($r$) with the xylem ratio ($-0.65$: Fig. 1), which correlated with main root diameter (0.63). A correlation coefficient with an absolute value of more than 0.62 was statistically meaningful according to the equation $t_{0.05,df6}=r/\sqrt{(1-r^2)/(n-2)}$, where $t$ represents $t$-values (1.943) of critical rate (0.05) and degree of freedom (6) obtained from a statistical $t$ table, and $n$ is sample number (8). These results conform well with previously reported findings that thin[5] and small[6] roots contained higher concentrations of saikosaponins than did big roots.

A positive correlation coefficient (0.71) was found between the saikosaponin a and Mg contents in non-bolting samples. The effect of Mg on saikosaponin biosynthesis in the plant has not been defined, but the two constituents are reported to coexist in high concentrations in root phloem tissue of *B. falcatum*.[1] Furthermore, wide phloem tissues are found in thin and flexible non-bolting roots possessing small xylem ratios, and the flexible Bupleuri Radix is considered, according to empirical evaluation standards, to be of good quality. These findings agree well with the present results showing that non-bolting samples were apt to have a greater total saikosaponin content ($1.85\pm0.90$ mg/g) than bolting samples ($1.40\pm0.62$ mg/g).

The standardized mean values of the sixteen variables in non-bolting and bolting samples were analyzed statistically. As shown in Fig. 2, the two groups were found to be characterized by nine variables: whole root dry weight (1), main root diameter (3), xylem ratio (4), Mg (5), P(7) and Mn (11) contents, and saikosaponins a (13), c (14) and d (15) and total saikosaponin (16) contents.

Furthermore, in order to search for effective variables for discriminating between non-bolting and bolting samples, discriminant analysis using the thirteen standardized variables (1)—(12) and (16), as shown in Table II, was carried out. It was found that all fifteen samples were correctly assigned to non-bolting and bolting groups (correlation ratio: 0.999). A 100% correct judgement rate was still obtained by the discriminant analysis using only four variables: (1), (4), (6) and (16).

The discriminant equation using the three morphological variables of dry weight ($x_1$), main root diameter ($x_3$) and xylem ratio ($x_4$), calculated from commercially available Bupleuri Radix was: $y_{1,3,4}{}^*=0.629x_1{}^*-0.170x_3{}^*+0.758x_4{}^*$, the correlation ratio and correct judge-

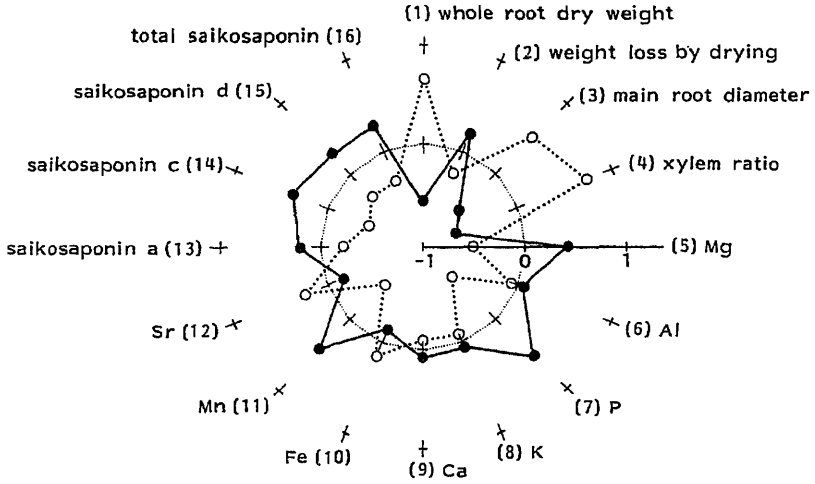


Fig. 2. Comparison of Non-bolting and Bolting Roots of *B. falcatum* Using Sixteen Standardized Variables

Non-bolting root ($n=8$); —●—; bolting root ($n=7$), ····○····; ··+··, total mean value ($n=15$). Each point of the sixteen variables represents the standardized mean value.

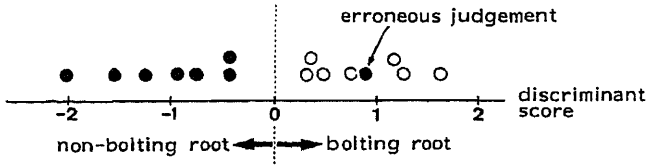


Fig. 3. Discriminant Scores Calculated from Three Variables from Non-bolting (8 Samples) and Bolting (7 Samples) Roots

Entered variables: (1) whole root dry weight, (3) main root diameter, (3) xylem ratio.
Discriminant equation:

$$y_{1,3,4} = 1.255x_1 - 0.327x_3 + 0.121x_4 - 6.871$$

$$(y_{1,3,4}{}^* = 0.629x_1{}^* - 0.170x_3{}^* + 0.758x_4{}^*).$$

The equations: $y_{1,3,4}$ and $y_{1,3,4}{}^*$ were calculated using original and standardized data, respectively.

ment rate from which were found to be 0.588 and 93.3% (14/15). As shown in Fig. 3, one non-bolting sample collected from field C, possessing a large dry weight and main root diameter was erroneously assigned to the bolting group.

The discriminant analysis was also performed using the three morphological variables (1), (3) and (4), and the total saikosaponin content (16). The correlation ratio obtained was 0.631 and the correct judgement rate, 93.3% (14/15).

It has been reported that *B. falcatum* roots could be classified histologically according to the arrangement of the xylem vessels.[7] In this study, samples were also classified according to the distribution pattern of xylem sclerenchyma, consisting mainly of sclerenchymatous cells and wood fibers with thick lignified cell walls. Thus, eight non-bolting samples could be classified into two types: I (four samples) and II-NB (four samples), and seven bolting samples also into two types: II-B (four samples) and III (three samples), as shown in Fig. 4. Type I was poor in xylem sclerenchyma and typical of non-bolting flexible roots. Type III was rich in xylem mechanical tissue, perhaps useful as the flower-stalk support, and typical of hard and thick bolting roots. Type II (II-NB and II-B) was histologically intermediate between types I and III.

The samples collected from fields A, B and C could be classified into all four histological types, but those from field D fitted into only types I, II-NB and II-B.

Table II. Discriminant Analyses of Non-bolting and Bolting Roots of *B. falcatum*

| Entered variables | Coefficients of discriminant equations (1)—(12), (16) | (1), (4), (6), (16) | (1), (3), (4) | (1), (3), (4), (16) | (5)—(12) | (13)—(15) |
|---|---|---|---|---|---|---|
| (1) Whole root dry weight | 0.388 | 0.562 | 0.629 | 0.586 | | |
| (2) Weight loss of drying | −0.226 | | | | | |
| (3) Main root diameter | −0.184 | | −0.170 | −0.766 | | |
| (4) Xylem ratio | 0.475 | 0.448 | 0.758 | 0.315 | | |
| (5) Mg | −0.124 | | | | −0.168 | |
| (6) Al | −0.421 | −0.586 | | | 0.623 | |
| (7) P | 0.115 | | | | 0.506 | |
| (8) K | 0.025 | | | | 0.202 | |
| (9) Ca | −0.032 | | | | −0.045 | |
| (10) Fe | 0.119 | | | | −0.532 | |
| (11) Mn | 0.141 | | | | 0.041 | |
| (12) Sr | 0.299 | | | | 0.808 | |
| (13) Saikosaponin a | | | | | | −0.207 |
| (14) Saikosaponin c | | | | | | 0.926 |
| (15) Saikosaponin d | | | | | | −0.316 |
| (16) Total saikosaponins | 0.456 | −0.376 | | 0.273 | | |
| Correlation ratio | 0.999 | 0.451 | 0.588 | 0.631 | 0.666 | 0.209 |
| Correct judgement rate (%) | 100 | 100 | 93.3 | 93.3 | 93.3 | 66.7 |

Each coefficient of the discriminant equations was calculated using standardized data.

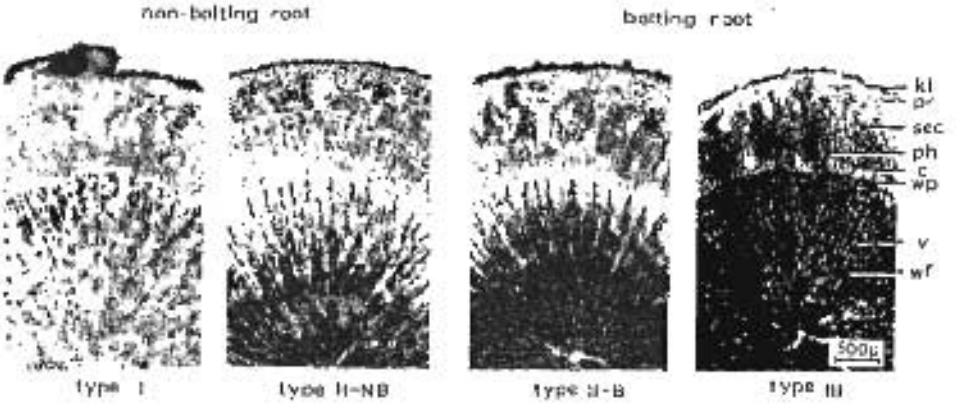


Fig. 4. Histological Types of *B. falcatum* Roots

Abbreviations: kl, cork layer; pr, pericycle; sec, secretory canal; ph, phloem; c, cambium; wp, wood parenchyma; v, vessel; wf, wood fiber.
Type I is typical of non-bolting flexible roots and type III is typical of hard bolting roots.

As shown in Fig. 5, the morphological and chemical properties of types I, II and III were statistically analyzed. The hexadecagonal figure obtained using the means of the sixteen characteristics of type II plants is very close to the regular hexadecagon of the total means of these sixteen variables. Thus type II tissue largely possessed intermediate values between the morphological and chemical characteristics of types I and III.

We have shown that type I with a small xylem ratio (4) contained more saikosaponins, (13), (14), (15) and (16), than type III with a large xylem ratio and main root diameter (3). Within the three types, total saikosaponin content appeared to decrease in amount along with the development of root sclerenchyma: types I, 2.14±1.18; II, 1.65±0.54; III,

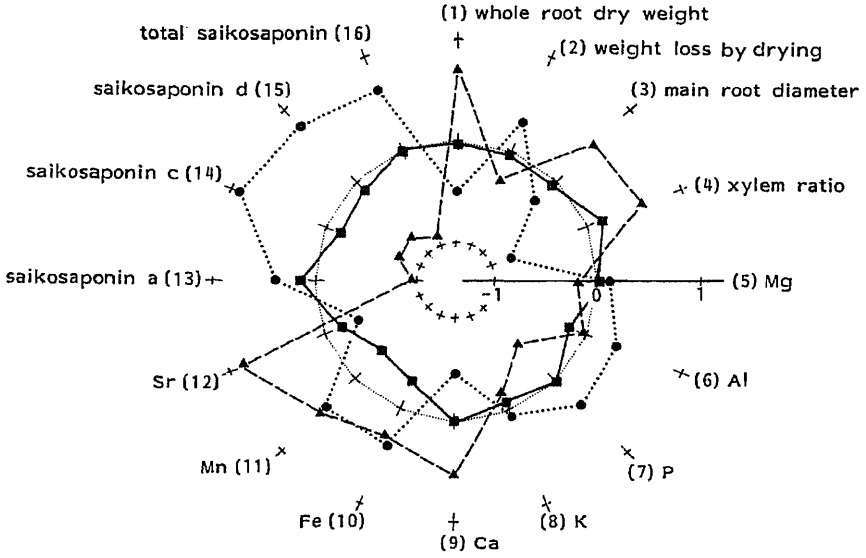


Fig. 5. Comparison of the Three Histological Types of *B. falcatum* Roots

Type I ($n=4$), ···●···; type II ($n=8$), —■—; type III ($n=3$), ---▲---; ··+··, total mean value ($n=15$). Each point of the sixteen variables represents standardized mean values. Type II was a combination of type II-NB and type II-B.

$0.96 \pm 0.28$ mg/g. Type I's saikosaponin c(14) content ($0.55 \pm 0.24$ mg/g) showed a statistically significant difference ($p<0.05$) from type III's ($0.25 \pm 0.09$ mg/g).

The present paper deals with a statistical comparison of various characteristics of non-bolting (rosette) and bolting roots of cultivated *B. falcatum*. It was found that no samples of 35 bolting roots examined were classified as type I with a small amount of xylem mechanical tissue. Thus, bolting growth is considered as a possible factor in the development of xylem sclerenchyma, which may be controlled by many factors, including genetic and environmental conditions. Concentrations of saikosaponins tended to be lower in bolting roots with a larger xylem ratio than in non-bolting roots with a smaller one. This is in agreement with the previous results[1,3] that bioactive saikosaponins were concentrated tissue-specifically in root phloem and pericycle.

**Acknowledgements** The authors are grateful to Dr. H. Ishii of Shionogi Research Laboratory and Mr. S. Fukuda of Nippon Tokushu Nosanbutsu Kyokai for supplying the authentic saikosaponins and cultivated *B. falcatum* roots.

## References

1) Part X: T. Tani, T. Katsuki, Y. Okazaki, and S. Arichi, *Chem. Pharm. Bull.*, **35**, 3323 (1987).
2) T. Tani, T. Katsuki, M. Kubo, and S. Arichi, *Shoyakugaku Zasshi*, **40**, 281 (1986).
3) T. Tani, T. Katsuki, M. Kubo, and S. Arichi, *J. Chromatogr.*, **360**, 407 (1986).
4) *a*) Y. Shimokawa, N. Ushio, N. Uno, and H. Ohashi, *Shoyakugaku Zasshi*, **34**, 209 (1980); *b*) Y. Shimokawa, N. Uno, N. Ushio, and H. Ohashi, *ibid.*, **34**, 221 (1980); *c*) Y. Shimokawa, I. Okuda, M. Kumano, and H. Ohashi, *ibid.*, **34**, 239 (1980).
5) H. Otsuka, S. Kobayashi, and S. Shibata, *Shoyakugaku Zasshi*, **31**, 195 (1977).
6) Y. Shimokawa and H. Ohashi, *Shoyakugaku Zasshi*, **34**, 235 (1980).
7) K. Kimura, K. Hata, and K. Sano, *Shoyakugaku Zasshi*, **17**, 36 (1963).

[Chem. Pharm. Bull. 35(11)4537—4543(1987)]

# Lipid A and Related Compounds. XVI.[1] Synthesis of Biologically Active Tetraacetyl-3-deoxy-D-*manno*-2-octulosonic Acid (KDO)-(α2→6)-D-Glucosamine-4-phosphates, Novel Analogs of the Nonreducing Sugar Moiety of Lipid A

SHIN-ICHI NAKAMOTO and KAZUO ACHIWA*

*School of Pharmaceutical Sciences, University of Shizuoka, Oshika 2-2-1, Shizuoka 422, Japan*

(Received May 13, 1987)

Synthesis of biologically active tetraacetyl-3-deoxy-D-*manno*-2-octulosonic acid-(α2→6)-D-glucosamine-4-phosphate analogs of lipid A is described.

**Keywords**——lipid A analog; KDO-linked glucosamine; 4-phosphorylated glucosamine; mitogenic activity; antitumor activity; lethal toxicity

Lipopolysaccharide (LPS) isolated from cell walls of various gram-negative bacteria possesses a variety of biological activities, *e.g.*, endotoxicity, adjuvanticity, antitumor activity and so on. These activities has been attributed to the hydrophobic moiety of LPS, termed lipid A.[2] 3-Deoxy-D-*manno*-2-octulosonic acid (KDO) occurs as a ketosidic component of the core region in all LPS and seems to play a biologically important role in being mitogenic and in amplifying the antitumor activity of lipid A.[3] However, the roles of KDO in the various biological activities of LPS are still unclear.

Recently, two research groups revealed that the C-2 position of KDO in the core region of LPS is attached to the C-6 position of the nonreducing moiety of lipid A from the Re mutant of *Salmonella minnesota* (**1a**)[4] and *Escherichia coli* (**1b**)[5] through a α2→6 linkage as shown in Chart 1. In addition, we and the other groups have found that the nonreducing

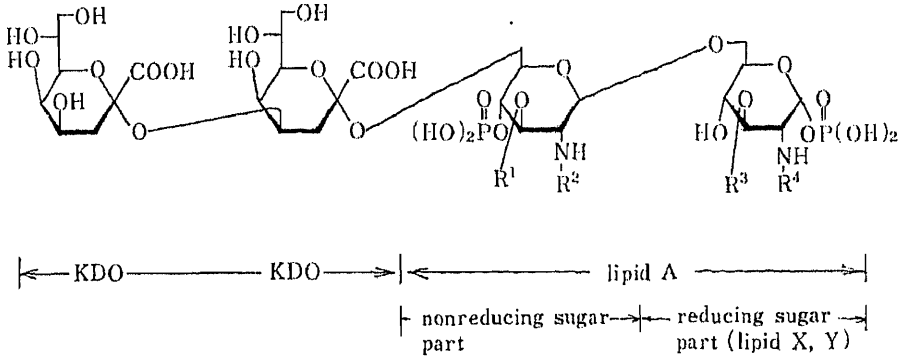


**1a**: $R^1=C_{14}$-O-$C_{14}$, $R^2=C_{14}$-O-$C_{12}$, $R^3=C_{14}$-OH, $R^4=C_{14}$-O-$C_{16}$
**1b**: $R^1=C_{14}$-O-$C_{14}$, $R^2=C_{14}$-O-$C_{12}$, $R^3=R^4=C_{14}$-OH

$C_{14}$-OH: (*R*)-3-hydroxytetradecanoyl $C_{14}$-O-$C_{12}$: (*R*)-3-dodecanoyloxytetradecanoyl
$C_{14}$-O-$C_{14}$: (*R*)-3-tetradecanoyloxytetradecanoyl $C_{14}$-O-$C_{16}$: (*R*)-3-hexadecanoyloxytetradecanoyl

Chart 1

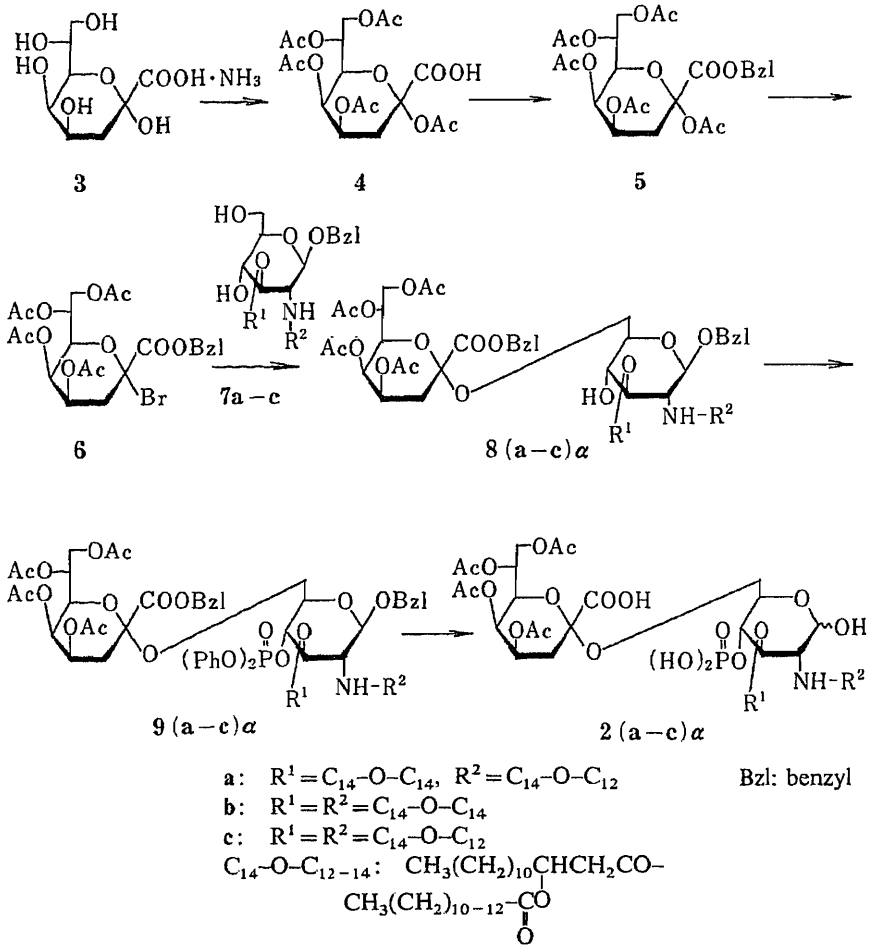


Chart 2

sugar moiety of lipid A is more important than the reducing sugar moiety (*cf.* lipid X and Y) for expressing the biological activities of LPS.[1c,h,6]

In a recent communication[1f] we reported the novel synthesis of tetraacetyl-KDO-(α2→6)-D-glucosamine-4-phosphate analogs (nonreducing sugar part) (**2a**—**c**) to clarify the effects of KDO on the biological activities of the nonreducing sugar part of lipid A. This paper describes these results in detail, as summarized in Charts 2 and 3.

The key disaccharide derivatives were synthesized by glycosidation of two monosaccharide components, **6** and **7a**—**c**, as shown in Chart 2. The component (**6**) as a glycosyl acceptor was prepared from ammonium KDO (**3**) (mp 122—124 °C, $[\alpha]_D^{24}$ +41.4 °), which was synthesized by a modification of the method of Hershberger *et al.*[7]

The hydroxyl groups of **3** were protected by acylation with acetic anhydride in the presence of 4-dimethylaminopyridine to give the pentaacetate (**4**) in 64% yield and further protection of the carboxyl group of **4** was carried out by esterification with phenyldiazomethane at room temperature to afford the ester (**5**) in 78% yield. Subsequent bromination at the C-2 position of **5** was accomplished by using $TiBr_4$ in dichloromethane at room temperature to give the bromide (**6**) as a syrup in almost quantitative yield. The bromide (**6**) was submitted to the next glycosidation without purification because of its instability.

On the other hand, the monosaccharide components (**7a**—**c**)[10] as glycosyl donors were prepared from benzyl 2-amino-2-deoxy-4,6-*O*-isopropyridene-β-D-glucopyranoside.[1a]

Glycosidation of **7a** with **6** freshly prepared from pentaacetyl-KDO (**4**) was carried out in

the presence of $Hg(CN)_2$–$HgBr_2$ and Molecular Sieves 4A in dichloromethane at room temperature for 24 h to give **8aα** and **8aβ** in 31 and 6% yields, respectively; excess addition of the 2-bromo-KDO derivative (**6**) to the glucosamine derivative (**7a**) (molar ratio; 1 : 0.75) was needed owing to the easy formation of the 2-debrominated derivative from 6. The structures of the glycosidic 2→6 linkages of **8aα** and **8aβ** were confirmed by the evidence presented later (see Chart 3).

Phosphorylation of **8aα** with diphenyl phosphorochloridate, pyridine and 4-dimethylaminopyridine in dichloromethane at room temperature for 4 h gave **9aα** in 92% yield. The infrared (IR) spectrum of **9aα** showed the characteristic absorption band of the diphenyl phosphoryl group at 958 $cm^{-1}$ and multiple signals assigned to the four phenyl groups were observed at 7.12—7.31 ppm in the proton nuclear magnetic resonance ($^1$H-NMR) spectrum. The protective benzyl and phenyl groups of **9aα** were then removed stepwise by hydrogenolysis catalyzed with 10% Pd-on-carbon at 35 °C for 5 h and $PtO_2$ at room temperature for 24 h in methanol to give the phosphate (**2aα**) in 54% yield. The phosphate (**2aα**) showed the characteristic blue color with the phosphate-specific spray reagent[8] and the $^1$H-NMR spectrum of **2aα** showed no proton signal due to phenyl groups. The related phosphates, **2bα** and **2cα**, were similarly synthesized from **7b** and **7c** as illustrated in Chart 2.

The stereochemistry of the 2→6 linkage in the glycosidation products (**8aα** and **8bβ**) was established by analysis of the $^1$H-NMR spectra of the modified compounds, **12α** and **12β**, bearing two 2,2,2-trichloroethoxycarbonyl (TCEC) substituents instead of the fatty acids on the 2-amino and 3-hydroxyl groups of **8**. In the KDO part of **8aα** and **8aβ**, the 3-$H_{eq}$ proton signals, which are reliable indicators of the α and β (2→6) linkages, overlapped with the methylene proton signals of fatty acids substituted on the glucosamine part, whereas **12α** and **12β** have no methylene proton signals of the fatty acids.

The latter compounds, **12α** and **12β**, were synthesized as shown in Chart 3. Glycosidation of the two components, **6** and **10**, was carried out by the procedure described above to yield **11α** (45%) and **11β** (4%). Each product was then phosphorylated by the above-mentioned procedure to give **12α** [$^1$H-NMR ($CDCl_3$) δ: 2.27 (dd, $J$ = 13.4, 5.9 Hz, 3-$H_{eq}$ of KDO] in 77% yield and **12β** [$^1$H-NMR ($CDCl_3$) δ: 2.47 (dd, $J$ = 11.7, 4.6 Hz, 3-$H_{eq}$ of KDO] in 68% yield. $^1$H-NMR spectroscopic analysis of the former indicated a smaller chemical shift value of the 3-$H_{eq}$ proton in the KDO residue, which is characteristic of an α-ketoside.[9] Subsequent deprotection of the TCEC group at the 2- and 3-position of the glucosamine skeleton of **12α**

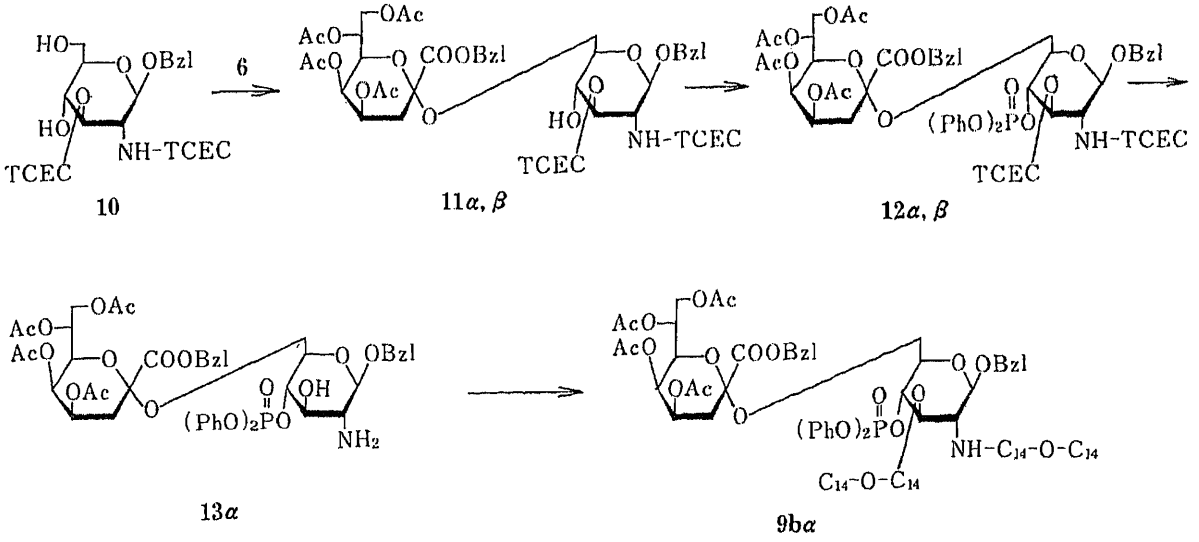


Chart 3

with zinc powder in acetic acid at room temperature for 5 h afforded **13α** in 41% yield. The simultaneous acylation[10] of the amino and hydroxyl groups of **13α** with (*R*)-3-tetradecanoyloxytetradecanoic acid gave **9bα** in 40% yield. The $^1$H-NMR and IR spectra and the optical rotation of **9bα** thus obtained were identical with those of **9bα** as indicated in Chart 2.

The antitumor activity, lethal toxicity and mitogenic activity of **2(a—c)α** were determined. Although the antitumor activity of **2(a—c)α** against ascities form of Ehrlich carcinoma in ddY mice was weaker than that of natural lipopolysaccharide, **2bα** was most effective. The lethal toxicity of **2cα** in $C_{57}$BL/6 mice loaded with galactosamine was most potent among these compounds, whereas **2bα** did not show lethality even at a high dose (50 g/mouse). On the other hand, these compounds (**2(a—c)α**) possess mitogenic activity comparable with that of lipid A.[1g,i]

## Experimental

All melting points were determined with a micro-melting point apparatus (Yanagimoto) and are uncorrected. Optical rotations were measured on a JASCO DIP-140 digital polarimeter. IR spectra were measured on a JASCO A-202 infrared spectrophotometer. $^1$H- and $^{13}$C-NMR spectra were recorded on a JEOL JNM-FX90Q (90 MHz) FT-NMR spectrometer using tetramethylsilane (TMS) as an internal standard. Chemical shifts were recorded in values ($\delta$) downfield from TMS, and the abbreviations of signal patterns are as follows: s, singlet; d, doublet; t, triplet; q, quartet; m, multiplet; br, broad. Thin layer chromatography (TLC) was performed on silica gel (Kiesel 60$F_{254}$ on aluminum sheets, Merck). All compounds were located by spraying the sheets with sulfuric acid and heating on a hot plate. Phosphorus-containing compounds were revealed by spraying with the phosphate-specific spray reagent.[8] Column chromatography was performed on silica gel (Kiesel gel 60, 70—230 mesh, Merck). Evaporations were carried out under reduced pressure at 35 °C. Reaction solvents were dried on Molecular Sieves 4A.

**2,4,5,7,8-Penta-*O*-acetyl-3-deoxy-α-D-*manno*-2-octulosonic Acid (4)**——A solution of **3** (3.0 g, 11.8 mmol) in pyridine (38.9 g, 0.49 mol) and acetic anhydride (43.5 g, 0.426 mol) was stirred at 5 C, and then 4-dimethylaminopyridine (0.5 g, 4.1 mmol) was added to the mixture. After 24 h, TLC (chloroform : methanol = 10 : 1) showed the reaction to be complete. Chloroform (300 ml) was added to the reaction solution. The mixture was cooled to 5 C and washed twice with 1 N hydrochloric acid (300 ml + 200 ml). The organic layer was washed with aqueous sodium hydrogen carbonate and water, dried ($MgSO_4$) and concentrated to dryness. The residual syrup (5.2 g) was purified on a column (50 ml) of silica gel (chloroform : methanol = 20 : 1) to yield the penta-*O*-acetate (**4**) (3.39 g, 64%), amorphous, $[\alpha]_D^{24}$ +93.6 ($c$ = 1.18, $CHCl_3$). IR (KBr): 1755, 1372, 1235, 1160, 1048, 1018 cm$^{-1}$. $^1$H-NMR ($CDCl_3$) $\delta$: 1.92—2.37 (17H, m, $COCH_3$ and H-3 of KDO), 6.77 (1H, brs, COOH).

**Benzyl 2,4,5,7,8-Penta-*O*-acetyl-3-deoxy-α-D-*manno*-2-octulosonate (5)**——A solution of **4** (2.24 g, 5 mmol) in dichloromethane (20 ml) was stirred at room temperature, and then a solution of phenyldiazomethane in petroleum ether [30 ml, 6.3% (w/v)] was added over 10 min. After 2 h, TLC (chloroform : isopropyl ether = 10 : 3) showed the reaction to be complete. The reaction mixture was adjusted to pH 4 with acetic acid and then washed successively with aqueous sodium hydrogen carbonate and water, dried ($MgSO_4$) and concentrated. The residual syrup (4.2 g) was purified on a column (50 ml) of silica gel (chloroform : methanol = 20 : 1) to yield the benzyl ester (**5**) (2.1 g, 78%), mp 96—98 C, $[\alpha]_D^{25}$ +91.9 ($c$ = 0.9, $CHCl_3$). IR (KBr): 1772, 1749, 1371, 1244, 1205, 1088, 1052, 1010 cm$^{-1}$. $^1$H-NMR ($CDCl_3$) $\delta$: 0.95—1.20 (16H, m, $COCH_3$ and H-3 of KDO), 7.32 (5H, s, Ph). $^{13}$C-NMR ($CDCl_3$) $\delta$: 20.59 ($CH_3CO$), 30.83 (C-3), 62.15 (C-8), 63.99 (C-6), 65.94 (C-5), 67.40 ($CH_2Ph$), 67.83 (C-4), 69.79 (C-7), 97.53 (C-2), 128.14 (arom.). *Anal.* Calcd for $C_{25}H_{30}O_{13}$: C, 55.76; H, 5.62. Found: C, 55.68; H, 5.65.

**Benzyl 4,5,7,8-Tetra-*O*-acetyl-2-bromo-3-deoxy-α-D-*manno*-2-octulosonate (6)**——A solution of **5** (269 mg, 0.5 mmol) in dichloromethane (5 ml) and ethyl acetate (0.5 ml) was stirred at room temperature. Then, Molecular Sieves 4A (160 mg) was added to the solution and the whole was stirred for 60 min. The reaction mixture was cooled to 5 °C, titanium tetrabromide (350 mg, 0.95 mmol) was added, and stirring was continued at room temperature for 16 h. The reaction was confirmed to be complete by TLC (chloroform : isopropyl ether = 10 : 3), then acetonitrile (2.8 ml) and anhydrous sodium acetate (1.0 g) were added to the reaction mixture and the whole was stirred at room temperature for 30 min to decompose the reagent. Toluene (10 ml) was added to the mixture with cooling, the whole was stirred for 30 min, and then the solids were filtered off and the filtrate was concentrated (vacuum pump) to give **6** (302 mg) (100%) as a syrup. This syrup was used for the following reaction without purification. *Rf* values on TLC (chloroform : acetone = 10 : 2): **5**, 0.22; **6**, 0.31; 2-deoxylate, 0.45.

**Benzyl 6-*O*-(Benzyl 4,5,7,8-tetra-*O*-acetyl-3-deoxy-α and β-D-*manno*-2-octulopyranosylonate)-2-deoxy-2-[(*R*)-3-dodecanoyloxytetradecanamido]-3-*O*-[(*R*)-3-tetradecanoyloxytetradecanoyl]-β-D-glucopyranoside (8aα and β)**——$Hg(CN)_2$ (180 mg, 0.49 mmol), $HgBr_2$ (36 mg, 0.14 mmol) and Molecular Sieves 4A (300 mg) were added to the

solution of **7a** (418 mg, 0.375 mmol) in dichloromethane (5 ml) and the mixture was stirred at room temperature for 2 h. Then, the bromide (**6**) (308 mg) derived from benzyl 2,4,5,7,8-penta-*O*-acetyl-3-deoxy-α-D-*manno*-2-octulosonate (269 mg, 0.50 mmol) in dichloromethane (1 ml) was added to the mixture and the whole was stirred at room temperature for 20 h. The reaction was confirmed to be complete by TLC (chloroform : isopropyl ether = 10 : 3) (the starting bromide was no longer detectable), then the reaction mixture was washed with 10% KI aqueous solution and water, dried ($MgSO_4$), and concentrated. The residual syrup was purified on a column (25 g) of silica gel (chloroform : isopropyl ether = 25 : 1) to give successively the HBr-eliminated product from the bromide (**6**), the α-glycosylate (**8aα**) (187 mg, 31%), the β-glycosylate (**8aβ**) (36 mg, 6%) and recovered **7a** (241 mg, 58%).

Characterizing Data for the α-Glycosylate (**8aα**): Syrup, $[\alpha]_D^{21}$ +9.2 ($c$ = 2.02, $CHCl_3$). IR (KBr): 3370, 2930, 1755, 1661, 1371, 1240, 1161, 1085, 1048, 699 $cm^{-1}$. $^1$H-NMR ($CDCl_3$) $\delta$: 0.88 (12H, t, $J$ = 3.2 Hz, $CH_3$), 1.27 (80H, s, $CH_2$), 1.81—2.46 (22H, m, $COCH_2$, $COCH_3$ and H-3 of KDO), 6.15 (1H, d, $J$ = 5.4 Hz, NH), 7.08—7.33 (10H, m, Ph). *Anal.* Calcd for $C_{90}H_{145}NO_{22}\cdot 4H_2O$: C, 64.91; H, 9.26; N, 0.84. Found: C, 65.08; H, 8.97; N, 0.90.

Characterizing Data for the β-Glycosylate (**8aβ**): Syrup, $[\alpha]_D^{22}$ +19.2 ($c$ = 0.24, $CHCl_3$). IR (KBr): 3380, 2935, 1750, 1660, 1371, 1235, 1162, 1089, 1048, 699 $cm^{-1}$. $^1$H-NMR ($CDCl_3$) $\delta$: 0.87 (12H, t, $J$ = 3.4 Hz, $CH_3$), 1.28 (80H, s, $CH_2$), 1.70—2.44 (22H, m, $COCH_2$, $COCH_3$ and H-3 of KDO), 5.84 (1H, d, $J$ = 5.4 Hz, NH), 7.22—7.38 (10H, m, Ph). *Anal.* Calcd for $C_{90}H_{145}NO_{22}\cdot 4H_2O$: C, 64.91; H, 9.26; N, 0.84. Found: C, 65.15; H, 9.01; N, 0.87.

**Benzyl 6-*O*-(Benzyl 4,5,7,8-tetra-*O*-acetyl-3-deoxy-α-D-*manno*-2-octulopyranosylonate)-2-deoxy-2-[(*R*)-3-tetradecanoyloxytetradecanamido]-3-*O*-[(*R*)-3-tetradecanoyloxytetradecanoyl]-β-D-glucopyranoside (8bα)**——Treatment of **7b** (434 mg, 0.380 mmol) as described for **8aα** gave **8bα** (250 mg, 31%), syrup, $[\alpha]_D^{24}$ +11.5 ($c$ = 1.46, $CHCl_3$).

**Benzyl 6-*O*-(Benzyl 4,5,7,8-tetra-*O*-acetyl-3-deoxy-α-D-*manno*-2-octulopyranosylonate)-2-deoxy-2-[(*R*)-3-dodecanoyloxytetradecanamido]-3-*O*-[(*R*)-3-dodecanoyloxytetradecanoyl]-β-D-glucopyranoside (8cα)**——Treatment of **7c** (220 mg, 0.202 mmol) as described for **8aα** gave **8cα** (81 mg, 25%), syrup, $[\alpha]_D^{24}$ +10.9° ($c$ = 3.25, $CHCl_3$).

**Benzyl 6-*O*-(Benzyl 4,5,7,8-tetra-*O*-acetyl-3-deoxy-α-D-*manno*-2-octulopyranosylonate)-2-deoxy-4-*O*-diphenylphosphono-2-[(*R*)-3-dodecanoyloxytetradecanamido]-3-*O*-[(*R*)-3-tetradecanoyloxytetradecanoyl]-β-D-glucopyranoside (9aα)**——Pyridine (30 mg, 0.38 mmol), 4-dimethylaminopyridine (43 mg, 0.35 mmol) and Molecular Sieves 4A (13 mg) were added to the solution of **8aα** (100 mg, 0.062 mmol) in dichloromethane (0.5 ml) with stirring at 5 C and after 30 min, diphenyl phosphorochloridate (92 mg, 0.34 mmol) was added to the mixture. The reaction mixture was stirred at room temperature for 4 h, after which time TLC (chloroform : isopropyl ether = 10 : 3) showed the reaction to be complete. The mixture was cooled to 5 C and the excess phosphorylating agent was destroyed by addition of a small amount of cold aqueous sodium hydrogen carbonate. After a short time, the organic layer was separated, washed with water and dried ($MgSO_4$). Solvents were removed under reduced pressure and the residue (208 mg) was purified on a column (10 g) of silica gel (chloroform : isopropyl ether = 20 : 1) to yield the diphenylphosphorylate (**9aα**) (106 mg, 93%), syrup, $[\alpha]_D^{22}$ +17.6 ($c$ = 1.42, $CHCl_3$). IR (KBr): 3400, 2930, 1755, 1235, 1221, 1192, 1162, 1043, 958 $cm^{-1}$. $^1$H-NMR ($CDCl_3$) $\delta$: 0.86 (12H, t, $J$ = 3.5 Hz, $CH_3$), 1.25 (80H, s, $CH_2$), 1.77—2.43 (22H, m, $COCH_2$, $COCH_3$ and H-3 of KDO), 6.10 (1H, d, $J$ = 5.7 Hz, NH), 7.12—7.31 (20H, m, Ph). *Anal.* Calcd for $C_{102}H_{154}NO_{25}P$: C, 67.12; H, 8.50; N, 0.77. Found: C, 66.88; H, 8.52; N, 0.72.

**Benzyl 6-*O*-(Benzyl 4,5,7,8-tetra-*O*-acetyl-3-deoxy-α-D-*manno*-2-octulopyranosylonate)-2-deoxy-4-*O*-diphenylphosphono-2-[(*R*)-3-tetradecanoyloxytetradecanamido]-3-*O*-[(*R*)-3-tetradecanoyloxytetradecanoyl]-β-D-glucopyranoside (9bα)**——Treatment of **8bα** (175 mg, 0.11 mmol) as described for **9aα** gave **9bα** (160 mg, 80%), syrup, $[\alpha]_D^{21}$ +17.2° ($c$ = 1.50, $CHCl_3$). *Anal.* Calcd for $C_{104}H_{158}NO_{25}P$: C, 67.40; H, 8.59; N, 0.76. Found: C, 67.23; H, 8.72; N, 0.77.

**Benzyl 6-*O*-(Benzyl 4,5,7,8-tetra-*O*-acetyl-3-deoxy-α-D-*manno*-2-octulopyranosylonate)-2-deoxy-4-*O*-diphenylphosphono-2-[(*R*)-3-dodecanoyloxytetradecanamido]-3-*O*-[(*R*)-3-dodecanoyloxytetradecanoyl]-β-D-glucopyranosie (9cα)**——Treatment of **8cα** (146 mg, 0.093 mmol) as described for **9aα** gave **9cα** (133 mg, 79%), syrup, $[\alpha]_D^{20}$ +15.6 ($c$ = 6.65, $CHCl_3$). *Anal.* Calcd for $C_{100}H_{150}NO_{25}P$: C, 66.83; H, 8.41; N, 0.98. Found: C, 66.90; H, 8.55; N, 1.01.

**6-*O*-(4,5,7,8-Tetra-*O*-acetyl-3-deoxy-α-D-*manno*-2-octulopyranosonic acid)-2-deoxy-2-[(*R*)-3-dodecanoyloxytetradecanamido]-3-*O*-[(*R*)-3-tetradecanoyloxytetradecanoyl]-4-*O*-phosphono-D-glucopyranose (2aα)**——A solution of **9aα** (63 mg, 0.035 mmol) in methanol (4 ml) was hydrogenated at 25°C under atmospheric pressure in the presence of 10% Pd-on-C catalyst (70 mg). The reaction was monitored by TLC (chloroform : methanol = 10 : 1, $Rf$ = 0.6). The catalyst was filtered off and $PtO_2$ (30 mg) was added to the filtrate. Hydrogenolysis was continued at room temperature for 18 h, when TLC (chloroform : methanol = 10 : 3, $Rf$ = 0.7) showed the reaction to be complete (there was no UV-absorbing material). The catalyst was then filtered off and the filtrate was concentrated to dryness. The residual solid (47 mg) was purified on a column (10 g) of silica gel (chloroform : methanol = 20 : 1) followed by lyophilization from dioxane to obtain the desired compound (**2aα**) (28 mg, 54%), mp 123—125 C, $[\alpha]_D^{22}$ +19.4 ($c$ = 0.32, $CHCl_3$). IR (KBr): 3450, 2935, 1751, 1630, 1372, 1250, 1108, 1051 $cm^{-1}$. *Anal.* Calcd for $C_{76}H_{134}NO_{25}P\cdot H_2O$: C, 60.41; H, 9.07; N, 0.93. Found: C, 60.11; H, 8.79; N, 0.79.

**6-*O*-(4,5,7,8-Tetra-*O*-acetyl-3-deoxy-α-D-*manno*-2-octulopyranosonic acid)-2-deoxy-2-[(*R*)-3-tetradecanoyloxytetradecanamido]-3-*O*-[(*R*)-3-tetradecanoyloxytetradecanoyl]-4-*O*-phosphono-D-glucopyranose (2bα)**——Treatment of **9bα** (85 mg, 0.046 mmol) as described for **2aα** gave **2bα** (26 mg, 37%), mp 116—120 C, $[\alpha]_D^{24}$ +14.2 ($c$ = 0.5, $CHCl_3$). *Anal.* Calcd for $C_{78}H_{138}NO_{25}P\cdot 2H_2O$: C, 60.21; H, 9.07; N, 0.90. Found: C, 60.05; H, 8.84; N, 1.00.

**6-*O*-(4,5,7,8-Tetra-*O*-acetyl-3-deoxy-α-D-*manno*-2-octulopyranosonic acid)-2-deoxy-2-[(*R*)-3-dodecanoyloxytetradecanamido]-3-*O*-[(*R*)-3-dodecanoyloxytetradecanoyl]-4-*O*-phosphono-D-glucopyranose (2cα)**——Treatment of **9cα** (128 mg, 0.071 mmol) as described for **2aα** gave **2cα** (36 mg, 35%), mp 122—124 °C, $[\alpha]_D^{25}$ +24.6° (*c* = 1.05, $CHCl_3$). *Anal.* Calcd for $C_{74}H_{130}NO_{25}P \cdot 3H_2O$: C, 58.51; H, 8.76; N, 0.92. Found: C, 58.71; H, 8.53; N, 0.76.

**Benzyl 6-*O*-(Benzyl 4,5,7,8-tetra-*O*-acetyl-3-deoxy-α and β-D-*manno*-2-octulopyranosylonate)-2-deoxy-2-(2,2,2-trichloroethoxycarbonyl)amino-3-*O*-(2,2,2-trichloroethoxycarbonyl)-β-D-glucopyranoside (11α and β)**——$Hg(CN)_2$ (72 mg, 0.2 mmol), $HgBr_2$ (10 mg, 0.04 mmol) and Molecular Sieves 4A (110 mg) were added to a solution of **10** (124 mg, 0.2 mmol) in dichloromethane (2 ml) and the mixture was stirred at room temperature for 1 h. Then the bromide (**6**, 114 mg) derived from benzyl 2,4,5,7,8-penta-*O*-acetyl-3-deoxy-α-D-*manno*-2-octulosonate (108 mg, 0.20 mmol) in dichloromethane (1 ml) was added to the mixture and the whole was stirred at room temperature for 20 h. It was confirmed by chloroform : isopropyl ether = 10 : 3) that the starting material (the bromide) had disappeared, then the reaction mixture was washed with 10% KI aqueous solution and water, dried ($MgSO_4$), and concentrated. The residual syrup (281 mg) was purified on a column (10 g) of silica gel (chloroform : isopropyl ether = 20 : 1) to yield the α-glycosylate (**11β**) (67 mg, 31%) and the β-glycosylate (**11α**) (8 mg, 4%), respectively.

Characterizing Data of the α-Glycoside (**11α**): Amorphous, $[\alpha]_D^{22}$ + 10.0° (*c* = 0.22, $CHCl_3$). IR (KBr): 3430, 1758, 1370, 1250, 1160, 1085, 1038, 820, 737, 700 $cm^{-1}$. $^1$H-NMR ($CDCl_3$) δ: 1.73—2.32 (14H, m, $COCH_3$ and H-3 of KDO), 7.17—7.38 (10H, m, Ph). *Anal.* Calcd for $C_{42}H_{47}Cl_6NO_{20}$: C, 45.92; H, 4.31; N, 1.28. Found: C, 45.85; H, 4.45; N, 1.12.

Characterizing Data of the β-Glycoside (**11β**): Amorphous, $[\alpha]_D^{23}$ + 18.4° (*c* = 1.1, $CHCl_3$). IR (KBr): 3430, 1758, 1370, 1250, 1160, 1085, 1052, 820, 739, 700 $cm^{-1}$. *Anal.* Calcd for $C_{42}H_{47}Cl_6NO_{20}$: C, 45.92; H, 4.31; N, 1.28. Found: C, 45.88; H, 4.52; N, 1.22.

**Benzyl 6-*O*-(Benzyl 4,5,7,8-tetra-*O*-acetyl-3-deoxy-α-D-*manno*-2-octulopyranosylonate)-2-deoxy-4-*O*-diphenylphosphono-2-(2,2,2-trichloroethoxycarbonyl)amino-3-*O*-(2,2,2-trichloroethoxycarbonyl)-β-D-glucopyranoside (12α)**——Pyridine (67 mg, 0.84 mmol), 4-dimethylaminopyridine (21 mg, 0.168 mmol) and Molecular Sieves 4A (30 mg) were added to a solution of **11α** (185 mg, 0.168 mmol) in benzene (1 ml) with stirring at 5 °C, and after 20 min diphenyl phosphorochloridate (226 mg, 0.84 mmol) was added. The reaction mixture was stirred at room temperature for 4 h, and monitored by TLC (dichloromethane : isopropyl ether = 10 : 3). After complete disappearance of the starting material, the reaction mixture was cooled, washed with aqueous sodium hydrogen carbonate and water, and dried ($MgSO_4$). The solvent was removed under reduced pressure and the residue was purified on a column (25 ml) of silica gel (chloroform : isopropyl ether = 20 : 1) to give the diphenylphosphate (**12α**) (171 mg, 77%), amorphous, $[\alpha]_D^{23}$ + 22.7° (*c* = 0.8, $CHCl_3$). IR (KBr): 3450, 1754, 1495, 1370, 1247, 1163, 1041, 961 $cm^{-1}$. $^1$H-NMR ($CDCl_3$) δ: 1.71—2.46 (14H, m, $COCH_3$ and H-3 of KDO), 2.27 (dd, *J* = 13.4, 5.9 Hz, 3-$H_{eq}$), 7.11—7.31 (20H, m, Ph). $^{13}$C-NMR ($CDCl_3$) δ: 98.6 (αC-2). *Anal.* Calcd for $C_{54}H_{56}Cl_6NO_{23}P$: C, 48.74; H, 4.24; N, 1.05. Found: C, 49.03; H, 4.33; N, 0.91.

**Benzyl 6-*O*-(Benzyl 4,5,7,8-tetra-*O*-acetyl-3-deoxy-β-D-*manno*-2-octulopyranosylonate)-2-deoxy-4-*O*-diphenylphosphono-2-(2,2,2-trichloroethoxycarbonyl)amino-3-*O*-(2,2,2-trichloroethoxycarbonyl)-β-D-glucopyranoside (12β)**——Treatment of **11β** (73 mg, 0.0664 mmol) as described for **12α** gave **12β** (60 mg, 68%), amorphous, $[\alpha]_D^{20}$ + 31.4° (*c* = 0.68, $CHCl_3$). $^{13}$C-NMR ($CDCl_3$) δ: 99.9 (βC-2). *Anal.* Calcd for $C_{54}H_{56}NO_{23}P$: C, 48.74; H, 4.24; N, 1.05. Found: C, 48.98; H, 4.31; N, 0.99.

**Benzyl 2-Amino-6-*O*-(benzyl 4,5,7,8-tetra-*O*-acetyl-3-deoxy-α-D-*manno*-2-octulopyranosylonate)-2-deoxy-4-diphenylphosphono-β-D-glucopyranoside (13α)**——A solution of **12α** (186 mg, 0.140 mmol) in acetic acid (1.9 ml) was stirred at room temperature. Zinc powder (156 mg, 2.39 mmol) was added to the solution in small portions over 30 min and then the mixture was stirred for 6 h, when TLC (chloroform : methanol = 10 : 1) showed the reaction to be complete. The solid was filtered off and the filtrate was concentrated to dryness. The residual syrup (274 mg) was purified on a column (10 g) of silica gel (chloroform : methanol = 25 : 1) to give **13α** (108 mg, 79%), amorphous, $[\alpha]_D^{24}$ + 29.0° (*c* = 2.26, $CHCl_3$). IR (KBr): 3440, 1753, 1591, 1492, 1372, 1222, 1190, 1162, 1092, 955, 698 $cm^{-1}$. $^1$H-NMR ($CDCl_3$) δ: 1.64—2.24 (14H, m, $COCH_3$ and H-3 of KDO), 7.19—7.38 (20H, m, Ph). *Anal.* Calcd for $C_{48}H_{54}NO_{19}P \cdot H_2O$: C, 56.75; H, 5.36; N, 1.38. Found: C, 56.55; H, 5.46; N, 1.35.

**Benzyl 6-*O*-(Benzyl 4,5,7,8-tetra-*O*-acetyl-3-deoxy-α-D-*manno*-2-octulopyranosylonate)-2-deoxy-4-*O*-diphenylphosphono-2-[(*R*)-3-tetradecanoyloxytetradecanoyl]amino-3-*O*-[(*R*)-3-tetradecanoyloxytetradecanoyl]-β-D-glucopyranoside (9bα)**——A solution of **13α** (70 mg, 0.071 mmol) in dichloromethane (0.7 ml) was stirred at −5 °C and (*R*)-3-tetradecanoyloxytetradecanoic acid (97 mg, 0.213 mmol), 4-dimethylaminopyridine (4 mg, 0.033 mmol) and *N*,*N*-dicyclohexylcarbodiimide (44 mg, 0.213 mmol) was added. The mixture was stirred at −5—5 °C for 1 h, at 5—20 °C for 3 h and at room temperature for 5 h. It was confirmed by TLC (chloroform : isopropyl ether = 10 : 3) that the reaction was complete, then the solid was filtered off and the filtrate was washed with water, dried ($MgSO_4$) and concentrated. The residual syrup (155 mg) was purified on a column (10 g) of silica gel (chloroform : isopropyl ether = 20 : 1) to give the diacylate (**9bα**) (52 mg, 40%), syrup, $[\alpha]_D^{24}$ + 16.9° (*c* = 1.35, $CHCl_3$). IR (KBr): 3420, 2930, 1758, 1236, 1220, 1191, 1164, 1045, 958, 698 $cm^{-1}$. $^1$H-NMR ($CDCl_3$) δ: 0.88 (12H, t, *J* = 3.0 Hz, $CH_3$), 1.25 (84H, s, $CH_2$), 1.80—2.60 (22H, m, $COCH_2$, $COCH_3$ and H-3 of KDO), 6.11 (1H, d, *J* = 5.6 Hz, NH), 7.05—7.40 (20H, m, Ph). *Anal.* Calcd for $C_{104}H_{158}NO_{25}P$: C, 67.40; H, 8.59; N, 0.76. Found: C, 67.27; H, 8.68; N, 0.88.

**Acknowledgement** The authors are indebted to Dr. K. Narita and the staff of the Analysis Center of this college for microanalysis. This work was supported in part by a Grant-in-Aid from Tokyo Biochemical Research Foundation.

## References

1) *a*) T. Takahashi, C. Shimizu, S. Nakamoto, K. Ikeda, and K. Achiwa, *Chem. Pharm. Bull.*, **33**, 1760 (1985); *b*) S. Nakamoto, T. Takahashi, K. Ikeda, and K. Achiwa, *ibid.*, **33**, 4098 (1985); *c*) T. Shimizu, S. Akiyama, T. Masuzawa, Y. Yanagihara, S. Nakamoto, T. Takahashi, K. Ikeda, and K. Achiwa, *ibid.*, **33**, 4621 (1985); *d*) K. Ikeda, S. Nakamoto, T. Takahashi, and K. Achiwa, *Carbohydr. Res.*, **145**, C5 (1986); *e*) T. Takahashi, S. Nakamoto, K. Ikeda, and K. Achiwa, *Tetrahedron Lett.*, **27**, 1819 (1986); *f*) S. Nakamoto and K. Achiwa, *Chem. Pharm. Bull.*, **34**, 2302 (1986); *g*) T. Shimizu, S. Akiyama, T. Masuzawa, Y. Yanagihara, S. Nakamoto, and K. Achiwa, *ibid.*, **34**, 2310 (1986); *h*) T. Shimizu, S. Akiyama, T. Masuzawa, Y. Yanagihara, S. Nakamoto, T. Takahashi, K. Ikeda, and K. Achiwa, *ibid.*, **34**, 5169 (1986); *i*) T. Shimizu, S. Akiyama, T. Masuzawa, Y. Yanagihara, S. Nakamoto, and K. Achiwa, *ibid.*, **35**, 873 (1987); *j*) K. Ikeda, T. Takahashi, H. Kondo, and K. Achiwa, *ibid.*, **35**, 1311 (1987); *k*) K. Ikeda, T. Takahashi, C. Shimizu, S. Nakamoto, and K. Achiwa, *ibid.*, **35**, 1383 (1987); *l*) T. Shimizu, S. Akiyama, T. Masuzawa, Y. Yanagihara, K. Ikeda, T. Takahashi, H. Kondo, and K. Achiwa, *Microbiol. Immunol.*, **31**, 381 (1987); *m*) T. Shimizu, S. Akiyama, T. Masuzawa, Y. Yanagihara, S. Nakamoto, and K. Achiwa, *Infection and Immunology*, **55**, 2287 (1987); *n*) K. Ikeda, S. Nakamoto, T. Takahashi, and K. Achiwa, *Chem. Pharm. Bull.*, **35**, 4436 (1987); *o*) S. Nakamoto, T. Takahashi, K. Ikeda and K. Achiwa, *ibid.*, **35**, 4517 (1987).
2) *a*) O. Westphal and O. Lüderitz, *Angew. Chem.*, **66**, 407 (1954); *b*) O. Lüderitz, C. Galanos, V. Lehmann, H. Mayer, E. T. Rietschel, and J. Weckesser, *Naturwissenschaften*, **65**, 578 (1978).
3) *a*) K. Amano, H. Hujita, T. Sato, H. Sasaki, Y. Yoshida, and F. Fukushi, *Jpn. J. Bacterol.*, **40**, 775 (1985); *b*) K. Tanamoto and J. H. Homma, *J. Biochem.* (Tokyo), **91**, 741 (1982).
4) R. Christian, G. Shulz, P. Waldstatten, and F. N. Unger, *Tetrahedron Lett.*, **25**, 3433 (1984).
5) U. Zähringer, B. Lindner, U. Seydel, E. T. Rietschel, H. Naoki, F. N. Unger, M. Imoto, S. Kusumoto, and T. Shiba, *Tetrahedron Lett.*, **26**, 6321 (1985).
6) *a*) S. Kusumoto, M. Yamamoto, and T. Shiba, *Tetrahedron Lett.*, **25**, 3727 (1984) and references cited therein; *b*) M. Kiso, H. Ishida, and A. Hasegawa, *Agric. Biol. Chem.*, **48**, 251 (1984); *c*) D. Charon, R. Chaby, A. Malinvaud, M. Montage, and L. Szabo, *Biochemistry*, **24**, 2736 (1985).
7) C. S. Hershberger, M. Davis, and S. B. Binkley, *J. Biol. Chem.*, **243**, 1585 (1968).
8) J. C. Dittmer and R. L. Lester, *J. Lipid Res.*, **5**, 126 (1964).
9) U. Zahringer, B. Lindner, U. Seydel, E. Th. Rietschel, H. Naoki, F. N. Unger, M. Imoto, S. Kusumoto, and T. Shiba, *Tetrahedron Lett.*, **26**, 6321 (1985).

[Chem. Pharm. Bull. 35(11)4544—4551(1987)]

# Analytical Studies on 1-(2-*o*-Chlorobenzoyl-4-chlorophenyl)-3-dimethylcarbamoyl-5-glycylaminomethyl-1*H*-1,2,4-triazole Hydrochloride Dihydrate. III.[1] High-Performance Liquid Chromatographic Method Applicable to Animal Feed

RIKIO IKENISHI* and TAKAYASU KITAGAWA

*Shionogi Research Laboratories, Shionogi & Co., Ltd., Sagisu 5–12–4, Fukushima-ku, Osaka 553, Japan*

(Received March 5, 1987)

An ion-pair reversed-phase high-performance liquid chromatographic (HPLC) assay method was developed for the sleep inducer 1-(2-*o*-chlorobenzoyl-4-chlorophenyl)-3-dimethylcarbamoyl-5-glycylaminomethyl-1*H*-1,2,4-triazole hydrochloride dihydrate (rilmazafone, **1**) in animal feed. This method is an ion-pair reversed-phase HPLC using an octadecylsilane chemically bonded silica gel column and dodecanesulfonic acid as an ion-pairing reagent. It can simultaneously assay drug **1** and its six degradation products. Dodecanesulfonic acid caused retention of three compounds (**1**, **6** and **7**) on the column through the ion-pair effect, with good separation from other neutral and acidic compounds.

The drug was extracted from the feed. After clean-up, the extract was subjected to HPLC, with **1** being assayed with a coefficient of variation of less than 4%. The degradation products can be simultaneously assayed with the same precision even when present at only 2—3 mg/kg. This method was used to confirm the stability of **1** in feed. An HPLC method to assay **1** alone was also established; it is more efficient than our previous fluorometric procedure.

**Keywords**——sleep inducer; rilmazafone; ion-pair high-performance liquid chromatography; dodecanesulfonic acid; degradation product; animal feed; stability assessment

In previous papers,[1,2] we have reported two methods, a colorimetry and a fluorometry, for assaying a sleep inducer, 1-(2-*o*-chlorobenzoyl-4-chlorophenyl)-3-dimethylcarbamoyl-5-glycylaminomethyl-1*H*-1,2,4-triazole hydrochloride dihydrate (rilmazafone, **1**[3]). We have now developed an analytical method using high-performance liquid chromatography (HPLC) for assaying **1** in feed samples used as test substance in animal toxicity tests. Compound **1** was mixed with animal feed, which was then sterilized. The feed sample was supplied to animals during the test and stored for 3—4 months. It was important to check whether or not any degradation products are formed under the preparation and storage conditions.[4] One objective of the analysis was to check the stability of **1** by using an HPLC method and another was to establish a more efficient method which would enable us to analyze samples more rapidly than was possible with our fluorometric procedure reported previously.[1] Since **1** was degraded to **2** and **3** in acid and to **4**—**7** in alkaline solution, these six compounds were assumed to be the degradation products of **1**. We established an ion-pair reversed-phase chromatography using octadecylsilane (ODS) chemically bonded silica gel column and 1-dodecanesulfonic acid sodium salt (DSAS) as an ion-pairing reagent. This paper describes the assay method applicable to the stability assessment of **1** and a simplified method for the determination of **1** alone. The latter method is more rapid than our previous fluorometric procedure.

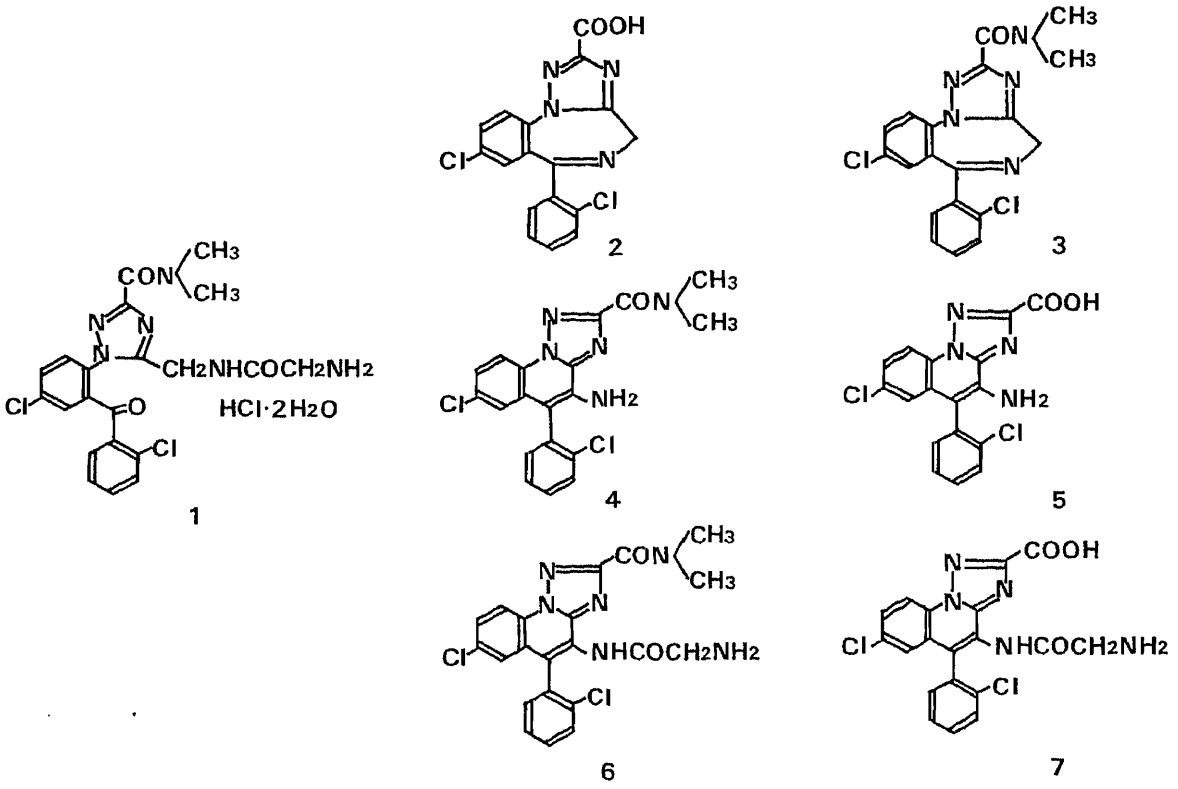


Chart 1

## Experimental

**Apparatus**——An Iwaki KM shaker, type V-S, was used for the extraction of **1** from feed. A Directmix, model TS-50 (Thermal Kagaku Sangyo Co., Ltd.) was used to dissolve the residue and for the liquid–liquid distribution. A Sakuma centrifuge, model 90-4, was used for the separation.

Liquid Chromatograph: A Shimadzu LC-4A pump equipped with a Shimadzu SPD-2AS UV detector and a Rheodyne model 7125 injection valve with a 100 $\mu$l sample loop were used.

Column: A stainless-steel column (30 cm × 4 mm i.d.) was packed with Nucleosil 10$C_{18}$ (Macherey-Nagel, 10 $\mu$m) by a slurry-packing method. The same two columns were connected in series in assay procedure A. A guard column, SPHERI-5, RP-18, OD-GU (Brownlee Labs., 5 $\mu$m) was joined in series in assay procedure B.

Data Integration System: Shimadzu Chromatopac C-R2AX data processor (ATTEN 3).

Chromatographic Conditions: The mobile phase used in assay procedure A was 0.1 M tartaric acid–$CH_3CN$–EtOH (210 : 140 : 50). The 0.1 M tartaric acid contained 5 mM DSAS and 0.29 mM $Et_3N$. The mobile phase used in assay procedure B was 0.1 M tartaric acid–$CH_3CN$–iso-PrOH (225 : 140 : 40). The 0.1 M tartaric acid contained 5 mM DSAS. The flow rates in assay procedures A and B were 1.2 and 1.0 ml/min, respectively. The wavelength was set at 254 nm with a sensitivity of 0.2 V/AU. HPLC analysis was performed at ambient temperature.

**Reagents and Materials**——The chemicals were of reagent grade. Solvents were purchased from E. Merck Co. (HPLC grade). Compound **1** and related compounds were supplied by our laboratories. Animal feed was Charles River CRF-1 (Oriental Yeast Co., Ltd.). Compound **1** was spiked with the powdered feed.

1 M Tartaric Acid: Dissolve 1.50 g of tartaric acid and 0.14 g of DSAS in water to make 10 ml.

0.1 M Tartaric Acid: Dissolve 7.5 g of tartaric acid and 0.68 g of DSAS in water to make 500 ml. For use in assay procedure A, add 20 $\mu$l of $Et_3N$ to the buffer.

Standard Solutions of **1** and Related Compounds for Assay Procedure A: Prepare two stock solutions of **1** and the related compounds by dissolving them in MeOH. Adjust the concentration of **1** to 400 $\mu$g/ml and those of the related compounds to 200 $\mu$g/ml for **2**—**6** and 50 $\mu$g/ml for **7**.[5] Mix the two stock solutions and dilute adequately to make four standard solutions (10, 20, 50 and 100 $\mu$g/ml for **1** and 1, 2, 5, 10 $\mu$g/ml for the related compounds).

Standard Solution of **1** for Assay Procedure B: Prepare a stock solution by dissolving **1** in $H_2O$. Dilute the solution to make five standard solutions (2, 4, 10, 20 and 40 $\mu$g/ml) in the mixed solvent ($H_2O/CH_3CN = 1 : 5$).

**Assay Procedure A**——Weigh 1.0 g of the spiked feed into a 20-ml centrifuge tube, add exactly 10 ml of MeOH and shake the mixture with a shaker for 45 min. After centrifugation at 2000 rpm for 10 min, transfer exactly 5 ml of the supernatant into a 12-ml centrifuge tube and evaporate off the solvent under a stream of $N_2$ at 30 C. Add exactly

1 ml of $CH_3CN$ and 0.1 ml of 1 M tartaric acid and vortex the mixture with a Directmix for 10 min. Add 5 ml of *n*-hexane and vortex the mixture with a Directmix for 10 min. After centrifugation at 2000 rpm for 5 min, discard the *n*-hexane layer with an aspirator. Filter the aqueous $CH_3CN$ layer with an Ekicrodisc 13CR membrane (0.45 $\mu$m, Gelman Sciences Japan Ltd.). Inject 10 $\mu$l of the filtrate into the column and proceed under the above operating conditions. Inject 10 $\mu$l each of four standard solutions into the column and proceed under the same conditions. Calculate the peak areas of the sample and the standard solutions. Make standard curves of **1** and the related compounds using the peak areas and the concentraions of each standard solution. Calculate the contents (mg/kg) in the feed according to the equation:

$$\text{content (mg/kg)} = \frac{\text{concentration } (\mu\text{g/ml}) \times 1.025 \times 2 \times 100}{\text{recovery value}} \quad (1)$$

In Eq. 1, 1.025 is the volume of the aqueous phase after extraction with *n*-hexane. Recovery values were 73.7% for **1**, 82.4% for **2**, 100.0% for **3** and **4**, 79.5% for **5** and 63.3% for **6**. These values, except for **7**, were reproducible between days. The recovery value for **7** was determined when it was assayed.[6]

**Assay Procedure B**——Weigh 1.0 g of the spiked feed into a 20-ml centrifuge tube, add exactly 10 ml of $CH_3CN$ and shake with a shaker for 45 min. After centrifugation at 2000 rpm for 10 min, transfer exactly 2.5 ml of the supernatant into a 12-ml centrifuge tube. Add exactly 0.5 ml of $H_2O$ and 5 ml of *n*-hexane, and shake the mixture with a shaker for 10 min. After centrifugation at 2000 rpm for 5 min, discard the *n*-hexane layer using an aspirator. Filter the aqueous $CH_3CN$ layer with an Ekicrodisc 13CR membrane. Inject 25 $\mu$l of the filtrate into the column and proceed under the above operating conditions. Inject 50 $\mu$l of the filtrate into the column for feed containing less than 50 mg/kg of **1**. Inject 25 $\mu$l each of five standard solutions into the column and proceed using the same conditions. Calculate the peak areas of the sample and standard solutions. Make a standard curve and calculate the content (mg/kg) in the feed according to Eq. 2 (the recovery value for **1** is 89.3%).

$$\text{content (mg/kg)} = \frac{\text{concentration } (\mu\text{g/ml}) \times 3 \times 4 \times 100}{89.3} \quad (2)$$

For a sample containing less than 50 mg/kg,

$$\text{content (mg/kg)} = \frac{\text{concentration } (\mu\text{g/ml}) \times 3 \times 2 \times 100}{89.3} \quad (3)$$

## Results and Discussion

### Chromatographic Conditions

Since **1** was stable in an acidic solution, a reversed-phase HPLC system with an acidic solution as the eluent was selected. The ion-pairing reagent was required to retain the basic compounds on an ODS column.

**Effect of Sodium Alkylsulfonate**——A ternary mixture of solvents, tartaric acid–$CH_3CN$–EtOH, was finally used. Various molecular sizes of sodium alkylsulfonates ($CH_3(CH_2)_nSO_3Na$; $n=6$—12) were added to the mobile phase system. Figure 1 shows the capacity factors ($k'$) of the seven compounds observed on elution with various alkylsulfonates. The $k'$ values of **1**, **6** and **7** increased as the carbon number of the alkyl chain increased, while **2**—**5** were not affected. The reagents had little effect on **4** and **5**, although they have the same basic $NH_2$ group. The dependence of the retention on the kind of substituent may be ascribed to the large difference of basic strength between the two kinds of compounds.[7] A good separation was obtained by the use of sulfonic acid of $n=11$, DSAS.

**Effect of DSAS Concentration**——The concentration of DSAS also affected the $k'$ values of **1**, **6** and **7**. As shown in Fig. 2, the three $k'$ values increased with increasing DSAS concentration. A good separation was obtained at 5 mM.

**Effect of Acid**——Various acids were also used. The $k'$ values differed among the acids (tartaric acid, malic acid, succinic acid and acetic acid). Separation was best with tartaric acid, and there was no interfering peak from feed components. The use of tartaric acid in the concentration range from 0.01 to 0.1 M caused little change of $k'$s.

**Effect of Solvent Composition**——When various amounts of EtOH were added to constant amounts of 0.1 M tartaric acid and $CH_3CN$, all $k'$s decreased as the EtOH content

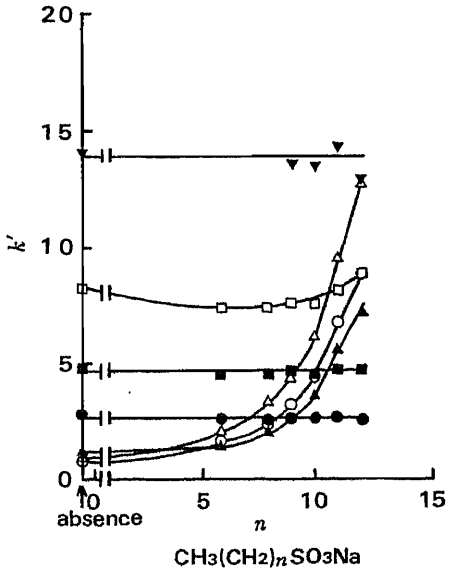


Fig. 1. Effect of Carbon Number of Alkylsulfonate on Capacity Factor ($k'$)

Column: Nucleosil $10C_{18}$, two 30 cm × 4 mm i.d.
Mobile phase: 0.1 M tartaric acid–$CH_3CN$–EtOH (210 : 140 : 50, v/v). (The 0.1 M tartaric acid contained 5 mM $CH_3(CH_2)_nSO_3Na$ and 0.29 mM $Et_3N$.)
Flow rate: 1.2 ml/min.
Amount injected: 10 μl.
—○—, compound 1; —●—, compound 2; —■—, compound 3; —▼—, compound 4; —□—, compound 5; —△—, compound 6; —▲—, compound 7.

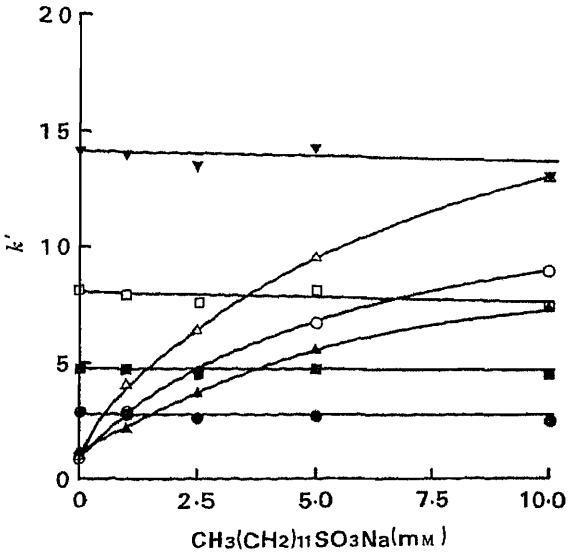


Fig. 2. Effect of Concentration of $CH_3(CH_2)_{11}SO_3Na$ on Capacity Factor ($k'$)

—○—, compound 1; —●—, compound 2; —■—, compound 3; —▼—, compound 4; —□—, compound 5; —△—, compound 6; —▲—, compound 7.

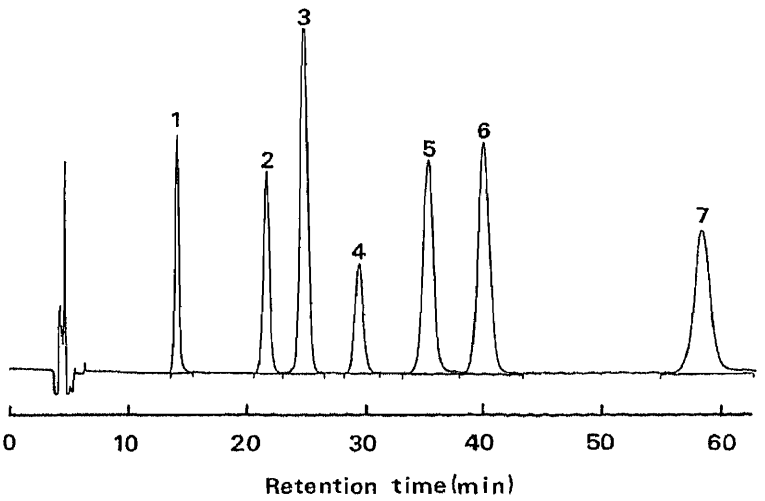


Fig. 3. Chromatogram of Compound 1 and Related Compounds

Column: Nucleosil $10C_{18}$, two 30 cm × 4 mm i.d.
Mobile phase: 0.1 M tartaric acid–$CH_3CN$–EtOH (210 : 140 : 50, v/v). (The 0.1 M tartaric acid contained 5 mM $CH_3(CH_2)_{11}SO_3Na$ and 0.29 mM $Et_3N$.)
Flow rate: 1.2 ml/min.
Amount injected: 10 μl.
1), compound 2; 2), compound 3; 3), compound 7; 4), compound 1; 5), compound 5; 6), compound 6; 7), compound 4.

increased. When the amount of $CH_3CN$ was increased in this system, all $k'$s also decreased and separation became insufficient. The best proportions were 12.5% EtOH and 35% $CH_3CN$.

A typical chromatogram obtained under the optimal conditions is shown in Fig. 3.

Triethylamine has been used as an effective agent to reduce the tailing of some benzodiazepines.[8] A small amount of triethylamine (0.29 mM) was therefore added to the system in method A. Essentially no change was observed in the elution patterns.

**Simultaneous Determination (Assay Procedure A)**

**Conditions for Clean-up. (a) Extraction of 1 and Related Compounds from Feed**——Methanolic solutions (10 ml) of the related compounds (1.5 $\mu$g/ml) were added to the spiked feed containing 150 mg/kg of **1**. Constant amounts of the compounds were recovered by shaking the mixture for more than 30 min. This MeOH extract also contained feed components, which amounted to about 70 mg. In order to avoid interference due to the feed components and column deterioration, the next two clean-up procedures were carried out.

**(b) Redissolution of MeOH Extract**——The MeOH extract was evaporated. The residue was dissolved in $CH_3CN$, followed by treatment according to the assay procedure. Although the recoveries of the compounds, except for **4**, were low, acidification improved the solubilities of these compounds. Figure 4 shows the effect of the concentration of tartaric acid on the dissolution. The recovered amounts of all the compounds increased as the concentration of tartaric acid increased. All the values were constant at over 0.5 M. Tartaric acid was used at 1 M. The time required for complete dissolution was 5 min.

**(c) Clean-up by Liquid–Liquid Distribution of $CH_3CN$ Extract**——The $CH_3CN$ extract (1.1 ml) containing aqueous tartaric acid solution was shaken with *n*-hexane. The two organic phases were cleanly separated and their volumes remained almost unchanged. A large part of the lipophilic components in feed was eliminated by this procedure and there was little loss of the samples. The effect of the amount of *n*-hexane (2.5, 5 and 7.5 ml) on the distribution was examined, and increased loss of **2**, **3** and **5** was found at more than 5 ml. The reproducibility of the recovery was constant over 5 min. This clean-up procedure was carried out with 5 ml of *n*-hexane for 10 min.

The $CH_3CN$ extract after pretreatment was subjected to HPLC. No interfering peaks were found after 13 min. Figure 5 shows a chromatogram of the extract of control feed which was obtained after this pretreatment.

**Recovery Value and Quantitation Limit**——Various amounts of **1** ranging from 50 to 300 $\mu$g were spiked into the feed. The feed samples were assayed by the above method. A linear relationship, which passed through the origin, was observed between the recovered and the

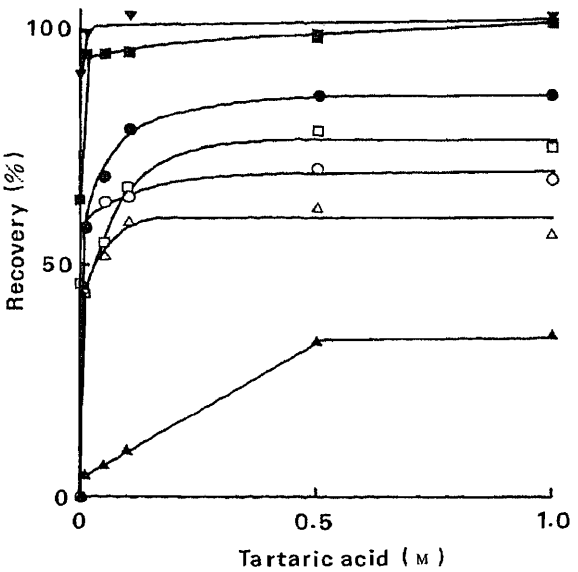


Fig. 4. Effect of Concentration of Tartaric Acid on Dissolution of Compound 1 and Related Compounds

—○—, compound 1; —●—, compound 2; —■—, compound 3; —▼—, compound 4; —□—, compound 5; —△—, compound 6; —▲—, compound 7.

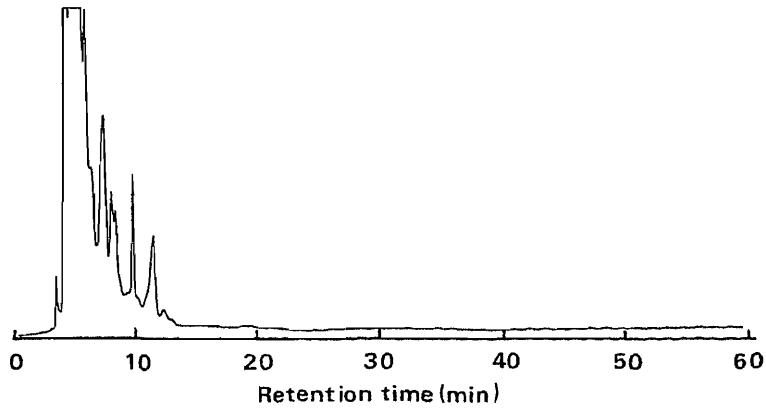


Fig. 5. Chromatogram of Extract from Control Feed

TABLE I. Recovery of Compound 1 from Feed

| n | 1st | | 2nd | |
|---|---|---|---|---|
| | Taken (μg) | Found (μg) | Taken (μg) | Found (μg) |
| 1 | 50 | 37.8 | 52 | 38.3 |
| 2 | 58 | 44.4 | 80 | 56.9 |
| 3 | 80 | 54.6 | 112 | 73.9 |
| 4 | 106 | 76.8 | 128 | 102.2 |
| 5 | 140 | 111.1 | 145 | 113.8 |
| 6 | 145 | 113.2 | 212 | 150.0 |
| 7 | 194 | 142.3 | 230 | 161.6 |
| 8 | 264 | 199.2 | 250 | 183.8 |
| 9 | 292 | 215.0 | 286 | 209.7 |

Regression equation
1st: $y=0.745x+0.415$, $n=9$, $s=4.14$, $r=0.998$.
2nd: $y=0.723x+1.090$, $n=9$, $s=6.16$, $r=0.995$.
Total: $y=0.733x+0.857$, $n=18$, $s=5.23$, $r=0.996$.

TABLE II. Recoveries and Quantitation Limits for the Related Compounds

| Compound | Regression equation ($x$=calcd. $y$=found) | n | s | Quantitation limit (mg/kg) |
|---|---|---|---|---|
| 2 | $y=0.858x-0.390$ | 18 | 0.264 | 2 |
| 3 | $y=0.980x+0.180$ | 18 | 0.376 | 2 |
| 4 | $y=0.988x+0.167$ | 17 | 0.373 | 3 |
| 5 | $y=0.818x-0.268$ | 15 | 0.255 | 3 |
| 6 | $y=0.627x+0.072$ | 16 | 0.261 | 3 |
| 7 | $y=0.374x+0.272$ | 7 | 0.983 | 3 |

added values. The recovery of **1** was calculated to be 73.7% (Table I). The related compounds were also tested. MeOH solutions were prepared containing 15 μg/ml of **1** and various concentrations of the related compounds ranging from 0.1 to 1.5 μg/ml. The solutions (10 ml) were added to the feed, and the assay procedure was carried out. The recoveries were calculated. The relationships between the recovered and the added amounts were linear and passed through the origin. Table II shows the regression equations. The recovery values, except for that of **7**, were reproducible. The slopes of the two straight lines of **7** given by interday analyses differed. Low solubility of **7** in $CH_3CN$ may have influenced the reproducibility and its recovery value had to be determined for every assay. Quantitation limits of the compounds were as follows: compounds **2** and **3**, 2 mg/kg; compounds, **4**—**7**, 3 mg/kg.

**Stability Assessment of 1 in Feed**

When the feed was sterilized in a $^{60}Co$ irradiation chamber for 48 h, the temperature rose to about 60 °C. Analysis of the sterilized feed showed complete recovery of compound **1**. No degradation products were detected. Compound **1** also maintained its stability during storage

TABLE III. Contents of Compound **1** in Three Lots of Feed by Assay Procedure B

| Labeled amount (mg/kg) | $n$ | Content (mg/kg) | | | | $\bar{x}\pm$S.D. | C.V. (%) |
|---|---|---|---|---|---|---|---|
| | | A | B | C | D | | |
| 17 | 1 | 16.93 | 16.56 | 19.28 | 16.62 | 17.40±0.91 | 5.24 |
| | 2 | 16.69 | 18.03 | 18.52 | 16.52 | | |
| | 3 | 17.67 | 17.05 | 17.22 | 17.99 | | |
| 50 | 1 | 47.07 | 47.87 | 47.72 | 43.57 | 47.06±1.44 | 3.06 |
| | 2 | 48.28 | 46.18 | 46.42 | 48.82 | | |
| | 3 | 48.51 | 47.73 | 46.24 | 46.35 | | |
| 150 | 1 | 150.7 | 138.3 | 169.0 | 146.1 | 149.0 ±7.66 | 5.14 |
| | 2 | 148.1 | 142.5 | 149.6 | 145.3 | | |
| | 3 | 143.0 | 152.6 | 152.3 | 150.8 | | |

for 3—4 months at 4 °C.

**Single Determination of 1 (Assay Procedure B)**

A guard column was substituted for one of the two columns in method A. Solvent EtOH in the mobile phase used in method A was replaced with iso-PrOH. Triethylamine was not added to the mobile phase, but this did not significantly change the retention or resolution. This column and solvent system and the simplified clean-up technique resulted in a reduction of the analysis time.

**Pretreatment of the Feed**——Compound **1** was extracted with $CH_3CN$. More than 85% of **1** was recovered by shaking the feed with $CH_3CN$ (10 ml) over 45 min. The $CH_3CN$ extract was treated by the clean-up procedure used in method A. No losses of **1** in $CH_3CN$ were observed with the use of *n*-hexane (1—10 ml) and shaking of the mixture for 2.5—20 min. The $CH_3CN$ extract after pretreatment was subjected to HPLC. No interfering peaks were found after 6.5 min.

**Recovery Value and Quantitation Limit**——The feed sample was prepared as described in method A and assayed. The calculated recovery was 89.3%, and this was reproducible. The lowest assayable concentration of **1** was 5 mg/kg.

**Analysis of Spiked Feed**

The feed sample was prepared regularly once every 3 or 4 months during the toxicity test. The content of **1** and its distribution state in feed were checked before use. The feed was sampled from four parts of the feed bag in the same manner as reported previously.[1] Analytical data for three lots of the feed samples (17, 50 and 150 mg/kg), shown in Table III, confirmed the proper concentration and sufficient uniformity of **1** in feed (coefficient of variation of less than 5%).

## Conclusion

Both method A and method B offered good precision, with coefficients of variation within 3—4% ($n=15$). Both methods are suitable for use in analysis to check standards of good laboratory practice. Method A consists of more complex procedures. When stability evaluation is a major objective, method A should be used. When assurance of the proper concentration and uniformity of **1** are required, method B is suitable because of its efficiency.

Method B, which consists of simpler procedures, is more efficient than our previous fluorometric method. Accuracy and precision are not significantly different between the two

methods, and a good correlation between the two results was obtained ($r=0.998$).

**Acknowledgement** The authors are grateful to Dr. K. Hirai and Mr. T. Ishiba for providing the samples.

**References and Notes**

1) R. Ikenishi, T. Kitagawa, and E. Hirai, *Chem. Pharm. Bull.*, **34**, 2873 (1986).
2) R. Ikenishi, T. Kitagawa, and E. Hirai, *Chem. Pharm. Bull.*, **32**, 748 (1984).
3) K. Hirai, H. Sugimoto, T. Ishiba, T. Fujishita, Y. Tsukinoki, and K. Hirose, *J. Heterocycl. Chem.*, **19**, 1363 (1982).
4) According to Good Laboratory Practice Standard, the content of the test substance should be determined periodically when its stability has not been evaluated.
5) Weigh 1 mg of **7**, add 10 ml of MeOH and reflux the solution till the crystals are completely dissolved. Dilute the solution to make 50 $\mu$g/ml.
6) Add 10 ml of the adequately diluted standard solution to the drug-free feed (1 g) and proceed as directed in assay procedure A. Calculate the recovery from the above calibration curve of **7**.
7) The p$K_a$ values of **1**, **6**, and **7**, which express a protonation equilibrium, were 6.98, 6.42 and 2.27, respectively. The p$K_a$ values of **4** and **5** for the same equilibrium were $-0.75$ and $-1.08$, respectively.
8) B. Kinberger and P. Wahrgren, *Anal. Lett.*, **15**(B6), 549 (1982).

[Chem. Pharm. Bull. 35(11)4552—4556(1987)]

# Detection of Anti-ribonucleic Acid Antibodies in Hyperthyroid Patients' Sera by a Solid-Phase Enzyme Immunoassay

NORIAKI KOBAYASHI

*Research and Development Center of Hygienic Sciences, Kitasato University, Shirokane, Minato-ku, Tokyo 108, Japan*

(Received March 13, 1987)

A solid-phase enzyme immunoassay for the measurement of anti-ribonucleic acid (RNA) antibodies in the sera from hyperthyroid patients was developed. Three antigens, calf liver RNA, poly (I)·(C) and poly (A)·(U), were fixed to 96-well enzyme immunoassay microtiter plates precoated with poly-L-lysine hydrobromide. Antibodies detected in the present assay cross-reacted with neither double strand-deoxyribonucleic acid (ds-DNA) nor single strand (ss)-DNA, and were RNA-specific.

In twenty (66.6%) out of 30 sera from hyperthyroid patients, anti-RNA antibodies were detected. Interestingly, in seven positive cases out of 8 patients with malignant thyrocele, the levels of antibodies against poly (I)·(C) and poly (A)·(U) were much higher than those against calf liver RNA, while antibodies against calf liver RNA were commonly high in hyperthyroid patients.

The present assay requires no radioactive materials, and is sensitive and specific. It is expected to be practically useful to measure anti-RNA antibodies. Furthermore, this assay may provide an aid to diagnose the disease type, *e.g.*, autoimmune or nonautoimmune, and the degree of the hyperthyroidosis.

**Keywords**——enzyme immunoassay; hyperthyroidosis; anti-RNA antibody; autoimmune disease

Since antibodies directed to ribonucleic acid (RNA) were first reported by Schur and Monroe[1] in the sera of systemic lupus erythematosus (SLE) patients, a variety of immunological techniques (radioimmunoassay, indirect hemagglutination, immunodispersion) for detecting the antibodies, as well as their incidence and clinical significance, have been investigated. Anti-RNA antibodies are now believed to be one of the autoantibodies secreted in such patients, and can be used as an index of disease activity in SLE.

In the present paper, we report the determination of anti-RNA antibodies in the sera of hyperthyroid patients by a newly established solid-phase enzyme immunoassay and we discuss their possible clinical significance in such patients.

## Materials and Methods

**Horseradish Peroxidase (HRPO) and Labeling**——Protein A (Sigma Chemical Co., St. Louis, MO) was conjugated with HRPO according to the method of Nakane and Kawaoi.[2] HRPO-labeled protein A was purified by Sephacryl S-200 column chromatography using 0.01 M phosphate buffer, pH 8.0, containing 0.8% NaCl as an eluent to remove conjugated HRPO.

**Solid-Phase Enzyme Immunoassay (EIA) for RNAs**——The standard method is described below.

**Coating of Microplate with Calf Liver RNA (n-RNA), Poly(I)·(C) and Poly(A)·(U)**——Ninety-six-well flat-bottomed plates for EIA (Coster, Cambridge, MA) were filled with 200 $\mu$l per well of 40 $\mu$g/ml of poly-L-lysine hydrobromide (PLL: Type 1B, Sigma Chemical Co., St. Louis, MO) in Tris–HCl buffer 0.1 M, pH 7.6). After incubation for 30 min at room temperature, the plates were washed twice with Tris–HCl buffer using a micromixer (model MX-2: Sanko Junyaku Co., Tokyo). Two hundred microliters of 10 $\mu$g/ml n-RNA, poly(I)·(C) or poly(A)·(U) in Tris–HCl buffer was added to each well, while 200 $\mu$l of Tris–HCl buffer was added to each control

background well. After incubation for 60 min at 37 °C, the plates were washed three times with Tris–HCl containing 0.85% NaCl and then filled with 250 μl per well of Tris–HCl containing 1% bovine serum albumin (BSA), 2% gelatin, 5% calf serum, 0.85% NaCl, and 0.1% Triton X-100 for 60 min at 37 °C to coat the active sites left on the wells.

**Procedure**——Two hundred microliters of diluted serum from a patient (1 : 40 and 1 : 80 in Tris–HCl containing 1% BSA, 0.85% NaCl, and 0.1% TX-100) or normal control serum was added to n-RNA, poly(I)·(C), poly(A)·(U), and control wells. Assay was performed in duplicate. After incubation for 60 min at 37 °C, the wells were washed three times with 250 μl of washing buffer (Tris–HCl containing 0.1% BSA, 0.85% NaCl, and 0.1% TX-100) and filled with 200 μl of 1 μg/ml of HRPO-protein A in 0.1 M Tris–HCl, pH 7.6 containing 1% BSA, and 0.85% NaCl. The plates were incubated for 60 min at room temperature and then washed with the washing buffer. The subsequent methods were as described by Kobayashi *et al.*[3] The amount of HRPO-protein A bound to immune complex on the surface of the microplate well was estimated from a dose–response curve in which optical densities at 492 nm were plotted against known amounts of HRPO-protein A.

**Hyperthyroid Patients**——The patients were 12 males and 18 females from 23 to 48 years old, of whom 25 had not previously received any therapy for hyperthyroidism. The other 5 were undergoing recurrence of hyperthyroidism. They exhibited high serum thyroid hormone and low serum thyroid stimulating hormone values and also satisfied one or more of 3 standard characteristics of the disease: 1) characteristic eye symptoms with elimination of other possible causes; 2) intake of radioisotope in 20 h— less than 30%; 3) thyrotropin-receptor antibody—less than 12%.

**Serum**——Blood samples were taken from a vein of the fasted patients, and were allowed to stand for 1 h at room temperature. After centrifugation, serum samples were obtained and kept at −20 °C.

**EIAs for Anti-double Strand-Deoxyribonucleic Acid (ds-DNA) and Anti-single Strand (ss)-DNA Antibodies**——EIAs for the measurement of antibodies against ds-DNA and ss-DNA were carried out by the use of HRPO-protein A in place of radioisotope-labeled anti-human immunoglobulin (anti-HGG) according to a modification of the method of Aotsuka *et al.*[4]

**Antiserum**——A rabbit was immunized intramuscularly (i.m.) with 1 mg of HGG (Miles Laboratories, Elkhart, IN) in complete Freund's adjuvant (CFA). Three booster immunizations with 1 mg of HGG in CFA were given i.m. weekly. The rabbit was bled seven days after the final injection. Anti-HGG serum thus obtained gave a single precipitin band against the immunogen. Proteins in anti-HGG serum were precipitated by addition of saturated ammonium sulfate (finally 50% saturation) and extensively dialyzed against 0.005 M borate buffer saline, pH 8.0. The final volume was adjusted to the original serum volume.

**Coupling to Sepharose 4B**——Five milliliters of 3 mg/ml of the purified anti-HGG, n-RNA, poly(I)·(C) or poly-(A)·(U) was coupled to 5 ml of Sepharose 4B (Pharmacia Fine Chemicals, Upsala, Sweden) according to the method of Porath *et al.*[5]

**Standard Serum for Anti-RNA Antibodies Measurement**——Pooled sera from aged NZB/W mice were used as a standard serum for the measurement of anti-RNA antibodies.

## Results

### EIA for the Measurement of Anti-RNA Antibodies

The first experiment was carried out to determine the optimal conditions for coating RNAs, n-RNA, poly(I)·(C), and poly(A)·(U), on the surface of microplate wells. Good results were obtained by pre-coating of the wells with PLL prior to antigen binding. A concentration of 10 μg/ml of antigen was enough to bind on the well surface, while 20 or more μg/ml of antigen did not bind well without pre-coating with PLL.

An attempt was also made to inhibit absorption of nonspecific human immunoglobulins on the wells. The use of Tris–HCl buffer containing 1% BSA, 2% gelatin, 5% calf serum, 0.85% NaCl, and 0.1% TX-100 was found to be effective for this purpose.

A dose–response curve using standard serum is plotted in Fig. 1. A similar curve was also obtained using the sera positive for anti-RNA antibodies.

### Specificity of EIA

Twenty sera which were positive for antibodies against RNA were subjected to EIAs for anti-ds-DNA and anti-ss-DNA antibodies. Only 4 sera gave a positive reaction against ds-DNA and no antibody against ss-DNA was detected. When these sera were passed through columns of n-RNA, poly(I)·(C), poly(A)·(U), and anti-HGG coupled to Sepharose 4B, no positive reaction was observed by EIA. These results confirmed that the RNA-binding

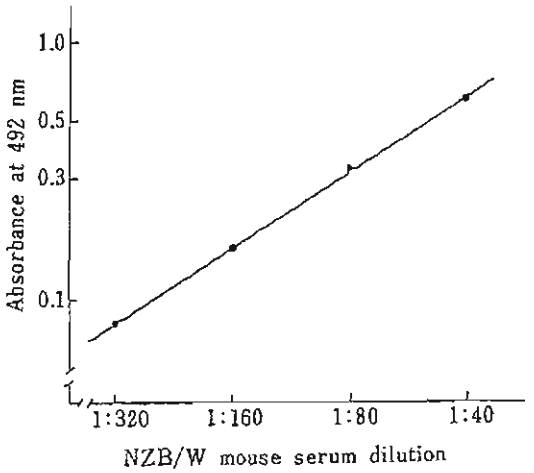


Fig. 1. Dose-Response Curve Using Pooled Sera from Aged NZB/W Mice as a Standard Serum

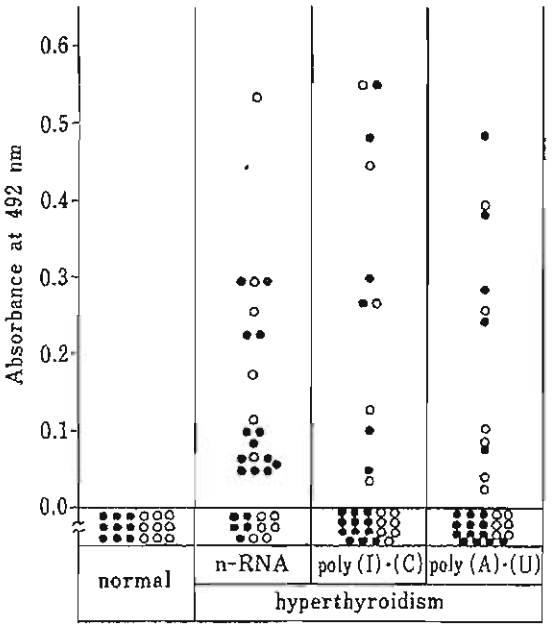


Fig. 2. Detection of Anti-RNA Antibodies against n-RNA, Poly(I)·(C), and Poly(A)·(U) in Normal Human Sera and Hyperthyroid Patients' Sera by EIA

○ and ● indicate male and female, respectively.

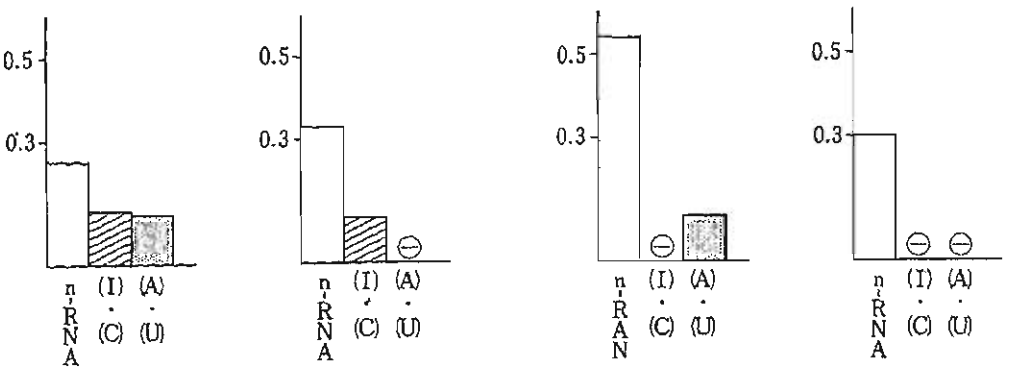


Fig. 3. Patterns of Anti-RNA Antibodies Found by EIA in Hyperthyroid Patients' Sera

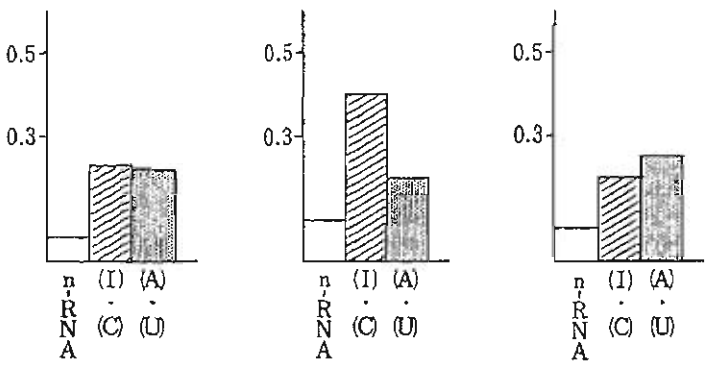


Fig. 4. Patterns of Anti-RNA Antibodies Found by EIA in Sera from Hyperthyroid Patients with Malignant Thyrocele

substances in the present assay were RNA-specific immunoglobulins.

**Anti-RNAs Antibodies in Hyperthyroid Patients**

In 20 (66.6%) out of 30 sera from hyperthyroid patients, anti-RNA antibodies were detected by EIA. The results of EIA using n-RNA, poly(I)·(C), and poly(A)·(U) as antigens are shown in Fig. 2. The patterns of positive reaction to n-RNA, poly(I)·(C), and poly (A)·(U) in patients' sera were found to vary from person to person. Some examples are presented in Fig.3. Antibodies against n-RNA were commonly detected in most of the hyperthyroid patients. However, in 7 out of 8 hyperthyroid patients with malignant thyrocele, the levels of antibodies against poly(I)·(C) and poly(A)·(U) were higher than that against n-RNA (Fig. 4).

## Discussion

A solid-phase enzyme immunoassay was developed for the measurement of anti-RNA antibodies in the sera from hyperthyroid patients. In this assay, pre-coating of the surface of microplate wells with PLL enhanced the binding of the antigen, as described previously.[3] The PLL is known to mediate coupling of negatively charged materials such as ds-DNA to a solid phase.[4] HRPO-protein A gave a lower non-specific reaction than HRPO-anti-HGG.[3]

Shirai *et al.*[6] reported that most monoclonal anti-DNAs antibodies cross-reacted with RNA. In order to examine the specificity of the present assay for measurement of anti-RNA antibodies, 22 sera positive for anti-RNA antibodies were subjected to EIA for anti-ds-DNA and anti-ss-DNA antibodies. No ds-DNA antibodies were detected and ss-DNA antibodies were weakly positive in only 4 sera. These results and the absorption study using affinity chromatography, in which positive sera passed through RNAs [n-RNA, poly(I)·(C), poly-(A)·(U)] and anti-HGG-Sepharose 4B gave no reaction in EIA, confirmed that substances responsible for this assay were RNA-specific immunoglobulins.

The presence of anti-RNA antibodies in the sera from SLE patients has been reported.[1] In the present study, we demonstrated the presence of anti-RNA antibodies in the sera from hyperthyroid patients for the first time. Anti-RNA antibodies were detected by EIA using n-RNA in 20 (66.6%) out of 30 sera from hyperthyroid patients. No anti-RNA antibody was detected in 10 sera from patients with lung cancer, hepatoma, and other malignant tumors. Further, the level of anti-RNA antibodies was remarkably decreased in the patients at one month after thyroidectomy. These results suggest that anti-RNA antibodies may be directed against RNA components that originated from the thyroid itself.

More interestingly, the levels of antibodies against poly(I)·(C) and poly(A)·(U) were considerably higher than that of anti-n-RNA antibodies in hyperthyroid patients with malignant thyrocele. As shown in Fig. 3, the positive pattern of antibodies against RNAs varied from individual to individual. These results indicate that the pattern of anti-RNAs antibodies may be available as a criterion for the judgement of disease type or degree of the disease in hyperthyroidosis. The clinical significance of anti-RNA antibodies has not been well investigated in comparison with that of anti-DNA antibodies. The presence of anti-RNA antibodies and their clinical significance should be further examined in patients with other diseases, and by the use of other types of synthetic RNAs.

In conclusion, we have developed an EIA procedure for the measurement of anti-RNA antibodies in sera from hyperthyroid patients. Anti-RNA antibodies were detected in 20 (66.6%) out of 30 sera from hyperthyroid patients. The positive pattern of antibodies against n-RNA, poly(I)·(C), and poly(A)·(U) was found to vary from patient to patient.

### References

1) P. H. Schur and M. Monroe, *Proc. Natl. Acad. Sci. U.S.A.*, 63, 1108 (1969).

2) P. K. Nakane and A. Kawaoi, *Immunochemistry*, **8**, 1175 (1971).
3) N. Kobayashi, H. Sugita, E. Terada, A. Ghoda, H. Okudaira, T. Ogita, and T. Miyamoto, *J. Immunol. Methods*, **73**, 267 (1984).
4) S. M. Aotsuka, K. Ikebe, and R. Yokohari, *J. Immunol. Methods*, **28**, 149 (1979).
5) J. Porath, R. Axen, and S. Ernback, *Nature* (London), **21S**, 1491 (1967).
6) S. Shirai, H. Satou, S. Hirose, and Y. Ishida, *New Medical World Weekly*, **1562** (August), 68 (1983).

[Chem. Pharm. Bull. 35(11)4557—4561(1987)]

# Stereoselectivity in the Mechanism of Acid Hydrolysis of Mitomycins

WILLY J. M. UNDERBERG*,[a] and JOS H. BEIJNEN[b]

*Department of Chemical Pharmacy, Subfaculty of Pharmacy, State University of Utrecht,[a] Catharijnesingel 60, 3511 GH Utrecht, The Netherlands and Slotervaart Hospital/Netherlands Cancer Institute,[b] Louwesweg 6, 1066 EC Amsterdam, The Netherlands*

(Received March 23, 1987)

The stereoselectivity in the acid hydrolysis mechanism of mitomycins was studied. The predominance of the 1,2-*cis*-mitosene degradation products occurring at low pH was ascribed to the directing force exerted on the incoming nucleophile by the protonated 2-amino function of an intermediate in the process as well as to steric hindrance due to the orientation of the $C_9$ urethane substituent in one of the degradation steps preceding the formation of the intermediate. The differences in electron density in the intermediate chromophore and the resulting differences in $pK_a$ value of the amino function involved are discussed.

**Keywords**——mitomycin; acid degradation; stereoselectivity; pH dependence

Mitomycins are a group of potent antitumor antibiotics, acting by covalent binding and cross-linking of deoxyribonucleic acid (DNA).[1,2] The compounds have the general structure given in Fig. 1 (I).[3,4] Activation of mitomycins *in vivo* may occur either after reduction[5,6] or under acidic conditions.[7-9] Under such conditions the compounds are converted into 2-amino-1-hydroxymitosenes (II, Fig. 1). During this conversion active intermediates exist that are responsible for the alkylating process. Both activation pathways show much similarity, only differing in the oxidation level of the reactive intermediate species. The *in vitro* degradation of the mitomycins has been studied extensively[10-26] and several mechanisms for this process have been suggested.[11-14,16,26] One of the interesting aspects of the process is the predominance of the 1,2-*cis*-2-amino-1-hydroxymitosene degradation products[22-25] in contrast to the occurrence of 1,2-*trans*-orientated amino alcohols during acid catalyzed ring opening of simple aziridines[27] as well as the pH dependence of the ratio between the *cis* and *trans* isomers.[16] The present study is focused on this aspect of the acid degradation of mitomycins.

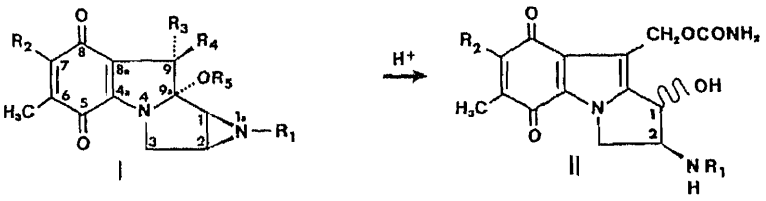


I II

| | $R_1$ | $R_2$ | $R_3$ | $R_4$ | $R_5$ |
|---|---|---|---|---|---|
| mitomycin A | H | $H_3CO$ | H | $CH_2OCONH_2$ | $CH_3$ |
| mitomycin B | $CH_3$ | $H_3CO$ | $CH_2OCONH_2$ | H | H |
| mitomycin C | H | $H_2N$ | H | $CH_2OCONH_2$ | $CH_3$ |
| porfiromycin | $CH_3$ | $H_2N$ | H | $CH_2OCONH_2$ | $CH_3$ |

Fig. 1. Structures of Mitomycins and Mitosene Degradation Products

### Experimental

Mitomycin A and mitomycin B were gifts from Dr. K. Shirahata, Kyowa Hakko Kogyo Chemical Co., Tokyo, Japan; mitomycin C was supplied by Bristol Myers, Amstelveen, The Netherlands and porfiromycin was obtained from Cyanamid, Pearl River, New York, U.S.A. Degradation studies were carried out at 25 C in 0.001 M acetate/phosphate buffers of various pH in the acid region, and the resulting mixtures were analyzed using high performance liquid chromatography (HPLC) procedures described earlier.[19,20] These stability indicating procedures enable the assay of the parent compounds as well as each individual degradation product. Half-wave potentials were determined at 25 C and pH 7.4 according to previously described procedures.[10]

## Results

The degradation of mitomycins in acid solution under the experimental conditions yields only two products, *cis*- and *trans*-2-amino-1-hydroxymitosene. The ratio between the concentrations of those two products is pH-dependent but, at a given pH, independent of the degradation stage. Figure 2 represents the pH dependences of the *cis/trans* ratios for mitomycins A, B and C and porfiromycin. The latter two show identical behavior with an inflexion in the curve at pH 2.8, whereas mitomycins A and B show this inflexion at pH 1.5. Figure 2 also demonstrates that at pH 1 the ratio for mitomycin B is 6.0, that for mitomycin A is 3.5, and those for mitomycin C and porfiromycin are 4.5. At pH 6 all compounds show ratios between 1.5 and 1.1. As reported earlier[16] the inflexion in the curve of mitomycin C (Fig. 2) agrees with the $pK_a$ of an intermediate in the acid hydrolysis of the compound. Consequently, the $pK_a$ values of the mitomycins A and B intermediates should be 1.5. The replacement of the 7-amino function by a methoxy group must account for this shift, since this replacement results in a different electron density in the chromophoric system. To establish these electron densities, half-wave potentials for the reduction of all mitosanes and mitosenes under investigation were determined (Table I). The results clearly indicate the decrease in electron density in mitomycins A and B and their mitosene degradation products in comparison to mitomycin C and porfiromycin and the corresponding mitosenes. Within the

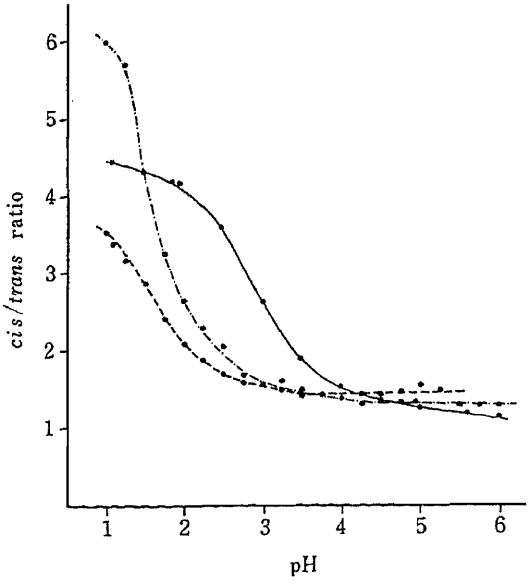


Fig. 2. pH Dependence of the Ratio between the Mole Fractions of 1,2-*cis* and 1,2-*trans* Mitosenes Originating from Mitomycin A (----), Mitomycin B (-----), and Mitomycin C and Porfiromycin (——)

TABLE I. Half-Wave Potentials for the Reduction of Mitomycins and Their Degradation Products in 0.1 M Phosphate Buffer pH 7.4 (25 °C)

| Compound | $E_{1/2}$ (mV) |
|---|---|
| Mitomycin A | −182 |
| Mitomycin B | −155 |
| Mitomycin C | −365 |
| Porfiromycin | −367 |
| Mitomycin A mitosenes | −315 |
| Mitomycin B mitosenes | −310 |
| Mitomycin C mitosenes | −475 |
| Porfiromycin mitosenes | −465 |

two groups, however, the values are the same. This indicates the same $pK_a$ value for the intermediates originating from mitomycin A and B but with a lower value than the also identical values for the intermediates originating from mitomycin C and porfiromycin.

## Discussion

The pH dependence of the *cis/trans* ratio of the mitosenes, resulting from mitomycin C degradation, was ascribed to the 2-amino function of an intermediate in the acid catalyzed degradation of the compound,[16] rather than to the $pK_a$ of the parent compound. Further evidence for the validity of this hypothesis is provided by the lower value of the inflexion in the pH dependences of these ratios for mitomycins A and B, having similar $pK_a$ values[20] but expected to possess lower electron densities in the chromophores. The degradation mechanism for mitomycin A and B is now presented in Fig. 3. Since porfiromycin and mitomycin C show identical curves, the $pK_a$ of the intermediate resulting from these compounds must be the same. The half-wave potentials for both compounds are also identical, which is in agreement with the similar $pK_a$ values for the intermediates resulting from both compounds.

The conclusion must be that the N-1a methyl substituent has no significant influence on

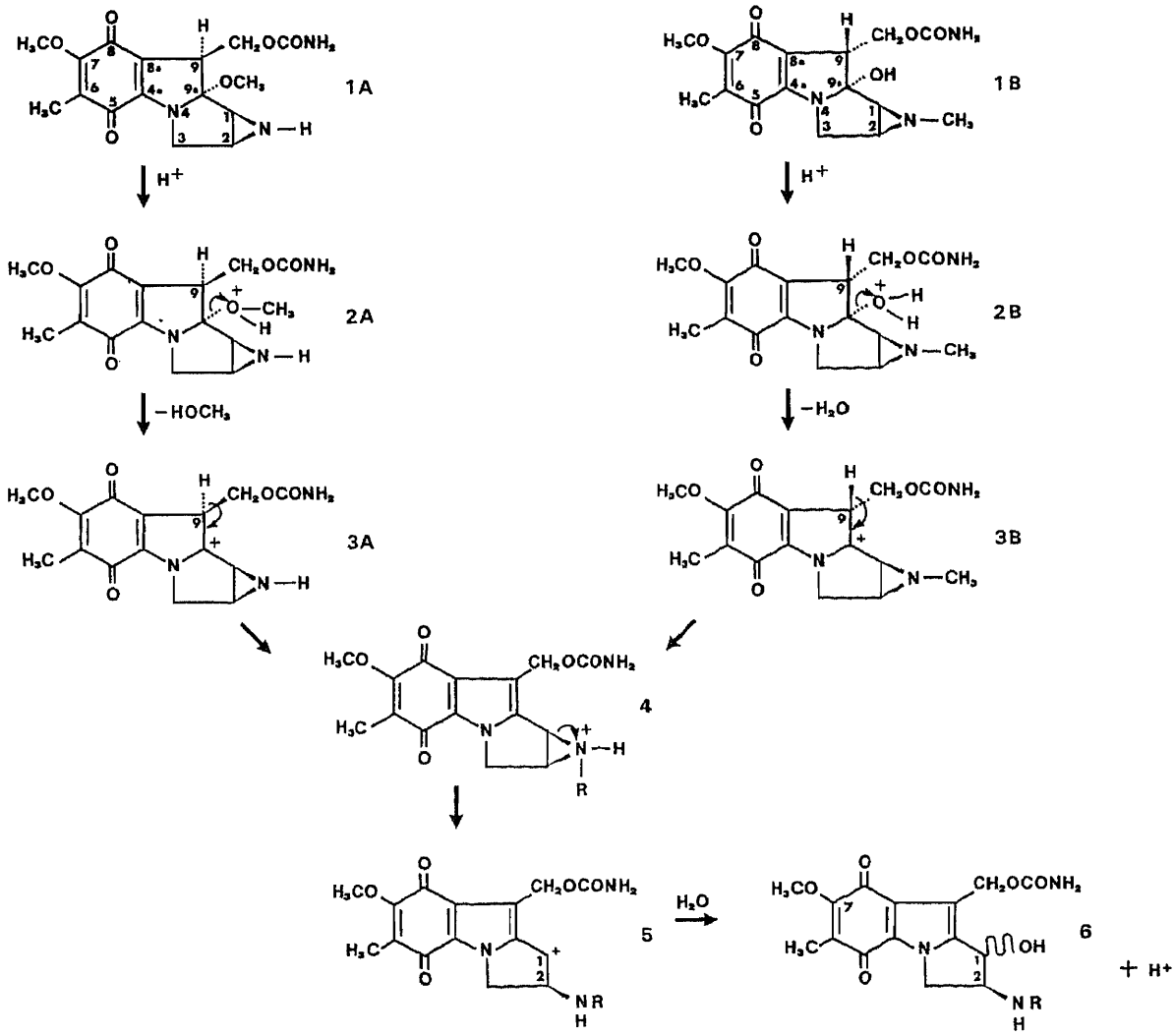


Fig. 3. Degradation Scheme of Mitomycin A (1A) and Mitomycin B (1B)

the stereospecificity of the hydrolysis, *i.e.*, the direction of the incoming nucleophile. The half-wave potentials of mitomycins A and B and their mitosene degradation products are much higher, due to the stronger electron-withdrawing properties of the 7-methoxy group in contrast to the electron-donating nature of the 7-amino substituent. A lower electron density in the chromophore results in an increased reduction capability of the quinoid moiety. Furthermore, a lower electron density decreases the stability of the protonated form of the intermediate (**5**, Fig. 3), due to the resulting decrease in inductive compensation of the positive charge at $C_1$. The half-wave potentials of the mitosene degradation products provide the best approach of the electron density in the intermediate **5** chromophore. Moreover, the replacement of the 7-amino function by a methoxy group diminishes the possibilities of mesomeric and tautomeric stabilization of the protonated intermediate **5**. These two changes, due to the presence of the 7-methoxy function, explain the decrease in $pK_a$ of **5** originating from mitomycins A and B, as well as the similarity of the $pK_a$ values, because the influences of the other substituents can be considered negligible.

Figure 2 shows that the *cis/trans* ratios for mitomycin C and porfiromycin degradation processes are identical at every pH. The identical $pK_a$ of the intermediates and the identical stereochemistry of the parent compounds are the explanation for this phenomenon. However, in spite of the identical $pK_a$ of the intermediates arising from mitomycins A and B, the *cis/trans* mitosene ratios for both compounds are significantly different, especially at low pH. Thus, another influence, apart from the protonated 2-amino group in **5**, must exist in directing the incoming nucleophile. This influence must be ascribed to the differences in structure of the two compounds. The presence of a hydroxy group at $C_{9a}$ in mitomycin B instead of the methoxy group in mitomycin A is unlikely to account for the difference between these ratios since the stereochemical orientation of the groups is identical and the cleavage of both groups is generally a very fast kinetic process. It is remarkable that the *cis* orientation of the $C_9$ urethane substituent with the 1,2-fused aziridine ring in mitomycin A parallels a lower ratio whereas the *trans* orientation in mitomycin B is accompanied by a higher *cis/trans* ratio of the diastereomeric degradation products. If the final orientation of the $C_1$ substituent were to occur solely in **5**, the only directing force would be the protonated 2-amino function, since in **5** the $C_9$ substituent has a coplanar orientation. Consequently, in this case, mitomycin A and mitomycin B should yield the mitosene degradation products in identical ratios. The additional stereospecificity must therefore have its origin in an earlier stage. The *cis/trans* ratio after degradation of 1,2-aziridinomitosene (**4**, Fig. 3) was found by Cheng and Remers[22] to be 3.2 at pH 1.30, while mitomycin B at this pH yields a ratio of 5.7.[22] This is in accordance with our observations with mitomycin B (Fig. 2). These data suggest that steric hindrance may determine in part the orientation of the $C_1$ substituent. The fact that no 9-epimitomycin B (9a-demethylmitomycin A) or 9-epi-9a-epimitomycin B and 9a-epimitomycin B are formed as degradation products of mitomycin A and mitomycin B, respectively, indicates that in this case also, the degradation steps preceding the formation of intermediate **4** (Fig. 3) are very fast. Consequently, the direction of the incoming nucleophile may in part be determined in one of these steps, resulting in the enhanced predominance of the *cis* stereospecificity at $C_1$ in mitomycin B.

Thus, in addition to the principle driving force (the protonated 2-amino function in intermediate **4**) *trans* orientation of the $C_9$ urethane substituent with the 1,2-fused aziridine ring results in an increase in the *cis/trans* mitosene ratio on degradation of mitomycin B.

## References

1) S. K. Carter and S. T. Crooke, "Mitomycin C: Current Status and New Developments," Academic Press, New York, 1979, p. 1.
2) W. A. Remers, "The Chemistry of Antitumor Antibiotics," John Wiley & Sons, New York, 1979, p. 221.

3) K. Shirahata and N. Hirayama, *J. Am. Chem. Soc.*, **105**, 7199 (1983).
4) U. Hornemann and M. J. Heins, *J. Org. Chem.*, **50**, 1301 (1985).
5) W. Szybalski and V. N. Iyer, "Antibiotics I, Mechanism of Action," Springer-Verlag, New York, 1967, p. 221.
6) H. W. Moore, *Science*, **197**, 527 (1977).
7) J. W. Lown, A. Begleiter, D. Johnson, and A. R. Morgan, *Can. J. Biochem.*, **54**, 110 (1976).
8) J. W. Lown and G. Wier, *Can. J. Biochem.*, **56**, 296 (1978).
9) K. A. Kennedy, J. D. McGurl, L. Leondaridis, and O. Alabaster, *Cancer Res.*, **45**, 3541 (1985).
10) E. R. Garrett, *J. Med. Chem.*, **6**, 488 (1963).
11) C. L. Stevens, K. G. Taylor, M. E. Munk, W. S. Marshall, K. Noll, G. D. Shah, L. G. Shah, and K. Uzu, *J. Med. Chem.*, **8**, 1 (1965).
12) B. S. Iyengar and W. A. Remers, *J. Med. Chem.*, **28**, 963 (1985).
13) R. A. McClelland and K. Lam, *J. Am. Chem. Soc.*, **107**, 5182 (1985).
14) W. J. M. Underberg and H. Lingeman, *J. Pharm. Sci.*, **72**, 549 (1983).
15) W. J. M. Underberg and H. Lingeman, *J. Pharm. Sci.*, **72**, 553 (1983).
16) J. H. Beijnen and W. J. M. Underberg, *Int. J. Pharm.*, **24**, 219 (1985).
17) J. H. Beijnen, J. Den Hartigh, and W. J. M. Underberg, *J. Pharm. Biomed. Anal.*, **3**, 59 (1985).
18) J. H. Beijnen, J. Den Hartigh, and W. J. M. Underberg, *J. Pharm. Biomed. Anal.*, **3**, 71 (1985).
19) J. H. Beijnen, H. Rosing, and W. J. M. Underberg, *Arch. Pharm. Chem. Sci. Ed.*, **13**, 58 (1985).
20) J. H. Beijnen, O. A. G. J. van der Houwen, H. Rosing, and W. J. M. Underberg, *Chem. Pharm. Bull.*, **34**, 2900 (1986).
21) U. Hornemann, P. J. Keller, and K. Takeda, *J. Med. Chem.*, **28**, 31 (1985).
22) L. Cheng and W. A. Remers, *J. Med. Chem.*, **20**, 767 (1977).
23) W. G. Taylor and W. A. Remers, *J. Med. Chem.*, **18**, 307 (1975).
24) W. G. Taylor and W. A. Remers, *Tetrahedron Lett.*, **39**, 3483 (1974).
25) M. Tomasz and R. Lipman, *J. Am. Chem. Soc.*, **101**, 6063 (1979).
26) I.-C. Chiu and H. Kohn, *J. Org. Chem.*, **48**, 2857 (1983).
27) O. C. Dermer and G. E. Ham, "Ethyleneimine and Other Aziridines," Academic Press, New York, 1969, p. 206.

[Chem. Pharm. Bull. 35(11)4562—4567(1987)]

# Synthesis of Disulfates of Unconjugated and Conjugated Bile Acids[1)]

JUNICHI GOTO, YOSHIHISA SANO, TOSHIYUKI CHIKAI and TOSHIO NAMBARA*

*Pharmaceutical Institute, Tohoku University, Aobayama, Sendai 980, Japan*

(Received April 18, 1987)

The disulfates of unconjugated, and glycine- and taurine-conjugated bile acids have been synthesized. Cholic acid derivatives appropriately protected were sulfated with sulfur trioxide–triethylamine complex in pyridine in the usual manner. Subsequent hydrolysis and/or sodium borohydride reduction provided the desired disulfates of cholates in satisfactory yields. Dihydroxylated bile acid disulfates were also prepared. The nuclear magnetic resonance spectral data for bile acid disulfates and related compounds are tabulated.

**Keywords**——sulfation; bile acid disulfate; glycine conjugate; taurine conjugate; *p*-nitrophenyl ester; active ester method

In recent years, considerable attention has been focused on the metabolic significance of sulfation of bile acids in hepatobiliary diseases. In order to aid research, the monosulfates of unconjugated and conjugated bile acids have been previously synthesized as standard samples.[2,3)] In addition, a novel method for simultaneous determination of the 3-sulfates in biological fluids by high-performance liquid chromatography (HPLC) has been developed.[4)] Recently, we disclosed the occurrence of bile acid 7-sulfates in urine from patients with primary biliary cirrhosis and congenital biliary atresia.[5)] Accordingly, it seems likely that disulfated bile acids are potential metabolites of bile acids in living animals. A particular interest in the relationship between bile acid metabolism and liver diseases prompted us to develop a new method for simultaneous determination of the disulfates using HPLC without prior deconjugation. For this purpose the 3,7-, 3,12- and 7,12-disulfated bile acids were required as authentic specimens.

Our initial effort was directed to the preparation of unconjugated, and glycine- and taurine-conjugated cholate 7,12-disulfates. Difficulties were encountered with selective acylation of the 3α-hydroxyl group of cholic acid since there was no marked difference in reactivity between the 3α- and 7α-hydroxyl groups, so 7-oxodeoxycholic acid methyl ester (**2**), obtainable from cholic acid by the known method,[6)] was used as a starting material. Selective acetylation of **2** proceeded with ease, providing a partially acylated product, on treatment with acetic anhydride and pyridine in benzene under mild conditions. The nuclear magnetic resonance (NMR) spectral data justified the structural assignment as the 3-monoacetate (**6**). The 3β-hydrogen appeared at *ca.* 4.5 ppm as a broad signal ($W_{1/2}=20$ Hz), while the 12β-hydrogen exhibited a signal ($W_{1/2}=7$ Hz) at *ca.* 3.9 ppm. Compound **6** was then reduced with sodium borohydride under ice-cooling to afford methyl cholate 3-acetate (**9**). Sulfation of **9** with sulfur trioxide–triethylamine complex in pyridine[7)] followed by alkaline hydrolysis furnished the desired cholic acid 7,12-disulfate (12).

The 7,12-disulfates of glycine- and taurine-conjugated bile acids were also synthesized in the same manner. 7-Oxodeoxycholic acid (**1**), derived from **2** by alkaline hydrolysis, was subjected to partial acetylation to give the 3-monoacetate (**5**). Condensation of **5** with *p*-nitrophenol was effected by use of *N,N'*-dicyclohexylcarbodiimide, yielding the *p*-nitrophenyl

ester. Further treatment with ethyl glycinate and taurine provided the glycine (**7**) and taurine (**8**) conjugates, respectively. Upon metal hydride reduction these conjugates were transformed into 7α-hydroxylated compounds (**10**, **11**), which, on sulfation followed by elimination of the protecting groups, were converted to the desired glycine- and taurine-conjugated cholate 7,12-disulfates (**13**, **14**).

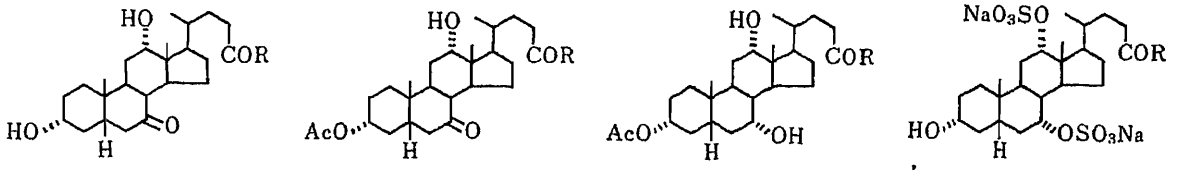

**1**: R=OH
**2**: R=$OCH_3$
**3**: R=$NHCH_2COOC_2H_5$
**4**: R=$NHCH_2CH_2SO_3H$
**5**: R=OH
**6**: R=$OCH_3$
**7**: R=$NHCH_2COOC_2H_5$
**8**: R=$NHCH_2CH_2SO_3H$
**9**: R=$OCH_3$
**10**: R=$NHCH_2COOC_2H_5$
**11**: R=$NHCH_2CH_2SO_3H$
**12**: R=ONa
**13**: R=$NHCH_2COONa$
**14**: R=$NHCH_2CH_2SO_3Na$

Chart 1. Cholate 7,12-Disulfates and Related Compounds

The synthesis of cholate 3,7-disulfates was then undertaken. Methyl cholate 3,12-diacetate, formed from **2** by usual acetylation with acetic anhydride in pyridine and metal hydride reduction, was converted to cholic acid 12-monoacetate (**15**) by brief exposure to 5% methanolic sodium hydroxide. In a similar fashion **15** was transformed into the *p*-nitrophenyl ester, which in turn was condensed with ethyl glycinate and taurine to yield the glycine (**17**) and taurine (**18**) conjugates. Treatment of the resulting cholate 12-monoacetates (**16**, **17**, **18**) with sulfur trioxide–triethylamine complex in pyridine and subsequent alkaline hydrolysis afforded the desired 3,7-disulfated cholates (**19**, **20**, **21**).

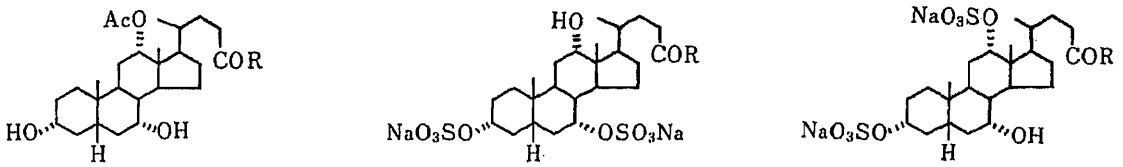

**15**: R=OH
**16**: R=$OCH_3$
**17**: R=$NHCH_2COOC_2H_5$
**18**: R=$NHCH_2CH_2SO_3H$
**19**: R=ONa
**20**: R=$NHCH_2COONa$
**21**: R=$NHCH_2CH_2SO_3Na$
**22**: R=ONa
**23**: R=$NHCH_2COONa$
**24**: R=$NHCH_2CH_2SO_3Na$

Chart 2. Cholate 3,7- and 3,12-Disulfates and Related Compounds

Next, preparation of cholate 3,12-disulfates was carried out. Condensation of **1** with *p*-nitrophenol yielded the *p*-nitrophenyl ester, which, on treatment with ethyl glycinate and taurine, were led to glycine (**3**) and taurine (**4**) conjugates, respectively. Compounds **2**, **3** and **4** were subjected to sulfation in the same manner as described above followed by borohydride reduction and elimination of the protecting groups, providing the desired cholate 3,12-disulfates (**22**, **23**, **24**).

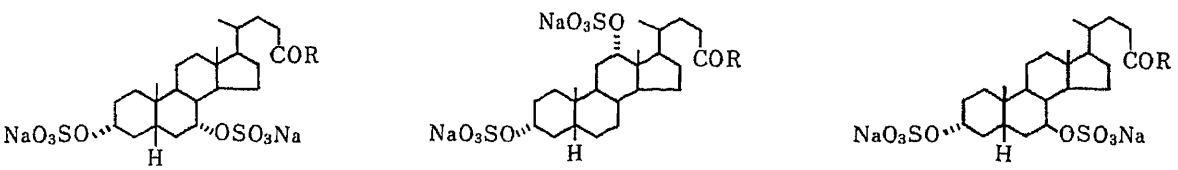

**25**: R=ONa
**26**: R=$NHCH_2COONa$
**27**: R=$NHCH_2CH_2SO_3Na$
**28**: R=ONa
**29**: R=$NHCH_2COONa$
**30**: R=$NHCH_2CH_2SO_3Na$
**31**: R=ONa
**32**: R=$NHCH_2COONa$
**33**: R=$NHCH_2CH_2SO_3Na$

Chart 3. Dihydroxylated Bile Acid Disulfates

TABLE I. NMR Spectral Data for Disulfated Bile Acids and Related Compounds

| Compd. | Solv.[a] | 18-$CH_3$ | 19-$CH_3$ | 21-$CH_3$[b] | 3β-H | 7β-H | 7α-H | 12β-H | $>NCH_2CO-$ | $>NCH_2CH_2S-$[c] | -NH- |
|---|---|---|---|---|---|---|---|---|---|---|---|
| **2** | C | 0.68 | 1.17 | 0.97 | 3.50 | | | 3.98 | | | |
| **3** | C | 0.67 | 1.15 | 1.01 | 3.56 | | | 3.92 | 3.93 d, 5.5 Hz | | 6.06 |
| **4** | M | 0.72 | 1.21 | 1.07 | 3.60 | | | 3.96 | | 3.01<br>3.60 | |
| **6** | C | 0.69 | 1.20 | 0.97 | 4.63 | | | 4.00 | | | |
| **7** | C | 0.70 | 1.18 | 1.03 | 4.65 | | | 4.00 | 4.00 d, 5.5 Hz | | 6.02 |
| **8** | M | 0.73 | 1.23 | 1.06 | 4.60 | | | 3.96 | | 2.98<br>3.59 | |
| **9** | C | 0.68 | 0.90 | 0.97 | 4.53 | 3.81 | | 3.94 | | | |
| **10** | C | 0.68 | 0.90 | 1.00 | 4.53 | 3.83 | | 3.95 | 3.98 d, 5.5 Hz | | 6.05 |
| **11** | M | 0.71 | 0.96 | 1.05 | 4.53 | 3.76 | | 3.90 | | 2.96<br>3.56 | |
| **12** | M | 0.76 | 0.92 | 1.07 | 3.28 | 4.42 | | 4.65 | | | |
| **13** | M | 0.76 | 0.92 | 1.08 | 3.29 | 4.42 | | 4.64 | 3.71 s | | |
| **14** | M | 0.76 | 0.92 | 1.07 | 3.30 | 4.43 | | 4.64 | | 2.94<br>3.56 | |
| **16** | C | 0.72 | 0.88 | 0.81 | 3.42 | 3.84 | | 5.06 | | | |
| **17** | C | 0.73 | 0.87 | 0.83 | 3.40 | 3.83 | | 5.02 | 3.96 d, 5.5 Hz | | 5.96 |
| **18** | M | 0.77 | 0.90 | 0.87 | 3.50 | 3.78 | | 5.03 | | 2.95<br>3.58 | |
| **19** | M | 0.71 | 0.94 | 1.01 | 4.13 | 4.43 | | 3.93 | | | |
| **20** | M | 0.71 | 0.94 | 1.02 | 4.12 | 4.42 | | 3.92 | 3.71 s | | |
| **21** | M | 0.71 | 0.93 | 1.01 | 4.12 | 4.42 | | 3.91 | | 2.94<br>3.57 | |
| **22** | M | 0.76 | 0.92 | 1.08 | 4.11 | 3.77 | | 4.66 | | | |
| **23** | M | 0.76 | 0.92 | 1.08 | 4.09 | 3.76 | | 4.64 | 3.71 s | | |
| **24** | M | 0.76 | 0.92 | 1.08 | 4.10 | 3.76 | | 4.63 | | 2.94<br>3.57 | |
| **25** | M | 0.68 | 0.94 | 0.95 | 4.13 | 4.42 | | | | | |
| **26** | M | 0.68 | 0.94 | 0.97 | 4.13 | 4.42 | | | 3.72 s | | |
| **27** | M | 0.69 | 0.95 | 0.96 | 4.14 | 4.43 | | | | 2.95<br>3.58 | |
| **28** | M | 0.76 | 0.93 | 1.06 | 4.22 | | | 4.65 | | | |
| **29** | M | 0.76 | 0.94 | 1.08 | 4.23 | | | 4.65 | 3.73 s | | |
| **30** | M | 0.76 | 0.93 | 1.06 | 4.21 | | | 4.63 | | 2.94<br>3.56 | |
| **31** | M | 0.69 | 0.97 | 0.95 | 4.20 | | 4.20 | | | | |
| **32** | M | 0.69 | 0.98 | 0.97 | 4.23 | | 4.23 | | 3.71 s | | |
| **33** | M | 0.69 | 0.97 | 0.97 | 4.23 | | 4.23 | | | 2.94<br>3.56 | |

*a*) C, $CDCl_3$; M, $CD_3OD$. *b*) Doublet, $J=6$ Hz. *c*) Triplet, $J=7$ Hz.

Finally, the disulfates of dihydroxylated bile acids (**25**—**33**) were synthesized from unconjugated, and glycine- and taurine-conjugated chenodeoxycholates, deoxycholates and ursodeoxycholates by sulfation with sulfur trioxide–triethylamine complex in pyridine.

These disulfates were purified by use of octadecyl silyl bonded silica instead of Amberlite XAD-2 resin, which is widely employed for the polar compounds in biological fluids, because the disulfates were partially decomposed into the monosulfates during the extraction procedure with the latter resin.

The NMR spectral data for the disulfates of bile acids and their derivatives are collected in Table I. These data may be helpful for the characterization of bile acids and related compounds.

Studies on the chromatographic separation of the disulfates of unconjugated and conjugated bile acids are being conducted in these laboratories and the details will be reported elsewhere in the near future.

## Experimental

All melting points were taken on a micro hot-stage apparatus and are uncorrected. Optical rotations were measured with a JASCO DIP-4 polarimeter in water. NMR spectra were recorded on a JEOL FX-100 spectrometer at 100 MHz with tetramethylsilane as an internal standard.

**General Procedure for Sulfation**——Sulfur trioxide–triethylamine complex[7] (1.5 g) was added to a solution of bile acid (1 g) in anhydrous pyridine (6 ml), and the solution was stirred at room temperature overnight. The reaction mixture was poured into ice-cooled petroleum ether (70 ml) and the solid product obtained was collected. After being washed with petroleum ether the product was dissolved in 1 N methanolic NaOH (30 ml) and the solution was refluxed for 2—10 h for deprotection. After filtration of the reaction mixture, the filtrate was concentrated *in vacuo* and diluted with ether (200 ml). The resulting precipitate was collected, redissolved in 0.5 M sodium phosphate buffer (pH 7.0, 2 ml) and passed through a column (23 × 22 mm i.d.) of PrePAK-500/$C_{18}$ (3 g, Waters Assoc., Milford, MA). The column was washed with water (5 ml), then the disulfate in the form of the sodium salt was eluted with 30% ethanol.

**General Procedure for Preparation of Glycine Conjugates**——*N,N'*-Dicyclohexylcarbodiimide (0.9 g) and *p*-nitrophenol (0.5 g) were added to a solution of bile acid (1 g) in anhydrous dioxane (10 ml)–AcOEt (20 ml), and the solution was stirred at room temperature overnight. After removal of the precipitate by filtration the filtrate was evaporated *in vacuo* and the oily residue obtained was chromatographed on silica gel (20 g). Elution with hexane–AcOEt (2 : 1—1 : 1) gave the *p*-nitrophenyl ester. Ethyl glycinate (500 mg) in pyridine (1 ml) was added to a solution of the *p*-nitrophenyl ester (1 g) in pyridine (4 ml) and the solution was stirred at room temperature for 3 h. The reaction mixture was poured into ice-water, acidified with 5% HCl and extracted with AcOEt. The organic layer was washed with water, dried over anhydrous $Na_2SO_4$ and evaporated down *in vacuo*. The oily residue was subjected to column chromatography on silica gel (20 g). Elution with hexane–AcOEt (1 : 2—1 : 10) gave the glycine conjugate.

**General Procedure for Preparation of Taurine Conjugates**——Taurine (400 mg) in water (4 ml) was added to a solution of bile acid *p*-nitrophenyl ester (1 g) in pyridine (20 ml) and the solution was stirred at room temperature overnight. The resulting solution was concentrated and the oily residue was subjected to column chromatography on silica gel (20 g). Elution with $CHCl_3$–MeOH (4 : 1—2 : 1) gave the taurine conjugate.

**Trisodium Cholate 7,12-Disulfate (12)**——Acetic anhydride (3 ml) in benzene (20 ml) was added to a solution of methyl 7-oxodeoxycholate[6] (**2**) (4 g) in pyridine (3 ml) and the solution was stirred at room temperature for 6.5 h. The reaction mixture was poured into ice-water, acidified with 5% HCl and extracted with AcOEt. The organic layer was washed successively with water, 5% $NaHCO_3$ and water, dried over anhydrous $Na_2SO_4$ and evaporated down *in vacuo*. Recrystallization of the crude product from acetone–hexane gave methyl 7-oxodeoxycholate 3-acetate (**6**) (2.9 g) as colorless needles. mp 176—177°C. A solution of **6** (1.9 g) in MeOH (50 ml) was treated with $NaBH_4$ (150 mg) under ice-cooling and the solution was stirred for 25 min. The reaction mixture was poured into ice-water, acidified with 5% HCl and extracted with AcOEt. The organic layer was washed with water, dried over anhydrous $Na_2SO_4$ and evaporated down *in vacuo*. Recrystallization of the crude product from acetone–hexane gave methyl cholate 3-acetate (**9**) (1.3 g) as colorless needles. mp 151—152°C. Compound **9** (1.2 g) was subjected to sulfation and the crude product was recrystallized from MeOH–ether to give **12** as colorless crystals. mp 164—166°C (dec.). $[\alpha]_D^{15}$ +33.0° ($c$=0.11). *Anal.* Calcd for $C_{24}H_{37}Na_3O_{11}S_2 \cdot 2H_2O$: C, 42.98; H, 6.16. Found: C, 43.01; H, 6.23.

**Trisodium Glycocholate 7,12-Disulfate (13)**——7-Oxodeoxycholic acid (**1**) (2 g) was subjected to partial acetylation in the same manner as described for **6** to give 7-oxodeoxycholic acid 3-acetate (**5**) (1.5 g). Compound **5** was condensed with ethyl glycinate to give ethyl glyco-7-oxodeoxycholate 3-acetate (**7**). Treatment of **7** in the same manner as described for **12** followed by recrystallization from MeOH–ether gave **13** (300 mg) as colorless crystals. mp 163—164°C (dec.). $[\alpha]_D^{17}$ +23.6° ($c$=0.11). *Anal.* Calcd for $C_{26}H_{40}NNa_3O_{12}S_2 \cdot 2H_2O$: C, 42.91; H, 6.09; N, 1.92. Found: C, 43.02; H, 6.25; N, 1.70.

**Trisodium Taurocholate 7,12-Disulfate (14)**——Compound **5** (600 mg) was condensed with taurine to give tauro-7-oxodeoxycholate 3-acetate (**8**). Treatment of **8** in the same manner as described for **12** followed by recrystallization from MeOH–ether gave **14** (150 mg) as colorless crystals. mp 150—152°C (dec.). $[\alpha]_D^{18}$ +17.5° ($c$=0.09). *Anal.* Calcd for $C_{26}H_{42}NNa_3O_{13}S_3 \cdot 2H_2O$: C, 40.15; H, 5.96; N, 1.80. Found: C, 40.22; H, 5.85; N, 1.85.

**Trisodium Cholate 3,7-Disulfate (19)**——Methyl cholate 3,12-diacetate (3 g) was dissolved in 5% methanolic KOH and the solution was stirred at room temperature for 30 min. The reaction mixture was poured into ice-water, acidified with 5% HCl and extracted with AcOEt. The organic layer was washed with water, dried over anhydrous $Na_2SO_4$ and evaporated down *in vacuo* to give cholic acid 12-acetate (**15**) in almost quantitative yield. Treatment of **15** with diazomethane followed by recrystallization from MeOH gave methyl cholate 12-acetate (**16**) (2.7 g) as colorless needles. mp 100—102°C. Compound **16** (1.5 g) was subjected to sulfation and the crude product was

recrystallized from MeOH–ether to give **19** as colorless crystals. mp 163.5—167 °C (dec.). $[\alpha]_D^{17}$ +4.8° ($c$=0.10). *Anal.* Calcd for $C_{24}H_{37}Na_3O_{11}S_2 \cdot 2H_2O$: C, 42.98; H, 6.16. Found: C, 43.12; H, 6.18.

**Trisodium Glycocholate 3,7-Disulfate (20)**——Compound **15** (1 g) was condensed with ethyl glycinate to give ethyl glycocholate 12-acetate (**17**) (850 mg). Compound **17** (800 mg) was subjected to sulfation and the crude product was recrystallized from MeOH–ether to give **20** (450 mg) as colorless crystals. mp 165—167 °C (dec.). $[\alpha]_D^{18}$ +23.6° ($c$=0.11). *Anal.* Calcd for $C_{26}H_{40}NNa_3O_{12}S_2 \cdot H_2O$: C, 45.15; H, 5.82; N, 2.02. Found: C, 45.02; H, 5.86; N, 2.05.

**Trisodium Taurocholate 3,7-Disulfate (21)**——Taurocholate 12-acetate (**18**) (1.5 g), obtainable from **15** by condensation with taurine, was subjected to sulfation and the crude product was recrystallized from MeOH–ether to give **21** (700 mg) as colorless crystals. mp 156—160 °C (dec.). $[\alpha]_D^{20}$ +19.1° ($c$=0.10). *Anal.* Calcd for $C_{26}H_{42}NNa_3O_{13}S_3$: C, 42.10; H, 5.71; N, 1.89. Found: C, 42.35; H, 5.81; N, 1.90.

**Trisodium Cholate 3,12-Disulfate (22)**——Compound **2** (1.8 g) was subjected to sulfation and the crude product obtained was reduced with $NaBH_4$ in the same manner as described for **9**. Recrystallization of the crude product from MeOH–ether gave **22** (700 mg) as colorless crystals. mp 163—164.5 °C (dec.). $[\alpha]_D^{20}$ +46.7° ($c$=0.11). *Anal.* Calcd for $C_{24}H_{37}Na_3O_{11}S_2 \cdot H_2O$: C, 44.17; H, 6.02. Found: C, 44.29; H, 6.12.

**Trisodium Glycocholate 3,12-Disulfate (23)**——Treatment of ethyl glyco-7-oxocdeoxycholate (**3**), obtainable from **1** (1.5 g) by condensation with ethyl glycinate, in the same manner as described for **22** followed by recrystallization from MeOH–ether gave **23** (750 mg) as colorless crystals. mp 167—168 °C (dec.). $[\alpha]_D^{20}$ +65.4° ($c$=0.10). *Anal.* Calcd for $C_{26}H_{40}NNa_3O_{12}S_2 \cdot 2H_2O$: C, 42.91; H, 6.09; N, 1.92. Found: C, 43.10; H, 6.03; N, 1.95.

**Trisodium Taurocholate 3,12-Disulfate (24)**——Treatment of tauro-7-oxodeoxycholate (**4**), obtainable from **1** (2 g) by condensation with taurine, in the same manner as described for **22** followed by recrystallization from MeOH–ether gave **24** (700 mg) as colorless crystals. mp 156—158 °C (dec.). $[\alpha]_D^{17}$ +72.7° ($c$=0.10). *Anal.* Calcd for $C_{26}H_{42}NNa_3O_{13}S_3 \cdot H_2O$: C, 41.10; H, 5.84; N, 1.84. Found: C, 41.02; H, 5.95; N, 1.80.

**Trisodium Chenodeoxycholate 3,7-Disulfate (25)**——Methyl chenodeoxycholate (2 g) was subjected to sulfation and the crude product was recrystallized from MeOH–ether to give **25** (1.3 g) as colorless crystals. mp 174.5—177 °C (dec.). $[\alpha]_D^{19}$ +0.2° ($c$=0.11). *Anal.* Calcd for $C_{24}H_{37}Na_3O_{10}S_2$: C, 46.60; H, 6.03. Found: C, 46.36; H, 6.01.

**Trisodium Glycochenodeoxycholate 3,7-Disulfate (26)**——Ethyl glycochenodeoxycholate (1.2 g) was subjected to sulfation and the crude product was recrystallized from MeOH–ether to give **26** (700 mg) as colorless crystals. mp 174.5—176 °C (dec.). $[\alpha]_D^{20}$ +18.4° ($c$=0.11). *Anal.* Calcd for $C_{26}H_{40}NNa_3O_{11}S_2 \cdot H_2O$: C, 45.01; H, 6.10; N, 2.02. Found: C, 44.92; H, 6.18; N, 2.05.

**Trisodium Taurochenodeoxycholate 3,7-Disulfate (27)**——Taurochenodeoxycholate (1.2 g) was subjected to sulfation and the crude product was recrystallized from MeOH–ether to give **27** (650 mg) as colorless crystals. mp 160—164 °C (dec.). $[\alpha]_D^{18}$ +9.3° ($c$=0.10). *Anal.* Calcd for $C_{26}H_{42}NNa_3O_{12}S_3 \cdot H_2O$: C, 41.99; H, 5.96; N, 1.88. Found: C, 42.05; H, 5.85; N, 1.80.

**Trisodium Deoxycholate 3,12-Disulfate (28)**——Methyl deoxycholate (1.8 g) was subjected to sulfation and the crude product was recrystallized from MeOH–ether to give **28** (1 g) as colorless crystals. mp 176—177 °C (dec.). $[\alpha]_D^{17}$ +67.0° ($c$=0.10). *Anal.* Calcd for $C_{24}H_{37}Na_3O_{10}S_2 \cdot H_2O$: C, 45.28; H, 6.17. Found: C, 45.04; H, 5.96.

**Trisodium Glycodeoxycholate 3,12-Disulfate (29)**——Ethyl glycodeoxycholate (800 mg) was subjected to sulfation and the crude product was recrystallized from MeOH–ether to give **29** (350 mg) as colorless crystals. mp 177—179 °C (dec.). $[\alpha]_D^{20}$ +40.0° ($c$=0.10). *Anal.* Calcd for $C_{26}H_{40}NNa_3O_{11}S_2 \cdot 3H_2O$: C, 42.79; H, 6.35; N, 1.92. Found: C, 42.51; H, 6.10; N, 1.84.

**Trisodium Taurodeoxycholate 3,12-Disulfate (30)**——Taurodeoxycholate (500 mg) was subjected to sulfation and the crude product was recrystallized from MeOH–ether to give **30** (200 mg) as colorless crystals. mp 165—168 °C (dec.). $[\alpha]_D^{18}$ +53.3° ($c$=0.10). *Anal.* Calcd for $C_{26}H_{42}NNa_3O_{12}S_3 \cdot 3H_2O$: C, 40.05; H, 6.20; N, 1.80. Found: C, 39.77; H, 6.18; N, 1.66.

**Trisodium Ursodeoxycholate 3,7-Disulfate (31)**——Methyl ursodeoxycholate (1.6 g) was subjected to sulfation and the crude product was recrystallized from MeOH–ether to give **31** (1.3 g) as colorless crystals. mp 182—184 °C (dec.). $[\alpha]_D^{17}$ +22.9° ($c$=0.11). *Anal.* Calcd for $C_{24}H_{37}Na_3O_{10}S_2 \cdot H_2O$: C, 45.28; H, 6.17. Found: C, 45.45; H, 6.55.

**Trisodium Glycoursodeoxycholate 3,7-Disulfate (32)**——Ethyl glycoursodeoxycholate (1 g) was subjected to sulfation and the crude product was recrystallized from MeOH–ether to give **32** (500 mg) as colorless crystals. mp 184—186 °C (dec.). $[\alpha]_D^{18}$ +43.9° ($c$=0.10). *Anal.* Calcd for $C_{26}H_{40}NNa_3O_{11}S_2 \cdot 3H_2O$: C, 42.79; H, 6.35; N, 1.92. Found: C, 42.61; H, 6.22; N, 1.87.

**Trisodium Tauroursodeoxycholate 3,7-Disulfate (33)**——Tauroursodeoxycholate (600 mg) was subjected to sulfation and the crude product was recrystallized from MeOH–ether to give **33** (230 mg) as colorless crystals. mp 166—168 °C (dec.). $[\alpha]_D^{19}$ +27.4° ($c$=0.11). *Anal.* Calcd for $C_{26}H_{42}NNa_3O_{12}S_2 \cdot 2H_2O$: C, 40.99; H, 6.09; N, 1.84. Found: C, 40.97; H, 6.10; N, 1.92.

**Acknowledgement** The authors are indebted to the staff of the Central Analytical Laboratory of this Institute for elemental analyses and spectral measurements. This work was supported in part by a Grant-in-Aid for Scientific Research from the Ministry of Education, Science and Culture of Japan.

## References and Notes

1) Part CCXXXII of "Studies on Steroids" by T. Nambara; Part CCXXXI: H. Hosoda, W. Takasaki, R. Tsukamoto and T. Nambara, *Chem. Pharm. Bull.*, **35**, 3336 (1987). The following trivial names are used in this paper: cholic acid = 3α,7α,12α-trihydroxy-5β-cholan-24-oic acid; chenodeoxycholic acid = 3α,7α-dihydroxy-5β-cholan-24-oic acid; deoxycholic acid = 3α,12α-dihydroxy-5β-cholan-24-oic acid; ursodeoxycholic acid = 3α,7β-dihydroxy-5β-cholan-24-oic acid.
2) J. Goto, H. Kato, F. Hasegawa and T. Nambara, *Chem. Pharm. Bull.*, **27**, 1402 (1979).
3) J. Goto, H. Kato, K. Kaneko and T. Nambara, *Chem. Pharm. Bull.*, **28**, 3389 (1980).
4) J. Goto, H. Kato, Y. Saruta and T. Nambara, *J. Chromatogr.*, **226**, 13 (1981).
5) J. Goto, T. Chikai and T. Nambara, *J. Chromatogr.*, **415**, 45 (1987).
6) L. F. Fieser and S. Rajagopalan, *J. Am. Chem. Soc.*, **71**, 3935 (1949).
7) K. Y. Tserng and P. D. Klein, *Steroids*, **33**, 167 (1979).

[Chem. Pharm. Bull. 35(11)4568—4573(1987)]

# Fabrication of Potentiometric Enzyme Sensors Based on a pH-Sensitive Polymer-Coated Ag Electrode

JUN-ICHI ANZAI, MASAHIKO SHIMADA, HONGDA FU, and TETSUO OSA*

*Pharmaceutical Institute, Tohoku University, Aobayama, Sendai 980, Japan*

(Received April 25, 1987)

A silver wire electrode coated with a poly(vinyl chloride)/tri-*n*-dodecylamine composite membrane was used to fabricate potentiometric enzyme sensors. The coated Ag electrode was further covered with a penicillinase or urease membrane to make a penicillin or urea sensor, respectively. The penicillin sensor was useful for determining penicillin at concentrations of millimolar level. Some operating variables such as pH and ionic concentration of the working buffer of the sensor were examined. The urea sensor could be used to determine urea in human blood.

**Keywords**——enzyme electrode; coated wire electrode; pH-sensitive electrode; poly(vinyl chloride)/tri-*n*-dodecylamine composite membrane; penicillin sensor; urea sensor

## Introduction

Much attention is currently being devoted to developing micro enzyme sensors.[1-5] We have reported that the ion-sensitive field effect transistor, which functions as a pH sensor, can be used for constructing micro enzyme sensors by covering it with enzyme membranes.[6-10] A coated wire electrode may be another possible material for constructing micro enzyme sensors. Coated wire electrodes are currently used for determining metal ions such as $Na^+$, $K^+$, and $Ca^{2+}$ in clinical laboratories, because of their ease of fabrication and low cost. The advantage of the coated wire electrode in miniaturizing the sensor body lies in the absence of internal reference solutions. Accordingly, if coated wire electrodes can be coupled with enzymes appropriately, we should be able to prepare micro enzyme sensors. We have already reported preliminary results on enzyme sensors based on a polymer-coated Ag electrode.[11] The present paper reports some performance characteristics of penicillin and urea sensors constructed by the use of a pH-sensitive Ag electrode coated with poly(vinyl chloride)/tri-*n*-dodecylamine membrane.

## Experimental

Poly(vinyl chloride) (PVC) (polymerization degree 1100), purchased from Wako Chemical Co., was used without further purification. Sodium tetraphenyl borate (NaTPB), tri-*n*-dodecylamine (TDA), and *o*-nitrophenyl *n*-octyl ether (NPOE) were of extra pure reagent grade. Penicillinase was purchased from Miles Co. Urease and bovine serum albumin (BSA) were obtained from Sigma Chemical Co., each as a crystallized and lyophilized powder. Glutaraldehyde, urea, and penicillin G potassium salt were of reagent grade. Human serum was purchased from Miles Scientific Co.

The structure of the enzyme sensor is illustrated in Fig. 1. The top of an Ag wire (0.5 mm diameter) mounted in a Teflon rod was coated with a pH-sensitive polymer membrane composed of PVC (31%), NPOE (63%), TDA (5.5%), and NaTPB (0.5%). The polymer membrane was prepared by pouring a small amount of tetrahydrofuran solution of the materials onto the surface of the Ag electrode and allowing the solvent to evaporate. The thickness of the polymer membrane was about 0.2 mm. The polymer layer of the electrode was further covered with an enzyme membrane, which was prepared from a mixture composed of equal amounts of 10% enzyme solution, 10% BSA solution,

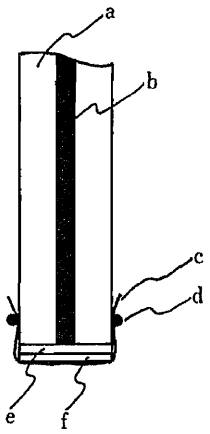


Fig. 1. Schematic Representation of the Enzyme Sensor
a) Teflon rod; b) Ag wire; c) Nylon mesh; d) O-ring; e) PVC/TDA membrane; f) enzyme membrane.

and 8% glutaraldehyde. After evaporation of the water, a thin layer of immobilized-enzyme membrane was formed on the electrode. The thickness of the enzyme membrane was about 5 $\mu$m. The sensitive layer was wrapped with nylon mesh.

All potentiometric measurements were carried out at 23 °C, using a high input impedance potentiometer (Takeda Riken Co., TR6843) and a reference saturated calomel electrode (SCE). Solutions were not stirred, and the probe was rinsed with the buffer solution after each measurement.

## Results and Discussion

### PVC/TDA-Coated Electrode

A pH-sensitive membrane electrode based on TDA was first reported by Simon *et al.*[12,13] The coated wire type of electrode using PVC/TDA membrane has been examined recently by Abe and Takizawa.[14] We used a series of $KH_2PO_4$/NaOH solutions ranging in pH from 4—9 to establish the pH response of the PVC/TDA-coated Ag electrode prior to enzyme immobilization. Figure 2 shows a typical pH response of the PVC/TDA-coated Ag electrode used in the present study. The calibration graph exhibited near Nernstian response over the pH range tested, with a response time of 20—30 s. The pH response of the electrode seems to be caused by the fact that $H^+$ is adsorbed by TDA at the membrane surface to form an electric double layer at the membrane/solution interface.

### Penicillin-Sensitive Electrode

A penicillin sensitive-electrode was prepared by covering the sensitive layer of the PVC/TDA-coated Ag electrode with a cross-linked penicillinase membrane. Figure 3 depicts typical response curves of the sensor for 0.01—10 mM penicillin G solutions. The probe was immersed in the buffer solution for about 30 min, then dipped into the sample solutions. The electrode potential changed markedly at the initial stage of the measurements and declined to reach the steady-state potentials in 5—10 min. The sensor showed no further change in potential, though, during the prolonged measurement, a potential drift was observed for the previously developed device.[11] This means that an AgCl layer is not required between the Ag wire and the polymer membrane for making high-performance potentiometric enzyme sensors. The positive shift of the potential means that the pH value around the pH-sensitive layer of the electrode shifted from the buffer condition to the acidic side. This can be reasonably explained on the basis of the enzymatic reaction (1) in the penicillinase membrane, where $H^+$ is liberated from penicilloic acid produced by the reaction. The output voltage, $\Delta E$, at the steady-state

$$\text{penicillin} + H_2O \xrightarrow{\text{penicillinase}} \text{penicilloate} + H^+ \qquad (1)$$

is plotted against the logarithm of substrate concentration in Fig. 4. The $\Delta E$ value clearly

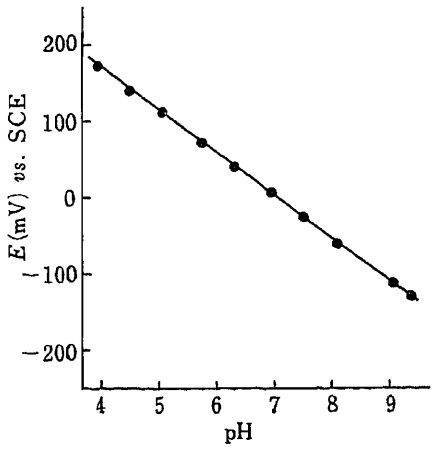


Fig. 2. pH Response of the PVC/TDA-Coated Ag Electrode

The pH value of the solutions was adjusted by adding various amounts of NaOH to a 50 mM $KH_2PO_4$ solution.

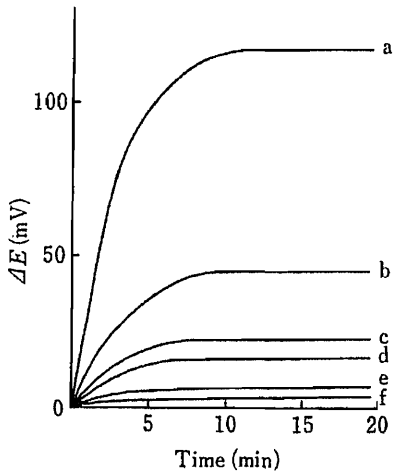


Fig. 3. Typical Response Curves of the Penicillin Sensor in 10 mM Phosphate Buffer (pH 7.0)

The penicillin G concentration was a) 10, b) 3.0, c) 1.0, d) 0.3, e) 0.1, or f) 0.01 mM.

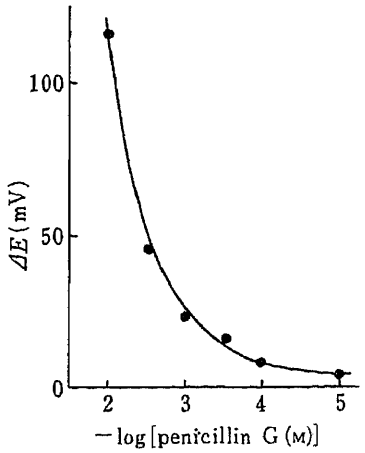


Fig. 4. Calibration Graph of the Penicillin Sensor

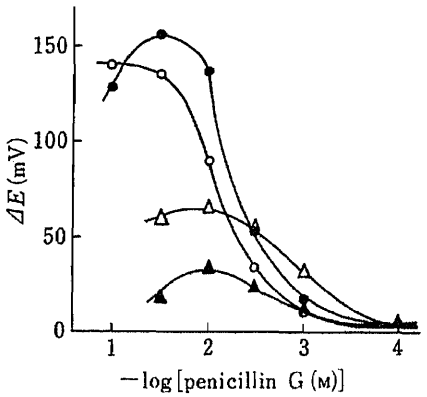


Fig. 5. Effects of Buffer pH on the Potentiometric Response of the Penicillin Sensor

Phosphate buffer (10 mM) was used. The buffer pH was 8.0 (—○—), 7.0 (—●—), 6.0 (—△—), or 5.2 (—▲—).

depends on the substrate concentration. The lower limit of detection with this sensor seems to be about 1 mM under the present operating conditions. The data shown in Figs. 3 and 4 imply that the sensor can be used to determine penicillin at millimolar levels.

The mechanism by which the penicillin sensor responds to the penicillin concentration in the sample solution is that the amount of $H^+$ liberated through the reaction (1) is detected as a pH change around the surface of the PVC/TDA membrane. Accordingly, the pH and concentration of the working buffer should be crucially important factors affecting the performance characteristics of the sensor. Figure 5 shows the effects of pH of the sample solutions on the potentiometric response of the penicillin sensor. The calibration curves obtained in pH 5.2, 6.0, 7.0, and 8.0 media (5 mM buffer) are shown. When the substrate concentration was below 1 mM, the effect of pH on the response was small. In the higher concentration regions, larger $\Delta E$ values were obtained in the cases of neutral or near-neutral

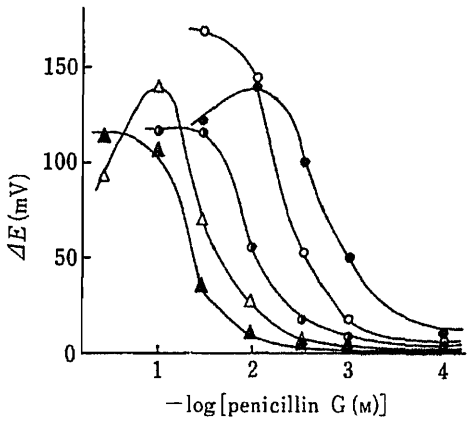


Fig. 6. Effects of Buffer Concentration on the Potentiometric Response of the Penicillin Sensor

Phosphate buffer containing 500 mM NaCl was used. The concentration of phosphate was 1 (—●—), 5 (—○—), 20 (—◑—), 50 (—△—), and 100 mM (—▲—).

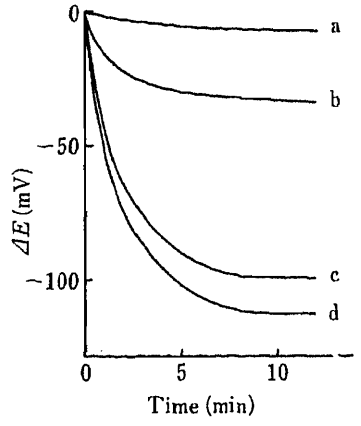


Fig. 7. Typical Response Curves of the Urea Sensor in 10 mM Phosphate Buffer (pH 7.0)

Urea concentration was a) 0.1; b) 1.0; c) 10; or d) 100 mM.

pH (pH 7.0 and 8.0). It should be noted here that, for the range of 1—10 mM substrate, a super-Nernstian response was obtained in pH 7.0 and 8.0 media, the slopes of the graphs being 100 mV/decade or more. This is presumably because the catalytic activity of the enzyme in the membrane is enhanced by the pH change arising from the progress of the enzymatic reaction in the membrane (*i.e.*, a positive feedback effect). In the present case, for example, the $\Delta E$ value of about 130 mV observed when the probe was dipped into the 30 mM sample solution of pH 8.0 corresponds to a shift of about two pH units to the acidic side from the buffer condition (pH 8.0), resulting in a pH of about 6.0 in the enzyme membrane. The optimum pH of penicillinase is known to be 6—7.[15] From Fig. 5, it is recommended to use pH 7—8 buffer for obtaining a high response.

Figure 6 shows the effects of buffer concentration on the response of the sensor. The calibration graphs were constructed in 1, 5, 20, 50, and 100 mM phosphate buffers, to which 500 mM NaCl was added to compensate the difference in ionic strength of the solutions, at pH 7. The dynamic range of the sensor shifted to the higher substrate concentration region with increase of the buffer concentration. This is presumably because, in the higher concentration buffer, the small pH change arising from the enzymatic reaction in the samples of low penicillin concentration is canceled by the higher buffer capacity. As discussed above, the effects of buffer concentration and pH on the potentiometric response of the sensor are basically the same as those previously reported for the ISFET-based enzyme sensors.[7]

**Urea-Sensitive Electrode**

A urea sensor was similarly fabricated by the use of the PVC/TDA-coated electrode coupled with a urease membrane. Figure 7 depicts typical response curves of the urea sensor for 0.01—100 mM urea solutions (10 mM phosphate buffer, pH 7.0). The electrode potential shifted in the negative direction, and reached the steady-state value after 5—10 min. The negative shift of the potential reflects a pH change of the medium around the electrode surface to the alkaline side, which can be reasonably explained based on the fact that urease catalyzes the decomposition reaction of urea to ammonia and carbon dioxide with consumption of $H^+$.

$$(NH_2)_2CO + 2H_2O + H^+ \xrightarrow{\text{urease}} 2NH_4^+ + HCO_3^- \qquad (2)$$

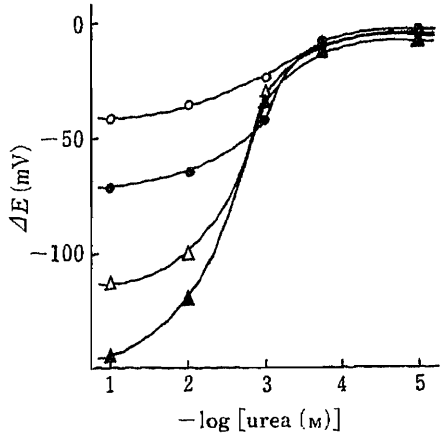


Fig. 8. Effects of Buffer pH on the Potentiometric Response of the Urea Sensor

Phosphate buffer (10 mM) was used. The pH value of the sample was 6.0 (—▲—), 7.0 (—△—), 8.0 (—●—), or 9.0 (—○—).

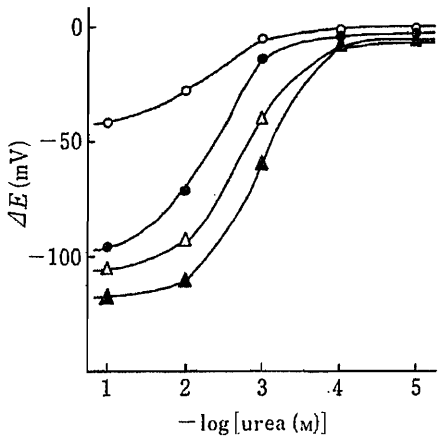


Fig. 9. Effects of Buffer Concentration on the Potentiometric Response of the Urea Sensor

The concentrations of phosphate buffer was 2.0 (—▲—), 5.0 (—△—), 10 (—●—), or 50 mM (—○—).

The effects of pH and strength of the working buffer on the response of the sensor are shown in Figs. 8 and 9. Figure 8 clearly indicates that the urea sensor exhibits a higher response in neutral or slightly acidic medium. The pH-dependence of the response of the sensor may arise from the facts that the activity curve of urease is bell-shaped with a maximum at pH 6.5—7.0, and that urease loses its catalytic ability precipitously around pH 9.0.[15] In the present case, the pH value of the membrane interior shifts in the alkaline direction as a result of $H^+$ consumption through the enzyme reaction (2). For example, $\Delta E$ of about 70 mV, obtained for 100 mM urea in pH 8 buffer, corresponds to about 1.2 pH unit shift to the alkaline side from the buffer condition, *i.e.*, about pH 9.2 in the membrane. This is the reason why the potentiometric response was reduced in pH 8.0 and also pH 9.0 buffers. From Fig. 9, it is clear that the response of the sensor is severely reduced in the higher concentration buffer. This is because the local pH change arising from the enzymatic reaction (2) is buffered easily by the higher concentration buffer. This behavior is characteristic of enzyme sensors based on pH-sensitive base electrodes.

We applied the urea sensor for determining urea in human serum. Serum was diluted 4-fold, 6-fold, and 10-fold with 10 mM phosphate buffer (pH 7.5), to which 160 mM NaCl was added to compensate the difference in ionic strength. The urea level of the samples was found to be 4.0 mM (4-fold), 4.1 mM (6-fold), and 4.1 mM (10-fold), in good agreement with the result obtained by the urease-indophenol method (4.2 mM).

Thus, we have demonstrated that penicillin and urea sensors can be constructed by the use of a pH-sensitive Ag electrode coated with PVC/TDA composite membrane. The long-term stability of the sensor, however, is not adequate. The potentiometric response of the sensors fell to *ca.* 60% of the original value in a week. Studies to miniaturize the sensor body and to improve in performance of the sensor are in progress in this laboratory.

**Acknowledgement** The authors are grateful to the Ministry of Education, Science and Culture of Japan for support of this work through a Grant-in-Aid for Special Project Research (No. 61127003).

## References

1) S. Caras and J. Janata, *Anal. Chem.*, **52**, 1935 (1980).
2) Y. Miyahara, T. Moriizumi, S. Shiokawa, H. Matsuoka, I. Karube, and S. Suzuki, *Nippon Kagaku Kaishi*, **1983**,

823.
3) S. Caras and J. Janata, *Anal. Chem.*, **57**, 1924 (1985).
4) D. C. Roberts, J. A. Osborn, and A. M. Yacynych, *Anal. Chem.*, **58**, 140 (1986).
5) S. Shiono, Y. Hanazato, and M. Nakato, *Anal. Sci.*, **2**, 517 (1986).
6) J. Anzai, T. Kusano, T. Osa, H. Nakajima, and T. Matsuo, *Bunseki Kagaku*, **33**, E131 (1984).
7) J. Anzai, Y. Ohki, T. Osa, H. Nakajima, and T. Matsuo, *Chem. Pharm. Bull.*, **33**, 2556 (1985).
8) J. Anzai, S. Tezuka, T. Osa, H. Nakajima, and T. Matsuo, *Chem. Pharm. Bull.*, **34**, 4373 (1986).
9) M. Esashi, T. Matsuo, J. Anzai, and T. Osa, Proceeding of the 5th Sensor Symposium, Tsukuba, 1985, p. 221.
10) J. Anzai, S. Tezuka, T. Osa, H. Nakajima, and T. Matsuo, *Chem. Pharm. Bull.*, **35**, 693 (1987).
11) J. Anzai and T. Osa, *Chem. Pharm. Bull.*, **34**, 3522 (1986).
12) P. Schulthess, Y. Shijo, H. V. Pharm, E. Pretsch, D. Amman, and W. Simon, *Anal. Chim. Acta*, **131**, 111 (1981).
13) D. Amman, F. Lanter, R. A. Steiner, P. Schultess, Y. Shijo, and W. Simon, *Anal. Chem.*, **53**, 2267 (1981).
14) H. Abe and S. Takizawa, Abstracts of Papers, 4th Sensor Symposium, Yokohama, 1985, p. 1.
15) H. Kitano, "Kagaku Zokan 84," Kagaku Dojin, Tokyo, 1980, p. 113.

[Chem. Pharm. Bull. 35(11)4574—4578(1987)]

# Assay of Purine Nucleoside Phosphorylase in Erythrocytes by Flow-Injection Analysis with Fluorescence Detection

YOHJI HAYASHI, KIYOSHI ZAITSU and YOSUKE OHKURA*

*Faculty of Pharmaceutical Sciences, Kyushu University 62, Maidashi, Higashi-ku, Fukuoka 812, Japan*

(Received May 11, 1987)

A sensitive assay for purine nucleoside phosphorylase (PNP) in human erythrocytes is described. Erythrocyte lysate is incubated with the substrate inosine in the presence of phosphate for the enzyme reaction, and the resulting mixture is deproteinized with perchloric acid and neutralized. The supernatant containing the reaction product, hypoxanthine, is applied to a flow-injection system in which immobilized enzyme columns of xanthine oxidase, urate oxidase and horseradish peroxidase are connected in series in that order in the flow line. Hydrogen peroxide formed in the enzymatic conversion of hypoxanthine is measured fluorimetrically by reaction with 3-(*p*-hydroxyphenyl)propionic acid in the system. The lower limit of determination (signal-to-noise ratio = 5) for hypoxanthine is 0.3 pmol in a 20-$\mu$l injection volume, which corresponds to a PNP activity of 0.117 $\mu$mol/min/ml erythrocytes. This method permits the assay of PNP in only 10 nl of human erythrocytes in 50 $\mu$l of erythrocyte lysate.

**Keywords**——purine nucleoside phosphorylase activity; flow-injection analysis; hypoxanthine determination; immobilized enzyme; xanthine oxidase; urate oxidase; horseradish peroxidase; fluorescence detection; hydrogen peroxide; 3-(*p*-hydroxyphenyl)propionic acid

Purine nucleoside phosphorylase (PNP; EC 2.4.2.1) catalyzes the conversion of purine nucleosides such as inosine, guanosine and their 2′-deoxyribonucleosides to purine bases and ribose 1-phosphate or 2-deoxyribose 1-phosphate. Deficiency of PNP is closely associated with immunodeficiency characterized by severely defective T-cell function with normal B-cell immunity.[1,2] Therefore, the assay of this enzyme activity in erythrocytes[3-7] or lymphocytes[8] is useful in the diagnosis of this disease.

PNP in erythrocytes and lymphocytes has been assayed by spectrophotometric[5-11] and radiochemical[3,4,12,13] methods. We have reported a sensitive fluorimetric flow-injection analysis (FIA) of hydrogen peroxide using an immobilized horseradish peroxidase (HRP) column,[14] and it was successfully applied to the flow-injection determination of adenosine and inosine in human plasma[15] and serum guanase activity using immobilized enzyme

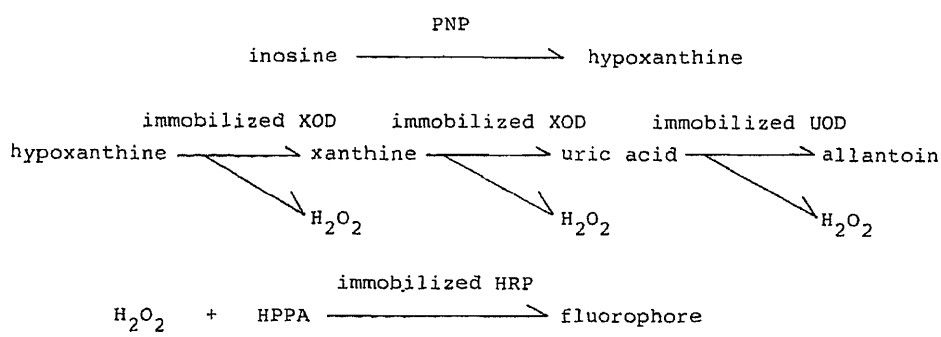


Chart 1

columns connected in series.[16] Based on the enzyme column technique, a highly sensitive FIA method for the assay of PNP in human erythrocytes has been developed. Hypoxanthine formed enzymatically from the substrate inosine is degraded to hydrogen peroxide by using immobilized xanthine oxidase (XOD) and urate oxidase (UOD, uricase) columns (Chart 1). The hydrogen peroxide is quantified by an immobilized HRP-mediated reaction using 3-(*p*-hydroxyphenyl)propionic acid (HPPA), an efficient fluorogenic substrate for HRP[17] (Chart 1).

## Experimental

**Chemicals and Reagents**——Double-deionized water was filtered through a Milli-QII system (Japan Millipore Ltd.; Tokyo, Japan) just before use. HPPA was obtained from Dojindo Laboratories (Kumamoto, Japan) and Otsuka Chemical Co. (Osaka, Japan). HRP (285 purpurogallin unit/mg), UOD (grade II, 4.0 U/mg, from *Candida* sp.) and XOD (0.4 U/mg, from cow's milk, in 3.2 M $(NH_4)_2SO_4$ suspension, 10 mM in ethylenediaminetetra acetic acid disodium (EDTA·2Na)) were from Sigma (St. Louis, U.S.A.), Toyobo Biochemicals (Osaka, Japan) and Boehringer Mannheim Yamanouchi (Tokyo, Japan), respectively. Inosine and hypoxanthine were purchased from Nakarai Chemicals (Kyoto, Japan). Unless otherwise noted, all other chemicals were of reagent grade.

**Preparation of Erythrocyte Lysate**——Venous blood samples (1 ml) obtained from healthy volunteers were collected in glass tubes containing 10 $\mu$l of 200 mM EDTA·2Na. Each blood sample was centrifuged for 10 min at 1000 *g*. Then, the plasma and the buffy coat were removed by centrifugation and the remaining erythrocytes (packed cells) were washed twice with 5 ml of ice-cold 150 mM NaCl. The erythrocytes were lysed with cold water to obtain a 5000-fold dilution.

**Enzyme Reaction and Sample Solutions for FIA**——The substrate solution was 1.0 mM inosine in 50 mM phosphate buffer (pH 6.0). The solution (450 $\mu$l) was preincubated at 37 °C for *ca.* 5 min and again incubated for exactly 10 min after adding 50 $\mu$l of the erythrocyte lysate. The reaction was stopped by addition of 100 $\mu$l of 4.0 M $HClO_4$. The resulting solution was mixed with 180 $\mu$l of 2 M $K_2CO_3$ to remove $KClO_4$ and centrifuged for 10 min at 1000 *g*. An aliquot (20 $\mu$l) of the supernatant (sample solution for testing) was applied to the flow-injection system. For the blank (reflecting endogenous uric acid, xanthine and hypoxanthine), the same procedure was carried out except that the erythrocyte lysate and the substrate solution were added to the $HClO_4$ solution, incubation being omitted.

**Flow-Injection System and Assay Procedure for Hypoxanthine**——A schematic flow diagram of the flow-injection system is shown in Fig. 1. The immobilized XOD, UOD and HRP columns were prepared as previously described[15] and connected in series in that order in the flow line using Teflon tubing (0.25 mm i.d.; Gasukuro Kogyo, Tokyo, Japan). The reagent solution, which was 5 mM HPPA in 0.1 M Tris–HCl buffer (pH 8.0), 0.15 M in NaCl, and 10 mM in EDTA·2Na and the carrier solution, which was the same as the reagent solution but without HPPA, were pumped separately with a Sanuki DM2M-1026 pump; the flow rates were both 0.25 ml/min. The sample solution for the test or blank was injected through a Rheodyne 7125 syringe-loading sample injector valve (20-$\mu$l loop) into the carrier stream. A mixing coil (1 m) and the three enzyme columns were immersed in a water bath at 37 °C. The fluorescence intensity was measured at an excitation wavelength of 305 nm and an emission wavelength of 405 nm with a Shimadzu RF 530 fluorescence spectromonitor equipped with a 12-$\mu$l flow cell and a Hitachi 056 chart recorder.

To prepare a calibration curve, hypoxanthine standard solutions (0.25—25 $\mu$M) were taken through the procedure. The concentration of hypoxanthine formed enzymatically was read on the calibration curve in terms of net peak height. PNP activity was expressed as micromoles of hypoxanthine formed per minute per milliliter of erythrocytes at 37 °C.

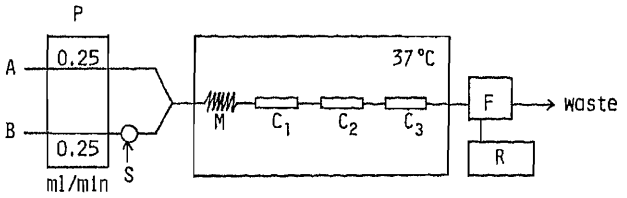


Fig. 1. Schematic Diagram of the Flow-Injection System

A, reagent solution; B, carrier solution; C, immobilized enzyme columns (1, XOD; 2, UOD; 3, HRP); F, fluorescence detector; P, pump; S, sample injector; M, mixing coil; R, recorder.

## Results and Discussion

The conditions of the FIA were optimum and essentially the same as described previously.[16] The PNP-catalyzed reaction requires inorganic phosphate, and thus phosphate buffer was used for the enzyme reaction. Although the relationship between pH and PNP activity was biphasic for an unknown reason, the pH at which the activity was highest was 6.0 (Fig. 2). Phosphate buffer gave a maximum and constant activity at concentrations of 25—75 mM. Therefore, 50 mM phosphate buffer of pH 6.0 was selected for the enzyme reaction. A maximum and constant activity was obtained with 0.75—2.0 mM inosine in the substrate solution, with an observed $K_m$ value of 95 $\mu$M; 1 mM in the substrate solution was employed as a saturating concentration for the enzyme reaction.

The amount of hypoxanthine formed enzymatically was strongly influenced by the incubation temperature in the reaction and higher temperatures resulted in faster formation of hypoxanthine up to at least 50 °C for the incubation time of 10 min (Fig. 3), though deactivation of the enzyme occurred on prolonged incubation; 37 °C was chosen for convenience. The enzyme reaction rate was linear with time up to at least 60 min at 37 °C. The amount of hypoxanthine formed during the incubation time of 10 min was proportional to the amount of erythrocytes up to at least 100 nl; 10 nl of erythrocytes (in 50 $\mu$l of erythrocyte lysate) was chosen for the standard procedure.

Components of the erythrocyte lysate had no effect on the determination of hypoxanthine; the recoveries of hypoxanthine added to the erythrocyte lysate in the concentration range of 1—400 $\mu$M were approximately 100%. Thus, a calibration curve was prepared by subjecting hypoxanthine standard solutions directly to the FIA. The calibration curve was linear up to 500 pmol per 20-$\mu$l injection volume and passed through the origin. The lower limit of determination (signal-to-noise ratio = 5) for hypoxanthine was 0.3 pmol in a 20-$\mu$l injection volume, which corresponds to a PNP activity of 0.117 unit.

Typical flow-injection peaks obtained with 10—80 pmol of hypoxanthine in a 20-$\mu$l injection volume and with the sample solutions for the test and blank are shown in Fig. 4. A rapid sampling rate (40 injections/h) could be attained.

Parallel tests with a spectrophotometric method[18] (enzyme reaction temperature 25 °C and pH 7.4) and the present method were performed on 15 different erythrocyte samples from

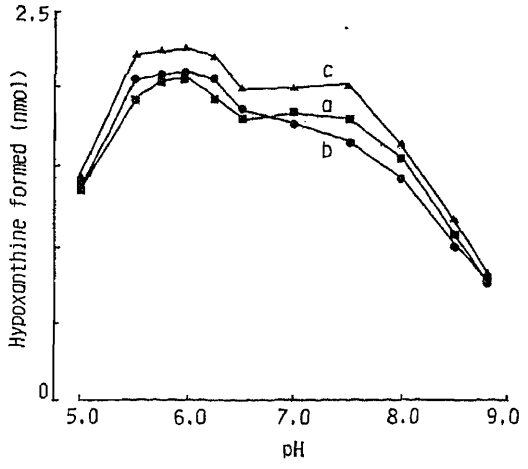


Fig. 2. Effect of pH of the Phosphate Buffer in the Enzyme Reaction on the Amount of Hypoxanthine Formed

PNP activities ($\mu$mol/min/ml): a, 20.9; b, 21.1; c, 22.6.

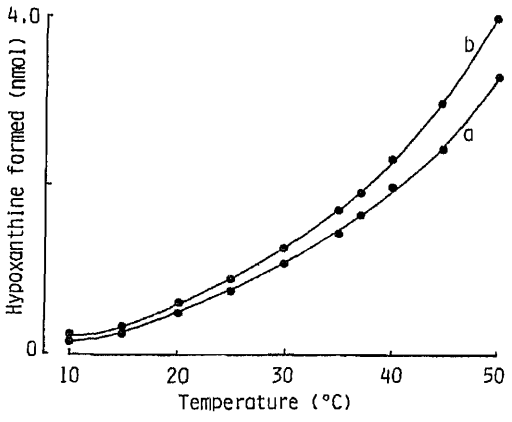


Fig. 3. Effect of Temperature of the Enzyme Reaction on the Amount of Hypoxanthine Formed

PNP activities ($\mu$mol/min/ml): a, 17.5; b, 20.9.

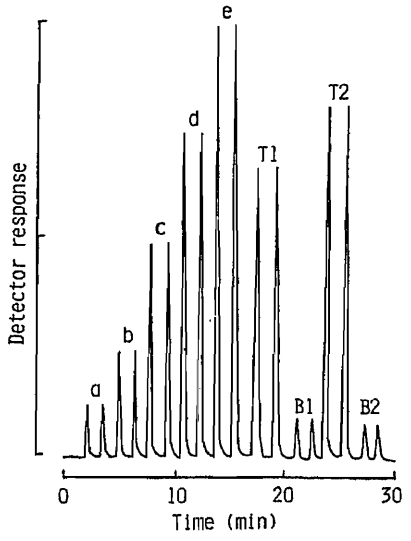


Fig. 4. Flow-Injection Peaks for Standard and Erythrocyte Samples

Amounts of hypoxanthine (pmol/20 μl): a, 10; b, 20; c, 40; d, 60; e, 80. T and B=test and blank, respectively. PNP activities (μmol/min/ml): 17.5 (obtained from T1 and B1), 22.6 (obtained from T2 and B2).

normal subjects (age, 21—56; male, 8; female 7). The linear regression equation and correlation coefficient for the two methods were $y$ (spectrophotometric method) $=0.34\ x$ (present method) $-0.7$ and 0.856, respectively. Mean PNP activities obtained by the spectrophotometric method and the present method were $6.29\pm0.87$ and $20.6\pm2.2$ (mean $\pm$ S.D.), respectively. The value obtained by the present method was about three times higher than that obtained by the spectrophotometric method. The discrepancy was considered to be due to the difference in the enzyme reaction temperatures and pHs (Figs. 2 and 3). The within-day precision of the present method was examined using erythrocytes with mean PNP activities of 17.5, 21.1 and 24.6 μmol/min/ml. The relative standard deviations were 0.85, 0.75 and 0.93% ($n=10$ each), respectively.

Uric acid (10 μM), ascorbic acid (100 μM) and glucose (10 mM) added to erythrocyte lysate at the abnormally high concentrations shown in parentheses had no effect on the hypoxanthine recovery.

To check the stability of the immobilized enzyme columns, hypoxanthine solutions (2.5 and 5 μM) were applied 50 times a week to the flow system. When not required for use, the columns were stored at 4°C after being filled with the following solutions: 3.2 M ammonium sulfate (pH 8.0) 10 mM in disodium EDTA for XOD; 50 (v/v)% glycerol (pH 10.2) 50 mM in glycine and 130 mM in sodium carbonate for UOD; and 0.1 M Tris–hydrochloric acid buffer (pH 8.5) 0.15 M in sodium chloride, 1 (w/v)% in bovine serum albumin and 25 mM in sodium merthiolate for HRP. The immobilized UOD and HRP columns were stable for at least one year; the XOD column was stable for 3 months, but a 10% loss of activity was detected after 4 months.

This study provides the first fluorimetric method for the assay of PNP. The method is highly sensitive and precise, and should be applicable to diagnosis and to biological investigations of PNP deficiency.

## References

1) E. R. Giblett, A. J. Ammann, D. W. Wara, R. Sandman and L. K. Diamond, *Lancet*, **1**, 1010 (1975).
2) J. W. Stoop, B. J. M. Zegers, G. F. M. Hendrickx, L. H. S. Heukelom, G. E. J. Staal, P. K. Bree, S. K. Wadman and R. E. Ballieux, *N. Engl. J. Med.*, **296**, 651 (1977).
3) L. H. S. Heukelom, J. W. N. Akkerman, G. E. J. Staal, C. H. M. M. Bruyn, J. W. Stoop, B. J. M. Zegers, P. K. Bree and S. K. Wadman, *Clin. Chim. Acta*, **74**, 271 (1977).
4) I. H. Fox, C. M. Andres, E. W. Gelfand and D. Biggar, *Science*, **197**, 1084 (1977).

5) G. E. J. Staal, M. J. M. Vlist, R. Geerdink, J. M. J. Veen, B. J. M. Zegers and J. W. Stoop, *Adv. Exp. Med. Biol.*, **122**, 367 (1980).
6) W. R. A. Osborne and C. R. Scott, *Am. J. Hum. Genet.*, **32**, 927 (1980).
7) J. M. Zabay, E. G. Concha, C. Ludena, C. Lozano, D. Salcedo, A. Bootello and P. Gonzalezporque, *Clin. Exp. Immunol.*, **50**, 610 (1982).
8) L. H. S. Heukelom, G. E. J. Staal, J. W. Stoop and B. J. M. Zegers, *Clin. Chim. Acta*, **72**, 117 (1976).
9) H. M. Kalckar, *J. Biol. Chem.*, **167**, 429 (1947).
10) F. Heinz, S. Reckel, R. Pilz and J. R. Kalden, *Enzyme*, **25**, 44 (1980).
11) A. P. Halfpenny and P. R. Brown, *J. Chromatogr.*, **199**, 275 (1980).
12) M. B. Weyden and L. Bailey, *Clin. Chim. Acta*, **82**, 179 (1978).
13) M. P. Uitendaal, C. H. M. M. Bruyn, T. L. Öei, P. Hösli and C. Griscelli, *Anal. Biochem.*, **84**, 147 (1978).
14) Y. Hayashi, K. Zaitsu and Y. Ohkura, *Anal. Sci.*, **1**, 65 (1985).
15) Y. Hayashi, K. Zaitsu and Y. Ohkura, *Anal. Chim. Acta*, **186**, 131 (1986).
16) Y. Hayashi, K. Zaitsu and Y. Ohkura, *Anal. Chim. Acta*, in press.
17) K. Zaitsu and Y. Ohkura, *Anal. Biochem.*, **109**, 109 (1980).
18) H. U. Bergmeyer, K. Gawehn and M. Grassl, "Methods of Enzymatic Analysis," Vol. 1, ed. by H. U. Bergmeyer, Verlag Chemie, Weinheim Academic Press, New York, 1974, p. 490.

[Chem. Pharm. Bull. 35(11)4579—4584(1987)]

# Inhibitory Effect of Bis[2-(*E*-2-alkenoylamino)ethyl] Disulfides and 2-(*E*-Octenoylamino)ethyl Carbamoylmethyl Sulfides on Carrageenin-Induced Paw Edema in Rats

TSUTOMU MIMURA,*[,a] HIROSHI NAKAJIMA,[a] YASUHIRO KOHAMA,[a] KAZUTAKE TSUJIKAWA,[a] SUSUMU ITOH,[a] TAKAO OHMURA,[b] MASAKAZU IWAI[b] and KAZUMASA YOKOYAMA[b]

*Faculty of Pharmaceutical Sciences, Osaka University,[a] Yamadaoka 1–6, Suita, Osaka 565, Japan and Central Research Laboratories, Green Cross Corporation, Ltd.,[b] Chuo-1-chome, Johto-ku, Osaka 536, Japan*

(Received April 6, 1987)

Two series of bis[2-(*E*-2-alkenoylamino)ethyl] disulfides (compds. I) and 2-(*E*-alkenoylamino)ethyl carbamoylmethyl sulfides (compds. II) were synthesized from 2-*trans* unsaturated fatty acids ($C_{6:1}$–$C_{14:1}$) and cystamine, and their effects on carrageenin-induced paw edema were studied. Several of compds. I and II showed significant anti-edema activity at a dose of 25 mg/kg, i.p. These derivatives were much more potent than the starting materials. The alkene chain length influenced the activity. The compounds (compds. I-3, I-8, II-3 and II-8) with $C_{8:1}$ and $C_{13:1}$ fatty acids showed the highest activity in both series. Compounds I-3 and II-3 with the $C_{8:1}$ fatty acid were also effective when administered orally at a dose of 10 mg/kg.

**Keywords**——cystamine; 2-*trans* unsaturated fatty acid; bis[2-(*E*-2-alkenoylamino)ethyl] disulfide; 2-(*E*-alkenoylamino)ethyl carbamoylmethyl sulfide; carrageenin-induced paw edema; anti-inflammatory drug

Previously, we reported that 2-(*E*-2-alkenoylamino)ethyl carbamoylmethyl sulfides (compds. II, Table I) had more potent anti-ulcerogenic activity than the starting materials, various 2-*trans* unsaturated fatty acids and cysteamine.[1] In this work, the anti-inflammatory activity of compds. II and its disulfide analogues (compds. I, Table I) was studied by using the carrageenin-induced paw edema model in rats.

## Experimental

**Materials**——Cystine, cysteine, cystamine dihydrochloride, cysteamine hydrochloride, methionine, methionine sulfone, methionine sulfate, ethionine and lanthionine were obtained from Nakarai Chemicals, Ltd. The following nine unsaturated fatty acids containing one *trans* double bond between the 2nd and 3rd carbons were obtained from Tokyo Kasei Co.: *trans*-2-hexenoic acid ($C_{6:1}$), *trans*-2-heptenoic acid ($C_{7:1}$), *trans*-2-octenoic acid ($C_{8:1}$), *trans*-2-nonenoic acid ($C_{9:1}$), *trans*-2-decenoic acid ($C_{10:1}$), *trans*-2-undecenoic acid ($C_{11:1}$), *trans*-2-dodecenoic acid ($C_{12:1}$), *trans*-2-tridecenoic acid ($C_{13:1}$), *trans*-2-tetradecenoic acid ($C_{14:1}$). The series of compds. I and II listed in Table I were synthesized as described previously.[1]

**Carrageenin-Induced Paw Edema**——Male SD rats (purchased from Japan Keari Co.) weighing 150—170 g were fasted for 24 h prior to experiments but were allowed water *ad libitum*. Carrageenin (Picnin-A, Zushikagaku) was suspended in 0.9% NaCl to make a 1.5% (w/v) suspension. The right hind paws were inoculated with 0.1 ml of the prepared carrageenin suspension while the left hind paws were injected with saline. At the indicated times, the volume of the swelling paws was measured by dipping the paws in mercury. The difference in volume between the carrageenin-inoculated and saline-injected paws was recorded as the amount of edema, and the swelling (percent) was calculated on the basis of the volume of the saline-injected paws. Samples were suspended in 5% acacia and were given intraperitoneally 30 min or orally 1 h before the carrageenin injection. Acacia was used as the control. As a positive control, a non-steroidal anti-inflammatory agent, phenylbutazone (Sigma) was given orally.

TABLE I. Bis[2-(*E*-2-alkenoylamino)ethyl] Disulfides and 2-(*E*-Alkenoylamino)ethyl Carbamoylmethyl Sulfides

(I) Bis[2-(*E*-2-alkenoylamino)ethyl] disulfides

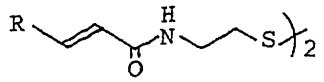

Compd. I-1, R = $C_3H_7$: bis[2-(*E*-2-hexenoylamino)ethyl] disulfide
Compd. I-2, R = $C_4H_9$: bis[2-(*E*-2-heptenoylamino)ethyl] disulfide
Compd. I-3, R = $C_5H_{11}$: bis[2-(*E*-2-octenoylamino)ethyl] disulfide
Compd. I-4, R = $C_6H_{13}$: bis[2-(*E*-2-nonenoylamino)ethyl] disulfide
Compd. I-5, R = $C_7H_{15}$: bis[2-(*E*-2-decenoylamino)ethyl] disulfide
Compd. I-6, R = $C_8H_{17}$: bis[2-(*E*-2-undecenoylamino)ethyl] disulfide
Compd. I-7, R = $C_9H_{19}$: bis[2-(*E*-2-dodecenoylamino)ethyl] disulfide
Compd. I-8, R = $C_{10}H_{21}$: bis[2-(*E*-2-tridecenoylamino)ethyl] disulfide
Compd. I-9, R = $C_{11}H_{23}$: bis[2-(*E*-2-tetradecenoylamino)ethyl] disulfide

(II) 2-(*E*-Alkenoylamino)ethyl carbamoylmethyl sulfides

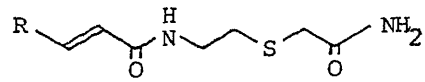

Compd. II-1, R = $C_3H_7$: 2-(*E*-hexenoylamino)ethyl carbamoylmethyl sulfide
Compd. II-2, R = $C_4H_9$: 2-(*E*-heptenoylamino)ethyl carbamoylmethyl sulfide
Compd. II-3, R = $C_5H_{11}$: 2-(*E*-octenoylamino)ethyl carbamoylmethyl sulfide
Compd. II-4, R = $C_6H_{13}$: 2-(*E*-nonenoylamino)ethyl carbamoylmethyl sulfide
Compd. II-5, R = $C_7H_{15}$: 2-(*E*-decenoylamino)ethyl carbamoylmethyl sulfide
Compd. II-6, R = $C_8H_{17}$: 2-(*E*-undecenoylamino)ethyl carbamoylmethyl sulfide
Compd. II-7, R = $C_9H_{19}$: 2-(*E*-dodecenoylamino)ethyl carbamoylmethyl sulfide
Compd. II-8, R = $C_{10}H_{21}$: 2-(*E*-tridecenoylamino)ethyl carbamoylmethyl sulfide
Compd. II-9, R = $C_{11}H_{23}$: 2-(*E*-tetradecenoylamino)ethyl carbamoylmethyl sulfide

Student's *t*-test was employed to assess the significance of differences between the mean values for the control group and the sample-administered groups. To evaluate the comparative activity of test samples in independent experiments, the mean inhibition rate (percent) of each sample from the control in the swelling (percent) values at 3,4 and 5 h (when the swelling (percent) value was highest in most cases) after the carrageenin injection was used.

## Results

### Effect of Intraperitoneally Administered Sulfur-Containing Amino Acids and Amines, and 2-*trans* Unsaturated Fatty Acids

The effect of intraperitoneally administered sulfur-containing amino acids and amines on the carrageenin-induced paw edema in rats is summarized in Table II. As shown in Table II, cystine, cystamine and ethionine given at a dose of 25 mg/kg showed significant inhibition, and the mean inhibition rates were 25.6, 22.2 and 13.1%, respectively. However, cysteine, cysteamine, methionine, methionine sulfone and lanthionine had no inhibitory activity. The effects of 2-*trans* unsaturated fatty acids with various alkene chains on the edema formation are summarized in Table III. 2-*trans* unsaturated fatty acids with carbon numbers of 7, 8, 9, 13 and 14 had significant inhibitory activity at a dose of 25 mg/kg. In particular, $C_{9:1}$ and $C_{13:1}$ showed higher mean inhibition rates of 20.0 and 21.2 respectively.

### Effect of Intraperitoneal Administration

The series of compds. I and II (Table I) were administered intraperitoneally at a dose of 25 mg/kg, and the effect on carrageenin-induced paw edema was examined. As shown in Table IV, compds. I-2, I-3, I-4, I-7, I-8, I-9, II-3, II-4, II-5, II-7, II-8 and II-9 had significant inhibitory activity on the edema formation. As to the structure (carbon number)–activity

TABLE II. Effect of Sulfur-Containing Amino Acids and Amines on Carrageenin-Induced Paw Edema in Rats

| Treatment[a] | Swelling (%)[b] | | | | | | | Mean inhibition rate[c] (%) |
|---|---|---|---|---|---|---|---|---|
| | 1 | 2 | 3 | 4 | 5 | 6 | 7 (h) | |
| Control | 11.6±2.0 | 24.3±2.4 | 41.2±3.6 | 47.9±3.2 | 43.8±2.5 | 40.1±3.1 | 36.4±2.1 | — |
| Cystine | 7.5±1.8 | 20.4±2.7 | 28.6±2.6[e] | 34.1±1.9[e] | 36.2±2.1[d] | 33.6±1.9 | 31.0±2.1 | 25.6 |
| Cysteine | 13.8±1.6 | 27.4±2.4 | 39.3±2.8 | 43.1±2.2 | 38.1±2.6 | 32.5±2.8 | 30.5±2.6 | 9.2 |
| Control | 5.8±1.3 | 41.3±3.9 | 59.0±3.0 | 58.4±3.1 | 58.0±2.5 | 56.4±2.7 | 52.8±2.5 | — |
| Cystamine | 5.2±0.9 | 28.9±2.1[d] | 43.6±3.8 | 46.8±3.5[d] | 46.1±2.5[e] | 45.3±2.0[d] | 45.8±2.8 | 22.2 |
| Cysteamine | 5.3±2.5 | 32.1±3.0 | 50.9±3.0 | 50.5±3.6 | 50.1±3.1 | 51.8±3.2 | 49.6±4.8 | 13.6 |
| Control | 8.8±1.1 | 12.8±0.8 | 33.8±1.3 | 51.7±2.1 | 46.6±1.5 | 48.9±1.8 | 53.0±2.9 | — |
| Methionine | 12.8±1.7 | 9.3±1.7 | 34.3±1.5 | 46.4±1.6 | 48.6±1.6 | 42.4±2.9 | 47.5±1.7 | 1.5 |
| Methionine sulfone | 12.5±2.2 | 13.7±2.1 | 37.4±2.5 | 46.4±1.4 | 50.6±1.7 | 46.9±1.5 | 49.5±2.3 | −3.0 |
| Control | 12.2±1.5 | 26.0±3.2 | 38.3±2.9 | 48.8±2.5 | 49.1±1.7 | 46.8±2.6 | 49.2±2.9 | — |
| Ethionine | 9.3±0.9 | 23.7±1.9 | 35.9±3.1 | 41.4±2.3[d] | 40.3±2.1[d] | 38.5±2.1[d] | 37.3±1.9[e] | 13.1 |
| Lanthionine | 10.1±2.1 | 20.1±1.8 | 44.1±2.1 | 48.2±2.5 | 48.0±2.0 | 47.7±2.2 | 50.5±2.2 | −3.9 |

*a*) Each sample was administered at 25 mg/kg intraperitoneally 30 min prior to carrageenin injection. *b*) All values represent mean±S.E. ($n=8$). *c*) Mean inhibition rate of each sample from the control in the swelling (%) value at 3, 4 and 5 h after carrageenin injection. Significantly different from the control group: *d*) $p<0.05$, *e*) $p<0.01$.

TABLE III. Effect of 2-*trans* Unsaturated Fatty Acids on Carrageenin-Induced Paw Edema in Rats

| Treatment[a] | Swelling (%)[b] | | | | | | | Mean inhibition rate[c] (%) |
|---|---|---|---|---|---|---|---|---|
| | 1 | 2 | 3 | 4 | 5 | 6 | 7 (h) | |
| Control | 7.4±1.8 | 36.0±2.3 | 48.3±1.9 | 49.2±1.4 | 48.0±1.3 | 47.0±1.7 | 45.5±1.4 | — |
| $C_{6:1}$ | 3.3±1.4 | 28.8±2.7 | 41.9±3.1 | 44.9±2.7 | 43.8±2.8 | 41.3±2.7 | 40.4±2.5 | 10.3 |
| $C_{7:1}$ | 5.7±6.0 | 35.7±4.7 | 39.3±2.0[e] | 44.9±1.4[d] | 44.1±1.0[d] | 44.6±1.3 | 43.4±2.2 | 11.8 |
| $C_{8:1}$ | 5.2±0.8 | 29.3±2.1[d] | 40.2±1.7[e] | 43.2±1.4[e] | 41.7±2.3[d] | 44.6±2.0 | 39.1±2.6 | 14.0 |
| Control | 5.8±1.5 | 33.3±2.6 | 47.9±1.9 | 49.3±1.5 | 49.7±1.7 | 48.7±2.1 | 46.0±1.8 | — |
| $C_{9:1}$ | 4.6±0.8 | 20.8±2.6[e] | 34.6±3.4[e] | 40.5±1.9[e] | 42.5±2.0[d] | 47.7±2.5 | 42.6±2.2 | 20.0 |
| $C_{10:1}$ | 3.1±1.8 | 32.5±2.7 | 45.9±1.9 | 46.1±2.5 | 45.6±2.9 | 45.7±3.1 | 48.0±3.0 | 6.3 |
| $C_{11:1}$ | 5.3±3.0 | 28.0±5.3 | 38.2±4.5 | 40.7±3.8 | 44.1±4.1 | 41.5±4.5 | 41.6±5.0 | 16.3 |
| Control | 4.0±1.9 | 32.1±3.5 | 45.2±2.5 | 49.4±2.4 | 49.7±2.5 | 48.7±2.5 | 45.6±2.7 | — |
| $C_{12:1}$ | 9.4±2.1 | 37.5±3.3 | 42.2±2.4 | 43.2±2.4 | 46.1±1.8 | 44.6±2.0 | 43.3±1.6 | 8.8 |
| $C_{13:1}$ | 0.1±1.4 | 24.4±2.2 | 37.2±2.2[d] | 37.6±2.3[e] | 38.8±2.2[e] | 38.8±2.3[d] | 37.1±2.7[d] | 21.2 |
| $C_{14:1}$ | 1.5±1.4 | 26.4±1.9 | 38.2±0.9[d] | 41.4±1.0[e] | 42.2±1.7[d] | 41.3±1.9[d] | 37.9±2.0[d] | 15.6 |

*a*) Each sample was administered at 25 mg/kg intraperitoneally 30 min prior to carrageenin injection. *b*) All values represent mean±S.E. ($n=8$). *c*) Mean inhibition rate of each sample from the control in the swelling (%) value at 3, 4 and 5 h after carrageenin injection. Significantly different from the control group: *d*) $p<0.05$, *e*) $p<0.01$.

relationship judged from the mean inhibition rates, the compounds (compds. I-3, I-8, II-3 and II-8) with carbon numbers of 8 and 13 showed the highest inhibitory activity in both series. The mean inhibition rates were 30—50%, and these compounds were much more potent than the starting materials.

**Effect of Oral Administration**

The effect of orally administered starting materials and compds. I-3, I-8, II-3 and II-8 on the edema formation was examined, and the results are shown in Table V. All of them had

TABLE IV. Effect of Compds. I and II on Carrageenin-Induced Paw Edema in Rats

| Treatment[a] | Swelling (%)[b] | | | | | | | Mean inhibition rate[c] (%) |
|---|---|---|---|---|---|---|---|---|
| | 1 | 2 | 3 | 4 | 5 | 6 | 7 (h) | |
| Control | 8.0±2.0 | 38.9±3.4 | 47.9±2.5 | 50.5±2.2 | 46.4±1.9 | 46.1±1.8 | 44.8±1.9 | — |
| Compd. I-1 | 9.4±1.7 | 38.8±2.9 | 46.1±2.6 | 46.0±3.5 | 45.9±3.0 | 44.6±3.2 | 40.9±2.7 | 4.6 |
| Compd. II-1 | 8.3±0.7 | 42.6±2.3 | 52.4±2.4 | 50.9±2.6 | 51.3±2.4 | 49.4±2.5 | 45.8±2.1 | −6.7 |
| Control | 2.6±1.4 | 28.3±1.5 | 43.1±1.1 | 45.6±0.9 | 48.2±1.2 | 46.9±2.1 | 43.4±1.0 | — |
| Compd. I-2 | 1.0±1.4 | 22.0±2.3[d] | 34.1±2.7[e] | 38.3±1.7[e] | 39.3±1.1[f] | 39.1±1.3[d] | 37.5±1.6[d] | 18.5 |
| Compd. II-2 | −0.7±1.2 | 20.6±3.8 | 40.5±1.3 | 44.4±0.9 | 46.2±0.9 | 45.3±0.9 | 43.0±0.7 | 4.2 |
| Control | 11.6±2.0 | 40.9±2.0 | 53.4±2.0 | 51.6±1.1 | 49.4±0.7 | 47.6±1.2 | 48.3±1.3 | — |
| Compd. I-3 | 13.9±3.3 | 27.5±2.8[e] | 32.1±3.1[f] | 36.3±1.7[f] | 35.7±1.8[f] | 38.4±1.2[f] | 41.8±1.8[e] | 32.4 |
| Compd. II-3 | 7.8±2.8 | 27.5±1.6[f] | 27.5±4.6[f] | 28.3±3.8[f] | 27.2±3.0[f] | 28.3±2.4[f] | 29.0±2.3[f] | 46.2 |
| Compd. I-4 | 6.9±2.1 | 27.4±2.5[f] | 38.4±1.8[f] | 38.5±1.6[f] | 40.1±2.2[e] | 38.8±2.1[e] | 41.0±2.0[e] | 24.1 |
| Compd. II-4 | 9.3±4.4 | 29.4±2.4[e] | 39.9±3.7[e] | 41.1±4.0[d] | 40.9±4.1[d] | 39.8±4.2 | 37.7±3.9[d] | 20.9 |
| Control | 2.6±1.4 | 28.3±1.5 | 43.7±1.1 | 45.6±0.9 | 48.2±1.2 | 46.9±2.1 | 43.4±1.0 | — |
| Compd. I-5 | 3.7±1.4 | 32.5±4.2 | 43.7±3.0 | 43.9±3.0 | 46.8±2.3 | 46.1±1.4 | 46.8±1.3 | 2.2 |
| Compd. II-5 | 2.1±0.7 | 32.5±1.6 | 50.2±1.4[e] | 51.0±1.6[d] | 54.6±1.2[e] | 52.4±1.8 | 51.6±2.0[e] | −13.3 |
| Control | 3.1±1.2 | 30.7±4.3 | 46.5±2.7 | 50.6±2.5 | 51.4±3.1 | 51.7±3.0 | 46.3±3.2 | — |
| Compd. I-6 | 7.9±2.9 | 34.8±4.1 | 44.2±3.6 | 47.1±4.1 | 47.5±3.8 | 46.5±3.0 | 42.7±2.8 | 6.5 |
| Compd. II-6 | 8.5±1.7[d] | 30.2±2.3 | 38.7±3.2 | 43.1±3.1 | 43.2±3.1 | 42.6±3.6 | 37.8±3.3 | 15.9 |
| Compd. I-7 | 6.5±1.5 | 31.5±2.0 | 40.2±1.9 | 40.0±1.5[e] | 42.0±1.9[d] | 42.5±1.3[d] | 40.1±1.6 | 17.6 |
| Compd. II-7 | 3.1±1.2 | 22.7±1.7 | 37.2±2.3[d] | 40.6±1.7[e] | 40.9±2.1[d] | 43.3±2.6 | 37.6±2.7 | 20.1 |
| Control | 4.8±2.5 | 33.5±2.7 | 43.8±2.3 | 48.2±2.3 | 48.0±1.9 | 45.7±2.0 | 44.9±2.2 | — |
| Compd. I-8 | 0.7±2.7 | 22.5±2.4[d] | 32.5±3.0[d] | 33.4±2.8[e] | 35.8±2.7[e] | 36.7±2.5[d] | 35.5±2.6[d] | 27.3 |
| Compd. II-8 | 2.5±2.2 | 13.0±4.0[e] | 19.6±2.6[f] | 24.3±2.8[f] | 26.5±2.4[f] | 28.3±2.7[f] | 27.9±2.6[f] | 49.9 |
| Compd. I-9 | 7.2±1.8 | 36.6±2.5 | 39.5±2.2 | 40.2±2.0 | 42.3±1.5[d] | 44.4±1.3 | 43.3±1.7 | 12.8 |
| Compd. II-9 | 8.3±2.6 | 27.6±4.5 | 34.7±4.1 | 36.5±3.6[d] | 38.5±3.6[d] | 38.7±3.9 | 37.0±3.9 | 21.6 |

*a*) Each sample was administered at 25 mg/kg intraperitoneally 30 min prior to the carrageenin injection. *b*) All values represent mean ± S.E. ($n=8$). *c*) Mean inhibition rate of each sample from the control in the swelling (%) value at 3, 4 and 5 h after carrageenin injection. Significantly different from the control group: *d*) $p<0.05$, *e*) $p<0.01$, *f*) $p<0.001$.

no effect at a dose of 25 mg/kg. Cystamine required a dose of 100 mg/kg to inhibit the edema formation significantly. The fatty acid $C_{8:1}$ had no inhibitory activity even at 100 mg/kg *p.o.*, while $C_{13:1}$ showed significant inhibition at 50 mg/kg *p.o.* Thus, the activities of the starting materials were influenced by the administration route. On the other hand, compds. I-3, I-8, II-3 and II-8 were also effective when administered orally (Table VI). Compounds I-3 and II-3 caused significant inhibition at 10 and 25 mg/kg *p.o.*; their activities were dose-dependent in the range of 5 to 25 mg/kg and were much more potent than those of the starting materials. However, the effects of compds. I-8 and II-8 were not dose-dependent. Phenylbutazone, used as a positive control, greatly inhibited the edema formation at a dose of 200 mg/kg, *p.o.*

## Discussion

We have reported that among various sulfur-containing amino acids, cystine and cystamine (with a disulfide bond) had ulceration-inhibitory activity, but the reduced forms of these compounds, cysteine and cysteamine, were ineffective.[1] Furthermore, S-alkyl analogues of cysteamine were found to be potent ulceration inhibitors.[1] It is known that cystamine shows radioprotective[2] and gastric mucosal defense[3] effects, and that sulfur-containing compounds such as D-penicillamine and SA-96 have anti-rheumatic action.[4] Thus, cys-

TABLE V. Effect of Cystamine, $C_{8:1}$, $C_{13:1}$ and Phenylbutazone on Carrageenin-Induced Paw Edema in Rats

| Treatment[a] | Dose (mg/kg) | Swelling (%)[b] 1 | 2 | 3 | 4 | 5 | 6 | 7 (h) | Mean inhibition rate[c] (%) |
|---|---|---|---|---|---|---|---|---|---|
| Control | — | 23.9±2.5 | 36.0±2.6 | 52.9±1.8 | 57.9±2.0 | 57.3±2.3 | 53.8±2.7 | 47.2±3.2 | — |
| Cystamine | 25 | 22.4±2.8 | 38.8±3.3 | 51.5±3.9 | 56.8±2.5 | 53.2±2.3 | 51.1±2.2 | 48.4±2.0 | 4.2 |
| | 50 | 20.1±1.6 | 30.0±2.3 | 47.2±2.4 | 56.6±1.3 | 53.9±1.3 | 52.0±1.1 | 50.5±1.1 | 6.3 |
| | 100 | 14.4±1.8[e] | 14.0±1.1[f] | 32.2±1.9[f] | 41.1±2.7[f] | 44.7±2.4[e] | 45.6±4.7 | 40.6±3.7 | 30.0 |
| Control | — | 25.6±2.7 | 31.1±2.7 | 40.0±2.8 | 45.0±2.4 | 49.1±1.9 | 47.7±1.9 | 43.9±1.1 | — |
| $C_{8:1}$ | 25 | 23.5±2.5 | 32.9±2.9 | 43.2±2.7 | 43.1±2.6 | 45.5±1.5 | 42.6±1.5 | 40.2±1.4 | 1.2 |
| | 100 | 24.7±1.4 | 23.8±3.0 | 31.6±4.1 | 40.0±4.0 | 44.1±2.7 | 42.1±2.3 | 39.9±2.6 | 14.1 |
| Control | — | 8.7±1.5 | 14.7±2.4 | 35.5±2.4 | 44.3±1.6 | 46.9±1.5 | 45.8±1.5 | 42.6±1.2 | — |
| $C_{13:1}$ | 25 | 5.4±1.3 | 12.6±1.8 | 34.5±2.0 | 42.7±1.9 | 42.9±1.9 | 42.4±2.2 | 41.7±2.5 | 5.0 |
| | 50 | 8.1±1.8 | 9.3±2.0 | 26.2±2.7[d] | 35.6±2.9[d] | 36.7±2.6[e] | 36.9±2.3[e] | 36.0±1.5[e] | 22.5 |
| Control | — | 5.8±1.3 | 41.3±3.9 | 59.0±3.0 | 58.4±3.1 | 58.0±2.5 | 56.4±2.7 | 52.8±2.5 | — |
| Phenyl-butazone | 200 | 5.0±0.7 | 17.2±0.6[f] | 23.8±2.6[f] | 25.2±0.4[f] | 30.3±0.3[f] | 33.7±0.6[f] | 36.0±0.6[f] | 54.8 |

*a*) Each sample was administered orally 1 h prior to the carrageenin injection. *b*) All values represent mean±S.E. ($n=8$). *c*) Mean inhibition rate of each sample from the control in the swelling (%) value at 3, 4 and 5 h after carrageenin injection. Significantly different from the control group: *d*) $p<0.05$, *e*) $p<0.01$, *f*) $p<0.001$.

TABLE VI. Effect of Compds. I-3, II-3, I-8 and II-8 on Carrageenin-Induced Paw Edema in Rats

| Treatment[a] | Dose (mg/kg) | Swelling (%)[b] 1 | 2 | 3 | 4 | 5 | 6 | 7 (h) | Mean inhibition rate[c] (%) |
|---|---|---|---|---|---|---|---|---|---|
| Control | — | 23.9±2.5 | 36.0±2.6 | 52.9±1.8 | 57.9±2.0 | 57.3±2.3 | 53.8±2.7 | 47.2±3.2 | — |
| Compd. | 5 | 24.6±2.3 | 39.8±3.1 | 51.4±2.7 | 53.4±2.4 | 53.1±2.1 | 51.9±1.8 | 49.0±1.4 | 6.0 |
| I-3 | 10 | 22.6±2.5 | 30.8±1.8 | 44.4±1.1[e] | 47.6±1.5[e] | 48.2±2.0[e] | 45.4±1.9[d] | 44.7±1.5 | 16.6 |
| | 25 | 21.3±1.2 | 27.1±1.9[d] | 39.3±2.5[f] | 40.8±1.2[f] | 41.2±1.0[f] | 40.6±1.1[e] | 36.4±1.1[e] | 27.8 |
| Control | — | 13.5±2.4 | 39.1±3.6 | 53.4±2.6 | 58.5±1.9 | 56.8±2.0 | 54.9±2.3 | 52.3±2.4 | — |
| Compd. | 5 | 14.8±2.2 | 37.2±3.8 | 46.5±4.3 | 51.0±4.0 | 50.8±3.5 | 51.0±2.1 | 48.4±1.4 | 12.1 |
| II-3 | 10 | 13.3±1.0 | 31.3±2.9 | 43.4±3.2[e] | 50.1±1.9[e] | 48.9±1.6[e] | 44.8±2.0[e] | 43.4±2.0[d] | 15.7 |
| | 25 | 9.4±0.8 | 24.4±2.3[e] | 35.0±2.1[f] | 39.4±1.7[f] | 41.2±1.7[f] | 40.2±2.0[f] | 39.5±2.3[e] | 31.5 |
| Control | — | 7.8±1.2 | 16.1±1.5 | 33.9±4.9 | 46.4±2.7 | 46.3±2.2 | 44.7±2.3 | 40.3±2.5 | — |
| Compd. | 2.5 | 6.0±0.7 | 12.1±0.9[d] | 29.8±1.4 | 42.7±2.2 | 44.9±1.8 | 44.2±1.8 | 41.8±2.0 | 7.7 |
| I-8 | 5 | 2.2±1.4[e] | 7.9±1.6[e] | 24.9±3.6 | 37.6±3.5 | 37.9±2.9[d] | 37.4±2.6 | 35.9±2.6 | 21.2 |
| | 10 | 0.4±0.5[f] | 7.3±1.1[f] | 26.5±2.2 | 34.5±1.6[e] | 38.3±1.7[d] | 36.5±1.3[e] | 34.5±1.5 | 21.6 |
| | 25 | 3.7±1.3[d] | 9.1±1.6[e] | 21.4±2.8[d] | 32.3±3.0[e] | 36.6±2.9[d] | 37.3±3.1 | 37.4±3.2 | 29.4 |
| Control | — | 6.1±0.8 | 24.5±1.9 | 44.7±2.6 | 48.3±1.1 | 47.8±1.1 | 45.4±1.3 | 42.6±1.4 | — |
| Compd. | 2.5 | 4.9±1.1 | 22.0±2.3 | 39.0±2.9 | 49.5±1.9 | 48.9±2.0 | 46.2±2.5 | 42.6±2.7 | 2.7 |
| II-8 | 5 | 3.5±1.1 | 14.5±1.4[e] | 31.0±2.6[d] | 42.6±2.2[d] | 42.7±2.0[d] | 41.3±2.1 | 38.3±2.4 | 17.7 |
| | 10 | 3.9±1.1 | 14.9±2.4[e] | 31.2±3.2[e] | 41.9±3.0 | 42.7±2.6 | 42.0±2.7 | 40.2±2.9 | 18.1 |
| | 25 | 4.1±1.0 | 18.0±1.3[d] | 36.5±1.9[d] | 42.7±1.5[e] | 41.8±1.5[e] | 41.3±1.3[d] | 37.6±1.9 | 14.2 |

*a*) Each sample was administered orally 1 h prior to the carrageenin injection. *b*) All values represent mean±S.E. ($n=8$). *c*) Mean inhibition rate of each sample from the control in the swelling (%) value at 3, 4 and 5 h after carrageenin injection. Signifincatly different from the control group: *d*) $p<0.05$, *e*) $p<0.01$, *f*) $p<0.001$.

teamine and cystamine derivatives may have anti-inflammatory effects. In a preliminary experiment, we screened sulfur-containing amino acids and amines for anti-inflammatory activity by using the carrageenin-induced paw edema model in rats. It was found that

cystamine and cystine had potent anti-edema activity. We next examined the effect of cystamine derivatives, 2-(*E*-2-alkenoylamino)ethyl disulfides (compds. I), and 2-(*E*-2-alkenoylamino)ethyl carbamoylmethyl sulfides (compds. II), on the carrageenin-induced paw edema in rats. Among compds. I and II, compds. I-3, I-8, II-3 and II-8 had stronger inhibitory effects at 25 mg/kg i.p. than the starting materials. The highest anti-edema activity was found with the compounds having carbon numbers of 8 and 13. Compounds I-3 and II-3 (with a carbon number of 8) showed dose-dependent inhibition, but compds. I-8 and II-8 (with a carbon number of 13) did not.

The anti-edema activities of compds. I-3 and II-3 were also observed after oral administration. The difference of administration route had no effect on the pharmacological activities, which were characteristically different from those of the starting materials. It was clear that the potent anti-edema activities of compds. I-3 and II-3 were due at least partly to the amide bond.

According to Vineger *et al.*[5] and Di Rosa and Willoughby,[6] carrageenin-induced paw edema can be classified into three phases which are mediated by histamine and serotonin (first phase), kinin (second phase) and prostaglandins (PGs, third phase). Since the series of compds. I and II inhibited mainly the second and third phases of carrageenin-induced paw edema, their action mechanism may be related to the metabolism of kinins and PGs. It is well known that most non-steroidal anti-inflammatory agents which act on the metabolism of PGs have the side effect of gastrointestinal damage.[7] This is because PGs cause increased vascular permeability in inflammation[8] while inhibiting gastric juice secretion.[9] From this point of view, compds. I-3 and II-3 may be superior as anti-edema compounds, since compds. I and II inhibit gastric juice secretion.[1]

**Acknowledgement** We are grateful to Ms. Aki Mitani for her technical assistance.

## References

1) M. Iwai, I. Kohda, C. Fudaya, Y. Naito, K. Yokoyama, H. Nakajima, K. Tsujikawa, M. Okabe and T. Mimura, *Chem. Pharm. Bull.*, **35**, 4616 (1987).
2) M. V. Vasin, B. I. Davydov and V. V. Antipov, *Radiobiologiya*, **11(4)**, 517 (1971).
3) P. Van Caneghem and M. L. Beaumariage, *Strahlentherapie*, **145(6)**, 663 (1973); S. Szabo, J. S. Trier and P. W. Frankel, *Science*, **214**, 200.(1981).
4) J. T. Lamont, A. S. Ventola, E. A. Maull and S. Szabo, *Gastroenterology*, **84**, 306 (1983); S. Szabo, *ibid.*, **87**, 228 (1984); H. Fujimura, Y. Hiramatsu, Y. Tamura, M. Yanagihara, A. Koda, H. Nagai, K. Uda, T. Iso and H. Yamauchi, *Nippon Yakurigaku Zasshi*, **76**, 117 (1980).
5) R. Vinegar, W. Schreiber and R. Hugo, *J. Pharmacol. Exp. Ther.*, **166**, 96 (1969).
6) M. Di Rosa and D. A. Willoughby, *J. Pharm. Pharmacol.*, **23**, 297 (1971); M. Di Rosa and L. Sorrentina, *Br. J. Pharmacol.*, **38**, 214 (1970).
7) F. J. Ingelfinger, *N. Engl. J. Med.*, **290**, 1196 (1974).
8) A. W. Ford-Hutchinson, J. R. Walker, E. M. Davidson and M. J. H. Smith, *Prostaglandins*, **16**, 253 (1978).
9) R. Magous, J. P. Bali, J. C. Rossi and J. P. Girard, *Biochem. Biophys. Res. Commun.*, **114**, 253 (1983).

[Chem. Pharm. Bull. 35(11)4585—4591(1987)]

# Inhibitory Effect of Bis[2-(*E*-2-octenoylamino)ethyl] Disulfide and 2-(*E*-Octenoylamino)ethyl Carbamoylmethyl Sulfide on Various Inflammation Models

TSUTOMU MIMURA,*[,a] HIROSHI NAKAJIMA,[a] YASUHIRO KOHAMA,[a] MASARU OKABE,[a] KAZUTAKE TSUJIKAWA,[a] SUSUMU ITOH,[a] TAKAO OHMURA,[b] MASAKAZU IWAI[b] and KAZUMASA YOKOYAMA[b]

*Faculty of Pharmaceutical Sciences, Osaka University,[a] Yamadaoka 1–6, Suita, Osaka 565, Japan and Central Research Laboratories, Green Cross Corporation, Ltd.,[b] Chuo-1-chome, Johto-ku, Osaka 536, Japan*

(Received April 13, 1987)

The anti-inflammatory action of bis[2-(*E*-2-octenoylamino)ethyl] disulfide (compd. I-3) and 2-(*E*-octenoylamino)ethyl carbamoylmethyl sulfide (compd. II-3) was evaluated in various experimental inflammation models. By using the xylene ear method in mice, the bradykinin-induced capillary permeability test in rat skin and the ultraviolet erythema method in guinea pigs, it was demonstrated that compd. I-3 had a significant inhibitory effect on the first phase of inflammation, but compd. II-3 did not. It was also shown that leucocyte emigration into the pouch fluid (the second phase), which accumulated after carboxymethyl cellulose injection in rats, was suppressed by the administration of both compounds. Moreover, granuloma formation (the third phase) generated by the felt pellet or croton oil method in rats was reduced by both compds. I-3 and II-3. Successive administrations of compd. II-3 caused hypertrophy of the spleen and thymus and atrophy of the kidney, but similar administrations of compd. I-3 did not.

**Keywords**——bis[2-(*E*-2-octenoylamino)ethyl] disulfide; 2-(*E*-octenoylamino)ethyl carbamoylmethyl sulfide; xylene ear method; capillary permeability test; ultraviolet erythema method; CMC pouch method; felt pellet induced granuloma; croton oil granuloma pouch; anti-inflammatory activity

In a previous paper,[1] we reported that among the series of bis[2-(*E*-2-alkenoylamino)ethyl] disulfides (compds. I) and 2-(*E*-alkenoylamino)ethyl carbamoylmethyl sulfides (compds. II), bis[2-(*E*-2-octenoylamino)ethyl] disulfide (compd. I-3) and 2-(*E*-octenoylamino)ethyl carbamoylmethyl sulfide (compd. II-3) were potent inhibitors of carrageenin-induced paw edema in rats. In general, the inflammation process is divided into 3 phases. The first phase is inhibited by anti-histamine and anti-serotonin agents, the first and the second phases by non-steroidal anti-inflammatory drugs and all phases by steroidal anti-inflammatory drugs. In this paper, we investigated whether or not compds. I-3 and II-3 would be effective in 6 kinds of experimental models involving the 3 inflammation phases.

## Experimental

**Materials**——Compounds I-3 and II-3 were synthesized as described previously.[2] Phenylbutazone (used as a reference control), prostaglandin $E_2$ (PG $E_2$), compound 48/80 and brilliant cresyl blue were products of Sigma Chemical Co. Pontamine sky blue (PSB), carboxymethyl cellulose (CMC) and sesame oil were obtained from Nakarai Chemical Ltd., histamine dihydrochloride and croton oil from Wako Pure Chemical Ind., Ltd., and serotonin creatinine sulfate and bradykinin from Seikagaku Kogyo Co., Ltd.

**Vascular Permeability Test Using Mouse Ear**——According to the method described by Fujimura *et al.*,[3] male

ddy mice weighing 15—20 g were injected intravenously with 5% PSB (0.1 ml/10 g body weight). Immediately after the injection, the left ear was pinched for 5 s between two felt pads which had been soaked in xylene beforehand. Fifteen minutes later, both ears were removed and placed between two plates (10 × 45 mm), each of which had a hole (6 mm diameter) in its center. The plates were then placed in the cuvette and the optical density value of the bluish color in the left ear was measured at 630 nm (the right ear was used as a blank). The dye concentration was calculated from the calibration curve and expressed as PSB concentration. One hour prior to the stimulation, a test sample to be tested was administered orally to the mouse.

**Capillary Permeability Test Induced by Various Phlogists in Rat Skin**——According to the methods of Thomas and West,[4] and Crunkhorn and Willis,[5] male SD rats weighing 150—180 g were fasted and had their backs shaved 24 h prior to experiments, but were supplied with water *ad libitum*. Histamine, serotonin, bradykinin, PG $E_2$ and compound 48/80 solutions were prepared at 1 mg/ml, 100, 50, 10 μg/ml and 1 mg/ml, respectively. Each phlogist (0.1 ml) and saline (0.1 ml) were administered intradermally at two points in the left and right back, respectively. Immediately, the rats were injected intravenously with 0.5% PSB (1 ml/kg). Forty-five minutes later, the rats were killed and skinned. The capillary permeability was expressed by multiplying the major and minor axes of the blue areas caused by the phlogist. A test sample was administered orally 1 h prior to the injection of each phlogist.

**Ultraviolet Erythema Method**——The procedure employed was basically that of Winder *et al.*[6] Male guinea pigs of Hartley strain weighing 250—350 g were used. Their backs were shaved 24 h prior to experiments by using a depilation mixture. A piece of felt with 3 holes (each 1 cm diameter) was used. The ultraviolet lamp (Wako Denki Rikagaku Co.) was used at a distance of 17 cm and the exposure time was 60 s, as described by Fujimura *et al.*[7] The erythema was evaluated by the method of Higuchi *et al.*[8] An exposed spot which develops no evident erythema scores 0.0, while one with a full circle of definite redness of any intensity scores 3.0. A spot with clear erythema over only a part of the spot scores 2.0, and one with the only slight and partial redness scores 1.0. The erythema was scored at 2 and 5 h after the ultraviolet exposure. The sample was administered intraperitoneally 1 h prior to the ultraviolet exposure.

**Anti-inflammatory Activity Test Using CMC Pouch Method**——According to the method described by Ishikawa and Mori,[9] 5 ml of $N_2$ gas was injected subcutaneously to the backs of male rats weighing 130—150 g one day before the injection of 5 ml of 2% CMC suspension in 0.9% NaCl into the $N_2$ gas sac. For the measurement of leucocyte number and protein content in the CMC fluid, 0.2 ml of the pouch fluid was collected in a tuberculin syringe 2, 4 and 6 h after the CMC injection. Leucocytes from 0.1 ml of the pouch fluid were stained with 0.05% brilliant cresyl blue in saline and were counted with a hemocytometer. The remaining pouch fluid (0.1 ml) was used for the determination of protein concentration using Folin–Lowry's method. A test sample was administered orally 1 h prior to the CMC injection.

**Felt Pellet-Induced Granuloma**——The basic procedure was as reported by Robert and Eezamic,[10] and Nakamura and Shimizu.[11] Eight male rats of SD strain, weighing 150—200 g were used for each group. Felt pellets, weighing 35 ± 1 mg (0.5—0.6 cm in diameter) each, were prepared from a felt pellets 0.6 cm thick and sterilized in an autoclave for 30 min at 120 °C. Two felt pellets were implanted into the subcutaneous space of the scapular region under pentobarbital anesthesia. On the 8th day after implantation, felt pellets, along with the surrounding inflammatory tissue, were removed from the animals. The removed granulomas were dried at 60 °C until they reached constant weight. The net weight increase was determined by subtracting the original weight of the felt pellet.

Adrenal glands, thymus, spleen, kidney and liver were also weighed immediately after the incision and were expressed as the weight per 100 g body weight. Test samples were orally administered at 24-h intervals for 8 d.

**Croton Oil Granuloma Pouch**——The procedure employed was basically that of Selye,[12] Itoga and Miyake.[13] Male rats of the SD strain weighing 150—180 g were used (10 animals per group). A pouch was formed by injecting 20 ml of $N_2$ gas subcutaneously into the back. One milliliter of 1% croton oil dissolved in sesame oil was injected into the pouch. On the 8th day of the injection, the animals were sacrificed and the wet weight of the pouch and the exudate were measured. The adrenal glands, thymus, spleen, kidney and liver were also weighed immediately after extirpation, and expressed as weight per 100 g body weight. Test samples were administered orally at 24-h intervals for 8 d.

**Statistics**——Student's *t*-test was employed to assess the significance of differences between the mean values for the control group and the sample-administered groups.

## Results

### Effect of Compds. I-3 and II-3 on the First Phase of Inflammation

**Vascular Permeability Test Using Mouse Ear**——As shown in Table I, compd. I-3 significantly inhibited the increase of vascular permeability caused by xylene at a dose of 25 mg/kg *p.o.* On the other hand, the same dose of compd. II-3 had no effect. Phenylbutazone, used as a reference control, caused significant inhibition at 150 mg/kg *p.o.*

TABLE I. Effect of Compds. I-3 and II-3 on Vascular Permeability (Xylene Ear Method in Mice)

| Treatment | Dose (mg/kg, *p.o.*) | No. of mice | Vascular permeability[a] PSB (mg/dl) |
|---|---|---|---|
| Control[b] | — | 7 | 3.13±0.16 |
| Compd. I-3 | 25 | 7 | 2.21±0.21[c] |
| Compd. II-3 | 25 | 7 | 2.80±0.24 |
| Phenylbutazone | 150 | 7 | 2.13±0.27[c] |

*a*) All values represent mean±S.E. *b*) 5% acacia in saline. Significantly different from the control group: *c*) $p<0.01$.

TABLE II. Effect of Compds. I-3 and II-3 on Capillary Permeability Induced by Bradykinin and PG $E_2$ in Rat Skin

| Treatment | Dose (mg/kg, *p.o.*) | No. of rats | Bradykinin Colored area[a] ($mm^2$) | PG $E_2$ Colored area[a] ($mm^2$) |
|---|---|---|---|---|
| Control[b] | — | 7 | 110.6± 7.2 | 104.5± 8.9 |
| Compd. I-3 | 25 | 7 | 80.0±10.2[c] | 101.6± 6.6 |
| Compd. II-3 | 25 | 7 | 105.9±12.6 | 106.1±13.3 |
| Phenylbutazone | 200 | 7 | 64.5±10.1[c] | 66.1± 7.0[d] |

*a*) All values (one point per rat) represent mean±S.E. *b*) 5% acacia in saline. Significantly different from the control group: *c*) $p<0.05$, *d*) $p<0.01$.

TABLE III. Effect of Compds. I-3 and II-3 on Ultraviolet-Induced Erythema in Guinea Pigs

| Treatment | Dose (mg/kg, i.p.) | No. of guinea pigs | Ultraviolet-induced erythema[a] | |
|---|---|---|---|---|
| | | | 2 | 5 (h) |
| Control[b] | — | 5 | 6.4±0.7 | 9.0±0.0 |
| Compd. I-3 | 25 | 5 | 2.8±1.0[c] | 7.2±0.7[c] |
| Compd. II-3 | 25 | 5 | 5.1±1.1 | 8.8±0.2 |
| Phenylbutazone | 50 | 5 | 1.5±0.4[e] | 7.0±0.5[d] |

*a*) Erythema was evaluated as follows: 3.0, complete erythema; 2.0, incomplete erythema; 1.0, slight erythema; 0.0, no erythema. All values (total score of 3 erythemas per guinea pigs) represent mean±S.E. *b*) 5% acacia in saline. Significantly different from the control group: *c*) $p<0.05$, *d*) $p<0.01$, *e*) $p<0.001$.

**Capillary Permeability Test with Various Phlogists in Rat Skin**——The effects of compds. I-3 and II-3 on capillary permeability are summarized in Table II. Compound I-3 significantly depressed the increase in capillary permeability induced by bradykinin at a dose of 25 mg/kg *p.o.*, but compd. II-3 did not. Neither affected the increase of permeability induced by PG $E_2$ (Table II), histamine, serotonin or compound 48/80 (data not shown). Phenylbutazone inhibited the increase in the permeability induced by bradykinin and PG $E_2$ at 200 mg/kg *p.o.* The inhibitory effect of phenylbutazone in the case of PG $E_2$ may be explained by the fact that at such a high dose, phenylbutazone has membrane-stabilizing activity.[5,14]

**Ultraviolet Erythema in Guinea Pigs**——The inhibitory effect of compds. I-3 and II-3 on ultraviolet erythema is summarized in Table III. These compounds were administered intraperitoneally, because this inflammation model would not be influenced by the stimulating

action of the administered sample.[15] Compound I-3 caused significant inhibition at a dose of 25 mg/kg i.p. at 2 and 5 h after the ultraviolet exposure, as did phenylbutazone at 50 mg/kg i.p., but compd. II-3 had no effect.

**Effect of Compds. I-3 and II-3 on the Second Phase of Inflammation**

**CMC Granuloma Pouch**——The inhibitory activity of compds. I-3 and II-3 on leucocyte emigration to the pouch fluid is summarized in Table IV. When compared with the control, a significantly lower leucocyte number was observed at 4 h (or 6 h) after the CMC injection in

Table IV. Effect of Compds. I-3 and II-3 on Leucocyte Emigration into Pouch Fluid (CMC Pouch Method)

| Treatment | Dose (mg/kg, *p.o.*) | No. of rats | Count of leucocytes per $mm^3$ of pouch fluid[a] | | |
|---|---|---|---|---|---|
| | | | 2 | 4 | 6 (h) |
| Control[b] | — | 7 | 1.6±0.5 | 12.9±1.9 | 34.8±5.3 |
| Compd. I-3 | 25 | 7 | 1.1±0.3 | 9.0±1.3 | 20.3±2.0[c] |
| Compd. II-3 | 25 | 7 | 1.6±0.2 | 5.7±1.3[d] | 24.2±2.0 |
| Phenylbutazone | 100 | 7 | 0.7±0.3 | 4.1±1.2[d] | 11.6±1.5[c] |

*a*) All values represent mean±S.E. *b*) 5% acacia in saline. Significantly different from the control group: *c*) $p<0.05$, *d*) $p<0.01$, *e*) $p<0.001$.

Table V. Effect of Compds. I-3 and II-3 on Protein Exudation into Pouch Fluid (CMC Pouch Method)

| Treatment | Dose (mg/kg, *p.o.*) | No. of rats | mg of protein per ml of pouch fluid[a] | | |
|---|---|---|---|---|---|
| | | | 2 | 4 | 6 (h) |
| Control[b] | — | 7 | 3.94±0.32 | 6.05±0.37 | 8.51±0.39 |
| Compd. I-3 | 25 | 6 | 3.57±0.20 | 5.73±0.28 | 8.44±0.26 |
| Compd. II-3 | 25 | 7 | 4.20±0.29 | 6.50±0.28 | 9.07±0.15 |
| Phenylbutazone | 100 | 7 | 3.14±0.18[c] | 3.96±0.17[d] | 5.88±0.35[d] |

*a*) All values represent mean±S.E. *b*) 5% acacia in saline. Significantly different from the control group: *c*) $p<0.05$, *d*) $p<0.001$.

Table VI. Effect of Successive Administration of Compds. I-3 and II-3 on Granuloma Formation (Felt Pellet Method in Rats)

| Treatment | Daily dose[a] (mg/kg, *p.o.*) | No. of rats | Granuloma[b] weight (mg) | Final body[b] weight (g) |
|---|---|---|---|---|
| Control[c] | — | 8 | 39.0±1.4 | 218.8±5.5 |
| Compd. I-3 | 10 | 8 | 35.3±1.8 | 217.3±5.5 |
| | 25 | 8 | 31.5±1.1[e] | 213.8±6.0 |
| Phenylbutazone | 200 | 8 | 21.6±2.6[e] | 230.1±8.8 |
| Control[c] | — | 8 | 53.9±2.5 | 204.6±2.6 |
| Compd. II-3 | 10 | 8 | 58.0±5.2 | 209.0±5.8 |
| | 25 | 8 | 43.6±2.5[d] | 198.9±4.1 |

*a*) Each sample was administered at 24-h intervals for 8 d. *b*) All values (2 granulomas per rat) represent mean±S.E. *c*) 5% acacia in saline. Significantly different from the control group: *d*) $p<0.01$, *e*) $p<0.001$.

the compd. I-3 (or II-3)-administered group at a dose of 25 mg/kg *p.o.* On the other hand, neither compound affected vascular permeability measured in terms of the protein concentration in the exudate (Table V). Phenylbutazone significantly inhibited both leucocyte emigration and vascular permeability at a dose of 100 mg/kg *p.o.*

**Effect of Compds. I-3 and II-3 on the Third Phase of Inflammation**

**Felt-Pellet Method**——Orally administered compds. I-3 and II-3 (25 mg/kg) significantly

TABLE VII. Effect of Successive Administration of Compds. I-3 and II-3 on Various Organ Weights (Felt Pellet Method in Rats)

| Treatment | Daily dose[a] (mg/kg, *p.o.*) | No. of rats | Relative organ weight[b] (mg/100 g final body weight) | | | | |
|---|---|---|---|---|---|---|---|
| | | | Adrenal | Thymus | Spleen | Kidney | Liver ($\times 10^3$) |
| Control[c] | — | 8 | 7.8±0.4 | 199.5± 9.3 | 231.0± 8.8 | 359.2± 9.3 | 3.73±0.12 |
| Compd. I-3 | 10 | 8 | 7.0±0.5 | 194.9± 6.4 | 231.4± 2.9 | 358.7± 4.7 | 4.03±0.12 |
| | 25 | 8 | 7.6±0.5 | 190.1±13.0 | 227.0±11.3 | 372.7±11.5 | 3.93±0.13 |
| Phenylbutazone | 200 | 8 | 8.8±0.2[d] | 186.6± 3.9 | 207.1± 7.9 | 372.2± 9.8 | 4.28±0.06[e] |
| Control[c] | — | 8 | 8.3±0.4 | 215.9± 7.5 | 271.4±13.9 | 408.6±11.2 | 4.18±0.06 |
| Compd. II-3 | 10 | 8 | 8.3±0.6 | 241.5±12.7 | 306.6±20.4 | 375.6± 3.6[d] | 4.42±0.06 |
| | 25 | 8 | 8.5±0.3 | 220.7±16.0 | 261.8±15.5 | 391.1± 7.3 | 4.07±0.11 |

*a*) Each sample was administered at 24-h intervals for 8 d. *b*) All values represent mean±S.E. *c*) 5% acacia in saline. Significantly different from the control group: *d*) $p<0.05$, *e*) $p<0.01$.

TABLE VIII. Effects of Successive Administration of Compds. I-3 and II-3 on Granuloma Formation and Exudation (Granuloma Pouch Method in Rats)

| Treatment | Daily dose[a] (mg/kg, *p.o.*) | No. of rats | Granuloma[b] weight (g) | Exudation[b] (ml) | Final body[b] weight (g) |
|---|---|---|---|---|---|
| Control[c] | — | 9 | 5.70±0.37 | 12.0±1.1 | 202.3±5.5 |
| Compd. I-3 | 10 | 9 | 5.35±0.37 | 10.2±1.3 | 204.8±4.3 |
| | 25 | 9 | 4.34±0.22[d] | 8.5±1.7 | 208.2±5.0 |
| Compd. II-3 | 10 | 9 | 5.16±0.19 | 14.2±0.4 | 199.4±6.5 |
| | 25 | 9 | 3.81±0.36[d] | 10.6±0.7 | 210.7±5.5 |
| Phenylbutazone | 200 | 9 | 4.43±0.25[d] | 10.2±1.5 | 207.9±5.1 |

*a*) Each sample was administered at 24-h intervals for 8 d. *b*) All values represent mean±S.E. *c*) 5% acacia in saline. Significantly different from the control group: *d*) $p<0.01$.

TABLE IX. Effect of Successive Administration of Compds. I-3 and II-3 on Various Organ Weights (Granuloma Pouch Method in Rats)

| Treatment | Daily dose[a] (mg/kg, *p.o.*) | No. of rats | Relative organ weight[b] (mg/100 g final body weight) | | | | |
|---|---|---|---|---|---|---|---|
| | | | Adrenal | Thymus | Spleen | Kidney | Liver ($\times 10^3$) |
| Control[c] | — | 9 | 8.8±0.8 | 194.3±10.6 | 375.2±15.6 | 386.4±5.6 | 4.21±0.08 |
| Compd. I-3 | 10 | 9 | 9.3±0.6 | 204.3±11.8 | 343.3± 8.8 | 380.3±9.1 | 4.25±0.10 |
| | 25 | 9 | 10.0±0.5 | 207.7± 8.5 | 351.0±10.1 | 379.8±6.6 | 4.03±0.05 |
| Compd. II-3 | 10 | 9 | 8.2±0.6 | 234.0±10.8[d] | 388.1±21.2 | 366.9±5.6[d] | 4.02±0.07 |
| | 25 | 9 | 9.2±0.7 | 186.5± 8.2 | 339.6±15.4 | 378.7±7.5 | 4.06±0.04 |
| Phenylbutazone | 200 | 9 | 10.0±1.8 | 159.0±12.8[d] | 442.2±38.2 | 387.6±5.6 | 5.43±0.10[e] |

*a*) Each sample was administered at 24-h intervals for 8 d. *b*) All values represent mean±S.E. *c*) 5% acacia in saline. Significantly different from the control group: *d*) $p<0.05$, *e*) $p<0.001$.

inhibited granuloma formation in the felt pellet method as a subacute inflammatory model (Table VI). Phenylbutazone significantly inhibited granuloma formation at a dose of 200 mg/kg. Various organs of rats from each group were weighed and the results are summarized in Table VII. Injection of compd. I-3 had no effect on the organ weight, while compd. II-3 (10 mg/kg) caused kidney atrophy. In the group given phenylbutazone, the weights of the adrenal glands and liver were increased.

**Croton Oil Granuloma Pouch Method**——This test was employed as a subacute inflammatory model which is not responsive to non-steroidal anti-inflammatory drugs. At a daily dose of 25 mg/kg for 8 d, compds. I-3 and II-3 both significantly suppressed granuloma formation in the granuloma pouch method (Table VIII). However, the exudate accumulation was not suppressed significantly by either compound. Phenylbutazone also inhibited granuloma formation. The thymus weight was found to be increased, and kidney weight was decreased by the administration of compd. II-3. The thymus weight was decreased and the liver weight was increased by the administration by phenylbutazone (Table IX).

## Discussion

In general, the inflammatory process can be divided into 3 phases. During the first phase, tissue damage caused by local stimulants and an enhancement of the vascular permeability take place. In the second phase, the emigration of leucocytes is observed. The third phase is characterized by granuloma formation and a regeneration of tissue. Since the inflammatory process involves many factors, the effectiveness of an anti-inflammatory drug should be evaluated by investigating the protective action in various inflammation models.

In this paper, we examined the effects of compds. I-3 and II-3 on 6 kinds of experimental models involving the 3 inflammation phases. Compound I-3 possessed a wide anti-inflammatory spectrum in the inflammation models used in the present study. From the results of the capillary permeability test in rats and the ultraviolet erythema test in guinea pigs, compd. I-3 was considered to suppress the arachidonic acid cascade. The reasons are as follows. 1) Compound I-3 inhibited the reaction caused by bradykinin, but did not compete with PG $E_2$. It was reported that bradykinin stimulates PG synthesis and acts in combination with the PGs generated in the inflammatory process.[16] 2) Non-steroidal anti-inflammatory drugs suppress the ultraviolet erythema *via* their inhibition of cyclooxygenase activity.[17] 3) Compound I-3 had no effect on the direct actions of histamine, serotonin and compound 48/80. Also, it was not a strong inhibitor of the third phase of inflammation and did not cause adrenal atrophy, in contrast to the steroid hormone.

On the other hand, compd. II-3 had a narrower anti-inflammatory spectrum than compd. I-3. This compound was inhibitory in 3 models (CMC pouch, felt pellet and croton oil granuloma pouch methods). However, successive administration had the serious drawbacks of causing spleen and thymus hypertrophy and kidney atrophy. The pathological examination of tissue slices of rats given compd. II-3 revealed abnormal arrangements of spleen and thymus cells, and glomerulonephritis in a few animals (data not shown). However, compd. I-3 did not cause such damage. Compound II-3 might affect the immune system and metabolic functions. The $LD_{50}$ values of compds. I-3 and II-3 were more than 2.5 g/kg, i.p. and 770 mg/kg, i.p. in mice, respectively.

It is possible that compds. I-3 and II-3 are both converted into the corresponding thiol compounds after administration, analogously to SA-96 and penicillamine. SA-96 inhibited arthritis, but not the early phase of inflammation.[18] On the other hand, compds. I-3 and II-3 inhibited the early phase of inflammation, but not arthritis (data not shown). Thus, compd. I-3 is a new compound with a wide anti-inflammatory spectrum and low toxicity.

**Acknowledgement** We are grateful to Ms. Aki Mitani for her technical assistance.

## References


1) T. Mimura, H. Nakajima, Y. Kohama, K. Tsujikawa, S. Itoh, T. Omura, M. Iwai and K. Yokoyama, *Chem. Pharm. Bull.*, **35**, 4579 (1987).
2) M. Iwai, I. Kohda, C. Fukaya, Y. Naito, K. Yokoyama, H. Nakajima, K. Tsujikawa, M. Okabe and T. Mimura, *Chem. Pharm. Bull.*, **35**, 4616 (1987).
3) H. Fujimura, S. Tsurumi and M. Hayashi, *Nippon Yakurigaku Zasshi*, **64**, 379 (1968).
4) G. Thomas and G. B. West, *Br. J. Pharmacol.*, **50**, 231 (1974).
5) P. Crunkhorn and A. L. Willis, *Br. J. Pharmacol.*, **41**, 49 (1971).
6) C. V. Winder, J. Wax, V. Burr, M. Been and C. E. Rosiere, *Arch. Int. Pharmacodyn. Ther.*, **116**, 261 (1958).
7) H. Fujimura, K. Tsurumi, Y. Hiramatsu, K. Go, K. Nakano and T. Shibuya, *Nippon Yakurigaku Zasshi*, **70**, 543 (1974).
8) S. Higuchi, Y. Osada, Y. Shioiri, S. Nakaike, M. Muramatsu, M. Tanaka, I. Arai, F. Amanuma, S. Otomo, H. Aihara and S. Tsurufuji, *Nippon Yakurigaku Zasshi*, **83**, 383 (1984).
9) H. Ishikawa and Y. Mori, *Eur. J. Pharmac.*, **7**, 201 (1969).
10) A. Robert and J. E. Eezamic, *Acta Endocrinol.*, **25**, 105 (1957).
11) H. Nakamura and M. Shimizu, *Eur. J. Pharmac.*, **27**, 198 (1974).
12) H. Selye, *Proc. Soc. Exp. Biol. Med.*, **82**, 328 (1957).
13) E. Itoga and Y. Miyake, *Nippon Yakurigaku Zasshi*, **66**, 316 (1970).
14) A. D. Inglot and E. Wolna, *Biochem. Pharmacol.*, **17**, 269 (1968).
15) H. Mizushima (ed.), "Ensho to Koenshoryoho," Ishiyaku Shuppan Ltd., Tokyo, 1982.
16) K. Ikeda, K. Tanaka and M. Katori, *Prostaglandins*, **10**, 747 (1975); B. B. Vargaftig and N. D. Hai, *J. Pharm. Pharmacol.*, **24**, 159 (1972).
17) A. K. Black, M. W. Greaves, C. N. Hensby and N. A. Plummer, *Br. J. Clin. Pharmacol.*, **4**, 643 (1977); M. W. Greaves and J. Soendergaard, *J. Invest. Dermatol.*, **54**, 365 (1970).
18) H. Fujimura, Y. Hiramatsu, Y. Tamura, M. Yanagihara, A. Koda, H. Nagai, K. Uda, T. Iso and H. Yamauchi, *Nippon Yakurigaku Zasshi*, **76**, 117 (1980).

[Chem. Pharm. Bull. 35(11)4592—4596(1987)]

# Intestinal Absorption of Tocopherol in Beagle Dog and Effect of Dosage Form[1)]

TADAKAZU TOKUMURA,*[,a] YOSHIHARU MACHIDA,[b] YUKI TSUSHIMA,[c] MASANORI KAYANO[d] and TSUNEJI NAGAI[b]

*Tsukuba Research Laboratories, Eisai Co., Ltd.,[a] 1–3 Tokodai 5-chome, Toyosato-machi, Tsukuba-gun, Ibaraki 300–26, Japan, Faculty of Pharmaceutical Sciences, Hoshi University,[b] Ebara 2–4–41, Shinagawa-ku, Tokyo 142, Japan, Products Formulation Research Laboratory, Eisai Co., Ltd.,[c] Minami 2–3–14, Honjo-shi, Saitama 367, Japan and Pharmaceutical Research Laboratories, Eisai Co., Ltd.,[d] 1, Takehaya-machi, Kawashima-cho, Hijima-gun, Gifu 483, Japan*

(Received February 20, 1987)

Intestinal absorption of *d*-α-tocopherol from four model preparations was investigated after oral administration to beagle dogs. The bioavailability of *d*-α-tocopherol from the model preparations was evaluated by determination of the plasma level after oral administration. It was found that the absorption of *d*-α-tocopherol was not affected by food, and that the difference in dosage forms caused a difference in bioavailability. The tablet showed lower availability than capsules filled with oily solution.

**Keywords**——*d*-α-tocopherol; dosage form; oral administration; beagle dog; plasma concentration; bioavailability; HPLC method

A water-insoluble drug is generally considered to be absorbed through the same process as lipids in the gastro-intestinal tract. When a pharmaceutical preparation of a water-insoluble drug is orally administered, most of the drug is absorbed through the following three steps, *i.e.*, dispersion, emulsification by the action of bile, pancreatic juice and peristalsis of the intestinal tract, and formation of mixed micelles.[2)]

On the other hand, it has been reported that different extents of bioavailability were observed on the oral administration of different preparations of a slightly water-soluble drug.[3,4)] In the case of slightly water-soluble drugs, dissolution from the preparations is considered to be the rate-determining step of absorption. If the micelle formation step in the absorption process of a water-insoluble drug corresponds to the dissolution step of a slightly water-soluble drug, the bioavailability of a water-insoluble drug may depend on the preparation employed. However, few bioavailability studies have been done on water-insoluble drug preparations. One reason for this is considered to be that the effect of physiological factors on the absorption of a water-insoluble drug is larger than that on a water-soluble or slightly soluble drug. This presents a problem in animal experiments to detect differences between preparations of water-insoluble drugs. Further, the rat has been the experimental subject in the majority of absorption studies on water-insoluble drugs, and observations in dogs or humans have been scant. However, a pharmaceutical preparation designed for humans cannot be administered directly to rats. Therefore, we examined the bioavailability of a water-insoluble drug, *d*-α-tocopherol, by administering several model preparations to beagle dogs, because a pharmaceutical preparation for humans can be administered directly and the dogs have a gallbladder. In addition, the effect of food, which is a

factor affecting the absorption of water-insoluble drugs, was examined. *d*-α-Tocopherol is well known to be absorbed through mixed micelle formation. In order to examine the differences of bioavailability four different model preparations, having markedly different properties, of *d*-α-tocopherol were prepared and used.

## Experimental

**Materials**——*d*-α-Tocopherol and tocol purified by Eisai Co., Ltd., were used. All other chemicals and solvents used were of analytical reagent grade.

**Absorption Study**——Four male beagle dogs with free access to water were used under fasted and non-fasted conditions. In the former case, the dogs were fasted for 18 h before drug administration and 12 h after drug administration. In the latter, the dogs were fasted from 18 h before drug administration and then given 100 g of Solid Feed DS (Oriental Yeast Co., Ltd., Tokyo, Japan) 1 h before drug administration. After drug administration the dogs were again fasted for 12 h. The concentration of endogenous *d*-α-tocopherol in dog plasma was determined under non-fasted conditions. The intervals between administrations were more than one week. The dose of *d*-α-tocopherol per dog was 300 mg unless otherwise stated. The following four preparations, A, B, C and D, were administered to the dogs with 30 ml of water.

Preparation A is a capsule containing 300 mg of *d*-α-tocopherol dissolved in 600 mg of polyoxyethylene derivative of hydrogenated castor oil (HCO-60) and 600 mg of polyethylene glycol 400 (PEG-400). This preparation forms micelles when added to water, and *d*-α-tocopherol is dissolved in water. Preparation B is a capsule containing 300 mg of *d*-α-tocopherol dissolved in 150 mg of cottonseed oil and 600 mg of decaglycerin monolaurate. This preparation forms an emulsion when added to water and *d*-α-tocopherol is dispersed in the water. Preparation C is a tablet containing 50 mg of *d*-α-tocopherol. This tablet was prepared as follows. *d*-α-Tocopherol was added to the same weight of silicic acid anhydride. After *d*-α-tocopherol was adsorbed, mannitol, polyvinylpyrrolidone K-30 and water were added and the mixture was granulated. The granules were dried for 18 h at 40 °C. Hydroxypropylcellulose and stearic acid were added to the dried granules, and tablets were prepared using a rotary tableting machine (Hata P-13). The weight, hardness and disintegration time in water of these tablets were 254.3 mg, 1.6 kg and 5—6 min, respectively. Preparation D is a capsule containing 300 mg of *d*-α-tocopherol dissolved in 390 mg of cottonseed oil.

At given intervals, a 2-ml blood sample was taken from the cephalic vein. The blood sample was centrifuged for 10 min at 3000 rpm. The plasma layer was removed and frozen at −20 °C until analysis. Then 200 μl of plasma, 1 ml of water and 1 ml of ethanol containing 2 μg of tocol as an internal standard were added to a light-resistant glass-stoppered centrifuge tube. The tubes were shaken for 3 min, then 5 ml of hexane was added, and the tubes were shaken for a further 20 min. After centrifugation for 10 min at 3000 rpm, the hexane phase was collected and evaporated to dryness under nitrogen on a water bath. The residue was dissolved in 200 μl of ethanol, and 20 μl of the solution was injected into a Shimadzu LC-5A high performance liquid chromatography (HPLC) instrument. The chromatograph was operated at a flow rate of 1.8 ml/min and the eluate was monitored spectrofluorometrically by using a fluorescence monitor (Shimadzu RF-530). The excitation wavelength and analyzed wavelength were 294 and 340 nm, respectively. A column of Nucleosil $C_{18}$ (5 μm in 4.5 mm × 25 cm) and methanol as the mobile phase were used for analysis. A standard curve was preparaed by analyzing plasma to which *d*-α-tocopherol had been added at various concentrations ranging from 5 to 50 μg/ml.

## Results and Discussion

### Endogenous *d*-α-Tocopherol

*d*-α-Tocopherol, a natural-type tocopherol, exists in blood and plasma of dogs. In order to determine the increase of plasma *d*-α-tocopherol concentration after oral administration, it was necessary to subtract endogenous *d*-α-tocopherol concentration. Figure 1 shows the time course of plasma concentration of *d*-α-tocopherol in non-fasted animals, when *d*-α-tocopherol was not administered. The concentrations ranged from 10 to 12 μg/ml. It was found that the *d*-α-tocopherol level was approximately constant. From this result, the concentration of endogenous *d*-α-tocopherol was considered to be equal to its plasma concentration just before the administration of *d*-α-tocopherol. The increase of *d*-α-tocopherol after oral administration was calculated by subtracting the concentration of endogenous *d*-α-tocopherol from each determined value.

### Dose of *d*-α-Tocopherol

The absorption mechanism of tocopherol from the gastro-intestinal tract is generally

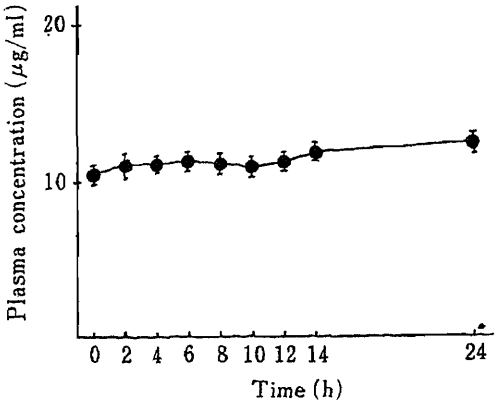


Fig. 1. Plasma Concentration of Endogenous *d*-α-Tocopherol in Non-fasted Dogs

Each point represents the mean±S.E. of 4 dogs.

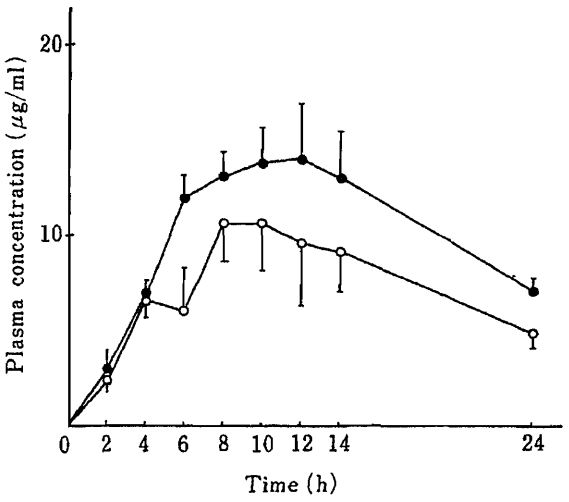


Fig. 2. Effect of Dose of *d*-α-Tocopherol on Plasma Concentration

(●), 300 mg; (○), 200 mg. Each point represents the mean±S.E. of 3 or 4 dogs.

considered to be a simple diffusion.[5,6] However, there were some reports suggesting the existence of specific proteins participating in the transport and uptake of tocopherol.[7,8] Further, it was reported that the efficiency of absorption decreased with increase in the dose of tocopherol in humans,[9] and it was also suggested that there might be a saturable process involved in the absorption.[10] Therefore, the effect of dose on the plasma concentration of *d*-α-tocopherol was examined. Figure 2 shows the plasma concentrations after oral administration of 200 and 300 mg of *d*-α-tocopherol as preparation A to fasted animals. The $AUC_{0-24h}$ and $C_{max}$ of the 200 mg dose were 171.1±39.2 μg·h/ml (mean±S.E.) and 11.7±2.5 μg/ml, respectively. When these values were compared with the values in the case of the 300 mg dose shown in Table II, $AUC_{0-24h}$ and $C_{max}$ were 1/1.4 and 1/1.3, respectively. It was confirmed from this result that the plasma concentration of *d*-α-tocopherol was proportional to the dose on oral administration. Therefore, the difference of plasma concentrations of *d*-α-tocopherol at a given dose is considered to be the result of differences between dosage forms or preparations.

**Absorption in the Non-fasted State**

Figure 3 shows the plasma concentration after oral administration of preparations A—D to non-fasted animals. No significant difference was observed among preparations A—D. The bioavailability parameters, $AUC_{0-24h}$, $C_{max}$ and $T_{max}$, as shown in Table I, were also statistically equal among the four preparations. However, the plasma concentration, $C_{max}$ and $AUC_{0-24h}$ of preparation C were smaller than those of preparations A, B and D. This tendency might be caused by the difference of dosage forms, *i.e.*, preparation C is a tablet and preparations A, B and D are capsules filled with solution.

**Absorption in the Fasted State**

Figure 4 shows the plasma concentrations of *d*-α-tocopherol after oral administration of preparations A—D to fasted animals. The plasma level of preparation C is lower than those of preparations A, B and D, and there was a significant difference between preparations B and C at 8 h. Table II shows the bioavailability parameters of preparations A—D in fasted animals. The $AUC_{0-24h}$ of preparation C was significantly smaller than those of preparations A and B. In the case of $C_{max}$, there was a significant difference between preparations B and C. The values of $T_{max}$ varied among the four preparations, but the reason for this was not clear. This result is similar to that in non-fasted animals. However, the difference among the

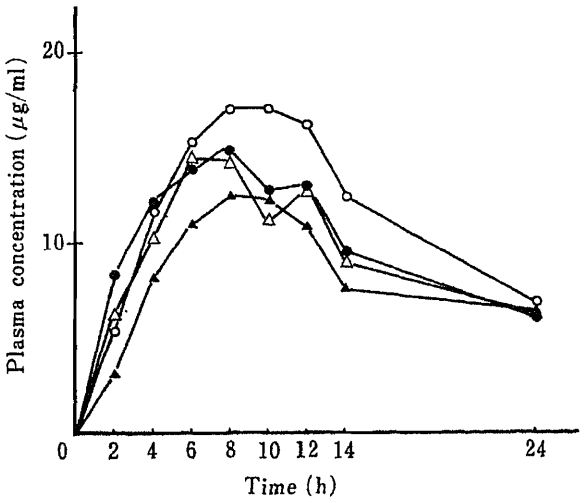


Fig. 3. Plasma Concentration of *d*-α-Tocopherol Following Oral Administration to Non-fasted Dogs

(●), preparation A; (○), preparation B; (▲), preparation C; (△), preparation D. Each point represents the mean of 4 dogs.

TABLE I. Bioavailability Parameters for Oral Administration of *d*-α-Tocopherol to Non-fasted Dogs

| Preparation | $AUC_{0-24h}$ (μg·h/ml) | $C_{max}$ (μg/ml) | $T_{max}$ (h) |
|---|---|---|---|
| A | 237.4±21.7 | 16.2±1.7 | 6.5±1.0 |
| B | 273.2±72.4 | 19.0±4.7 | 8.5±1.5 |
| C | 193.6±54.0 | 13.0±3.4 | 9.0±0.6 |
| D | 217.9±39.1 | 16.4±3.0 | 8.0±1.4 |

Each value represents the mean±S.E. of 4 dogs.

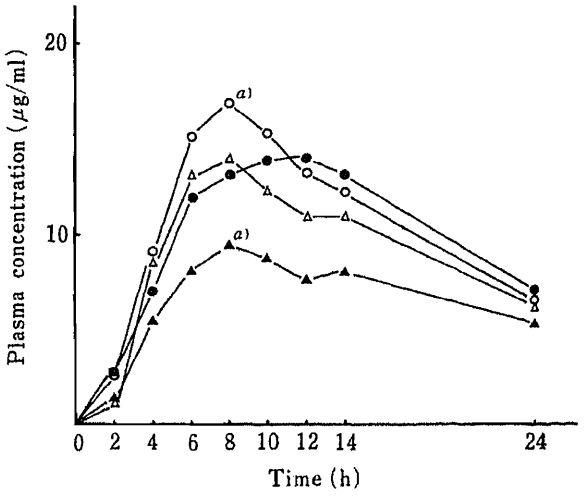


Fig. 4. Plasma Concentration of *d*-α-Tocopherol after Oral Administration to Fasted Dogs

(●), preparation A; (○), preparation B; (▲), preparation C; (△), preparation D. Each point represents the mean of 3 or 4 dogs. *a*) $p<0.02$.

TABLE II. Bioavailability Parameters for Oral Administration of *d*-α-Tocopherol to Fasted Dogs

| Preparation | $AUC_{0-24h}$ (μg·h/ml) | $C_{max}$ (μg/ml) | $T_{max}$ (h) |
|---|---|---|---|
| A | 240.4±36.6[a)] | 15.1±2.5 | 10.0±1.2 |
| B | 250.3±10.9[a)] | 17.5±0.5[b)] | 8.5±1.0 |
| C | 157.7±35.9[a)] | 11.4±0.9[b)] | 11.5±4.2 |
| D | 217.9±47.4 | 14.4±3.1 | 7.3±0.7 |

Each value represents the mean±S.E. of 3—4 dogs. *a*) $p<0.05$. *b*) $p<0.02$.

preparations was clearer in fasted animals than in non-fasted animals. Therefore, fasted animals should be preferable to detect differences in bioavailabilities among the preparations.

**Effect of Food on Absorption**

Figure 5 compares the bioavailability parameters in non-fasted and fasted animals on the basis of the data in Tables I and II. There is no significant difference between the results in non-fasted and fasted animals for each preparation.

Intestinal absorption of tocopherol, as already described, is considered to be similar to the absorption of lipids. Therefore, it was easy to predict the effect of bile secretion on the absorption of *d*-α-tocopherol. However, no effect of food on the absorption of *d*-α-

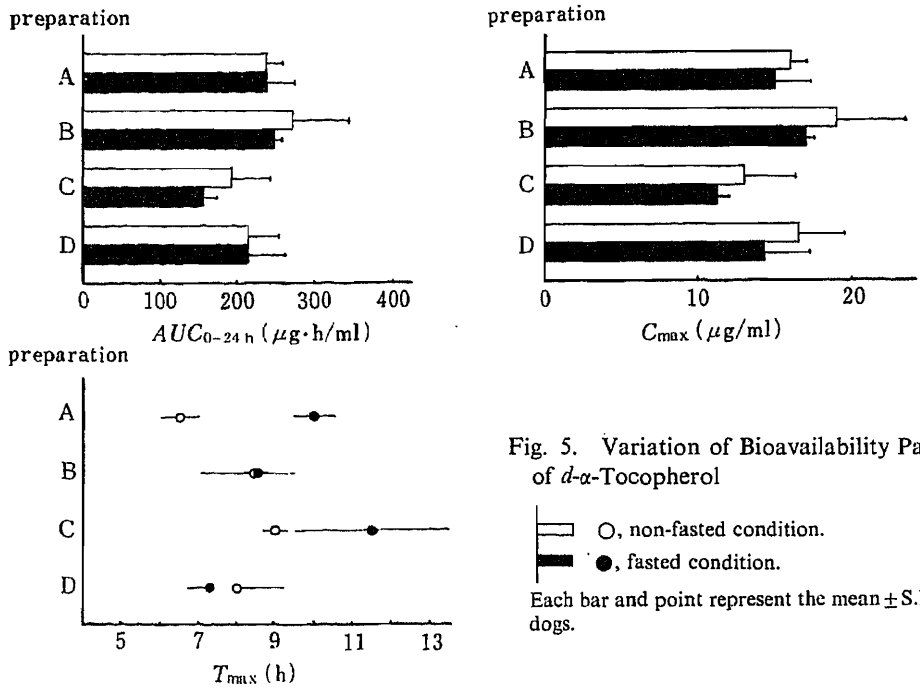


Fig. 5. Variation of Bioavailability Parameters of *d*-α-Tocopherol

○, non-fasted condition.
●, fasted condition.
Each bar and point represent the mean ± S.E. of 3—4 dogs.

tocopherol was observed. it is considered from this result that the amount of bile salts in the intestinal tract of fasted animals is enough, since *d*-α-tocopherol easily forms mixed micelles with bile salts.

Thus, the bioavailability of *d*-α-tocopherol from the four model preparations was evaluated by the determination of the plasma level of *d*-α-tocopherol after oral administration. It was found that the absorption of *d*-α-tocopherol was not affected by food, and that differences of the dosage forms did cause differences of bioavailability. In the case of *d*-α-tocopherol, a solid dosage form such as preparation C was less effective than solution-type dosage forms such as preparations A, B and D.

**Acknowledgement** The authors are very grateful to Miss Azusa Koseki, Mr. Takeshi Igawa, Mr. Kazuhiro Inouye, Mr. Masafumi Teshigawara and Mr. Yosiyuki Harada for their assistance in the experimental work.

## References and Notes

1) This work was presented at the 106th Annual Meeting of the Pharmaceutical Society of Japan, Chiba, April 1986.
2) N. Kanamori, K. Kataoka, S. Nishii, A. Yamaji, H. Kishi, E. Hiraoka, T. Okamoto and T. Kishi, *Yakuzaigaku*, **45**, 119 (1985).
3) T. Tokumura, Y. Tsushima, K. Tatsuishi, M. Kayano, Y. Machida and T. Nagai, *Chem. Pharm. Bull.*, **33**, 2962 (1985).
4) I. Sugimoto, A. Kuchiki, H. Nakagawa, K. Tohgo, S. Kondo, I. Iwane and K. Takahashi, *Drug. Dev. Ind. Pharm.*, **6**, 137 (1980).
5) D. Hollander, E. Rim and K. S. Muralidhara, *Gastroenterology*, **68**, 1492 (1975).
6) M. T. MacMahon and G. R. Thompson, *Eur. J. Clin. Invest.*, **1**, 288 (1971).
7) O. V. Rajaram, P. Fatterpaker and A. Sreenivasan, *Biochem. Biophys. Chem. Commun.*, **52**, 459 (1973).
8) O. V. Rajaram, P. Fatterpaker and A. Sreenivasan, *Biochem. J.*, **140**, 509 (1974).
9) M. S. Losowsky, J. Kelleher and B. E. Walker, *Ann. N. Y. Acad. Sci.*, **203**, 212 (1972).
10) J. Kelleher, T. Davis and C. L. Smith, *Int. J. Vit. Nutr. Res.*, **42**, 394 (1972).

[Chem. Pharm. Bull. 35(11)4597—4604(1987)]

# Effect of Water Extracts of Crude Drugs in Decreasing Blood Ethanol Concentrations in Rats

KIYOSHI SAKAI,*[,a] TOSHIKO YAMANE,[a] YUKIKO SAITOH,[a] CHIE IKAWA[a] and TOSHIAKI NISHIHATA[b]

*Osaka University of Pharmaceutical Sciences,[a] 2-10-65 Kawai, Matsubara, Osaka 580, Japan, and Faculty of Pharmaceutical Sciences, Osaka University,[b] 1-6 Yamadaoka, Suita, Osaka 565, Japan*

(Received February 23, 1987)

Oral administration of ethanol to rats at a dose of 3 g/kg decreased the alcohol dehydrogenase (ADH) activity in liver cytosol. The effects of water extracts of eight crude drugs, which are believed to have protective activities against alcohol toxicity, on the blood ethanol concentration and on the ADH activity in liver cytosol were examined. Water extracts of these crude drugs caused a rapid elimination of ethanol from the blood of normal rats when they were administered orally at 30 min before oral ethanol administration or simultaneously with ethanol. The rapid elimination of ethanol seems to be due to the effect of the water extracts in inhibiting the decrease of ADH activity in rat liver cytosol, and in supplementing nicotinamide adenine dinucleotide (a coenzyme in ethanol metabolism). Among the eight crude drugs, water extracts of only three crude drugs (Mori Albae Fructus, Alpiniae Katsumadai semen and Dolichoris semen) decreased the blood ethanol concentration and inhibited the decrease of ADH activity in liver cytosol when they were administered at 30 min after ethanol. Water extracts of the other crude drugs did not accelerate the ethanol elimination or inhibit the decrease of the ADH activity when administered 30 min after ethanol.

**Keywords**——crude drug; water extract; blood ethanol concentration; lactate; pyruvate; alcohol dehydrogenase; aldehyde dehydrogenase

The incidence of hepatic disorders owing to alcohol consumption has been increasing.[1,2] There have been many reports on the influence of synthetic drugs on ethanol metabolism.[3-5] Some crude drugs have been used as protective drugs against alcohol toxicity. However, the mechanism involved has not been clarified. It has been reported[6] that more than 90% of ethanol is metabolized, predominantly in the liver, by alcohol dehydrogenase (ADH) followed by aldehyde dehydrogenase (ALDH). Thus, it is of interest to investigate the effect of crude drugs on alcohol concentration in the blood and on ADH activity.

In the present study, we examined the effect of water extracts of eight crude drugs on blood ethanol concentration in rats after oral administration of ethanol, and also investigated the effect of these extracts on the activities of ADH and ALDH in the liver of rats. These crude drugs are believed to be protective against alcohol toxicity.[7,8] Since these crude drugs are often administered as decoctions, their water extracts were examined.

## Experimental

**Materials**——Hoveniae semen seu Fructus (Rhamnaceae), Farina Nelumbinis Rhizoma (Nymphaeaceae), Mori Albae Fructus (Moraceae), Alpiniae Katsumadai semen (Zingiberaceae), Dolichoris semen (Leguminosae), Trapae Fructus (Onagraceae), Phaseoli Munginis semen (Leguminosae) and Nelumbinis semen (Nymphaeaceae) were obtained from Tochimototenkaido Co. at the Osaka Market in 1983. They were finely chopped and extracted with boiling water (ten-fold excess by weight). Each solution was evaporated under reduced pressure to obtain the residue. Five extractions were performed from samples of each crude drug, and each of the extracts was tested separately. The

TABLE I. Yields[a] and Doses[b] of Water Extracts of Eight Crude Drugs in Rats

| Crude drugs | Code | Yield (%) | Dose (mg/kg body weight) |
|---|---|---|---|
| Hoveniae semen seu Fructus | A | 24.4±0.7 | 487.8±14.0 |
| Farina Nelumbinis Rhizoma | B | 12.9±0.9 | 420.3±30.8 |
| Mori Albae Fructus | C | 42.9±1.4 | 858.2±29.5 |
| Alpiniae Katsumadai semen | D | 8.1±0.3 | 60.4± 2.2 |
| Dolichoris semen | E | 22.7±1.2 | 417.5±22.9 |
| Trapae Fructus | F | 14.1±1.3 | 93.8± 8.5 |
| Phaseoli Munginis semen | G | 17.2±0.8 | 1289.8±63.2 |
| Nelumbinis semen | H | 22.2±0.8 | 332.4±12.4 |

*a*) Yield was determined as the average of 5 extractions. *b*) Dose was determined on the basis of the yield of water extract from the crude drug and the dose of crude drog used in humans, calculated per kg body weight. Each value represents the mean±S.E. ($n=5$).

yields of water extracts of the eight crude drugs are listed in Table I. The dose given to rats was determined from the dose for humans, by calculating the dose per kg body weight according to references 7 and 8. Other reagents used were of analytical grade.

**Animal Study**——Wistar male rats, weighting 250 to 300 g, were fasted for 24 h prior to experiment, but water was given freely. Rats were anesthetized with urethane (500 mg/kg). Administrations of ethanol and water extracts of crude drugs were performed with a gastric catheter. The extracts were dissolved in 1.0 ml of distilled water, and the solutions were administered 30 min before ethanol, simultaneously with ethanol, or 30 min after ethanol.

After administration of ethanol at a dose of 3.0 g/kg,[9] 0.25 ml of blood was collected from the jugular vein at 0.5, 1, 1.5, 2, 3, 4, 5 and 6 h. Two milliliters of 0.33 N hydroperchloric acid was added to 0.25 ml of blood to assay ethanol concentration in the supernatant after centrifugation.[10]

In another experement, 6 ml of blood was collected at 1 h after ethanol administration. Four milliliters of 1 N hydroperchloric acid was added to 4 ml of blood to assay lactate and pyruvate levels in the supernatant after centrifugation.[11] Two milliliters of blood was centrifuged at $900\times g$ to obtain serum for assay of glutamate oxaloacetate transaminase (GOT) and glutamate pyruvate transaminase (GPT) activities.

Just after the final collection of blood in the above experiments, the whole liver was removed and rinsed gently with 0.25 M sucrose solution at 4 °C. It was sliced, and homogenized with approximately 7 volumes of 0.25 M sucrose solution in a Potter-Elvehjem homogenizer. The homogenate was centrifuged at $600\times g$ for 10 min, followed by further centrifugation of the supernatant at $10000\times g$ for 10 min. The supernatant, obtained by centrifugation at $10000\times g$, was further centrifuged at $105000\times g$ for 60 min to obtain the cytosolic fraction, which was used for measurement of ADH and ALDH activities.

To estimate the absorption of ethanol, the *in situ* rat gastric and jejunal loop method was employed.[12] For this study, the whole stomach and about 10 cm of the jejunum of a rat were ligated at both ends. Briefly, at 30 min after administration of ethanol at a dose of 3 g/kg into the loop, the intestinal loop and gastric loop were removed to measure the remaining amount of ethanol in these loops. Test samples were administered together with ethanol.

**Assays**——Ethanol concentration was determined by using an assay kit (F-kit ethanol®, Boehringer Mannheim Yamanouchi). The limit of determination of ethanol in blood was 2 mM. Serum GOT and GPT were measured by the method of Reitman and Frankel,[13] by using an assay kit (S. TA-Testwako®, Wako Pure Chemical Co., Ltd.). Activities of ADH and ALDH were measured by the method of Lebsack *et al.*[14] Assay of pyruvate level was performed by using an assay kit (Pyruvate Test®, Boehringer Mannheim Yamanouchi) and assay of lactate level was also performed using an assay kit (Lactate Test®, Boehringer Mannheim Yamanouchi), based on the method of Gutmann and Wahlefeld.[15] Assay of protein concentration was performed by the method of Lowry *et al.*[16]

**Statistical Analyses**——Statistical analyses were performed by means of Student's *t*-test.

## Results and Discussion

### Effect of Water Extracts of Crude Drugs on Blood Ethanol Concentrations in Rats after Oral Administration

When each water extract was administered orally 30 min before oral administration of ethanol to rats, significantly lower concentrations of ethanol in the blood were observed in comparison to those after administration of ethanol alone (Fig. 1). The simultaneous

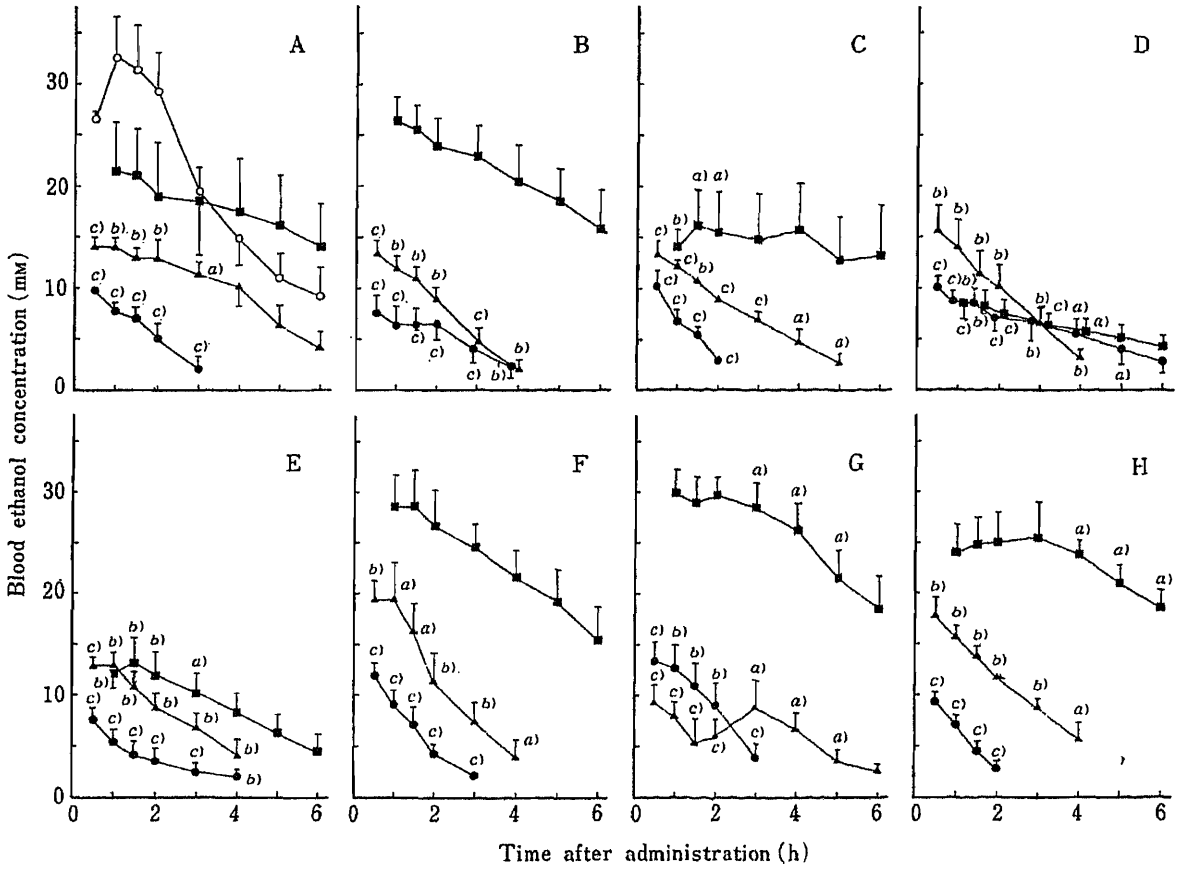


Fig. 1. Effect of Water Extracts of Crude Drugs on Rat Blood Ethanol Concentration after Oral Administration of Ethanol at a Dose of 3 g/kg

Water extracts were administered orally 30 min before ethanol (●), simultaneously (▲), or 30 min after ethanol (■). Open circles represent results after administration of ethanol alone. Water extracts were obtained from the following crude drugs: A, Hoveniae semen seu Fructus; B, Farina Nelumbinis Rhizoma; C, Mori Albae Fructus; D, Alpiniae Katsumadai semen; E, Dolichoris semen; F, Trapae Fructus; G, Phaseoli Munginis semen; H, Nelumbinis semen.

Each value represents the mean ± S.E. ($n=5$). *a*) $p<0.05$ *versus* control (open circles); *b*) $p<0.01$; *c*) $p<0.001$.

administration of each water extract with ethanol also decreased blood ethanol concentrations significantly. There were no significant differences among the effects of the various extracts.

The administration of water extracts of Mori Albae Fructus, Alpiniae Katsumadai semen and Dolichoris semen 30 min after ethanol administration also caused a significant decrease of blood ethanol concentrations (in the case of the water extract of Mori Albae Fructus, only at an early stage) (Figs. 1C, D and E). The water extracts of the other five crude drugs did not cause a dramatic change of blood ethanol concentration. These differences of effectiveness among water extracts may suggest that the effective components are different among the crude drugs.

A decrease of ethanol absorption could account for the effect observed in the cases of prior and simultaneous administrations. Thus, the effect of the water extracts on ethanol absorption was examined by using the *in situ* loop method, in which disappearance of ethanol from gastric and jejunal loops was measured 30 min after administration of ethanol with the extracts. As shown in Table II, the water extracts did not change the disappearance of ethanol from the gastric and intestinal loops, *i.e.*, disappearance (absorption) of ethanol at 30 min

TABLE II. Disappearance of Ethanol from Rat Gastric and Jejunal Loops 30 min after Ethanol Administration (3 g/kg) into the Loops, and Effect of Water Extracts of Crude Drugs Administered Simultaneously with Ethanol

| Code[a] | Amount of ethanol disappeared (%) | |
|---|---|---|
| | From gastric loop | From jejunal loop |
| None (ethanol alone) | 82.4±6.1 | 76.7± 6.2 |
| A | 84.2±9.6 | 82.4± 2.2 |
| B | 79.5±6.9 | 77.2± 4.5 |
| C | 88.3±7.4 | 82.5± 8.1 |
| D | 78.9±7.3 | 79.1± 8.9 |
| E | 83.2±6.2 | 72.9±10.6 |
| F | 71.7±9.0 | 70.4± 5.8 |
| G | 81.9±4.6 | 78.7± 9.7 |
| H | 83.1±4.2 | 73.9±11.5 |

*a*) See Table I. Each value represents the mean±S.E. ($n=3$).

TABLE III. Effect of Administration of Water Extracts of Eight Crude Drugs on the Ratio of Lactate to Pyruvate in Blood in Rats at 1 h after Ethanol Administration

| Code[a] | [Lactate]/[pyruvate] ratio | | |
|---|---|---|---|
| | Time of administration of water extracts[b] | | |
| | Before | Simultaneously | After |
| A | 35.0± 7.0[c] | 22.4± 9.3[c] | 25.6± 1.1[c] |
| B | 19.1± 6.2[c] | 15.1± 0.4[c] | 18.8± 6.9[c] |
| C | 20.1± 3.8[c] | 18.7± 3.3[c] | 21.5± 3.7[c] |
| D | 43.8± 2.8[c] | 34.4± 3.9[c] | 34.6± 1.1[c] |
| E | 25.1± 2.8[c] | 22.3± 1.7[c] | 73.0±24.0 |
| F | 35.5± 3.0[c] | 55.7±19.4 | 48.0±14.6 |
| G | 41.0± 6.6[c] | 22.7± 4.4[c] | 73.3±21.6 |
| H | 30.1±13.5[c] | 23.7± 3.8[c] | 26.7±7.1[c] |
| Without administration of water extracts | | 71.0± 3.2 | |

*a*) See Table I. *b*) Before=30 min before ethanol; simultaneously=simultaneous administration; after=30 min after ethanol. Each value represents the mean±S.E. ($n=5$). *c*) $p<0.05$ *versus* value without administration of any water extract.

after administration into the loop was about 70 to 90% (Table II). It has been reported that more than 90% ethanol in blood is metabolized in the liver.[6] Thus, the decrease of ethanol concentration in blood caused by the administration of the water extracts may be due to an acceleration of ethanol elimination, probably predominantly by an acceleration of ethanol metabolism in the liver.

It has been reported that nicotinamide adenine dinucleotide (NAD) is required as a coenzyme in ethanol metabolism to acetic acid *via* acetaldehyde in the liver, and that the rate-limiting step is often oxidation of reduced nicotinamide adenine dinucleotide (NADH),[17] which is produced from NAD by ethanol metabolism. Oxidation of NADH to NAD is performed by metabolism of lactate to pyruvate in the liver.[18] Therefore, it has been widely accepted that determination of the lactate/pyruvate ratio in blood provides a parameter of the NADH/NAD redox state[19]; *i.e.*, a decrease of the ratio indicates that lactate is metabolized to pyruvate along with production of NAD. Thus, in the present study, the ratio in the blood of rats 1 h after ethanol administration was measured to estimate the ethanol metabolism (Table III).

The administration of each water extract 30 min before ethanol administration caused a significant decrease of the ratio, in comparison with that after administration of ethanol alone. Simultaneous administration of water extracts with ethanol also decreased the ratio, the decrease was not statistically significant in the case of Trapae Fructus.

The ratio was also decreased significantly by the administration of water extracts of crude drugs 30 min after ethanol administration, except for water extracts of Dolichoris semen and Phaseoli Munginis semen. However, these results do not correlate with the changes of blood ethanol concentrations on administration of each water extract 30 min after ethanol; *i.e.*, some extracts decreased the ratio even when ethanol elimination was not accelerated (Fig. 1 and Table III). These results indicate that water extracts of the eight crude drugs seem to supply sufficient NAD as a coenzyme for ethanol metabolism in liver. However, the possibility remains that an effect on the enzyme itself and/or on liver function may be involved.

TABLE IV. Effect of Oral Administration of Water Extracts of Crude Drugs on Serum GOT and GPT Levels in Rats at 1 h after Ethanol Administration (3 g/kg body weight)

| Code[a] | Time of administration of water extract | GOT | GPT |
|---|---|---|---|
| | | KU | |
| None | | 68.6±11.4 | 12.9±3.8 |
| Ethanol alone | | 72.2±12.4 | 13.7±6.5 |
| A | 30 min before ethanol | 76.9±21.4 | 15.8±7.1 |
| | Simultaneously with ethanol | 73.8±12.9 | 14.6±4.8 |
| | 30 min after ethanol | 86.2±24.7 | 10.6±5.2 |
| B | Before | 65.7±17.4 | 10.9±5.6 |
| | Simultaneously | 71.5±24.4 | 14.1±3.7 |
| | After | 82.6±34.2 | 15.9±4.7 |
| C | Before | 76.8±36.2 | 11.0±6.3 |
| | Simultaneously | 62.7±26.1 | 15.7±4.4 |
| | After | 62.9±16.5 | 12.6±2.3 |
| D | Before | 83.9±26.1 | 15.7±3.2 |
| | Simultaneously | 74.8±39.6 | 13.1±1.9 |
| | After | 76.9±26.4 | 17.4±6.8 |
| E | Before | 74.0±16.2 | 14.1±2.0 |
| | Simultaneously | 86.2±31.5 | 16.8±1.9 |
| | After | 68.8±21.4 | 14.1±2.8 |
| F | Before | 64.3±11.5 | 9.6±3.1 |
| | Simultaneously | 73.7±10.9 | 11.6±4.7 |
| | After | 79.1±30.5 | 13.6±1.7 |
| G | Before | 73.9±14.2 | 10.9±2.6 |
| | Simultaneously | 88.0±24.1 | 11.3±5.7 |
| | After | 71.0± 6.9 | 12.5±1.2 |
| H | Before | 60.2±13.8 | 10.7±4.1 |
| | Simultaneously | 69.1±19.6 | 16.1±3.2 |
| | After | 72.1±24.8 | 10.2±2.9 |

*a*) See Table I. Each value represents the mean±S.E. ($n=5$). KU: Karmen units.

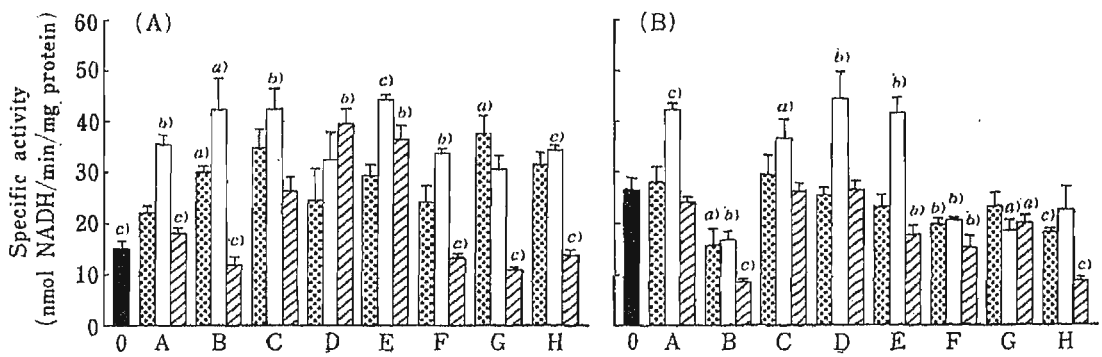


Fig. 2. Effect of Water Extracts of the Crude Drugs on ADH Activity in Rat Liver Cytosol at 1 h (A) and 6 h (B) after Oral Ethanol Administration

An extract was administered orally at 30 min before ethanol ( ▨ ), simultaneously ( □ ), or at 30 min after ethanol ( ▨ ). Ethanol was administered alone as a control ( ■ ). Cytosolic ADH activity (nmol NADH/min/mg-protein) without ethanol was 26.0±2.0 ($n=5$). Water extracts were obtained from the crude drugs indicated by capital letters (see the legend to Fig. 1).

Each value represents the mean±S.E. ($n=5$). *a*) $p<0.05$ *versus* the value without ethanol; *b*) $p<0.01$; *c*) $p<0.001$.

To examine the effect of ethanol and the water extracts on liver function, serum GOT and GPT were measured at 1 h after ethanol administration. As shown in Table IV, administration of ethanol and the water extracts did not change the levels of serum GOT and GPT. Thus, it is considered that serious disorder of liver function was not caused.

**Effect of Water Extracts of Crude Drugs on Activities of ADH and ALDH in Rat Liver after Oral Administration of Ethanol**

In rats after an oral administration of ethanol alone (control), ADH activity in rat liver cytosol was decreased at 1 h in comparison to that before ethanol administration (Fig. 2A), but recovery of the activity was observed at 6 h (Fig. 2B).

It has been reported[6] that more than 90% of the ethanol in blood is metabolized in the liver and that the first step of ethanol metabolism is the conversion of ethanol to acetaldehyde by ADH. Since it is considered that this activity correlates directly to blood ethanol concentration, the effect of oral administration of the water extracts on ADH activity in liver cytosol was investigated at 1 and 6 h after ethanol administration (Fig. 2).

When a water extract was administered 30 min before ethanol or simultaneously with ethanol, the decrease of ADH activity in the cytosol by the ethanol administration was inhibited at 1 h (Fig. 2).

When water extracts were administered 30 min after an ethanol administration, water extracts of Mori Albae Fructus, Alpiniae Katsumadai semen and Dolichoris semen also inhibited the decrease of ADH activity in the cytosol at 1 h, but water extracts of the other five crude drugs did not (Fig. 2A). These results seem to be consistent with the effect on the decrease of blood ethanol concentration at an early stage when the water extracts were administered 30 min after ethanol (Figs. 1 and 2A).

The effect of the water extracts after absorption seems to involve predominantly the ADH activity. However, it is not clear why water extracts of some crude drugs did not inhibit the decrease of ADH activity when they were administered after ethanol. One possibility is that gastrointestinal absorption of effective components in the water extracts is obstructed by the preadministration of ethanol, or alternatively the ADH activity in liver cytosol may be influenced in a different manner by the water extract of each crude drug. Further, it is important to clarify how the water extracts after their absorption inhibit the decrease of ADH activity induced by ethanol. Further studies are planned.

The ADH activity at 6 h after ethanol administration was not significantly different from

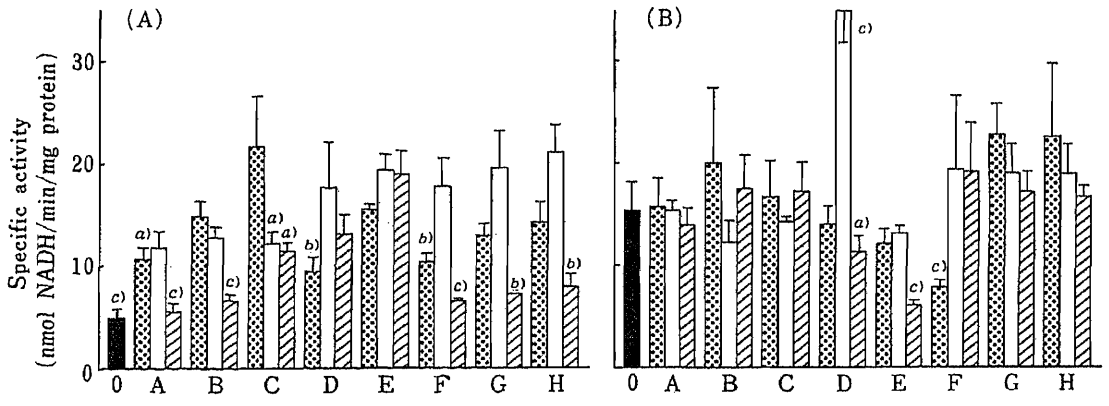


Fig. 3. Effect of Water Extracts of Crude Drugs on ALDH Activity in Rat Liver Cytosol at 1 h (A) and 6 h (B) after Ethanol Administration

ALDH activity (nmol NADH/min/mg-protein) without ethanol was 15.7±2.0 ($n=5$). Capital letters and symbols are defined in the legend to Figs. 1 and 2.

Each value represents the mean±S.E. ($n=5$). *a*) $p<0.05$ *versus* the value without ethanol; *b*) $p<0.01$; *c*) $p<0.001$.

that without ethanol administration, when water extracts were administered (Fig. 2B), except that water extracts of Farina Nelumbinis Rhizoma and Nelumbinis semen given at 30 min after ethanol, decreased the ADH activity at 6 h after ethanol administration. This is consistent with the slow elimination of blood ethanol observed at the later stage after ethanol administration (Figs. 1B and H).

The decrease of ADH activity in rat liver cytosol caused by oral ethanol administration may be a result of a change of liver function, even though there was no change of serum GOT or GPT (Table III). Thus, it is necessary to investigate other functions of the liver such as gluconeogenesis,[20] glycogenolysis[21] and thiol content.[22] We recently found that there was a significant increase of glycogenolysis when 100 mM ethanol was perfused in isolated rat liver (unpublished data).

Acetaldehyde produced from ethanol by ADH is metabolized to acetic acid by ALDH in the liver, and this metabolite is also cytotoxic. Thus, it is of importance to measure the activity of ALDH in liver cytosol to estimate the rate of metabolism of acetaldehyde to acetic acid, because ALDH is located in cytosol as well as mitochondria of the liver.[3] The administration of ethanol alone decreased the activity of ALDH in the cytosol at 1 h, but recovery of ALDH activity was observed at 6 h (Fig. 3), as was also observed for the ADH activity (Fig. 2).

Water extracts, when they were administered 30 min before ethanol or simultaneously with ethanol, inhibited the decrease of the ALDH activity 1 h after ethanol administration (Fig. 3A). However, the water extracts of these crude drugs except for Mori Albae Fructus, Alpiniae Katsumadai semen and Dolichoris semen failed to inhibit the decrease of the ALDH activity at 1 h after ethanol administration when they were administered 30 min after the ethanol (Fig. 3A), as also found with the ADH activity (Fig. 2A). The ALDH activity 6 h after ethanol administration was similar to that without ethanol administration, with only a few exceptions (Fig. 3B).

In conclusion, the blood ethanol concentration after oral administration seems to be dependent on the activity of ADH in liver cytosol, and the protective effect of the water extracts of the eight crude drugs against alcohol toxicity may be due to their effect in accelerating the elimination of ethanol from blood by inhibiting the alcohol-induced decrease of ADH activity and also by providing sufficient NAD as a coenzyme.

## References


1) G. J. Gabuzda, *Am. J. Clin. Nutr.*, **6**, 280 (1958).
2) E. Rubin and C. S. Lieben, *Science*, **162**, 690 (1968).
3) J. J. Hjelle, J. H. Grubbs, D. G. Beer and D. R. Petersen, *J. Pharmacol. Exp. Ther.*, **219**, 821 (1981).
4) T. K. Li and H. Theorell, *Acta Chem. Scand.*, **23**, 892 (1969).
5) R. A. Deitrich, *J. Biol. Chem.*, **247**, 7232 (1972).
6) M. Nakanishi, *Saishin Igaku*, **31**, 2086 (1976).
7) Kososhin-igaku Commission, "Chuyakudaijiten," Shanhaikagakugijutsu Shuppan, Hongkong, 1978, pp. 1511, 1582, 1742, 1803, 1967, 1992, 2271 and 2691.
8) Kobechuigaku Kenkyukai, "Kanyaku No Rinsho-Oyo," Ishiyaku Shuppan, Tokyo, 1979, pp. 125, 127, 209, 249, 355 and 388.
9) Y. Shigeta, H. Ishii, S. Takagi, S. Iraoka and T. Kamiya, *Saishin Igaku*, **31**, 2108 (1976).
10) H. O. Beutler and G. Michal, *Z. Anal. Chem.*, **284**, 113 (1977).
11) R. Czok and W. Lamprecht, "Methods of Enzymatic Analysis," 2nd English ed., Volume 4, ed. by H. U. Bergmeyer, Verlag Chemie Weinheim Academic Press, Inc., New York and London, 1974, p. 1446.
12) T. Nishihata, K. Kamikawa, H. Takahata and A. Kamada, *J. Pharmacobio-Dyn.*, **7**, 143 (1984).
13) S. Reitman and S. Frankel, *Am. J. Clin. Path*, **28**, 56 (1975).
14) M. E. Lebsack, D. R. Petersen and A. C. Collins, *Biochem. Pharmacol.*, **26**, 1151 (1976).
15) I. Gutmann and A. W. Wahlefeld, "Methods of Enzymatic Analysis," 2nd English ed., Volume 3, ed. by H. U. Bergmeyer, Verlag Chemie Weinheim Academic Press, Inc., New York and London, 1974, p. 1464.
16) O. H. Lowry, N. J. Rosebrough, A. L. Farr and R. J. Randall, *J. Biol. Chem.*, **193**, 265 (1951).
17) H. Theorell and B. Chance, *Acta Chem. Scand.*, **5**, 1127 (1951).

18) T. Yuhki, T. Hashimoto, K. Kuruya, T. Ogasahara and T. Takini, "Alcohol Metabolism and Liver," Vol. 2, Ishiyaku Press, Tokyo, 1982, p. 56.
19) H. Hasumura, R. Teschke and C. S. Lieber, *Protein, Metabolism and Enzyme*, **21**, 711 (1976).
20) T. Nishihata, M. Sudoh, M. Yamazaki and A. Kamada, *Chem. Pharm. Bull.*, **34**, 5086 (1986).
21) P. F. Blackmore, F. T. Brumely, J. C. Murk and J. H. Exton, *J. Biol. Chem.*, **253**, 4851 (1978).
22) D. P. Jones, H. Thor, M. T. Smith, S. A. Jwell and S. Orrenius, *J. Biol. Chem.*, **258**, 6390 (1983).

[Chem. Pharm. Bull. 35(11)4605—4608(1987)]

# Effect of 1-Alkyl- or 1-Alkenylazacycloalkanone Derivatives on Penetration of Mitomycin C through Rat Skin

HIROKAZU OKAMOTO, HIROKO TSUKAHARA, MITSURU HASHIDA and HITOSHI SEZAKI*

*Faculty of Pharmaceutical Sciences, Kyoto University, Yoshida Shimoadachi-cho, Sakyo-ku, Kyoto 606, Japan*

(Received March 16, 1987)

The effects of five new compounds containing an azacyclo ring and a terpene or an alkyl chain, *i.e.*, 1-geranylazacyclohexan-2-one (6GU), 1-(3,7-dimethyloctyl)azacycloheptan-2-one (7GS), 1-(3,7,11-trimethyldodecyl)azacycloheptan-2-one (7FS), 1-geranylgeranylazacycloheptan-2-one (7GGU), and 1-geranylgeranylazacyclohexan-2-one (6GGU), on percutaneous penetration of mitomycin C (MMC) through rat skin *in vitro* were investigated in comparison with those of 1-farnesylazacycloheptan-2-one (7FU) and 1-dodecylazacycloheptan-2-one (Azone). In an *in vitro* diffusion experiment, 6GU, 7GS, 7FU, 7FS, 7GGU, 6GGU, and Azone significantly enhanced MMC penetration through rat skin compared with the control. The size of the azacyclo ring had little effect on the potency of these penetration enhancers. On the other hand, the changes in the length of the hydrophobic chain resulted in some variation in the activity of these compounds. Azone and 7FU, which have a hydrophobic chain of length of twelve carbons, were the most effective among enhancers with an azacycloheptanone ring, and 7GGU, with the longest hydrophobic chain, showed the weakest MMC penetration-enhancing activity. Among the compounds with an azacyclohexanone ring, 6GGU (with a longer hydrophobic chain) was more effective than 6GU (with a shorter hydrophobic chain). Saturation of the double bonds of the farnesyl group of 7FU decreased the enhancing ability.

**Keywords**——percutaneous absorption; percutaneous penetration enhancer; 1-dodecylazacycloheptan-2-one (Azone); 1-alkenylazacycloalkanone derivative; mitomycin C; terpene

The topical application of antitumor agents for the treatment of diseases such as cutaneous cancer and psoriasis has many advantages; in particular, the systemic toxicity of the drug may be reduced. However, one of the problems in topical application of antitumor agents is the poor skin penetration of such compounds, *e.g.* mitomycin C (MMC).

One approach to improve the low skin penetrability of a drug is the use of a penetration enhancer to reduce the barrier function of the skin. Some compounds such as 2-pyrrolidone and decyl methyl sulfoxide have been reported as potential percutaneous penetration enhancers, and recently 1-dodecylazacycloheptan-2-one (Azone) has received considerable attention as a percutaneous absorption enhancer for a wide range of drugs.[1-3] Both the long alkyl chain moiety and the mild polar ring moiety of Azone seem to be necessary for its action as a penetration promoter.

In the previous report, four types of percutaneous absorption enhancers with azacyclo ring moieties and terpene chains were designed. Some of these substances improved the percutaneous penetration of MMC through the skin of hairless mouse and rat, and were almost equipotent to Azone in this regard.[4] In the present study, five new compounds with different structural characteristics were designed and their effects on the percutaneous penetration of MMC through the rat skin were investigated.

## Experimental

**Materials**——Mitomycin C (MMC) was obtained from Kyowa Hakko Kogyo Co., Japan. 1-Dodecylazacycloheptan-2-one (Azone) was kindly supplied by Nelson Research Center, U.S.A. 1-Geranylazacyclohexan-2-one (6GU), 1-(3,7-dimethyloctyl)azacycloheptan-2-one (7GS), 1-farnesylazacycloheptan-2-one (7FU), 1-(3,7,11-trimethyldodecyl)azacycloheptan-2-one (7FS), 1-geranylgeranylazacycloheptan-2-one (7GGU), 1-geranylgeranylazacyclohexan-2-one (6GGU) were synthesized by Kuraray Co., Japan. All other reagents used were of analytical grade.

**Percutaneous Penetration Experiments**——Transdermal delivery rates of MMC were determined in the same manner as described in the previous report.[4] The full thickness dorsal skin of male Wistar rats (230—250 g) was obtained after the removal of the hair with electric clippers, followed by the careful removal of adipose tissue. The freshly excised skin was mounted in a sink-type diffusion cell with an available diffusion area of 8.04 $cm^2$ as described by Loftsson and Bodor.[5] The receptor compartment of each cell was filled with 48 ml of saline containing 100 ppm of kanamycin sulfate. Test formulations were prepared by suspending MMC in ethanol with or without the compounds listed in Fig. 1. These compounds were contained at concentration of 3.3 v/v%. One milliliter of MMC suspension was applied to each donor compartment. In all the experiments, the donor cell was sealed with a silicone stopper to prevent evaporation of the test sample. The diffusion cell was placed in a thermostated chamber maintained at 37 °C and the receptor medium was stirred with a magnetic stirrer. At appropriate intervals, 1 ml of the receptor medium was withdrawn and replaced with an equal volume of fresh medium. Diffusion experiments were carried out for 30 h. At the end of each experiment, the drug in the donor phase was recovered with ethanol (25 ml).

The concentration of MMC appearing in the receptor medium was measured by high-pressure liquid chromatography (HPLC) as described by Sasaki *et al.*[6] MMC recovered from the donor phase with ethanol was measured by spectrophotometric analysis at 360 nm after centrifugation and adequate dilution.

## Results and Discussion

The structures of enhancers examined in this investigation are shown in Fig. 1. Saturation of the side chain of 7FU yields the structure of 7FS, which can be considered as Azone methylated at three positions in its alkyl chain. Similarly, saturation of the side chain of 1-geranylazacycloheptan-2-one (7GU) (reported in previous paper) gives 7GS. All these

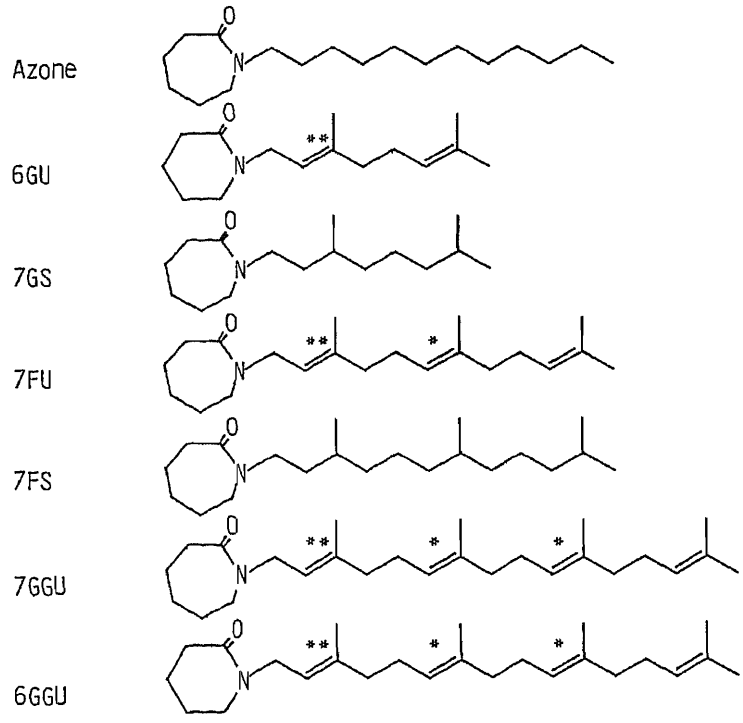


Fig. 1. The Structures of Azone and the Newly Developed Compounds

*, *trans*: *cis* = 10: 0; **, *trans*: *cis* = 7: 3.

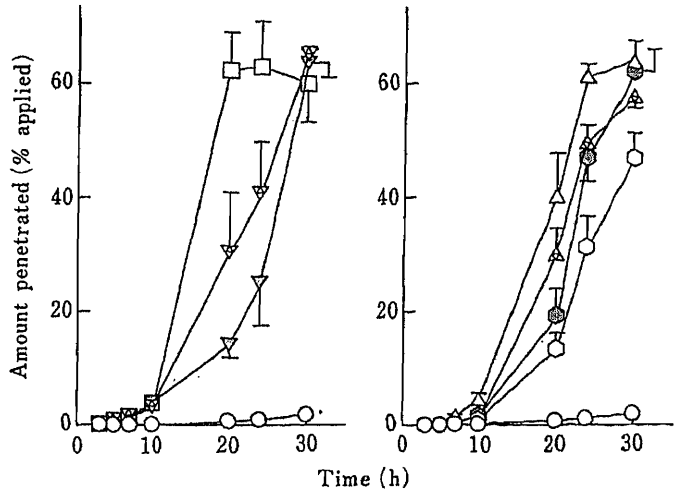


Fig. 2. The Penetration of MMC through Rat Skin at 37 °C

One milliliter of MMC suspension (total concentration, 10 mM) in ethanol with or without (control (○, $n=6$)) a test compound listed in Fig. 1 was applied. Azone (□, $n=3$), 6GU (▽, $n=4$), 7GS (▼, $n=7$), 7FU (△, $n=5$), 7FS (▲, $n=5$), 7GGU (⬡, $n=7$), and 6GGU (⬢, $n=4$) were used at the concentration of 3.3 v/v%. Each point represents the mean value and vertical bars indicate standard errors of the mean. The absence of a vertical bar means that the standard error is smaller than the size of the symbol.

compounds are oils at room temperature.

Figure 2 shows the permeation profiles of MMC through rat skin when applied with or without the compounds listed in Fig. 1. The decrease in the amount of MMC in the receptor at 30 h in the system with Azone indicates that MMC may decompose in the receptor phase. The pH–rate profile for the decomposition of MMC was reported to show a minimum degradation rate at pH 7.5—8.0.[7] We did not, however, follow the pH of the receptor saline during our experiment. A peak with shorter retention time than that of MMC was observed on a chromatogram. This peak was much smaller than that of MMC. The absorption spectra (240—420 nm) of the donor and receptor solutions were each recorded at the end of every experiment. A clear peak of MMC was recognized at 360 nm and in some cases a small peak or shoulder was observed at 280 nm. The decomposition of MMC in this study, if any, seems to be minor and should not result in misinterpretation of the penetration-enhancing activity.

6GU, 7GS, 7FU, 7FS, 7GGU, and 6GGU as well as Azone markedly enhanced MMC penetration through rat skin ($p<0.001$ in all comparisons at 30 h). At 30 h after beginning the penetration experiment, Azone produced no significant difference in amount of MMC in the receptor compartment as compared with 6GU, 7GS, 7FU, 7FS, 7GGU, and 6GGU. Azone, however, enhanced the penetration of MMC when compared with 6GU and 7GGU at 24 h and compared with 6GU, 7FS, 7GGU, and 6GGU at 20 h (at least $p<0.05$ in all comparisons). 7GGU (with a geranylgeranyl chain) was less effective than Azone, 6GU, 7GS, 7FU, or 7FS.

The amount of MMC remaining in the donor phase at the end of the experiment (control value, 68.35%) was significantly decreased by these compounds ($p<0.001$ in all comparisons). Azone decreased this amount (0.93%) significantly more than 7FS (4.07%), 7GGU (12.84%), or 6GGU (6.15%). 6GU (4.77%), 7GS (1.75%), and 7FU (1.21%) were not significantly different from Azone in this regard.

To examine the structure–activity relationship of these penetration enhancers, sets of two compounds were compared for ability to promote MMC penetration by means of the paired $t$-test. Data on 7GU, 7FU, 1-geranylazacyclopentan-2,5-dione (5GUDO), and 1-farnesylazacyclopentan-2-one (5FU) are cited from previous reports[4,8] (represented by asterisks

in the discussion below). The amounts of MMC in the receptor medium at 20, 24, and 30 h and that remaining in the donor phase at 30 h were compared (the criterion of statistical significance was set at $p<0.05$). The consistency of the two series of experiments was warranted by the facts that no significant difference was observed in the results of comparisons of the control experiments, the effects of Azone and the effects of 7FU.

The size of the azacyclo ring had little effect on the potency of these penetration enhancers (7GU* = 6GU, 7FU* = 5FU*, 7GGU = 6GGU). But the polar group of the ring moiety had an important effect (7GU* > 5GUDO* at 20 and 30 h, 6GU > 5GUDO* at 30 h), as reported previously.

The length of hydrophobic chain caused greater apparent variation in the activity of these compounds as penetration enhancers. Comparisons of the enhancers with an azacycloheptane ring showed that the closer to twelve carbons the length of the hydrophobic chain was (Azone and 7FU), the more effective the penetration enhancer was, and the compound with the longest hydrophobic chain (7GGU) showed the weakest MMC penetration-enhancing activity (7GU* > 7GGU at 30 h, 7FU > 7GGU at 20, 24, and 30 h, 7GS > 7FS at 30 h). In the compounds with an azacyclohexanone ring, on the other hand, the compound with a longer hydrophobic chain (6GGU) was more effective than that with a shorter hydrophobic chain (6GU) at 24 h.

In the alkyl methyl derivatives of sulfoxides, the optimum chain length was reported to be ten carbons.[1] The balance of hydrophilicity and hydrophobicity in a molecule may have a major effect on the activity as a penetration enhancer. A different polar group may require a different hydrophobic group for maximum penetration enhancing activity.

6GU with a geranyl chain showed a longer lag time, as did 7GU* and 5GUDO* in a previous report, than the others. The enhancers with a geranyl chain seems to need a longer period to attain the steady state of penetration of MMC.

The effect of saturation of the hydrophobic chain was also examined. Saturation of the double bonds of the farnesyl group decreased the activity (7FU > 7FS at 30 h), whereas saturation of the double bonds of the geranyl group had no significant effect (7GU* = 7GS).

Through our two series of experiments, several 1-alkyl- or 1-alkenylazacycloalkanone derivatives were proved to be potent penetration enhancers for MMC. Further investigation is in progress in our laboratory to elucidate the mechanisms of action of these compounds.

**References and Notes**

1) J. Hadgraft, *Pharm. Int.*, **5**, 252 (1984).
2) R. B. Stoughton, *Arch. Dermatol.*, **118**, 474 (1982).
3) R. B. Stoughton, *Drug Dev. Ind. Pharm.*, **9**, 725 (1983).
4) H. Okamoto, M. Ohyabu, M. Hashida and H. Sezaki, *J. Pharm. Pharmacol.*, **39**, 531 (1987).
5) T. Loftsson and N. Bodor, *J. Pharm. Sci.*, **70**, 756 (1981).
6) H. Sasaki, E. Mukai, M. Hashida, T. Kimura and H. Sezaki, *Int. J. Pharmaceut.*, **15**, 49 (1983).
7) H. Sasaki, E. Mukai, M. Hashida, T. Kimura and H. Sezaki, *Int. J. Pharmaceut.*, **15**, 61 (1983).
8) 7GU, 7FU, 5GUDO, and 5FU were abbreviated as GAH, FAH, GAPD, and FAP, respectively, in previous reports.

[Chem. Pharm. Bull. 35(11)4609—4615(1987)]

# New Methods for Preparing Cyclodextrin Inclusion Compounds. I. Heating in a Sealed Container

YOSHINOBU NAKAI,* KEIJI YAMAMOTO, KATSUHIDE TERADA, and DAIICHI WATANABE

*Faculty of Pharmaceutical Sciences, Chiba University, 1-33, Yayoicho, Chiba 260, Japan*

(Received May 6, 1987)

A new method for preparing a solid inclusion compound was developed. A physical mixture of benzoic acid and α- or β-cyclodextrin (CD) or the ground mixture was sealed in a container after adsorbing a definite amount of water vapor, then heated to a temperature ranging from 43 to 142 °C. The results of powder X-ray diffraction and infrared spectroscopy showed that the crystalline inclusion compound was produced when the container was heated at over 70 °C. The combining molar ratio of benzoic acid to α-CD in the inclusion compound prepared by this method was higher than that obtained by the coprecipitation method. Physical mixtures of benzoic acid and α- or β-CD were also sealed in a stainless steel vessel under nitrogen gas pressure, then heated to 127 °C. The pressurized samples had a higher combination ratio than the non-pressurized samples.

**Keywords**——cyclodextrin; inclusion complex formation; heating; X-ray diffraction; combining ratio; infrared spectrum

It is well known that cyclodextrins (CDs) form inclusion compounds with many kinds of drugs and improve the physical and chemical properties of the drugs.[1] Solid inclusion compounds have been prepared by coprecipitation,[2] kneading,[3] freeze-drying,[2] and co-grinding.[4] In the present study, we attempted to obtain inclusion compounds by heating mixtures of α- or β-cyclodextrin and a drug. As inclusion compounds were obtained by this method, the physicochemical properties were compared with those of inclusion compounds by the coprecipitation method in terms of powder X-ray diffraction and infrared (IR) spectroscopy.

## Experimental

**Materials**——α-CD and β-CD were purchased from Nakarai Chemicals Ltd. and Andou Kasei Co., respectively. The CD hydrates were obtained by recrystallization from distilled water. The dried α- and β-CDs were prepared by heating the CD hydrates at 110 °C for 3 h *in vacuo* for grinding. Benzoic acid was of JPX grade.

**Preparation of Physical Mixture and Ground Mixture**——The physical mixture was prepared by simple blending of benzoic acid and α- or β-CD with a mortar and pestle. The molar mixing ratio of benzoic acid to CD was 1 : 1 or 1 : 2. A ground mixture was obtained by grinding the physical mixture for 5 min using a vibrational mill as described previously.[5] The ground mixtures were stored in an atmosphere of 48.3% relative humidity at 40 °C, and allowed to adsorb water vapor until adsorption equilibrium was attained.[6] A Hiranuma AQ-3C aquacounter was used to determine the water content.

**Heating in a Sealed Container**——Two methods were used. In one, about 1 g of the mixture was sealed in a glass ampule (the volume was 2.25 ml), which was heated at a definite temperature (43—142 °C). In the other, about 1 g of the physical mixture of benzoic acid with α- or β-CD hydrate was sealed in a stainless steel vessel (the volume was 27.5 ml), which was heated at 127 °C for 10—90 min with or without pressurization by $N_2$ gas. The $N_2$ gas pressure was measured with a pressure gauge (Nagano, SUS 316). The amount of benzoic acid combining with CD was determined spectrophotometrically after washing the contents of the vessel with ethyl ether to remove the excess benzoic acid.

**Preparation of Inclusion Compounds by the Coprecipitation Method**——An aqueous solution containing benzoic acid and α-CD hydrate or benzoic acid and β-CD hydrate was agitated vigorously for 5 h at 60 °C. The solution was filtered and the filtrate was allowed to stand for 2 d at room temperature to allow the crystallization of the inclusion compound. After filtration, the coprecipitate was dried for 24 h at room temperature and washed with ethyl ether, then dried again for 24 h at room temperature. The amount of benzoic acid in the inclusion compounds was determined spectrophotometrically.

**Powder X-Ray Diffraction Measurement**——A Rigaku Denki 2027 diffractometer was used. The measurement conditions were the same as those reported in the previous paper.[5]

**Thermal Analysis**——A Shimadzu DT-20B unit was used for thermogravimetry (TG). The heating rate was 1 K/min. A Perkin-Elmer DSC-1B was used for differential scanning calorimetry (DSC) at a scanning speed of 4 K/min using a liquid cell.

**IR Absorption Spectroscopy**——A Hitachi 295 infrared spectrophotometer was used. The measurements were made by the nujol method.

## Results and Discussion

### Effects of Heating on the Crystal Properties of α- and β-CD

The α-CD hydrate contained 6 water molecules as water of crystallization (9.99% water content).[7] The amorphous α-CD hydrate (10.2% water content) was prepared by grinding of dried α-CD and water vapor adsorption. Figure 1 shows the X-ray diffraction patterns of various α- and β-CDs. Two kinds of amorphous α-CDs, namely dried and $H_2O$-adsorbed,

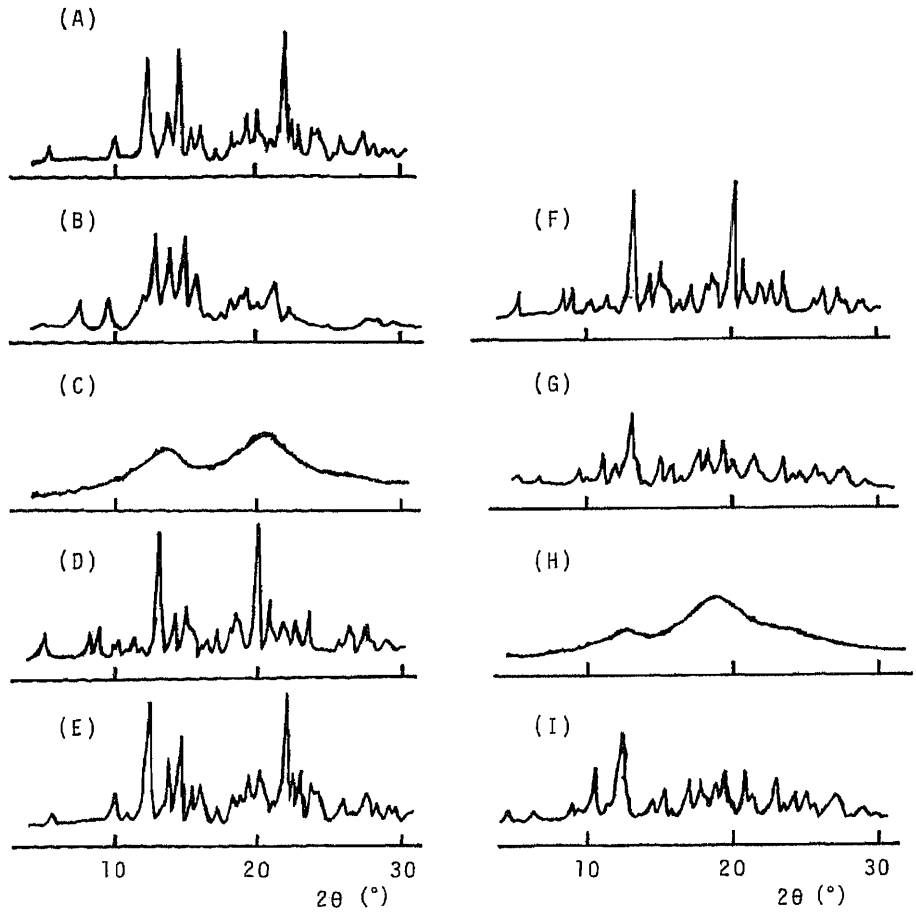


Fig. 1. Powder X-Ray Diffraction Patterns of Various CDs

(A), α-CD hydrate (form A); (B), dried α-CD; (C), ground amorphous α-CD ($H_2O$ adsorbed); (D), heated A at 90 °C for 1 h; (E), heated C at 70 °C for 1 h; (F), heated C at 90 °C for 1 h; (G), β-CD hydrate; (H), ground amorphous β-CD ($H_2O$ adsorbed); (I), heated H at 90 °C for 1 h.

have the same halo patterns (curve C), while the crystalline α-CD hydrate and the dried α-CD showed different X-ray diffraction patterns from each other (curves A and B). The X-ray diffraction patterns of α-CDs after heating in glass ampules are also shown in Fig. 1 (curves D to F). The hydrated samples of the crystalline and amorphous α-CD showed changes in X-ray diffraction patterns on heating, while no change was observed for the dried crystalline and the dried amorphous α-CD. The polymorphic transition of the crystalline α-CD hydrate from form A to B on heating was ascertained from the facts that the endothermic peak appeared at 78 °C on the DSC curve, and that the water content did not change before and after the heating. It was also found that the amorphous α-CD hydrate recrystallized to form A of α-CD hydrate on heating at below 78 °C (curve E), and to form B of the hydrate on heating at over 78 °C (curve F). On the other hand, β-CD hydrate showed no polymorphic transition. Only the crystallization of amorphous β-CD hydrate to crystalline β-CD hydrate was observed, as shown in Fig. 1 (curves G-I).

**Formation of Inclusion Compound by Heating of Physical Mixture of Benzoic Acid with α- or β-CD Hydrate in Ampules**

Figure 2 shows the powder X-ray diffraction patterns of the mixtures of benzoic acid and either α- or β-CD hydrate before and after heating in glass ampules. The diffraction patterns after heating were consistent with the patterns of the respective inclusion compounds obtained by the coprecipitation method. Irrespective of the kind of CDs and the initial mixing ratio of benzoic acid to CDs, it was found that the inclusion compounds were formed by heating in the

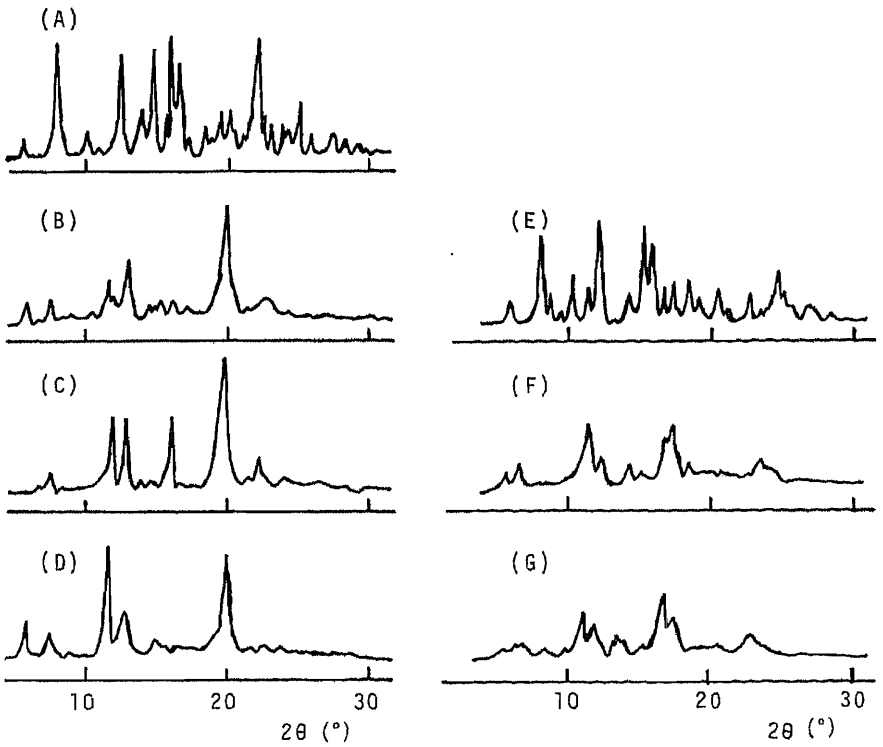


Fig. 2. Powder X-Ray Diffraction Patterns of Benzoic Acid (BA)–CD Hydrate System

(A), physical mixture of BA and α-CD hydrate (initial mixing molar ratio (IMR) of BA to CD = 1 : 1; (B), mixture of BA and α-CD hydrate heated at 90 °C for 30 min (IMR = 1 : 2); (C), mixture of BA and α-CD hydrate heated at 90 °C for 30 min (IMR = 1 : 1); (D), BA–α-CD inclusion compound prepared by the coprecipitation method; (E), physical mixture of BA and β-CD hydrate (IMR = 1 : 1); (F), mixture of BA and β-CD hydrate heated at 90 °C for 30 min (IMR = 1 : 1); (G), BA–β-CD inclusion compound prepared by the coprecipitation method.

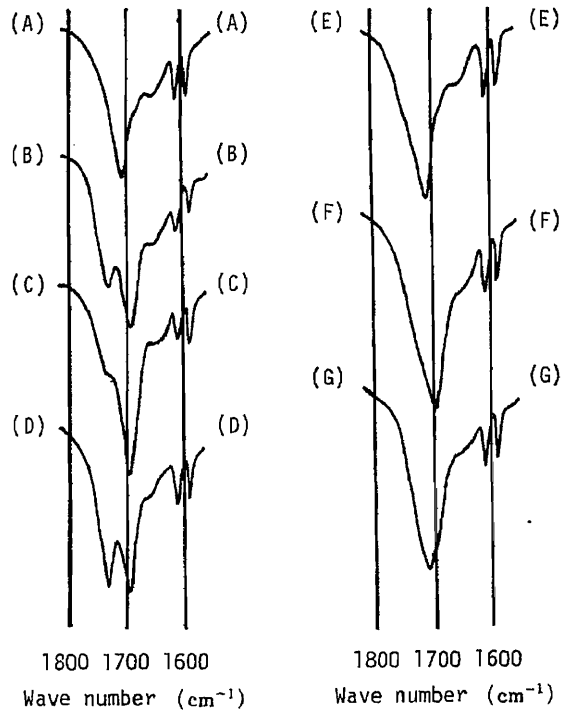


Fig. 3. IR Spectra of BA–CD Hydrate Systems

(A)–(G), same as in Fig. 2.

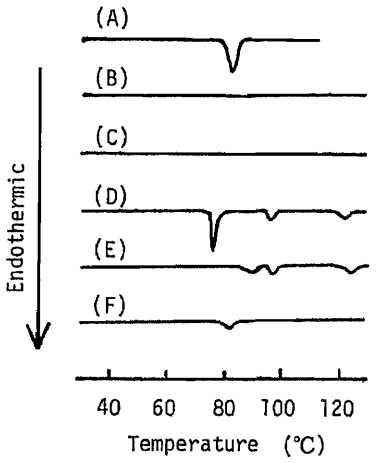


Fig. 4. DSC Curves of CD and BA–CD Hydrate Systems

(A), α-CD hydrate (form A); (B), α-CD hydrate (form B); (C), β-CD hydrate; (D), physical mixture of BA and α-CD hydrate (form A) (IMR = 1 : 1); (E), physical mixture of BA and α-CD hydrate (form B) (IMR = 1 : 1); (F), physical mixture of BA and β-CD hydrate (IMR = 1 : 1).

ampules.

For β-CD, the combining ratio of benzoic acid to β-CD was 1 : 1 in both the coprecipitation complex and the complex obtained by heating in ampules. For α-CD, the combining ratio of benzoic acid to α-CD was 1 : 2 in the coprecipitation complex. In the heating method, however, the combining ratio varied with the experimental conditions; increasing initial mixing ratio and increasing heating temperature caused an increase in the combining ratio of the inclusion compound, and finally the combining ratio approached about 4 : 5. As the combining ratio increased, the water content of the inclusion compound decreased.

IR spectra of the various complexes are shown in Fig. 3. As the benzoic acid molecules are dimerized by strong hydrogen bonding in the crystal, the carbonyl stretching vibration band appeared at 1704 $cm^{-1}$, as reported previously.[8] The carbonyl bands of benzoic acid in the α-CD inclusion compound prepared by the coprecipitation method appeared at 1740 and 1698 $cm^{-1}$. These bands are considered to be due to free and hydrogen-bonded carbonyls, respectively.[9] The α-CD inclusion compound of 1 : 2 ratio obtained by the heating method showed nearly the same IR spectrum to that obtained by the coprecipitation method except for minor intensity differences. However, benzoic acid in the α-CD inclusion compound having a higher combining ratio showed a strong carbonyl absorption band at 1698 $cm^{-1}$ and a shoulder at 1740 $cm^{-1}$. It was suggested that the hydrogen-bonded dimer was dominant for benzoic acid in the α-CD inclusion compound of high combining ratio, and the molecular interaction mode was somewhat different from that of the 1 : 2 inclusion compound.

The IR spectra of β-CD systems were in good accordance with those of the coprecipitate and the heated complexes, indicating the practical usefulness of the heating method for preparing inclusion compounds similar to those obtained by the coprecipitation method.

Figure 4 shows the DSC curves of α- and β-CD hydrate and the physical mixtures of benzoic acid with α- or β-CD hydrate. The endothermic peaks at 78 °C in the α-CD hydrate

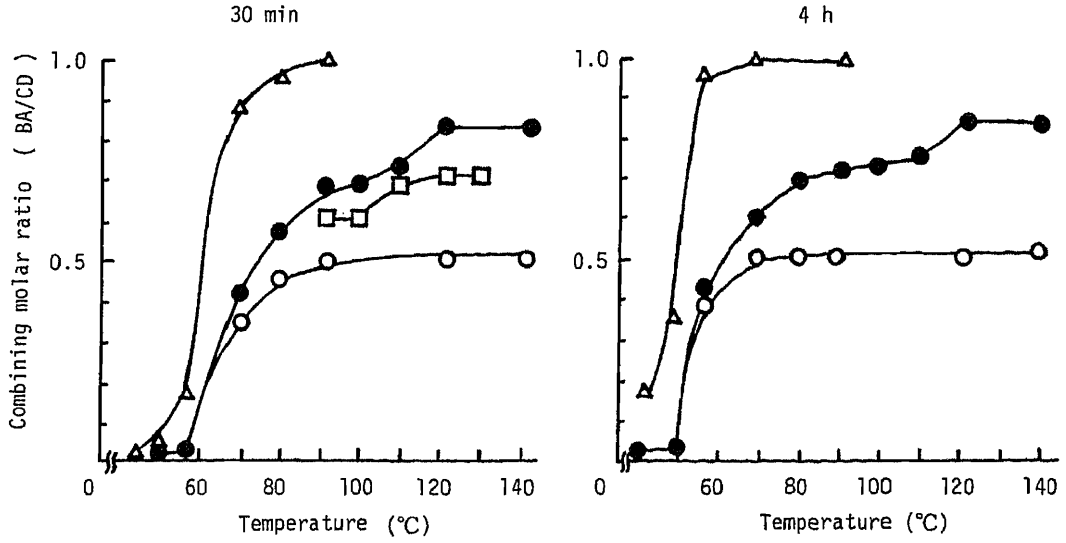


Fig. 5. Combining Molar Ratio of BA to CDs after Heating in Ampules for 30 min or 4 h at Various Temperatures

○, BA–α-CD hydrate (form A) (IMR = 1 : 2); ●, BA–α-CD hydrate (form A) (IMR = 1 : 1); □, BA–α-CD hydrate (form B) (IMR = 1 : 1); △, BA–β-CD hydrate (IMR = 1 : 1).

(form A) and in the α-CD hydrate (form A)–benzoic acid system were due to the transformation into polymorphous α-CD (form B). The β-CD hydrate did not show any peaks below 130 °C. The small endothermic peaks, at 93 °C in curve D, at 87 and 93 °C in curve E and at 82 °C in curve F could be attributed to the inclusion of benzoic acid in CD molecules. The endothermic peaks at 121 °C in curves D and E were due to the melting of excess benzoic acid crystals.

Figure 5 shows the combining ratios of benzoic acid with α-CD or β-CD in various mixtures after heating in ampules at a definite temperature (43—142 °C) for 30 min or 4 h. The physical mixture of benzoic acid with β-CD hydrate changed to the inclusion compound of 1 : 1 combining ratio after heating at 70 °C for 4 h or at 90 °C for 30 min. The mixture of benzoic acid with α-CD hydrate (form A) formed the inclusion compound of 1 : 2 combining ratio after heating at 70 °C for 4 h or at 90 °C for 30 min, when the initial mixing ratio of benzoic acid to α-CD was 1 : 2. In the case of the mixtures of benzoic acid with α-CD hydrate, where the initial mixing ratio was 1 : 1, the higher combining ratio inclusion compounds were obtained, while only the 1 : 2 inclusion compound was obtained by the coprecipitation method. In the α-CD–benzoic acid complex crystal, it was suggested that the α-CD molecules had a channel structure and that the benzoic acid molecules existed in that structure.[10] In the inclusion complex obtained by the heating method, the benzoic acid appeared to exist in a more than stoichiometric ratio with respect to the channel structure.

**Heating of Physical Mixtures of Benzoic Acid with Amorphous CDs and Heating of Ground Mixtures**

Figure 6 shows the effects of heating in ampules on the powder X-ray diffraction patterns of physical mixtures of benzoic acid with amorphous α-CD hydrate and on those of ground mixtures of benzoic acid with α-CD stored in an atmosphere of 55% relative humidity after grinding. After heating at 60 °C for 30 min, the ground mixture crystallized into the inclusion compound (curves E—H). From the changes in the X-ray pattern of the physical mixture, however, both the transformation to the inclusion compound and the crystallization of α-CD (form B) were observed. As the heating temperature was increased, the X-ray diffraction patterns came to coincide with that of the inclusion compound even in the case of the physical

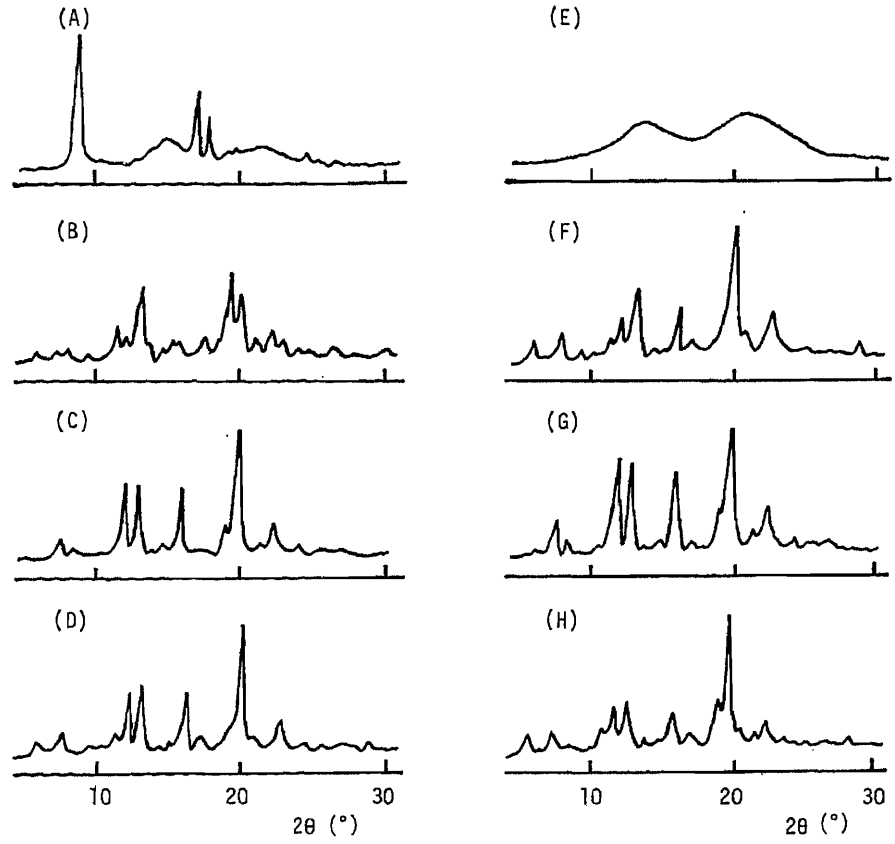


Fig. 6. Powder X-Ray Diffraction Patterns of BA–Amorphous CD Systems

(A), physical mixture of BA and amorphous α-CD (IMR = 1 : 1); (B), heated A at 60 °C for 30 min; (C), heated A at 90 °C for 30 min; (D), heated A at 125 °C for 30 min; (E), ground mixture of BA and α-CD (IMR = 1 : 1); (F), heated E at 60 °C for 30 min; (G), heated E at 90 °C for 30 min; (H), heated E at 125 °C for 30 min.

TABLE I. Combining Molar Ratio of Benzoic Acid to Cyclodextrins after Heating in Ampules at Various Temperatures for 30 min (mol of benzoic acid/mol of CD)

| | Heated for 30 min at | | |
|---|---|---|---|
| | 60 °C | 90 °C | 125 °C |
| Physical mixture with amorphous α-CD[a)] | 0.57 | 0.72 | 0.81 |
| Ground mixture with α-CD[a)] | 0.86 | 0.70 | 0.80 |
| Physical mixture with amorphous β-CD[a)] | 0.90 | 1.00 | |
| Ground mixture with β-CD[a)] | 1.00 | 1.00 | |

a) IMR = 1 : 1.

mixture. When β-CD was used instead of α-CD, similar results were obtained, *i.e.*, the formation of the β-CD benzoic acid inclusion compound by heating in ampules was observed.

Table I shows the combining ratio of benzoic acid to α-CD or β-CD after the heating of various mixtures. In the physical mixture with amorphous α-CD hydrate, increasing heating temperature caused an increase of the combining ratio, as observed in the physical mixture with α-CD hydrate. In the ground mixture with α-CD, the combining ratio did not depend on the heating temperature. This result is ascribed to the occurrence of molecular interaction

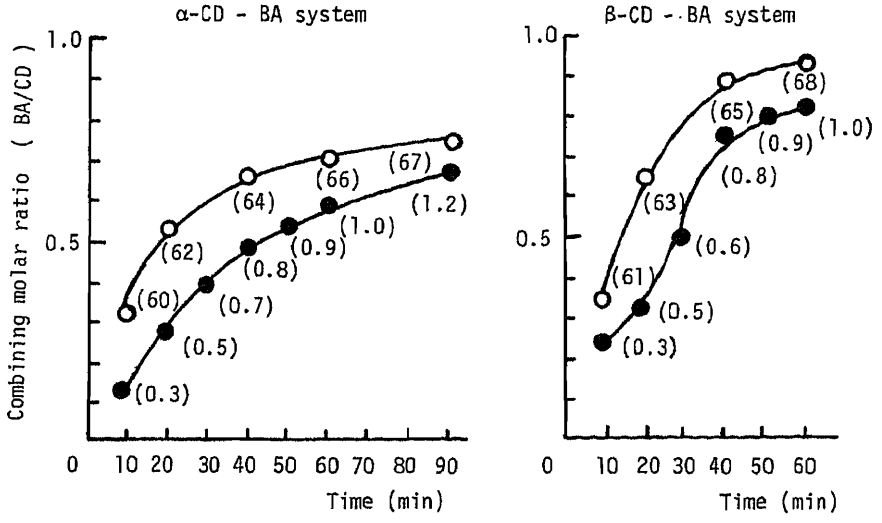


Fig. 7. Effect of $N_2$ Pressure on the Combining Molar Ratio of BA to CD after Heating at 127°C in a Stainless Steel Vessel

O, under pressure; ●, without pressure. Numbers in parentheses indicate gas pressure ($kg \cdot cm^{-2}$).

between benzoic acid and CD molecules during the grinding. In the case of β-CD mixtures, a constant ratio of 1 : 1 was observed, regardless of the heating temperature and the dispersed state.

**Effects of $N_2$ Gas Pressure on the Inclusion Formation by Heating**

Figure 7 shows the relationship between the combining ratio and the heating time with or without $N_2$ gas pressure. The mixtures used were the benzoic acid–α-CD hydrate physical mixture (initial mixing molar ratio = 1 : 1) and the benzoic acid–β-CD hydrate physical mixture (initial mixing molar ratio = 1 : 1). A high $N_2$ gas pressure caused an increase in the combining ratio of the inclusion complex, although the complex formation rates were different from the cases when the samples were heated in ampules. The data in Fig. 7 also indicate an important role of the water vapor pressure on the inclusion formation. Finally, when physical mixtures of benzoic acid with dried CDs were heated in a stainless steel vessel, the pressure change was very small and the inclusion complex was not obtained.

In conclusion, the sealed heating method is a new and effective method to prepare inclusion compounds of organic molecules with CDs, as it is very simple and does not require any dissolution process. Further investigations are in progress to extend this method to other organic molecules and to elucidate the mechanism of the inclusion phenomenon.

**References and Notes**

1) K. Uekama, *Yakugaku Zasshi*, **101**, 857 (1981).
2) M. Kurozumi, N. Nambu, and T. Nagai, *Chem. Pharm. Bull.*, **23**, 3062 (1975).
3) M. Turuoka, T. Hashimoto, H. Seo, S. Ichimasa, O. Ueno, T. Fujinaga, M. Otagiri, and K. Uekama, *Yakugaku Zasshi*, **101**, 360 (1981).
4) Y. Nakai, S. Nakajima, K. Yamamoto, K. Terada, and T. Konno, *Chem. Pharm. Bull.*, **26**, 3419 (1978).
5) Y. Nakai, K. Yamamoto, K. Terada, and Y. Ueno, *Chem. Pharm. Bull.*, **34**, 315 (1986).
6) Y. Nakai, K. Yamamoto, K. Terada, and I. Sasaki, *Yakugaku Zasshi*, **106**, 420 (1986).
7) K. Lindner and W. Saenger, *Acta Crystallogr., Sect. B*, **38**, 203 (1982).
8) Y. Nakai, S. Nakajima, K. Yamamoto, K. Terada, and T. Konno, *Chem. Pharm. Bull.*, **28**, 1552 (1980).
9) G. Allen, G. Watkinson, and K. H. Webb, *Spectrochim. Acta*, **22**, 807 (1966).
10) *a*) K. Harata, *Denpun Kagaku*, **26**, 198 (1979); *b*) Y. Ikeda, K. Matsumoto, K. Kunihiro, T. Fuwa, and K. Uekama, *Yakugaku Zasshi*, **102**, 83 (1982).

[Chem. Pharm. Bull. 35(11)4616—4625(1987)]

# Inhibitory Effect of 2-(*E*-2-Alkenoylamino)ethyl Alkyl Sulfides on Gastric Ulceration in Rats. I. Effect of 2-(*E*-2-Alkenoylamino)ethyl Carbamoylmethyl Sulfides on Gastric Secretion and Various Ulceration Models in Rats

MASAKAZU IWAI,*[,a] ISAO KOHDA,[a] CHIKARA FUKAYA,[a] YOICHIRO NAITO,[a] KAZUMASA YOKOYAMA,[a] HIROSHI NAKAJIMA,[b] KAZUTAKE TSUJIKAWA,[b] MASARU OKABE[b] and TSUTOMU MIMURA[b]

*Central Research Laboratories, The Green Cross Corporation,[a] Miyakojima-ku, Osaka 534, Japan and Faculty of Pharmaceutical Sciences, Osaka University,[b] Yamadaoka 1–6, Suita, Osaka 565, Japan*

(Received March 23, 1987)

Bis[2-(*E*-2-alkenoylaminoethyl)] disulfides (I) and 2-(*E*-2-alkenoylamino)ethyl carbamoylmethyl sulfides (II) with various alkenyl chain lengths were synthesized and their inhibitory effects on gastric secretion in rats were compared. There was a relationship between the alkenyl chain length of a series of sulfide derivatives (II) and their biological activities (C10 and C11 alkenyl derivatives were the most effective compounds). On the other hand, variation of the alkenyl chain length did not affect the anti-ulcerogenic activity of the disulfide derivatives (I). The derivatives (II) showed stronger biological activity than (I) when the same alkenyl group was present in both.

The administration of 2-(*E*-2-decenoylamino)ethyl carbamoylmethyl sulfide (II-5) or 2-(*E*-2-undecenoylamino)ethyl carbamoylmethyl sulfide (II-6) at a dose of 20 mg/kg (i.p.) caused significant inhibition of various experimental ulcerations caused by stress, aspirin and HCl–ethanol. Oral administration of both acetamides (II-5, II-6) also caused 50—60% inhibition of ulceration in the water-immersion stress model at a dose of 20 mg/kg, although the activity was not as strong as that after i.p. injection. An improvement in anti-ulcerogenic activity was observed when acetamides were administered as a suspension in 10% HCO-60. Both acetamides (II-5, II-6) caused a dose-dependent decrease of the ulcer index of restrained and water-immersion stress-loaded rats in the dosage range from 0.5 mg/kg *p.o.* to 5 mg/kg *p.o.* The lethal dose 50% values ($LD_{50}$) for both acetamides were over 8 g/kg (*p.o.* or i.p.).

**Keywords**——bis[(2-(*E*-2-alkenoylaminoethyl)] disulfide; 2-(*E*-2-alkenoylamino)ethyl carbamoylmethyl sulfide; anti-ulcerogenic activity; antisecretory activity

We have reported that human immunoglobulin G (IgG) showed anti-ulcerogenic[1] and anti-inflammatory[2] activity after reductive cleavage of interchain disulfide bonds, though the native IgG showed no such activity. It was suggested that the chemical modification of S–S bonds in the hinge region was essential. On the other hand, we have reported the anti-ulcerogenic activity of various saturated[3] and unsaturated[4] fatty acids and investigated the relationship between alkyl or alkenyl chain lengths and biological activities.

In the present article, we describe our primary results in attempting to develop a new anti-ulcerogenic drug. As a first step, commercially available sulfur-containing amino acids and amines were chosen and their gastric secretion-inhibitory activity in pylorus-ligated rats were observed. Among the chemicals tested, cystamine showed the strongest activity. Therefore, alkenyl amino derivatives (I) were synthesized from various *trans*-2-unsaturated fatty acids and cystamine, and their pharmacological activities were tested together with those of the 2-(*E*-2-alkenoylamino)ethyl carbamoylmethyl sulfides (II) which were obtained by reduction and alkylation of the derivatives (I).

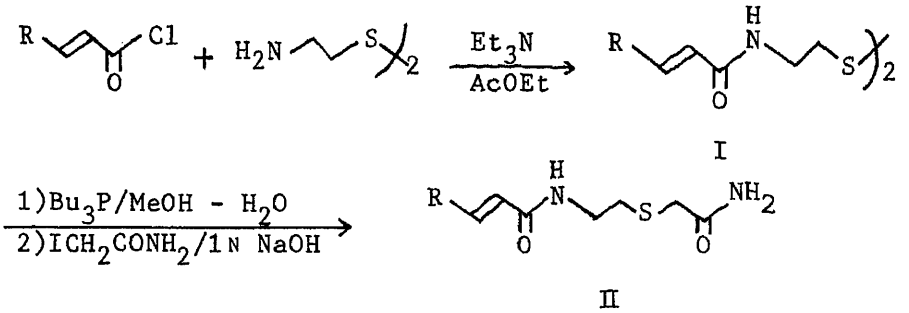

bis[2-(*E*-2-alkenoylaminoethyl)]disulfides (I)

I-1: R=$C_3H_7$ I-2: R=$C_4H_9$ I-3: R=$C_5H_{11}$ I-4: R=$C_6H_{13}$ I-5: R=$C_7H_{15}$
I-6: R=$C_8H_{17}$ I-7: R=$C_9H_{19}$ I-8: R=$C_{10}H_{21}$ I-9: R=$C_{11}H_{23}$

2-(*E*-2-alkenoylamino)ethyl carbamoylmethyl sulfides (II)

II-1: R=$C_3H_7$ II-2: R=$C_4H_9$ II-3: R=$C_5H_{11}$ II-4: R=$C_6H_{13}$ II-5: R=$C_7H_{15}$
II-6: R=$C_8H_{17}$ II-7: R=$C_9H_{19}$ II-8: R=$C_{10}H_{21}$ II-9: R=$C_{11}H_{23}$

Chart 1

## Experimental

**Reagents**——Cystine, cysteine, methionine, ethionine, taurine, hypotaurine, methionine sulfone, cystamine dihydrochloride and cysteamine hydrochloride were from Nakarai Chemicals Ltd., Japan. Lanthionine and methionine sulfate were obtained from Tokyo Kasei Co., Japan. Test samples were suspended in 5% gum arabic in saline and were administered intraperitoneally at doses of 5, 10, and 25 mg/kg to the test animals.

**Synthesis of Bis[(2-(*E*-2-alkenoylaminoethyl)] Disulfide Derivatives (I)**——The following nine unsaturated fatty acids, containing one *trans* double bond between carbon numbers 2 and 3, were obtained from Tokyo Kasei Co., Japan: *trans*-2-hexenoic acid (C6 : 1), *trans*-2-heptenoic acid (C7 : 1), *trans*-2-octenoic acid (C8 : 1), *trans*-2-nonenoic acid (C9 : 1), *trans*-2-decenoic acid (C10 : 1), *trans*-2-undecenoic acid (C11 : 1), *trans*-2-dodecenoic acid (C12 : 1), *trans*-2-tridecenoic acid (C13 : 1) and *trans*-2-tetradecenoic acid (C14 : 1).

We synthesized the desired bis[(2-(*E*-2-alkenoylaminoethyl)] disulfides (I) from cystamine and the nine 2-*trans*-unsaturated fatty acids according to the method shown in Chart 1. First, the unsaturated fatty acid halides, obtained by reaction between the unsaturated fatty acids and thionyl chloride, were reacted with cystamine to give (I). After reduction of the disulfide bond in cystamine with tributylphosphine, the generated SH groups were alkylated with iodoacetamide to afford 2-(*E*-2-alkenoylamino)ethyl carbamoylmethyl sulfides (II).

The synthetic procedures, infrared data and $^1$H nuclear magnetic resonance ($^1$H-NMR) spectrum data for the 18 objective compounds are given below.

**Synthesis of Bis[(2-(*E*-2-hexenoylaminoethyl)] Disulfide (I-1)**——A mixture of *trans*-2-hexenoic acid (15 g) and thionyl chloride (20 ml) was refluxed for 15 h. After the reaction, excess thionyl chloride was distilled off and the residue was distilled under reduced pressure to afford the acid chloride [(11.3 g, 64%, b.p. 77—78 °C (34 mmHg)].

A solution of this acid chloride (9.6 g) in ethyl acetate (15 ml) was added dropwise to an ice-cooled solution of cystamine (5.0 g) and triethylamine (10.1 ml) in ethyl acetate (150 ml). The reaction was carried out for 30 min at 0 °C. The mixture was then left overnight at room temperature. Water (100 ml) was added, and the precipitated solid was collected by filtration. Compound I-1 was obtained by recrystallization from ethyl acetate (10.8 g, 57%). mp 137—138 °C (pale yellow crystals). IR $\nu_{max}^{KBr}$ cm$^{-1}$: 3300, 3050, 2950, 2860, 1665, 1620, 1540, 1465, 975. $^1$H-NMR ($CDCl_3$) $\delta$: 0.90 (t, 6H, $J$=7 Hz), 2.13 (dt, 4H, $J$=6, 6 Hz), 2.80 (t, 4H, $J$=6 Hz), 3.58 (dt, 4H, $J$=6, 6 Hz), 5.85 (dt, 2H, $J$=16, 1 Hz), 6.80 (dt, 2H, $J$=16, 16 Hz), 6.90 (br, 2H).

**Synthesis of 2-(*E*-2-Hexenoylamino)ethyl Carbamoylmethyl Sulfide (II-1)**——Compound I-1 (2.0 g) was suspended in 60 ml of a 9 : 1 (v/v) mixture of methanol and water, and then tributylphosphine (1.3 g) was added dropwise to the suspension under an $N_2$ gas atmosphere. The reaction was carried out for 30 min at 0 °C and the mixture was allowed to stand for an additional hour at room temperature. Iodoacetamide (2.3 g) was then added, and 1 N NaOH (12.2 ml) was added dropwise to the cooled mixture. The whole was stirred for 1 h at room temperature. Water (100 ml) was added, and the white precipitate was collected by filtration. After recrystallization from ethanol-water, II-1 was obtained (1.8 g, 67%). mp 143—144.5 °C (white crystals). IR $\nu_{max}^{KBr}$ cm$^{-1}$: 3380, 3300, 3180, 2950, 2860, 1645, 1620, 1542, 1460, 975. $^1$H-NMR ($CDCl_3+CF_3COOH$) $\delta$: 0.94 (t, 3H, $J$=7 Hz), 2.28 (dt, 2H, $J$=6, 6 Hz), 2.88 (t, 2H, $J$=7 Hz), 3.45 (s, 2H), 3.60 (t, 2H, $J$=7 Hz), 6.00 (d, 1H, $J$=15 Hz), 7.08 (dt, 1H, $J$=15, 6 Hz), 7.0—8.60 (br, m, 3H).

**Synthesis of Bis[(2-(*E*-2-heptenoylaminoethyl)] Disulfide (I-2)**——The procedures used for I-1 were repeated with *trans*-2-heptenoic acid (15 g) to obtain I-2 (12.3 g, 65%). mp 124—125 °C (white crystals). IR $\nu_{max}^{KBr}$ cm$^{-1}$: 3300, 3050, 2950, 2850, 1665, 1620, 1540, 1465, 978. $^1$H-NMR ($CDCl_3$) $\delta$: 0.90 (br, 6H), 2.20 (br, 4H), 2.85 (t, 4H, $J$=7 Hz), 3.65

(dt, 4H, $J$=7, 7 Hz), 5.89 (dt, 2H, $J$=15, 1 Hz), 6.86 (dt, 2H, $J$=15, 6 Hz), 6.80 (br, 2H).

**Synthesis of 2-(*E*-2-Heptenoylamino)ethyl Carbamoylmethyl Sulfide (II-2)**——The procedures used for II-1 were repeated with I-2 (2.0 g) to obtain II-2 (1.5 g, 57%). mp 143—144 °C (white crystals). IR $\nu_{max}^{KBr}$ cm$^{-1}$: 3380, 3300, 3180, 2950, 2850, 1645, 1620, 1540, 1460, 975. $^1$H-NMR (DMSO-$d_6$+$CDCl_3$) $\delta$: 0.90 (br t, 3H, $J$=6 Hz), 2.20 (br, 2H), 2.67 (t, 2H, $J$=7 Hz), 3.10 (s, 2H), 3.30 (dt, 2H, $J$=7, 7 Hz), 5.83 (d, 1H, $J$=15 Hz), 6.65 (dt, 1H, $J$=15, 6 Hz), 6.90 (br, 1H), 7.30 (br, 1H), 7.90 (br t, 1H, $J$=7 Hz).

**Synthesis of Bis[(2-(*E*-2-octenoylaminoethyl)] Disulfide (I-3)**——The procedures used for I-1 were repeated with *trans*-2-octenoic acid (3.9 g) to obtain I-3 (3.4 g, 85%). mp 131—133 °C (white crystals). IR $\nu_{max}^{KBr}$ cm$^{-1}$: 3300, 3050, 2950, 2850, 1665, 1620, 1545, 975. $^1$H-NMR ($CDCl_3$+$CF_3COOH$) $\delta$: 0.90 (br t, 6H, $J$=6 Hz), 2.15 (br, 4H), 2.85 (t, 4H, $J$=7 Hz), 3.60 (dt, 4H, $J$=7, 7 Hz), 5.90 (dt, 2H, $J$=16, 1 Hz), 6.80 (dt, 2H, $J$=16, 7 Hz), 6.90 (br, 2H).

**Synthesis of 2-(*E*-2-Octenoylamino)ethyl Carbamoylmethyl Sulfide (II-3)**——The procedures used for II-1 were repeated with I-3 (3.0 g) to obtain II-3 (1.0 g, 77%). mp 146.5—147 °C (needle-shaped white crystals). IR $\nu_{max}^{KBr}$ cm$^{-1}$: 3370, 3300, 3170, 2920, 2850, 1645, 1625, 1600, 1540, 975. $^1$H-NMR (DMSO-$d_6$+$CDCl_3$) $\delta$: 0.90 (br t, 3H, $J$=6 Hz), 2.10 (br, 2H), 2.65 (t, 2H, $J$=7 Hz), 3.10 (s, 2H), 3.40 (dt, 2H, $J$=7, 7 Hz), 5.85 (d, 1H, $J$=16 Hz), 5.65 (dt, 1H, $J$=16, 7 Hz), 7.40 (br, 1H), 7.90 (br, 2H).

**Synthesis of Bis[(2-(*E*-2-nonenoylaminoethyl)] Disulfide (I-4)**——The procedures used for I-1 were repeated with *trans*-2-nonenoic acid (5.0 g) to obtain I-4 (1.9 g, 27%). mp 127—129 °C (white crystals). IR $\nu_{max}^{KBr}$ cm$^{-1}$: 3300, 3150, 2930, 2850, 1665, 1620, 1540, 1465, 975. $^1$H-NMR ($CDCl_3$) $\delta$: 0.90 (br t, 6H, $J$=6 Hz), 2.20 (br, 4H), 2.90 (t, 4H, $J$=6 Hz), 3.65 (dt, 4H, $J$=6, 6 Hz), 5.90 (d, 2H, $J$=15 Hz), 6.90 (dt, 2H, $J$=15, 6 Hz), 6.7 (br, 2H).

**Synthesis of 2-(*E*-2-Nonenoylamino)ethyl Carbamoylmethyl Sulfide (II-4)**——The procedures used for II-1 were repeated with I-4 (1.0 g) to obtain II-4 (1.0 g, 78%). mp 150—151 °C (white crystals). IR $\nu_{max}^{KBr}$ cm$^{-1}$: 3370, 3300, 3190, 2930, 2840, 1665, 1640, 1620, 1545, 1490, 975. $^1$H-NMR (DMSO-$d_6$+$CDCl_3$) $\delta$: 0.88 (br, 3H), 2.15 (br, 2H), 2.70 (t, 2H, $J$=7 Hz), 3.12 (s, 2H), 3.20 (t, 2H, $J$=7 Hz), 5.85 (d, 1H, $J$=16 Hz), 6.68 (dt, 1H, $J$=16, 6 Hz), 6.9 (br, 1H), 7.35 (br, 1H), 7.88 (br, 1H).

**Synthesis of Bis[(2-(*E*-2-decenoylaminoethyl)] Disulfide (I-5)**——The procedures used for I-1 were repeated with *trans*-2-decenoic acid (15 g) to obtain I-5 (10.75 g, 75%). mp 136—136.5 °C (white crystals). IR $\nu_{max}^{KBr}$ cm$^{-1}$: 3300, 3050, 2920, 2850, 1665, 1620, 1540, 975. $^1$H-NMR ($CDCl_3$+$CF_3COOH$) $\delta$: 0.90 (br, 6H), 2.30 (br, 4H), 2.90 (t, 4H, $J$=7 Hz), 3.80 (t, 4H, $J$=7 Hz), 6.00 (d, 2H, $J$=15 Hz), 7.10 (dt, 2H, $J$=15, 16 Hz), 7.20 (br, 2H).

**Synthesis of 2-(*E*-2-Decenoylamino)ethyl Carbamoylmethyl Sulfide (II-5)**——The procedures used for II-1 were repeated with I-5 (2.0 g) to obtain II-5 (2.1 g, 84%). mp 151—151.5 °C (white crystals). IR $\nu_{max}^{KBr}$ cm$^{-1}$: 3370, 3300, 3170, 2920, 2850, 1650, 1620, 1540, 970. $^1$H-NMR (DMSO-$d_6$+$CDCl_3$) $\delta$: 0.90 (br t, 3H, $J$=6 Hz), 2.15 (br, 2H), 2.65 (t, 2H, $J$=6 Hz), 3.10 (s, 2H), 3.40 (dt, 2H, $J$=6, 6 Hz), 5.80 (d, 1H, $J$=16 Hz), 6.65 (dt, 1H, $J$=16, 7 Hz), 6.90 (br, 1H), 7.30 (br, 1H), 7.90 (br, 1H).

**Synthesis of Bis[(2-(*E*-2-undecenoylaminoethyl)] Disulfide (I-6)**——The procedures used for I-1 were repeated with *trnas*-2-undecenoic acid (12.3 g) to obtain I-6 (9.14 g, 68%). mp 133—133.5 °C (white crystals). IR $\nu_{max}^{KBr}$ cm$^{-1}$: 3300, 3050, 2920, 2850, 1650, 1620, 1600, 1545, 957. $^1$H-NMR ($CDCl_3$+$CF_3COOH$) $\delta$: 0.90 (br t, 6H), 2.40 (br, 4H), 2.90 (t, 4H, $J$=7 Hz), 3.80 (br t, 4H, $J$=7 Hz), 6.10 (d, 2H, $J$=16 Hz), 7.10 (dt, 2H, $J$=16, 7 Hz), 7.80 (br, 2H).

**Synthesis of 2-(*E*-2-Undecenoylamino)ethyl Carbamoylmethyl Sulfide (II-6)**——The procedures used for II-1 were repeated with I-6 (2.0 g) to obtain II-6 (2.0 g, 81%). mp 150.5—151.0 °C (white crystals). IR $\nu_{max}^{KBr}$ cm$^{-1}$: 3350, 3300, 3150, 2950, 2850, 1650, 1620, 1540, 1460, 970. $^1$H-NMR (DMSO-$d_6$+$CDCl_3$) $\delta$: 0.90 (br t, 3H, $J$=6 Hz), 2.10 (br, 2H), 2.70 (t, 2H, $J$=7 Hz), 3.30 (s, 2H), 3.35 (dt, 2H, $J$=7, 7 Hz), 5.85 (d, 1H, $J$=16 Hz), 6.70 (dt, 1H, $J$=16, 7 Hz), 7.20 (br, 1H), 7.90 (br, 2H).

**Synthesis of Bis[(2-(*E*-2-dodecenoylaminoethyl)) Disulfide (I-7)**——The procedures used for I-1 were repeated with *trans*-2-dodecenoic acid (15 g) to obtain I-7 (10.0 g, 83%). mp 136—137 °C (pale red crystals). IR $\nu_{max}^{KBr}$ cm$^{-1}$: 3300, 3050, 2930, 2850, 1665, 1620, 1545, 1465, 980. $^1$H-NMR ($CDCl_3$+$CF_3COOH$) $\delta$: 0.90 (br t, 6H, $J$=6 Hz), 2.30 (br, 4H), 2.90 (t, 4H, $J$=6 Hz), 3.82 (br t, 4H, $J$=6 Hz), 6.02 (d, 2H, $J$=16 Hz), 7.12 (dt, 2H, $J$=16, 16 Hz), 7.80 (br, 2H).

**Synthesis of 2-(*E*-2-Dodecenoylamino)ethyl Carbamoylmethyl Sulfide (II-7)**——The procedures used for II-1 were repeated with I-7 (2.0 g) to obtain II-7 (2.0 g, 82%). mp 143—144 °C (needle-shaped white crystals). IR $\nu_{max}^{KBr}$ cm$^{-1}$: 3380, 3300, 3180, 2850, 1650, 1620, 1545, 1460, 975. $^1$H-NMR ($CDCl_3$+$CF_3COOH$) $\delta$: 0.90 (br, 3H), 2.30 (br, 2H), 2.90 (t, 2H, $J$=6 Hz), 3.48 (s, 2H), 3.72 (t, 2H, $J$=6 Hz), 6.02 (d, 1H, $J$=15 Hz), 7.12 (dt, 1H, $J$=15, 6 Hz), 6.80—8.20 (br, m, 3H).

**Synthesis of Bis[(2-(*E*-2-tridecenoylaminoethyl)] Disulfide (I-8)**——The procedures used for I-1 were repeated with *trans*-2-tridecenoic acid (8.4 g) to obtain I-8 (3.28 g, 67%). mp 131—134 °C (pale yellow crystals). IR $\nu_{max}^{KBr}$ cm$^{-1}$: 3300, 3050, 2950, 2850, 1670, 1630, 1550, 980. $^1$H-NMR ($CDCl_3$+$CF_3COOH$) $\delta$: 0.90 (br, 6H), 2.30 (br, 4H), 2.90 (br, 4H), 3.90 (br, 4H), 6.10 (br d, 2H, $J$=15 Hz), 7.20 (br, 2H).

**Synthesis of 2-(*E*-2-Tridecenoylamino)ethyl Carbamoylmethyl Sulfide (II-8)**——The procedures used for II-1 were repeated with I-8 (3.7 g) to obtain II-8 (2.04 g, 45%). mp 151—152 °C (pale yellow crystals). IR $\nu_{max}^{KBr}$ cm$^{-1}$: 3400, 3330, 3200, 2950, 2850, 1650, 1630, 1550, 1460, 980. $^1$H-NMR ($CDCl_3$+$CF_3COOH$) $\delta$: 0.90 (br, 3H), 2.40 (br, 2H), 3.00 (br, 2H), 3.53 (s, 2H), 3.80 (br, 2H), 6.10 (br d, 1H, $J$=15 Hz), 7.00—8.90 (br, m, 3H).

**Synthesis of Bis[(2-(*E*-2-tetradecenoylaminoethyl)] Disulfide (I-9)**——The procedures used for Compound I-1 were repeated with *trans*-2-tetradecenoic acid (15 g) to obtain I-9 (4.2 g, 25%). mp 134—136.5 °C (white crystals). IR $\nu_{max}^{KBr}$ cm$^{-1}$: 3300, 2860, 1665, 1625, 1545, 1465, 985. $^1$H-NMR ($CDCl_3 + CF_3COOH$) $\delta$: 0.90 (br t, 6H, $J$=6 Hz), 2.35 (br, 4H), 2.92 (t, 4H, $J$=6 Hz), 3.84 (br t, 4H, $J$=6 Hz), 6.04 (d, 2H, $J$=16 Hz), 7.13 (dt, 2H, $J$=16, 7 Hz), 6.80—8.20 (br, m, 2H).

**Synthesis of 2-(*E*-2-Tetradecenoylamino)ethyl Carbamoylmethyl Sulfide (II-9)**——The procedures used for II-1 were repeated with I-9 (1.5 g) to obtain II-9 (1.5 g, 82%). mp 154—155 °C (white crystals). IR $\nu_{max}^{KBr}$ cm$^{-1}$: 3380, 3300, 3180, 2950, 2850, 1665, 1650, 1622, 1545, 1460. $^1$H-NMR ($CDCl_3 + CF_3COOH$) $\delta$: 0.90 (br t, 3H, $J$=6 Hz), 2.35 (br, 2H), 2.90 (t, 2H, $J$=7 Hz), 3.49 (s, 2H), 3.74 (t, 2H, $J$=7 Hz), 6.05 (d, 1H, $J$=16 Hz), 7.12 (dt, 1H, $J$=16, 7 Hz), 6.80—8.10 (br, m, 3H).

**Assay of Gastric Juice Secretion-Inhibitory Activity in Rats**——The assay was performed as follows. Male Wistar rats weighing 160—180 g, fasted for 48 h, were anesthetized with ethyl ether and the pylorus was ligated. Each sample was dissolved or suspended in 5% gum arabic in saline and administered intraperitoneally immediately after pylorus ligation. As a control, 5% gum arabic solution alone was administered. At 4 h after the pylorus ligation, the contents of the stomach were collected and the volume of gastric juice, total acid output and total peptic activity were determined by the methods described in our previous paper.[1]

**Experimental Gastric Ulcers in Rats**——i) Stress-Induced Gastric Ulcer: Male Wistar rats weighing 230—250 g, fasted for 48 h, were used as experimental animals. The rats were subjected to stress following the method of Takagi and Okabe,[5] in which animals were immobilized in a stress cage and immersed vertically in a water bath at 22±1 °C to the level of the xiphoid process for 7 h. Each sample was suspended in 5% gum arabic or 10% HCO-60 (Nikko Chemicals) in saline and administered intraperitoneally or perorally immediately before the stress treatment. The animals were sacrificed 7 h later. The stomach was then removed, inflated with 10 ml of saline and immersed in 1% formalin solution for 5 min. This formalin treatment was performed in all the following experiments. Subsequently, the stomach was incised along the greater curvature and examined for gastric lesions.

The total length (mm) of all lesions in the glandular portion of the stomach was used as an ulcer index.

ii) Aspirin-Induced Gastric Ulcer: Male Wistar rats weighing 160—180 g were deprived of food for 24 h. According to the method of Okabe *et al.*,[6] the rats were orally given 150 mg/kg of aspirin (Nakarai Chemicals, Ltd.) suspended in 5% gum arabic solution immediately after the pylorus ligation. Each sample was suspended in 5% gum arabic in saline and administered intraperitoneally immediately after the pylorus ligation. At 7 h after the pylorus ligation, rats were sacrificed and their stomachs removed. After the formalin treatment, the lesions in the glandular portion of the stomach were examined and the sum of the lengths (mm) of all lesions was used as an ulcer index.

iii) HCl–Ethanol-Induced Gastric Ulcer: Male Wistar rats weighing 160—190 g, fasted for 24 h, were used as experimental animals. This ulcer model was induced according to the method of Mizui and Doteuchi.[7] Each rat received 1.5 ml of 150 mM HCl-60% ethanol solution. Test samples were suspended in 5% gum arabic in saline and administered intraperitoneally 2 h before the HCl–ethanol administration. The animals were sacrificed 1 h later and their stomachs were removed to examine the lesions in the glandular portion. The sum of the length (mm) of all lesions was used as an ulcer index.

**Acute Toxicity Test in Mice**——Acute toxicity was studied in male ddY mice, weighing 18—21 g. Five mice in each group were used for the experiment. Test samples, suspended in 10% HCO-60 in saline, were administered at doses of 125, 500, 2000 and 8000 mg/kg perorally or intraperitoneally at a volume of 40 ml/kg. After the administration of a single dose of each test sample, the behavior of the animals was also observed for 6 h, then they were caged and bred as usual for 7 d. Numbers of dead animals and the change of body weight in each mouse were observed every day until the end of the experiment.

**Statistics**——Results are expressed as the mean±S.E. Student's $t$ test was applied to evaluate the significance of differences between the mean of the control group and the means of sample-administered groups.

## Results

### Inhibitory Effects of Various Sulfur-Containing Amino Acids and Amines on Gastric Secretion in Rats

The inhibitory effect of various samples, given at doses of 5, 10, and 25 mg/kg i.p., on gastric juice secretion in pylorus-ligated rats, was examined by measuring the volume, total acid output and total peptic activity of gastric juice, collected for 4 h during the experiment.

At a dose of 25 mg/kg i.p., all of the test sample-injected groups, except for the cysteine and cysteamine groups, showed a significant inhibition in the volume, total acid output and total peptic activity of gastric juice when compared to the control group. At a dose of 10 mg/kg i.p., only cystamine and lanthionine showed a significant gastric juice secretion-

Table I. Effect of Various Sulfur-Containing Amino Acids and Amines on Gastric Secretion in Pylorus-Ligated Rats (4 h)

| Treatment | Dose (mg/kg) | Gastric volume (ml/100 g b.w.) | Total acid output (μeq/100 g b.w.) | Total peptic activity (mg as tyrosine/100 g b.w.) |
|---|---|---|---|---|
| 1) Control[a] | — | 2.89±0.22 | 201.8±11.6 | 206.8±10.3 |
| Cystine | 25 | 2.05±0.09[c] | 146.4± 8.5[c] | 165.5± 3.5[c] |
| Cysteine | 25 | 2.53±0.13 | 171.0± 9.7 | 176.5±12.0 |
| Methionine | 25 | 2.13±0.20[b] | 145.7± 6.9[c] | 166.9± 8.8[b] |
| Taurine | 25 | 1.72±0.08[d] | 123.6± 4.2[d] | 145.0± 3.5[d] |
| 2) Control[a] | — | 2.62±0.28 | 260.8±30.3 | 184.2±15.4 |
| Hypotaurine | 25 | 1.66±0.31[b] | 157.3±39.3 | 114.5±15.9[c] |
| Ethionine | 25 | 1.52±0.22[b] | 105.9±18.6[d] | 102.7±18.4[c] |
| Methionine sulfate | 25 | 1.66±0.32[b] | 136.5±33.7[b] | 107.5±14.5[c] |
| 3) Control[a] | — | 2.79±0.35 | 271.1±39.0 | 232.8±26.7 |
| Cystamine | 25 | 1.36±0.16[c] | 120.6±19.9[c] | 125.6±14.2[c] |
| Cysteamine | 25 | 2.02±0.26 | 165.8±31.0 | 175.0±22.2 |
| Lanthionine | 25 | 1.76±0.23 | 142.3±21.5[b] | 152.9±16.4[b] |
| Methionine sulfone | 25 | 1.72±0.30[b] | 155.0±33.5 | 143.6±23.0[b] |
| 4) Control[a] | — | 2.26±0.24 | 223.5±29.0 | 194.2±20.2 |
| Methionine | 10 | 1.90±0.18 | 170.7±19.2 | 148.4±22.4 |
| Ethionine | 10 | 1.89±0.26 | 191.8±23.7 | 228.0±24.7 |
| Lanthionine | 10 | 1.02±0.20[c] | 122.9±16.6[c] | 152.1±18.6 |
| Methionine sulfone | 10 | 1.64±0.18 | 186.9±19.8 | 182.8±18.9 |
| Cystamine | 10 | 0.78±0.14[d] | 84.0±14.5[d] | 110.3±10.9[c] |
| 5) Control[a] | — | 2.90±0.26 | 371.3±35.1 | 235.2±20.2 |
| Cystine | 10 | 2.54±0.30 | 328.2±33.4 | 190.2±22.9 |
| Taurine | 10 | 3.04±0.20 | 379.0±38.6 | 224.6±12.3 |
| Hypotaurine | 10 | 3.14±0.26 | 413.5±41.3 | 237.4±19.1 |
| Methionine sulfate | 10 | 2.49±0.39 | 310.2±56.3 | 184.5±13.9 |
| 6) Control[a] | — | 2.60±0.23 | 288.8±38.7 | 205.3±17.1 |
| Lanthionine | 5 | 2.92±0.25 | 339.3±25.1 | 204.4±14.7 |
| Cystamine | 5 | 2.51±0.14 | 286.2±18.1 | 190.8±10.0 |

All values represent the mean±S.E. of 8 rats. *a*) Acacia, 5% in saline. Each sample was intraperitoneally administered immediately after pylorus ligation. Significantly different from the control group: *b*) $p<0.05$, *c*) $p<0.01$, *d*) $p<0.001$.

inhibitory activity; they gave 62% and 45% inhibitions of total acid output, respectively. Cystamine was more potent than lanthionine, but the difference was not significant.

Thus, cystamine was the strongest gastric secretion-inhibitory material among the various sulfur-containing amino acids and amines tested (Table I).

**Inhibitory Effects of Several Disulfides (I-1—I-9) and Sulfides (II-1—II-9) on Gastric Secretion in Rats**

In order to examine the gastric juice secretion-inhibitory activity for each of the eighteen synthesized derivatives, each test sample was given intraperitoneally to rats at a dose of 25 mg/kg immediately after pylorus ligation.

All sulfides (II), which were alkylated with iodoacetamide, showed stronger activity than the disulfides (I), no matter what the length of the alkenyl chains (Table II). The correlation between the length of the alkenyl chain of the unsaturated fatty acid in II-1—II-9 and the total acid output inhibitory activity was examined; the results are shown in Fig. 1. Compounds II-5 and II-6, containing 10 or 11 carbons in the alkenyl chain of the unsaturated fatty acid, showed stronger inhibitory activity than cystamine or unsaturated fatty acid having the same carbon number alone.

We found a correlation between the pharmacological activity and the carbon number of

TABLE II. Effect of Various Bis[2-(*E*-2-alkenoylaminoethyl)] Disulfides and 2-(*E*-2-Alkenoylamino)ethyl Carbamoylmethyl Sulfides on Gastric Secretion in Pylorus-Ligated Rats (4 h)

| Treatment | Dose (mg/kg) | Gastric volume (ml/100 g b.w.) | Total acid output (μeq/100 g b.w.) | Total peptic activity (mg as tyrosine/100 g b.w.) |
|---|---|---|---|---|
| Control[a] | — | 3.05±0.20 | 326.0±26.1 | 184.5±13.7 |
| I-1 | 25 | 2.61±0.28 | 287.7±33.7 | 161.7±16.9 |
| II-1 | 25 | 2.32±0.38 | 253.3±53.1 | 157.4±21.7 |
| I-2 | 25 | 2.50±0.35 | 267.9±48.5 | 136.0±13.3 |
| II-2 | 25 | 2.14±0.41 | 194.7±38.0[b] | 138.2±19.5 |
| Control[a] | — | 3.50±0.24 | 394.5±36.5 | 214.0±15.4 |
| I-3 | 25 | 2.72±0.29 | 289.8±36.2 | 156.8±11.9 |
| II-3 | 25 | 1.95±0.41[c] | 180.2±39.8[d] | 120.1±18.6[c] |
| I-4 | 25 | 3.09±0.29 | 318.6±33.8 | 177.9±15.3 |
| II-4 | 25 | 1.75±0.44[c] | 170.1±49.0[c] | 120.4±24.8[c] |
| Cystamine | 25 | 1.80±0.39[d] | 192.2±49.6[c] | 129.9±20.8[c] |
| Control[a] | — | 2.49±0.32 | 289.3±36.5 | 150.9±13.5 |
| I-5 | 25 | 2.44±0.36 | 320.8±54.9 | 150.2±19.4 |
| II-5 | 25 | 0.93±0.13[d] | 91.1±15.1[d] | 81.5± 8.1[d] |
| I-9 | 25 | 1.68±0.38 | 187.5±49.6 | 125.4±23.0 |
| II-9 | 25 | 1.90±0.30 | 207.6±35.9 | 135.1±16.6 |
| Control[a] | — | 2.98±0.26 | 331.4±34.9 | 184.2±13.2 |
| I-6 | 25 | 2.10±0.26[b] | 229.2±30.5[b] | 139.9±15.8[b] |
| II-6 | 25 | 0.97±0.20[d] | 97.4±24.3[d] | 70.9±11.1[d] |
| I-7 | 25 | 2.20±0.43 | 243.5±49.7 | 143.3±22.7 |
| II-7 | 25 | 1.50±0.24[d] | 167.9±31.9[c] | 108.3±12.3[d] |
| Cystamine | 25 | 1.42±0.16[d] | 150.0±18.9[d] | 99.0± 7.8[d] |
| Control[a] | — | 2.37±0.36 | 223.4±58.0 | 138.4±15.3 |
| I-8 | 25 | 1.66±0.41 | 177.9±50.3 | 116.4±21.0 |
| II-8 | 25 | 1.02±0.14[c] | 108.1±18.1 | 73.9± 7.4[c] |

All values represent the mean±S.E. of 8 rats. *a*) Acacia, 5% in saline. Each sample was intraperitoneally administered immediately after pylorus ligation. Significantly different from the control group: *b*) $p<0.05$, *c*) $p<0.01$, *d*) $p<0.001$.

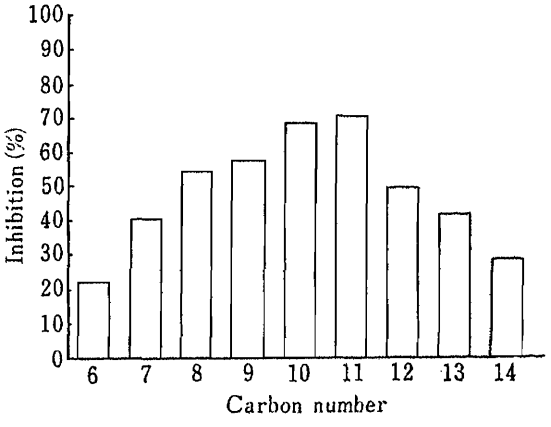


Fig. 1. Effect of Carbon Number of Unsaturated Fatty Acids in Various 2-(*E*-2-Alkenoylamino)ethyl Carbamoylmethyl Sulfides on Gastric Secretion in Pylorus-Ligated Rats (4 h)

Each column represents percent inhibition of total acid output in various 2-(*E*-2-alkenoylamino)ethyl carbamoylmethyl sulfide-treated groups against that in the control group. Each sample was administered intraperitoneally (25 mg/kg) immediately after pylorus ligation.

the unsaturated fatty acid in the synthesized sulfides. Namely, the peak of gastric secretion-inhibitory activity was observed at 10 or 11 carbons in the unsaturated fatty acid (Fig. 1).

**Anti-ulcer Activity of 2-(*E*-2-Decenoylamino)ethyl Carbamoylmethyl Sulfide (II-5) and 2-(*E*-2-Undecenoylamino)ethyl Carbamoylmethyl Sulfide (II-6) on Various Experimental Ulceration Models in Rats**

The effects of II-5 and II-6, which exhibited the strongest gastric secretion-inhibitory

TABLE III. Effect of 2-(*E*-2-Decenoylamino)ethyl Carbamoylmethyl Sulfide and 2-(*E*-2-Undecenoylamino)ethyl Carbamoylmethyl Sulfide on Stress-, Aspirin- and HCl·Ethanol-Induced Ulceration in Rats

| Ulceration | Treatment | Dose (mg/kg) | Ulcer index | Inhibition (%) |
|---|---|---|---|---|
| Stress-induced ulceration (7 h) | Control[a] | — | 29.1 ± 3.0 | — |
| | II-5[b] | 20 | 13.3 ± 5.1[e] | 54.3 |
| | II-6[b] | 20 | 9.0 ± 2.7[f] | 69.1 |
| | Cimetidine[b] | 80 | 5.4 ± 1.8[g] | 81.4 |
| Aspirin-induced ulceration (7 h) | Control[a] | — | 17.1 ± 2.8 | — |
| | II-5[c] | 20 | 8.6 ± 2.5[e] | 49.7 |
| | II-6[c] | 20 | 4.0 ± 1.1[g] | 76.4 |
| | Cimetidine[c] | 80 | 2.9 ± 0.7[g] | 83.0 |
| HCl·ethanol-induced ulceration (1 h) | Control[a] | — | 41.3 ± 7.4 | — |
| | II-5[d] | 20 | 12.5 ± 3.0[f] | 69.7 |
| | II-6[d] | 20 | 12.2 ± 3.4[f] | 70.5 |
| | Cimetidine[d] | 80 | 31.3 ± 12.7 | 24.2 |

All values represent the mean ± S.E. of 8 rats. *a*) Acacia, 5% in saline. *b*) Each sample was intraperitoneally administered immediately before the restraint and water-immersion stress loading. *c*) Each sample was intraperitoneally administered immediately after pylorus ligation. *d*) Each sample was intraperitoneally administered 2 h before the per oral administration of 150 mM HCl, 60% ethanol (1.5 ml/rat) to rats. Significantly different from the control group: *e*) $p<0.05$, *f*) $p<0.01$, *g*) $p<0.001$.

activity, on water-immersion stress-, aspirin-, and HCl–ethanol-induced gastric ulcers in rats were examined.

**Stress-Induced Gastric Ulcer**——At 20 mg/kg i.p., the ulcer index of the animals treated with II-5 and II-6 was significantly less ($p<0.05$) than that of the control group, and the inhibitory activity of II-6 was more potent than that of II-5. Cimetidine was used as a positive control (Table III).

**Aspirin-Induced Gastric Ulcer**——As shown in Table III, II-5 and II-6 showed a significant decrease in their ulcer indices at a dose of 20 mg/kg i.p., and II-6 was more effective than II-5. Compound II-6 showed almost the same activity as cimetidine, which was used as a positive control.

**HCl–Ethanol-Induced Gastric Ulcer**——Both II-5 and II-6 showed the same inhibitory ratio (about 70%) for HCl–ethanol-induced gastric ulcer at a dose of 20 mg/kg i.p. Cimetidine, used as a positive control, did not show a significant inhibition, even at a dose of 80 mg/kg i.p.

**Effect of Dispersive Agents for II-5 and II-6 on Stress-Induced Gastric Ulcer in Rats**

Compounds II-5 and II-6 were hardly soluble in water, so we used them as a suspension in 5% gum arabic solution. In order to examine the effect of dispersive agents for these two derivatives, we used gum arabic and HCO-60 (a detergent; Nikko Chemicals), and compared their inhibitory effects on water immersion stress-loaded rats. Peroral administration, in 5% gum arabic, gave a weaker activity than intraperitoneal administration; however, the inhibition of ulceration was substantial (about 50—60%) at a dose of 20 mg/kg. At a dose of 5 mg/kg, the inhibition was as low as 40% (not significantly different from the control).

Compounds II-5 and II-6 showed more potent inhibitory activity when they were suspended in 10% HCO-60 in saline than when they were suspended in 5% gum arabic solution (Table IV).

The relationship between the administered dose and the antiulcer activity of II-5 and II-6 was examined by using restrained and water-immersion stress-loaded rats. Both acetamides

TABLE IV. Effect of 2-(*E*-2-Decenoylamino)ethyl Carbamoylmethyl Sulfide and 2-(*E*-2-Undecenoylamino)ethyl Carbamoylmethyl Sulfide on Stress-Induced Ulceration in Rats

| Treatment | Dose (mg/kg) | Ulcer index | Inhibition (%) |
|---|---|---|---|
| Control[a] | — | 16.8±2.6 | — |
| II-5 | 20 | 8.4±1.1[c] | 50.0 |
| | 5 | 9.7±2.1 | 42.3 |
| II-6 | 20 | 6.7±0.8[d] | 60.1 |
| | 5 | 10.4±1.6 | 38.1 |
| Control[b] | — | 18.1±3.7 | — |
| II-5 | 20 | 7.9±1.2[c] | 56.4 |
| | 5 | 9.2±2.5 | 49.2 |
| II-6 | 20 | 6.7±1.1[d] | 63.0 |
| | 5 | 8.4±1.9[c] | 53.6 |

All values represent the mean±S.E. of 8 rats. *a*) Acacia, 5% in saline. *b*) HCO-60, 10% in saline. Each sample was perorally administered immediately before the restraint and water-immersion stress loading. Significantly different from the control group: *c*) $p<0.05$, *d*) $p<0.01$.

TABLE V. Effect of Various 2-(*E*-2-Alkenoylamino)ethyl Carbamoylmethyl Sulfides on Stress-Induced Ulceration in Rats

| Treatment | Dose (mg/kg) | Ulcer index | Inhibition (%) |
|---|---|---|---|
| Control[a] | — | 15.1±1.3 | — |
| II-1 | 5 | 13.3±2.3 | 11.9 |
| II-5 | 5 | 7.5±1.4[c] | 50.3 |
| II-6 | 5 | 7.0±1.1[d] | 53.6 |
| Control[a] | — | 15.6±1.9 | — |
| II-2 | 5 | 10.8±1.7 | 30.9 |
| II-3 | 5 | 11.4±1.2 | 26.6 |
| II-4 | 5 | 9.4±1.5[b] | 39.5 |
| Control[a] | — | 18.6±2.4 | — |
| II-7 | 5 | 14.3±2.8 | 23.1 |
| II-8 | 5 | 17.6±1.4 | 5.4 |
| II-9 | 5 | 18.5±3.2 | 0.5 |

All values represent the mean±S.E. of 8 rats. *a*) HCO-60, 10% in saline. Each sample was perorally administered immediately before the restraint and water-immersion stress loading. Significantly different from the control group: *b*) $p<0.05$, *c*) $p<0.01$, *d*) $p<0.001$.

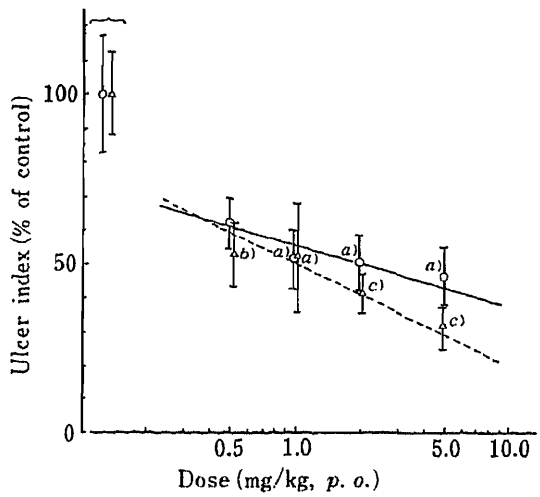


Fig. 2. Dose-Response Curves for the Inhibitory Effect of 2-(*E*-2-Decenoylamino)ethyl Carbamoylmethyl Sulfide and 2-(*E*-2-Undecenoylamino)ethyl Carbamoylmethyl Sulfide on Stress-Induced Ulceration in Rats

Each point represents the mean±S.E. of 8 rats. Significantly different from each control group: *a*) $p<0.05$, *b*) $p<0.01$, *c*) $p<0.001$. ○—○, II-5; △--△, II-6; ⌒⌒, control (10% HCO-60 in saline).

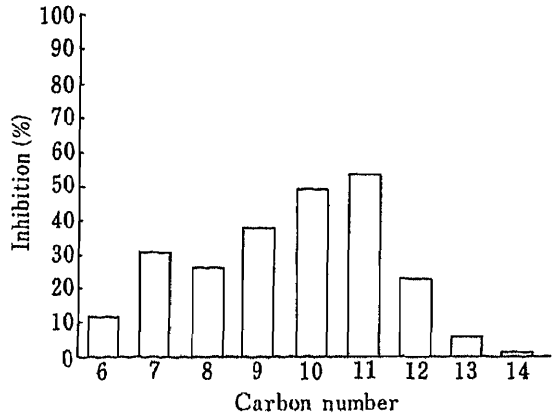


Fig. 3. Effect of Carbon Number of Unsaturated Fatty Acids in Various 2-(*E*-2-Alkenoylamino)ethyl Carbamoylmethyl Sulfides on Stress-Induced Ulceration in Rats (7 h)

Each column represents percent inhibition of ulcer index in various 2-(*E*-2-alkenoylamino)ethyl carbamoylmethyl sulfide-treated groups against that in the control group. Each sample was administered perorally (5 mg/kg) immediately before the restraint and water-immersion stress loading.

showed a dose-dependent decrease of the ulcer index between the dosage range from 0.5 to 5 mg/kg *p.o.* (Fig. 2). The $ED_{50}$ values (Fig. 2) were about 2 mg/kg (1—5 mg/kg) for II-5 and about 1 mg/kg (0.5—2.5 mg/kg) for II-6.

**Effect of Carbon Number of Unsaturated Fatty Acid in Various Sulfides on Stress-Induced Gastric Ulceration in Rats**

Compounds II-1—II-9 were suspended with 10% HCO-60 solution and administered at a

dose of 5 mg/kg *p.o.* to rats, which were then restrained for 7 h during water-immersion stress loading. The ulcer indices obtained are shown in Table V. The correlation between the inhibition ratio (%) of ulcer index (treated *vs.* control) and the alkenyl chain length of the unsaturated fatty acid in various sulfides is summarized in Fig. 3.

The strongest inhibitory activity was observed between the carbon numbers of 10 and 11 gave the most potent activity.

**Acute Toxicity Test of II-5 and II-6 in Mice**

No deaths or toxic symptoms were observed in mice at any dose examined (*p.o.* or i.p.) during the experimental period. The increase of body weight was unaffected when the test samples were administered perorally. However, when the test samples were administered intraperitoneally, a slight inhibition of body weight gain was observed a few days after the sample administration in the higher dosage groups (8000 and 2000 mg/kg) of both compounds.

## Discussion

We have found that reduction and alkylation of interchain disulfide bonds of native IgG result in the appearance of gastric secretion-inhibitory activity. Alkylation of thiols was necessary, because the heavy and light chains in which SH groups were left free showed no inhibitory activity.[1)]

In the research described in this paper, we studied the effect of modification of the SH group of simple thiol-containing amino acids and amines. Comparison of cystine and cysteine, cystamine and cysteamine indicated that the compounds which had free SH groups showed no anti-gastric secretion activity; compounds which had masked SH groups were, however, effective. Among various amino acids and amines containing a thiol, cystamine showed the strongest activity. We have already reported that *trans*-2-unsaturated fatty acids inhibited gastric secretion.[4)] Therefore, we prepared derivatives of cystamine using *trans*-2-unsaturated fatty acids with various chain lengths. Disulfide (I) and sulfide (II) derivatives were screened for pharmacological activity, and it was found that compounds (II) which has a carbamoylmethylated sulfide moiety showed stronger inhibitory activity than those having disulfides (I) in the stress ulceration model. Moreover, there was a relationship between the chain length of 2-alkenoic acid and the biological activity; the compounds containing a 2-alkenoic acid with a chain length of 10 to 11 carbon atoms (II-5, II-6) showed the strongest activity.

Therefore, in the next step, we tested II-5 and II-6 in other experimental ulcer models induced by aspirin and HCl–ethanol. Both compounds showed potent inhibitory activity in both models. In the formation of stress-induced, pylorus-ligation and aspirin-induced ulcers, the reduction of gastric membrane defensive factors is reported to be important, in addition to the influence of gastric acid as an offensive factor.[8,9)] Further study will be necessary to elucidate the mechanism of action of our compounds.

These compounds also showed anti-ulcerogenic activity when the administration route was changed from peritoneal to peroral, at a dose of 20 mg/kg in the water-immersed stress model. At a dose of 5 mg/kg, both compounds showed approximately 40% inhibition, which was not statistically significant when compared with the control group. However, when dispersed in 10% HCO-60 and administered orally, both compounds showed more potent activity than when administered with 5% gum arabic. The results suggested that the compounds were better dispersed in 10% HCO-60 than 5% gum arabic and were better absorbed.

A dose-dependent decrease of ulcer index was observed in the restrained and water-immersion stress-loaded rats at the dosage range from 0.5 to 5 mg/kg *p.o.* for both

compounds. This activity is comparable with that of commonly used anti-peptic ulceration drugs.

Since no toxic symptoms were observed at any dose tested in mice (perorally or intraperitoneally), these derivatives may be practically useful as anti-peptic-ulceration drugs.

**References**

1) T. Mimura, T. Terada, M. Iwai, I. Kohda, S. Take, K. Maeda and S. Aonuma, *J. Pharmacobio-Dyn.*, **6**, 397 (1983).
2) T. Mimura, K. Tsujikawa, H. Nakajima, M. Okabe, Y. Kohama, M. Iwai and K. Yokoyama, *J. Pharmacobio-Dyn.*, **9**, 46 (1986).
3) T. Mimura, H. Tsujibo, N. Muto, S. Otsuka and S. Aonuma, *Chem. Pharm. Bull.*, **28**, 1077 (1980).
4) T. Mimura, I. Kohda, K. Maeda, M. Iwai, Y. Sasaki, S. Aonuma and T. Momose, *J. Pharmacobio-Dyn.*, **6**, 527 (1983).
5) K. Takagi and S. Okabe, *Jpn. J. Pharmacol.*, **18**, 9 (1968).
6) S. Okabe, K. Takeuchi, K. Nakamura and K. Takagi, *Jpn. J. Pharmacol.*, **24**, 363 (1974).
7) T. Mizui and M. Doteuchi, *Jpn. J. Pharmacol.*, **33**, 939 (1983).
8) H. Kitagawa, M. Fujiwara and Y. Osumi, *Gastroenterology*, **7**, 298 (1979).
9) S. Okabe, K. Takeuchi, N. Nakamura and K. Takagi, *Jpn. J. Pharmacol.*, **24**, 363 (1974).

[Chem. Pharm. Bull. 35(11)4626—4631(1987)]

# Evidence That Lipid Peroxidation by Doxorubicin Does Not Initiate the Beat Inhibition of Cultured Mouse Myocardial Cells

KYOKO TAKAHASHI,*,[1] TADANORI MAYUMI and TAKEO KISHI

*Faculty of Pharmaceutical Sciences, Kobe-Gakuin University, Nishi-ku, Kobe 673, Japan*

(Received May 1, 1987)

In order to elucidate the biochemical mechanism by which doxorubicin (DX) induces cumulative dose-dependent cardiomyopathy, the effect of DX on beating and on lipid peroxide level in myocardial cells was investigated by using a mouse myocardial cell culture system. Inhibition by DX of the beating of cultured myocardial cells was dose- and exposure time-dependent. When incubated with DX for 0.5 h, the number of beating cells decreased to 74% at 172 $\mu$M, 52% at 345 $\mu$M and 37% at 517 $\mu$M, and the lipid peroxide level in the cells increased significantly at 345 $\mu$M DX or more. At the low dose of 3.5 $\mu$M DX, though the number of beating cells decreased to 72% at 24 h, the lipid peroxide level in the cells was about the same as that without DX at 24 h, and increased to about 1.5 times that of the control at 48 h. Under the same conditions as above, 120 $\mu$M $\alpha$-tocopherol (Toc) added in advance of the treatment reduced by 86% the lipid peroxidation by DX, but did not protect the beating from DX toxicity. In contrast, 120 $\mu$M coenzyme $Q_{10}$ ($CoQ_{10}$) reduced the lipid peroxidation by only 33%, but increased the number of beating cells at 48 h from 42% to 68%. We conclude that the lipid peroxidation by DX does not initiate the beat inhibition of cultured myocardial cells, and that the protective effect of $CoQ_{10}$ on beating is also based on biochemical actions other than reduction of the lipid peroxidation.

**Keywords**——doxorubicin; cardiotoxicity; lipid peroxidation; coenzyme $Q_{10}$; $\alpha$-tocopherol; cardiac cell culture

## Introduction

Doxorubicin (adriamycin, DX) is a member of the anthracycline antibiotics that has been widely accepted as a major chemotherapeutic agent in the treatment of a variety of malignancies.[2] The usefulness of this drug has been limited not only by common toxicities of antineoplastic agents such as bone-marrow suppression, but also by cardiotoxicity.[3,4] The biochemical mechanism by which DX induces myocardial toxicity has been a subject of extensive investigations but still remains unresolved. One of the proposed mechanisms for DX cardiotoxicity is an increase in lipid peroxides in the myocardium. Myers *et al.*[5] studied the effect of DX on lipid peroxidation in mice and observed the accumulation of lipid peroxides in the myocardium of DX-treated animals. Further, they showed that $\alpha$-tocopherol (Toc) significantly reduced the incidence and severity of DX cardiomyopathy. On the other hand, there are many reports indicating that coenzyme $Q_{10}$ ($CoQ_{10}$) is also benefical for cardiac damage induced by DX.[6-10] Takeshige *et al.*[8] suggested that the reduced form of $CoQ_{10}$ might act as an antioxidant.

In the present paper, we describe the changes of lipid peroxide levels in cultured mouse myocardial cells and their beating status after DX addition, and compare the effects of $CoQ_{10}$ and Toc on both these parameters.

## Experimental

**Materials**——DX was kindly donated by Kyowa Hakko Co., Chiyoda-ku, Tokyo, Japan. $CoQ_{10}$, Toc and their

solvent (HCO-60) were supplied by courtesy of Eizai Co., Bunkyo-ku, Tokyo, Japan. The other agents were of analytical reagent grade.

**Mouse Embryo Cardiac Cell Culture**——The method of myocardial cell culture was described elsewhere.[10] In brief, hearts from 14- to 16 day-old mouse embryos (ICR strain) were minced and digested with 5 ml of 0.125% trypsin–0.025% collagenase solution at 37 °C for 15—20 min. The dispersed myocardial cells were filtered then collected by centrifugation at $200 \times g$ for 10 min. Cardiac cells $2—4 \times 10^5$ per dish were seeded into Petri dishes (35 mm i.d.) each containing 1 ml of Ham's F-12 medium supplemented with 10% newborn calf serum. The cells were incubated at 37 °C in a humidified atmosphere of 5% $CO_2$–95% air. Two different cell types, myocardial cells and fibroblast-like cells, could be easily distinguished under a phase-contrast microscope. In our experiments, the ratio of myocardial cells to fibroblast-like cells was 4 : 1. The following studies were started after a 24 h preincubation, during which period 90% of cultured myocardial cells showed rhythmical spontaneous beating.

**Measurement of Beating**——The beating status of cultured myocardial cells was monitored with an inverted phase-contrast microscope at a magnification of 150 to 400 in a chamber controlled at 37 °C. In each culture dish, about twenty cells or clusters, which were beating regularly at the mean beating rate of 102 beats/min, were selected for each experiment, and their beating rates, shapes and locations in the dish were recorded before application of the test agents. Beating of each cell or cluster was usually counted for 60 s at the time indicated. Each experiment was repeated at least three times by using separately prepared cell cultures, and the results were averaged.

**Measurement of Lipid Peroxides**——Lipid peroxide content was determined fluorometrically by Yagi's method.[11] 1,1,3,3-Tetraethoxypropane was employed as the standard, and the total amount of lipid peroxides was expressed as picomoles of malondialdehyde (MDA) equivalent per microgram of cellular protein. The sample for the MDA determination was prepared as follows. At the time indicated, the medium containing DX was removed from the dish. Then, the cells attached to the dish were washed 3 times with 0.5 ml of cold phosphate-buffered saline (PBS, pH 7.4), and then dissolved in 0.5 ml of 0.1 M sodium hydroxide solution for 30 min. Two-thirds of the sodium hydroxide solution was diluted with distilled water to a final volume of 2 ml. This solution (2 ml) was added to 1 ml of 2% (w/v) 2-thiobarbituric acid and heated for 60 min on a boiling water bath. After cooling of the mixture, 5 ml of *n*-butanol was added and the whole was mixed vigorously. The butanol phase was separated by centrifugation and its fluorescence intensity was measured at an excitation wavelength of 515 nm and an emission wavelength of 553 nm. The rest of the solution was used for the measurement of protein content by the method of Lowry *et al.*[12]

## Results

### Effects of $CoQ_{10}$ and Toc on the Beat Inhibition by DX

Effects of $CoQ_{10}$ and Toc on the beat inhibition by DX were compared and are summarized in Tables I and II. As shown in a previous report,[10] the inhibition by DX was dose- and time-dependent and 50% cessation of beating was observed at 430 $\mu$M DX (0.5 h), 280 $\mu$M DX (1 h), 70—100 $\mu$M DX (4 h) or 3.5 $\mu$M DX (36 h). Thus, the preventive effects of $CoQ_{10}$ and Toc were compared in the presence of high and low doses of 140 $\mu$M DX and 3.5 $\mu$M DX, respectively.

In the presence of 140 $\mu$M DX, the number of beating cells and the beating rate decreased to 68% and 44% of the initial values at 1 h and to 26% and 15% at 4 h, respectively. $CoQ_{10}$ added in advance did not substantially protect beating of the cells at 1 h after the DX addition, but did provide significant protection at 4 h. At 4 h, $CoQ_{10}$ increased the number of beating cells from 26% to 48% and the beating rates from 15% to 27%. On the other hand, Toc added in advance did not affect the cell beating at all.

When cultures were incubated with 3.5 $\mu$M DX, $CoQ_{10}$ did not appreciably protect beating cells at 24 h, but did so significantly at 48 and 72 h. $CoQ_{10}$ increased the number of beating cells from 42% to 68% at 48 h and from 5% to 16% at 72 h. The protective effect of $CoQ_{10}$ against the decrease of beating rate by DX was not statistically significant. However, Toc did not protect the beating, *i.e.*, the beating cell number or the beating rate, from DX toxicity at all, but stimulated the DX toxicity. Toc decreased the number of beating cells from 72% to 49% at 24 h incubation with 3.5 $\mu$M DX. Further, significant differences were observed between the effects of $CoQ_{10}$ and Toc on the beating with incubation at 3.5 $\mu$M DX for 24—72 h (Tables I and II).

TABLE I. Protective Effects of $CoQ_{10}$ and Toc against Cessation of Beating Induced by DX

| DX ($\mu$M) | Incubation time (h) | Beating cell number (%) None | $CoQ_{10}$ | Toc |
|---|---|---|---|---|
| 3.5 | 24 | 58/81 (72) | 63/81 (78) | 40/81 (49)[b,c] |
| | 48 | 34/81 (42) | 55/81 (68)[c] | 29/81 (36)[e] |
| | 72 | 4/81 (5) | 13/81 (16)[a] | 2/81 (3)[d] |
| 140 | 1 | 55/81 (68) | 60/81 (74) | 37/54 (69) |
| | 4 | 21/81 (26) | 39/81 (48)[b] | 20/54 (37) |

Beating cell number is given as the ratio of beating cells at the indicated time to that at 0 h. Figures in parentheses are the percentages. The control medium (none) contained the solvent for $CoQ_{10}$ and Toc solution. In other cases, 120 $\mu$M $CoQ_{10}$ or 120 $\mu$M Toc and the solvent were added to the medium at the seeding time. Values with superscripts *a*, *b*) and *c*) are significantly different from the corresponding control values (none) with $p<0.01$, $p<0.005$ and $p<0.001$ (by $X^2$-test), respectively. Values with superscripts *d*) and *e*) are significantly different from the corresponding $CoQ_{10}$ with $p<0.005$ and $p<0.001$ (by $X^2$-test), respectively.

TABLE II. Protective Effects of $CoQ_{10}$ and Toc on Inhibition for Beating Rate by DX

| DX ($\mu$M) | Incubation time (h) | Beating rate (%) None | $CoQ_{10}$ | Toc |
|---|---|---|---|---|
| 3.5 | 24 | 75±7 (81) | 86±7 (81) | 58±9[b] (81) |
| | 48 | 35±7 (81) | 51±7 (81) | 27±5[c] (81) |
| | 72 | 5±3 (81) | 9±3 (81) | 1±0.5[c] (81) |
| 140 | 1 | 44±4 (81) | 42±4 (81) | 37±5 (54) |
| | 4 | 15±3 (81) | 27±4[a] (81) | 19±4 (54) |

Beating rate is given as the rate of beating cells at the indicated time to that at 0 h. Beating rates of none, $CoQ_{10}$ and Toc at 0 h were 40 to 200 beats/min (average 104), 40 to 170 beats/min (average 99) and 30 to 170 beats/min (average 96), respectively. Beating rates are expressed as averaged beating rates (mean ± S.E.) of individual cells, and figures in parentheses are the numbers of observed cells. The control medium (none) contained the solvent for $CoQ_{10}$ and Toc solution. In other cases, 120 $\mu$M $CoQ_{10}$ or 120 $\mu$M Toc and the solvent were added to the medium at the seeding time. The value with superscript *a*) is significantly different from the corresponding control (none) with $p<0.02$ (by Student's *t*-test). Values with superscripts *b*) and *c*) are significantly different from the corresponding $CoQ_{10}$ with $p<0.02$ and $p<0.01$ (by Student's *t*-test), respectively.

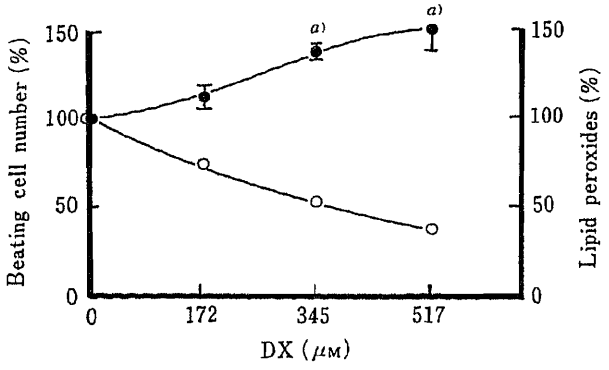


Fig. 1. Effect of DX on Lipid Peroxidation and Beating of Cardiac Cells

Open circles and closed circles show beating cell number and lipid peroxide content, respectively. Beating cell numbers are given as the ratios of beating cells at 0.5 h after the addition of various concentrations of DX to those at 0 h. Data on lipid peroxide contents are expressed as mean percentage ± S.E. of 10 experiments with respect to the content (1.54 pmol/$\mu$g protein) after incubation without DX for 0.5 h.

*a*) Significant differences from the control (without DX) with $p<0.01$ by Student's *t*-test.

## The Beat Inhibition and the Lipid Peroxidation by DX

The above results are interesting in connection with the relation of the beat inhibition with lipid peroxidation, since Toc is a more effective antioxidative agent than $CoQ_{10}$. Thus, we investigated whether or not DX stimulated the formation of lipid peroxides under our experimental conditions. Figure 1 shows the effects of DX on the lipid peroxidation and the beating of the cells. The data in Fig. 1 were determined at 0.5 h after DX addition. Accordingly, the results reflect the acute toxicity of DX at high doses. Under such conditions, the number of beating cells decreased to 74% of the initial value at 172 $\mu$M DX, 52% at 345 $\mu$M DX and 37% at 517 $\mu$M DX. However, a significant increase in lipid peroxides in the cells was observed only at 345 $\mu$M or more DX.

When the cells were incubated with a low dose of 3.5 $\mu$M DX, the number of beating cells decreased to 79% at 24 h, 29% at 48 h and 6% at 72 h, as shown in the previous report.[10]

TABLE III. Effects of DX on the Lipid Peroxide Contents in Cardiac Cells

| DX ($\mu$M) | Incubation time (h) | Lipid peroxide content[a] (pmol/$\mu$g protein) |
|---|---|---|
| None | 4 | 1.29±0.233 (11) |
| | 24 | 1.93±0.268 (9) |
| | 48 | 2.01±0.177 (9) |
| 3.5 | 24 | 1.78±0.0156 (10) |
| | 48 | 3.07±0.237[c] (10) |
| 140 | 4 | 2.02±0.181[b] (13) |

*a*) The total content of lipid peroxides was calculated in MDA eq and is expressed as the mean±S.E. (figures in parentheses are the numbers of experiments). Values with superscripts *b*) and *c*) are significantly higher than the corresponding controls with $p<0.02$ and $p<0.01$ (by Student's *t*-test), respectively.

TABLE IV. Effects of $CoQ_{10}$ and Toc on Lipid Peroxidation by Low and High Doses of DX

| DX ($\mu$M) | Incubation time (h) | Lipid peroxide content (%) | | |
|---|---|---|---|---|
| | | None | $CoQ_{10}$ | Toc |
| 3.5 | 48 | 153±12 (8) | 102± 8[a] (8) | 21±2[c] (8) |
| 140 | 4 | 154±19 (4) | 167±30 (4) | 56±6[b] (4) |

The control medium (none) contained the solvent for $CoQ_{10}$ and Toc solution. In other cases, 120 $\mu$M $CoQ_{10}$ or 120 $\mu$M Toc and the solvent were added to the medium at the seeding time. Lipid peroxide contents are expressed as mean percentage±S.E. with respect to the content in the case incubated without DX for 48 h or 4 h (none). The averaged contents of none (without DX) were 1.20 pmol/$\mu$g protein at 4 h and 2.77 pmol/$\mu$g protein at 48 h. Figures in parentheses are the number of experiments. Values with superscripts *a*, *b*) and *c*) are significantly different from the corresponding control values (none) with $p<0.05$, $p<0.02$ and $p<0.001$ (by Student's *t*-test), respectively.

Under the same conditions, the addition of 3.5 $\mu$M DX did not significantly increase lipid peroxides in the cells at 24 h, but increased them to about 1.5 times the control at 48 h (Table III). When incubated with a high dose of 140 $\mu$M DX for 4 h, the lipid peroxides in the cells increased to 2.02 pmol/$\mu$g protein compared with 1.29 pmol/$\mu$g protein in the control (Table III).

The effects of $CoQ_{10}$ and Toc on the lipid peroxidation by 3.5 $\mu$M DX are shown in Table IV. The data were expressed as percent of the control incubated without DX for 48 h. Addition of 120 $\mu$M Toc in advance of the DX treatment reduced lipid peroxides in the cells to 20% of the initial level, but did not protect the beating from DX toxicity at all (Tables I and II). In contrast, addition of 120 $\mu$M $CoQ_{10}$ decreased lipid peroxides only to the same level as the initial level, but significantly increased the number of beating cells at 48 h from 42% to 68% (Tables I and IV). Such effects of $CoQ_{10}$ and Toc on the beating and the lipid peroxidation were obtained in the case of 140 $\mu$M DX at 4 h (Tables I, II and IV). Namely, Toc prevented the lipid peroxidation by DX more effectively than $CoQ_{10}$, but did not prevent the beat inhibition by DX.

## Discussion

The biochemical mechanisms by which DX induces cardiomyopathy are still obscure despite a number of investigations using *in vivo* and *in vitro* systems. However, lipid peroxidation by DX is an attractive candidate mechanism. DX can be converted to free radical semiquinones *via* the acceptance of one electron from reduced nicotinamide adenine dinucleotide phosphate (NADPH)–cytochrome P-450 reductase[4,13-15] and the free radical thus formed may subsequently transfer an electron to molecular oxygen, thereby generating superoxide ion. Activities of catalase and superoxide dismutase of detoxifying activated oxygen in the heart are much weaker than in the liver.[13] In addition, Se-glutathione (GSH) peroxidase in the heart may be depleted by DX treatment.[16,17] Myers *et al.*[5] first reported the stimulation of lipid peroxidation in the myocardium of mouse induced with DX *in vivo*, and showed that Toc caused a significant reduction of the incidence and severity of histological changes observed in DX cardiomyopathy.

Recently, several reports have suggested that Toc is ineffective in preventing DX

cardiotoxicity *in vivo*[18,19] and *in vitro*.[20,21] Thus, we investigated whether DX stimulated the formation of lipid peroxides under our experimental conditions. If some biochemical abnormalities cause the cardiotoxicity, they must develop before or in parallel to the functional and structural alterations of myocardial tissue by DX. We[10] have previously reported that the beating status of myocardial cells is a sensitive and reliable parameter in a mouse myocardial cell culture system for studies on the cardiotoxicity of DX, and we showed that functional alterations by DX in this system were similar to those seen *in vivo*. Lampidis *et al.*[22] also showed that structural and functional alterations induced by DX in cultured rat heart cells are similar to those seen *in vivo*, and can be related to DX dose and exposure time. The doses of 3.5 and 140 $\mu$M DX in our work seem to correspond to their low (or intermediate) and high doses, *i.e.*, the levels for so-called chronic and acute toxicities, respectively.

The lipid peroxidation in myocardial cells was significantly enhanced by incubations with low and high doses of DX. At the dose of 3.5 $\mu$M DX, however, a pronounced increase in the lipid peroxide level in the cells was observed after the beat inhibition. When the cells were incubated with DX for 0.5 h, the concentration of DX required for the stimulation of lipid peroxidation in the cells was high in comparison with that for the beat inhibition. These results suggested that the accumulation of lipid peroxides in the cells does not trigger DX toxicity.

On the other hand, $CoQ_{10}$ has been reported to partially reduce DX cardiotoxicity.[6-8] Takeshige *et al.*[8] have suggested that the reduced form of $CoQ_{10}$ acts as an antioxidant in beef heart mitochondria. Thus, the effects of $CoQ_{10}$ and Toc on the beat inhibition by DX were compared using this system. Though Toc showed a much stronger antioxidative effect than $CoQ_{10}$, Toc did not protect the beating from DX toxicity. In contrast, $CoQ_{10}$ significantly increased the number of beating cells and beating rate despite the fact that there was no or a slight reduction in the lipid peroxide level. These results provide further support for the view that the stimulation of the lipid peroxidation by DX is not directly involved in the inhibition of beating of the cultured myocardial cells, and that the protective effect of $CoQ_{10}$ is not based on depression of lipid peroxide formation.

Several types of biochemical actions of DX, except for the lipid peroxidation described above, have been found and suggested as possible mechanisms of DX cardiotoxicity. These include: (a) mitochondrial dysfunction,[23,24] (b) inhibition of nucleic acid synthesis,[25,26] (c) membrane perturbation,[27,28] or (d) disturbance of electolyte balance,[29,30] (e) interaction with contractile proteins.[31] However, there is little evidence to show why the cumulative and dose-dependent toxicity of DX is severe in the heart but not in other tissues.

The myocardium is a strongly energy-consuming tissue, and the energy for the myocardial function is generated and supplied mainly through the mitochondrial respiratory chain, which is aboundant in heart mitochondria *in vivo*.[24] Thus, the effect of DX on heart mitochondria has been studied intensively. In 1974, Gosalvez *et al.*[32] showed that DX inhibited mitochondrial respiration. Iwamoto *et al.*[24] reported that DX inhibited mitochondrial succinoxidase and NADH-oxidase activities from beef heart. We have proved previously that $CoQ_{10}$ prevents the inhibition of succinoxidase and NADH-oxidase activities by DX.[6] Further, we have shown that DX depresses the adenosine triphosphate (ATP) content in cultured myocardial cells.[10]

We have shown here that although Toc is ineffective, $CoQ_{10}$ partially prevents the inhibition of the beating of myocardial cells by low and high doses of DX (Tables I and II). It seems reasonable that $CoQ_{10}$ protects the cells from DX toxicity more effectively than Toc, since $CoQ_{10}$ can act not only as a radical-scavenger against lipid peroxidation in the cells, but also as an essential cofactor in the mitochondrial electron transport chain. Namely, the beating improvement by $CoQ_{10}$ may be mainly derived from its action on electron transfer and energy conservation in mitochondria.

**Acknowledgments** The authors wish to thank Prof. T. Hama, Dean of the Faculty of Pharmaceutical Sciences, Kobe-Gakuin University, for his valuable comments on the present study.

**References and Notes**

1) Present address: *Third Department of Internal Medicine, Osaka University Medical School, Fukushima-ku, Osaka 553, Japan.*
2) R. C. Young, R. F. Ozols and C. E. Myers, *New Eng. J. Med.*, **305**, 139 (1981).
3) M. R. Bristow, M. E. Billingham, J. W. Mason and J. R. Daniels, *Cancer Treat. Rep.*, **62**, 873 (1978).
4) C. Praga, G. Beretta, P. L. Vigo, G. R. Lenaz, G. Bonadonna, R. Canetta, R. Castellani, E. Villa, C. G. Gallagher, H. von Melchner, M. Hayat, P. Ribaud, G. De Wasch, W. Mattsson, R. Heinz, R. Walder, K. Kolaric, R. Buehner, W. Ten Bokkel-Huyninck, N. I. Perevodchikova, L. A. Manziuk, H. J. Senn and A. C. Mayr, *Cancer Treat. Rep.*, **63**, 827 (1979).
5) C. E. Myers, W. P. McGuire, R. H. Liss, I. Ifrim, K. Grotzinger and R. C. Young, *Science*, **197**, 165 (1977).
6) E. P. Cortes, M. Gupta, A. Chou, V. C. Amin and K. Folkers, *Cancer Treat. Rep.*, **62**, 887 (1978).
7) T. Kishi, T. Watanabe and K. Folkers, *Proc. Natl. Acad. Sci. U.S.A.*, **73**, 4653 (1976).
8) K. Takeshige, R. Takayanagi and S. Minakami, "Biomedical and Clinical Aspects of Coenzyme Q," Vol. 2, ed. by Y. Yamamura, K. Folkers and Y. Ito, Elsevier, North-Holland Biochemical Press, Amsterdam, 1980, pp. 15—20.
9) G. Zbinden, E. Bachmann and H. Bolliger, "Biomedical and Clinical Aspects of Coenzyme Q," ed. by K. Folkers and Y. Yamamura, Elsevier, North-Holland Biochemical Press, Amsterdam, 1977, pp. 219—228.
10) K. Takahashi, Y. Fujita, T. Mayumi, T. Hama and T. Kishi, *Chem. Pharm. Bull.*, **35**, 326 (1987).
11) K. Yagi, *Biochem. Med.*, **15**, 212 (1976).
12) O. H. Lowry, N. J. Rosebrough, A. L. Farr and R. J. Randall, *J. Biol. Chem.*, **193**, 265 (1951).
13) N. R. Bachur, S. L. Gordon, M. V. Gee and H. Kon, *Proc. Natl. Acad. Sci. U.S.A.*, **76**, 954 (1979).
14) N. Domae, H. Sawada, E. Matsuyama, T. Konishi and H. Uchino, *Cancer Treat. Rep.*, **65**, 79 (1981).
15) K. Fujita, K. Shinpo, K. Yamada, T. Sato, H. Niimi, M. Shamoto, T. Nagatsu, T. Takeuchi and H. Umezawa, *Cancer Res.*, **42**, 309 (1982).
16) J. H. Doroshow and J. Reeves, *Biochem. Pharmacol.*, **30**, 259 (1981).
17) R. D. Olson, J. S. MacDonald, C. J. van Boxtel, R. C. Boerth, R. D. Harbison, A. F. Slonim, R. W. Freeman and J. A. Oates, *J. Pharmacol. Exp. Ther.*, **215**, 450 (1980).
18) N. R. Bachur, S. L. Gordon and M. V. Gee, *Cancer Res.*, **38**, 1745 (1978).
19) J. H. Doroshow, G. Y. Locker and C. E. Myers, *J. Clin. Invest.*, **65**, 128 (1980).
20) M. R. Bristow, "Biomedical and Clinical Aspects of Coenzyme Q," Vol. 2, ed. by Y. Yamamura, K. Folkers and Y. Ito, Elsevier, North-Holland Biochemical Press, Amsterdam, 1980, pp. 179—188.
21) S. S. Legha, Y. Wang, B. Mackays, M. Ewer, G. N. Hortobagyi, R. S. Benjamin and M. K. Ali, *Ann. N. Y. Acad. Sci.*, **393**, 411 (1982).
22) T. J. Lampidis, I. C. Henderson, M. Israel and G. P. Canellos, *Cancer Res.*, **40**, 3901 (1980).
23) M. E. Ferrero, E. Ferrero, G. Gaja and A. Bernelli-Zazzera, *Biochem. Pharmacol.*, **25**, 125 (1976).
24) Y. Iwamoto, I. L. Hansen, T. H. Porter and K. Folkers, *Biochem. Biophys. Res. Commun.*, **58**, 633 (1974).
25) B. A. Chabner, C. E. Myers, C. N. Coleman and D. G. Johns, *New Eng. J. Med.*, **292**, 1159 (1975).
26) V. N. Iyer and W. Szybalski, *Science*, **145**, 55 (1964).
27) J. A. Siegfried, K. A. Kennedy, A. C. Sartorelli and T. R. Tritton, *J. Biol. Chem.*, **258**, 339 (1983).
28) T. R. Tritton and G. Yee, *Science*, **217**, 248 (1982).
29) M. Gosalvez, G. D. V. van Rossum and M. F. Blanco, *Cancer Res.*, **39**, 257 (1979).
30) H. M. Olson, D. M. Young, D. J. Prieur, A. F. Leroy and R. L. Reagan, *Am. J. Pathol.*, **77**, 439 (1974).
31) A. Someya, T. Akiyama, M. Misumi and N. Tanaka, *Biochem. Biophys. Res. Commun.*, **85**, 1542 (1978).
32) M. Gosalvez, M. Blanco, J. Hunter, M. Miko and B. Chance, *Eur. J. Cancer*, **10**, 567 (1974).

## Notes

[Chem. Pharm. Bull. 35(11)4632—4636(1987)]

# Magnesium Salt-Induced Opening of α,β-Epoxy Sulfoxides: A Synthesis of α-Chloro Ketones, α-Alkoxy Ketones, and α,β-Unsaturated Ketones from Carbonyl Compounds through α,β-Epoxy Sulfoxides[1)]

TSUYOSHI SATOH, ATSUSHI SUGIMOTO and KOJI YAMAKAWA*

*Faculty of Pharmaceutical Sciences, Science University of Tokyo, Ichigaya-funagawara-machi, Shinjuku-ku, Tokyo 162, Japan*

(Received May 6, 1987)

Magnesium chloride in alcohols was found to be effective to promote the opening of α,β-epoxy sulfoxides, giving a variety of compounds such as α-chloro ketones, α-alkoxy ketones, or α,β-unsaturated ketones. The products of the reaction were dependent upon the combination of the substituents on the epoxy group of α,β-epoxy sulfoxides, magnesium salt, solvent, and reaction conditions.

**Keywords**——α,β-epoxy sulfoxide; epoxide; α-chloro ketone; α-alkoxy ketone; α,β-unsaturated ketone; magnesium chloride

α-Halo ketones are useful intermediates for preparing heterocyclic compounds, including products obtained *via* the Favorskii rearrangement.[2)] Recently, we have reported a novel and versatile method for homologation of carbonyl compounds through α,β-epoxy sulfoxides[3)]; the α,β-epoxy sulfoxides (**3**), derived from carbonyl compounds (**2**) and 1-chloroalkyl phenyl sulfoxides (**1**) in nearly quantitative yields, on treatment with strong nucleophiles (such as selenolate, thiolate, and amine) gave dialkyl ketones (**4**: Nu = H) or α-substituted ketones (**4**) in quite good yields (Chart 1). In contrast to these results, it was found that weak nucleophiles such as alcoholates or acetate were rather intert toward the α,β-epoxy sulfoxides.[3f)] However, we recently found that magnesium chloride and magnesium perchlorate in alcohols were very effective to promote the opening of α,β-epoxy sulfoxides, giving a variety of products such as α-chloro ketones, α-alkoxy ketones, or α,β-unsaturated ketones. In this paper, we present the details of these results.

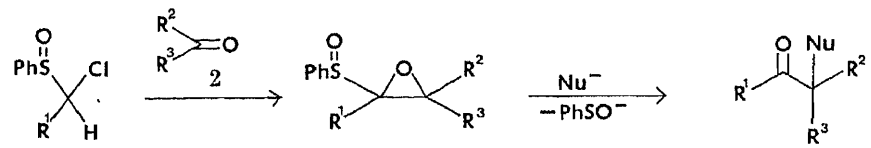


1 3 4

Chart 1

We chose four kinds of α,β-epoxy sulfoxides (**3**) with respect to the substituents on the epoxy group ($R^1$—$R^3$). The first (**3a**) has no branch at C-1 of $R^1$ and has a hydrogen as $R^2$ or $R^3$. The second (**3b**, **3c**) has no branch at C-1 of $R^1$ and has alkyl groups as $R^2$ and $R^3$. The third (**3d**, **3e**) has a branch at C-1 of $R^1$ and has a hydrogen as $R^2$ or $R^3$. The last (**3f**, **3g**) has branch at C-1 of $R^1$ and has alkyl groups as $R^2$ and $R^3$.

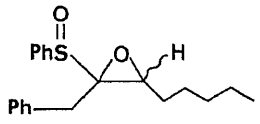
3a

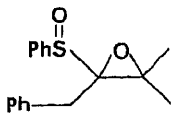
3b

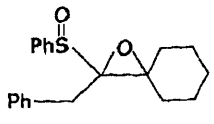
3c

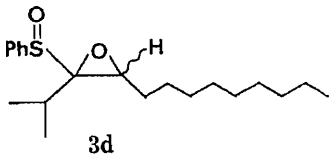
3d

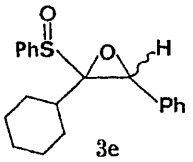
3e

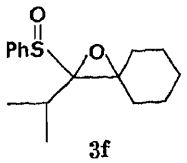
3f

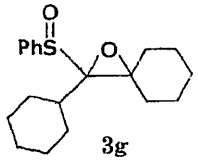
3g

The reaction was simply carried out with 2 eq of magnesium chloride or magnesium perchlorate in 2-propanol or l-propanol under heating. Representative results are summarized in Table I. In these reactions, the reactivities of the diastereomers of the α,β-epoxy sulfoxides (**3a**, **3d**, **3e**) appeared to be nearly equal under the conditions used.

Entries 1, 2, 4, 8, 11, 12, and 14 show that all the α,β-epoxy sulfoxides except **3f** and **3g** gave α-chloro ketones in good yields. Although many procedures are available for preparing α-bromo ketones[4] the synthesis of α-chloro ketones[4,5] still presents some problems. Thus, the present procedure offers a useful method for preparing relatively simple α-chloro ketones.

Entries 3, 5—7, and 9 show that when the reaction was carried out in normal alcohol, α-alkoxy ketones rather than α-chloro ketones were obtained. As the magnesium salt, magnesium chloride was found to be a better promoter than magnesium perchlorate; however, **3a** gave a complex mixture on treatment with magnesium chloride in l-propanol.

In entry 9, **3c** gave both α-chloro ketone (**11**) and α-alkoxy ketone (**12**). This result implies that these reactions are quite sensitive to the reaction conditions as well as to the substituents on the epoxy group.

All attempts to obtain α-chloro ketones or α-alkoxy ketones from **3f** and **3g** were fruitless; the reaction gave α,β-unsaturated ketones (**16** and **17**) in moderate yields. However, we had already obtained better results in the synthesis of α,β-unsaturated carbonyl compounds from α,β-epoxy sulfoxides by the use of lithium perchlorate as a promoter.[6]

In conclusion, a novel procedure for the preparation of synthetically useful α-chloro ketones and α-alkoxy ketones has been developed from carbonyl compounds with carbon homologation. Because of the ease of handling of all intermediates in this procedure, the low price of the reagents and the high yields of the products, the present method offer a simple and useful approach to the synthesis of α-chloro ketones and β-alkoxy ketones.

## Experimental

**General**——Infrared (IR) spectra were measured directly on an NaCl plate or in KBr disks with a Hitachi 215 spectrometer. $^1$H Nuclear magnetic resonance (NMR) spectra were measured in $CDCl_3$ solution with a JEOL FX-100 spectrometer using $Me_4Si$ as an internal standard. Electron-impact mass spectra (MS) were obtained on a Hitachi M-80 double-focusing spectrometer at 70 eV by direct insertion.

Magnesium chloride and magnesium perchlorate: Commercially available anhydrous $MgCl_2$ and $Mg(ClO_4)_2$ were used without further purification.

**α,β-Epoxy Sulfoxides**——All α,β-epoxy sulfoxides, except **3d** and **3e**, used in this study were reported in reference 3*c*. α,β-Epoxy sulfoxides (**3d** and **3e**) were prepared according to the procedure reported in reference 3*c* in nearly quantitative yields. **3d**: (*Z*)-Isomer; colorless oil. IR $\nu_{max}^{neat}$ cm$^{-1}$: 1050 (SO). $^1$H-NMR $\delta$: 0.39 (3H, d, $J$=7 Hz), 0.89 (3H, t, $J$=7 Hz), 1.07 (3H, d, $J$=7 Hz), 2.02 (2H, m), 2.48 (1H, septet, $J$=7 Hz), 3.21 (1H, t, $J$=6 Hz), 7.3—7.8 (5H, m). (*E*)-Isomer; colorless oil. IR $\nu_{max}^{neat}$ cm$^{-1}$: 1050 (SO). $^1$H-NMR $\delta$: 0.75 (3H, d, $J$=7 Hz), 0.99 (3H, t, $J$=7 Hz), 1.06 (3H, d, $J$=7 Hz), 2.25 (1H, septet, $J$=7 Hz), 3.55 (1H, dd, $J$=7, 4.5 Hz), 7.3—7.8 (5H, m). **3e**: (*Z*)-Isomer; mp 93.5—94 °C. IR $\nu_{max}^{KBr}$ cm$^{-1}$: 1045 (SO). $^1$H-NMR $\delta$: 0.5—2.5 (11H, m), 4.44 (1H, s), 7.1—7.8 (10H, m). (*E*)-Isomer; mp 97—98 °C. IR $\nu_{max}^{KBr}$ cm$^{-1}$: 1055 (SO). $^1$H-NMR $\delta$: 0.5—1.9 (11H, m), 4.61 (1H, s), 7.29 (5H, s), 7.4—7.9 (5H, m).

TABLE I. Reaction of α,β-Epoxy Sulfoxides with Magnesium Salt

| Entry | α,β-Epoxy sulfoxide | Magnesium salt | Solvent | Conditions[a] | Product | Yield[b] (%) |
|---|---|---|---|---|---|---|
| 1 | **3a** | $MgCl_2$ | 2-PrOH | 1 h | 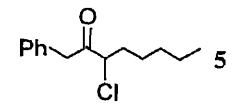 **5** | 86 |
| 2 | **3a** | $MgCl_2$ | AcOH | 100 °C 30 min | **5** | 94 |
| 3 | **3a** | $Mg(ClO_4)_2$ | 1-PrOH | 42 h | 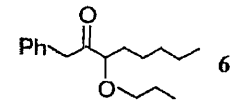 **6** | 72 |
| 4 | **3b** | $MgCl_2$ | 2-PrOH | 4 h | 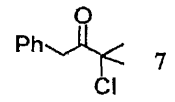 **7** | 78 |
| 5 | **3b** | $MgCl_2$ | 1-PrOH | 70 °C, 5 h | 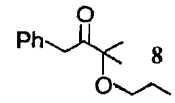 **8** | 61 |
| 6 | **3b** | $MgCl_2$ | $EtO(CH_2)_2OH$ | 70 °C, 4 h | 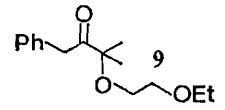 **9** | 75 |
| 7 | **3b** | $Mg(ClO_4)_2$ | 1-PrOH | 4 h | **8** + 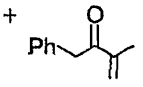 **10**[c] | 40 42 |
| 8 | **3c** | $MgCl_2$ | 2-PrOH | 9 h | 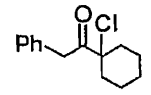 **11** | 70 |
| 9 | **3c** | $MgCl_2$ | 1-PrOH | 2.5 h | **11** + 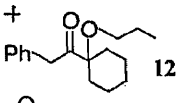 **12** | 22 55 |
| 10 | **3c** | $Mg(ClO_4)_2$ | 1-PrOH | 4.5 h | 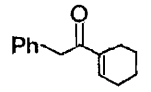 **13**[c] | 72 |
| 11 | **3d** | $MgCl_2$ | 1-PrOH | 70 °C, 5 h | 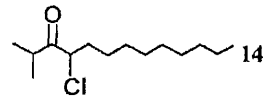 **14** | 76 |
| 12 | **3d** | $MgCl_2$ | MeOH | 70 °C, 2 d | **14** | 85 |
| 13 | **3d** | $Mg(ClO_4)_2$ | 1-PrOH | 20 h | Many products | |
| 14 | **3e** | $MgCl_2$ | 1-PrOH | 16 h | 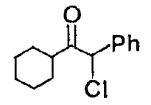 **15** | 78 |
| 15 | **3f** | $MgCl_2$ | 1-PrOH | 1.5 h | 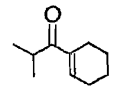 **16**[c] | 64 |
| 16 | **3g** | $MgCl_2$ | 1-PrOH | 8 h | 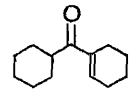 **17**[c] | 82 |

*a*) Unless otherwise noted, the reaction was carried out in refluxing solvent. *b*) Isolated yield after silica gel column chromatography. *c*) See reference 6.

**General Procedure for the Formation of α-Chloro Ketones and α-Alkoxy Ketones from α,β-Epoxy Sulfoxides**——A typical procedure is described for the synthesis of 3-chloro-1-phenyl 2-octanone (**5**). $MgCl_2$ (0.32 mmol) was added to a solution of the α,β-epoxy sulfoxide (**3a**) (53 mg; 0.16 mmol) in 2 ml of 2-propanol, and the reaction mixture was stirred and refluxed under $N_2$ for 1 h. The solvent was evaporated off under vacuum and ether and water were added to the residue. The whole was extracted with ether and the organic layer was washed with sat. aq. $NH_4Cl$. The product was purified by silica gel column chromatography developed with a mixture of hexane:AcOEt = 50:1 to give **5** (33 mg; 86%) as a colorless oil. IR $\nu_{max}^{neat}$ $cm^{-1}$: 1730 (CO). $^1$H-NMR $\delta$: 0.85 (3H, t, $J$=7 Hz), 1.0-2.2 (8H, m), 3.92, 3.96 (each 1H, d, $J$=16 Hz), 4.27 (1H, dd, $J$=7.5, 6.5 Hz), 7.0—7.5 (5H, m). MS $m/z$ (%): 238 ($M^+$, 3), 168 ($[M-C_5H_{10}]^+$, 6), 119 ($[M-C_6H_{12}Cl]^+$, 8), 91 ($[M-C_7H_{12}ClO]^+$, 100). Found: $m/z$ 238.1123. Calcd for $C_{14}H_{19}ClO$: M, 238.1123.

**1-Phenyl-3-propoxy-2-octanone (6)**——Colorless oil. IR $\nu_{max}^{neat}$ $cm^{-1}$: 1730 (CO), 1110 (COC). $^1$H-NMR $\delta$: 0.6—1.8 (16H, m), 3.30 (2H, m), 3.70 (1H, t, $J$=7 Hz), 3.81 (2H, s), 7.0—7.4 (5H, m). MS $m/z$ (%): 262 ($M^+$, 0.8), 204 ($[M-C_3H_6O]^+$, 0.3), 143 ($[M-C_8H_7O]^+$, 90), 101 (45), 91 (53), 83 (100). Found: $m/z$ 262.1921. Calcd for $C_{17}H_{26}O_2$: M, 262.1931.

**3-Chloro-3-methyl-1-phenyl-2-butanone (7)**——Colorless oil. IR $\nu_{max}^{neat}$ $cm^{-1}$: 1725 (CO). $^1$H-NMR $\delta$: 1.72 (6H, s), 4.05 (2H, s), 7.04—7.40 (5H, m). MS $m/z$ (%): 196 ($M^+$, 10), 119 ($[M-C_3H_6Cl]^+$, 10), 91 ($[M-C_4H_6ClO]^+$, 100). Found: $m/z$ 196.0655. Calcd for $C_{11}H_{13}ClO$: M, 196.0654.

**3-Methyl-1-phenyl-3-propoxy-2-butanone (8)**——Colorless oil. IR $\nu_{max}^{neat}$ $cm^{-1}$: 1725 (CO), 1080 (COC). $^1$H-NMR $\delta$: 0.96 (3H, t, $J$=7 Hz), 1.32 (6H, s), 1.64 (2H, m), 3.26 (2H, t, $J$=7 Hz), 3.90 (2H, s), 7.0—7.4 (5H, m). MS $m/z$ (%): 220 ($M^+$, 0.3), 192 ($[M-CO]^+$, 0.2), 161 ($[M-C_3H_7O]^+$, 2), 101 (57), 91 ($[M-C_7H_{13}O]^+$, 22), 59 (100). Found: $m/z$ 220.1438. Calcd for $C_{14}H_{20}O_2$: M, 220.1461.

**3-(2-Ethoxyethoxy)-3-methyl-1-phenyl-2-butanone (9)**——Colorless oil. IR $\nu_{max}^{neat}$ $cm^{-1}$: 1725 (CO), 1090 (COC). $^1$H-NMR $\delta$: 1.22 (3H, t, $J$=7 Hz), 1.33 (6H, s), 3.40—3.68 (6H, m), 3.98 (2H, s), 7.22 (5H, m). MS $m/z$ (%): 250 ($M^+$, trace), 205 ($[M-C_2H_5O]^+$, trace), 131 ($[M-PhCH_2CO]^+$, 100). Found: $m/z$ 250.1563. Calcd for $C_{15}H_{22}O_3$: M, 250.1567.

**1-Chloro-1-(1-oxo-2-phenylethyl)cyclohexane (11)**——Colorless oil. IR $\nu_{max}^{neat}$ $cm^{-1}$: 1720 (CO). $^1$H-NMR $\delta$: 1.0—2.2 (10H, m), 4.03 (2H, s), 7.24 (5H, m). MS $m/z$ (%): 236 ($M^+$, 10), 119 ($[M-C_6H_{10}Cl]^+$, 13), 91 ($[M-C_7H_{10}ClO]^+$, 100). Found: $m/z$ 236.0952. Calcd for $C_{14}H_{17}ClO$: M, 236.0966.

**1-(1-Oxo-2-phenylethyl)-1-propoxycyclohexane (12)**——Colorless oil. IR $\nu_{max}^{neat}$ $cm^{-1}$: 1715 (CO), 1080 (COC). $^1$H-NMR $\delta$: 0.97 (3H, t, $J$=7 Hz), 1.0—2.0 (12H, m), 3.17 (2H, t, $J$=7 Hz), 3.86 (2H, s), 7.22 (5H, m). MS $m/z$ (%): 260 ($M^+$, trace), 201 ($[M-C_7H_7O]^+$, trace), 141 ($[M-PhCH_2CO]^+$, 77), 99 (100). Found: $m/z$ 260.1762. Calcd for $C_{17}H_{24}O_2$: M, 260.1774.

**4-Chloro-2-methyl-3-tridecanone (14)**——Colorless oil. IR $\nu_{max}^{neat}$ $cm^{-1}$: 1725 (CO). $^1$H-NMR $\delta$: 0.88 (3H, t, $J$=7 Hz), 1.14, 1.15 (each 3H, d, $J$=7 Hz), 3.05 (1H, septet, $J$=7 Hz), 4.30 (1H, dd, $J$=7.5, 6.5 Hz). MS $m/z$ (%): 246 ($M^+$, 3), 120 ($[M-C_9H_{18}]^+$, 6), 71 ($[M-C_{10}H_{20}Cl]^+$, 100). Found: $m/z$ 246.1743. Calcd for $C_{14}H_{27}ClO$: M, 246.1748.

**2-Chloro-1-cyclohexyl-2-phenylethanone (15)**——Colorless oil. IR $\nu_{max}^{neat}$ $cm^{-1}$: 1735 (CO). $^1$H-NMR $\delta$: 0.7—1.9 (10H, m), 2.60 (1H, m), 5.45 (1H, s), 7.35 (5H, s). MS $m/z$ (%): 236 ($M^+$, 0.4), 125 ($[M-C_7H_{11}O]^+$, 10), 111 ($[M-C_7H_6Cl]^+$, 37), 83 ($[M-C_8H_6ClO]^+$, 100). Found: $m/z$ 236.0965. Calcd for $C_{14}H_{17}ClO$: M, 236.0966.

**Acknowledgements** The authors are grateful to Miss Noriko Sawabe and Mrs. Noriko Yamatani of this laboratory for the NMR and mass spectral measurements.

## References

1) α,β-Epoxy sulfoxides as useful intermediates in organic synthesis. XII. Part XI: T. Satoh, K. Iwamoto and K. Yamakawa, *Tetrahedron Lett.*, **28**, 2603 (1987).
2) K. Sato and M. Oohashi, *Yuki Gosei Kagaku Kyokai Shi*, **32**, 435 (1974); P. J. Chenier, *J. Chem. Educ.*, **55**, 286 (1978).
3) *a*) T. Satoh, Y. Kaneko, T. Kumagawa, T. Izawa, K. Sakata and K. Yamakawa, *Chem. Lett.*, **1984**, 1957; *b*) T. Satoh, Y. Kaneko, K. Sakata and K. Yamakawa, *ibid.*, **1985**, 585; *c*) T. Satoh, Y. Kaneko, T. Izawa, K. Sakata and K. Yamakawa, *Bull. Chem. Soc. Jpn.*, **58**, 1983 (1985); *d*) T. Satoh, T. Kumagawa and K. Yamakawa, *ibid.*, **58**, 2849 (1985); *e*) T. Satoh, Y. Kaneko, K. Sakata and K. Yamakawa, *ibid.*, **59**, 457 (1986); *f*) T. Satoh, S. Motohashi and K. Yamakawa, *ibid.*, **59**, 946 (1986); *g*) T. Satoh, T. Kumagawa and K. Yamakawa, *Tetrahedron Lett.*, **27**, 2471 (1986); *h*) T. Satoh, Y. Kaneko and K. Yamakawa, *ibid.*, **27**, 2379 (1986); *i*) T. Satoh, S. Motohashi and K. Yamakawa, *ibid.*, **27**, 2889 (1986); *j*) T. Satoh, Y. Kaneko and K. Yamakawa, *Bull. Chem. Soc. Jpn.*, **59**, 2463 (1986); *k*) T. Satoh, T. Kumagawa, S. Sugimoto and K. Yamakawa, *ibid.*, **60**, 301 (1987).
4) Recent papers on α-halo ketones: S. Motohashi, M. Satomi, Y. Fujimoto and T. Tatsuno, *Synthesis*, **1982**, 1021; *idem*, *Chem. Pharm. Bull.*, **31**, 1788 (1983); T. Kageyama, Y. Tobito, A. Katoh, Y. Ueno and M. Okawara,

*Chem. Lett.*, **1983**, 1481; Y. D. Vankar and G. Kumaravel, *Tetrahedron Lett.*, **25**, 233 (1984); W. Oppolzer and P. Dudfield, *ibid.*, **26**, 5037 (1985); S. T. Purrington, N. V. Lazaridis and C. L. Bumgardner, *ibid.*, **27**, 2715 (1986); T. Umemoto, K. Kawada and K. Tomita, *ibid.*, **27**, 4465 (1986).

5) G. A. Olah, L. Ohannesian, M. Arvanaghi and G. K. S. Prakash, *J. Org. Chem.*, **49**, 2032 (1984).

6) T. Satoh, M. Itoh, T. Ohara and K. Yamakawa, *Bull. Chem. Soc. Jpn.*, **60**, 1839 (1987).

[Chem. Pharm. Bull.
35(11)4637—4641(1987)]

# Benzylpiperazine Derivatives. VII.[1] Studies on the Role of the Nitrogen Atom in the Cerebral Vasodilating Activity of 1-Benzyl-4-diphenylmethylpiperazine Derivatives

HIROSHI OHTAKA,* TOSHIRO KANAZAWA, KEIZO ITO and GORO TSUKAMOTO

*Pharmaceuticals Research Center, Kanebo Ltd., 5-90, Tomobuchi-cho 1-chome, Miyakojima-ku, Osaka 534, Japan*

(Received April 20, 1987)

1-Benzyl-4-diphenylmethylpiperidine derivatives were prepared to investigate the role of the nitrogen atom in their cerebral vasodilating activity. The pharmacological test results revealed that the piperidine derivatives are roughly equipotent to the piperazine derivatives in our test system. Structure–activity analyses are presented.

**Keywords**——1-benzyl-4-diphenylmethylpiperidine; Leuckart–Wallach reaction; piperidine; piperazine; bioisosterism; regression analysis; adaptive least-square method; cerebral vasodilating activity

We have previously reported the syntheses and cerebral vasodilating activities of 1-benzyl-4-diphenylmethylpiperazines.[2] Among these compounds, 1-[bis(4-fluorophenyl)methyl]-4-(2,3,4-trimethoxybenzyl)piperazine dihydrochloride (KB-2796) was selected as the most promising compound, and is now under clinical trial.

The quantitative structure–activity relationship (QSAR) results suggested that a monoprotonated species, protonated at the benzylic nitrogen atom, is important for high cerebral vasodilating activity, and indicated that an electron-donating group on the benzyl moiety increases the electron density of the nitrogen, increases the amount of monoprotonated species, and enhances the activity.[3]

These considerations prompted us to synthesize piperidine analogs to investigate the role of the nitrogen atom attached to the diphenylmethyl residue.

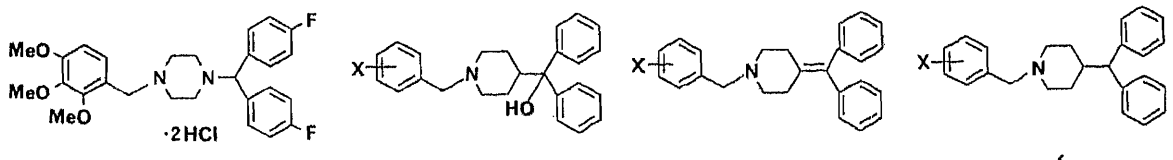


KB-2796 2 4 6

Chart 1

## Chemistry

The compounds for biological testing were prepared as follows; namely, ethyl 1-benzylisonipecotate was subjected to the Grignard reaction to give α-(1-benzyl-4-piperidyl)-diphenylmethanol (**2a**) as an oil,[4] which was dehydrated[5] with acid to give **4a**,[6] while the conversion of **2a** to **6a**[7] was achieved by treatment of **2a** with phosphorus and hydrogen iodide.[8] Furthermore, compounds **2b**, **4b**—**c** and **6b**—**d** were prepared from α-(4-piperidyl)diphenylmethanol (**1**),[9] 4-diphenylmethylenepiperidine (**3**)[10] and 4-diphenylmethylpiperidine (**5**),[11] respectively, *via* a route involving Leuckart–Wallach reaction.

TABLE I. 1-Benzyl-4-diphenylmethylpiperidine Derivatives

| Compd. No. | X | Yield (%) | mp (°C) | Recrystn.[a] solvent | Formula | Analysis (%) Calcd (Found) C | H | N | Potency[b] |
|---|---|---|---|---|---|---|---|---|---|
| **2a**[c] | H | | | [d] | | | | | |
| **2b** | 2,3,4-$(OMe)_3$ | 18 | 53—56 | — | $C_{28}H_{33}NO_4 \cdot 0.4H_2O$ | 73.95 (73.98 | 7.49 7.42 | 3.08 3.13) | 1.00[e] |
| **2c** | 2,4-$(OMe)_2$ | 22 | 61—63 | — | $C_{27}H_{31}NO_3 \cdot 0.7H_2O$ | 75.39 (75.41 | 7.59 7.41 | 3.26 3.28) | 1.37 (D) |
| **4a**[f] | H | 32 | 261—264 (dec.) | E–Et | $C_{25}H_{25}N \cdot HCl$ | 79.87 (80.03 | 6.97 7.06 | 3.73 3.75) | 0.78 |
| **4b** | 2,3,4-$(OMe)_3$ | 54 | 230—233 (dec.) | E–A | $C_{28}H_{31}NO_3 \cdot HCl \cdot 0.25H_2O$ | 71.48 (71.51 | 6.96 6.82 | 2.98 2.99) | 1.05 (D) |
| **4c** | 2,4-$(OMe)_2$ | 8 | 119—122 (dec.) | E–Et | $C_{27}H_{29}NO_2 \cdot HCl \cdot 0.75EtOH$ | 72.98 (72.73 | 7.09 7.22 | 2.99 3.02) | 0.96 (D) |
| **6a**[g] | H | 33 | 179—185 (dec.) | E | $C_{25}H_{27}N \cdot C_4H_4O_4 \cdot 0.5H_2O$ | 74.65 (74.66 | 6.91 6.83 | 3.00 3.06) | 0.67 |
| **6b** | 2,3,4-$(OMe)_3$ | 46 | 225—227 (dec.) | E–Et | $C_{28}H_{33}NO_3 \cdot HCl$ | 71.86 (71.87 | 7.32 7.30 | 2.99 2.98) | 1.00 (D) |
| **6c** | 2,4-$(OMe)_2$ | 45 | 199—202 (dec.) | E–Et | $C_{27}H_{31}NO_2 \cdot HCl$ | 74.04 (74.02 | 7.36 7.42 | 3.20 3.18) | 1.10 (D) |
| **6d**[h] | 4-$NMe_2$ | 15 | 236—238 (dec.) | M–Et | $C_{27}H_{32}N_2 \cdot 2HCl \cdot 0.1H_2O$ | 70.61 (70.46 | 7.51 7.28 | 6.10 6.13) | 1.08 (D) |

*a*) The following abbreviations are used: A, AcOEt; E, EtOH; Et, $Et_2O$; M, MeOH. *b*) The potency is expressed as the ratio of cerebral vasodilating activity to that of papaverine taken as 1. (D) stands for duration of action. *c*) See ref. 4. *d*) Used in the next step without further purification. *e*) Arrhythmia was observed. *f*) See ref. 7. *g*) For the hydrochloride see ref. 7. *h*) See ref. 15.

## Results and Discussion

The compounds prepared were tested for cerebral vasodilating activity by the method reported previously.[12] The results are summarized in Table I.

The compounds substituted with electron-donating groups exhibited strong activity as well as a long duration of action, whereas unsubstituted derivatives (**4a** and **6a**) were less active and did not show any long-lasting action. Table I suggests that the potency of the compound depends on the kind of substituent on the benzyl moiety, and the mode of connection between the piperidine ring and the diphenylmethyl group has little effect on the potency. When the substituent on the benzyl moiety is the same, the piperidine analogs are roughly equipotent to the piperazine analogs reported previously.[2]

These results suggest that the piperidine derivatives interact with the active site in the same manner as piperazines. Thus, the relative potency (log RP)[3] was calculated by the use of Eq. 1, assuming that the slopes of the log(dose)–response curves of these two series of compounds are the same.

$$\log RP = -\log(\text{dose}) + 1.36\text{CVA} \quad (1)$$

where the dose (1 mg/kg) is expressed on a molar basis, the value of 1.36 is the observed slope of the log(dose)–response curve of piperazines[3] and CVA (ceveral vasodilating activity) is the potency relative to papaverine listed in Table I.

Relationships between structure and log RP of 9 piperidine derivatives were examined by regression analysis and Eq. 2 was obtained. It is essentially identical to Eq. 3[3] obtained previously for 35 piperazine derivatives. Equation 2 shows that the electron-donating effect of

the substituent is predominantly important, as in the case of the piperazine series.

$$\log RP = -0.708(\pm 0.298)\Sigma\sigma + 6.672 \quad (2)$$
$$n=9,\ r=0.904,\ s=0.094,\ F=31.60$$

$$\log RP = -0.998(\pm 0.286)\Sigma\sigma - 0.073(\pm 0.036)MR + 6.593 \quad (3)$$
$$n=35,\ r=0.809,\ s=0.220,\ F=30.27$$

Next, all 44 compounds (35 piperazines and 9 piperidines) were subjected to regression analysis, and Eq. 4 was obtained.

$$\log RP = -0.952(\pm 0.231)\Sigma\sigma - 0.074(\pm 0.032)MR + 6.618 \quad (4)$$
$$n=44,\ r=0.819,\ s=0.201,\ F=41.88$$

In these equations $\Sigma\sigma$ represents the electronic effect of the substituent X, while $MR$, the larger value of $MR_Y$ and $MR_Z$, represents the steric effect of the substituents Y and Z. The values of these parameters were taken from the literature.[13]

The use of an indicator variable for distinction between the piperazine series and the piperidine series did not give any statistically significant result. The calculated potencies using Eq. 4 are summarized in Table II. The correlation matrix of the parameters used in Eq. 4 is shown in Table III, indicating low colinearity of the variables.

Next, the relationship between structure and duration of action was taken into consideration. The data suggest that the compounds with an electron-donating group exhibit long-lasting effects. The adaptive least-square (ALS) analysis[14] between $\Sigma\sigma$ and duration of 9 piperidines gave a significant result, Eq. 5, which is similar to Eq. 6[3] obtained previously for 34 piperazine derivatives.

$$Y = -2.898\Sigma\sigma - 1.195 \quad (5)$$
$$n=9,\ R_s=0.756,\ \varepsilon=0.467,\ n_{mis}=1,\ t=3.055,\ p<0.05$$

TABLE II. Structural Features and Cerebral Vasodilating Activities of 1-Benzyl-4-diphenylmethylpiperidine Derivatives

| Compd. No. | X | Parameter[a] | | log RP | | Duration | | |
|---|---|---|---|---|---|---|---|---|
| | | $\Sigma\sigma$ | $MR$ | Obsd.[b] | Eq. 4 | Obsd. | Recog.[c] | Pred.[d] |
| **2b** | 2,3,4-$(OMe)_3$ | −0.42 | 1.03 | 7.02 | 6.94 | 0 | 1 | 1 |
| **2c** | 2,4-$(OMe)_2$ | −0.54 | 1.03 | 7.05 | 7.06 | 1 | 1 | 1 |
| **4a** | H | 0.00 | 1.03 | 6.64 | 6.54 | 0 | 0 | 0 |
| **4b** | 2,3,4-$(OMe)_3$ | −0.42 | 1.03 | 7.10 | 6.94 | 1 | 1 | 1 |
| **4c** | 2,4-$(OMe)_2$ | −0.54 | 1.03 | 6.98 | 7.06 | 1 | 1 | 1 |
| **6a** | H | 0.00 | 1.03 | 6.58 | 6.54 | 0 | 0 | 0 |
| **6b** | 2,3,4-$(OMe)_3$ | −0.42 | 1.03 | 7.03 | 6.94 | 1 | 1 | 1 |
| **6c** | 2,4-$(OMe)_2$ | −0.54 | 1.03 | 7.14 | 7.06 | 1 | 1 | 1 |
| **6d** | 4-$NMe_2$ | −0.83 | 1.03 | 7.13 | 7.33 | 1 | 1 | 1 |

*a*) $\sigma$(2-OMe)=$\sigma$(4-OMe)=−0.27. $MR$ stands for the larger value of $MR_Y$ and $MR_Z$. *b*) Calculated using Eq. 1. *c*) From Eq. 7. *d*) Using the leave-one-out technique.

TABLE III. Correlation Matrix of Parameters Used in Eq. 4

| | $\Sigma\sigma$ | $MR$ |
|---|---|---|
| $\Sigma\sigma$ | 1.000 | |
| $MR$ | −0.100 | 1.000 |

$$Y = -1.774\Sigma\sigma - 0.128MR - 0.302 \quad (6)$$
$$n=34,\ R_s=0.620,\ \varepsilon=0.773,\ n_{mis}=6,\ t=4.47,\ p<0.001$$

Next, all 43 compounds (34 piperazines and 9 piperidines) were analyzed by using the ALS method to obtain Eq. 7.

$$Y = -2.253\Sigma\sigma - 0.157MR - 0.484 \quad (7)$$
$$n=43,\ R_s=0.623,\ \varepsilon=0.653,\ n_{mis}=8,\ t=5.09,\ p<0.001$$

In these expressions, $Y$ is the discriminant score for the classification, $n$ represent the number of compounds, $n_{mis}$ is the number misclassified, $R_s$ is the Spearman rank coefficient, $t$ is the $t$-statistics and $p$ is the level of significance. In Eq. 7, 81% of the compounds were correctly classified. To confirm the validity of the ALS results, the leave-one-out technique was applied and the predictive results classified 76% of the compounds correctly. The results are summarized in Table II.

Thus, it was confirmed that the QSAR for both the piperazine series and the piperidine series can be expressed in one model where the electronic nature of the substituent X and the steric nature of the substituents Y and Z affect the potency and duration of cerebral vasodilating activity.

Compound **6d** (SC-30552) shows rather high cerebral vasodilating activity. However, it was reported to be an antihypertensive agent whose action is mediated through calcium blockade in vascular smooth muscle.[15] Our biological test results (intravenous administration) suggest the bioequivalence of piperazine and piperidine, though the difference of lipophilicity of the whole molecule would result in some changes of the pharmacokinetics, such as absorption and distribution.

In conclusion, the nitrogen atom attached to the diphenylmethyl group in the 1-benzyl-4-diphenylmethylpiperazine derivatives plays no special role in the activity, but is exchangeable for a carbon atom. Thus, the mode of connection between the piperidine moiety and diphenylmethyl group has little effect on the activity. However, the pharmacokinetics would be changed when the nitrogen atom is replaced with a carbon atom owing to the increase of total lipophilicity of the molecule.

## Experimental

Melting points were determined on a Yamato capillary melting point apparatus, model MP-21, and are uncorrected. $^1$H Nuclear magnetic resonance ($^1$H-NMR) spectra were determined on a Hitachi R-24A NMR spectrometer using tetramethylsilane (TMS) as an internal standard. Silica gel 60 $F_{254}$ (Merck) TLC plates were used for thin layer chromatography. For column chromatography, Silica gel 60 (Merck) was used. Yield, melting point and elementary analysis data for **2b**, **c**, **4a**—**c** and **6a**—**d** are listed in Table I.

**1-Benzyl-4-diphenylmethylpiperidine Fumarate (6a)**——A solution of ethyl 1-benzylisonipecotate (8.6 g) in dry $Et_2O$ (20 ml) was added dropwise to the Grignard reagent [prepared from bromobenzene (24.1 g) and magnesium turnings (3.66 g) in dry ether (30 ml)] and the mixture was stirred for 2 h at room temperature. A solution of $NH_4Cl$ (15 g) in water (40 ml) was added and the deposited solid was filtered off. The organic layer was separated, and usual work-up of the organic layer gave crude **2a** as an brown oil (12.6 g).

A mixture of the crude **2a** (5 g), red phosphorus (2.1 g) and 57% HI was refluxed for 7.5 h. The cooled mixture was made basic with 10% NaOH and the product was extracted with AcOEt. Usual work-up of the organic layer gave free **6a** as a brown oil (4 g). $Et_2O$ was added to an EtOH (50 ml) solution of free **6a** and fumaric acid (1.67 g), and the deposited solid was collected and recrystallized from EtOH to give **6a** (2.15 g).

**1-Benzyl-4-diphenylmethylenepiperidine Hydrochloride (4a)**——A solution of the crude **2a** (4.0 g) in 20% $H_2SO_4$ (20 ml) was refluxed for 1.5 h. The cooled mixture was made basic with 10% NaOH and extracted with AcOEt. After usual work-up of the extract, the product was chromatographed on silica gel with $CHCl_3$–MeOH (10 : 1) to give free **4a**. Concentrated HCl (1 ml) was added to a solution of free **4a** (2 g) in EtOH (10 ml) and the solvent was evaporated off. Recrystallization of the residue from EtOH–$Et_2O$ gave **4a** (1.25 g).

**α-[1-(2,4-Dimethoxybenzyl)-4-piperidyl]diphenylmethanol (2c)**——**2c** was prepared in the same manner as described for **2a** and obtained as a powder by lyophilization.

**1-(2,3,4-Trimethoxybenzy)-4-diphenylmethylenepiperidine Hydrochloride (4b)**——2,3,4-Trimethoxybenzaldehyde (0.94 g) and **3** (1.2 g) were heated in an oil bath at 120°C. Formic acid (0.24 ml) was added dropwise to the molten mixture and the mixture was stirred for 1 h. The cooled mixture was diluted with benzene, washed with 20% NaOH and water, and then dried over $MgSO_4$. After removal of the solvent, the residue was dissolved in EtOH (10 ml). Concentrated HCl (1 ml) was added to the solution and the solvent was evaporated off. Recrystallization of the residue from EtOH–AcOEt gave **4b** (1.21 g).

Compounds **4c** and **6b—d** were prepared in the same manner as described for **4b**. Compound **2b** was prepared in a similar manner and obtained as a powder by lyophilization.

**Biological Testing Method**[12]—— The cerebral blood flow-increasing activity was measured by using the amount of vertebral blood flow as an index. Mongrel dogs of either sex (body weight 11 to 18 kg) were anesthetized with sodium pentobarbital (30 mg/kg, by intravenous injection) and artificially ventilated. The right vertebral artery was isolated from the surrouding tissues and a flow probe was attached to it and led to an electromagnetic flow meter (MVF-2100, Nihon Koden Co., Ltd.). The blood flow was periodically measured.

Each of the test compounds was dissolved in a 2% tartaric acid solution containing 20% dimethylacetamide, and administered to the right femoral vein at a dose of 1 mg/kg. The potency was expressed in terms of the ratio of the maximum change of blood flow induced by the test compound to that induced by papaverine. A compound was judged to be long-acting when it exhibited more than 20 times longer duration of action than papaverine.

## References and Notes


1) H. Ohtaka, T. Kanazawa, K. Ito and G. Tsukamoto, *Chem. Pharm. Bull.*, **35**, 4124 (1987).
2) H. Ohtaka, T. Kanazawa, K. Ito and G. Tsukamoto, *Chem. Pharm. Bull.*, **35**, 3270 (1987).
3) H. Ohtaka and G. Tsukamoto, *Chem. Pharm. Bull.*, **35**, 4117 (1987).
4) M. Suzuki, Tokkyo Koho 33-7629 [*Chem. Abstr.*, **54**, 2365*f* (1960)]; *idem*, *ibid.*, 33-7630 [*Chem. Abstr.*, **54**, 2365*g* (1960)].
5) N. Sperber, F. J. Villani, M. Sherlock and D. Papa, *J. Am. Chem. Soc.*, **73**, 5010 (1951).
6) C. M. Lee, A. H. Beckett and J. K. Sugden, *Tetrahedron*, **22**, 2721 (1966).
7) M. Yamato, K. Hashigaki, K. Hiramatsu and K. Tasaka, *Chem. Pharm. Bull.*, **31**, 521 (1983).
8) J. S. Gillespie, Jr., S. P. Acharya and D. A. Shamblee, *J. Org. Chem.*, **40**, 1838 (1975).
9) E. L. Schumann, M. G. Van Campen, Jr. and R. C. Pogge, U. S. Patent 2804422 [*Chem. Abstr.*, **52**, 1558*f* (1958)].
10) K. W. Wheeler, J. K. Seyer, F. P. Palopoli and F. J. McCarty, U. S. Patent 2898339 [*Chem. Abstr.*, **54**, 581*f* (1960)].
11) E. Sury and K. Hoffmann, *Helv. Chim. Acta*, **37**, 2133 (1954).
12) H. Ohtaka, M. Miyake, T. Kanazawa, K. Ito and G. Tsukamoto, *Chem. Pharm. Bull.*, **35**, 2774 (1987).
13) C. Hansch, A. Leo, S. H. Unger, K. H. Kim, D. Nikaitani and E. J. Lien, *J. Med. Chem.*, **16**, 1207 (1973).
14) I. Moriguchi, K. Komatsu and Y. Matsushita, *J. Med. Chem.*, **23**, 20 (1980); I. Moriguchi and K. Komatsu, Abstracts of Papers, 8th Symposium on Structure-Activity Relationships, Tokyo, Oct. 1981, p. 55.
15) J. Y. Lee, L. F. Rozek, J. H. Sanner and F. M. Radzialowski, *Meth. and Find. Exptl. Clin. Pharmacol.*, **5**, 235 (1983).

[Chem. Pharm. Bull. 35(11)4642—4644(1987)]

# Determination of Barbaloin in Rat Serum

YASUKO ISHII,* HISAYUKI TANIZAWA and YOSHIO TAKINO

*Shizuoka College of Pharmacy, 2-2-1, Oshika, Shizuoka 422, Japan*

(Received March 30, 1987)

A procedure for assay of barbaloin by thin layer chromatography (TLC)–densitometry was developed. The method is based on measuring the yellow-green fluorescence, which is produced by the reaction of barbaloin and borax (Schoutelen's reaction), on the TLC plate with a fluorophotometer. The limit of detection was about 0.01 μg of barbaloin, corresponding to about 0.033 μg/ml of barbaloin in rat serum. This method was applied for the determination of barbaloin in serum after oral administration of barbaloin (100 mg/kg) to rats. The serum concentration of barbaloin was extremely low; the peak concentration was only 0.34 μg/ml.

**Keywords**——barbaloin; serum concentration; fluorophotometry; TLC–densitometry; Aloe

The main laxative component in both Cape aloe and *Aloe arborescence* MILL. var. *natalensis* BERGER (kidachi-aloe in Japanese) has been proved to be barbaloin, an anthraquinone glycoside, by us.[1] However, neither the action mechanism nor the pharmacodynamics of barbaloin have been investigated, until now.

We have already developed a method for the determination of barbaloin by fluorophotometry based on Schoutelen's reaction, which takes place between barbaloin and borax.[2] In this paper, we describe the development of a thin layer chromatography (TLC)–densitometry procedure, with fluorophotometric detection, that is suitable for the determination of barbaloin in rat serum after oral administration.

## Experimental

**Material**——Male Wistar rats (180—200 g) were purchased from Shizuoka Laboratory Animal Center. The animals were deprived of food but given free access to water for 18 h prior to the experiments. Barbaloin and reagents used were the same as in the previous paper.[2]

**TLC–Densitometry**——TLC was done on Merck precoated Kieselgel 60 plates (0.25 mm thick). As a developing solvent for TLC, the following mixture was used: $CHCl_3$–95% ethanol–$H_2O$ (60 : 30 : 2, v/v). The detection of the spots ($Rf$=0.52) on the TLC plate was done by spraying 0.1 M borax solution (in 50% methanol aqueous solution) followed by blowing hot air for 1 min. Immediately, the TLC plate was covered with a clean glass plate to prevent discoloration of the yellow-green fluorescent spots. TLC densitograms were obtained by using a Shimadzu CS-910 chromatogram scanner with a fluorescence spectrophotometer under the following conditions: excitation wavelength, 383 nm; emission wavelength, 550 nm; scanning mode, linear scanning. The peak areas (fluorescence intensities) of spots were calculated by using an integrator.

**Determination of Barbaloin in Rat Serum**——Barbaloin was dissolved in distilled water to 20 mg/ml, and administered orally at a dose of 100 mg/kg to rats. At definite times after the administration of barbaloin, rat blood was taken from a polyethylene tube canulated into the right carotid artery of a rat under anesthesia with ether. Serum was obtained by centrifugation at 3000 rpm for 15 min after clotting. The serum (2 ml) was treated with 5 ml of ethyl acetate saturated with water for the extraction of barbaloin. This extraction was repeated 4 times. The combined ethyl acetate layer was evaporated to dryness under reduced pressure. The residue was redissolved in 0.2 ml of 50% aqueous methanol and a 30 μl aliquot was used as a sample for TLC.

## Results and Discussion

### Effect of the Drying Time of TLC Plates

As Schoutelen's reaction requires heating to complete the reaction, we used hot air as a heating source and for drying the TLC plate. The effect of drying time of the TLC plates with hot air after spraying the 0.1 M borax solution on the fluorescence intensity of barbaloin (0.5 $\mu$g) was first examined. The fluorescence intensity (expressed as the integration value) depended markedly on the drying time. The decrease was 77% at 2 min, and over 98% at 3 min based on the integration value at 1 min as the standard. One minute was not a sufficient time for full drying of the TLC plate. Therefore, it seemed that moderate wetness was required for the stability of the fluorescence developed by borax and barbaloin. We adopted 1 min as the standard drying time of TLC plates.

### Reproducibility

The reproducibility of the integration value was tested. When barbaloin (0.05 $\mu$g) was spotted at 4 sites on the same plate, the coefficient of variation (C.V.) was 0.55% ($n=4$). This result is similar to that in the previous fluorophotometry of barbaloin.

### Calibration Curve

The calibration curve obtained is shown in Fig. 1. There was a good linear relationship between the amounts (0.028—0.113 $\mu$g) of barbaloin applied and the integration values.

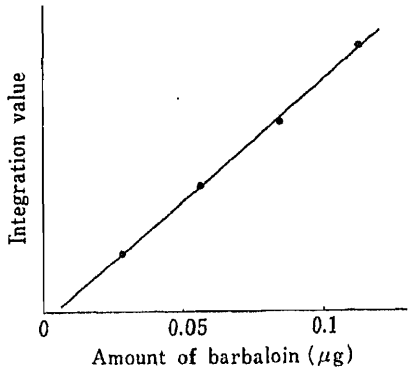


Fig. 1. Calibration Curve for Barbaloin
$r=0.9993$.

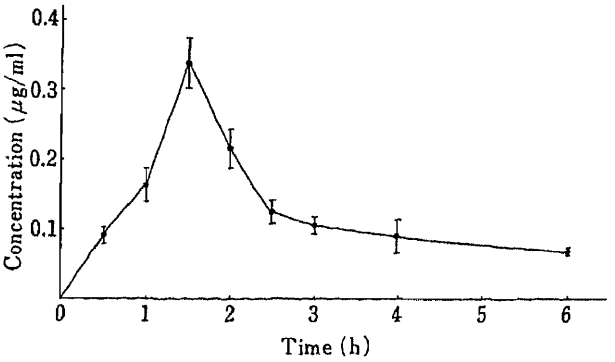


Fig. 2. Serum Concentration of Barbaloin after Oral Administration of Barbaloin (100 mg/kg) to Rats
Each point represents the mean ± S.D. of 4 animals.

TABLE I. Recovery of Barbaloin Added to Rat Serum

| Added amount ($\mu$g) | Recovered amount ($\mu$g) | Recovery (%) |
|---|---|---|
| 0.2152 | 0.2206 | 102.5 |
| 0.4444 | 0.4112 | 92.5 |
| 0.6375 | 0.6219 | 97.6 |
| 0.4173 | 0.4270 | 102.3 |
| 0.3850 | 0.3919 | 101.8 |
| Mean | | 99.3 |
| C.V.[a] | | 4.35 |

a) C.V., coefficient of variation (%).

The limit of detection was about 0.01 μg of barbaloin, so that the assay is more sensitive than fluorophotometry (limit=2 μg).[2] As this limit corresponds to about 0.033 μg/ml of barbaloin in rat serum, the assay should be applicable to practical animal experiments (*in vivo*).

The slope of the calibration curve differed somewhat with each TLC plate. Therefore, an individual calibration curve was made for each TLC plate.

**Recovery of Barbaloin Added to Rat Serum**

The recovery of barbaloin added to rat serum was investigated. The *Rf* value of barbaloin was 0.52 and no fluorescent spot was found on the TLC plate in the case of normal rat serum. As shown in Table I, the mean recovery percentage obtained with 5 plates was 99.3% and the C. V. (%) was 4.35%. This satisfactory result proved that our new method based on the application of fluorophotometry to TLC–densitometry is suitable for the determination of barbaloin in rat serum.

**Time Course of Barbaloin in Rat Serum**

Figure 2 shows the time course of barbaloin in serum of male rats after oral administration at a dose of 100 mg/kg. Barbaloin was first recognized in serum at 30 min after administration (0.092 μg/ml) and the maximum concentration, 0.337 μg/ml, was reached at 90 min. The serum concentration of barbaloin decreased smoothly thereafter, up to 3 h. Barbaloin was still detectable at 6 h. The maximal serum concentration of barbaloin (0.34 μg/ml) was extremely low, and at least three possibilities may be considered to explain this. One is low absorbability of barbaloin from the rat gastrointestinal tract, another is high degradability of barbaloin by rat gastrointestinal flora and the third is high transferability of barbaloin from rat serum to tissues. Further work is necessary to elucidate the pharmacodynamics of barbaloin.

**References**

1) Y. Ishii, H. Tanizawa, C. Ikemoto and Y. Takino, *Yakugaku Zasshi*, **101**, 254 (1981).
2) Y. Ishii, H. Tanizawa and Y. Takino, *Chem. Pharm. Bull.*, **32**, 4946 (1984).

[Chem. Pharm. Bull. 35(11)4645—4649(1987)]

# Enhanced Absorption of Phenobarbital from Suppositories Containing Amino Acid and Choline Salts of Phenobarbital

REIKO IWAOKU and MASAHIRO NAKANO*

*Department of Pharmaceutical Services, Kumamoto University Hospital, 1-1-1 Honjo, Kumamoto 860, Japan*

(Received March 9, 1987)

Dissolution and permeation patterns of phenobarbital (PB) from basic amino acid and choline salts of PB indicated that drug dissolution from the salts was faster than that of PB itself. Release of the drug from Vosco H15 suppositories containing the salts was faster than that from the suppository containing PB itself. After rectal administration of suppositories containing the salts to rabbits, the blood levels were significantly ($p<0.05$) higher than those following administration of the suppository containing PB itself during a period from 30 min to 2 h.

**Keywords**——phenobarbital; amino acid salt; choline salt; Vosco H15; suppository; dissolution pattern; release pattern; blood level; rabbit; rectal absorption

## Introduction

Phenobarbital (PB) is often used in the form of suppositories in the treatment of febrile convulsion in infants. Bioavailability of the drug following rectal administration of a PB suppository has been studied in pediatric patients.[1] Since rapid absorption of the drug is required in the treatment of febrile convulsion, we have been examining possible methods to attain fast absorption of the drug from suppositories. The use of $\beta$-cyclodextrin inclusion complexes or povidone coprecipitates has been reported by us.[2,3]

In the present work, the use of basic amino acid and choline salts to attain fast drug absorption from suppositories was examined since faster dissolution of the drug from salts was expected and increased rectal absorption of drugs by the employment of basic amino acid salts has been reported.[4]

## Experimental

**Materials**——PB(pharmacopeial grade) and a fatty suppository base (VoscoH15) were purchased from Maruishi Seiyaku Co. L-Lysine and L-arginine were obtained from Wako Junyaku Kogyo Co., while 50% choline aqueous solution was from Katayama Kagaku Co. Other chemicals used were of commercial reagent grade.

**Preparation of Amino Acid and Choline Salts of PB**——L-Lysine salt of PB (PB-Lys) was prepared as follows. A solution of 10 mmol L-lysine dissolved in 10 ml of water was added to a solution of 10 mmol of PB in a mixture of 50 ml of methanol and 50 ml of water at room temperature under stirring. The resultant solution was stirred for 1 h, then filtered, and the filtrate was freeze-dried. The residue was sieved through a No. 100 sieve (149 $\mu$m). L-Arginine salt of PB (PB-Arg) was prepared in a similar way.

Choline salt of PB (PB-Cho) was prepared by adding 10 mmol of PB and a small amount of water to a 50% choline aqueous solution (2.1 ml) containing 10 mmol choline. The solution was stirred for 1 h at room temperature, and the solvent was evaporated off under reduced pressure. The residue was further dried in a vacuum desiccator and then sieved through a No. 100 sieve (149 $\mu$m).

**Differential Thermal Analysis (DTA)**——A differential scanning calorimeter-thermal gravimetric analyzer (DSC-TG standard type, CN8089A1 Rigaku Denki, Tokyo) was used for thermal analysis. The temperature was increased at 10 °C/min.

**Preparation of Suppositories**——PB itself or an amino acid or choline salt of PB was suspended in the

suppository base after the base had been melted at 40 °C. The molten mass was then poured into a suppository mold (Erweka). In each batch, a sufficient amount of PB was suspended to give 50 mg of the drug in each suppository Suppositories were solidified at room temperature and then in a refrigerator.

**Measurement of Drug Content**——PB in a whole suppository was dissolved in 200 ml of a mixture of saline, ethanol and 0.05 M borax solution (1 : 2 : 7), then a 0.5 ml aliquot was diluted with the same solution. Absorbance at 241 nm was measured with a spectrophotometer (Shimadzu UV-240), and the drug content was calculated.

**Measurement of Dissolution Patterns**——Powder of PB, PB-Lys, PB-Arg, or PB-Cho, each corresponding to 50 mg as PB, was added to 300 ml of saline in a flask kept at 37.0 ± 0.2 °C by means of a thermostated water bath. The suspension was stirred with a magnetic bar at a rate of 100 rpm. One milliliter of the solution was pipeted at predetermined time intervals through a cotton plug and its absorbance at 241 nm was measured after dilution with 9 ml of a mixture of ethanol and 0.05 M borax solution (2 : 7).

**Measurement of Permeation Patterns**——An apparatus for the measurement of drug release from suppositories, model TMS-103, Toyama Sangyo Co., was employed for the measurement of permeation patterns. A 300 ml portion of saline or phosphate buffer, pH 7.4, was warmed to 37.0 ± 0.1 °C in the flask and 3 ml of saline was put into the cylindrical cell. A Millipore filter disk, SSWP 04700, was employed as a membrane. Powder of PB or its salt, each corresponding to 50 mg of the drug, was put into the cell. The rotation rate of the steel rod was 25 rpm, while the solution in the flask was stirred with a magnetic bar at 100 rpm. PB in the outer solution was determined as described in the dissolution studies.

**Measurement of Release Patterns**——Release patterns of PB from suppositories containing PB or its salt were determined by using the same apparatus, membrane and release media as in the permeation studies according to the procedures reported by Muranishi *et al.*[5] PB in the outer solution was determined as described for the dissolution studies.

**Measurement of Blood Levels**——Male albino rabbits weighing 2.5—3.5 kg were fasted for 24 h prior to rectal drug administration. The animal was secured in a supine position without anesthesia, and a test suppository was inserted into the rectum, then the anus was closed with a clip (Medama Clip®, Kokuyo Co.) to prevent possible leakage. At predetermined intervals, a 0.5 ml blood sample was withdrawn from the ear vein. An interval of more than 14 d was allowed prior to the next experiment.

Assay of PB in blood samples was performed by a gas chromatographic procedure.[6] A gas chromatograph (Hitachi 063) equipped with a flame ionization detector and a glass column packed with 3% silicone OV—17 on Chromosorb WAW DMCS 80—100 mesh was used.

## Results and Discussion

### Thermogram Patterns

Thermal characteristics of amino acid and choline salts of PB and PB itself measured by DTA are shown in Fig. 1. A sharp endothermic peak at around 178 °C was observed with PB itself whereas endothermic (see Fig. 1, choline salt of PB) peaks were not observed at this position with the salts.

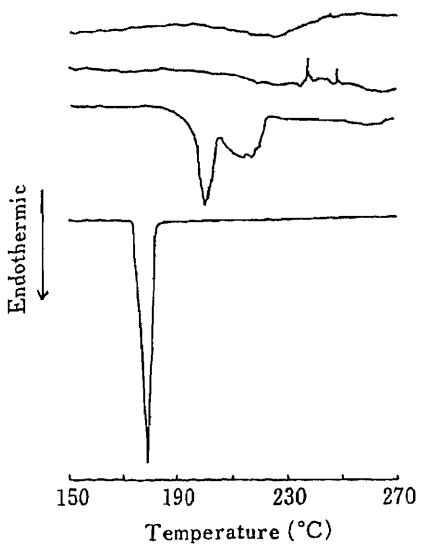


Fig. 1. Thermogram Patterns

From top to bottom: L-lysine salt, L-arginine salt, and choline salt of phenobarbital and phenobarbital itself.

**Dissolution Patterns**

Dissolution patterns of PB in the form of salts and PB acid are shown in Fig. 2. Dissolution from the salts was almost completed in one minute while 50% of the drug was dissolved from the PB powder in 5 min. Among the three salts, no significant difference in dissolution pattern was observed. Dissolution patterns of PB in phosphate buffer, pH 7.4, were very similar to those in saline.

Dissolution rates of PB from these salts were greater than those from β-cyclodextrin complex.[2] Dissolution rates of PB from povidone coprecipitates[3] appear to be comparable to those from the salts.

**Permeation Patterns**

Permeation profiles of PB through a membrane from a small amount of saline solution into a large volume of saline solution are shown in Fig. 3. As expected from the dissolution patterns shown in Fig. 2, PB permeated faster from the salts than from PB itself. Permeation patterns of PB in phosphate buffer, pH 7.4, were very similar to those in saline. There was no significant difference in permeation pattern among the three salts. Permeation rates of PB from these salts were greater than those from β-cyclodextrin complex,[2] or povidone

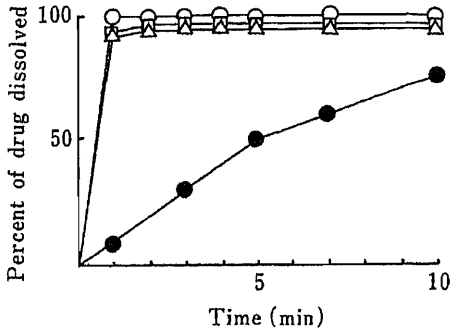


Fig. 2. Dissolution Patterns of Phenobarbital from Salts in Saline

Points are the averages of five experiments. ○, choline salt; □, L-arginine salt; △, L-lysine salt; ●, phenobarbital itself.

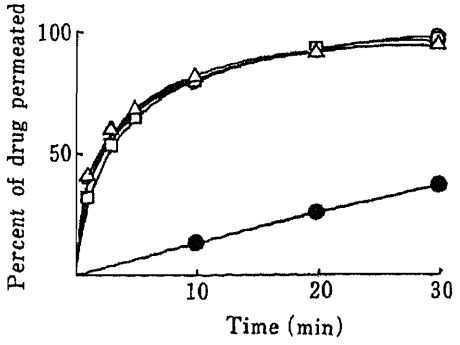


Fig. 3. Permeation Patterns of Phenobarbital to Outer Saline after Dissolution from Salts in Inner Saline

Points are averages of five experiments. ○, choline salt; □, L-arginine salt; △, L-lysine salt; ●, phenobarbital itself.

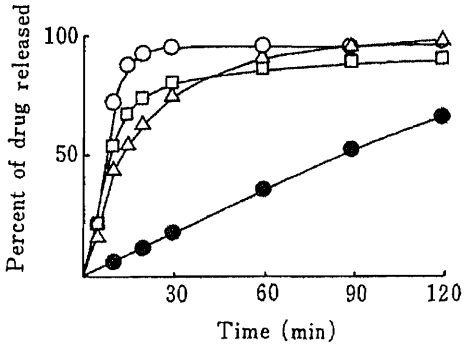


Fig. 4. Release Patterns of Phenobarbital from Vosco H15 Suppositories in Saline

Points are averages of five experiments. ○, choline salt; □, L-arginine salt; △, L-lysine salt; ●, phenobarbital itself.

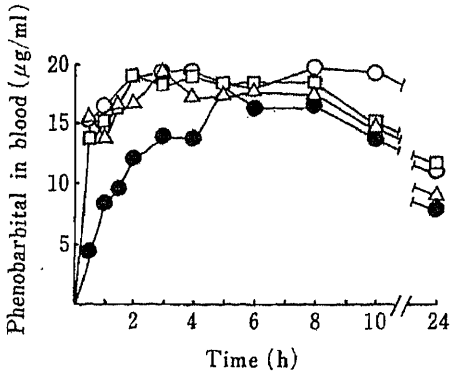


Fig. 5. Blood Levels following Rectal Administration of Phenobarbital in Vosco H15 Suppositories

Points are average of seven rabbits. ○, choline salt; □, L-arginine salt; △, L-lysine salt; ●, phenobarbital itself.

TABLE I. Pharmacokinetic Parameters after Rectal Administration of Phenobarbital Suppositories (Mean±S.E.M., $n=7$)

| Suppository | $t_{max}$ (h) | $C_{max}$ (μg/ml) | $AUC_{0-10h}$ (μg·h/ml) | Relative bioavailability |
|---|---|---|---|---|
| PB itself | 7.86±0.94 | 18.12±1.18 | 139.6±11.6 | 1.00 |
| PB-Lys | 4.93±1.24 | 20.73±0.98 | 175.9± 9.5 | 1.26 |
| PB-Arg | 5.14±1.08 | 20.90±1.62 | 174.9±10.7 | 1.25 |
| PB-Cho | 7.14±1.16 | 20.97±1.28 | 182.1± 9.3 | 1.30 |

coprecipitates.[3]

**Weight and Drug Contents of Suppositories**

Average weights and S.E.M. ($n=24$) of each suppository formulation were 1.1343±0.0043 g for PB itself, 1.1501±0.0039 g for PB-Lys, 1.1515±0.0040 g for PB-Arg, and 1.1383±0.0016 g for PB-Cho. Average drug contents and S.E.M.($n=5$) of each suppository formulation were 43.40±0.44 mg for PB, 43.52±0.11 mg for PB-Lys, 45.74±0.96 mg for PB-Arg, and 47.08±0.25 mg for PB-Cho.

**Release Patterns**

Release patterns of PB from Vosco H15 suppositories in saline are shown in Fig. 4. Release rates from suppositories containing the salt were greater than those from suppositories containing PB itself, reflecting the permeation patterns shown in Fig. 3. Among the three salts examined, the choline salt exhibited faster release than the others. Release patterns of the drug in phosphate buffer, pH 7.4, were very similar to those in saline. Release rates of PB from suppositories containing these salts were greater than those from suppositories containing povidone coprecipitates.[3] No direct comparison can be made between the results of the present study and those on β-cyclodextrin complex[2] since the suppository bases used were different in the two studies.

**Blood Level Patterns**

Blood levels of PB following administration of suppositories to rabbits are shown in Fig. 5. Coefficients of variation in blood levels were within 12.5—20.5%. Blood levels following administration of the suppositories containing the salts were significantly ($p<0.05$) greater than those following administration of the suppository containing PB itself during a period from 30 min to 2 h.

The pharmacokinetic parameters, $t_{max}$, $C_{max}$ and $AUC_{0-10h}$, determined directly from the plots are shown in Table I. $AUC_{0-10h}$ may be regarded as a parameter of the rate of absorption of PB from the suppositories. Although the $t_{max}$ values varied somewhat among the three suppositories containing each salt, no significant difference was found in $C_{max}$ and $AUC_{0-10h}$ values among the three salts. Relative bioavailability was improved significantly to 1.25—1.30 when the salts were employed.

Although unionized forms of drugs are considered to be favorable for permeation through lipoidal membranes on the basis of the pH partition hypothesis, faster absorption and an improved rate of bioavailability were observed after rectal administration of the suppository containing an amino acid salt or choline salt of the drug compared with rectal administration of the suppository containing PB itself. This observation may be rationalized on the basis that rates of release of the drug from the suppositories play an important role in the absorption of PB from suppositories.

No clear difference in absorption rates is apparent among the present study, β-cyclodextrin complex study,[2] and povidone coprecipitate study[3] since the suppository bases

or experimental designs were somewhat different among the studies.

**Acknowledgement** The authors are grateful to Miss Takayo Syudoh for her technical assistance.

## References

1) M. Matsukura, A. Higashi, T. Ikeda, and I. Matsuda, *Pediat. Pharmacol.*, **1**, 259 (1981).
2) R. Iwaoku, K. Arimori, M. Nakano, and K. Uekama, *Chem. Pharm. Bull.*, **30**, 1416 (1982).
3) R. Iwaoku, Y. Okamatsu, S. Kino, K. Arimori, and M. Nakano, *Chem. Pharm. Bull.*, **32**, 1091 (1984).
4) H. Yaginuma, T. Nakata, H. Toya, T. Murakami, M. Yamazaki, A. Kamada, H. Shimazu, and I. Makita, *Chem. Pharm. Bull.*, **29**, 3326 (1981).
5) S. Muranishi, Y. Okubo, and H. Sezaki, *Yakuzaigaku*, **39**, 1 (1979).
6) H. Sato, *Igaku No Ayumi*, **107**, 330 (1978).

[Chem. Pharm. Bull. 35(11)4650—4655(1987)]

# Comparative Study of the Interaction between Sulfamethizole and Ibufenac, Sulindac or Mepirizole at the Renal Level in Rats

KAZUMOTO CHIBA, SATOSHI KIKUCHI, KOUZOU MINO, SEIKUN NISHIMURA, SHOZO MIYAZAKI and MASAHIKO TAKADA*

*Faculty of Pharmaceutical Sciences, Higashi-Nippon-Gakuen University, Kanazawa, Ishikari-Tobetsu, Hokkaido 061-02, Japan*

(Received March 16, 1987)

The effects of three non-steroidal anti-inflammatory drugs, ibufenac, sulindac and mepirizole, on the renal excretion of sulfamethizole in rats were investigated, in order to clarify the mechanisms involved. The clearance ratio of sulfamethizole was markedly decreased after infusion of ibufenac, while sulindac or mepirizole had no effect on the clearance ratio of sulfamethizole. From this result, it is speculated that the decrease of renal excretion of sulfamethizole caused by ibufenac is mainly due to competitive interaction between sulfamethizole and ibufenac at the renal secretory level. The correlation between the chemical structures of some anionic non-steroidal anti-inflammatory drugs and the characteristics of renal tubular transport is discussed.

**Keywords**——drug interaction; ibufenac; sulindac; mepirizole; sulfamethizole; proximal tubular secretion; renal excretion; non-steroidal anti-inflammatory drug; rat

Many drugs are excreted by renal tubular secretion. It is well known that *p*-aminohippurate (PAH) inhibits the tubular secretion of penicillin, and this interaction had been used therapeutically.[1] Probenecid inhibits the renal clearance of indomethacin and this interaction is also probably clinically significant.[2] Thus, in considering pharmacokinetic drug interactions, we must take mutual interactions during renal excretion into account.

Recently, many new non-steroidal anti-inflammatory (NSAI) drugs have been introduced clinically for the therapy of various diseases. These NSAI drugs are frequently coadministered with various chemotherapeutic drugs, and pharmacokinetic drug interactions in such drug combinations must be taken into account in establishing dosage schedules.

We have already reported pharmacokinetic drug interactions between sulfamethizole and nine NSAI drugs at the renal level in rats.[3-6] In this paper, we deal with the interactions between sulfamethizole (SMZ) and ibufenac, sulindac or mepirizole at the renal level in rats, examined by the renal clearance technique. Furthermore, the correlation between the chemical structures of some NSAI drugs and the characteristics of the renal tubular transport is discussed.

## Experimental

**Materials**——Ibufenac (mp 83—86 C) was kindly supplied by Kaken Pharmaceutical Co., Ltd., Osaka, Japan. Sulindac (mp 200—205 C), mepirizole (mp 88—91 C) and sulfamethizole (SMZ, mp 207—208 C) were purchased from commercial sources. All other chemicals were of reagent grade and were used without further purification.

**Renal Clearance Experiment**——Standard methods for determining renal clearance[7] were employed. Male Wistar rats weighing 250—350 g were used in these experiments. Sodium pentobarbital at the dose of 30 mg/kg was used for anesthetization. After intubation and catheterization of the left femoral vein and right femoral artery, the rats were primed with SMZ (20 mg/body) and inulin (40 mg/body) through the left femoral vein, and sustained infusion of SMZ (0.35 mg/min) and inulin (0.2 mg/min) in saline was continued throughout the experiment. The left

ureter was catheterized with polyethylene tubing (PE-10) by the retroperitoneal approach procedure.[8] Constant urine flow was usually obtained within 1 h after the start of infusion. After attainment of constant urine flow, three control clearance periods were carried out. Immediately thereafter, an anti-inflammatory drug (2 mg/body) was primed through the femoral vein for blockade of proximal tubular secretion of SMZ, and sustained infusion of the anti-inflammatory drug (0.35 mg/min) was continued. About 30 min after primed infusion of the anti-inflammatory drug, three experimental clearance periods were carried out. Drug clearance ($C$, ml/min) was calculated as $C=UV/P$, where $U$, $P$ and $V$ indicate the urine and plasma concentrations of the drug in mg/ml, and the urine flow rate in ml/min, respectively. To estimate the renal handling of the drug, clearance ratio ($CR$) has been conventionally used and was expressed as $CR=C/GFR$, where $GFR$ is the glomerular filtration rate in ml/min. SMZ was used as an aqueous solution of sodium sulfamethizole. Each anti-inflammatory drug was used as a suspension in 0.5% Tween 80.

**Analytical Method**——For the determination of SMZ, 60 $\mu$l of MeOH and 100 $\mu$l of $H_2O$ were added to 50 $\mu$l of plasma. The mixture was shaken and centrifuged at 3000 rpm for 10 min. Then 10 $\mu$l of the supernatant or 10 $\mu$l of urine sample was taken, 420 $\mu$l of $H_2O$ and 10 $\mu$l of internal standard solution (sulfamethoxazole) were added, and the mixture was filtered through a Millipore Filter HV (0.45 $\mu$m diameter). A 20 $\mu$l aliquot of the filtrate was subjected to high-performance liquid chromatography (HPLC). For the determination of SMZ, a high-performance liquid chromatograph (Shimadzu LC-5A) equipped with an ultraviolet (UV) detector (245 nm, Shimadzu SPD-2A) was used with a stationary phase of Zorbax $C_8$ (5—6 $\mu$m particle diameter) packed in 25 cm × 4.6 mm i.d. stainless-steel tubing. The mobile phase was 0.2 M sodium phosphate (monobasic pH = 5.6) mixed with acetonitrile in a volume ratio of 3/2, and the flow rate was maintained at 0.5 ml/min.

Inulin was determined by a modification of the method described by Dische and Borenfreund.[9] The temperature at which the reaction mixture was left standing was modified at 40 °C (room temperature is recommended in the original procedure[9]).

## Results

### Interactions between SMZ and Ibufenac, Sulindac or Mepirizole at the Renal Level

Renal clearance experiments were carried out to investigate whether the renal excretion of SMZ could be altered by ibufenac, sulindac or mepirizole infusion. The results are shown in

TABLE I. Effect of Non-steroidal Anti-inflammatory Drugs on Renal Clearance of SMZ in Rats

| Coadministered compound | Rat body weight | | Time (min) | $V^{a)}$ (ml/min) | $GFR^{b)}$ (ml/min) | SMZ | | | |
|---|---|---|---|---|---|---|---|---|---|
| | | | | | | $U^{c)}$ (mg/ml) | $P^{d)}$ (mg/ml) | $C^{e)}$ (ml/min) | $CR^{f)}$ |
| Ibufenac | Rat A 210 g | Control | 30—20 | 0.054 | 1.01 | 7.53 | 0.273 | 1.49 | 1.48 |
| | | | 20—10 | 0.066 | 1.02 | 6.83 | 0.300 | 1.50 | 1.47 |
| | | | 10— 0 | 0.062 | 0.984 | 5.48 | 0.252 | 1.35 | 1.37 |
| | | Exptl. | 30—40 | 0.086 | 1.14 | 3.51 | 0.271 | 1.11 | 0.974 |
| | | | 40—50 | 0.070 | 1.23 | 3.99 | 0.232 | 1.20 | 0.976 |
| | | | 50—60 | 0.080 | 1.05 | 3.18 | 0.245 | 1.04 | 0.990 |
| Sulindac | Rat B 260 g | Control | 30—20 | 0.210 | 1.92 | 1.83 | 0.143 | 2.69 | 1.40 |
| | | | 20—10 | 0.184 | 1.62 | 1.62 | 0.152 | 1.96 | 1.21 |
| | | | 10— 0 | 0.208 | 2.03 | 1.92 | 0.162 | 2.46 | 1.21 |
| | | Exptl. | 30—40 | 0.215 | 2.13 | 2.04 | 0.157 | 2.80 | 1.31 |
| | | | 40—50 | 0.200 | 1.93 | 1.84 | 0.152 | 2.42 | 1.25 |
| | | | 50—60 | 0.232 | 2.24 | 1.93 | 0.150 | 2.99 | 1.33 |
| Mepirizole | Rat C 240 g | Control | 30—20 | 0.140 | 1.17 | 3.48 | 0.267 | 1.82 | 1.56 |
| | | | 20—10 | 0.114 | 0.818 | 1.78 | 0.180 | 1.13 | 1.38 |
| | | | 10— 0 | 0.142 | 1.06 | 3.27 | 0.288 | 1.61 | 1.52 |
| | | Exptl. | 30—40 | 0.126 | 0.975 | 1.92 | 0.162 | 1.49 | 1.53 |
| | | | 40—50 | 0.118 | 1.06 | 1.99 | 0.146 | 1.61 | 1.52 |
| | | | 50—60 | 0.116 | 1.27 | 2.07 | 0.140 | 1.72 | 1.35 |

*a*) Urine flow rate. *b*) Glomerular filtration rate. *c*) Urine concentration. *d*) Plasma concentration. *e*) Drug clearance. *f*) Clearance ratio. Exptl.: experimental.

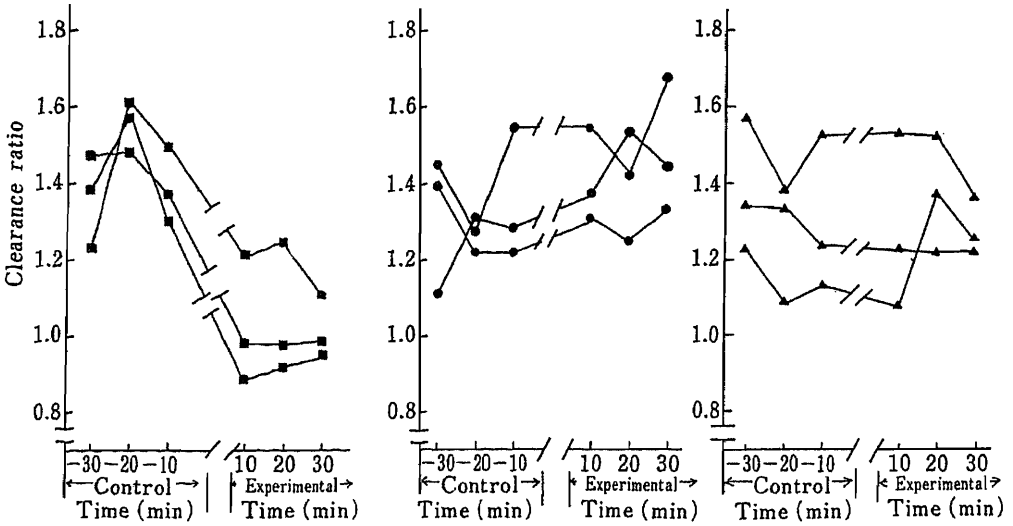


Fig. 1. Clearance Ratio of SMZ before and after Blockade of Proximal Tubular Secretion by Ibufenac, Sulindac or Mepirizole in Rats

■, SMZ with ibufenac; ●, SMZ with sulindac; ▲, SMZ with mepirizole.

Fig. 1. The data from renal clearance experiments in individual rats are exemplified in Table I.[10] As shown in Fig. 1 and Table I, a marked decline in the clearance ratio of SMZ was observed after ibufenac infusion. However, SMZ excretion was not affected by sulindac or mepirizole at the dosage level of this experiment, as shown in Fig. 1 and Table I.

## Discussion

Ibufenac, a phenylacetic acid derivative, was introduced into clinical drug therapy of rheumatic diseases in 1963 as a new type of NSAI drug.[11] However, after several years of clinical application, this drug had to be withdrawn owing to its serious hepatotoxicity. Since the development of ibufenac, many new NSAI drugs structurally related to ibufenac have been developed and used clinically. Thus, ibufenac occupies a key position in the development of NSAI drugs.

There was a marked difference in the clearance ratio of SMZ before and after ibufenac infusion, as shown in Fig. 1. This result indicates that renal tubular secretion of SMZ might be decreased by competition with ibufenac for the same transport process. The result for ibufenac is in agreement with previous results obtained for chemically analogous NSAI drugs such as 4-biphenylacetic acid[5] and diclofenac.[6] Sulindac is also a new NSAI drug belonging to the category of indeneacetic acid derivatives structurally related to indomethacin, and has been widely used clinically. There was no difference in the clearance ratio of SMZ before and after sulindac infusion, as shown in Fig. 1. This fact suggests that no interaction occurs between SMZ and sulindac at the renal level.

Mepirizole is a cationic NSAI drug belonging to the category of pyrimidinyl pyrazole derivatives, and is quite different from both ibufenac and sulindac in regard to chemical and physicochemical characteristics. As also shown in Fig. 1, mepirizole did not interact with SMZ at the renal level. This result raises the possibility that mepirizole might not be transported by the same transport process as proposed for SMZ.[12]

One of the major aims of our recent researches is to demonstrate whether or not the various NSAI drugs interact with SMZ at the renal level, and to elucidate the approximate correlation between the tubular secretory activities and the chemical structural features of

(propionic acid derivatives)

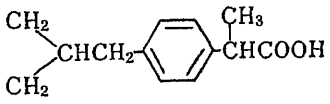

ibuprofen

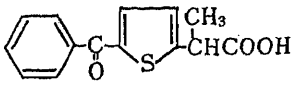

tiaprofenic acid

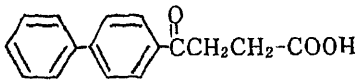

fenbufen

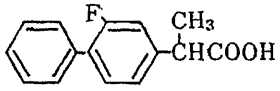

flurbiprofen

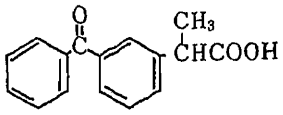

ketoprofen

(indeneacetic acid derivative)

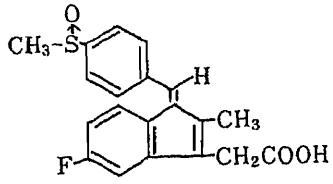

sulindac

(phenylacetic acid derivatives)

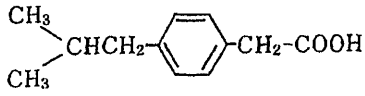

ibufenac

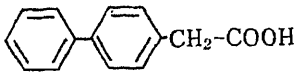

4-biphenylacetic acid

(barbituric acid derivative)

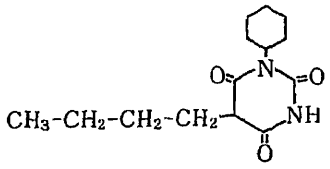

bucolome

(pyrimidinyl pyrazole derivative)

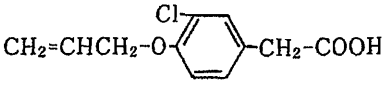

alclofenac

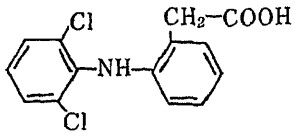

diclofenac (as Na salt)

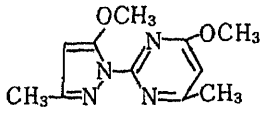

mepirizole

Chart 1

NSAI drugs. Several reports and reviews on the correlation between molecular features of organic anions and the renal excretory patterns have been published.[13-15] So far, twelve NSAI drugs (eleven anionic drugs and a cationic drug) including three NSAI drugs examined in this paper have been subjected to renal clearance experiments.[3-6] The chemical structures of the NSAI drugs examined are illustrated in Chart 1.

All renal clearance experiments were carried out under conditions such that SMZ excretion might be inhibited by each NSAI drug if the two drugs interact at the renal level. The date are summarized in Table IV. In order to assess the effect of NSAI drugs on the renal handling of SMZ comparatively, the degree of inhibition (degree of decrease of the clearance ratio of SMZ after NSAI drug infusion) was indicated by the symbols defined in Table II. As for the correlation between degree of inhibition of SMZ excretion and the chemical structures of anionic NSAI drugs, a few conclusions can be drawn from the results of the present study and our preceding reports[3-6] as follows.

(1) Propionic acid derivatives (except flurbiprofen) potently inhibit the renal excretion of SMZ. Among the five derivatives examined, only flurbiprofen does not inhibit renal excretion of SMZ.

(2) Phenylacetic acid derivatives potently inhibit the renal excretion of SMZ.

(3) Introduction of an isobutyl group at the *p*-position on the α-phenyl ring of phenylacetic acid causes a moderate decrease of inhibition of SMZ excretion as compared with the effects of the other substituted derivatives.

Since only one barbituric acid derivative and one indeneacetic acid derivative were tested here, additional trials will be necessary.

TABLE II. Effect of Non-steroidal Anti-inflammatory Drugs on Renal Clearance Ratio of SMZ in Rats

| Chemical group | Non-steroidal anti-inflammatory drug | The clearance ratio of SMZ | | Degree of inhibition[a] |
|---|---|---|---|---|
| | | Control | Experimental | |
| Propionic acid derivatives | Ibuprofen ($n=3$) | 1.23±0.127 | 0.945±0.0616 | ++ |
| | Fenbufen ($n=3$) | 1.68±0.0425 | 0.841±0.0486 | +++ |
| | Ketoprofen ($n=3$) | 1.51±0.0885 | 0.886±0.0645 | +++ |
| | Flurbiprofen ($n=3$) | 1.19±0.0435 | 1.21 ±0.0488 | − |
| | Tiaprofenic acid ($n=3$) | 1.78±0.00755 | 0.787±0.0418 | +++ |
| Phenylacetic acid derivatives | Ibufenac ($n=3$) | 1.44±0.0145 | 1.03 ±0.145 | ++ |
| | 4-Biphenylacetic acid ($n=3$) | 1.07±0.0629 | 0.702±0.0571 | +++ |
| | Alclofenac ($n=3$) | 1.75±0.0525 | 0.862±0.0449 | +++ |
| | Diclofenac ($n=3$) | 1.84±0.0220 | 0.734±0.0538 | +++ |
| Indeneacetic acid derivative | Sulindac ($n=3$) | 1.31±0.0929 | 1.44 ±0.131 | − |
| Barbituric acid derivative | Bucolome[b] ($n=2$) | 0.951[b] | 0.850[b] | + |
| Pyrimidinyl pyrazole derivative | Mepirizole ($n=3$) | 1.32±0.172 | 1.29 ±0.164 | − |

Numbers in parenthesis indicate numbers of rats used in renal clearance experiments. Each value is the mean±S.D. *a*) Degree of inhibition was classified into four categories according to the percentage of decline in clearance ratio (*CR*) of SMZ after non-steroidal anti-inflammatory drug administration, as follows: +++, over 40%; ++, 20—40%; +, 5—20%; −, below 5%. *b*) Each value is the arithmetic mean.

It is generally agreed that certain organic anions are secreted through the proximal tubules by the PAH transport process, and competition for tubular transport of such organic anions is established as the process underlying the depression of the secretion of one compound by another.[13,16] Each anionic NSAI drug might inhibit renal proximal tubular secretion of SMZ by competing with it in the anionic transport process proposed for SMZ and these NSAI drugs.

The reason why SMZ excretion was not affected by flurbiprofen is obscure. Flurbiprofen is the only compound containing fluorine among the five propionic acid derivatives examined. The introduction of fluorine into the propionic acid derivatives might affect the renal handling. Sulindac also contains fluorine in the molecular structure and dose not affect SMZ excretion. Elucidation of the correlation between the introduction of fluorine into propionic acid derivatives or indeneacetic acid derivatives and the renal handling requires more extensive study.

As mentioned above, the interactions between SMZ and the anionic NSAI drugs at the renal level were partially elucidated by means of renal clearance experiments. However, in order to obtain more precise information about the correlation between the renal secretory characteristics and the chemical structures of anionic NSAI drugs, more intensive and detailed studies using renal cortical slices or membrane vesicles isolated from the renal cortex will be necessary.

Mepirizole was the only organic cationic drug used in this study, and did not interact with SMZ at the renal level. Certain organic cations such as tetraethylammonium bromide or *N*-methylnicotinamide are well known to be excreted into urine by proximal tubular secretion.[17,18] The organic cation transport system is clearly separated from the anion transport system.[18] Competitive inhibitors of the transport of organic cations do not inhibit the transport of organic anions such as PAH. Mepirizole might be excreted into urine by a cation transport process different from the anion transport process proposed for SMZ and

anionic NSAI drugs.

## References and Notes


1) K. H. Beyer, L. Peters, R. Woodward and W. F. Verwey, *J. Pharmacol. Exptl. Ther.*, **82**, 310 (1944).
2) M. D. Skeith, P. A. Simkin and L. A. Healey, *Clin. Pharmacol. Ther.*, **9**, 89 (1968).
3) K. Chiba, M. Yoshida, A. Ishihara, J. Sudo, T. Tanabe, S. Miyazaki and M. Takada, *Chem. Pharm. Bull.*, **33**, 3415 (1985).
4) K. Chiba, S. Nishimura, S. Kikuchi, N. Higuchi, S. Miyazaki and M. Takada, *Chem. Pharm. Bull.*, **33**, 5100 (1985).
5) K. Chiba, S. Kikuchi, N. Higuchi, S. Miyazaki and M. Takada, *Chem. Pharm. Bull.*, **34**, 4389 (1986).
6) K. Chiba, S. Kikuchi, S. Nishimura, N. Higuchi, S. Miyazaki and M. Takada, *Chem. Pharm. Bull.*, **35**, 882 (1987).
7) M. Fujimoto, *Nippon Rinsho*, **25**, 1154 (1967).
8) J. Sudo, A. Ishihara and T. Tanabe, *Chem. Pharm. Bull.*, **31**, 4524 (1983).
9) Z. Dische and E. Borenfreund, *J. Biol. Chem.*, **192**, 583 (1951).
10) The values of *GFR* (glomerular filtration rate) and *C* (clearance) in our previous papers[3-6] should be changed to one-tenth of the reported values, because *GFR* and *C* are usually expressed in ml/min.
11) S. S. Adams, E. E. Cliffe, B. Lessel and J. S. Nicholson, *Nature* (London), **200**, 271 (1963).
12) T. Arita, R. Hori, M. Takada, S. Akuzu and A. Misawa, *Chem. Pharm. Bull.*, **19**, 937 (1971).
13) J. V. Møller and M. I. Sheikh, *Pharmacol. Rev.*, **34**, 315 (1983).
14) A. Despopoulos, *Am. J. Physiol.*, **203**, 19 (1962).
15) A. Despopoulos, *J. Theor. Biol.*, **8**, 163 (1965).
16) K. H. Beyer, *Pharmacol. Rev.*, **2**, 227 (1950).
17) M. Mintum, K. J. Himmelstein, R. L. Schroder, M. Gibaldi and D. D. Shen, *J. Pharmacokinet. Biopharm.*, **8**, 373 (1980).
18) B. R. Rennick, *Am. J. Physiol.*, **240**, F83 (1981).

[Chem. Pharm. Bull. 35(11)4656—4660(1987)]

# Fluorescence of 1,4-Dihydropyridine Derivatives Relevant to Age Pigments

KIYOMI KIKUGAWA,* TAKAMI NAKAHARA and KEIZO SAKURAI

*Tokyo College of Pharmacy, 1432–1 Horinouchi, Hachioji, Tokyo 192–03, Japan*

(Received May 6, 1987)

1,4-Disubstituted-1,4-dihydropyridine-3,5-dicarbaldehydes, models of fluorogens in age pigments, show a high intensity of fluorescence comparable to that of quinine sulfate. Relationships between the structures and fluorescence emission of the 1,4-dihydropyridine derivatives were studied. Loss of substituents at the 1- or 4-positions had little effect on the fluorescence. Reduction of one of the aldehyde groups to an alcoholic group greatly decreased the fluorescence intensity. When the aldehyde groups were replaced by acetyl groups, the fluorescence was greatly decreased. A derivative without aldehyde or carbonyl groups at the 3- and 5-positions was virtually non-fluorescent. Thus, the aldehyde groups at the 3- and 5-positions are requisite for the high intensity of fluorescence of the 1,4-dihydropyridines.

**Keywords**——1,4-dihydropyridine; 1,4-dihydropyridine-3,5-dicarbaldehyde; 3-hydroxymethyl-1,4-dihydropyridine-5-carbaldehyde; 3,5-diacetyl-1,4-dihydrolutidine; fluorescence; age pigment

Fluorescent lipofuscin granules develop in cells or tissues as they age.[1,2] It has been assumed that accumulation of age pigments is due to lipid oxidation in cells or subcellular organisms.[3,4] Lipid oxidation produces lipid hydroperoxides which in turn degrade into many secondary products including malonaldehyde and monofunctional aldehydes.[5] Among the secondary products, malonaldehyde produces fluorescence by reaction with primary amines or proteins. Two models have been proposed for the fluorogens: conjugated Schiff bases[6] and 1,4-disubstituted-1,4-dihydropyridine-3,5-dicarbaldehydes.[7] The latter class of compounds may include the fluorogens produced in biological systems, since they can be produced under physiological conditions.[7]

1,4-Disubstituted-1,4-dihydropyridine-3,5-dicarbaldehydes (I: $R_1$, $R_2$=alkyl) formed by reaction of malonaldehyde and primary amines $R_2NH_2$ in the absence and presence of monofunctional aldehydes $R_1CHO$ exhibit high intensity of fluorescence, comparable to that of quinine sulfate.[8] In order to obtain information of the relationship between the structures and fluorescence emission of 1,4-dihydropyridines, we prepared several 1,4-dihydropyridine derivatives to compare their fluorescence characteristics.

## Experimental

**Methods**——Ultraviolet (UV) absorption spectra were measured with a Shimadzu UV-200S double beam spectrophotometer. Fluorescence spectra were taken with a Hitachi 650-40 fluorescence spectrophotometer. Fluorescence intensity was measured at the concentration range in which the fluorescence linearly increased, and was compared with the intensity of 0.1 μM quinine sulfate in 0.1 N sulfuric acid (excitation at 350 nm and emission at 450 nm). Relative molar intensity of fluorescence was expressed with respect to quinine sulfate. Mass spectra (MS) were taken with a Hitachi M-80 double focusing mass spectrometer. Nuclear magnetic resonance (NMR) spectra were taken in $CDCl_3$ or $d_6$-dimethyl sulfoxide on a JEOL PS-100 machine with tetramethylsilane as an internal standard. Column chromatographies were done with silicic acid (Mallinkrodt) or silica gel for chromatography (Wako Pure Chemical Industries, Ltd.). Thin-layer chromatography was carried out by the use of Wakogel B-0 (Wako Pure Chemical Industries, Ltd.). Malonaldehyde (TMP hydrolysate) was prepared from tetramethoxypropane (TMP) according to the method described elsewhere.[8]

TABLE I. Compounds Ia—c, IIa and IIIa—d

| Compd. | Recrystn. solvent | Yield (%) | mp (°C) | Formula and analyses[a] | MS *m/z* (rel. intensity) | NMR ppm (Hz) $CDCl_3$[b] $d_6$-dimethylsulfoxide[c] |
|---|---|---|---|---|---|---|
| Ia | Chloroform–methanol | 5.8 | 215—217 | $C_8H_9NO_2$: C, H, N | $M^+$ 151 (50), $M^+-1$ [H] 150 (100), $M^+-29$ [CHO] 122 (16) | 9.39 (2H, s, CHO), 6.68 (2H, s, 2,6-H), 3.27 (3H, s, $NCH_3$), 3.18 (2H, s, 4-H)[b] |
| Ib | 1-Butanol–*n*-hexane | 5.3 | 155—168 | $C_8H_9NO_2$: C, H, N | $M^+$ 151 (10), $M^+-15$ [$CH_3$] 136 (100) | 9.32 (2H, s, CHO), 7.32 (2H, br s, 2,6-H), 3.67 (1H, q, 4-H), 0.93 (3H, d, 4-$CH_3$)[c] |
| Ic | Ethyl acetate–*n*-hexane | 10.7 | 129—137 | $C_{20}H_{17}NO_2$: C, H, N | $M^+$ 303 (26), $M^+-77$ [phenyl] 226 (50), $M^+-77-77$ 149 (19), benzyl 91 (100) | 9.31 (2H, s, CHO), 6.97 (2H, s, 2,6-H), 7.2—7.6 (10H, m, phenyl), 5.08 (1H, s, 4-H), 4.76 (2H, s, $CH_2$)[b] |
| IIa | — | 28.0 | — | $C_9H_{13}NO_2 \cdot 0.25$ $CH_3OH$: C, H, N | $M^+$ 167 (20), $M^+-15$ [$CH_3$] 152 (100), $M^+-15-17$ [OH] 135 (20) | 9.10 (1H, s, CHO), 7.13 (1H, s, 2-H), 6.03 (1H, s, 6-H), 3.97 (2H, s, $CH_2$), 3.38 (1H, q, 4-H), 3.13 (3H, s, $NCH_3$), 0.98 (3H, d, 4-$CH_3$)[c] |
| IIIa[d] | Methanol | 22.4 | 216—220 | $C_{11}H_{15}NO_2$: C, H, N | $M^+$ 193 (80), $M^+-1$ [H] 192 (100), $M^+-15$ [$CH_3$] 178 (65), $M^+-43$ [$COCH_3$] 150 (35) | |
| IIIb | Methanol | 16.6 | 155—156 | $C_{12}H_{17}NO_2$: C, H, N | $M^+$ 207 (7), $M^+-15$ [$CH_3$] 192 (100), $M^+-15-43$ [$COCH_3$] 149 (7) | 3.83 (1H, q, 4-H), 2.25 (12H, br s, $CH_3$), 0.97 (3H, d, 4-$CH_3$)[c] |
| IIIc | Ethyl acetate–*n*-hexane | 19.7 | 127—132 | $C_{14}H_{21}NO_2$: C, H, N | $M^+ + 1$ 236 (5), $M^+-15$ [$CH_3$] 220 (6), $M^+-43$ [$COCH_3$ and propyl] 192 (100) | 3.88 (1H, t, 4-H), 2.23 (12H, br s, $CH_3$), 1.1 (4H, m, $(CH_2)_2$), 0.80 (3H, t, $CH_3$)[c] |
| IIId | Chloroform–*n*-hexane | 11.3 | 124—126 | $C_{16}H_{25}NO_2$: C, H, N | $M^+ + 1$ 264 (4), $M^+-43$ [$COCH_3$] 220 (4), $M^+-71$ [pentyl] 192 (100) | 3.86 (1H, t, 4-H), 2.22 (12H, br s, $CH_3$), 1.1 (8H, m, $(CH_2)_4$), 0.80 (3H, t, $CH_3$)[c] |

*a*) Analyses are indicated only by the symbols of the elements whose analytical results were within ±0.3% of the theoretical values. *b, c*) Solvents for NMR spectroscopy of the samples are indicated. *d*) Reported melting points are 220 °C (ref. 9), 201—205 °C (ref. 11) and 204—205 °C (ref. 12).

**1,4-Dihydropyridine-3,5-dicarbaldehydes (Ia—c)**——Compounds Ia—c were synthesized according to the method previously described.[8d] Thus, a mixture of 0.1 M TMP hydrolysate, 0.05 M $R_1CHO$ and 0.05 M $R_2NH_2$ in 1 l of 0.1 M phosphate buffer (pH 7)–methanol (1 : 1) was incubated at 37 °C for 50 h. The mixture was extracted with chloroform (for Ia and Ic) or ethyl acetate (for Ib) in the presence of sodium chloride. The extract was evaporated to dryness *in vacuo*, and the residue was crystallized (Ia) or purified by column chromatography (Ib and Ic). For column chromatography, the residue was applied to a column (3.2 × 35 cm) of silica gel and eluted with chloroform or a chloroform–methanol system. The fluorescent fractions were collected and evaporated *in vacuo*, and the residue was crystallized (Table I).

**1,4-Dimethyl-3-hydroxymethyl-1,4-dihydropyridine-5-carbaldehyde (IIa)**——A mixture of 3.0 g of I ($R_1 = R_2 = CH_3$)[8a] and 3.0 g of sodium borohydride in 300 ml of methanol was kept at room temperature overnight. The mixture was evaporated to a small volume and extracted with 200 ml of chloroform twice. The extract was evaporated to dryness *in vacuo* and the residue was applied to a column (2.8 × 10 cm) of silicic acid. The column was eluted with chloroform and successively with chloroform–methanol (49 : 1). The green fluorescent fractions were collected and evaporated to dryness *in vacuo*. The residue was dissolved in 5 ml of methanol and applied to 15 thin-layer plates (20 × 20 cm). The plates were developed with chloroform–methanol (9 : 1). The green fluorescent zones, whose *Rf* value (0.65) was smaller than that of the starting compound (*Rf* 0.80), were excised and extracted with chloroform–methanol (8 : 2). The extract was evaporated to dryness and kept at −20 °C. The solid material IIa was obtained (Table I).

**3,5-Diacetyl-1,4-dihydrolutidines (IIIa—d)**——Compounds IIIa—d were prepared by Nash's method.[9] A mixture of 0.1 M acetylacetone, 0.05 M ammonium acetate and 0.05 M $R_1CHO$ in 1 l of 0.08 M phosphate buffer (pH 7) was incubated at 37 °C for 50 h. The products were extracted with ethyl acetate (for IIIa and IIIb) or chloroform (IIIc and IIId), the extract was evaporated to dryness *in vacuo* and the residue was crystallized (Table I).

**1-Phenyl-2-propyl-3,5-diethyl-1,4-dihydropyridine (IVa)**——Compound IVa was synthesized by the reaction of 1-butanal and aniline in acetic acid–water according to the method described previously.[10] bp 2.5 mmHg 156—158 °C (ref. 10; bp 0.5 mmHg 125 °C). MS *m/z* (rel intensity); $M^+$ 255 (4), $M^+ - 43$ [propyl] 212 (100).

## Results and Discussion

The structures of 1,4-dihydropyridine derivatives prepared for comparison of fluorescence are shown in Chart 1. 1,4-Dihydropyridine-3,5-dicarbaldehydes without a substituent at the 4-position (Ia) or the 1-position (Ib), and the derivative in which the alkyl substituent at the 1-position was replaced by an aryl substituent (Ic) were prepared according to the previously reported method[8d] (Table I). Compound Ic revealed the same fluorescence spectrum as the previously reported 1,4-disubstituted derivatives I[8c,d] (Table II). While Ib showed the same fluorescence spectrum, Ia showed excitation and emission maxima shifted to slightly higher wavelength. The fluorescence intensities of Ia—c were comparable to that of quinine sulfate as well as those of the previously reported 1,4-disubstituted compounds I,[8c,d] although the intensity of Ia was somewhat lower. When 1,4-dimethyl-1,4-dihydropyridine-3,5-dicarbaldehyde I ($R_1 = R_2 = CH$) was reduced with sodium borohydride, compound IIa in which one of the aldehyde groups was converted into an alcoholic group was obtained (Table I). The fluorescence intensity of IIa was one-thousandth of that of the original compound, although the wavelengths of maximum excitation and emission were little changed (Table II).

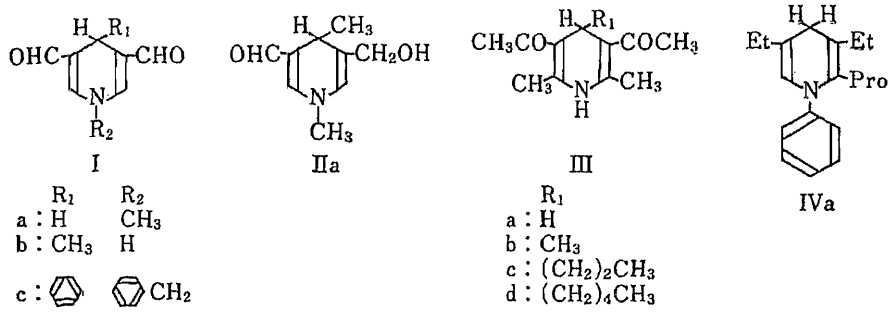


Chart 1

TABLE II. Spectral Data for I, II, III and IV

| Compd. | UV absorption spectrum 0.1 M phosphate (pH 7)[a] ethanol[b] $\lambda_{max}$ (nm) (mε) | Fluorescence spectrum 0.1 M phosphate (pH 7)[a] ethanol[b] | | |
|---|---|---|---|---|
| | | Excitation maximum (nm) | Emission maximum (nm) | Relative molar intensity[c] |
| I ($R_1$ = alkyl or aryl, $R_2$ = alkyl)[d] | 231—245 (20—26), 256—273 (7—11), 384—406 (9—12)[a] | 390—403 | 449—466 | 0.44—1.70[a] |
| Ia | 238 (19.0), 268 (7.6), 410 (11.1)[a] | 413 | 480 | 0.37[a] |
| Ib | 234 (21.2), 256 (6.2), 385 (11.5)[a] | 390 | 457 | 0.82[a] |
| Ic | 262 (14.6), 391 (11.3)[a] | 397 | 458 | 0.67[a] |
| IIa | 361 (11.0)[a] | 404 | 465 | 0.0013[a] |
| IIIa[e] | 256 (13.2), 280 (7.1), 413 (8.3)[a] | 394 | 454 | 0.05[a] |
| IIIb | 258 (15.8), 388 (9.3)[a] | 397 | 490 | 0.002[a] |
| IIIc | 259 (16.0), 383 (9.5)[a] | 399 | 498 | 0.002[a] |
| IIId | 258 (15.8), 383 (9.4)[a] | 400 | 498 | 0.003[a] |
| IVa[f] | 247 (9.5), 340 (9.1)[b] | 375 | 424 | $2 \times 10^{-7}$[b] |

*a, b*) Solvents for spectral measurement of the samples are indicated. *c*) Relative molar intensity of fluorescence with respect to quinine sulfate in 0.1 N sulfuric acid. *d*) All the data are summarized from the previous papers (ref. 8*c,d*). *e*) Reported absorption maxima are 412 (7.7) (ref. 9) and 251 (10.6), 277 (6.4), 406 (7.0) (ref. 12). *f*) Reported absorption maxima are 245 (8.0), 340 (12.0) (ref. 10).

3,5-Diacetyl-1,4-dihydrolutidines (IIIa—d) were prepared according to the method of Nash[9] (Table I). Among them, IIIa has no substituents at the 1- and 4-positions, and IIIb—d have an alkyl group at the 4-position and no substituent at the 1-position. Compounds IIIa—d emitted weaker fluorescence than I did. While IIIa showed fluorescence similar to those of I, IIIb—d exhibited excitation and emission maxima shifted to slightly higher wavelength. The fluorescence intensity of IIIa was about 5% of that of quinine sulfate, but those of IIIb—d were less than 0.3% of the intensity of quinine sulfate (Table II). The 1,4-dihydropyridines without carbonyl or aldehyde groups at the 3- and 5-positions (IVa)[10] emitted virtually no fluorescence (Table II). From these results, it is concluded that the high intensity of fluorescence of I was caused by the presence of aldehyde groups at the 3- and 5-positions, and the substituents at the 1- or 4-position did not greatly affect the fluorescence intensity.

In earlier studies it has been shown that 1,4-dihydropyridine derivatives usually fluoresce.[13] 3,5-Diacetyl-1,4-dihydrolutidines[9] and 3,5-diacetyl-1,4-dihydropyridines[14] are fluorescent. From the present experiments, it was found that 1,4-dihydropyridine-3,5-dicarbaldehydes I showed much higher intensity of fluorescence than other 1,4-dihydropyridines. The aldehyde and carbonyl groups at the 3- and 5-positions of 1,4-dihydropyridines contributed to the fluorescence emission, and in particular the aldehyde groups were requisite for the high intensity of fluorescence. It is interesting that the fluorescence intensity of I was diminished by borohydride treatment,[8c,d] which resulted in the formation of II with much lower intensity of fluorescence. The fluorescence of polylysine modified with malonaldehyde was lost after treatment with borohydride,[15] which presumably reduced the aldehyde group of the 1,4-dihydropyridine-3,5-dicarbaldehyde fluorogens.

## References

1) B. L. Strehler, "Adv. Gerontol. Res.," Vol. 1, ed. by B. L. Strehler, Academic Press, New York, 1964, p. 343.
2) M. Elleder, "Age Pigments," ed. by R. S. Sohal, Elsevier/North-Holland Biomedical Press, Amsterdam, 1981, p. 203.
3) K. S. Chio, R. Reiss, B. Fletcher and A. L. Tappel, *Science*, **166**, 1535 (1969).

4) C. J. Dillard and A. L. Tappel, *Lipids*, **6**, 715 (1971).
5) E. N. Frankel, *Prog. Lipid Res.*, **22**, 1 (1982).
6) A. L. Tappel, "Free Radicals in Biology," Vol. IV, ed. by W. A. Pryor, Academic Press, New York, 1980, p. 1.
7) K. Kikugawa, *Adv. Free Radical Biol. Med.*, **2**, 389 (1986).
8) *a*) K. Kikugawa, T. Maruyama, Y. Machida and T. Kurechi, *Chem. Pharm. Bull.*, **29**, 1423 (1981); *b*) K. Kikugawa, Y. Machida, M. Kida and T. Kurechi, *Chem. Pharm. Bull.*, **29**, 3003 (1981); *c*) K. Kikugawa and Y. Ido, *Lipids*, **19**, 600 (1984); *d*) K. Kikugawa, Y. Ido and A. Mikami, *J. Am. Oil Chem. Soc.*, **61**, 1574 (1984).
9) T. Nash, *Biochem. J.*, **55**, 416 (1953).
10) D. Craig, L. Schaefgen and W. P. Tyler, *J. Am. Chem. Soc.*, **70**, 1624 (1948).
11) J. M. Erikson and H. G. Biggs, *J. Chem. Educ.*, **50**, 631 (1973).
12) B. J. Compton and W. C. Purdy, *Can. J. Chem.*, **58**, 2207 (1980).
13) U. Eisner and J. Kuthan, *Chem. Rev.*, **72**, 1 (1972).
14) *a*) N. Sugiyama, G. Inouye and K. Ito, *Bull. Chem. Soc. Jpn.*, **35**, 927 (1962); *b*) Y. Kurabayashi, K. Kubota, Y. Omote and N. Sugiyama, *Nippon Kagaku Zasshi*, **86**, 106 (1965).
15) K. Kikugawa, K. Takayanagi and S. Watanabe, *Chem. Pharm. Bull.*, **33**, 5437 (1985).

[Chem. Pharm. Bull. 35(11)4661—4663(1987)]

# Parsonine, a Pyrrolizidine Alkaloid from *Parsonsia laevigata*

FUMIKO ABE and TATSUO YAMAUCHI*

*Faculty of Pharmaceutical Sciences, Fukuoka University, 8-19-1 Nanakuma, Jonan-ku, Fukuoka 814-01, Japan*

(Received May 28, 1987)

A pyrrolizidine alkaloid was isolated from the stems of *Parsonsia laevigata* ALSTON, a plant upon which the larvae of *Idea leuconoe* ERICHSON feed, and its structure was determined to be 1-(2′*S*,3′*S*)-2′,3′-dihydroxy-2′-isopropylbutanoyloxymethyl-5,6-dihydropyrrolizin-7-one.

**Keywords**——*Parsonsia laevigata*; Apocynaceae; pyrrolizidine alkaloid; 2,3-dihydroxy-2-isopropylbutanoic acid; viridifloric acid; 1-hydroxymethyl-5,6-dihydropyrrolizin-7-one; danaidone homologue

Genus *Parsonsia* belongs to Apocynaceae. In Japan, one species, *P. laevigata* ALSTON, grows in the southern islands, and it is known that the larvae of *Idea leuconoe* ERICHSON feed upon this plant. Three triterpenes were isolated from the leaves of *P. laevigata* by Ogihara *et al.*,[1] and pyrrolizidine alkaloids have been isolated from other species of *Parsonsia*.[2] In the course of our studies on the constituents of Apocynaceae plants, we have examined the alkaloids of *P. laevigata*. This paper deals with the isolation and structure determination of parsonine, a pyrrolizidine alkaloid, from the stems.

When the MeOH percolate of the stems was extracted with $CHCl_3$, the $CHCl_3$-soluble fraction showed a positive reaction to the Dragendorff reagent. The $CHCl_3$ extractives were fractionated by means of chromatographies on a silica gel column and a Sephadex LH-20 column, and a crystalline compound (I) was isolated.

Compound I, mp 117—118 °C, showed the molecular formula $C_{15}H_{21}NO_5$ on elementary analysis and fast atom bombardment (FAB)-mass spectroscopy (MS) (*m/z* 318.135, $M^+ + Na$). Upon usual acetylation, a monoacetate (I-1) was formed. On the basis of the presence of an esterified carbonyl carbon signal at $\delta$ 174.2 among 15 signals in the carbon-13 nuclear magnetic resonance ($^{13}$C-NMR) spectrum, as well as the molecular formula, I was considered to be a pyrrolizidine alkaloid composed of necic acid and necine moieties. In the electron impact (EI)-mass spectrum (MS), a base peak was observed at *m/z* 134 ($C_8H_8NO$), suggesting the necic acid to be composed of a 7-carbon unit. The presence of an isopropyl group and a secondary carbinyl carbon bearing a methyl group was also suggested by decoupling experiments in the proton nuclear magnetic resonance ($^1$H-NMR) spectrum.

In a comparison of I-1 with I by $^1$H-NMR and $^{13}$C-NMR, the secondary carbinyl proton signal and the corresponding carbon signal in I-1 were shifted downfield by +1.18 ppm and +3.0 ppm, respectively, while the tertiary carbinyl carbon showed an upfield shift of −1.7 ppm, indicating the presence of a glycol moiety composed of secondary and tertiary carbinols. The necic acid moiety was therefore considered to be a 2,3-dihydroxy-2-isopropylbutanoic acid such as viridifloric acid (2*S*, 3*S* or 2*R*, 3*R*) or trachelanthic acid (2*S*, 3*R* or 2*R*, 3*S*), of which the former was preferred based on a comparison of the $^1$H- and $^{13}$C-NMR spectra with those of lycopsamine and intermedine.[3]

In the nuclear Overhauser effect (NOE) difference NMR measurements initiated by irradiation of the hydroxymethylene protons at $\delta$ 5.31, the signals at $\delta$ 6.52, 6.99, 4.30, and

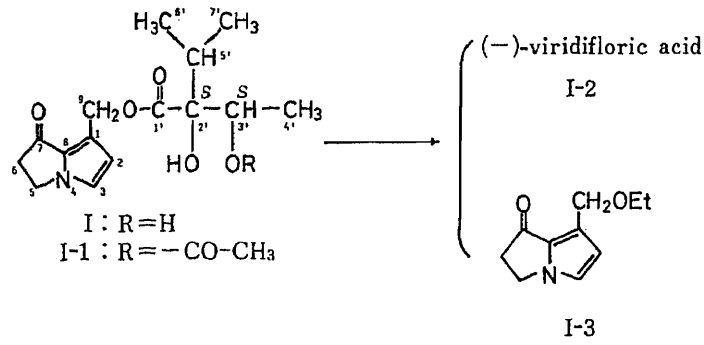


Chart 1

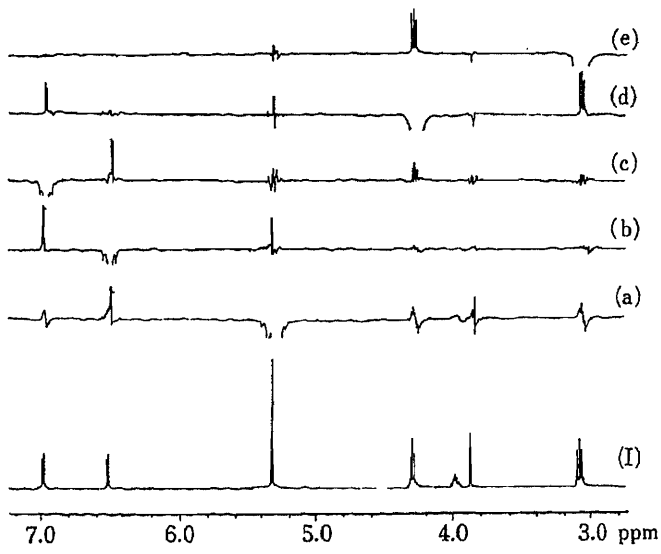


Fig. 1. NOE Difference NMR Spectra of I

(a), irradiated at $\delta$ 5.31; (b), irradiated at $\delta$ 6.52; (c), irradiated at $\delta$ 6.99; (d), irradiated at $\delta$ 4.30; (e), irradiated at $\delta$ 3.09.

3.09 showed responses, and these signals were assignable at H-9, H-2, H-3, H-5 and H-6, respectively (Fig. 1). The carbonyl group was allocated to C-7 based on the chemical shift at $\delta$ 189.1 (conjugated carbonyl) and the ultraviolet (UV) absorption at 288 nm. In the long range $^{13}C$–$^{1}H$ two dimensional (2D)-NMR spectrum in the $^{3}J$ mode, cross peaks between H-2/C-8 and C-9, H-3/C-8 and C-1, H-9/C-2, C-8 and C-1′ were observed as well as those between H-6′ and H-7′/C-2′, 2′-OH/C-1′, H-4′/C-2′ in the necic acid moiety, and thus, all the $^{1}H$ and $^{13}C$ peaks were assignable.

In order to confirm the structure, I was subjected to alkaline hydrolysis with 1% KOH in EtOH to afford I-2 as a necic acid, and I-3[4] from the pyrrolizidine moiety. Compound I-2 was identified as (2*S*,3*S*)-2,3-dihydroxy-2-isopropylbutanoic acid ((−)-viridifloric acid) based on the physical constants, NMR and chemical ionization (CI)-MS. Compound I-3 showed the molecular formula $C_{10}H_{13}NO_2$, and showed the presence of an ethoxyl group in the $^{1}H$-NMR spectrum. While a 2H singlet peak was assignable to primary carbinyl protons at C-9, other $^{1}H$- and $^{13}C$-NMR signals due to the pyrrolizidine framework showed almost the same chemical shifts as those of I. The structure of I-3 was assigned as 1-ethoxymethyl-5,6-dihydropyrrolizin-7-one. Thus, the structure of I was established and I was named parsonine.

It is a well known fact that male butterflies of Danaus, belonging to the same family as Idea, contain danaidone (1-methyl-5,6-dihydropyrrolizin-7-one) in their hair pencils as a courtship pheromone.[5] It seems noteworthy that I is the only pyrrolizidine alkaloid having a dienone system so far found among the homologous alkaloids from the higher plants.

## Experimental

Melting points were taken on a hot stage apparatus and are uncorrected. $^1$H-NMR and $^{13}$C-NMR spectra were recorded on a JEOL GX-400 spectrometer. Samples for NMR measurements were dissolved in $CDCl_3$ unless otherwise mentioned. Chemical shifts are given in $\delta$ values referred to internal tetramethylsilane, and the following abbreviations are used: s=singlet, d=doublet, dd=doublet of doublets, q=quartet, dq=doublet of quartets, m=multiplet. EI-MS, FAB-MS, and CI-MS were recorded on a JEOL D-300-FD spectrometer. UV spectra were taken in MeOH on a Shimadzu 200S double-beam spectrometer. The following solvent systems were employed for silica gel and Sephadex LH-20 column chromatography, and thin layer chromatography (TLC); solv. 1, benzene–acetone (10:1—7:1); solv. 2, $CHCl_3$; solv. 3, $CHCl_3$–MeOH–$H_2O$ (7:1:2, bottom layer).

**Extraction and Isolation of I**——Air-dried and powdered stems of *Parsonsia laevigata* ALSTON (2.4 kg) collected at Kikai-Jima, Kagoshima Prefecture, in July, 1983, were percolated with MeOH. The MeOH percolate was concentrated *in vacuo* to 1 l, and diluted with $H_2O$ (1 l), then the mixture was filtered. The filtrate was extracted with $CHCl_3$. The $CHCl_3$ extractives (9.8 g) were chromatographed on a silica gel column with solv. 1 and solv. 3, and the fraction containing I was further chromatographed on a Sephadex LH-20 column with solv. 2 to afford I as prisms from EtOAc–hexane (287 mg).

**Parsonine (I)**——mp 117—118 °C, $[\alpha]_D^{26}$ +5.3° (*c*=0.45, MeOH). *Anal.* Calcd for $C_{15}H_{21}NO_5$: C, 61.00; H, 7.17; N, 4.74. Found: C, 61.23; H, 7.37; N, 4.58. UV $\lambda_{max}^{MeOH}$ ($\varepsilon$): 287 nm (18700). FAB-MS *m/z*: 318.135 (Calcd for $C_{15}H_{21}NO_5$+Na: 318.135). EI-MS *m/z*: 296.149 (Calcd for $C_{15}H_{21}NO_5$+H: 296.150), 267, 250, 134 (base peak, $C_8H_8NO$). $^1$H-NMR $\delta$: 6.52 (1H, d, *J*=2 Hz, H-2), 6.99 (1H, d, *J*=2 Hz, H-3), 4.30 (2H, t, *J*=6 Hz, H-5), 3.09 (2H, t, *J*=6 Hz, H-6), 5.31 (2H, s, H-9), 3.98 (1H, dq, *J*=5, 6 Hz, H-3′), 1.21 (3H, d, *J*=6 Hz, H-4′), 2.17 (1H, m, H-5′), 0.88, 0.91 (3H each, d, *J*=6 Hz, H-6′, 7′), 2.55 (1H, d, *J*=5 Hz, 3′-OH), 3.91 (1H, s, 2′-OH). $^{13}$C-NMR $\delta$: 118.7 (C-1), 117.1 (C-2), 122.7 (C-3), 42.2 (C-5), 39.5 (C-6), 189.1 (C-7), 130.0 (C-8), 59.5 (C-9), 174.2 (C-1′), 83.3 (C-2′), 70.6 (C-3′), 17.3 (C-4′), 32.5 (C-5′), 16.1, 17.7 (C-6′, 7′). Upon acetylation of I with pyridine and $Ac_2O$ at room temperature, I-monoacetate (I-1) was obtained as prisms from hexane–AcOEt, mp 120—122 °C. EI-MS *m/z*: 338.161 (Calcd for $C_{17}H_{23}NO_6$+H: 338.160), 320, 267, 250, 134, 106. $^1$H-NMR $\delta$: 5.16 (1H, q, *J*=6 Hz, H-3′), 2.02 (3H, s, $-OCOCH_3$). $^{13}$C-NMR $\delta$: 81.6 (C-2′), 73.6 (C-3′), 15.1 (C-4′), 170.2, 21.2 ($-OCOCH_3$).

**Alkaline Hydrolysis of I**——Compound I (80 mg) was refluxed with 2 ml of 1% KOH in EtOH for 1 h. The mixture was concentrated *in vacuo* and then diluted with $H_2O$. After partition with $CHCl_3$, the $CHCl_3$ extract was passed through a silica gel column with solv. 1 to isolate I-3 (24 mg).[4] I-3: A solid. EI-MS *m/z*: 179.094 (Calcd for $C_{10}H_{13}NO_2$: 179.095), 150, 135, 106. $^1$H-NMR $\delta$: 6.55 (1H, d, *J*=2 Hz, H-2), 6.96 (1H, d, *J*=2 Hz, H-3), 4.26 (2H, t, *J*=6 Hz, H-5), 3.05 (2H, t, *J*=6 Hz, H-6), 4.63 (2H, s, H-9), 3.57 (2H, q, *J*=7 Hz, $-OCH_2CH_3$), 1.22 (3H, t, *J*=7 Hz, $-OCH_2CH_3$). $^{13}$C-NMR $\delta$: 116.9 (C-1, 2), 122.5 (C-3), 42.0 (C-5), 39.5 (C-6), 189.1 (C-7), 130.0 (C-8), 65.7 (C-9), 63.6, 15.2 ($-OCH_2CH_3$). The $H_2O$ layer, after $CHCl_3$ extraction, was acidified with dil. $H_2SO_4$ and extracted with BuOH to give I-2 (30 mg). I-2: mp 119—121 °C, $[\alpha]_D^{26}$ −2.3° (*c*=2.2, MeOH), ((−)-viridifloric acid: mp 121.5—124 °C, $[\alpha]_D$ −0.8°,[3b] mp 122—123 °C, $[\alpha]_D$ −1.4°,[3c] (+)-trachelanthic acid: mp 92—93 °C, $[\alpha]_D$ +2.3°)[3d]. CI-MS (isobutane) *m/z*: 163.097 (Calcd for $C_7H_{14}O_4$+H: 163.097). EI-MS *m/z*: 149, 118, 103 (base peak). $^1$H-NMR (in pyridine-$d_5$) $\delta$: 4.56 (1H, q, *J*=6 Hz, H-3′), 1.69 (3H, d, *J*=6 Hz, H-4′), 2.65 (1H, m, H-5′), 1.23, 1.33 (3H each, d, *J*=6 Hz, H-6′, 7′). $^{13}$C-NMR (in pyridine-$d_5$) $\delta$: 177.7 (C-1′), 83.6 (C-2′), 70.8 (C-3′), 18.7 (C-4′), 33.1 (C-5′), 18.5, 17.0 (C-6′, 7′).

**Acknowledgements** We thank Mr. S. Yoshitome and Mr. T. Iwamoto, then teachers of Kikai High School, for collection of *Parsonsia laevigata*. Our thanks are also due to Misses Y. Iwase and S. Hachiyama of Fukuoka University, for NMR and MS measurements. This work was supported in part by a grant from the Central Research Institution of Fukuoka University.

## References and Notes

1) K. Ogihara, M. Higa, K. Hokama, and T. Suga, *Phytochemistry*, **26**, 783 (1987).
2) J. A. Edgar and C. C. J. Culvenor, *Experientia*, **31**, 393 (1975); J. A. Edgar, N. J. Eggers, A. J. Jones, and G. B. Russell, *Tetrahedron Lett.*, **21**, 2657 (1980).
3) *a*) J. N. Roitman, *Aust. J. Chem.*, **36**, 769 (1983); *b*) C. C. J. Culvenor and L. W. Smith, *ibid.*, **19**, 1955 (1966); *c*) T. Furuya and K. Araki, *Chem. Pharm. Bull.*, **16**, 2512 (1968); *d*) C. C. J. Culvenor, *Aust. J. Chem.*, **7**, 287 (1954).
4) An unidentified product having the same molecular formula with one ethoxyl group and one methyl group accompanied I-3.
5) J. A. Edgar and C. C. J. Culvenor, *Nature* (London), **248**, 614 (1974).

## Communications to the Editor

[Chem. Pharm. Bull. 35(11)4664—4667(1987)]

# INCORPORATION OF RADIOACTIVITY INTO FATTY ACIDS IN PIGS AFTER SUCCESSIVE ADMINISTRATION OF $^{14}$C-SEDECAMYCIN

Junya Okada* and Sadao Kondo
Animal Health Products Division, Takeda Chemical Industries, Ltd.,
17-85, Jusohonmachi 2-chome, Yodogawa-ku, Osaka 532, Japan

The major radioactive components found in pig adipose tissue after successive administration of the macrolide antibiotic $^{14}$C-sedecamycin were isolated and chemically identified. Eighty-nine percent of the whole radioactivity in the adipose tissue was extracted into the lipid fraction, and 82% of the lipid radioactivity was recovered in the fatty acid fraction, 92% of which was found in palmitate, oleate, and stearate. No significant radioactivity was found in linoleic acid. These results indicate that some metyl carbons of sedecamycin are incorporated into fatty acids, presumably via the usual pathway of de novo biosynthesis in mammals.

KEYWORDS —— macrolide; sedecamycin; methyl carbon; pig fat; incorporation; fatty acid

Since 1985, sedecamycin (SCM), a 17-membered macrolide antibiotic produced by Streptomyces rochei var. volubilis,[1] has been used to treat swine dysentery at a feed level of 25 to 75 ppm. Our residue studies using high-performance liquid chromatography had shown that there was no appreciable residue in the adipose tissue, even when SCM was given to pigs for 14 days at a feed level of 500 ppm.[2] However, when radiolabeled-SCM was successively administered to pigs for 14 days, radioactivity found in adipose tissue increased up to the 10th administration, and remained at almost the same level for 14 days after withdrawal, whereas that in various specimens such as blood, liver, kidney, etc., declined within short periods.[3] In view of public health the radioactive components were isolated and identified to determine whether they are nontoxic endogenous substances.

## MATERIALS AND METHOD

Labeled Compound—— $^{14}$C-SCM was prepared by Dr. T. Suzuki of the Applied Microbiology Laboratories of our company according to the fermentation method of Sawada et al.[4] using (methyl-$^{14}$C)-methionine as a substrate. The positions of radiocarbons are shown in Chart 1. Its chemical and radiochemical purities were 91.5 and 100%, respectively. The specific radioactivity was 51.75 KBq/mg (3104.95 dpm/μg).

Adipose Tissue—— The subcutaneous adipose tissue of the dorso-lateral region was excised from a pig (10 weeks old, 40.2 kg) which received 3 mg/kg/day of $^{14}$C-SCM for 14 days and was killed 8 h after the last administration at Southwest Bio-Labs Inc. (Las Cruces, NM) for Hoffmann-La Roche. The radioactivity per gram of the tissue was equivalent to 0.21 μg of SCM and the

total radioactivity in the whole adipose tissue was estimated to be 0.075% of the dosage, assuming that adipose constitutes 15% of body weight.

Radioassay—— Radioactivity was determined with a scintillation cocktail (DPO 15 g, bis-MSB 1 g in 1 l of toluene) on an Aloka scintillation counter LSC-910.

Extraction of Radioactive Components—— Ten grams of the adipose tissue was extracted 3 times with a mixture of 20 ml of chloroform, 20 ml of methanol, and 10 ml of water by Bligh and Dyer's method.[5] The lower layer containing lipids was evaporated and the lipids were hydrolyzed by refluxing for 2 h with 0.5 N KOH in 95% ethanol. After the ethanol was evaporated off, the residue was redissolved in water and extracted with ethyl acetate, then with ethyl ether at pH 3-4.

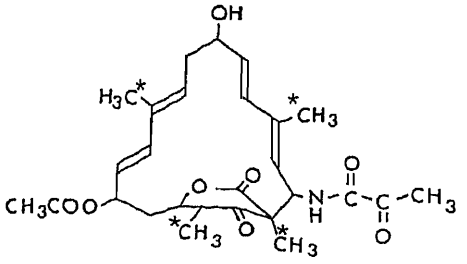


* = $^{14}C$

Chart 1. Sedecamycin (SCM)

Reversed-Phase Chromatography of Fatty Acids—— A column bed was prepared by packing 100 g of silanized Celite 545,[6] coated with 78 g of liquid paraffin (LP) into a glass column (3 cm id × 40 cm). An aliquot of the fatty acid extract (corresponding to 0.5 to 1.5 g of adipose tissue), mixed with 4.14 g of LP and 6.25 g of silanized Celite 545,[7] was applied to the column. Elution was carried out stepwise with 65% to 80% acetone saturated with LP.[8] Two ml of the eluate (10 ml) was titrated with 0.01 N methanolic KOH using bromothymol blue as an indicator.[8]

Isolation of Fatty Acids—— Each of four peaks from 8 chromatographic runs was pooled, concentrated to remove acetone, and extracted with ethyl ether at pH 3-4. An aliquot of the concentrated ether extract was subjected to radioassay, GLC, and mass spectroscopy.

Catalytic Hydrogenation—— A portion of unsaturated fatty acid was hydrogenated in ethanol with 5% Pd/C as a catalyst under atmospheric pressure of hydrogen.

GLC of Fatty Acids—— Fatty acids esterified with $CH_2N_2$ were determined with GLC under the following conditions: model G80 (Yanaco); liquid phase, 15% DEGS; column support, Chromosorb W (AW DMCS 80/100 mesh); carrier, He; detector, FID.

Electron Impact Mass Spectroscopy (EIMS)—— Me esters of fatty acids were measured on a Shimadzu GCMS9020-DF/SCAP 1123 data processing system.

## RESULTS AND DISCUSSION

Eighty-nine percent of the radioactivity in the adipose tissue (654 dpm/g) was transferred to the chloroform layer as lipids. Eighty-two percent of the lipid radioactivity, that is, 73% of the whole tissue radioactivity, was extracted as free fatty acids after being saponified.

The fatty acid fraction was chromatographed on silanized Celite 545 and separated into four peaks ($P_1$ to $P_4$) (Fig. 1). In this chromatographic run, 92% of the titrable acids and 97% of the radioactivity were recovered. $P_2$, $P_3$, and $P_4$ contained 7.3, 73.0, and 18.4% of the recovered radioactivity, respectively, while $P_1$ comprised only 1.3%. Therefore, $P_2$ to $P_4$ were analyzed by GLC and EIMS for the elucidation of the components. $P_2$ consisted of linoleic (83.1%), myristic (6.7%), palmitoleic (10.1%), and linolenic (trace) acids. $P_3$ contained oleic (59.8%), palmitic (38.2 %), linoleic (0.8%), and stearic (1.2%) acids. $P_4$ contained stearic acid (>98%).

Aliquots of the extract obtained from 9.1 g of the starting adipose tissue were subjected to chromatography and the corresponding peaks were pooled for isolating fatty acids. Myristic (33

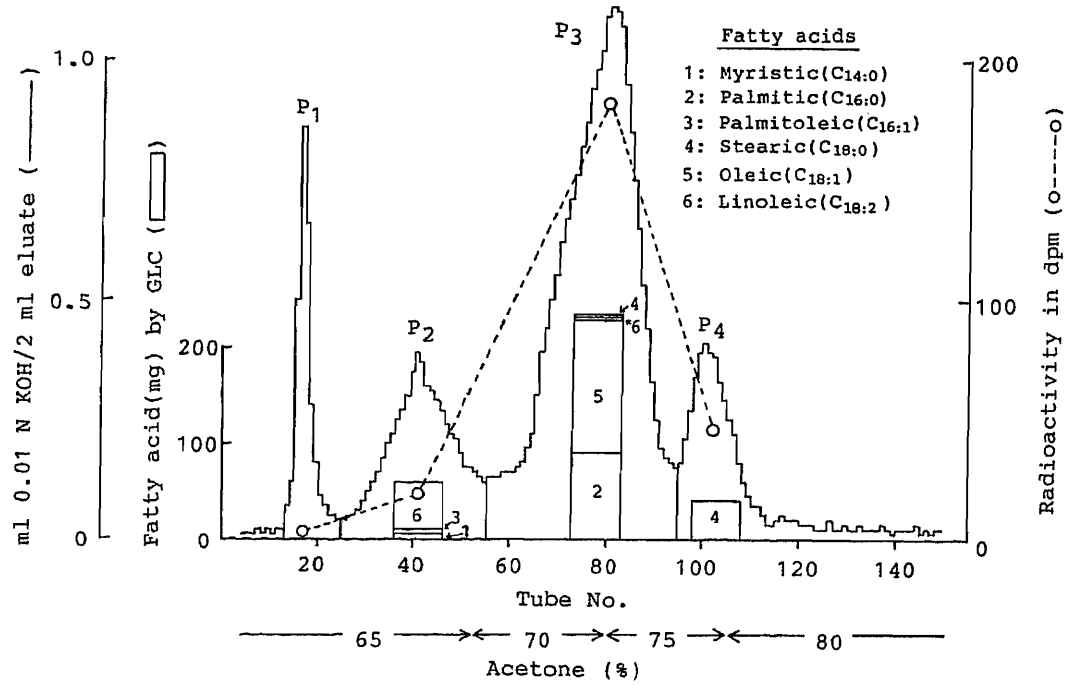


Fig. 1. Reversed-Phase Chromatography of Fatty Acid Mixture Obtained from 0.5 g of Pig Adipose Tissue on Silanized Celite 545

Table I. Specific Radioactivity of Fatty Acids after Crystallization

| Acid | n [a] | Solvent [b] | dpm/mg | Acid | n | Solvent | dpm/mg |
|---|---|---|---|---|---|---|---|
| Stearic | 1 | None | 0.684 | Palmitic | 5 | Hexane | 0.929 |
| | 2 | Aq. EtOH [c] | 0.716 | | 6 | Pet. E | 0.950 |
| | 3 | Pet. E [d] | 0.894 | | 7 | EtOH | 0.943 |
| | 4 | Aq. Acetone [e] | 0.904 | | 8 | EtOAc | 0.935 |
| | 5 | Hexane | 1.000 | Oleic-derived | 1 | Hexane | 0.556 |
| | 6 | EtOH | 1.023 | stearic | 2 | EtOH | 0.616 |
| | 7 | EtOAc | 1.016 | | 3 | Pet. E | 0.623 |
| Palmitic | 1 | Acetone | 0.840 | | 4 | EtOAc | 0.648 |
| | 2 | Aq. EtOH [f] | 0.880 | Linoleic-derived | 1 | Hexane | NA [h] |
| | 3 | Pet. E | 0.924 | stearic | 2 | EtOH | NA |
| | 4 | Aq. Acetone [g] | 0.936 | | 3 | Pet. E | NA |

a) Number of crystallization. b) Crystallization solvent. c) Water-EtOH (2:5, v/v). d) Petroleum ether. e) Water-acetone (1:3, v/v). f) Water-EtOH (1:2, v/v). g) Water-acetone (3:8, v/v). h) No significant radioactivity.

mg), palmitic (120 mg, derived from palmitoleate on hydrogenation), and stearic (800 mg, derived from linoleate) acids were obtained by rechromatography on hydrogenated products of $P_2$. Palmitic acid (1.7 g) was isolated from $P_3$ by cold crystallization.[7] Stearic acid (700 mg) derived from oleate was obtained by rechromatography of hydrogenated products of the oleate-enriched remainder of $P_3$. Stearic acid (1 g) was obtained from $P_4$.

Each acid was repeatedly crystallized from petroleum ether, hexane, ethyl acetate, (aq) acetone, or (aq) ethanol. Stearic, palmitic, and oleic-derived stearic acids showed constant specific radioactivity after several crystallizations (Table I). From the contents and the specific radioactivities of the acids, it is calculated that 92% of the radioactivity is attributable to oleic (38.3%), palmitic (35.2%), and stearic (18.6%) acids. On the other hand, no significant radioactivity was found in linoleic-derived stearic acid. The yields of myristic and palmitoleic-derived palmitic acids were too small for repeating crystallizaton.

These data clearly indicate that the methyl carbons of SCM are incorporated into fatty acid of pig adipose tissue. The fatty acids are considered to be biosynthesized presumably through the formation of acetyl-CoA; otherwise radioactivity would not be incorporated into such extensive fatty acids. The finding that linoleic acid contains no radioactivity accords with the well-known fact that the acid can not be synthesized in mammals. The difference in the specific radioactivity among stearate, palmitate, and oleic-derived stearate is undoubtedly caused by the difference in the metabolic pool sizes of the acids.

ACKNOWLEDGEMENT The authors thank Hoffmann-La Roche for generously providing the adipose tissue. They are grateful to Dr. Z. Suzuoki, Dr. S. Harada, Dr. S. Tanayama, Mr. T. Kawakami, and Dr. T. Kobayashi of the Central Research Division of our company for their valuable suggestions.

## REFERENCES AND NOTES

1) S. Harada, E. Higashide, T. Fugono, and T. Kishi, Tetrahedron Lett., 1969, 2239.
2) J. Okada, S. Yamamoto, H. Yamamoto, and S. Kondo, "Residue of Macrolide Antibiotic Sedecamycin and Its Metabolites in Swine Blood and Tissues," J. Agr. Food Chem., in press.
3) A private communication from Dr. A. MacDonald of Hoffmann-La Roche, Nutley, NJ.
4) H. Sawada, T. Suzuki, S Akiyama, and Y. Nakao, Appl. Microbiol. Biotechnol., 26, 522 (1987).
5) E. G. Bligh and W. J. Dyer, Can. J. Biochem. Physiol., 37, 911 (1959).
6) R. T. Krause, J. Assoc. Off. Anal. Chem., 68, 726 (1985).
7) M. Kayama and M. Hirata, Yukagaku, 33, 426 (1984).
8) G. A. Howard and A. J. P. Martin, Biochem. J., 46, 532 (1950).

(Received July 29, 1987)

## Communications to the Editor

[Chem. Pharm. Bull. 35(11)4668—4671(1987)]

# INDOLE ALKALOIDS ISOLATED FROM GELSEMIUM ELEGANS (THAILAND): 19-(Z)-AKUAMMIDINE, 16-EPI-VOACARPINE, 19-HYDROXYDIHYDRO-GELSEVIRINE, AND THE REVISED STRUCTURE OF KOUMIDINE

Shin-ichiro Sakai,*,[a] Sumphan Wongseripipatana,[b] Dhavadee Ponglux,[b] Masaki Yokota,[a] Koreharu Ogata,[c] Hiromitsu Takayama,[a] and Norio Aimi[a]

Faculty of Pharmaceutical Sciences,[a] and Chemical Analysis Center,[c] Chiba University, 1-33, Yayoi, Chiba 260, Japan, Faculty of Pharmaceutical Sciences, Chulalongkorn University,[b] Bangkok 10500, Thailand

Structures of the new indole alkaloids, 19-(Z)-akuammidine, 16-epi-voacarpine, 19-hydroxydihydrogelsevirine isolated from the root of Gelsemium elegans have been determined by the spectral method, X-ray analysis and chemical correlation. Koumidine was revised to show the 19-(Z) ethylidene configuration in the structure.

KEYWORDS——Gelsemium elegans; Loganiaceae; indole alkaloid; 19-(Z)-akuammidine; 16-epi-voacarpine; 19-hydroxydihydrogelsevirine; koumidine; X-ray analysis

Recently, research on the isolation and structure of the several new alkaloids from G. elegans Benth. (Loganiaceae) has been reported by a few research groups of China. They also reported structures of koumidine 1,[1] akuammidine 2,[1] humantenine 5[2] and other indole alkaloids[3,4] isolated from the same plant.

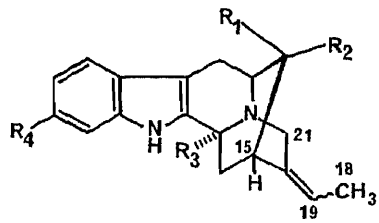


koumidine 1 $R_1=CH_2OH$, $R_2=R_3=R_4=H$, C-19 E form(a) or Z-form(b)

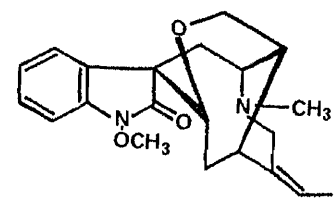


humantenine 5

16-epi-voacarpine 3 $R_1=CH_2OH$, $R_2=CO_2CH_3$, $R_3=OH$, $R_4=H$, C-19 E form

akuammidine 2 $R_1=CO_2CH_3$, $R_2=CH_2OH$, $R_3=R_4=H$, C-19 E form(a) and Z-form(b)

gardnerine 4 $R_1=CH_2OH$, $R_2=R_3=H$, $R_4=OCH_3$, C-19 E form

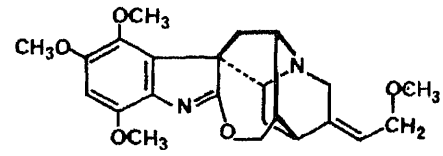


gardneramine 6

The (Z)-ethylidene configuration of humantenine 5 was determined by X-ray analysis.[2] Gardneramine 6 and its analogous alkaloids having the Z-form ethylidene configuration were isolated by us in 1971 as the first examples of 19-(Z)-ethylidene indole alkaloids, from the bark of Gardneria nutans (Loganiaceae).[5] Among Gardneria alkaloids, both the E and Z ethylidene configurations are found. Of the Gelsemium alkaloids, the configuration of the ethylidene part of 1 and 2 has not been reported. We need a careful structural elucidation for the ethylidene configuration of Gelsemium alkaloids. Therefore we reinvestigated this point.

Here we describe the revised structure of koumidine is 19-(Z)-ethylidene type structure **1b** instead of the previously reported 19-(E)-form **1a**. The so-called akuammidine isolated from G. elegans has the 19-(Z)-ethylidene type structure **2b** instead of 19-(E)-form **2a**. The new bases, 16-epivoacarpine **3** and 19-hydroxydihydrogelsevirine **7**, were isolated from the roots of G. elegans (Thailand) together with the known bases, gelsemine, gelsevirine, koumine, gelsenicine, 14-hydroxygelsenicine, humantenine, 14-hydroxygelsedine (isolated from seeds), and two unknown bases [A($C_{20}H_{24}N_2O$), B ($C_{19}H_{22}N_2O_4$)].

So-called akuammidine isolated from the roots of G. elegans showed mp 240-242°C, $[\alpha]_D^{16}$= +9°(c=0.16, MeOH) and the same mass spectral fragment pattern as authentic akuammidine (19 E form ) **2a**. However, the $^1$H-NMR and $^{13}$C-NMR spectra of the alkaloid were similar but not completely identical to the spectra of the authentic akuammidine **2a**. The $^{13}$C-NMR chemical shifts of C-15 (6.3ppm lower shift than E form) and C-21 (2.9ppm higher shift than E-form) of the isolated akuammidine **2b** compared with that of authentic C-19(E)-akuammidine **2a** can be reasonably interpreted in terms of the γ-gauche effect due to C-18 on the double bond of Z-configuration. A difference NOE experiment also supported the presence of the 19-(Z)-configuration: a 12% enhancement between C-15H and C-18 methyl group (C-15⟶C-18) of **2a** and a 23% enhancement between C-15H and C-19H (C-15⟶C-19) for the isolated alkaloid **2b**. Finally, we determined the structure of the Z-form **2b** by X-ray analysis.[6] The R value is 4.8%. Both akuammidines **2a,b** exhibited exactly the same CD curves, and therefore 19-(Z)-akuammidine **2b** also has the same absolute configuration as the common indole alkaloids.

Koumidine isolated from the roots of the same plant had mp 200-201°C(dec.) $[\alpha]_D^{21}$= -9°(c=0.10, MeOH) and all the other spectral data agreed well with those given in the literature.[1] The base gave rise to a ring closed indolenine derivative [7] by mesylation followed by a reaction with NaOMe. The $^{13}$C-NMR spectra of a koumidine was compared with that of the known base, gardnerine **4**. The signal due to C-15 of koumidine was observed at 7.6 ppm higher shift but that of C-21 was observed at 2.1 ppm lower field than the corresponding signals of **4**. The difference NOE experiment of the koumidine exhibited 13% NOE enhancement between C-15H and C-19H(C-19⟶C-15). These data showed the 19-(Z)-ethylidene configuration for the revised koumidine **1b**.

The new base 16-epi-voacarpine **3** showed mp 162-165°C, $[\alpha]_D^{22}$= +42.3°(c=0.20, $CHCl_3$). Acetylation of **3** gave rise to two products (**8** and **9**). The Nb-acetyl-2-acyl indole derivative **8** exhibited a typical 2-acyl indole UV absorption at 314 nm and $^1$H-NMR signal for an acetoxy group (s, δ 1.45, $C\underline{H}_3$) shielded by an indole skeleton.[9]

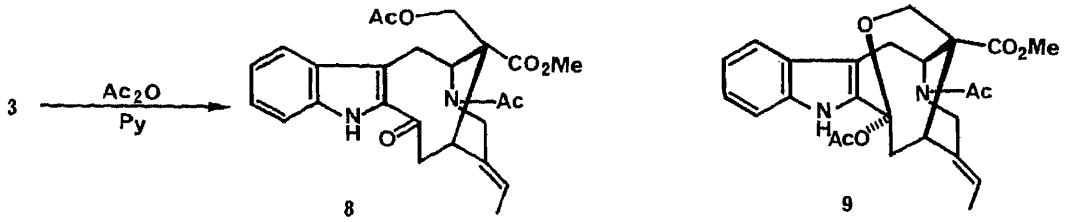


The mass spectrum[10] of the new base 3 showed a fragment pattern similar to that of voacarpine.[11] About 10% enhancement (C-15⟶C-18) observed in an NOE difference experiment between C-15H and C-18 methyl group showed the E-form of the ethylidene group in 3.

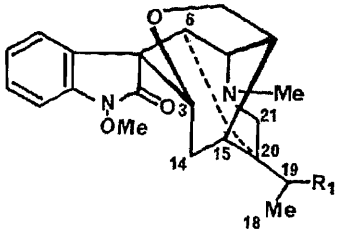


$R_1$ = C-19(R), OH 7
$R_1$ = C-19(S), OH 10
$R_1$ = H, $\Delta^{18,19}$ 11
gelsevirine
$R_1$ = =O 12

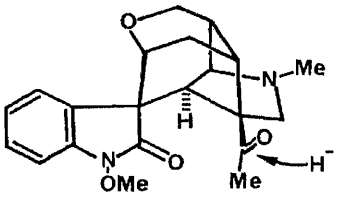


A-form 12

19-Hydroxydihydrogelsevirine 7 is an amorphous solid and showed $[\alpha]_D^{21}$= +1° (c=0.11, MeOH), $C_{21}H_{26}N_2O_4$.[12] From the $^1$H-NMR spectrum, base 10 showed the presence of Na-OMe, -O-C(3)-H, -O-$CH_2$ and Nb-Me signals. The secondary alcohol group (MeCHOH-) was revealed by signals at δ5.13 (1H, q, J=6.6Hz) and δ1.09 (3H, d, J=6.6Hz) instead of the vinyl group in gelsevirine 11. The $^{13}$C-NMR spectrum[12] of 7 showed very similar signals to those of gelsevirine 11 except that $\Delta^{18,19}$ vinyl carbons and high field shifts of C-6 (3.6 ppm) and C-21 (7.5 ppm) were observed as the result of the "γ-gauche effect" due to the C-19 secondary alcohol group. Swern's oxidation[13] of 7 gave rise to a ketone derivative which was obtained by the Wacker oxidation to the gelsevirine N-oxide.[14] Upon the reduction by $NaBH_4$, the ketone 12 gave a diastereomeric alcohol 10 as the major product, which is accompanied with trace amounts of 7. This stereospecific reduction enabled us to determine the stereochemistry of the isomeric alcohol 10 results from the reduction through a less hinderd form A of ketone 12 to the (S)-alcohol 10. Therefore, 7 takes the R configuration at C-19.

**ACKNOWLEDGMENTS** The authors are grateful to the Ministry of Education, Science and Culture of Japan for financial support [Grant-in-Aid for scientific Research (No.61470146) and Overseas Scientific Survey (No.60043014)] of this research.

## REFERENCES AND NOTES

1) a) Chu-tsin Liu, Qi-wen Wang and Chi-hao Wang, J. Am. Chem. Soc., 103, 4634 (1981); b) Francoise Khuong-Huu, Angle Chiaroni and Claude Riche, Tetrahedron

Lett., **22**, 733 (1981); c) Rao Zhu-Li and Liang Dong-Gai, Acta Physica Sinica, **31**, 547 (1982); d) Jin Hao-Lun and Xu Ren-Sheng, Acta Chimica Sinica, **40**, 1129 (1982); e) Liu Zhujin and Yu Qiansheng, Youji Huaxu, **1**, 36 (1986); f) Shin-ichiro Sakai, Etsuji Yamanaka, Mariko Kitajima, Masaki Yokota, Norio Aimi, Sumphan Wongseripipatana and Dhavadee Ponglux, Tetrahedron Lett., **27**, 4585 (1986).

2) Yang Jun-Shan and Chen Yu-Wu, Yaoxue Xuebao, **19**, 686 (1984).

3) Yang Jun-Shan and Chen Yu-Wu, Yaoxue Xuebao, **18**, 104 (1983).

4) In this paper, $CD_3OD$ was used as the solvent for measurements of the $^{13}C$-NMR of E and Z-akuammidine(**2a** and **2b**) because of the low solubility of **2b** in $CDCl_3$. A. Koskinen and M. Lounasmaa, "Progress in the Chemistry of Organic Natural Products", Vol.43, ed. by W. Herz, H. Grisebach, G. W. Kirby, Springer Verlag, 1983, p.326.

5) Norio Aimi, Shin-ichiro Sakai, Youichi Iitaka and Akiko Itai, Tetrahedron Lett., **1971**, 2061.

6) Crystals of **2b**(19-Z form) belong to the orthorhombic space group $P2_12_12_1$ with cell constants of a = 13.962(5)Å, b = 20.498(8)Å, c = 6.668(2)Å and Z = 4. A total of 2189 unique independent intensities were measured within the range of $3° \leqq 2\theta \leqq 120°$, 155°on a 4-circle diffractometer (Rigaku AFC-5) using CuK$\alpha$ radiation ($\lambda$=1.54Å). The structure was solved by the direct method using MULTSN 80 (UNICS III system) and refined anisotropically (isotropically for H) by the least-squares method,[7] using the 1886 reflections for which $/Fo/ > 3\sigma /Fo/$.

7) T. Sakurai and K. Kobayashi, Rep. Inst. Phys. & Chem. Res., 55, 69 (1979).

8) **Indolenine derivative:** mp 258-259°C, UV($\lambda$max, nm); 259, 219 213, Mass(m/z, %); 276($M^+$, 100), 275(48), 181(24), 168(58).

9) **8:** mp 138-140°C, UV( max,$\lambda$nm); 314, 238, 203, Mass(m/z, %); 452($M^+$, 71), 409(100), 309(34), 280(38), 194(43), 178(74), 172(77), $^1H$-NMR; $\delta$ 3.65(s. $CO_2CH_3$), 1.45(s. $CH_3CO_2CH_2$-), 2.12(s. N-$COCH_3$, **9:** mp 143-145°C, UV($\lambda$max, nm); 291, 282, 275, 224, Mass (m/z, %); 452($M^+$, 38), 393(87), 351(43), 333(100), 307(32), 247(43), $^1H$-NMR($CDCl_3$, 270MHz); $\delta$ 3.65(s. $CO_2CH_3$), 1.91(s. $CH_3CO_2C$-O), 2.20(s. N-$COCH_3$).

10) **3:** Mass(m/z, %); 368($M^+$, 62), 351(29), 337(28), 309(19), 265(65), 185(81), 184(100), $^{13}C$-NMR($CDCl_3$, 68MHz); C-2(s. 137.1), C-3(s. 80.5), C-5(d. 57.5), C-6(t. 21.3), C-7(s. 107.0), C-8(s. 125.7), C-9(d. 119.5), C-10(d. 115.7), C-11(d. 122.0), C-12(d. 110.9), C-13(s. 136.3), C-14(t. 36.5), C-15(d. 33.7), C-16(s. 53.2), C-17(t. 63.3), C-18(q. 12.7), C-19(d. 118.5), C-20(s. 135.4), C-21(t. 48.1), $CO_2Me$(s. 175.8), $CO_2CH_3$(q. 52.1).

11) Manfred Hesse, "Indole alkaloid," ed. by H. Budzikiewicz, Verlag Chem., **1973**, p.161.

12) **10:** High resolution Mass; Calcd. for $C_{21}H_{26}N_2O_4$ 370.1890, Found. 370.1889, $^{13}C$-NMR($CDCl_3$, 68MHz); C-2(s. 174.2), C-3(d. 69.1), C-5(d. 71.8), C-6(d. 47.5), C-7(s. 53.3), C-8(s. 127.9), C-9(d. 128.4), C-10(d. 123.0), C-11(d. 128.5), C-12(d. 107.2), C-13(s. 139.2), C-14(t. 22.6), C-15(d. 35.7), C-16(d. 38.6), C-17(t. 61.6), C-18(q. 19.4), C-19(d. 64.3), C-20(s. 56.8), C-21(t. 58.8), Nb-Me(q. 40.7), N-OMe(q. 63.3).

13) $(COCl)_2$/DMSO/$NEt_3$ in $CH_2Cl_2$, 85% in the yield of **12** (mp 225-227°C).

14) i) MCPBA, ii) $PdCl_2$, $O_2$ in DMF-$H_2O$, iii) $NaHSO_3$, 44% in the yield of **12**.

(Received September 3, 1987)

## Communications to the Editor

[Chem. Pharm. Bull. 35(11)4672—4675(1987)]

# REDUCTION OF OXIMES OF α-SUBSTITUTED β-KETOESTERS WITH SODIUM CYANOBOROHYDRIDE: STEREOSELECTIVE SYNTHESIS OF 3,4-CIS-SUBSTITUTED AZETIDIN-2-ONES[1)]

Takuo Chiba,* Takenori Ishizawa, Jun-ichi Sakaki, and Chikara Kaneko*
Pharmaceutical Institute, Tohoku University, Aobayama, Sendai 980

erythro-3-Hydroxyamino-2-alkylbutanoate and its derivatives were prepared stereoselectively by reduction of the oximes of the corresponding β-ketoesters with sodium cyanoborohydride in acidic media. Cyclization of the β-amino acids obtained by reduction and successive hydrolysis gave 3,4-cis-substituted azetidin-2-ones.

KEYWORDS——3,4-cis-substituted azetidin-2-one; erythro-β-amino acid; β-hydroxyiminoester; diastereoselective reduction; sodium cyanoborohydride; diastereofacial selectivity

Though many methods for the introduction of functionalized alkyl groups (e.g. the 1-hydroxyethyl group) into azetidin-2-ones have been described these methods invariably afforded 3,4-trans-azetidin-2-ones. For examples, direct aldol condensation with acetaldehyde[2)] and acetylation followed by reduction[3)] of 4-substituted azetidin-2-ones both proceeded stereoselectively to give thermodynamically more stable trans-3,4-substituted azetidinones, which are used to synthesize thienamycin and related trans-carbapenems. The discovery of carpetimycin A[4)] and its analogues has, however, aroused much interest in the synthesis of 3,4-cis-substituted azetidinones, which can serve as building blocks for these cis-carbapenems. Though several useful methods have been elaborated for construction of cis-azetidinones, they are not so highly stereoselective[5,6)] or have limited utility for introducing a variety of functionalities into the 4-substituent.[7,8)]

In this paper, we report highly stereoselective synthesis of erythro-β-amino acids (D) from α-substituted β-ketoesters (A) which are the important precursors for cis-3,4-azetidin-2-ones. We expected that a six-membered chelate complex (B')

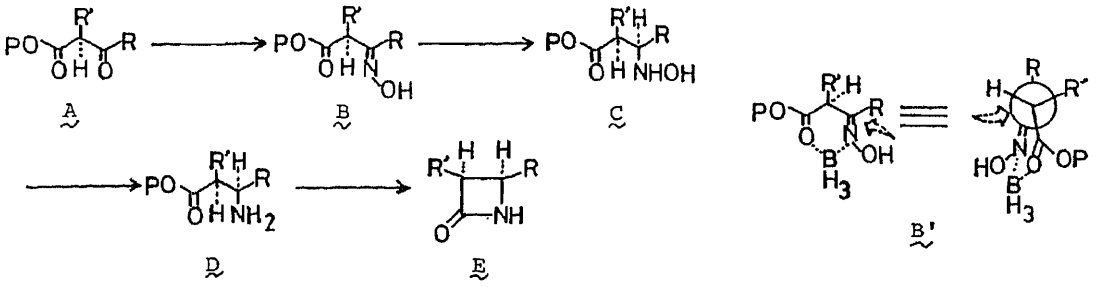

Chart 1 P is a protecting group.

could be formed, when β-hydroxyiminoester (B) is reduced with sodium cyanoborohydride in acidic media, and could control the direction of the attack of the reducing reagent from the less-hindered side giving the desired erythro-β-hydroxyaminoesters (C), whose further hydrogenation over Raney nickel and deblocking of the ester group afford the desired erythro-β-amino acids (D) ready for cyclization to the final azetidinones (E). The advantage of this strategy is obvious, because the desired functionality of R and R' of the starting material (A) can be readily introduced at an early stage.

To verify our strategy, we first examined the synthesis of 3,4-dimethylazetidin-2-one from tert-butyl 2-methylacetoacetate (1). Thus, the oxime (2) was reduced by sodium cyanoborohydride in acidic media at 0°C and the crude product (3) was hydrogenated further over Raney nickel to give a single amino ester (4) as almost the sole product. After acidic hydrolysis of 4, the acid (5) was cyclized by usual method[9] to give azetidinone [6: oil, $\delta(CDCl_3)$: 1.18, d (J=7 Hz, $CH_3$) and 1.22, d (J=6Hz, $CH_3$), $\nu_{CO}$=1755 $cm^{-1}$][10] in 62% yield. A large coupling constant (J=5.0Hz) between protons at the 3- and 4-positions of 6 clearly demonstrates their cis-relationship. A small amount (ca. 1/20 to 6) of another isomer [probably trans-isomer: $\delta(CDCl_3)$: 1.25 (3H, d, J=7Hz), 1.33 (3H, d, J=6Hz), 2.74 (1H, ddq, J=7, 2, 1Hz), 3.36 (1H, dq, J=6, 2Hz)] was detected from the spectrum, whose proportion increased up to ca. 20%, when the reduction step (2→3) was carried out at room temperature.[11] This remarkable stereoselectivity in the reduction step (step b) is due to involvement of the expected cyclic species (B'). Though we tentatively consider borane as the chelating species, proton may also participate in constructing an equally rigid cyclic system.[12]

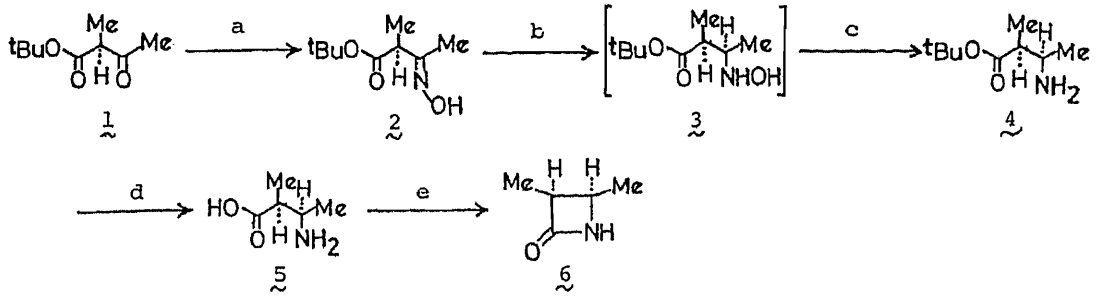


1 2 3 4 5 6

Chart 2 Reagents: a, $NH_2OH$, MeOH, 0°C; b, $NaBH_3CN$, AcOH-THF(2:1), 0°C; c, $H_2$, Raney-Ni, MeOH; d, conc. HCl; e, DCC or $Ph_3P$, $(2\text{-PyS})_2$, $CH_3CN$

Usual silylation of tert-butyl acetoacetate (7) afforded silyl enol ether (8) as a single isomer[13], which by trimethylsilyl trifluoromethanesulfonate ($TfOSiMe_3$) catalyzed aldol condensation[15] with 2,2-dimethoxypropane led to 2-(1-methoxyisopropyl)acetoacetate [9: oil, $\delta(CDCl_3)$: 1.34 (3H, s, $CH_3$), 1.37 (3H, s, $CH_3$), 3.22 (3H, s, $OCH_3$)]. Conversion of 7 to 10 proceeded in almost quantitative yield.[16] Sequential reactions used to convert 2 to 6 were then applied to 10 to give 3-(1-methoxyisopropyl)-4-methylazetidin-2-one [13: mp 60-61°C, $\delta(CDCl_3)$: 1.49 (3H, d, J=7Hz, $CH_3$), 3.20 (1H, d, J=5Hz, 3-H), 3.85 (1H, dq, J=5, 7Hz, 4-H)] as the sole product in 32% overall yield from 10. When the reduction step (10 to the hydroxylamine) was carried out at 0°C, no trans-isomer was detected even in the mother liquor fraction of 13. This indicates again that the involvement of cyclic

intermediate (B') is valid and diastereofacial selectivity in the cyclic species is more pronounced when R' becomes more bulky than the methyl group.

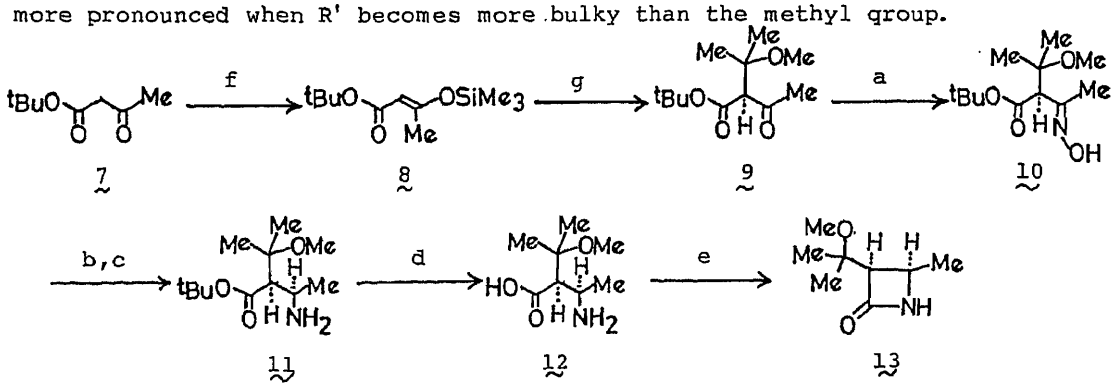

Chart 3 Reagents: a-e are the same in Chart 2; f, $Me_3SiCl$, $Et_3N$, THF, reflux; g, $Me_2C(OMe)_2$, $TfOSiMe_3$, $CH_2Cl_2$, -45°C

The same aldol condensation using acetal (1,1-dimethoxyethane) instead of the ketal also proceeded smoothly. Thus, the two-step procedure using this acetal was applied to 7, the product (14) was obtained in 90% yield as an inseparable mixture of diastereomers in nearly equal amount. The mixture was then transformed to β-lactam (17) in 42% overall yield. Two isomers (both 3,4-cis) were separated by silica gel column chromatography to give a readily crystallizable major one [(S*)-17: mp 62-63°C] and an oily minor one [(R*)-17] in ca. 4:3 ratio.

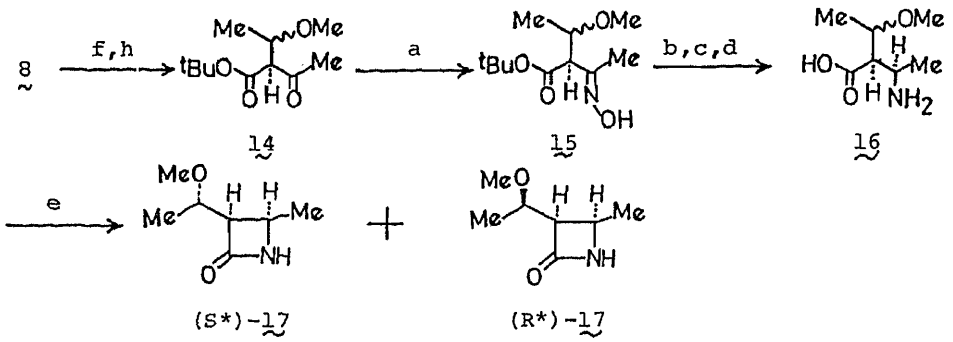

Chart 4 Reagents: a-f are the same in Chart 3; h, $MeCH(OMe)_2$, $TfOSiMe_3$, $CH_2Cl_2$, -45°C

Inspection of NMR spectra of both isomers ($J_{3,4}$=5.5Hz for both isomers) revealed that the coupling constants $C_3$ and $C_1$, are larger (11.0Hz) for the major one than for the minor one (7.0Hz) and these data are in good accordance with those of the related β-lactams reported by McCombie et al.[17] Thus, the relative stereochemistries of both isomers are assigned as ($S^*$) for the major one and ($R^*$) for the minor one. It has also been shown that the use of benzyl ester instead of tert-butyl ester likewise proceeds under the same stereocontrol and use of 4-benzyloxyacetoacetates provides 4-benzyloxymethylazetidinones.[18] These facts

suggests that the present methodology can be used for the synthesis of a variety of 3,4-cis-substituted azetidin-2-one derivatives. Further work is now in progress in applying the method to the synthesis of chiral azetidinones.

ACKNOWLEDGEMENTS This work was supported in part by the Ministry of Education, Science, and Culture, Japan (Grant-in-Aid, No. 62870084).

REFERENCES AND NOTES

1) Part VIII of "Studies on Amino Acid Derivatives", Part VII; Ref. 14.
2) D. B. R. Johnston, S. M. Schmitt, F. A. Bouffard, and B. G. Christensen, J. Am. Chem. Soc., 100, 313 (1978).
3) T. N. Salzmann, R. W. Ratcliffe, B. G. Christensen, and F. A. Bouffard , J. Am. Chem. Soc., 102, 6161 (1980).
4) M. Nakayama, A. Iwasaki, S. Kimura, T. Mizoguchi, S. Tanabe, A. Murakami, I. Watanabe, M. Okuchi, H. Itoh, Y. Saino, F. Kobayashi, and T. Mori, J. Antibiot., 33, 1388 (1980); A. Imada, Y. Nozaki, K. Kintaku, K. Okonogi, K. Kitano, and S. Harada, ibid., 33, 1417 (1980).
5) N. Natsugari, Y. Matsushita, N. Tamura, K. Yoshioka, and M. Ochiai, J. Chem. Soc., Perkin Trans. I, 1983, 403.
6) D. Ha, D. J. Hart, and T. Yang, J. Am. Chem. Soc., 106, 4819 (1984).
7) T. Iimori, Y. Takahashi, T. Izawa, S. Kobayashi, and M. Ohno, J. Am. Chem. Soc., 105, 1659 (1983).
8) N. Oguni, S. Tomago, and K. Inami, Chemistry Express, 1, 579 (1986).
9) Cyclization of these β-amino acids can be effected either by usual DCC method or by Mukaiyama-Ohno's procedure.[a] a: S. Kobayashi, T. Iimori, T. Izawa, and M. Ohno, J. Am. Chem. Soc., 103, 2406 (1981).
10) New compounds were identified by either elemental analysis or by high-resolution mass spectra, and the structures were supported by acceptable spectral data.
11) Actual isolation of the trans-isomer was failed, since it exhibited almost the same property as cis-isomer on chromatography.
12) Almost exclusive formation of the erythro diastereomers has been observed under the same reduction conditions for the systems (F[a] and G[b]). In both cases the unsaturated bond to be reduced has groups capable of complexing with borane (or proton) to form similar cyclic species. a: G. Rosini, A. Medici, and M. Soverini, Synthesis, 1979, 789; b: D. G. Melillo, I. Shinkai, T. Liu, K. Ryan, and M. Sletzinger, Tetrahedron Lett., 21, 2783 (1980).

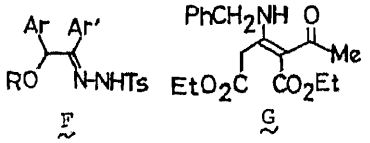


F G

13) Oil, bp 75-76°C (5mmHg), δ($CDCl_3$): 0.29 (9H, s, $SiMe_3$), 1.49 (9H, s, t-Bu), 2.21 (3H, s, $CH_3$), 5.04 (1H, s, -CH=). Since tert-butyl formylacetate[14] afforded stereoselectively an [E]-sily enol ether ($J_{2,3}$=12Hz) under the same condition, the stereochemistry of 8 is also assigned as the [E]-isomer.
14) T. Chiba, J. Sakaki, T. Takahasi, K. Aoki, A. Kamiyama, C. Kaneko, and M. Sato, J. Chem. Soc., Perkin Trans. I, 1987 , 1845.
15) S. Murata, M. Suzuki, and R. Noyori, J. Am. Chem. Soc., 102, 3248 (1980).
16) When 8 reacted with 2,2-dimethoxypropane in the presence of a catalytic amount of $TfOSiMe_3$, a significant amount of the simple hydrolysis product (7) was obtained. Since 7 could be recycled, however, the overall yield of 10 from 7 is almost quantitative based on the consumed 7.
17) S. W. McCombie, A. K. Ganguly, V. M. Girijavallabhan, P. D. Teffrery, S. Lin, and P. Pinto, Tetrahedron Lett., 22, 3489 (1981).
18) Major isomer corresponding to (S*)-cis-form, mp 54.5-56°C, δ($CDCl_3$): 1.31(3H, d, J=6Hz), 3.25 (3H, s), 3.28 (1H, ddd, J=11, 5, 2Hz), 3.59 (1H, t, J=9Hz), 3.64 (1H, dd, J=11, 6Hz), 3.89 (1H, dd, J=9, 3Hz), 3.94 (1H, ddd, J=9, 5, 3Hz), 4.53 (1H, d, J=12Hz), 4.57 (1H, d, J=12Hz), 6.03-6.16 (1H, brs), 7.25-7.30 (5H, m).

(Received September 10, 1987)

## Communications to the Editor

[Chem. Pharm. Bull. 35(11)4676—4679(1987)]

# THE FIRST EXAMPLES OF ISOLATED N-UNSUBSTITUTED 1H-1,4-BENZODIAZEPINES

Haruki Sashida, Mamoru Kaname, and Takashi Tsuchiya*
School of Pharmacy, Hokuriku University,
Kanagawa-machi, Kanazawa 920-11, Japan

The photolysis in the presence of sodium methoxide of the 4-azidoquinolines (5a-g) having a carbonyl group or its analogue in the 2- or 8-position resulted in ring expansion to give the stable N-unsubstituted 1H-1,4-benzodiazepines (6a-g). These were assumed to be stabilized by intramolecular hydrogen bonding between the NH and the 2- or 9-acyl groups. It is known that the N-unsubstituted 1H-1,4-benzodiazepines having no acyl group are too unstable to be isolated.

KEYWORDS ——— 4-azidoquinoline; photolysis; ring expansion; N-unsubstituted 1H-1,4-benzodiazepine; hydrogen bonding

Among the six benzodiazepine isomers due to the isomeric positions of the two nitrogen atoms, the 1,4-benzodiazepines have been most widely studied owing to their biological activities,[1] but only a few examples of fully unsaturated compounds have been reported[2] prior to our recent work.[3] Therefore, we were interested in finding new routes to fully unsaturated 1,4-benzodiazepines as part of our continuing studies on diazepines.[4] We have recently reported[3] the first formation of the N-unsubstituted 1H-1,4-benzodiazepines (3) via the azirine intermediates (2) by irradiation of the 4-azidoquinolines (1) in the presence of sodium methoxide. However, the 1H-1,4-benzodiazepines (3) are extremely unstable and thus can not be isolated, although they are tautomerized to the stable 3H-isomers (4) by further treatment with sodium methoxide. We report here that the N-unsubstituted 1H-1,4-benzodiazepines (6) having a carbonyl group or its analogue in the 2- or 9-position derived from the corresponding 4-azidoquinolines (5) can be isolated as stable crystals. Apparently, they are stabilized by intramolecular hydrogen bonding.

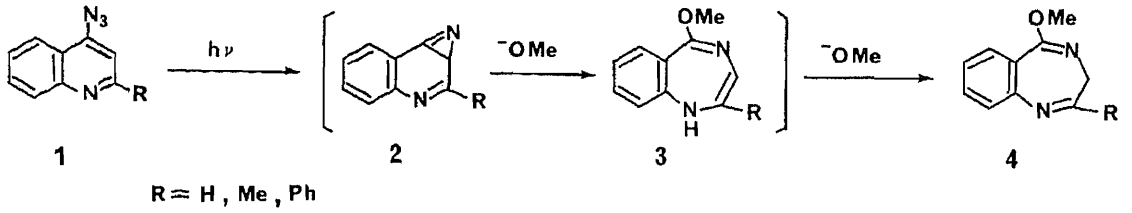


1 2 3 4

R = H, Me, Ph

Chart 1

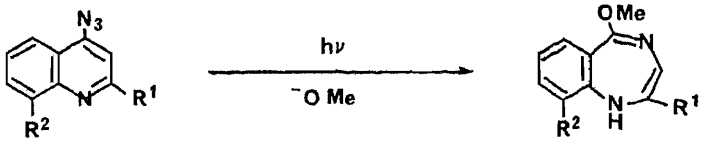

5a–g 6a–g

| | $R^1$ | $R^2$ |
|---|---|---|
| a : | $CONH_2$ | H |
| b : | COMe | H |
| c : | $CO_2Me$ | H |
| d : | H | $CONH_2$ |
| e : | H | COMe |
| f : | H | $SO_2Me$ |
| g : | H | $NO_2$ |

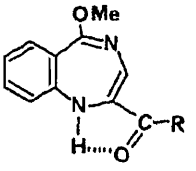

7

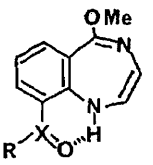

8

XOR = $CONH_2$, COMe, $SO_2Me$, $NO_2$

Chart 2

Irradiation (400 W, high-pressure Hg lamp; Pyrex filter) of the 4-azido-2-carbamoylquinoline[5] (5a: 0.5 g) in methanol-dioxane (1:1) containing sodium methoxide (3-4 mol eq) for ca. 20 min resulted in the formation of 2-carbamoyl-5-methoxy-1H-1,4-benzodiazepine (6a) in 65% yield as a stable crystal.[6] Under similar conditions, the 2-acetyl- (6b) and 2-methoxycarbonyl- 1H-1,4-benzodiazepines (6c) were also obtained from the corresponding 4-azidoquinolines[7] (5b,c) in 35% and 20% yields, respectively, as the sole characterizable products.

The $^1$H-NMR spectra of the products 6a-c showed NH proton signals at $\delta$ 5.4-5.6 and no signals due to methylene or methine protons, and $^{13}$C-NMR spectra of 6a-c exhibited no signals due to $sp^3$ carbon, except for the methyl carbons. These data are consistent with the proposed 1H-structure and rule out other possible 3H- and 5H-structures. In the IR spectra of 6a-c, both the carbonyl and the NH sbsorptions appeared at lower wave-lengths; C=O (6a: 1658; 6b: 1652; 6c: 1698 $cm^{-1}$) and NH (ca. 3350 $cm^{-1}$). These lower-frequency shifts clearly depend on hydrogen bonding between the 1-NH hydrogen and the CO oxygen, as illustrated in the structure 7. These spectral data strongly suggest that the 1H-1,4-benzodiazepines (6a-c) are stabilized by this hydrogen bonding. The similar hydrogen

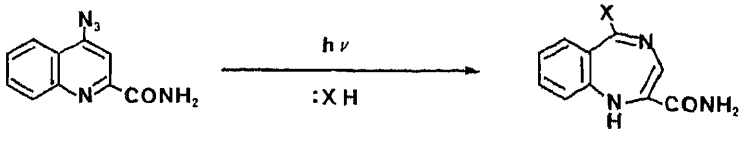

5a 9a–f

HX; a: $HNEt_2$, b:  , c: 

d:  , e: 

Chart 3

bonding effect has also been observed in 2-acyl-1H-azepines.[8]

Similarly, the 4-azidoquinolines (5d-g) having a carbonyl, sulfonyl, or nitro group in the 8-position, upon irradiation under similar conditions, afforded the corresponding 9-substituted 5-methoxy-1H-1,4-benzodiazepines (6d-g) in 20-60% yields.[9] These products 6d-g are also assumed to be stabilized by the hydrogen bonding shown in structure 8.

The products 6a-g thus obtained are the first examples of isolated N-unsubstituted 1H-1,4-benzodiazepines, although the N-acetyl compounds have been prepared from the 3H-benzodiazepines (4) by treatment with acetyl chloride in pyridine. In addition, the 1H-benzodiazepines (6) did not undergo tautomerization to 3H-isomers by further treatment with sodium methoxide, in contrast to the case of the compounds 3.

Next, we examined the photochemical behavior of 4-azidoquinolines in the presence of nucleophiles other than sodium methoxide. Photolysis of the 4-azidoquinolines (1) having no carbonyl group in the presence of amines or thiols only resulted in decomposition to give no characterizable products, presumably because the initially formed unstable 1H-benzodiazepines of type 3 could not be tautomerized by the weak bases used in the reaction, and thus were decomposed during isolation. However, 4-azido-2-carbamoylquinoline (5a), upon irradiation for 20-30 min in dioxane containing an amine (diethylamine, piperidine, or morpholine), gave the corresponding 5-amino-1H-1,4-benzodiazepines (9a-c) in 85-95% yields.[10] Similarly, photolysis of 5a in dioxane-water (1:1) containing a sodium thiolate (2-propanethiolate or benzenethiolate: ca. 10 mol eq) and 18-crown-6 (1-2 mol eq) resulted in the formation of 5-isopropylthio- (9d) or 5-phenylthio-2-carbamoyl-1H-1,4-benzodiazepine (9e) in 20-30% yield.[11] The products 9a-e may also be stabilized by hydrogen bonding, thus allowing isolation.

## REFERENCES AND NOTES


1) G.A. Archer and L.H. Sternbach, Chem. Rev., 68, 747 (1968); L.H. Sternbach, Angew. Chem., Int. Ed. Engl., 10, 34 (1971); J.T. Sharp, "Comprehensive Heterocyclic Chemistry," Vol. 7, ed. by A.R. Katritzky and C.W. Rees, Pergamon Press, Oxford, 1984, p. 593.

2) P. Nedenskov and M. Mandrap, Acta Chem. Scand., B, 31, 701 (1977); K.R. Randles and R.C. Storr, J. Chem. Soc., Chem. Commun., 1984, 1485.

3) H. Sashida, A. Fujii, H. Sawanishi, and T. Tsuchiya, Heterocycles, 24, 2147 (1986); H. Sashida, A. Fujii, and T. Tsuchiya, Chem. Pharm. Bull., 35, 3182 (1987).

4) For examples, see J. Kurita, K. Iwata, and T. Tsuchiya, Chem. Pharm. Bull., 35, 3166 (1987); H. Sawanishi, K. Tajima, and T. Tsuchiya, ibid., 35, 3175 (1987); and refs. cited therein.

5) S. Kamiya, S. Sueyoshi, M. Miyahara, K. Yanagimachi, and T. Nakashima, Chem. Pharm. Bull., 28, 1485 (1980).

6) Satisfactory elemental analyses and spectral data were obtained for all products reported; e.g., 6a; mp 159-160 °C; IR (KBr): 3420 and 3356 (NH), 1658 (C=O) $cm^{-1}$; $^1$H-NMR ($CDCl_3$) $\delta$ : 3.87 (3H, s, 5-OMe), 5.6 (3H, br, 1-NH and 2-$CONH_2$), 6.56 (1H, s, 3-H), 6.5-7.4 (4H, m, Ar-H); $^{13}$C-NMR $\delta$ : 54.36 (q, 5-OMe), 123.85

(s, 2-C), 164.89 (s, 5-C), 129.89 (d, 3-C), 181.90 (s, C=O), Ph-C [119.77 (d), 122.42 (d), 124.72 (d), 129.90 (s), 133.54 (d), 155.07 (s)]; 6b: mp 116-118 °C; 6c: mp 143-145 °C.

7) 4-Azidoquinolines (5b-g) were prepared from the corresponding 4-chloroquinolines by treatment with sodium azide.

8) N.R. Ayyangar, A.K. Purohit, and B.D. Tilak, J. Chem. Soc., Chem. Commun., 1981, 399.

9) Compound 6d: mp 110-112 °C; IR (KBr): 3352, 3284; 3256, and 3188 (NH), 1674 (C=O) $cm^{-1}$; $^1$H-NMR $\delta$ : 3.76 (3H, s, 5-OMe), 5.32 (1H, dd, J=6 and 7 Hz, 2-H), 5.72 (1H, d, J=6 Hz, 3-H), 6.2 (2H, br, $CONH_2$), 6.70 (1H, dd, J=8 and 8 Hz, 7-H), 7.34 (2H, d, J=8 Hz, 6- and 8-H), 8.0 (1H, br d, J=7 Hz, 1-NH); 6e: mp 83-85 °C; 6f: mp 107-109 °C; 6g: mp 133-135 °C.

10) Compound 9a: mp 183-185 °C; IR (KBr): 3344, 3264, 3176 (NH), 1668 (C=O) $cm^{-1}$; $^1$H-NMR $\delta$ : 1.18 and 3.38 (6H, t, and 4H, q, J=7 Hz, 2 N-Et), 5.6 (1H, br, 1-NH), 5.7 (2H, br, $CONH_2$), 6.9 (1H, s, 3-H), 6.7-7.4 (4H, m, Ar-H); 9b: mp 193-195 °C; 9c: mp 200-201 °C.

11) Compound 9d: mp 165-166 °C; IR (KBr): 3504, 3328, 3192 (NH), 1664 (C=O) $cm^{-1}$; $^1$H-NMR $\delta$ : 1.40 [6H, s, $CH(\underline{Me})_2$], 3.78 [1H, m, $C\underline{H}(Me)_2$], 5.6 (1H, br, 1-NH), 5.8 (2H, br, $CONH_2$), 6.90 (1H, s, 3-H), 6.5-7.5 (4H, m, Ar-H); 9e: mp 178-179 °C.

(Received September 19, 1987)

## Communications to the Editor

[Chem. Pharm. Bull. 35(11)4680—4682(1987)]

# THE STRUCTURES OF $AH_{15}$ AND $AH_{18}$, NEW BI- AND TRI-PHENYLETHYLCHROMONES FROM AGALWOOD

Kiyoshi Iwagoe,[a] Sanetaka Kodama,[a] Tenji Konishi,[a] Shiu Kiyosawa,*[,a] Yasuhiro Fujiwara,[a] and Yasuo Shimada[b]
Kyoto Pharmaceutical University,[a] Nakauchi-cho, Misasagi, Yamashina-ku, Kyoto, 607, Japan, and Mitsuboshi Seiyaku Company,[b] 153, Gose-shi, Nara, 639-22, Japan

New bi- and tri-2-(2-phenylethyl)chromones, tentatively named $AH_{15}$ and $AH_{18}$ were isolated from Agalwood "Jinkō" and their structures were determined.

KEYWORDS——— bi-2-(2-phenylethyl)chromone; tri-2-(2-phenylethyl)-chromone; agalwood; Aquilariaceae; $^1$H-NMR; $^{13}$C-NMR

New bi- and tri-2-(2-phenylethyl)chromones, $AH_{15}$ and $AH_{18}$ were isolated from the acetone extracts of agalwood "Jinkō" from Kalimantan, along with other related compounds.[1)]

This paper describes the characterization of these structures.

$AH_{15}$, $C_{34}H_{30}O_9$, colorless needles, mp 244-245°C, $[\alpha]_D$ +5.8° (MeOH) appeared to be a bi-2-(2-phenylethyl)chromone derivative according to their IR (KBr), UV (MeOH) and $^1$H-NMR spectra : 1668, 1625, 1590 cm$^{-1}$ and 244 nm, $\varepsilon$ =36321 ($\gamma$-pyrone ring); $\delta$ 6.11, 6.16 (each s, 3-H). The structure of monomeric one (Unit A) of the dimer appeared to be agarotetrol on the basis of four methine proton signals at $\delta$ 3.89, 4.33, 4.59 and 5.34, and the vicinal coupling systems of 5/6 trans, 6/7 cis, and 7/8 trans (Table I). The doublet signal of the methine proton in the downfield position at $\delta$ 5.34 should be assigned to 5-H because of the effect of bonding of the ether at $C_5$ to another monomeric unit (Unit B), as in the case of $AH_{10}$.[1c)]

The structure and the assignments of protons of Unit B were elucidated by measuring the nuclear Overhauser effect (NOE) difference and $^1$H-$^{13}$C shift-correlated spectra. Irradiation of the 5-H at $\delta$ 5.34 gave appreciable NOE increase of the 5'-H as a well defined doublet signal at $\delta$ 7.23 and further irradiation of 5'-H indicated an NOE increase of 8'-H along with an increase of 5-H. The presence of the hydroxyl group linked at 7'-position was confirmed by the respective irradiation of phenolic and aquatic protons at $\delta$ 9.95 and 3.40 which gave an NOE increase of 8'-H.

Accordingly, the structure of Unit B was assumed to be a 6,7-disubstituted one. The above results and the $^{13}$C-NMR spectrum support the conclusion that $AH_{15}$ is (5S,6S,7R,8S)-2-(2-phenylethyl)-6,7,8-trihydroxy-5,6,7,8-tetrahydro-5-[2-(2-

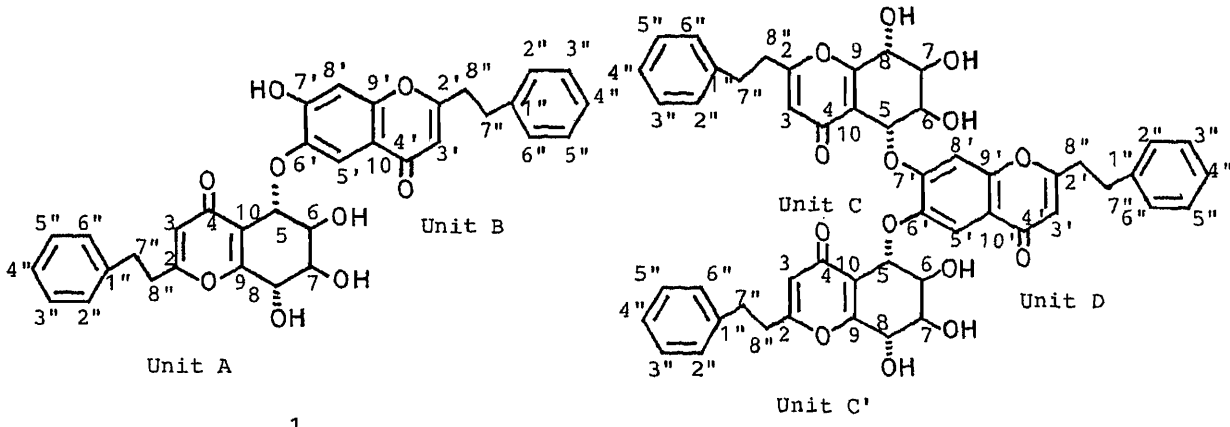


1 2

phenylethyl)-7-hydroxy-chromonyl-6-oxy]chromone, 1.

$AH_{18}$ (2), $C_{51}H_{46}O_{14}$, a white powder (mp 147-148°C), $[\alpha]_D$ -109.1° (MeOH), IR (KBr): 1658, 1600 $cm^{-1}$, UV (MeOH): 250 nm, $\varepsilon$ =39215 showed peaks at m/z 883 ($M^+$+H) and 905 ($M^+$+Na) in the FD-MS. The $^1$H-NMR spectrum of 2 (300 MHz, in DMSO-$d_6$) showed three proton signals at $\delta$ 6.107, 6.136, 6.142 (each s, 3-H) and three sets of phenylethyl groups, indicating the structure of a tri-2-(2-phenylethyl)chromone derivative of 2. Two units (Unit C and C') of the trimer appeared to be 5,6,7,8-tetrahydroxy-2-(2-phenylethyl)-5,6,7,8-tetrahydrochromone derivatives, identical with each other because of the presence of the respective pair of the adjacent two proton signals for each proton of the methine and three hydroxyl groups attached to hexenyl ring of the chromone (Table I). The structures of the two units, Unit C and C' were characterized as agarotetrol linked at $C_5$ by the ether bond to another monomeric unit (Unit D) on the basis of the chemical shifts and coupling systems of the four methine protons similar to those of $AH_{10}$ and $AH_{15}$ (Table I).

It appears that the structure of Unit B is 6.7-dialkoxy-2-(2-phenylethyl)chromone, based on the two singlet proton signals ($\delta$ 7.85 and 7.73) assumed to be located at the $C_5$ and $C_8$ positions of the chromone ring.

The above results were supported by the $^{13}$C-NMR spectrum, indicating the presence of one pair of signals for each carbon 5-8 position of 5-alkoxy-agarotetrol, and three set signals of $C_2$, $C_4$ and $C_{1''}$, respectively (Table II).

Accordingly, $AH_{18}$ was concluded to be bi-(5S,6S,7R,8S)-2-(2-phenylethyl)-6,7,-8-trihydroxy-5,6,7,8-tetrahydro-5-[2-(2-phenylethyl)chromonyl-6,7-dioxy]chromone, 2.

$AH_{18}$ was first isolated from agalwood as the trimer of 2-(2-phenylethyl)chromone. As it relates to the biogenesis of polymerization of 2-(2-phenylethyl)chromones it is noteworthy that these di- and trimers were found to be agarotetrol- and isoagarotetrol-linked at $C_5$ and $C_8$ by the ether bond to $C_6$ and $C_7$ positions of another monomeric unit, 2-(2-phenylethyl)chromone derivatives, except for the structure of the C-C linkage, $AH_{11}$.[1c,d]

Table I. $^1$H-NMR Spectral Data for $AH_{15}$ and $AH_{18}$ ( $\delta$ in DMSO-$d_6$)

| | $AH_{15}$ (1) | | $AH_{18}$ (2) | |
|---|---|---|---|---|
| | Unit A | Unit B | Unit C and C' | Unit D |
| 5,5'-H | 5.34 d<br>J=8.0 | 7.23 d<br>J=2.0 | 5.41 d J=7.0<br>5.56 d J=7.0 | 7.85 s |
| 6-H | 4.33 dd<br>J=8.0,2.0 | | 4.26 ddd J=7.0,6.5,2.0<br>4.35 ddd J=7.0,6.5,2.0 | |
| 7-H | 3.89 dd<br>J=3.6,2.1 | | 3.85 ddd J=4.0,4.0,2.0<br>3.89 ddd J=4.0,4.0,2.0 | |
| 8,8'-H | 4.59 d<br>J=3.7 | 6.94 d<br>J=2.0 | 4.56 dd J=5.0,4.0<br>4.59 dd J=5.0,4.0 | 7.73 s |
| 6-OH | | | 5.44 d J=6.5<br>5.48 d J=6.5 | |
| 7-OH | | 9.95 s | 5.31 d J=4.0<br>5.32 d J=4.0 | |
| 8-OH | | | 5.45 d J=5.0<br>5.45 d J=5.0 | |
| 3-H | 6.16 s | 6.11 s | 6.142 s, 6.136 s | 6.107 s |
| $CH_2CH_2$ | 2.51 m(4H),2.94 m(4H) | | 2.64 m(6H),2.92 m(6H) | |
| $C_6H_5$ | 6.96 dd J=7.5,2.0<br>7.17 m(4H),7.21 m(4H) | | 6.95 m(3H),7.12 m(6H),7.20 m(6H) | |

Table II. $^{13}$C-NMR Spectral Data for $AH_{15}$ and $AH_{18}$ [a)]

| | $AH_{15}$ (1) (DMSO-$d_6$) | | $AH_{18}$ (2) (DMSO-$d_6$) | | |
|---|---|---|---|---|---|
| Carbon | Unit A | Unit B | Unit C and C' | | Unit D |
| 2,2' | 167.82 | 167.46 | 167.96 | 167.68 | 167.64 |
| 3,3' | 113.11 | 108.60 | 112.81 | 112.81 | 109.30 |
| 4,4' | 177.81 | 176.35 | 177.87 | 177.79 | 175.81 |
| 5,5' | 77.96 | 108.79 | 77.09 | 76.87 | 108.64 |
| 6,6' | 68.87 | 149.58 | 68.64 | 68.56 | 147.84 |
| 7,7' | 73.19 | 154.40 | 73.14 | 73.04 | 154.93 |
| 8,8' | 64.17 | 99.89 | 64.10 | 64.01 | 104.02 |
| 9,9' | 159.40 | 154.40 | 159.72 | 159.25 | 151.82 |
| 10,10' | 124.72 | 121.81 | 121.75 | 121.61 | 116.90 |
| 1" | 139.59 | 139.83 | 139.66 | 139.72 | 139.93 |
| 2",6" | 128.19 | 128.19 | 127.92 | 127.92 | 127.92 |
| 3",5" | 127.88 | 127.88 | 127.69 | 127.69 | 127.69 |
| 4" | 126.06 | 126.06 | 125.87 | 125.87 | 125.74 |
| 7" | 31.45 | 31.74 | 31.30 | 31.45 | 31.85 |
| 8" | 34.16 | 34.52 | 33.78 | 33.95 | 34.75 |

a) Assignments of $C_5$-$C_8$ were established by $^1$H-$^{13}$C shift-correlated spectrum.

REFERENCES

1) a) Y. Shimada, T. Tominaga, T. Konishi, and S. Kiyosawa, Chem. Pharm. Bull., 30, 3791 (1982); b) Y. Shimada, T. Konishi, S. Kiyosawa, M. Nishi, K. Miyahara, and T. Kawasaki, ibid., 34, 2766 (1986); C) K. Iwagoe, T. Konishi, S. Kiyosawa, Y. Shimada, K. Miyahara, and T. Kawasaki, ibid., 34, 4889 (1986); d) K. Iwagoe, T. Konishi, S. Kiyosawa, Y. Shimada, K. Miyahara, and T. Kawasaki, Abstracts of Papers, The 107th Annual Meeting of Pharmaceutical Society of Japan, Kyoto, April 1987, P. 366.

(Received September 25, 1987)

## Communications to the Editor

[Chem. Pharm. Bull. 35(11)4683—4686(1987)]

# THE ABSOLUTE CONFIGURATION OF REGELIDINE, A NOVEL 6-NICOTINOYL DIHYDROAGAROFURAN SESQUITERPENE ALKALOID FROM TRIPTERYGIUM REGELII[1)]

Hitoshi Hori,[a] Guo-Mao Pang,[a,2)] Kenzo Harimaya,[a] Yoichi Iitaka,[b] and Seiichi Inayama*,[a]

Pharmaceutical Institute, School of Medicine, Keio University,[a] 35 Shinanomachi, Shinjuku-ku, Tokyo 160, Japan and Faculty of Pharmaceutical Sciences, The University of Tokyo,[b] Bunkyo-ku, Tokyo 113, Japan

Regelidine (1), a new nicotinoyl sesquiterpene alkaloid, was isolated from the roots of Tripterygium regelii. The structure of 1 was determined on the basis of $^{1}H$-, $^{13}C$-NMR spectrometry and X-ray crystallography. The absolute configuration of 1 was deduced unambiguously by the anomalous dispersion method.

KEYWORDS ——— regelidine; sesquiterpene; alkaloid; Tripterygium regelii; $^{1}H$-NMR; $^{13}C$-NMR, X-ray diffraction; absolute configuration

In our preceding paper,[3)] regelin and regelinol isolated from Tripterygium regelii (Celastraceae) were reported as new antitumor triterpenoids. A novel nicotinoyl sesquiterpene alkaloid referred to regelidine (1) has been isolated from the same plant, along with these major triterpinoid constituents.[1,4)]

Following the preliminary communication concerning the novel structure of maytoline as the prototype of a new family of alkaloids,[5)] the structures of more than 20 related alkaloids from the family Celastraceae have been reported. But their structures have not been fully confirmed, although in most cases the presence of a $C_{15}$ nucleus and a nicotinic acid group has been recognized. Furthermore, their absolute configurations were not yet defined unambiguously, when those structures and relative configurations were assigned.[6,7)] We now describe the structure of regilidine (1) and its absolute configuration determined by X-ray analysis[8)] as shown in Figs. 1 and 2.

The ethanol extract of the dried roots (5 kg) of T. regelii was percolated successively with n-hexane, ethyl acetate and n-butanol. The ethyl acetate percolate was chromatographed on silica gel. The 50% chloroform-petroleum ether eluate was separated by rechromatography on alumina, leading to the isolation of 1 (13 mg, 0.00026%). Crystallization of 1 from chloroform gave colorless prisms of mp 292-294°C, $[\alpha]_D^{26.4}$ +50° (c, 0.6; $CHCl_3$). The empirical formula, $C_{35}H_{37}O_8N$ was determined by high-resolution MS: m/z ($M^+$) 599.2513 (Theor. 599.2518). The IR spectrum showed the peaks at $\nu_{max}^{KBr}$ ($cm^{-1}$) 3515, 1720 and 1596 for the hydroxyl group, carbonyl ester and aromatic rings, respectively. The UV spectrum absorbed

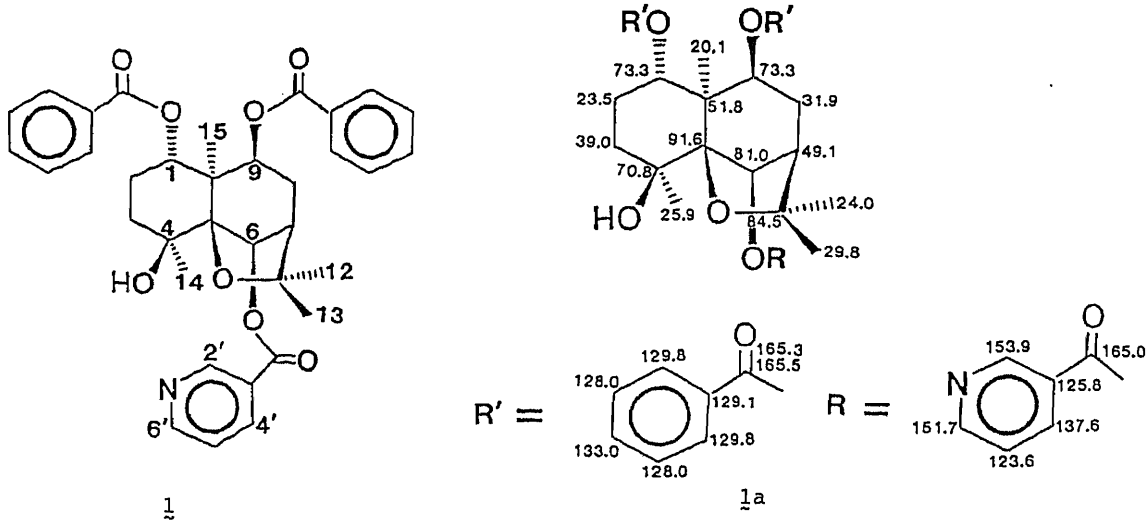


1 1a

Fig. 1. The Structure of Regilidine (1) and Its $^{13}$C-NMR Chemical Shifts

at $\lambda_{max}^{EtOH}$ nm (ε): 227 (25000), 252 (2400), 258 (2400), 265 (3400), 270 (3200) and 280 (1600). Fragmentation peaks were present at m/z 124, 106, assignable to a nicotinoyl group, and at m/z 105 as the base peak for benzoyl ions.[9] One nicotinoyl and two benzoyl esters were confirmed from the $^1$H-NMR spectrum of 1, which contained signals at δ 9.40 (1H, d, J = 1.5, nicotinoyl H-2'), 8.82 (1H, dd, J = 5, 1.5, nicotinoyl H-6'), 8.53 (1H, dt, J = 8, 1.5, nicotinoyl H-4') and 7.82-7.22 (m, 10H, benzoyl x 2 and 1H, nicotinoyl H-5') in the aromatic region. As well as nicotinoyl and benzoyl proton signals, the NMR spectrum of 1 contained signals assignable to protons on the carbon atoms carrying three secondary ester groups, δ 5.73 (1H, s, H-6 ax.), 5.63 (1H, dd, J = 12, 4, H-1 ax.), 5.16 (1H, d, J = 7, H-9 eq.), and to four tertiary methyl groups, δ 1.59 (3H, s, Me-13), 1.56 (3H, s, Me-15), 1.54 (3H, s, Me-12), 1.41 (3H, s, Me-14). The $^{13}$C-NMR assignments shown in 1a, were closely compatible with the INEPT spectrum and with the reported values in several similar systems.[10,11] This also indicated the presence of two benzoyl, ($\delta_c$ for C=O: 165.3, 165.5), one nicotinoyl ($\delta_c$: 165.0), four tert-methyl groups ($\delta_c$: 24.0, 29.8, 25.9, 20.1), and four quat carbons ($\delta_c$: 70.8, 91.6, 84.5, 51.8). 1 was thus shown to be a triester of a $C_{15}H_{22}O_5$ sesquiterpene tetraol belonging to the dihydroagarofuran[12,13] named regelidine. Unfortunately, the nature of the esterificating acids on these three positions could not be elucidated only on the NMR basis because the ring effects created by benzoate and nicotinate groups resemble each other to closely to be distinguished.[10]

X-ray diffraction measurements were made on a Philips four-circle diffractometer using graphite monochromated CuKα radiation. The crystal data of 1 are as follows: $C_{35}H_{37}O_8N$, MW = 599.7; Monoclinic, space grou $P2_12_12_1$; lattice constants; a = 12.059(7), b = 28.489(15), c = 8.986(5) Å; U = 3087 Å$^3$; $D_{calc}$ = 1.290 gcm$^{-3}$; Z = 4. Intensities of 3194 reflections out of 3359 were measured within the 2θ range of 6° through 156°. Intensities of 773 Friedel pairs were also measured in the 2θ range of 25° through 60°. The crystal structure was

determined by the direct method and refined the atomic parameters by the block-diagonal matrix least-squares method to an R value of 0.046 including 37 hydrogen atoms.[14] An attempt has been made to determine the absolute configuration by the anomalous dispersion method. Since the dispersion corrections for the atomic scattering factors of carbon, nitrogen and oxygen are small, it was not possible to draw definite conclusion. However, seven structure factors out of nine for which the difference of the structure factors between the Friedel pair is greater than the 2 ($F_{obs}$) value and both the ratios of $r_{obs} = |F_{obs}(hk\ell)|/|F_{obs}(\bar{h}\bar{k}\bar{\ell})|$ and $r_{calc} = |F_{calc}(hk\ell)|/|F_{calc}(\bar{h}\bar{k}\bar{\ell})|$ differ more than 1% from unity, showing clearly the close similarity of $r_{obs}$ and $r_{calc}$. This indicates the absolute configuration to be as shown in Fig. 2, which is also in accordance with that derived by chemical correlation.[15]

From Fig. 2, the oxygenation pattern on the dihydroagarofuran skeleton (C-1 eq., C-4 eq., C-6 eq., C-9 ax.) is apparent. It is of interest to note that the location of the nicotinoyl ester group at C-6 was found for the first time in the structures of sesquiterpene alkaloids belonging to the family Celastraceae. The absolute configuration of the ent type dihydroagarofuran polyester (1) has now been established unequivocally. Hence, the similar nicotinoyl sesquiterpene alkaloids found so far, mostly in the Celastraceae plants,[16] appear to have the same ent type absolute configuration. A further study of the biogenetic consideration of 1 is now in progress.

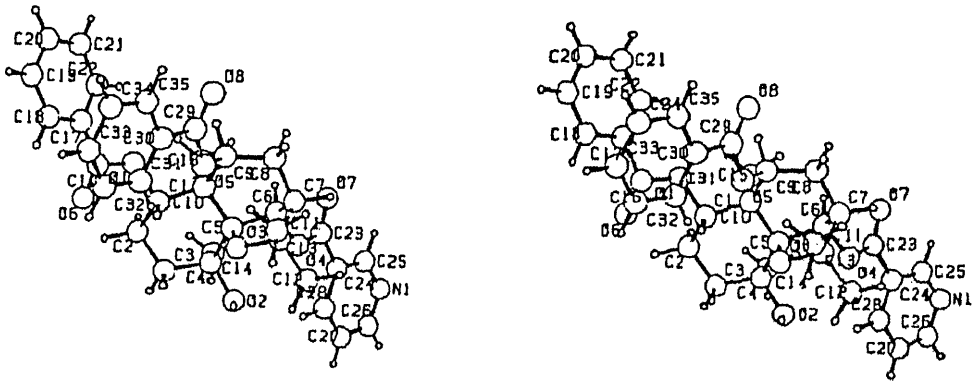


Fig. 2. The Absolute Configuration of Regelidine (1)

ACKNOWLEDGEMENTS The authors are grateful to Dr. Moroi of Daiichi Pharmaceutical Co., Ltd., Mrs. M. Tomoda of Sophia University, Dr. S. Manabe, Mr. M. Nakamura and Miss S. Takei of the Joint Laboratory, School of Medicine, Keio University for measurements of the NMR, MS and IR spectra, respectively.

## REFERENCES AND NOTES


1) Presented at the 31st Symposium on the Chemistry of Perfume, Terpene and Essential Oils, Kyoto, Abstracts p. 262, and p. 265, Sept. 11 (1987).
2) Visiting Research Associate of Keio University on leave from China Jilin Province Institute of Pharmaceutical Industry.
3) H. Hori, G-M. Pang, K. Harimaya, Y. Iitaka and S. Inayama, Chem. Pharm. Bull., 35, 2125 (1987).
4) The plant material was collected at Chang Bai Shan Mountain in Fusong Prefecture, Jilin Province, China in September 1985.
5) S.M. Kupchan, R.M. Smith and R.F. Bryan, J. Am. Chem. Soc., 92, 6667 (1970).
6) R.F. Bryan and R.M. Smith, J. Chem. Soc. (B), 2159 (1971).
7) G. Baudouin, F. Tillequin and M. Koch, Heterocycles, 22, 2221 (1984).
8) The previously reported X-ray crystallographic diffraction method was used to determine the esterification sites in the respective polyester structure and the relative configuration of the molecule [M.J. Begley et al., J. Chem. Soc., Perkin Trans. 1, 535 (1986); references loc. cit].
9) S.M. Kupchan and R.M. Smith, J. Org. Chem., 42, 115 (1977).
10) R.L. Baxter, W.M.L. Crombie, L. Crombie and D.J. Simmonds, J. Chem. Soc., Perkin Trans. 1, 2972 (1979).
11) H.J. den Hertog Jr and C. Kruk, Tetrahedron Lett., 26, 2219 (1974).
12) R.M. Smith in "The Alkaloids" ed., R.H.F. Manske, Academic Press, New York, Vol. 16, 215 (1977); R. Bruning and H. Wagner, Phytochemistry, 17, 1821 (1978).
13) K. Yamada, Kagaku No Ryoiki, Zoukan, 128 57 (1980).
14) A list of atomic parameters will be deposited with the Cambridge Crystallographic Data File and Fo-Fc; thermal parameters and other tables may be obtained from one of the authors (Y.I.) upon request.
15) H.C. Barrett and G. Buchi, J. Am. Chem. Soc., 89, 5665 (1967).
16) Y. Takaiashi et al. have reported very recently that the structures of similar alkaloids isolated from Tripterigium wilfordii Hook. file var regelii have been determined by two-dimensional NMR spectroscopy [Chem. Pharm. Bull., 35, 3534 (1987)]. However, their absolute configurations as well as several non-nicotinoyl dihydroagarofuran constituents in the same plant were not established rigorously [Abstracts of Papers, the 32nd Annual Meeting of the Japanese Society of Pharmacognosy, Okayama, p. 39, Oct. 11 (1985); the 106th Annual Meeting of the Pharmaceutical Society of Japan, Chiba, p. 199, Apr. 2 (1986)].


(Received October 6, 1987)